

# Iron-Catalyzed C–H/N–H Activations for Annulation of Allenes, Alkynes, and Bicyclopropylidenes

**Dissertation**

for the award of the degree

“Doctor rerum naturalium”

of the Georg-August-University of Göttingen



within the doctoral program of chemistry

of the Georg-August-University School of Science (GAUSS)

submitted by

**Jiayu Mo**

from Liuzhou, Guangxi Province, China

Göttingen, 2020



## **Thesis Committee**

Prof. Dr. Lutz Ackermann, Institute of Organic and Biomolecular Chemistry,  
University of Göttingen

Prof. Dr. Alexander Breder, Institute of Organic Chemistry, University of  
Regensburg

## **Examination Board**

Reviewer: Prof. Dr. Lutz Ackermann, Institute of Organic and Biomolecular  
Chemistry, University of Göttingen

Second Reviewer: Prof. Dr. Alexander Breder, Institute of Organic and  
Biomolecular Chemistry, University of Regensburg

## **Further Members of the Examination Board**

Prof. Dr. Dr. h.c.mult. Lutz F. Tietze, Institute of Organic and Biomolecular  
Chemistry, University of Göttingen

Prof. Dr. Marina Bennati, Institute of Organic and Biomolecular Chemistry,  
University of Göttingen; Max Planck Institute for Biophysical Chemistry,  
Göttingen

Prof. Dr. Ricardo Mata, Institute of Physical Chemistry, University of Göttingen

Jun.-Prof. Dr. Johannes C. L. Walker, Institute of Organic and Biomolecular  
Chemistry, University of Göttingen

**Date of the Oral Examination: 26.10.2020**



## **Acknowledgements**

I would like to express the deepest appreciation to my supervisor Prof. Dr. Lutz Ackermann, who gave me constant encouragement, excellent guidance and patience during my Ph.D. study. Without his persistent help this dissertation would not have been possible.

I also want to express my sincere appreciation to China Scholarship Council (CSC) for the financial support of my doctoral research in Germany.

I am grateful to Prof. Dr. Alexander Breder for accepting to be my second supervisor. I also would like to thank Prof. Dr. Dr. h.c.mult. Lutz F. Tietze, Prof. Dr. Marina Bennati, Prof. Dr. Ricardo Mata, and Jun.-Prof. Dr. Johannes C. L. Walker for agreeing to take part in my defense.

I would like to thank people who I have the opportunity to cooperate in our group: Dr. Thomas Müller, Dr. Joao Carlos Agostinho de Oliveira, Dr. Antonis Messinis, Dr. Gianpiero Cera, Dr. Gandeepan Parthasarathy. My deepest thanks also go to Dr. Serhiy Demeshko and Prof. Dr. Franc Meyer for their invaluable contributions of our collaboration on iron chemistry. I also thank Dr. Torben Rogge, Julia Struwe, Dr. Julian Koeller, Ralf Alexander Steinbock, Nikolaos Kaplaneris, Uttam Dhawa and Dr. Svenja Warratz for their helpful suggestions concerning several instruments.

I deeply thank Dr. Torben Rogge, Alexej Scheremetjew, Leonardo Massignan, Nate Ang, Long Yang, Jun Wu, and Shou-Kun Zhang for their patience and time to proofread this thesis. My sincere thanks also go to Dr. Joachim Loup, Dr. Torben Rogge, Long Yang, Julia Struwe, Nikolaos Kaplaneris, Dr. Lars Finger, Wei Wang, Dr. Xuefeng Tan, and Shou-Kun Zhang to correct supporting information and manuscripts of my projects.

I thank Dr. Gianpiero Cera, Dr. Joachim Loup, Dr. Youai Qiu, Dr. Yulei Wang, Dr. Holm Frauendorf and Dr. Michael John for their suggestion on my projects.

I would also like to thank Dr. Christopher Golz for his assistance with X-ray diffraction analysis, as well as to all the members of the analytical departments (NMR and mass spectrometry) at the IOBC for their continuous support to our research work.

My deep thanks also go to Ms. Gabriele Keil-Knepel and Ms. Bianca Spitalieri for their kindly assistance with administrative tasks. I thank Mr. Stefan Beußhausen for the technical assistance with instruments and Mr. Karsten Rauch for his support to our lab work.

I thank all the group members in Ackermann Group, particularly the past and current members in Lab 302, 308 and 123: Dr. Santhi Vardhana Yetra, Dr. Lars Finger, Dr. Thomas Müller, Dr. Julian Koeller, Dr. Joachim Loup, Zhigao Shen, Dr. Gandeepan Parthasarathy, Dr. Qingqing Bu, Dr. Alexandra Schischko, Dr. Gianpiero Cera, Dr. Wei Wang, Shou-Kun Zhang, Alexej Scheremetjew, Prof. Dr. Yan Zhang, Prof. Dr. Huawen Huang and Dr. Samaresh Chandra Sau.

Last but not the least, I want to express my special thanks to my family and my friends for their continuous support and encouragement.

## Contents

1. Introduction .....	1
1.1 Transition Metal-Catalyzed C–H Activation.....	2
1.1.1 The Concept of Transition Metal-Catalyzed C–H Activation.....	2
1.1.2 Advantages of Transition Metal-Catalyzed C–H Activation .....	2
1.1.3 Mechanisms of Transition Metal-Catalyzed C–H Activation .....	4
1.2 Iron-Catalyzed C–H Activation .....	6
1.2.1 Early Reports on Iron-Catalyzed C–H Activation.....	7
1.2.2 Iron-Catalyzed C–H Activation with Organometallic Reagents.....	10
1.2.3 Iron-Catalyzed C–H Activation with Organic Electrophiles .....	12
1.2.4 Iron-Catalyzed C–H Annulation Reactions .....	17
1.3 Transition Metal-Catalyzed C–H/C–C Activation.....	21
2. Objectives .....	28
3. Results and Discussion.....	31
3.1 Iron-Catalyzed C–H/N–H Allene Annulation .....	31
3.1.1 Optimization Studies .....	31
3.1.2. Impact of Directing Group on C–H Functionalization.....	34
3.1.3. Substrate Scope and Limitations.....	37
3.1.4 Traceless Removal of TAM Group .....	44
3.1.5 Mechanistic Studies .....	45
3.1.6 Proposed Mechanism.....	50
3.2 Iron-Catalyzed C–H/N–H Propargyl Acetate Annulation .....	52

3.2.1 Optimization Study and Substrate Scope .....	52
3.2.2 Traceless Electrochemical Removal of TAH Group .....	53
3.2.3 Mechanistic Studies .....	55
3.2.4 Proposed Mechanism.....	59
3.3 Iron-Catalyzed C–H/C–C Activation with Bicyclopropylidenes .....	60
3.3.1 Optimization Studies .....	60
3.3.2 Impact of the N-Substituent on the C–H/C–C Activation .....	64
3.3.3 Substrate Scope and Limitations.....	66
3.3.4 Removal of TAH Group .....	73
3.3.5 Mechanistic Studies .....	74
3.3.6 Proposed Mechanism.....	78
4. Summary and Outlook .....	80
5. Experimental Part .....	83
5.1 General Remarks.....	83
5.2 General Procedures.....	87
5.3 Iron-Catalyzed C–H/N–H Annulation with Allenes .....	90
5.3.1 Analytical Data – Products with Different N-Substituted Triazolyl Moieties .....	90
5.3.2 Analytical Data – Products <b>89</b> .....	97
5.3.3 Analytical Data – Products <b>90</b> .....	106
5.3.4 Analytical Data – Products of TAM Benzamide Annulation with Different Allene Acetates .....	111
5.3.5 Traceless Removal of TAM Group .....	115
5.3.6 Mechanistic Studies .....	116

5.4 Iron-Catalyzed C–H/N–H Annulation with Propargyl Acetates .....	127
5.4.1 Analytical Data – Products <b>92</b> .....	127
5.4.2 Traceless Removal of TAH Group.....	128
5.4.3 Mechanistic Studys .....	129
5.5 Iron-Catalyzed C–H/C–C Activations .....	132
5.5.1 Analytical Data – Products with Different N-Substituted Triazolyl Moieties .....	132
5.5.2 Analytical Data – Isoquinolone <b>95</b> .....	138
5.5.3 Analytical Data – Impact of CF <sub>3</sub> -Substitution of Benzamide .....	145
5.5.4 Analytical Data – Substrate Scope with BCP <b>94</b> .....	150
5.5.5 Analytical Data – Bispiro-Fused Isoquinolone <b>96</b> .....	152
5.5.6 Removal of TAH Group .....	161
5.5.7 Mechanistic Studies .....	162
5.6 Mössbauer Measurement .....	170
5.7 X-Ray Crystallographic Analysis .....	176
5.7.1 Data Analysis for Crystal Structure of <b>89la</b> .....	176
5.7.2 Data Analysis for Crystal Structure of <b>120</b> .....	180
6. References .....	186
NMR Spectra .....	200

## List of Abbreviations

Ac	acetyl
acac	acetyl acetate
Alk	alkyl
AMLA	ambiphilic metal ligand activation
aq	aqueous
Ar	aryl
atm	atmosphere
BHT	2,6-di- <i>tert</i> -butyl-4-methylphenol
BIES	base-assisted internal electrophilic substitution
Bn	benzyl
Bu	butyl
calc.	calculated
<i>cat.</i>	catalytic
CMD	concerted metalation deprotonation
Cy	cyclohexyl
$\delta$	Chemical shift
d	doublet
dbm	1,3-diphenyl-1,3-propanedione
dd	doublet of doublets
DCB	dichlorobenzene
DCE	dichloroethane
DCP	Dicumyl peroxide
DCIB	dichloroisobutane
DME	dimethoxyethane
DMSO	dimethylsulfoxide
dppbz	1,2-bis(diphenylphosphino)benzene
dppe	1,2-bis(diphenylphosphino)ethane
dppen	1,2-bis(diphenylphosphino)ethene
dt	doublet of triplets
DG	directing group

EWG	electron withdrawing group
EI	electron ionization
equiv	equivalent
ESI	electrospray ionization
Et	ethyl
g	gram
GC	gas chromatography
h	hour
hept	heptyl
hex	hexyl
HRMS	high resolution mass spectrometry
Hz	Hertz
<i>i</i>	iso
IMes	1,3-bis(2,4,6-trimethylphenyl)imidazole-2-ylidene
IPr	1,3-bis(2,6- <i>iso</i> -propylphenyl)imidazole-2-ylidene
IR	infrared spectroscopy
<i>J</i>	coupling constant
KIE	kinetic isotope effect
L	ligand
LDA	lithium diisopropylamide
<i>m</i>	<i>meta</i>
m	multiplet
M	molar
[M] <sup>+</sup>	molecular ion peak
Me	methyl
Mes	mesityl
mg	milligram
MHz	megahertz
min	minute
mL	milliliter
mmol	millimole
M. p.	melting point

MS	mass spectrometry
<i>m/z</i>	mass to charge ratio
NMR	nuclear magnetic resonance
<i>o</i>	<i>ortho</i>
Oct	octyl
OLED	organic light emitting diode
<i>p</i>	<i>para</i>
Pent	pentyl
Ph	phenyl
phen	1,10-phenanthroline
PMB	<i>para</i> -methoxybenzyl
PMP	<i>para</i> -methoxyphenyl
Piv	pivaloyl
ppm	parts per million
Pr	propyl
q	quartett
Q	8-aminoquinoline
RT	room temperature
R <sub>L</sub>	large substituent
s	singlet and second
SET	single electron transfer
SPS	solvent purification system
<i>t</i>	<i>tert</i>
t	triplet
<i>T</i>	temperature
TAH	triazolylmethyl
TAM	triazolyldimethylmethyl
TEMPO	2,2,6,6-tetramethylpiperidine- <i>N</i> -oxide
TFA	Trifluoroacetic acid
THF	tetrahydrofuran
THP	tetrahydropyranyl
TLC	thin layer chromatography

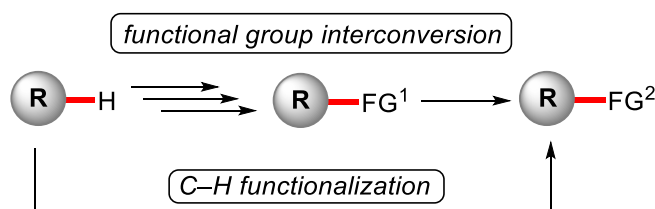
TM	transition metal
TMEDA	<i>N,N,N',N'</i> -tetramethylethylenediamine
TMS	trimethylsilyl
TS	transition state
X	(pseudo-)halide

## 1. Introduction

Organic synthesis is a powerful tool for molecular construction with notable applications to material sciences,<sup>[1]</sup> natural product syntheses<sup>[2]</sup> and life-saving pharmaceuticals.<sup>[3]</sup> In light of these transformative advantages, tremendous efforts have been devoted to the development of novel methods for molecular syntheses, which has resulted in diverse applications with countless benefits for society.<sup>[4]</sup> However, despite indisputable progress, organic syntheses, which has been dominated by the transformation of functional groups,<sup>[5]</sup> continues to be perceived as a polluting science due to *inter alia* waste generation, resource and energy consumption, and the use of often toxic and dangerous chemicals.

In 1988, *Warner* and *Anastas* included catalysis as one of the “12 Principles of Green Chemistry”.<sup>[6]</sup> During the past century, catalysis has been recognized as a foundation of the chemical industries with significant achievements in developing economically, environmentally and technologically beneficial transformations.<sup>[7]</sup>

A significant stimulus in organic synthesis was made by the emergence of direct functionalizations of omnipresent C–H bonds.<sup>[8]</sup> C–H functionalizations are environmentally-benign and economically-attractive, since they prevent lengthy synthetic operations and reduce waste generation by activating the inert C–H bonds directly instead of using pre-functionalized substrates (Scheme 1).

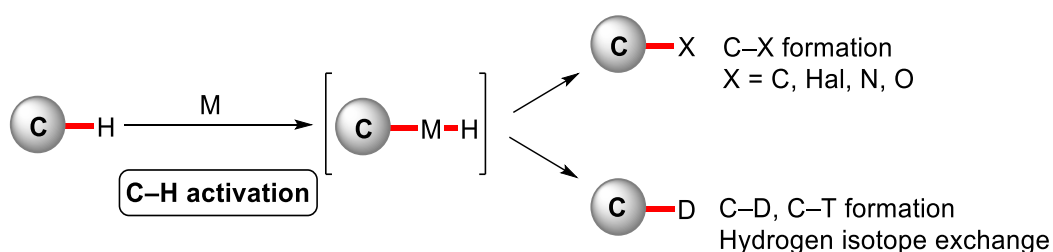


**Scheme 1** Traditional functional group interconversion *versus* C–H functionalization.

## 1.1 Transition Metal-Catalyzed C–H Activation

### 1.1.1 The Concept of Transition Metal-Catalyzed C–H Activation

Transition metal-catalyzed C–H activation involves the transformation of otherwise inert C–H bonds into C–Met bonds.<sup>[9]</sup> In this concept, the formation of an organometallic complex through C–H coordination of the inner-sphere of a metal is often important.<sup>[10]</sup> The intermediate produced by C–H activation can further undergo subsequent reactions to afford the functionalized products (Scheme 1.1).

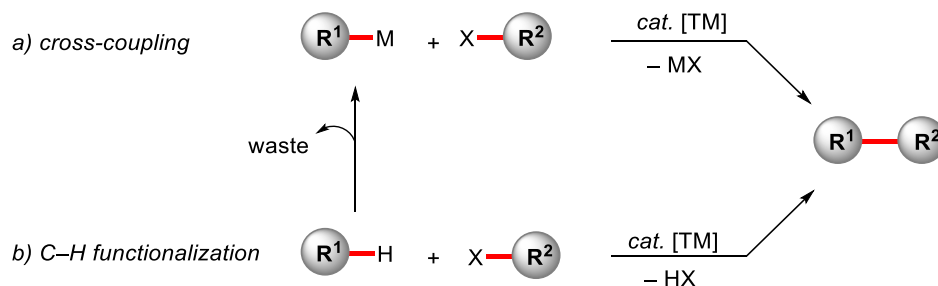


**Scheme 1.1** C–H activation.

### 1.1.2 Advantages of Transition Metal-Catalyzed C–H Activation

Transition metal-catalyzed cross-couplings, such as the *Suzuki-Miyaura*, *Negishi* and *Mizoroki-Heck* reactions, are an important tool in organic synthesis for the formation of C–C bonds, which have been awarded the 2010 Nobel Prize in chemistry.<sup>[11]</sup> However, despite indisputable progress, cross-coupling reactions continue to be severely limited, due to *inter alia* the requirement of pre-functionalized substrates and organometallic compounds, which significantly decrease the user-friendliness, sustainability and step-economy. From this point of view, the direct activation of omnipresent C–H bonds would be a highly desirable alternative to conventional cross-couplings due to the avoidance of pre-functionalized substrates (Scheme 1.2).

## 1. Introduction



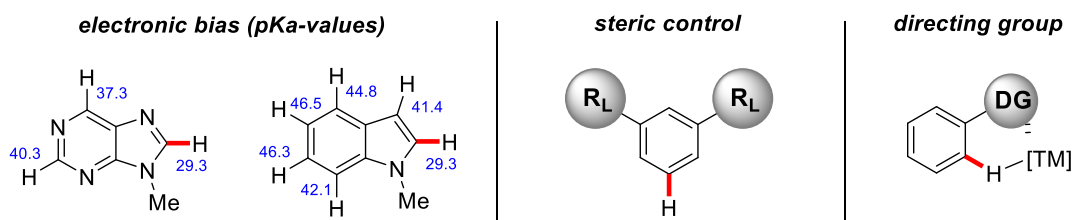
**Scheme 1.2** Comparison of cross-coupling and C–H functionalization.

In order to achieve an efficient direct C–H functionalization, a transition metal catalyst, which can directly react with a C–H bond to generate a C–M bond under mild conditions, is highly desirable. Partially, due to the high dissociation energy of C–H bonds ( $\sim 110 \text{ kcal mol}^{-1}$  for C(aryl)–H and  $\sim 105 \text{ kcal mol}^{-1}$  for alkanes),<sup>[12]</sup> harsh conditions would be required to cleave the bond directly, thus resulting in a narrow substrate scope.<sup>[13]</sup> Additionally, the metallated intermediates can easily react with a number of different chemicals thereby allowing for a range of applications.<sup>[14]</sup>

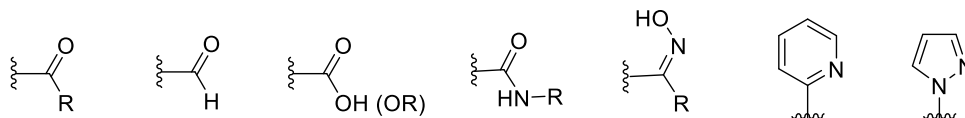
The fact that C–H bonds are omnipresent in organic molecules and have comparable dissociation energies represents a challenge for controlling the selectivity in direct C–H activation. To tackle this issue, various strategies have been developed based on the transition metal catalyst's mode of action, for example 1) electronic bias,<sup>[15]</sup> 2) steric control,<sup>[16]</sup> and 3) directing group-assisted C–H activation<sup>[17]</sup> (Scheme 1.3a). Since approaches based on electronic and steric biases highly depend on the nature of the substrates, this strategy is typically limited in terms of viable scope. In sharp contrast, by a directing group (DG) which coordinates to the metal center of the catalyst and directs the catalyst to a proximal position, selective C–H activation could be achieved with a broad variety of substrates. Furthermore, considerable attention has been devoted to the development of weakly coordinating,<sup>[18]</sup> removable<sup>[19, 17c]</sup> or transient<sup>[20]</sup> directing groups (Scheme 1.3b).

## 1. Introduction

### a) approaches for selective C–H activation



### b) selected examples of directing groups



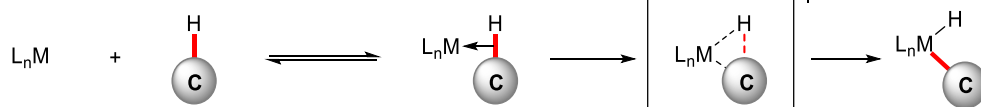
**Scheme 1.3** Positional selectivity in C–H activation.

### 1.1.3 Mechanisms of Transition Metal-Catalyzed C–H Activation

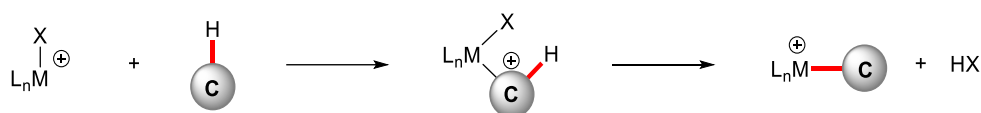
As a better understanding of the elementary C–H cleavage step would allow for the design of more efficient catalytic C–H functionalizations, intensive studies have been devoted to elucidate various C–H activation modes.<sup>[21]</sup> Depending on the metal fragment, C–H metalation can proceed *via* several distinct reaction pathways:<sup>[21a]</sup> a) oxidative addition with electron-rich, low-valent complexes of late transition metals, b) electrophilic substitution with late transition metals in higher oxidation states where the metal acts as a Lewis acid, c)  $\sigma$ -bond metathesis with early transition metals, typically involving an alkyl- or hydride-metal complex, as well as lanthanides and actinides,<sup>[21b]</sup> d) 1,2-addition with unsaturated M=X bonds, such as metal imido, oxo and alkylidene complexes, and e) base-assisted metalation most commonly with carboxylate ligands (Scheme 1.4).<sup>[21a]</sup>

## 1. Introduction

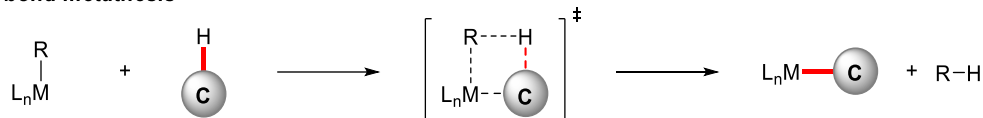
### a) oxidative addition



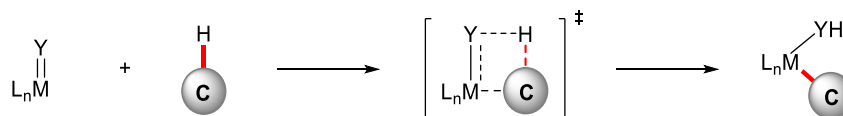
### b) electrophilic substitution



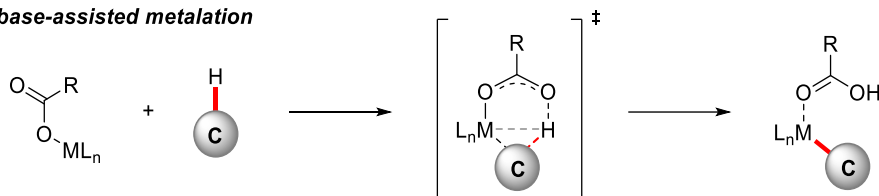
### c) $\sigma$ -bond metathesis



### d) 1,2-addition



### e) base-assisted metalation

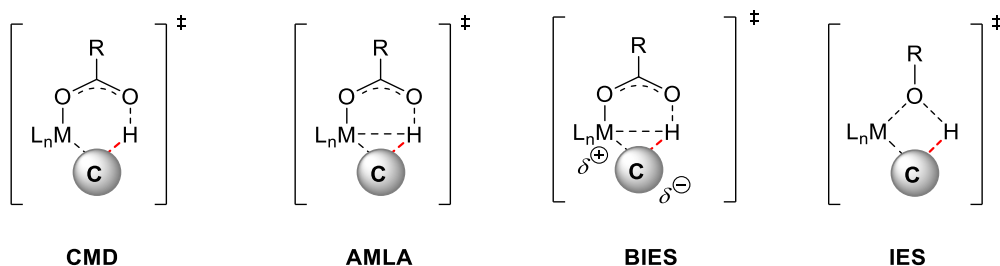


**Scheme 1.4** Viable modes of organometallic C–H activation.

Over the past few years, several transition states of base-assisted C–H metalation were proposed (Scheme 1.5).<sup>[21a]</sup> The concerted metalation-deprotonation (CMD)<sup>[22]</sup> describes the synergistic interaction between the metal center, the carboxylate-ligand and the C–H bond *via* a six-membered transition state. For the ambiphilic metal-ligand activation (AMLA),<sup>[23]</sup> a similar transition state has been proposed. Both transition states are characterized by a preference for kinetically C–H-acidic substrates. As an explanation for the preference of electron-rich substrates in several catalytic transformations, the concept of base-assisted internal electrophilic substitution (BIES) has been

## 1. Introduction

proposed by *Ackermann*.<sup>[24]</sup> In contrast to the six-membered transition states, the term internal electrophilic substitution (IES)<sup>[25]</sup> which was proposed for the reaction involving alkoxide bases featured a transition state with a highly strained four-membered ring, basically a  $\sigma$ -bond metathesis. Based on *Ackermann's* BIES, *Carrow* coined this mechanistic manifold very recently as e-CMD.<sup>[26]</sup>



**Scheme 1.5** Proposed transition states for base-assisted C–H metalations.

## 1.2 Iron-Catalyzed C–H Activation

Transition metal-catalyzed C–H functionalization has been recognized as a powerful tool for molecular syntheses.<sup>[9, 14, 17a]</sup> Thus far, C–H functionalizations were often achieved with precious transition metal catalysts, for instance, palladium, iridium, rhodium and ruthenium. However, these noble late transition metals normally feature high costs,<sup>[27]</sup> a low natural abundance<sup>[28]</sup> and a high toxicity,<sup>[29]</sup> which highly decreases the sustainability and economic efficiency of the approach. As a direct consequence, the development of transformations under 3d transition metal catalysis,<sup>[30]</sup> and especially iron,<sup>[31]</sup> has attracted considerable attention due to their high Earth-abundance, cost-efficiency, and low toxicity.<sup>[32]</sup>

Owing to the electron configuration of iron, iron catalysts can access various oxidation from –2 to +6 and spin states and can easily undergo single electron transfer (SET) processes. These properties enable iron catalysts to be employed in a wide range of transformations.<sup>[33]</sup>

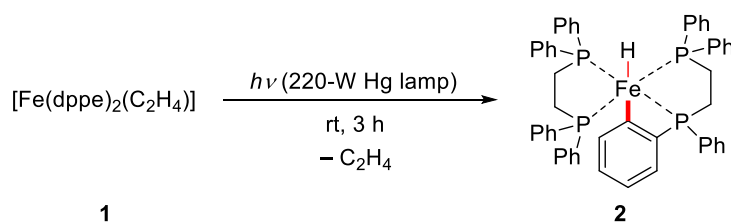
## 1. Introduction

In general, iron in low oxidation states exhibits nucleophilic properties, which enables a number of organic transformations, such as nucleophilic substitutions, reductions, cycloisomerizations, or cross coupling reactions,<sup>[34]</sup> while in higher oxidation states, iron behaves as a Lewis acid, thus activating unsaturated bonds.<sup>[35]</sup>

Inspired by early studies of catalytic C–C bond formations,<sup>[36]</sup> the scientific community focused their attention on the development of efficient iron catalysts systems for sustainable C–H activation strategies. Indeed, low-valent iron species were found to be effective for the activation of C(sp<sup>2</sup>)–H as well as C(sp<sup>3</sup>)–H bonds under mild reaction conditions, providing an environmentally benign and atom-economical alternative for the construction of novel C–C and C–Het bonds.<sup>[31]</sup>

### 1.2.1 Early Reports on Iron-Catalyzed C–H Activation

In 1968, an early example of stoichiometric organometallic C–H activation was reported, in which an *ortho*-C–H bond was oxidatively added to an iron(0) center to form the hydride ferracycle complex **2** through irradiation of the [Fe(dppe)<sub>2</sub>·C<sub>2</sub>H<sub>4</sub>] complex **1** (Scheme 1.6).<sup>[37]</sup>

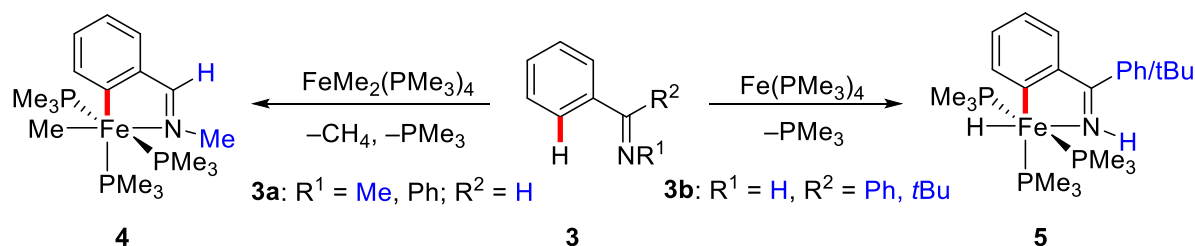


**Scheme 1.6** Stoichiometric organometallic C–H activation.

Stoichiometric cyclometallations of organic compounds with iron complexes were subsequently described.<sup>[38]</sup> A representative example is the stoichiometric cyclometallation of aryl imines with Fe(PMe<sub>3</sub>)<sub>4</sub> or FeMe<sub>2</sub>(PMe<sub>3</sub>)<sub>4</sub>, which was reported by *Klein*.<sup>[39]</sup> C–H activation of benzaldimine **3a** by FeMe<sub>2</sub>(PMe<sub>3</sub>)<sub>4</sub>

## 1. Introduction

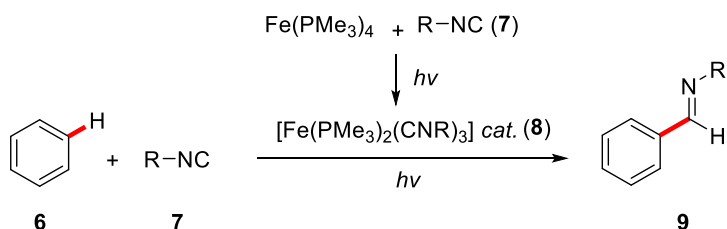
proceeds *via*  $\sigma$ -bond metathesis, while cyclometallation was proposed to proceed *via* nitrogen-assisted C–H oxidative addition when  $\text{Fe}(\text{PMe}_3)_4$  and ketimine **3b** were employed (Scheme 1.7).



**Scheme 1.7** Directed stoichiometric C–H activation.

Two notable aspects of this stoichiometric C–H activation are: 1) Nitrogen-directed  $\text{C}(\text{sp}^2)\text{--H}$  activation is possible, ideally with iron(0) through oxidative addition or with a methyliron(II) species *via*  $\sigma$ -bond metathesis, and 2) the iron(0) complex displayed a higher reactivity towards C–H bond activation as compare to N–H bond cleavage.

In 1987, Jones disclosed the first example of iron-catalyzed C–H functionalization.<sup>[40]</sup> The catalyst **8** generated from  $\text{Fe}(\text{PMe}_3)_4$  and isocyanide **7** enable the successful transformation of aldimine **9** from benzene **6** (Scheme 1.8). The key to success in this reaction was the low concentration to avoid substrate inhibition and the use of UV irradiation for the generation of active iron species.

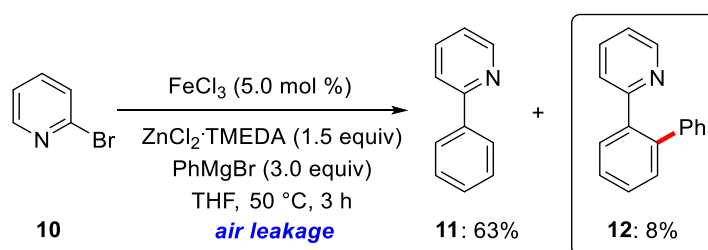


**Scheme 1.8** Iron-catalyzed C–H functionalization of benzene.

In 2006, Nakamura disclosed an example of iron-catalyzed direct C–H activation was disclosed by through a serendipitous observation during iron-

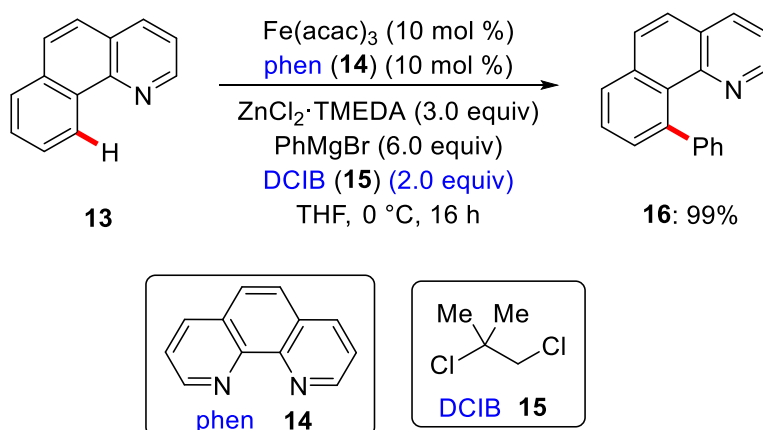
## 1. Introduction

catalyzed cross-coupling reactions (Scheme 1.9).<sup>[41]</sup> Here, a C–H functionalized product, 2-biphenylpyridine **12**, was observed in the cross-coupling of 2-bromopyridine **10** and a phenylzinc reagent. In order to develop an efficient iron-catalyzed C–H activation system, the authors analyzed the reaction, which resulted in a number of significant observations: 1) an oxidant is necessary for catalyst turnover, 2) a nitrogen-based ligand is crucial for this transformation, and 3) the coupling partner is an *in situ* formed organic zinc reagent rather than the Grignard reagent.



**Scheme 1.9** Iron-catalyzed C–H arylation.

Two years later, *Nakamura* reported an iron-catalyzed direct C–H activation with phenanthroline **14** as the ligand and dichloroisobutane **15** (DCIB) as the oxidant of choice (Scheme 1.10).<sup>[42]</sup>



**Scheme 1.10** Iron-catalyzed direct C–H activation.

Subsequent studies using monodentate directing groups,<sup>[43]</sup> such as imines, amides, ketones, esters, and pyridines, led to major advancement in the field of

## 1. Introduction

iron-catalyzed C(sp<sup>2</sup>)–H arylations and alkylations. A breakthrough in iron-catalyzed C–H functionalization was represented by the application of bidentate<sup>[9a, 9g]</sup> directing groups, which not only provided an access to unprecedented C(sp<sup>3</sup>)–H activations, but also significantly diversified possible transformations. Major progress in the field of bidentate directing group-assisted iron-catalyzed C–H functionalizations was achieved by *Nakamura*<sup>[31a]</sup> with 8-aminoquinoline (Q) group and by *Ackermann*<sup>[31b]</sup> with the easily accessible triazolyldimethylmethyl (TAM) group.

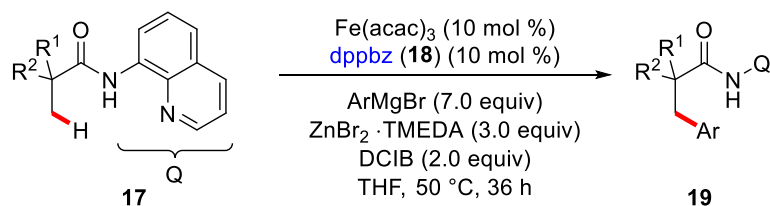
### 1.2.2 Iron-Catalyzed C–H Activation with Organometallic Reagents

At an early stage, major progress in this research field was achieved by the development of direct arylations of C(sp<sup>2</sup>)–H bonds using monodentate directing groups, including: 1) functionalizations of olefinic C(sp<sup>2</sup>)–H bonds,<sup>[43g]</sup> 2) without zinc additives,<sup>[43h]</sup> 3) replacing Grignard reagents with metallic magnesium,<sup>[43e]</sup> and 4) the use of synthetically useful imines<sup>[43c, 43h, 43j]</sup> and amides<sup>[43f]</sup> as the directing group.

C(sp<sup>3</sup>)–H functionalizations were realized by bidentate directing group assistance through low-valent iron catalysis. In this context, *Nakamura* reported on 8-aminoquinoline group-assisted direct arylations of aliphatic amides **17** with *in situ* generated aryl zinc reagents (Scheme 1.11a).<sup>[44]</sup> In contrast, *Ackermann* developed a powerful method employing the TAM group, a highly effective bidentate directing group, for the direct arylation of aromatic and aliphatic amides **20** and **23** (Scheme 1.11b).<sup>[45]</sup> It is worth noting that a bidentate phosphine ligand, such as dppbz **18** or dppe **21**, was necessary for these transformations, whereas nitrogen-based ligands turned out to be ineffective. Recently, *Ackermann* successfully used environmental friendly electricity as oxidant instead of DCIB for the iron-catalyzed C–H arylation.<sup>[46]</sup>

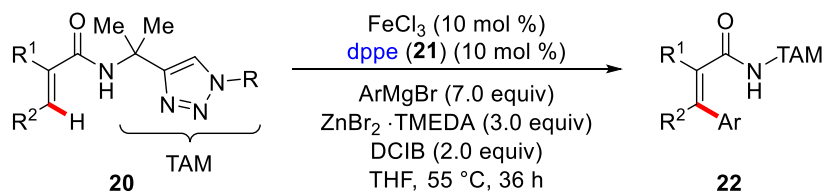
## 1. Introduction

a) Nakamura

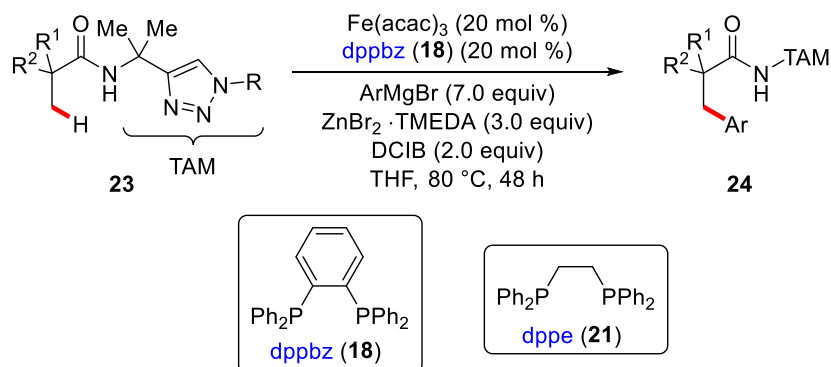


b) Ackermann

$C(sp^2)$ -H arylation



$C(sp^3)$ -H arylation

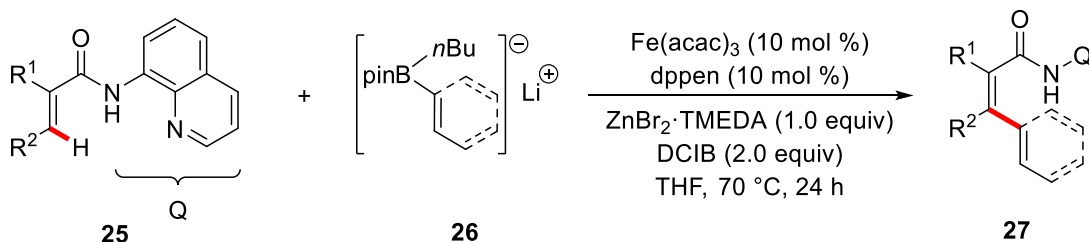


**Scheme 1.11** Bidentate directing group-assisted iron-catalyzed C–H arylation.

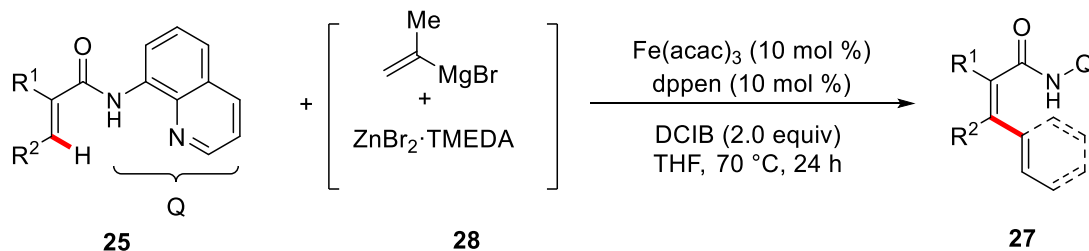
In addition, lithium borate salts **26** proved to be a viable alternative to Grignard reagents for the low-valent iron-catalyzed C–H alkenylation (Scheme 1.12a).<sup>[47]</sup> Since various alkenylboronates are easily available and the corresponding magnesium reagents are usually difficult to prepare, this transformation shows a broader substrate scope as compared to the approach using alkenylmagnesium bromide **28** (Scheme 1.12b).<sup>[48]</sup>

## 1. Introduction

### a) alkenylation with lithium borate salts



### b) alkenylation with Grignard reagents



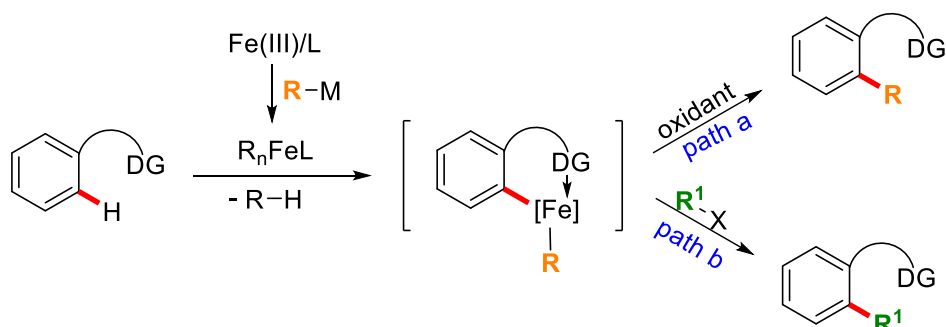
**Scheme 1.12** Iron-catalyzed C–H alkenylation.

Apart from arylations and alkenylations, considerable achievements were also accomplished in iron-catalyzed C–H alkylations using alkyl aluminium reagents<sup>[49]</sup> or *in situ* alkyl formed zinc reagents.<sup>[48, 50]</sup>

### 1.2.3 Iron-Catalyzed C–H Activation with Organic Electrophiles

Despite indisputable progress in iron-catalyzed C–H activations with nucleophilic coupling partners, in most of the cases, stoichiometric amounts of expensive and toxic DCIB is needed as an oxidant to guarantee an efficient transformation (Scheme 1.13, path a). Recently, a major advancement in iron-catalyzed C–H activation was represented by reacting the *in situ* generated iron species with various organic electrophiles, thus avoiding the use of external oxidants (scheme 1.13, path b). In this context, C–H transformations including alkylation,<sup>[51]</sup> allylation<sup>[51a, 52]</sup> and alkynylation<sup>[53]</sup> were accomplished, employing electrophiles in bidentate directing group-assisted low-valent iron catalysis.

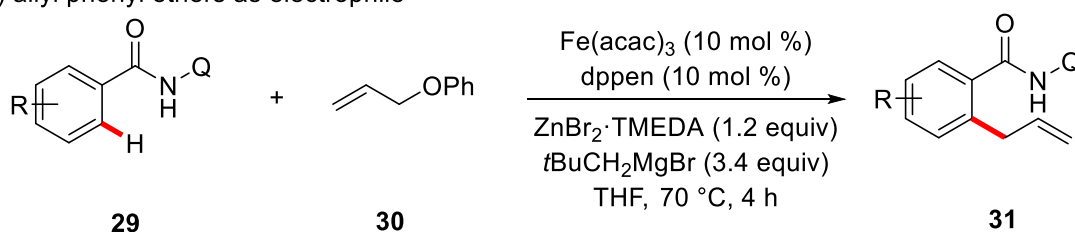
## 1. Introduction



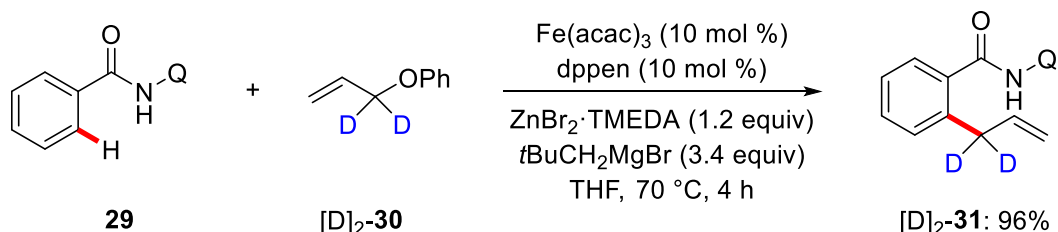
**Scheme 1.13** Bidentate directing group assisted iron-catalyzed C–H arylation.

*Nakamura* reported iron-catalyzed C–H allylations with allyl phenyl ethers **30** as the organic electrophiles (Scheme 1.14a).<sup>[52]</sup> The fact that allyl phenyl ether **30** could be used as the electrophile in iron-catalyzed C–H functionalizations, was serendipitously discovered during their optimization of oxidants for iron-catalyzed arylations of *N*-phenylpyrazole with diarylzinc. In this approach, C–H methylations and arylations in the presence of organozinc reagents, such as  $\text{Me}_2\text{Zn}$  or  $\text{Ph}_2\text{Zn}$ , was observed, suggesting that an appropriate organometallic base was crucial for the transformation. To further gain insights into the catalyst's mode of action, deuterated allyl phenyl ether  $[\text{D}]_2\text{-30}$  was subjected

a) allyl phenyl ethers as electrophile



b) evidence for  $\text{S}_{\text{N}}2$ -type mechanism

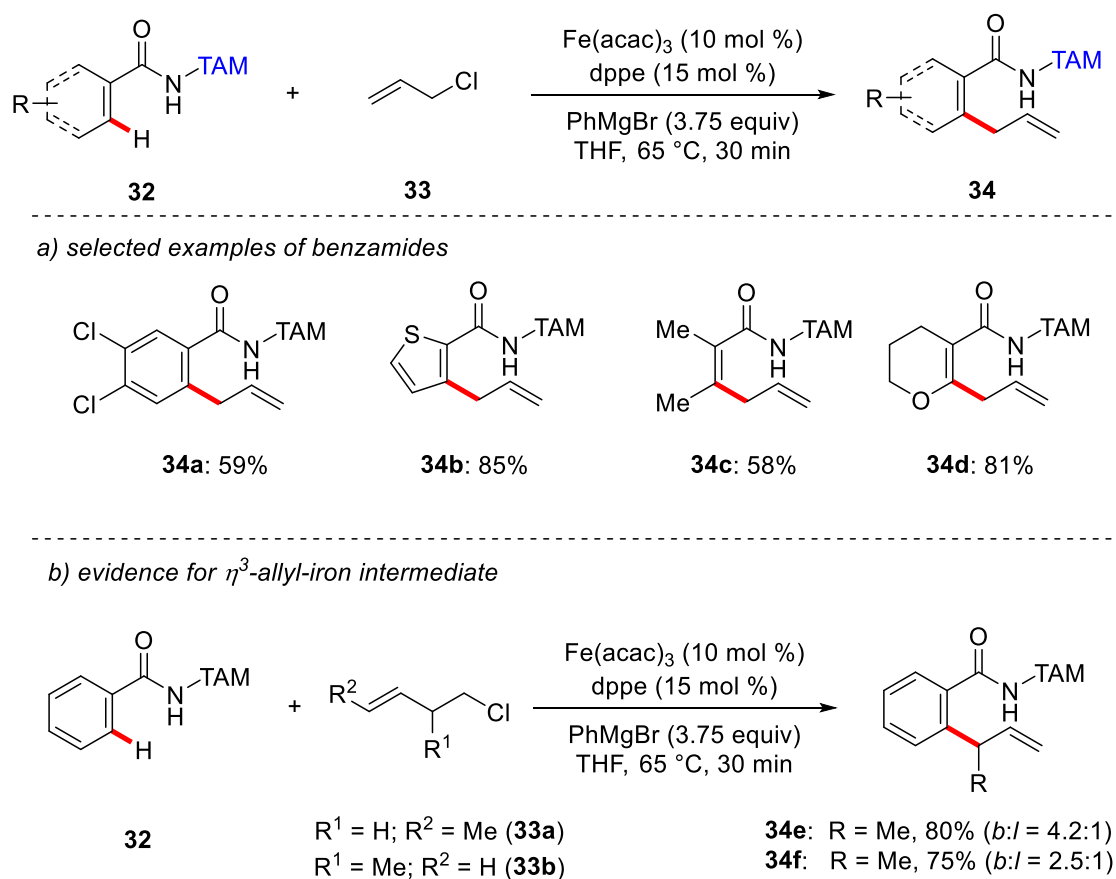


**Scheme 1.14** Iron-catalyzed C–H allylations with allyl phenyl ethers.

## 1. Introduction

to the reaction. Selectively  $\gamma,\gamma$ -deuterated-product  $[D]_2\text{-}\mathbf{31}$  was observed, providing strong support for a  $S_N2$ -type mechanism (Scheme 1.14b).

In a report by *Ackermann*, a widely applicable method for C–H allylations employing the user-friendly TAM group was disclosed.<sup>[51a]</sup> Various aromatic, heteroaromatic and olefinic benzamides **32** were found to be applicable in the transformation (Scheme 1.15a). Notably, the branched allylated product **34e/34f** was formed with comparable levels of regioselectivity with (*E*)-crotyl chloride **33a** or the secondary allyl chloride **33b**, providing support for the formation of a  $\eta^3$ -allyl intermediate (Scheme 1.15b).<sup>[54]</sup>

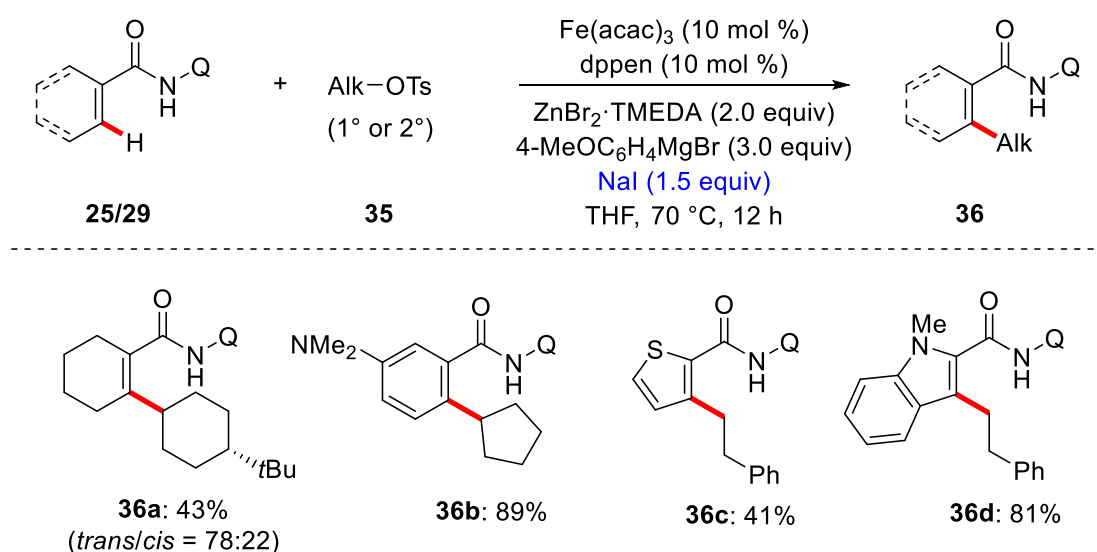


**Scheme 1.15** Iron-catalyzed C–H allylation with allyl halides.

The concept was further expanded to iron-catalyzed C–H alkylation and benzylation using alkyl and benzyl electrophiles.

## 1. Introduction

For the alkylation reported by *Nakamura*, an excess of NaI was crucial for suppressing the undesired C–H arylation, thereby allowing for an efficient transformation (Scheme 1.16).<sup>[51c]</sup> Interestingly, the diastereochemical information was partially deteriorated in **36a** when using diastereochemically well-defined *trans*-4-*tert*-butylcyclohexyl tosylate **35a**. In addition, the catalytic activity was completely inhibited when the radical scavenger TEMPO was added. These observations highlight the radical character of the C–O cleavage process.<sup>[55]</sup>



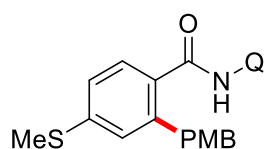
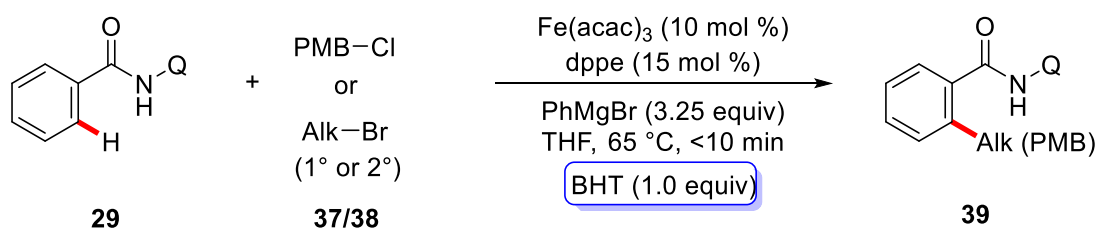
**Scheme 1.16** Iron-catalyzed C–H alkylation with tosylates.

In a contribution by *Cook*, alkyl and benzyl halides were employed for alkylations and benzylations in which NaI or zinc salt as additives were not necessary (Scheme 1.17a).<sup>[51b]</sup> The key to success in this reaction was the slow addition of the Grignard reagent and the use of BHT in the transformation of secondary alkyl halides **38**. In addition, based on the slow addition procedure and the short reaction time, the authors proposed that a phenyliron species formed by transmetallation from PhMgBr, which immediately undergoes turnover-limiting coordination of the amide substrate, followed by rapid, irreversible C–H cleavage. Furthermore, *Ackermann* described an approach for methylation, alkylation and benzylation utilizing the modular click-triazole-

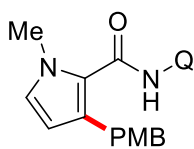
## 1. Introduction

based TAM as the directing group (Scheme 1.17b).<sup>[51a]</sup> This powerful procedure enabled the C–H alkylations with alkyl iodides, bromides, and even chlorides as the electrophile. Detailed studies revealed the reaction to proceed *via* a SET-induced C–Hal cleavage.

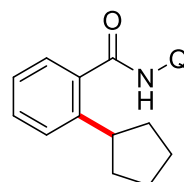
### a) Cook



**39a**: 80%

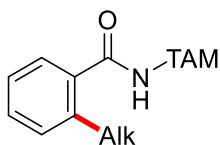
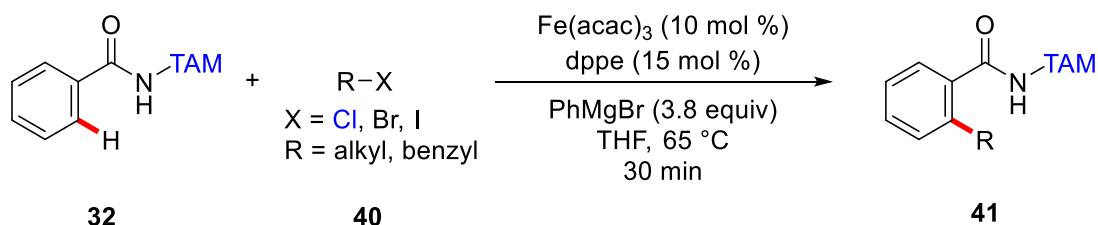


**39b**: 61%

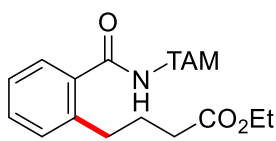


**39c**: 73%

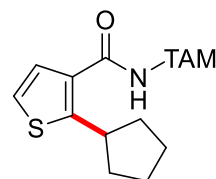
### b) Ackermann



Alk = Me, X = I (**41a**): 75%  
Alk = Bn, X = Cl (**41b**): 76%



**41c**: 60%



**41d**: 53%

**Scheme 1.17** Iron-catalyzed alkylation and benzylation of amides with halides.

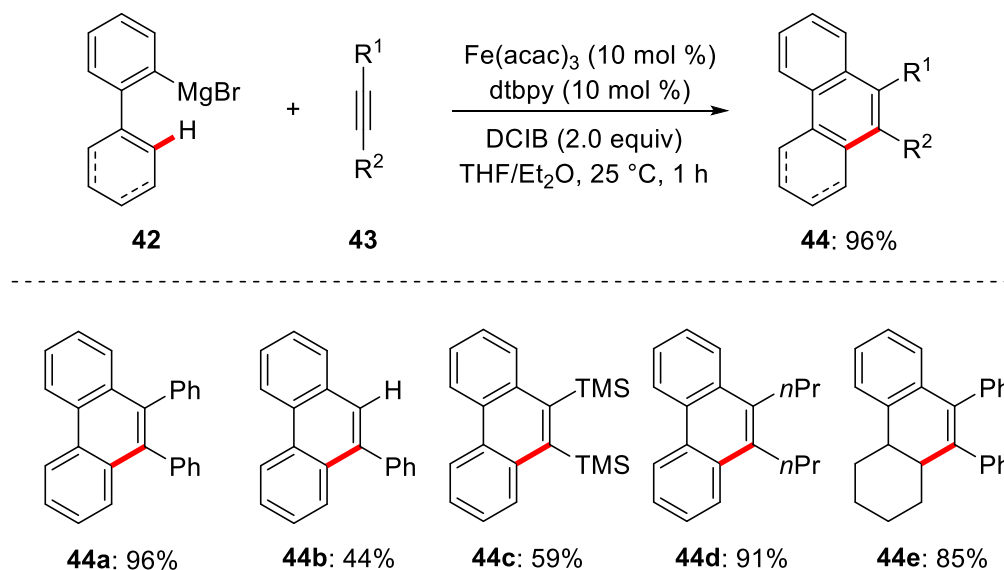
### 1.2.4 Iron-Catalyzed C–H Annulation Reactions

Apart from their application to C–H alkylation, arylation and allylation reactions, low-valent iron species, which can be coordinated by the  $\pi$ -systems of alkynes,<sup>[56]</sup> can promote C–H annulation reactions.

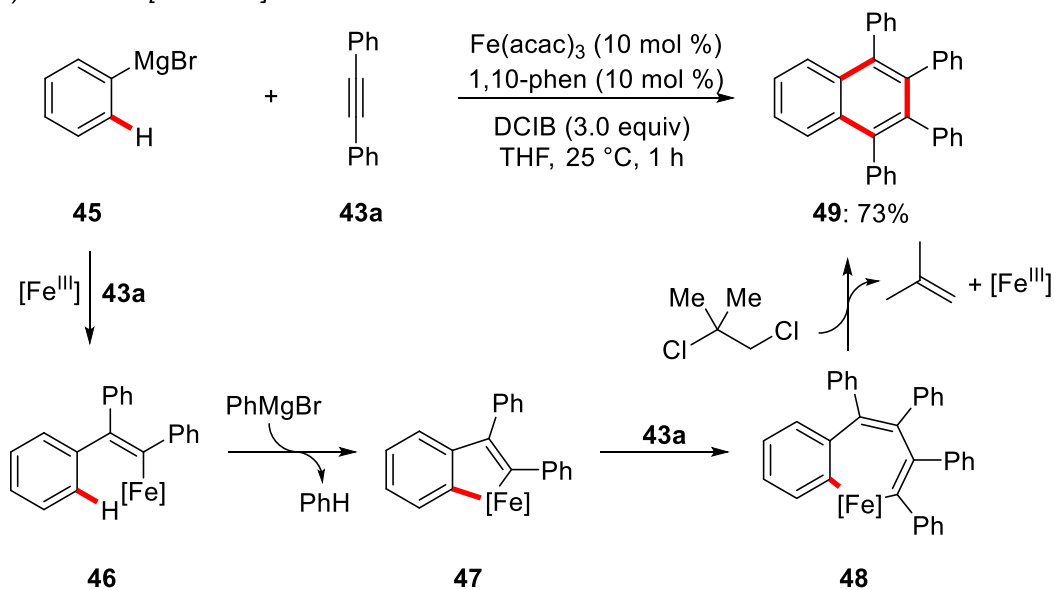
Thus, *Nakamura* reported the iron-catalyzed oxidative [4 + 2] annulation of 2-biaryl Grignard reagents **42** with alkynes **43** for the synthesis of phenanthrene derivatives **44** (Scheme 1.18a).<sup>[57]</sup> Notably, not only internal alkynes but also terminal alkynes could be transformed. In addition, a similar approach for iron-catalyzed oxidative [2 + 2 + 2] annulations of aryl Grignard reagents **45** with two molecules of an internal alkyne **43a** was achieved by the authors.<sup>[58]</sup> Mechanistically, the reaction was proposed to proceed through iron-catalyzed carbometalation of the alkyne **43a** with the aryl Grignard reagent **45**, subsequent with intramolecular C–H activation to form the five-membered ferracycle **46**. Then insertion of a second molecule of alkyne **43a** takes place to form intermediate **48**, which undergoes reductive elimination and oxidation to afford the final product **49** and regenerate the active iron species (Scheme 1.18b). Furthermore, a combination of arylindium reagents with alkyl Grignard reagents was found to be a viable alternative for the synthesis of phenanthrene derivatives under redox-neutral conditions.<sup>[59]</sup>

## 1. Introduction

### a) [4 + 2] benzannulation



### b) oxidative [2 + 2 + 2] annulation

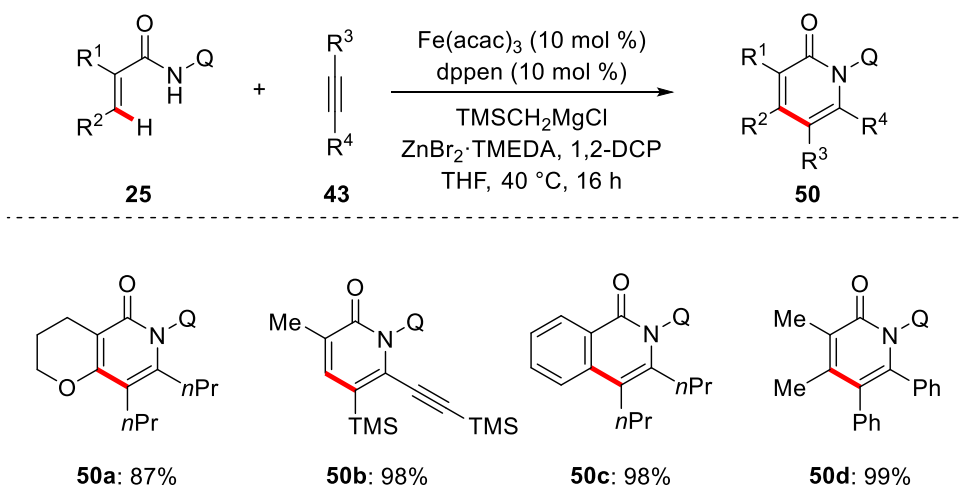


**Scheme 1.18** Iron-catalyzed annulation of alkynes with aryl Grignard reagents.

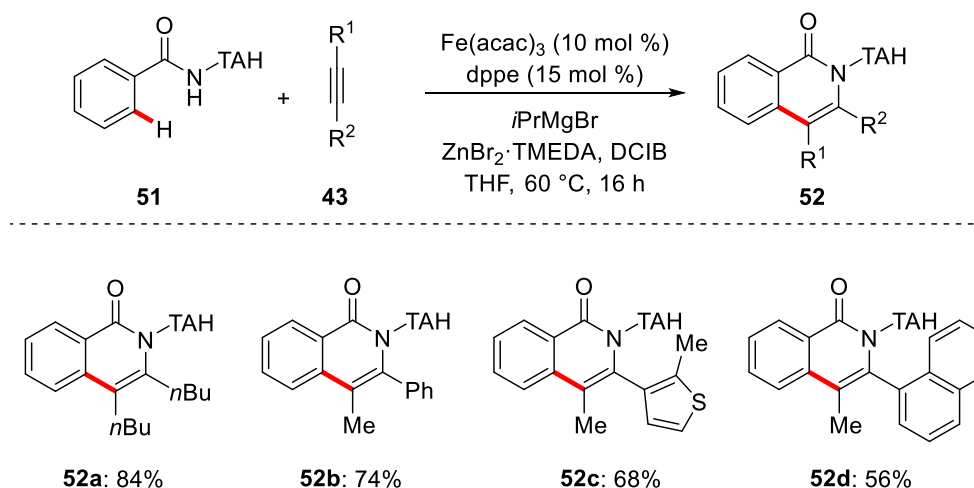
*Nakamura*<sup>[60]</sup> and *Ackermann*<sup>[61]</sup> reported iron-catalyzed formations of pyridone **50** and isoquinolone derivatives **52** by assistance of the well-established Q and the modular triazolylmethyl (TAH) groups, respectively (Scheme 1.19). In contrast to iron-catalyzed transformations using organometallic reagents<sup>[45]</sup> or organic electrophiles,<sup>[51a]</sup> which prefer the bulky TAM group, the TAH group was shown to be more suitable for oxidative annulations.

## 1. Introduction

### a) Nakamura



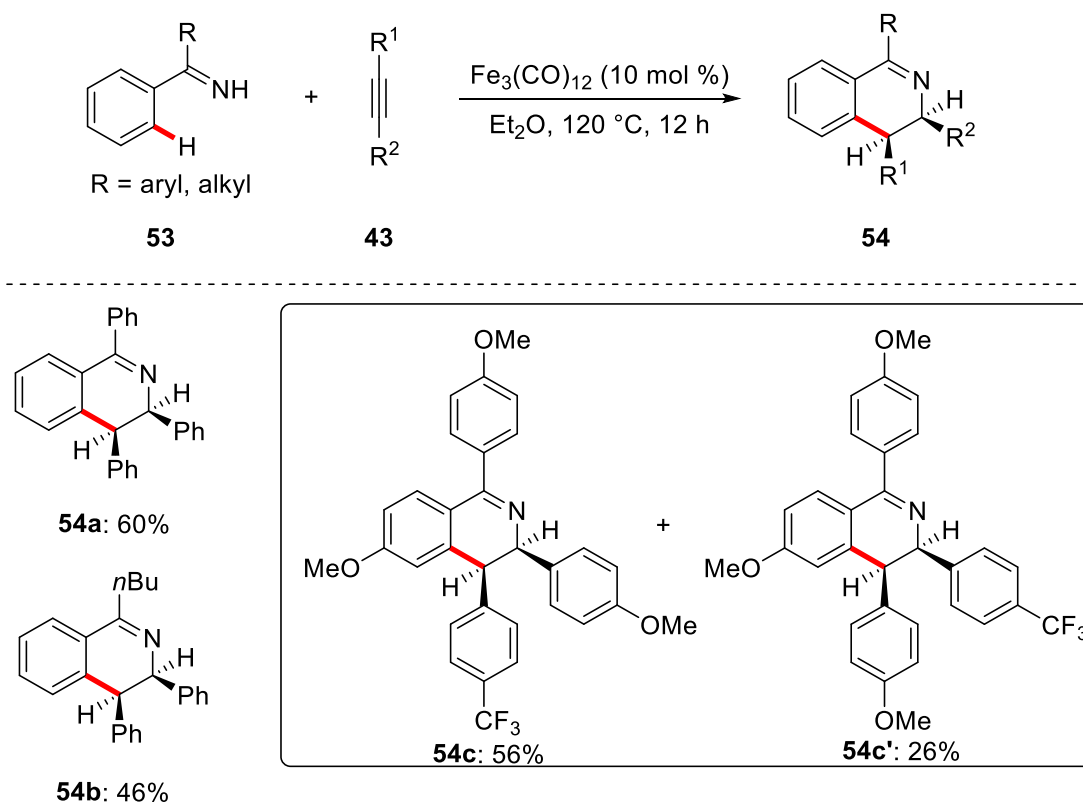
### b) Ackermann



**Scheme 1.19** Iron-catalyzed C–H annulations.

Inspired by the work of *Reed* on iron(0)-mediated imine cyclometallations,<sup>[62]</sup> *Wang* developed Fe<sub>3</sub>(CO)<sub>12</sub> catalyzed redox-neutral cyclizations of internal alkynes **43** with imines **53** for the synthesis of 3,4-dihydroisoquinolines **54** (Scheme 1.20).<sup>[63]</sup> Despite this transformation featured neat reaction conditions, the coupling partners were limited in diarylethynes and poor regio-selectivity was observed when asymmetric alkyne was employed.

## 1. Introduction



**Scheme 1.20** Iron-catalyzed C–H redox-neutral [4+2] cyclization.

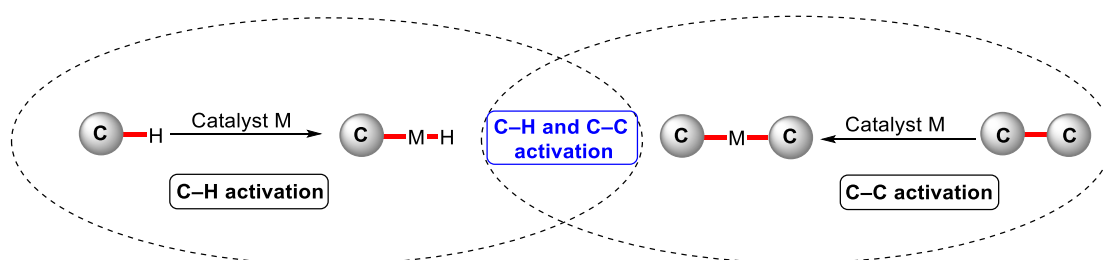
Despite considerable progress, iron-catalyzed C–H annulation reactions, thus far limited to alkynes as coupling partners, employing unsaturated coupling partners such as allenes and BCPs have not been developed.

Allenes have been recognized as increasingly useful building blocks in modern synthetic chemistry,<sup>[64]</sup> due to *inter alia* their transformative utility,<sup>[65]</sup> and various bioactive compounds and functional materials containing an allene moiety.<sup>[66]</sup> However, compared to alkyne and alkene transformations,<sup>[67]</sup> the application of allenes in catalyzed C–H activation remains underdeveloped, and thus far dominated by precious 4d and 5d transition metals.<sup>[68]</sup>

Bicyclopropylidenes (BCPs) featuring two cyclopropane rings were identified as a useful structural motif for six membered ring formation.<sup>[69]</sup> However, their applications in C–H activation are narrow with three ruthenium-catalyzed C–H hydroarylations being reported, in which the cyclopropane rings are conserved.<sup>[70]</sup>

### 1.3 Transition Metal-Catalyzed C–H/C–C Activation

Transition metal-catalyzed C–H activation has gained significant attention for efficient C–C and C–Het formations. The past decade has witnessed the emergence of selective C–C cleavages as a powerful tool for the construction of increasingly complex molecules,<sup>[71]</sup> despite C–C bonds usually being less sterically accessible and having less favorable orbital interactions with transition metal catalyst compared to C–H bonds.<sup>[72]</sup> Significant progress in this field was recently made by merging C–H activation with challenging C–C activation,<sup>[73]</sup> which provided a new strategy for overcoming synthetic challenges and a method for the convenient preparation of novel molecules (Scheme 1.21).



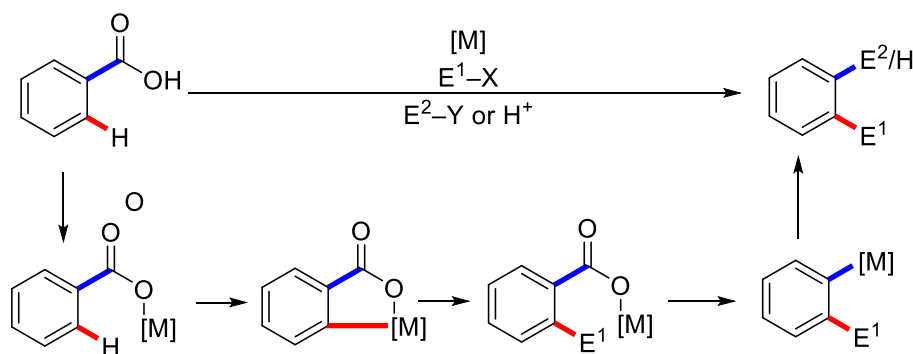
**Scheme 1.21** Merging C–H activation with C–C activation.

To date, several mode of actions have been suggested for this novel strategy depending on the different kinds of substrates, including mainly: 1) combination of decarboxylation and C–H activation,<sup>[74]</sup> 2) merging decarbonylation with C–H activation,<sup>[75]</sup> and 3) functionalization of strained carbocycles<sup>[76]</sup> (Scheme 1.22). The tandem reactions of decarboxylation and concomitant C–H activation is highly desirable, due to the abundance and availability of aromatic carboxylic acids. For a successful transformation, a fine-tuning of the experimental conditions is required to avoid protodecarboxylation without C–H activation as well as C–H bond activation without decarboxylation (Scheme 1.22a). The decarbonylation of aldehydes through dual C–H and C–C activation became attractive to the scientific community after Wilkinson's catalyst was found to be effective for this transformation.<sup>[75a, 75d–75f]</sup> Typically, the

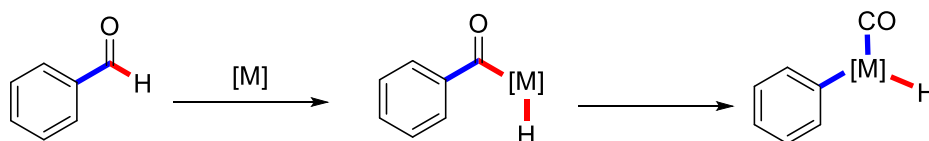
## 1. Introduction

decarbonylation includes two elementary steps. First, C–H activation of the aldehyde occurs, followed by C–C cleavage and CO extrusion (Scheme 1.22b). The strain-release of highly strained carbocycles enabled C–C cleavages by the assistance of transition metals (Scheme 1.22c),<sup>[77]</sup> which provided access to novel molecules.<sup>[78]</sup>

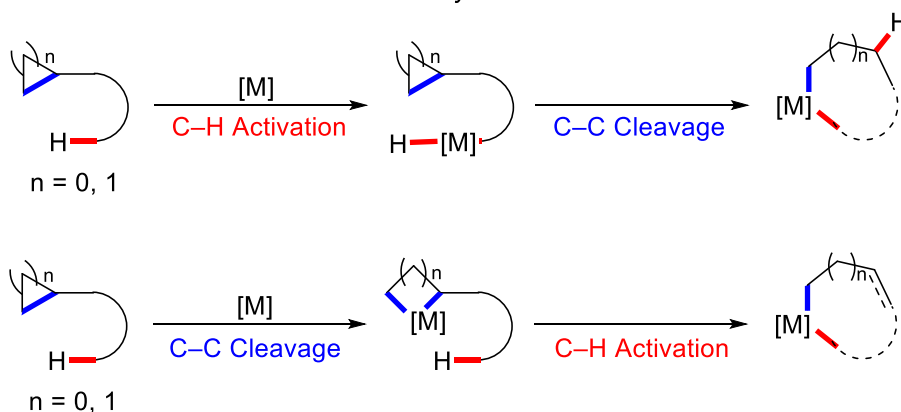
a) decarboxylation accompanied by C–H activation



b) decarbonylation accompanied by C–H activation



c) C–H and C–C activation of strained carbocycles

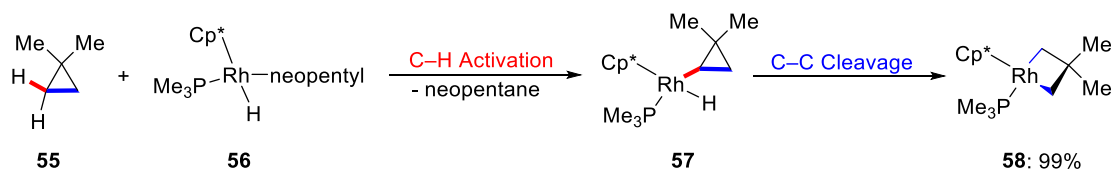


**Scheme 1.22** Manifolds of merging C–H activation and C–C cleavage.

The first example of this dual activation mode was reported by *Bergman* during a study on the mechanism of the formation of rhodacyclobutane **58** (Scheme 1.23).<sup>[79]</sup> The C–H bond of 1,1-dimethylcyclopropane **55** was activated by the rhodium species **56** at low temperature. Subsequently, by warming up the

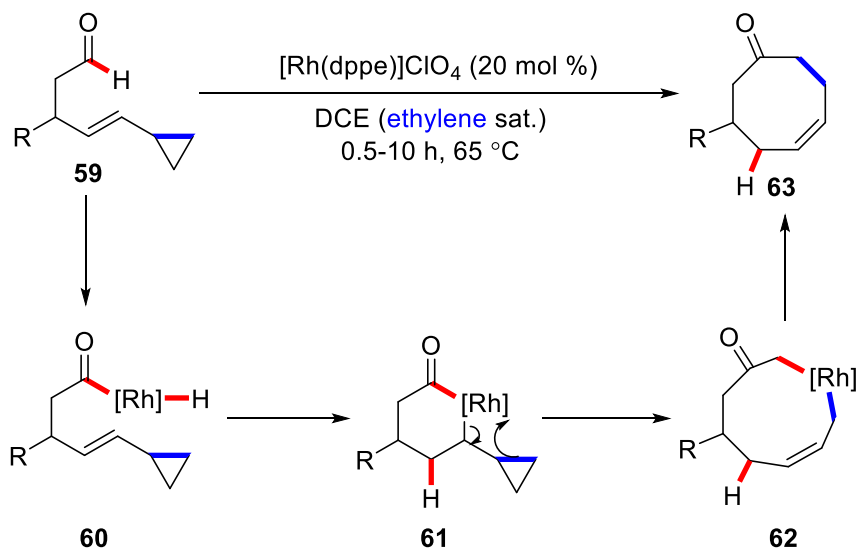
## 1. Introduction

reaction mixture, C–C bond insertion took place to give the thermodynamic product **58**.



**Scheme 1.23** Dual activation of C–H and C–C bonds.

Inspired by the pioneering work of *Bergman*, strained ring systems for C–H and C–C dual activations have thus been intensively studied.<sup>[80]</sup> In 2000, *Shair* reported the rhodium-catalyzed intramolecular C–H activation and C–C cleavage for the formation of cyclooctenone **63**.<sup>[81]</sup> The C–H activation of the aldehyde moiety in **59** takes place first, then intermediate **60** undergoes intramolecular hydrometallation to form intermediate **61**. After ring opening and reductive elimination, the final product **63** is obtained (Scheme 1.24). In order to avoid decarbonylation and guarantee high yields ethylene was necessary.

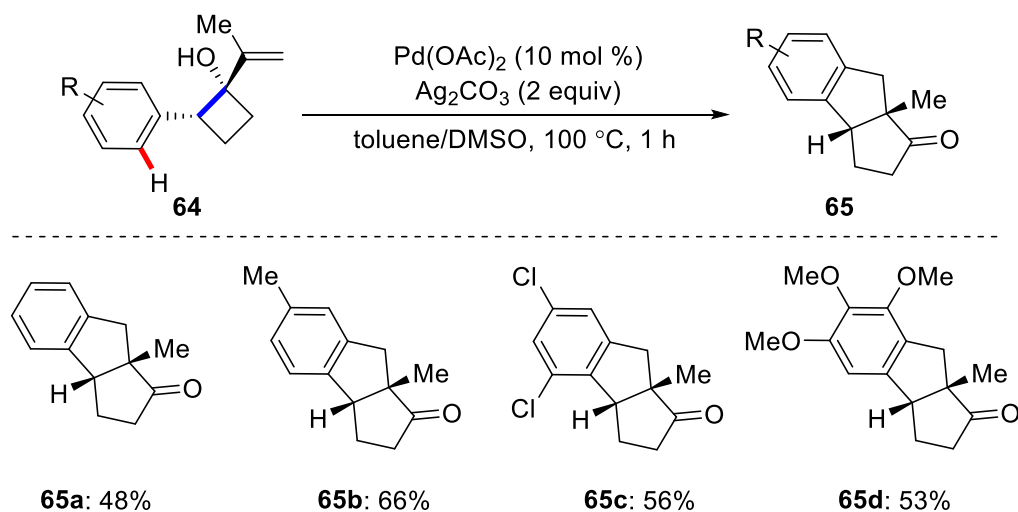


**Scheme 1.24** Synthesis of cyclooctenone through dual C–H and C–C activation.

In 2011, *Orellana* disclosed the synthesis of benzodiquinanes **65** through palladium-catalyzed oxidative ring expansion of 1-vinyl-1-cyclobutanols **64** (Scheme 1.25).<sup>[82]</sup> The generally moderate yields observed in this

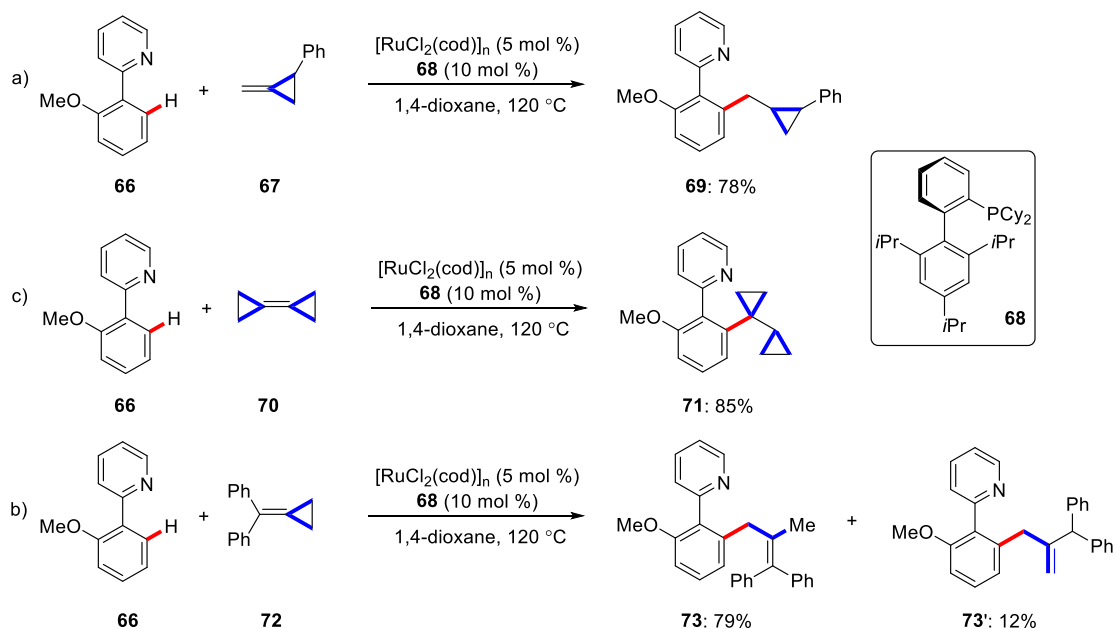
## 1. Introduction

transformation suggested the existence of other pathways, which led to several byproducts.



**Scheme 1.25** Palladium-catalyzed oxidative ring expansion reaction.

The dual activation strategy was also viable for intermolecular reactions using rhodium or ruthenium catalysts.<sup>[83]</sup> An early example of a dual activation manifold for intermolecular reactions was disclosed by *Ackermann* during their research on ruthenium-catalyzed hydroarylations of methylenecyclopropanes

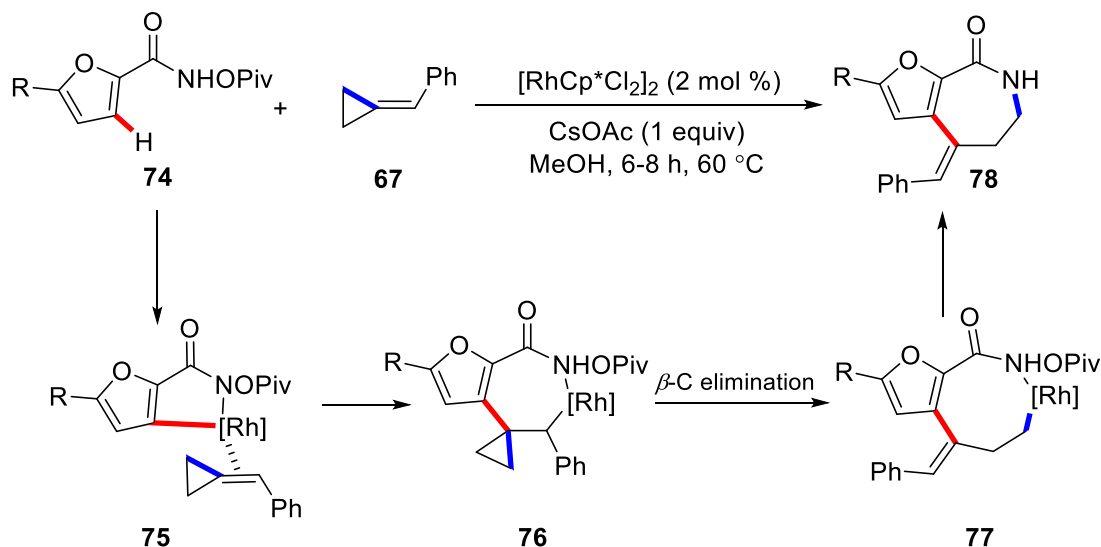


**Scheme 1.26** Ruthenium-catalyzed hydroarylation reactions.

## 1. Introduction

**67** (Scheme 1.26a).<sup>[70b, 70c]</sup> It is worth noting that in the reactions with methylenecyclopropanes **67** or bicyclopropylidenes **70**, the strained rings were conserved (Scheme 1.26a and 1.26b), while in the hydroarylation with benzhydrylidene cyclopropane **72** C–C cleavage occurred (Scheme 1.26c).

In 2013, *Wu* developed an intermolecular tandem C–H and C–C activation during their research on rhodium-catalyzed C–H annulations of benzamide with methylenecyclopropanes (Scheme 1.27).<sup>[84]</sup> From a mechanism perspective, C–H activation proceeds through a concerted metalation-deprotonation sequence, followed by coordination and insertion of methylenecyclopropane **67** to furnish **75**, the arylrhodium intermediate **76** then undergoes  $\beta$ -C-elimination and reductive elimination to yield product **77**.



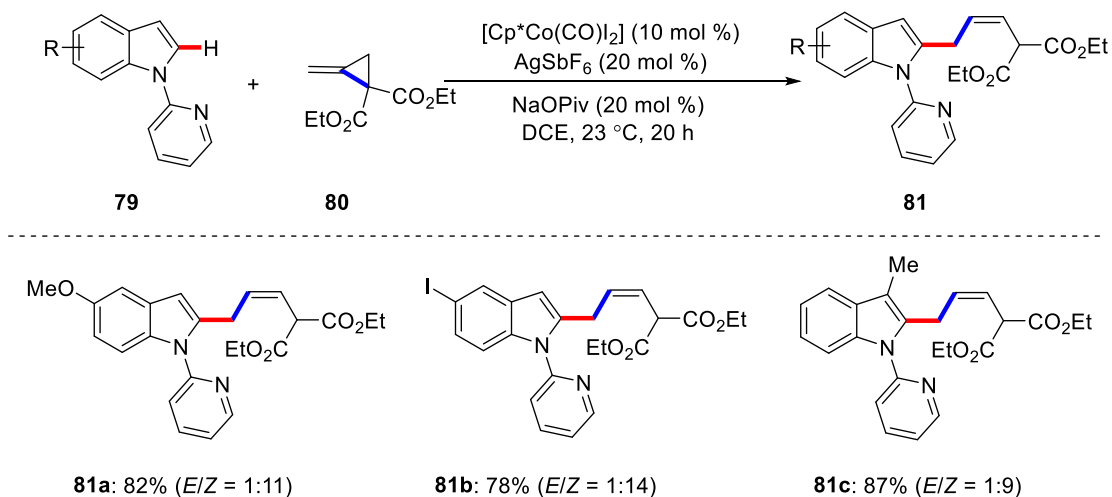
**Scheme 1.27** Intermolecular tandem C–H and C–C activation.

During the past years, 3d metal catalysis was proven to be an ideal alternative for tandem C–H and C–C activations.<sup>[24c, 85]</sup> In 2016, *Ackermann* disclosed the first example of cobalt-catalyzed C–H activation and C–C cleavage (Scheme 1.28a).<sup>[85d]</sup> The reaction featured a high catalytic efficacy at room temperature. In addition, this transformation resulted in an unprecedented diastereoselectivity affording the thermodynamically less stable *Z*-alkenes **81**

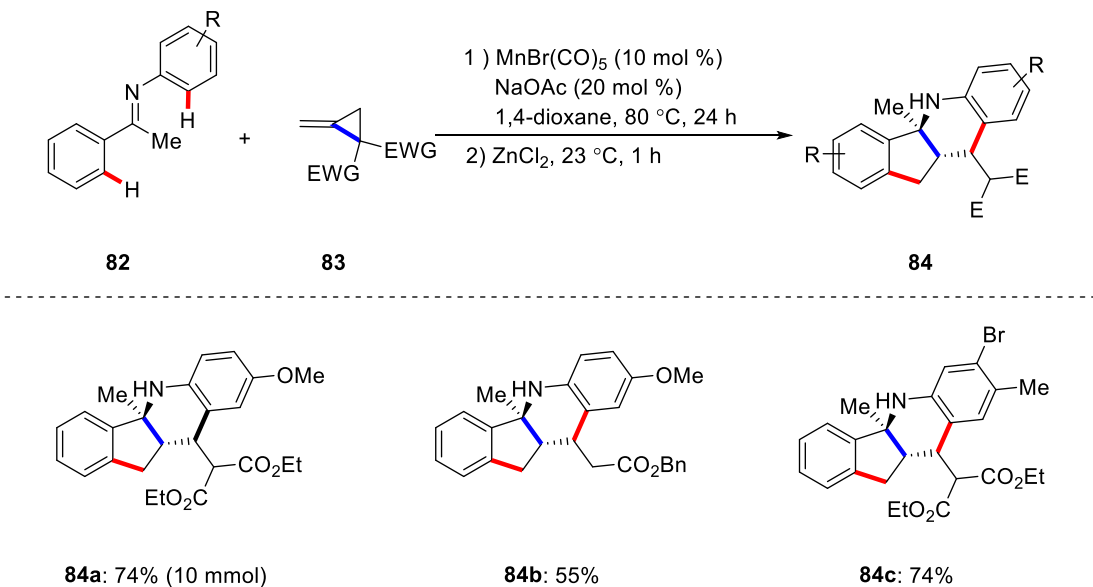
## 1. Introduction

as the product. One year later, *Ackermann* reported the formation of tetracyclic compounds **84** through manganese-catalyzed stereoselective C–H/C–C activation with methylenecyclopropane **83** (Scheme 1.28b).<sup>[24c]</sup> Excellent levels of positional selectivity as well as diastereoselectivity were achieved in this transformation.

### a) Cobalt-catalyzed C–H /C–C activation



### b) Manganese-catalyzed C–H /C–C activation

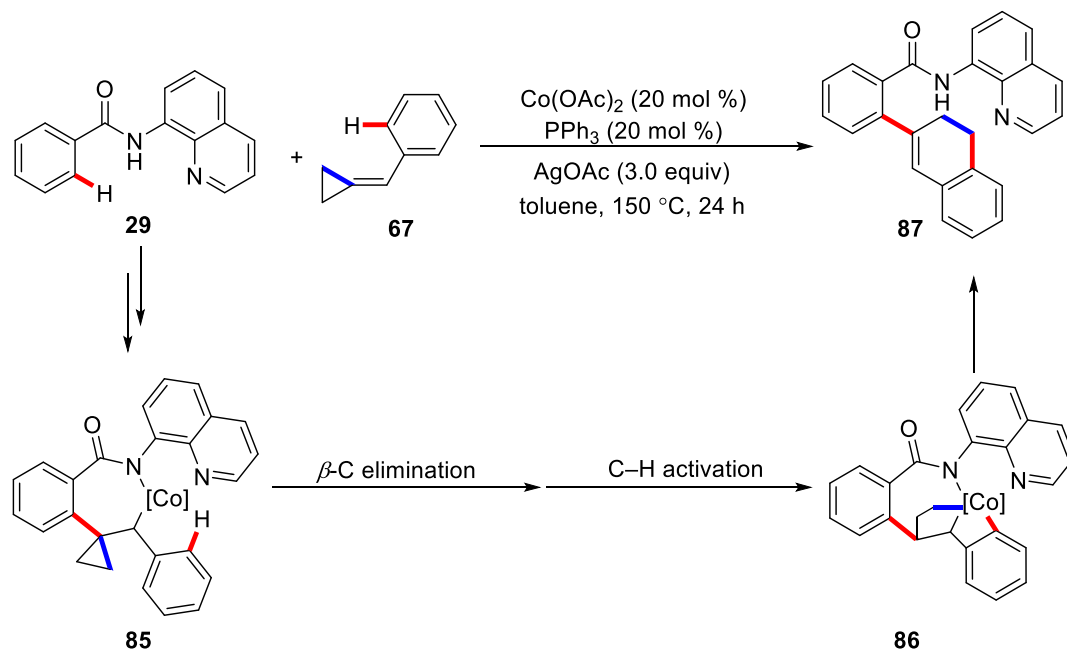


**Scheme 1.28** 3d metal-catalyzed tandem C–H and C–C activation.

Tandem C–H activation/C–C cleavage reactions can also occur under assistance of bidentate directing groups, using cobalt acetate as the catalyst

## 1. Introduction

(Scheme 1.29).<sup>[85a]</sup> Instead of a reductive elimination to form a C–N bond, which is observed in the rhodium-catalyzed annulation of alkylidenecyclopropanes annulations,<sup>[84]</sup> a second C–H activation occurred to form the ring opening product **87** under cobalt catalysis.



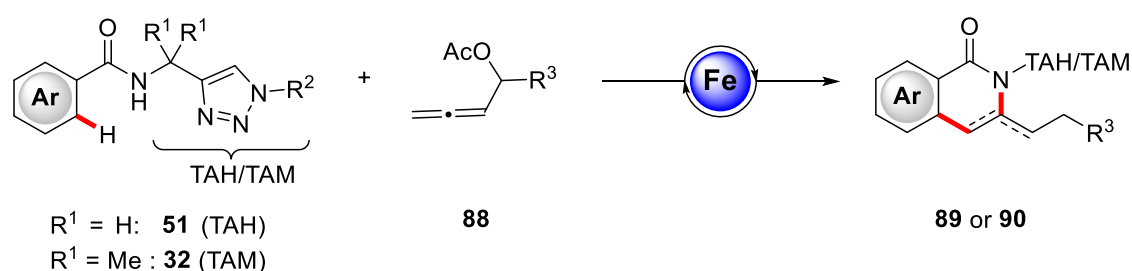
**Scheme 1.29** Cobalt-catalyzed C–H/C–C/C–H activation.

## 2. Objectives

Transition metal-catalyzed C–H activations have emerged as a powerful platform for efficient and sustainable C–C and C–Het bond formations. While most transformations were accomplished with precious and toxic 4d and 5d metal catalysts, sustainable catalytic manifolds by 3d metal catalysis,<sup>[30]</sup> and especially iron-catalyzed C–H transformations,<sup>[31, 33, 86]</sup> have attracted significant attention due to their Earth-abundance, cost-efficiency, and low toxicity.<sup>[32]</sup>

Despite considerable progress, iron-catalyzed C–H annulation reactions<sup>[57–61, 63]</sup> continue to be challenging transformation with major limitations in: 1) types of coupling partners with only alkynes were reported thus far, 2) the requirement of an excess of DCIB as an external oxidant, 3) lack of product diversity, due to a narrow substrate scope in some cases, 4) not fully elucidated reaction mechanism, and 5) absence of efficient protocols for removal of the TAH group.

Therefore, it is highly desirable to establish a novel approach for low-valent iron-catalyzed C–H annulations with allenes under redox-neutral conditions (Scheme 2.1).

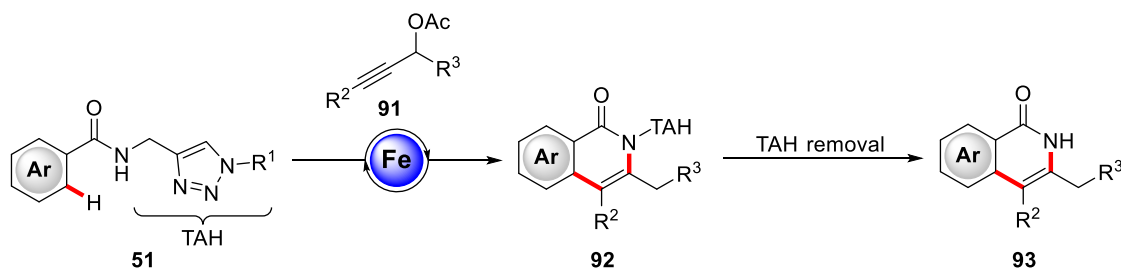


**Scheme 2.1** Iron-catalyzed redox-neutral annulation with allenes.

Remaining limitations in iron-catalyzed C–H alkyne annulation, such as the lack of detailed mechanistic studies and efficient procedures to remove the TAH group, promoted us to develop iron-catalyzed C–H annulations with propargyl acetates with the main purpose to shed light on the mechanism of iron-

## 2. Objectives

catalyzed redox-neutral annulations with alkynes and the removal of TAH group (Scheme 2.2).

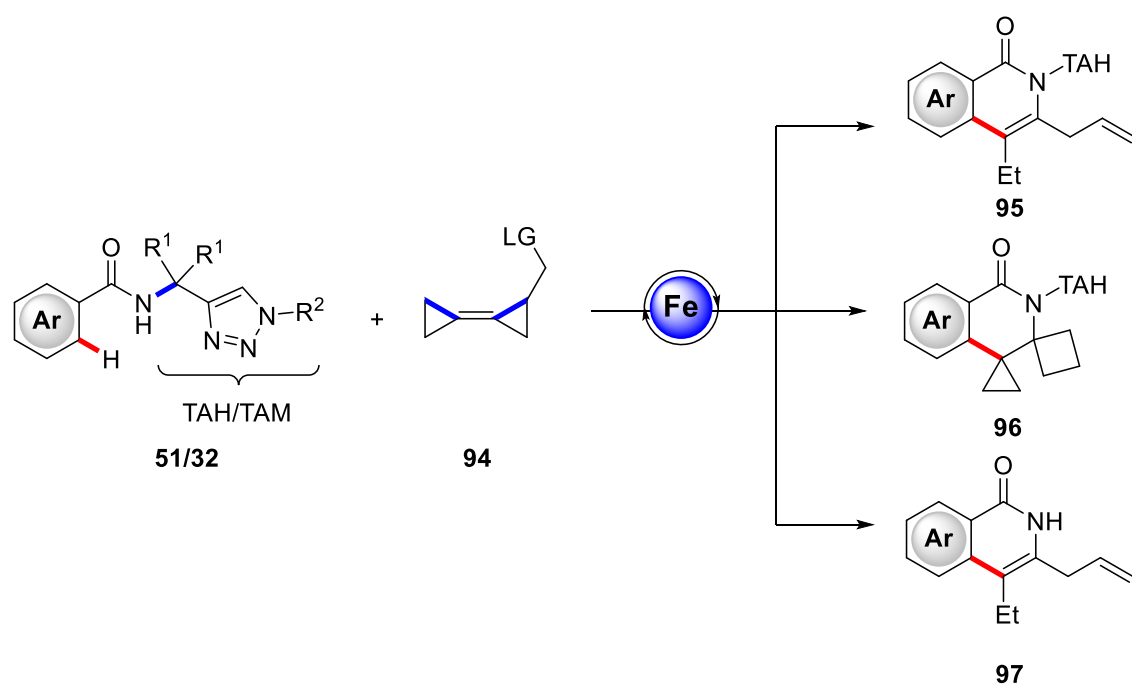


**Scheme 2.2** Iron-catalyzed redox-neutral annulation with alkynes.

A significant stimulus in C–H activation chemistry was recently gained by merging C–H activation with challenging C–C cleavages.<sup>[71, 73]</sup> While considerable progress has been achieved, this methodology was still limited by 1) the requirement of precious metals,<sup>[83–84]</sup> 2) activated vinylcyclopropanes,<sup>[24c, 85b–85d]</sup> and 3) harsh oxidative conditions.<sup>[85a]</sup> Thus, a protocol to overcome these limitations would be highly desirable.

To combine C–H activation with challenging C–C activation under iron catalysis as well as to further diversify the application of BCPs in C–H activation, the application of bicyclopropylidene derivatives in iron-catalyzed C–H/C–C activation should prove highly valuable (Scheme 2.3).

## 2. Objectives



**Scheme 2.3** Iron-catalyzed C-H/C-C activation with BCPs.

## 3. Results and Discussion

### 3.1 Iron-Catalyzed C–H/N–H Allene Annulation

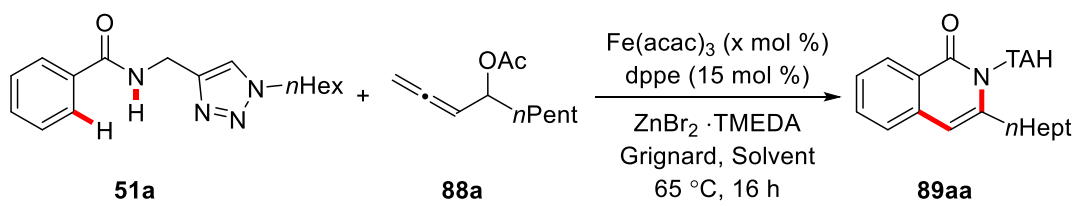
Iron-catalyzed C–H oxidative annulations have emerged as a powerful tool for N-heterocycle constructions. While these strategies were limited to alkynes as the coupling partners and highlighted the requirement of an excess of DCIB as the external oxidant, a study of iron-catalyzed C–H oxidative annulations with alternative coupling partners under redox-neutral conditions would be highly considerable.

#### 3.1.1 Optimization Studies

The optimization studies began by probing various reaction conditions for the envisioned iron-catalyzed C–H functionalization of benzamide **51a** with allene **88a** (Table 3.1). The investigation on the amount of solvent and the addition order of allenes (see general procedure **GPA'**) indicated that a high concentration of Grignard reagent and zinc salts was required for the formation of the active iron catalyst (entries 1–3). In addition, the use of biomass-derived solvent<sup>[87]</sup> 2-MeTHF delivered product **89aa** in moderate yield (entry 4). *i*-PrMgBr proved to be the additive of choice (entries 5 and 6). The allene annulation smoothly occurred at room temperature and with reduced catalyst loading (entries 7–10).

### 3. Results and Discussion

**Table 3.1** Optimization of iron-catalyzed C–H activation with allenes **88a**.

				
Entry	X mol %	Grignard reagent	Solvent (y mL)	Yield/%
1	15	<i>i</i> PrMgBr	THF (1.0)	44 <sup>[b]</sup>
2	15	<i>i</i> PrMgBr	THF (0.4)	91
3	15	<i>i</i> PrMgBr	THF (0.4)	46 <sup>[c]</sup>
4	15	<i>i</i> PrMgBr	2-MeTHF (0.4)	59 <sup>[b]</sup>
5	15	MeMgBr	THF (0.4)	71
6	15	<i>i</i> PrMgCl	THF (0.4)	64
7	15	<i>i</i> PrMgBr	THF (0.4)	66 <sup>[d]</sup>
8	1	<i>i</i> PrMgBr	THF (0.4)	38
9	5	<i>i</i> PrMgBr	THF (0.4)	35
10	10	<i>i</i> PrMgBr	THF (0.4)	82

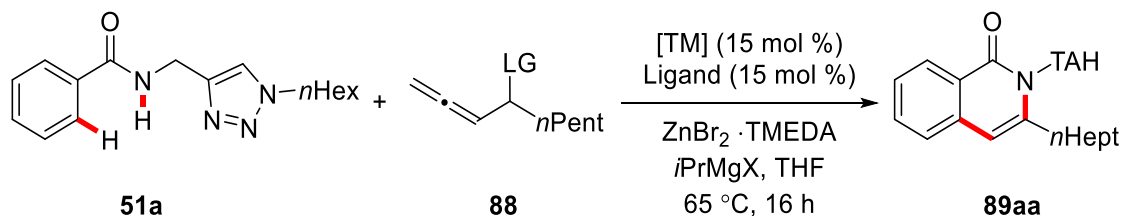
<sup>[a]</sup> Reaction conditions: **51a** (0.30 mmol), **88a** (3 equiv), Fe(acac)<sub>3</sub> (x mol %), dppe (15 mol %), ZnBr<sub>2</sub>·TMEDA (2 equiv), Grignard reagent (3.0 M, 3 equiv), Solvent (y mL), 65 °C, 16 h; yields of isolated products. [b] used **51a** (0.15 mmol) [c] adding **88a** at the same time with catalyst. [d] 25 °C.

To further optimize the reaction, different types of catalyst, ligand and leaving group were tested in the transformation (Table 3.2). The unique power of the iron catalysis regime was reflected by cobalt, manganese and nickel catalysts falling short in providing the desired product **89aa** (entries 1–5). Various simple phosphine and nitrogen-based ligand were also tested, but failed to provide the

### 3. Results and Discussion

desired product **89aa** in synthetically useful yields (entries 6–12). The investigation on different leaving groups revealed allenyl acetate **88a** to be optimal for an external-oxidant-free C–H annulation (entries 13–17).

**Table 3.2** Optimization of iron-catalyzed C–H activation with allenes **88**.



Entry	[TM]	Ligand	LG	Yield [%]
1	---	dppe	OAc ( <b>88a</b> )	---
2	CoCl <sub>2</sub>	dppe	OAc ( <b>88a</b> )	---
3	MnCl <sub>2</sub>	dppe	OAc ( <b>88a</b> )	---
4	Ni(acac) <sub>2</sub>	dppe	OAc ( <b>88a</b> )	---
5	Fe(acac) <sub>3</sub>	dppe	OAc ( <b>88a</b> )	91
6	Fe(acac) <sub>3</sub>	dppen	OAc ( <b>88a</b> )	25
7	Fe(acac) <sub>3</sub>	dppz	OAc ( <b>88a</b> )	trace
8	Fe(acac) <sub>3</sub>	PPh <sub>3</sub>	OAc ( <b>88a</b> )	---
9	Fe(acac) <sub>3</sub>	dppp	OAc ( <b>88a</b> )	---
10	Fe(acac) <sub>3</sub>	Xantphos	OAc ( <b>88a</b> )	---
11	Fe(acac) <sub>3</sub>	phen	OAc ( <b>88a</b> )	---
12	Fe(acac) <sub>3</sub>	2,2'-bipyridine	OAc ( <b>88a</b> )	---
13	Fe(acac) <sub>3</sub>	dppe	Cl ( <b>88b</b> )	16

### 3. Results and Discussion

14	Fe(acac) <sub>3</sub>	dppe	OP(O)(OEt) <sub>2</sub> ( <b>88c</b> )	16
15	Fe(acac) <sub>3</sub>	dppe	OC(O)Ph ( <b>88d</b> )	30
16	Fe(acac) <sub>3</sub>	dppe	OC(O)OMe ( <b>88e</b> )	35
17	Fe(acac) <sub>3</sub>	dppe	OH ( <b>88f</b> )	---

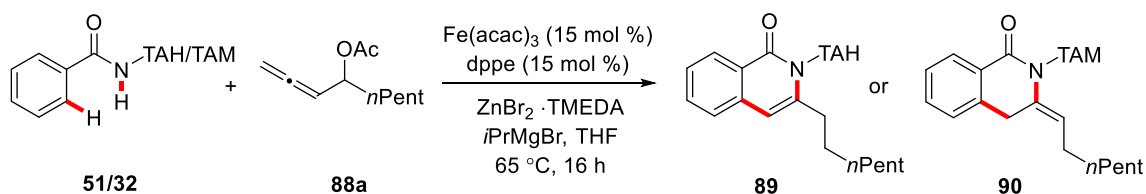
<sup>[a]</sup> Reaction conditions: **51a** (0.30 mmol), **88** (0.90 mmol), [TM] (15 mol %), Ligand (15 mol %), ZnBr<sub>2</sub>·TMEDA (0.60 mmol), *i*-PrMgBr (3.0 M, 0.90 mmol), THF (0.40 mL), 65 °C, 16 h; yields of isolated products.

#### 3.1.2. Impact of Directing Group on C–H Functionalization

With the optimized condition in hand, we further tested the impact of various bidentate directing group on this transformation (Table 3.3). Thus, a variety of methylene-tethered triazoles TAH delivered the desired isoquinolones **89aa–89da** in high yields (entries 1–4), tolerating among others a reactive alkyl chloride **51d** without any cross-coupling products being observed. In addition, the modular nature of the triazole group further enabled the synthesis of the non-aromatic *exo*-methylene dihydroisoquinolines **90** through the judicious choice of the TAM group which was proved to be invalid for iron-catalyzed C–H annulation with alkynes<sup>[61]</sup> (entries 5–7). However, other bulky groups at the triazole directing group did not give the desired product (entries 8–9).

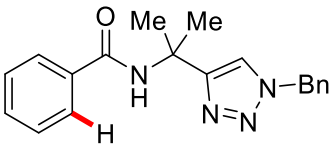
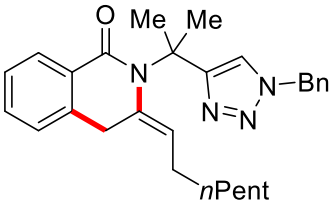
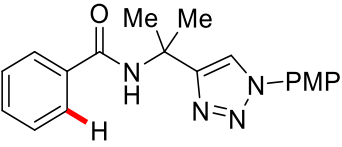
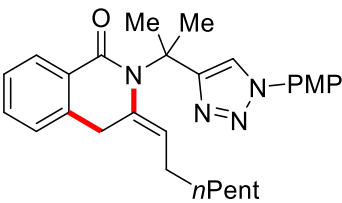
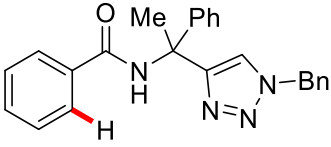
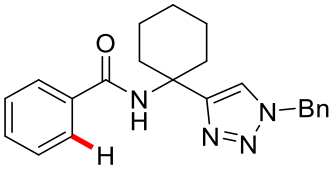
### 3. Results and Discussion

**Table 3.3** Impact of directing group on C–H functionalization.



Entry	51/32	89/90	Yield [%]
1	<p>51a</p>	<p>89aa</p>	91
2	<p>51b</p>	<p>89ba</p>	82
3	<p>51c</p>	<p>89ca</p>	80
4	<p>51d</p>	<p>89da</p>	69
5	<p>32a</p>	<p>90aa</p>	93

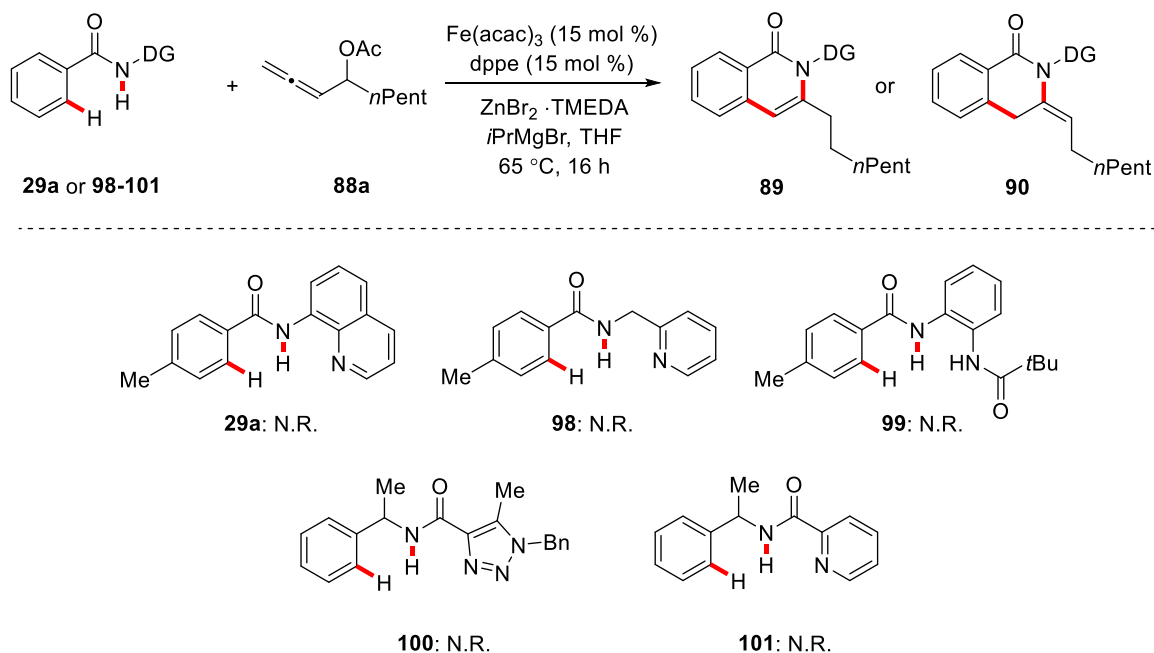
### 3. Results and Discussion

6	 <p><b>32b</b></p>	 <p><b>90ba</b></p>	76
7	 <p><b>32c</b></p>	 <p><b>90ca</b></p>	73
8	 <p><b>32d</b></p>	---	---
9	 <p><b>32e</b></p>	---	---

<sup>[a]</sup> Reaction conditions: **51/32** (0.30 mmol), **88a** (0.90 mmol), Fe(acac)<sub>3</sub> (15 mol %), dppe (15 mol %), ZnBr<sub>2</sub>·TMEDA (0.60 mmol), *i*PrMgBr (3 M, 0.90 mmol), THF (0.40 mL), 65 °C, 16 h; yields of isolated products.

No transformation was observed when employing bidentate directing groups which were otherwise widely used in 3d transition metal catalyzed system (Scheme 3.1). These observations suggested that the structure as well as the electronic properties of the directing group are crucial to achieve successful C–H activation catalyzed by the *in situ* generated low-valent iron species.

### 3. Results and Discussion



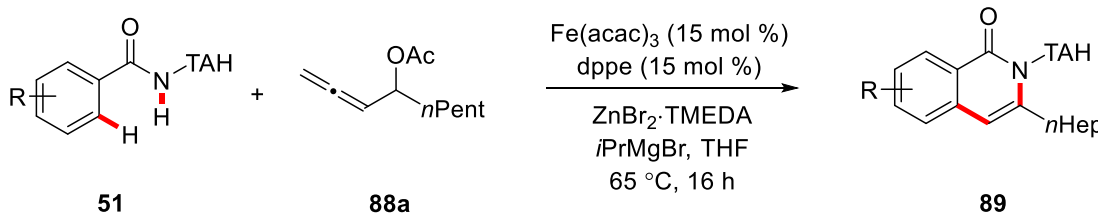
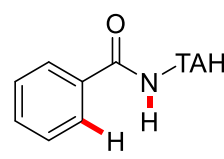
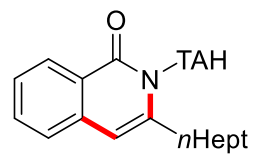
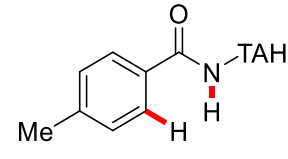
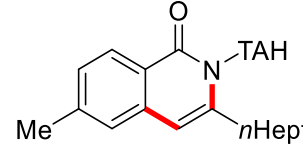
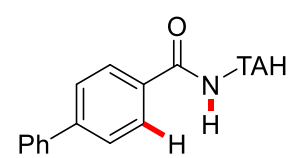
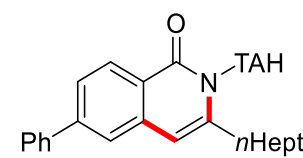
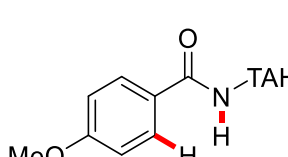
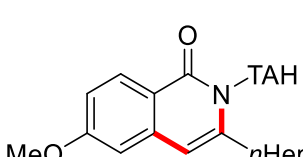
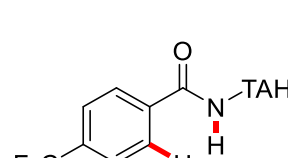
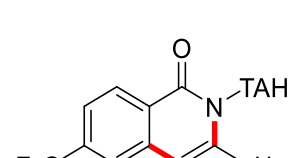
**Scheme 3.1** Limitations on directing group.<sup>[a]</sup>

#### 3.1.3. Substrate Scope and Limitations

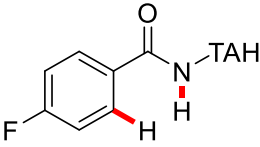
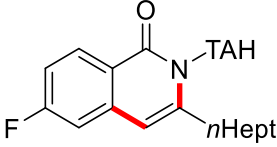
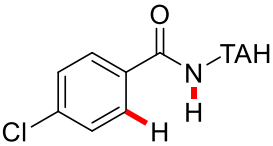
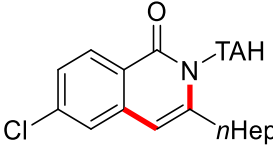
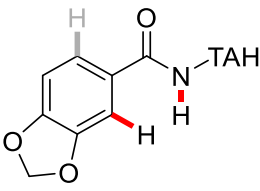
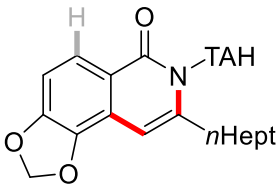
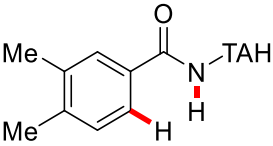
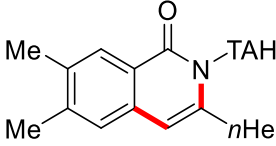
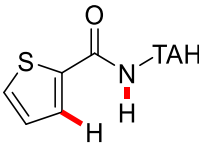
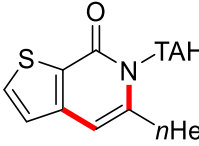
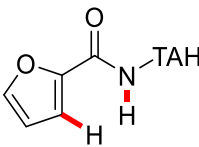
Under the optimized iron-catalyzed C–H activation conditions, we next explored its versatility with a range of substituted TAH-benzamides **51** (Table 3.4). With regard to *para*-substituted TAH-benzamides **51e–51j**, the corresponding isoquinolone products **89ea–89ja** were obtained in moderate to high yields, (entries 2–7). Likewise, chloro at the *para*-position **51j** were efficiently converted to synthetically useful isoquinolones without any dehalogenation product being observed (entry 7). Di-substituted benzamides **51k** and **51l** yielded the corresponding products **89ka** and **89la** in good regioselectivity (entries 8 and 9). Furthermore, thiophenyl-derived benzamide **51m** furnishing the desired products **89ma** in moderate yield, while furanyl-derived benzamide **51n** proved to be unsuitable for the transformation (entries 10 and 11). Unfortunately, the olefinic C(sp<sup>2</sup>)–H and aliphatic C(sp<sup>3</sup>)–H bond were incompatible for this transformation (entries 12–14).

### 3. Results and Discussion

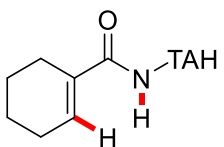
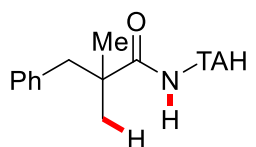
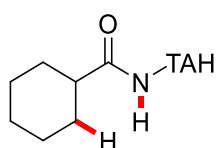
**Table 3.4** Substrate scope of TAH benzamide **51**.

			
Entry	51	89	Yield [%]
1	 <b>51a</b>	 <b>89aa</b>	91
2	 <b>51e</b>	 <b>89ea</b>	80
3	 <b>51f</b>	 <b>89fa</b>	70
4	 <b>51g</b>	 <b>89ga</b>	82
5	 <b>51h</b>	 <b>89ha</b>	65

### 3. Results and Discussion

6	 <b>51i</b>	 <b>89ia</b>	51
7	 <b>51j</b>	 <b>89ja</b>	56
8	 <b>51k</b>	 <b>89ka</b>	67 (1.2:1)
9	 <b>51l</b>	 <b>89la</b>	69
10	 <b>51m</b>	 <b>89ma</b>	67
11	 <b>51n</b>	---	---

### 3. Results and Discussion

12	 <b>51o</b>	---	---
13	 <b>51p</b>	---	---
14	 <b>51q</b>	---	---

<sup>[a]</sup> Reaction conditions: **51** (0.30 mmol), **88a** (0.90 mmol), Fe(acac)<sub>3</sub> (15 mol %), dppe (15 mol %), ZnBr<sub>2</sub>·TMEDA (0.60 mmol), *i*PrMgBr (3.0 M, 0.90 mmol), THF (0.40 mL), 65 °C, 16 h; yields of isolated products.

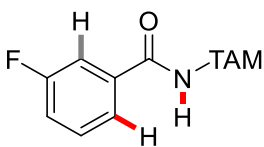
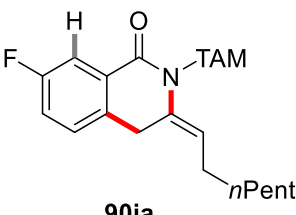
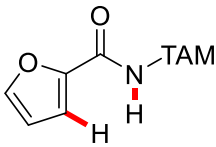
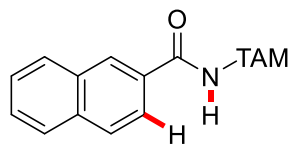
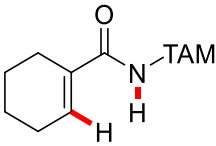
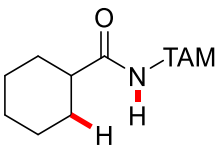
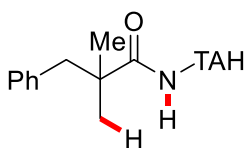
The modular nature of the triazole group TAM provided an access to various *exo*-methylene isoquinolines **90** with ample scope (Table 3.5). Differently decorated aromatic amides delivered the desired products **90fa–90ja** with high levels of positional selectivity control, with the reaction occurring at the less sterically congested site (entries 1–6). However, other types of C(sp<sup>2</sup>)–H bond, such as in furanyl-, naphthyl-, olefinic and C(sp<sup>3</sup>)–H bonds fell short in the envisioned iron-catalyzed annulations (entries 7–11).

### 3. Results and Discussion

**Table 3.5** Substrate scope of TAM benzamide.

Entry	32	90	Yield [%]
1	<p>32a</p>	<p>90aa</p>	93
2	<p>32f</p>	<p>90fa</p>	68
3	<p>32g</p>	<p>90ga</p>	81
4	<p>32h</p>	<p>90ha</p>	71
5	<p>32i</p>	<p>90ia</p>	90

### 3. Results and Discussion

6	 <b>32j</b>	 <b>90ja</b>	76
7	 <b>32k</b>	---	---
8	 <b>32l</b>	---	---
9	 <b>32m</b>	---	---
10	 <b>32n</b>	---	---
11	 <b>32o</b>	---	---

<sup>[a]</sup> Reaction conditions: **32** (0.30 mmol), **88a** (0.90 mmol), Fe(acac)<sub>3</sub> (15 mol %), dppe (15 mol %), ZnBr<sub>2</sub>·TMEDA (0.60 mmol), *i*PrMgBr (3.0 M, 0.90 mmol), THF (0.40 mL), 65 °C, 16 h; yields of isolated products.

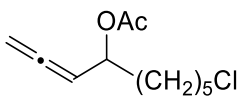
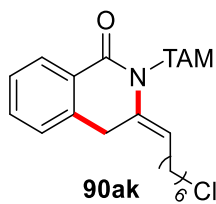
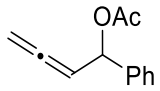
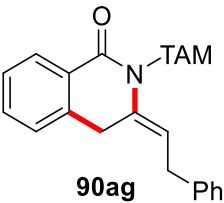
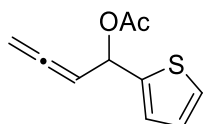
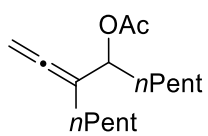
### 3. Results and Discussion

Furthermore, the versatile iron catalyst further enabled the efficient conversion of decorated allenes **88** and TAM-benzamide **32a** to furnish the corresponding *exo*-methylene isoquinolines **90** with moderate to high yields (Table 3.6). Allenyl acetates bearing alkyl groups with different chain-lengths and functional group were efficiently converted (entries 1–4). Allenes with aromatic substituted at the  $\alpha$ -position of acetate group or the di-substituted allene failed to give the product (entries 5–7).

**Table 3.6** Substrate scope of TAM substrate **32a** with various allenes **88**.

Entry	<b>88</b>	<b>90</b>	Yield [%]
1	 <b>88h</b>	 <b>90ah</b>	76
2	 <b>88i</b>	 <b>90ai</b>	87
3	 <b>88j</b>	 <b>90aj</b>	78

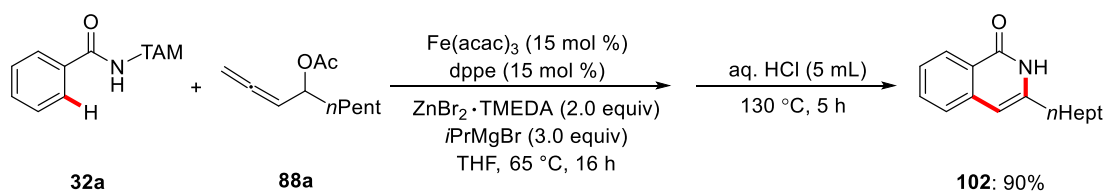
### 3. Results and Discussion

4	 <b>88k</b>	 <b>90ak</b>	68
5	 <b>88g</b>	 <b>90ag</b>	Trace
6	 <b>88l</b>	---	---
7	 <b>88m</b>	---	---

<sup>[a]</sup> Reaction conditions: **32a** (0.30 mmol), **88** (0.90 mmol), Fe(acac)<sub>3</sub> (15 mol %), dppe (15 mol %), ZnBr<sub>2</sub>·TMEDA (0.60 mmol), *i*PrMgBr (3.0 M, 0.90 mmol), THF (0.40 mL), 65 °C, 16 h; yields of isolated products.

#### 3.1.4 Traceless Removal of TAM Group

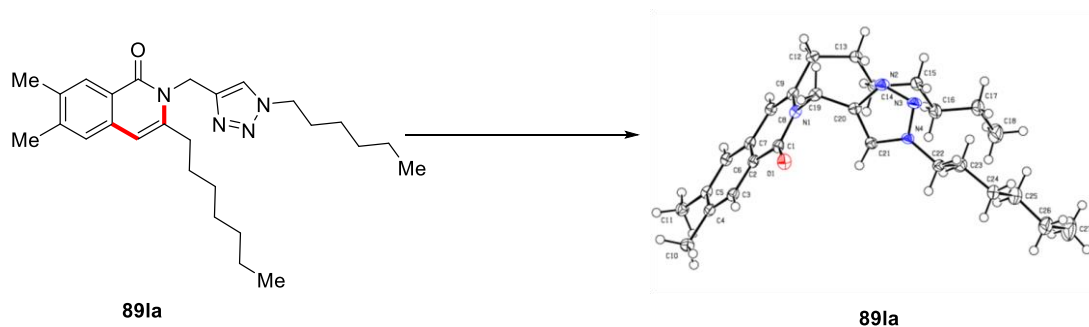
The TAM directing group was tracelessly removed in a user-friendly one-pot fashion further illustrate the synthetic utility of the iron-catalyzed redox-neutral C–H annulation with allenes (Scheme 3.2).



**Scheme 3.2** Traceless removal of TAM group.

### 3. Results and Discussion

Crystals suitable for X-ray diffraction were then grown by slow evaporation, unambiguously confirming the connectivity of product **89la** (Scheme 3.3).



**Scheme 3.3** Molecular structure of **89la** with thermal ellipsoids at 50% probability level. The crystal structure was measured and solved by Dr. Christopher Golz.

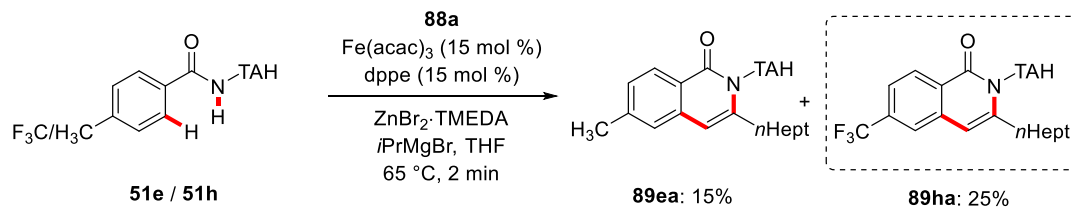
#### 3.1.5 Mechanistic Studies

Given the unique features of the developed iron-catalyzed C–H annulation, we became intrigued by studying its mode of action. Mechanistic approaches including experiment, Mössbauer spectroscopy and DFT computation were carefully conducted to reveal the detail mechanism.

#### Competition Experiment

Intermolecular competition experiments revealed an inherent higher reactivity of electron-deficient arenes **51h** (Scheme 3.4), indicating a ligand-to-ligand hydrogen transfer (LLHT)<sup>[24d, 46, 88]</sup> mechanism which prefer a kinetically C–H-acidic substrates to be operative for the C–H activation. Different from  $\sigma$ -bond metathesis with early transition metals and base-assisted metalation most commonly with carboxylate ligands, the LLHT was reported in the cases with late transition metals and normally with nitrogen ligands.

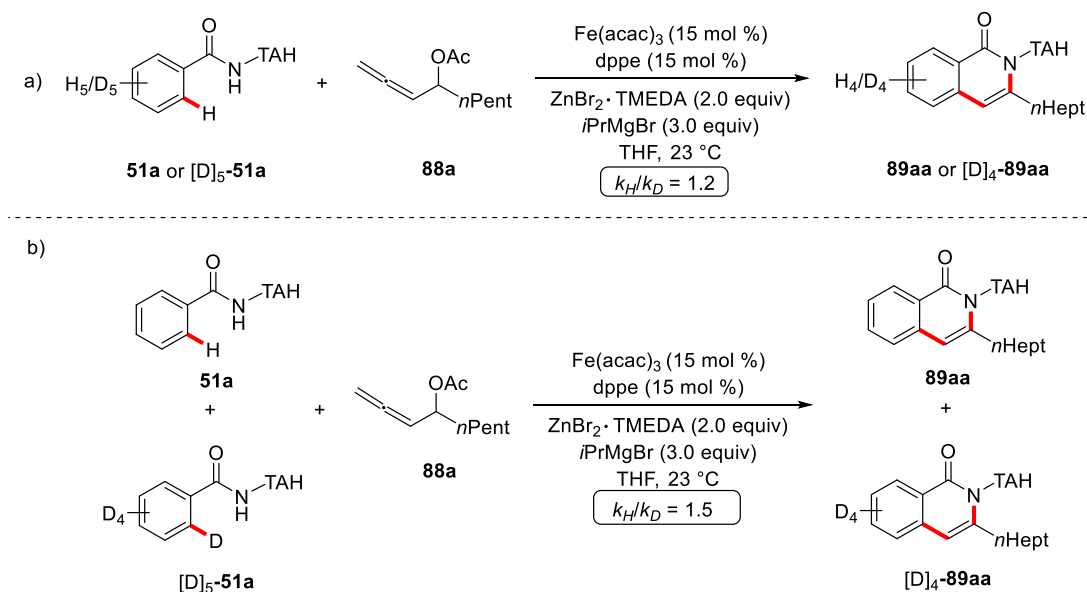
### 3. Results and Discussion



**Scheme 3.4** Competition reaction of iron-catalyzed C–H/N–H annulation.

#### Reactions with Isotopically-labelled Substrates

A C–D functionalization with the isotopically labelled substrate  $[\text{D}]_5\text{-51a}$  either by independent reactions using *in situ* React-IR measurement (Scheme 3.5a) or an intermolecular KIE measurement through a one-pot reaction fashion (Scheme 3.5b), showed no significant kinetic isotope effect ( $k_{\text{H}}/k_{\text{D}} = 1.2$  or  $1.5$ ), providing support for a facile C–H cleavage which is not the rate-determining step of the overall reaction.

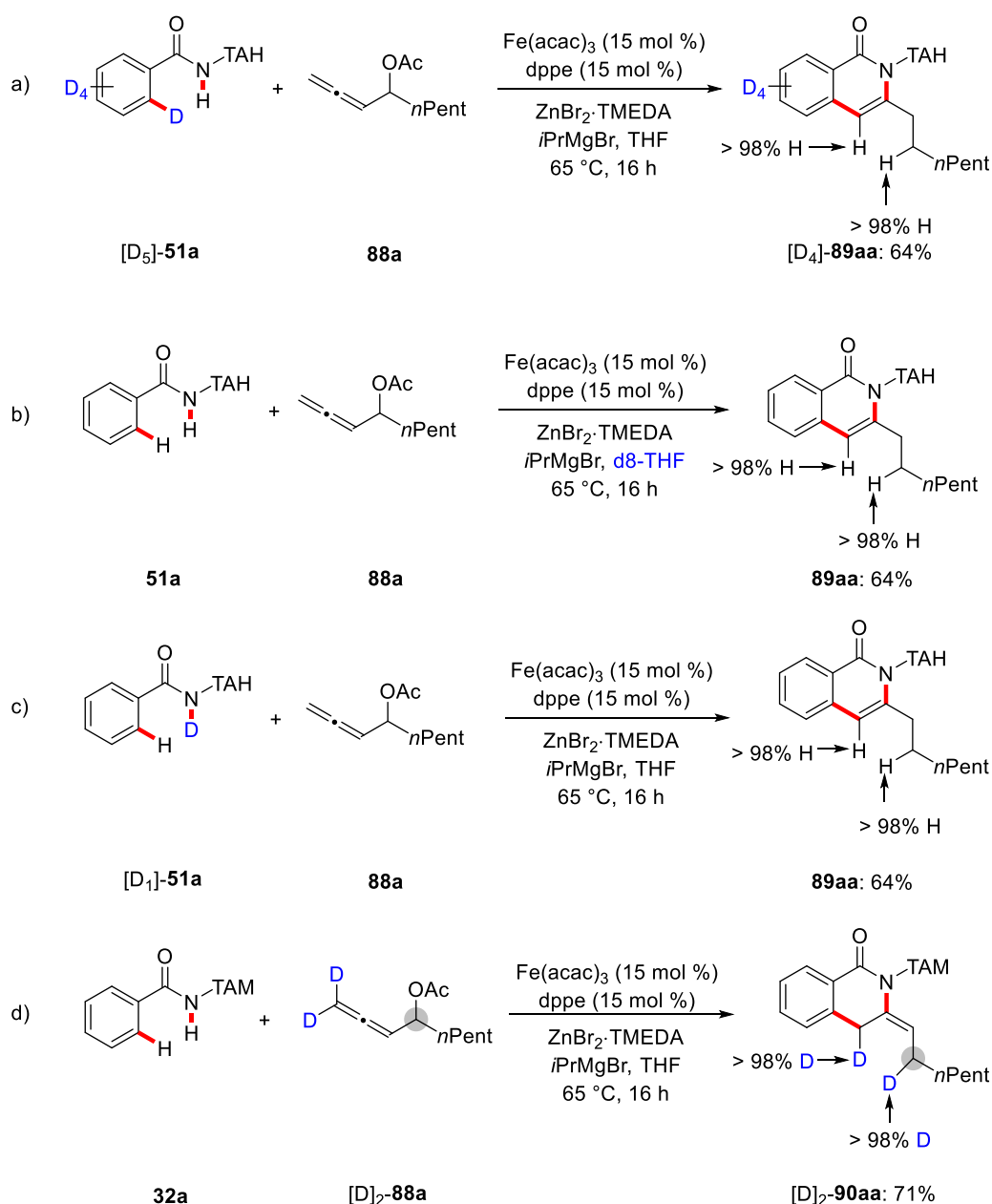


**Scheme 3.5** KIE studies of iron-catalyzed C–H annulation with allenes **88a**.

No deuterium scrambling was observed when isotopically labelled substrate  $[\text{D}]_5\text{-51a}$  was employed (Scheme 3.6a). Furthermore, deuterium scrambling was not observed when using deuterium-labelled solvent (Scheme 3.6b) or isotopically labelled substrate  $[\text{D}]_1\text{-51a}$  (Scheme 3.6c). In contrast, the

### 3. Results and Discussion

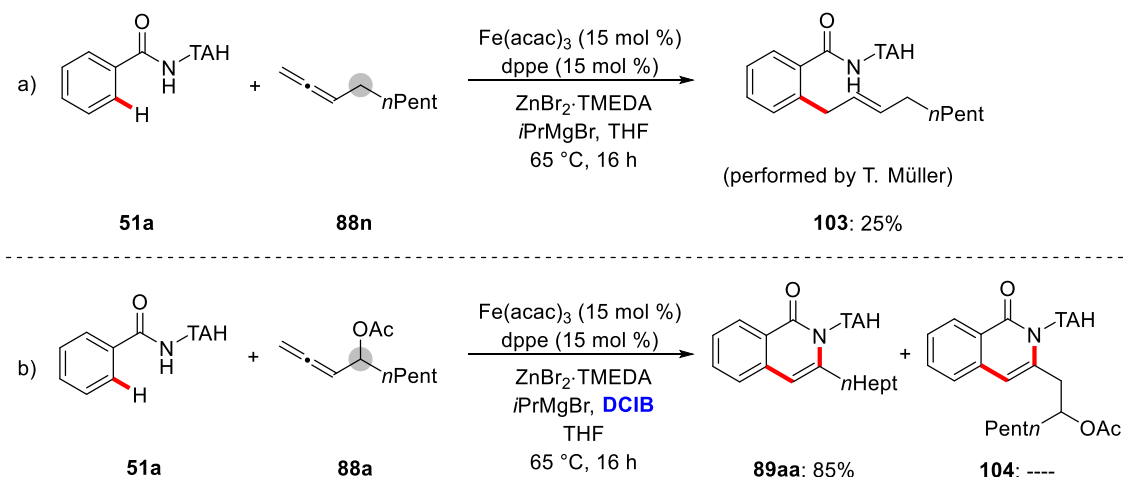
specifically deuterium-labelled allene **[D]<sub>2</sub>-88a** resulted in the site-selective deuterium incorporation in the products **[D]<sub>2</sub>-90aa** (Scheme 3.6d), highlighting the key role of the C–O/C–H cleavage within an external oxidant-free allene annulation process. In addition, the same result was deuterium scrambling was observed in the product, when TAH benzamide **51a** was reacted with **[D]<sub>2</sub>-88a**, which was performed by Dr. T. Müller.<sup>[89]</sup>



**Scheme 3.6** Experiments with isotopically-labelled substrates.

### 3. Results and Discussion

To further unveil the role of the acetate leaving group, two control experiment were conducted, one was employing alkyl allene **88n** under the standard condition, which was performed by Dr. T. Müller (Scheme 3.7a), the other one was using the standard allene **88a** but adding DCIB as an additional oxidant (Scheme 3.7b). To the end, the reaction under otherwise identical reaction conditions led to the corresponding hydroarylation product **103**, while the reaction in the presence of DCIB gave the standard product **89aa**. These observations highlighted an oxidation-induced reductive elimination occurring during the annulation process.



**Scheme 3.7** Role of leaving groups in iron-catalyzed C–H annulation.

#### Mössbauer Spectroscopic Studies

As to the catalyst's mode of action, detailed step-to-step Mössbauer spectroscopic studies were conducted to unveil the oxidation and spin states of the iron intermediate species (Table 3.7). In order to avoid the influence of iron-catalyzed  $\beta$ -H-elimination of Grignard reagent, MeMgBr was used instead of *i*PrMgBr for the Mössbauer measurement. As the amount of Grignard reagent and zinc salts was largely excess comparing with iron catalyst in the standard condition, 9 equivalent of MeMgBr and 6 equivalent of ZnBr<sub>2</sub>·TMEDA were used here to create similar reduce environment for iron catalyst. To this end, the

### 3. Results and Discussion

presence of high-spin iron(II) intermediate species were supported by these observations.<sup>[90]</sup> This research was performed in collaboration with the research group of Prof. Dr. F. Meyer. After sample preparation, the data was recorded and interpreted by Dr. S. Demeshko.

**Table 3.7** Mössbauer parameters of reaction mixtures.

Entry	Reaction	Valence of Iron/ Spin State	$\delta$ (mm s <sup>-1</sup> )	$\Delta E_Q$ (mm s <sup>-1</sup> )	rel. int. (%)
1	<sup>57</sup> FeCl <sub>2</sub> + THF	+2 <sup>HS</sup>	1.26	3.05	100
2	Entry 1 + MeMgBr	+1.4 <sup>[91]</sup>	0.29	0.88	100
3	Entry 2 + ZnBr <sub>2</sub> ·TMEDA	+2 <sup>HS</sup>	1.01	2.69	69
		+2 <sup>HS</sup>	1.36	2.56	31
		+2 <sup>HS</sup>	0.92	1.42	23
4	Entry 3 + dppe	+2 <sup>HS</sup>	0.98	2.57	40
		+2 <sup>HS</sup>	1.24	2.68	37
		n.a. <sup>[a]</sup>	0.26	1.01	43
5	Entry 4 + <b>51a</b>	+2 <sup>HS</sup>	1.14	2.45	36
		+2 <sup>HS</sup>	1.00	3.17	21
6	Entry 5 + <b>88a</b>	n.a. <sup>[a]</sup>	0.24	1.43	28
		+2 <sup>HS</sup>	0.68	1.94	29
		+2 <sup>HS</sup>	1.12	2.60	43

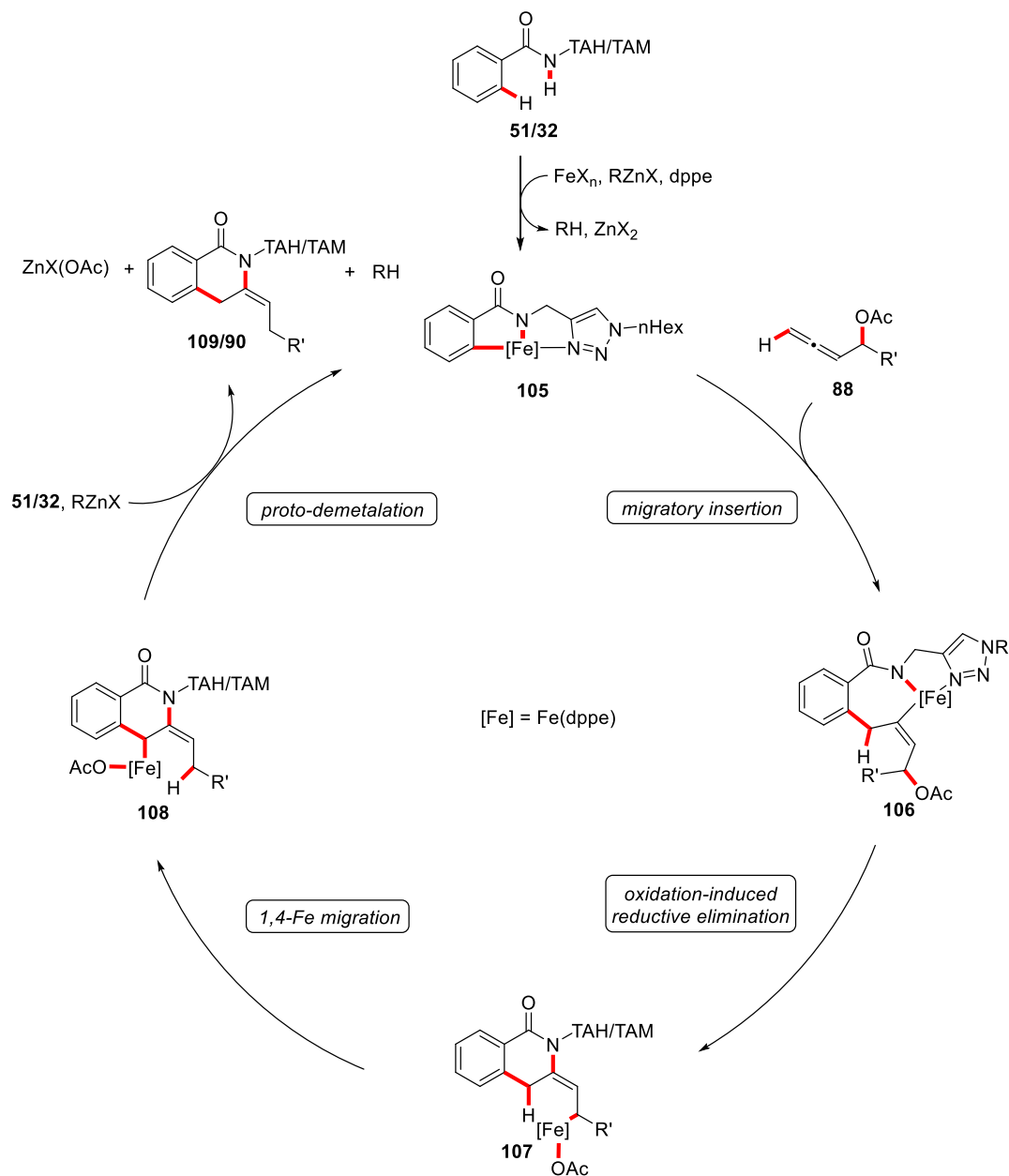
<sup>[a]</sup> n.a. = not assigned. The data were recorded and interpreted by Dr. S. Demeshko.

### 3. Results and Discussion

#### 3.1.6 Proposed Mechanism

Based on the mechanistic findings, the iron-catalyzed allene annulation is proposed to be initiated by facile C–H metalation *via* LLHT, along with allene migratory insertion (Scheme 3.8). Thereafter, oxidation-induced reductive elimination takes place to generate the iron allyl complex **107**. Based on the selective deuterium transposition, the iron allyl complex **107** was proposed to undergo a unique intramolecular C–H activation by 1,4-iron migration<sup>[92]</sup> which was considered as the key step to generate the stabilized allylic-benzylic iron intermediate **108**. Proto-demetalation with the amide motif of the substrate **51/32** delivers the intermediate **109** or the final product **90**. The intermediate **109** finally undergoes isomerization to furnish the corresponding isoquinolone **89**. The crucial 1,4 iron migration was further supported by computational studies that were conducted by Dr. J. C. A. Oliveira.<sup>[89]</sup>

### 3. Results and Discussion



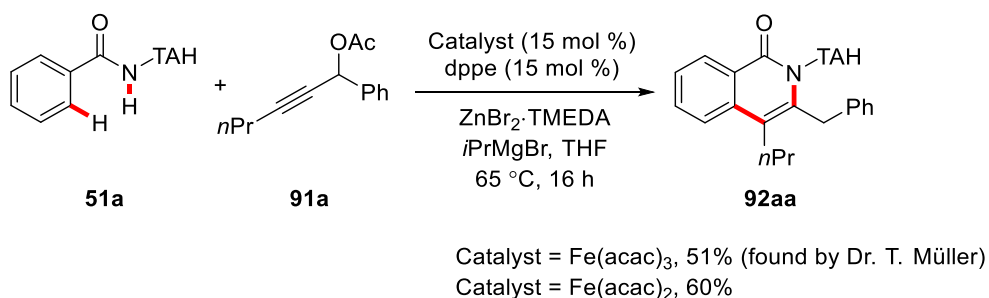
**Scheme 3.8** Proposed mechanism for iron-catalyzed C–H annulation with allenes **88**.

### 3.2 Iron-Catalyzed C–H/N–H Propargyl Acetate Annulation

While a previous report on iron-catalyzed alkyne annulations<sup>[61]</sup> showed limitations in substrate scope and a procedure to remove the TAH group was not available, it was valuable to investigate the reactivity of propargyl acetates in iron-catalyzed C–H annulations.

#### 3.2.1 Optimization Study and Substrate Scope

Under the standard reaction condition for the allene annulations (Chapter 3.1.1), a similar reactivity was accomplished with propargyl acetates **91a**, the reaction was found by Dr. T. Müller. The yield increased to 60% when using  $\text{Fe}(\text{acac})_2$  instead of  $\text{Fe}(\text{acac})_3$ . This finding suggested that an iron(II) catalyst may be more reactive than iron(III) catalysts (Scheme 3.9).



**Scheme 3.9** Test reaction of propargyl acetate **91a**.

For consistency and reproducibility, the optimization studies and the substrate scope were performed by Dr. T. Müller.<sup>[93]</sup>

These experiments showed that: As in the allene annulation reactions (Chapter 3.1.1), dppe proved to be the ligand of choice and  $\text{FeCl}_2$  showed higher activity in the catalytic reaction. The propargyl acetate annulation required more solvent and a lower reaction temperature. Furthermore, the propargyl acetate annulations with the TAH-substrates showed similar reactivity as was observed with the allenes. However, the TAM-substrates, which were compatible for allene annulations, fell short in providing the target products here. The

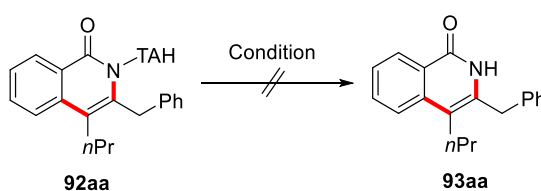
### 3. Results and Discussion

inherently decreased reactivity of the TAM-substrate can be partially attributed to the increased steric bulk of propargyl acetates as compared to the allenes.

#### 3.2.2 Traceless Electrochemical Removal of TAH Group

Efforts first have been made to chemically remove the TAH group. Unfortunately, all attempts failed to deliver the target product **93aa** (Table 3.8).

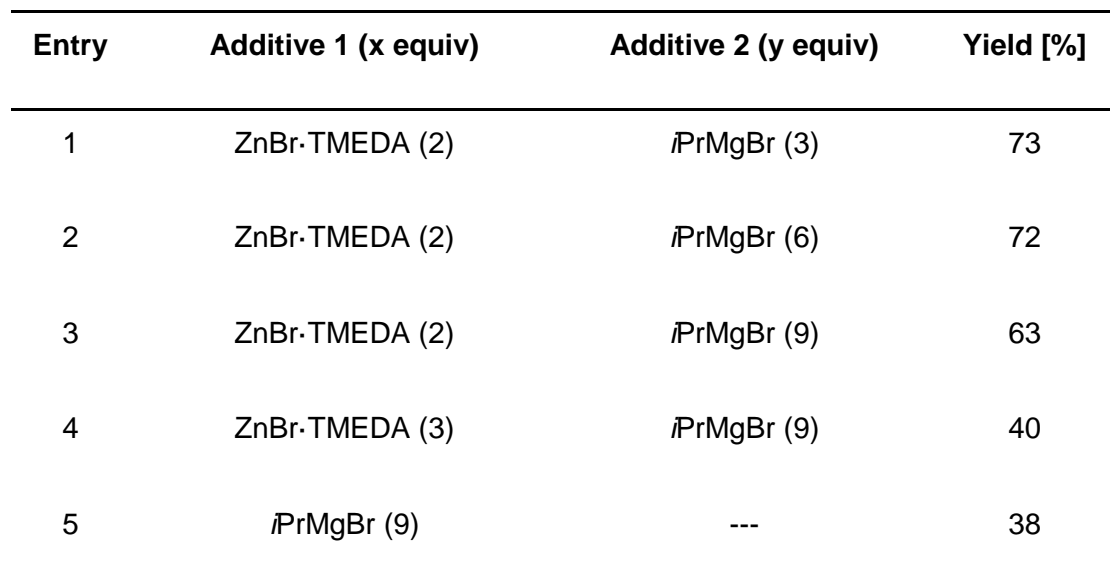
**Table 3.8** Failed attempts for removal of TAH group.



Entry	Conditions
1	1) LDA (2 equiv) /THF, -78 °C, 5 min 2) O <sub>2</sub> , -78 °C, 3) 10 min 4) NH <sub>4</sub> Cl/H <sub>2</sub> O, -78–23 °C, 1 h
2	1) BBr <sub>3</sub> (5.3 equiv), DCM, 0–23 °C, 16 h 2) PhI(TFA) <sub>2</sub> , MeCN/THF/H <sub>2</sub> O, 0 °C, 2 h
3	BF <sub>3</sub> Et <sub>2</sub> O (1.5 equiv), dry MeOH, 130 °C, 16 h
4	NOBF <sub>4</sub> (2.0 equiv), MeCN, 50 °C, 16 h
5	H <sub>2</sub> O <sub>2</sub> (5 mL), CF <sub>3</sub> COOH (4 mL), 40 °C, 18 h
6	Conc. aq. HCl (1 mL), THF, 130 °C, 16 h
7	Conc. aq. HCl (1 mL), THF, 130 °C, 16 h
8	H <sub>2</sub> SO <sub>4</sub> (1 mL), THF, 130 °C, 16 h

9	sat. NaOH (1 mL), THF, 130 °C, 16 h
---	-------------------------------------

**Table 3.9** Optimization of traceless removal of the TAH group.



### 3. Results and Discussion

6	MgBr <sub>2</sub> (10)	---	n.r.
7	ZnBr <sub>2</sub> ·TMEDA (10)	---	n.r.
8	ZnBr <sub>2</sub> (10)	---	n.r.
9	<i>n</i> Bu <sub>4</sub> NBF <sub>4</sub> (4)	---	n.r.
10 <sup>[b]</sup>	H <sub>2</sub> O	---	n.r.
11 <sup>[b]</sup>	aq. NH <sub>4</sub> Cl	---	n.r.

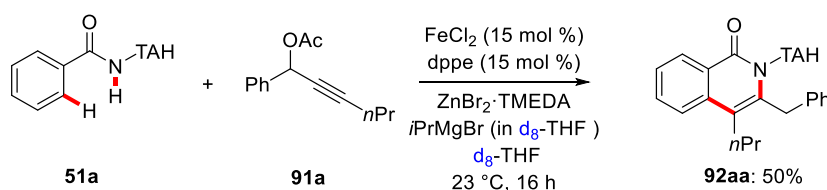
<sup>[a]</sup> Reaction conditions: **92aa** (0.30 mmol), additive 1 (x equiv), additive (y equiv), THF (2 mL), 60 °C, 16 h; yields of isolated products. <sup>[b]</sup> 2 mL of additive 1 was used.

#### 3.2.3 Mechanistic Studies

Mechanistic experiments were performed by Dr. T. Müller<sup>[93]</sup> including 1) intermolecular competition experiments, 2) reactions with the isotopically-labelled substrates, and 3) Hammett-plot analysis of the initial rates of the iron catalyzed C–H activation with a range of propargyl acetates.

These experiments showed that a LLHT mechanism could be possible and that the C–H activation event is not the rate-determining step. Furthermore, no deuterium was incorporated into the product **92aa** by using various isotopically-labelled substrates, such as [D<sub>5</sub>]-benzamide, [D]-benzamide, [D<sub>6</sub>]-*i*PrMgBr, [D<sub>20</sub>]-dppe. A change in the rate-determining step could exist.

Furthermore, when the standard reaction was conducted in the presence of

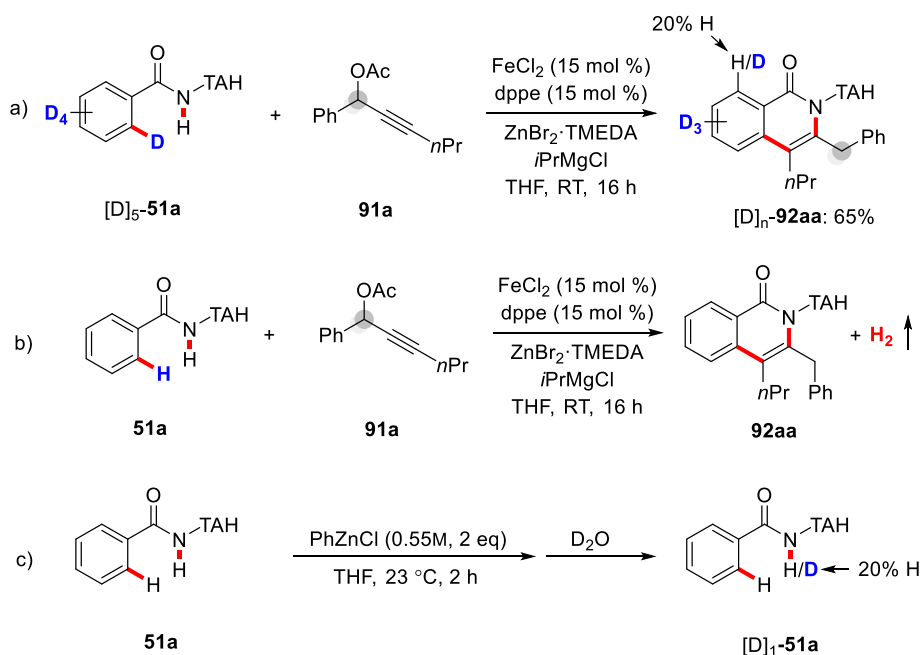


**Scheme 3.10** Reaction with isotopically-labelled solvent.

### 3. Results and Discussion

isotopically-labelled solvent, no deuterium was incorporated into the product (Scheme 3.10).

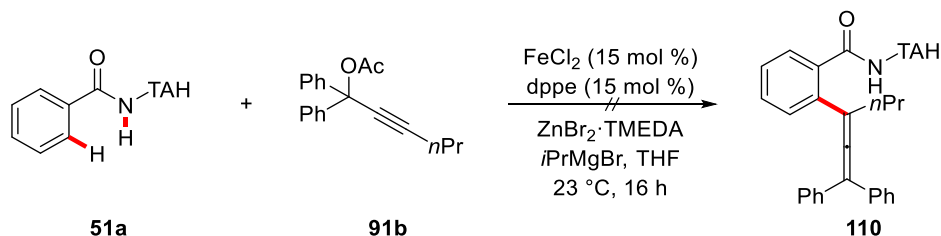
While no deuterium incorporation in product **92aa** was observed in the reaction with [D<sub>5</sub>]-**51a** (Scheme 3.11a, performed by Dr. T. Müller), the following experiments were conducted to understand where the proton at the *ortho*-position of the benzamide **51a** was ending in. H<sub>2</sub> was detected by headspace GC analysis in the standard catalytic reaction (Scheme 3.11b). In addition, the proton of amide in the substrate **51a** can be deprotonated by PhZnCl (Scheme 3.11c). Thus, H<sub>2</sub> could be formed through  $\beta$ -hydride elimination of the Fe-alkyl complex **111** (Scheme 3.13) or by-reaction of iron reacting with Grignard reagent. To further confirm, a DFT calculation was conducted by Dr. J. C. A. Oliveira. These results showed that the formation of H<sub>2</sub> through  $\beta$ -hydride elimination of iron-alkyl complex **111** is less possible during the C–H activation event (Scheme 3.13). Based on these findings, we proposed that the proton of benzamide **51a** which participate in C–H activation would be transferred to the isopropyl group in complex **111** then form propane gas (Scheme 3.13).



**Scheme 3.11** Detection of H<sub>2</sub> and deprotonation of benzamide **51a**.

### 3. Results and Discussion

In order to capture the intermediate, a reaction with di-phenyl substituted propargyl acetate **91b** was performed (Scheme 3.12). Unfortunately, no transformation was observed under the standard conditions.



**Scheme 3.12** Reaction with di-phenyl substituted propargyl acetate **91b**.

#### Mössbauer Spectroscopy Studies

To further gain insights into the catalyst's mode of action, Mössbauer spectroscopic studies were conducted to unveil the oxidation and spin states of the iron intermediate species (Table 3.10). In order to avoid the influence of iron-catalyzed  $\beta$ -H-elimination of Grignard reagent, MeMgBr was used instead of  $i\text{PrMgBr}$  for the Mössbauer measurement. As the amount of Grignard reagent and zinc salts was largely excess comparing with iron catalyst in the standard condition, 9 equivalent of MeMgBr and 6 equivalent of  $\text{ZnBr}_2 \cdot \text{TMEDA}$  were used here to create similar reduced environment for the iron catalyst. Our observations provided strong support for the presence of high-spin iron(II) intermediate species.<sup>[90]</sup> This research work was performed in collaboration with the research group of Prof. Dr. F. Meyer. After sample preparation, the data were recorded and interpreted by Dr. S. Demeshko.

### 3. Results and Discussion

**Table 3.10** Mössbauer parameters of reaction mixtures.

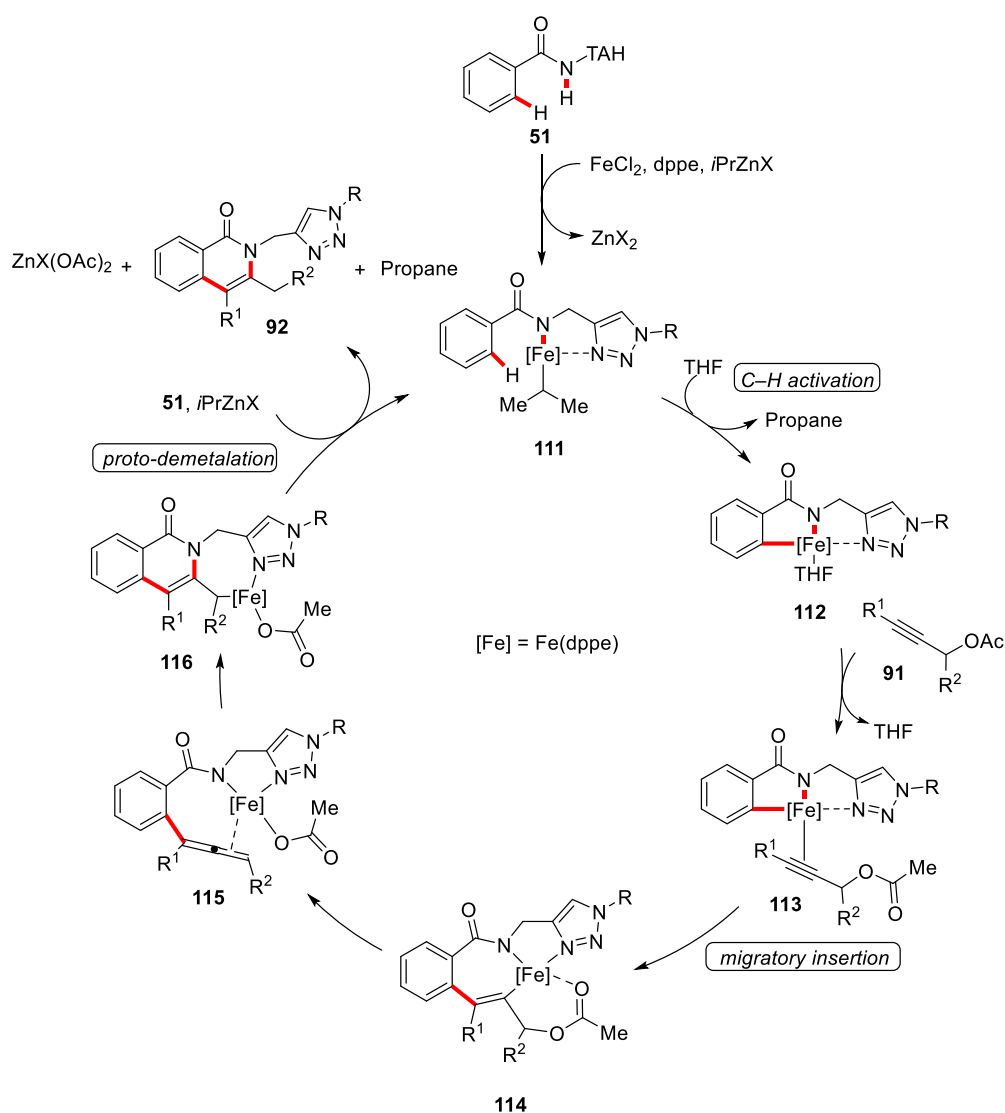
Entry	Reaction	Valence of Iron/ Spin State	$\delta$ (mm s <sup>-1</sup> )	$\Delta E_Q$ (mm s <sup>-1</sup> )	rel. int. (%)
1	<sup>57</sup> FeCl <sub>2</sub> + THF	+2 <sup>HS</sup>	1.26	3.05	100
2	Entry 1 + MeMgBr	+1.4 <sup>[91]</sup>	0.29	0.88	100
3	Entry 2 + ZnBr <sub>2</sub> ·TMEDA	+2 <sup>HS</sup> +2 <sup>HS</sup>	1.01 1.36	2.69 2.56	69 31
		+2 <sup>HS</sup>	0.92	1.42	23
4	Entry 3 + dppe	+2 <sup>HS</sup> +2 <sup>HS</sup>	0.98 1.24	2.57 2.68	40 37
		n.a. <sup>[a]</sup>	0.26	1.01	43
5	Entry 4 + <b>51a</b>	+2 <sup>HS</sup> +2 <sup>HS</sup>	1.14 1.00	2.45 3.17	36 21
6	Entry 5 + <b>91a</b>	+2 <sup>HS</sup> +2 <sup>HS</sup>	1.00 0.95	2.94 2.29	48 52

<sup>[a]</sup> n.a. = not assigned. The data were recorded and interpreted by Dr. S. Demeshko.

### 3. Results and Discussion

#### 3.2.4 Proposed Mechanism

Based on our studies, a plausible catalytic cycle was proposed (Scheme 3.13). The catalytic cycle consists of: a) a reversible, facile C–H activation *via* LLHT, b) alkyne migratory insertion, c) exergonic  $\beta$ -O-elimination, d) allene migratory insertion, and e) proto-demetalation to deliver the desired isoquinolone product **92** and regenerate the active iron species **111**.



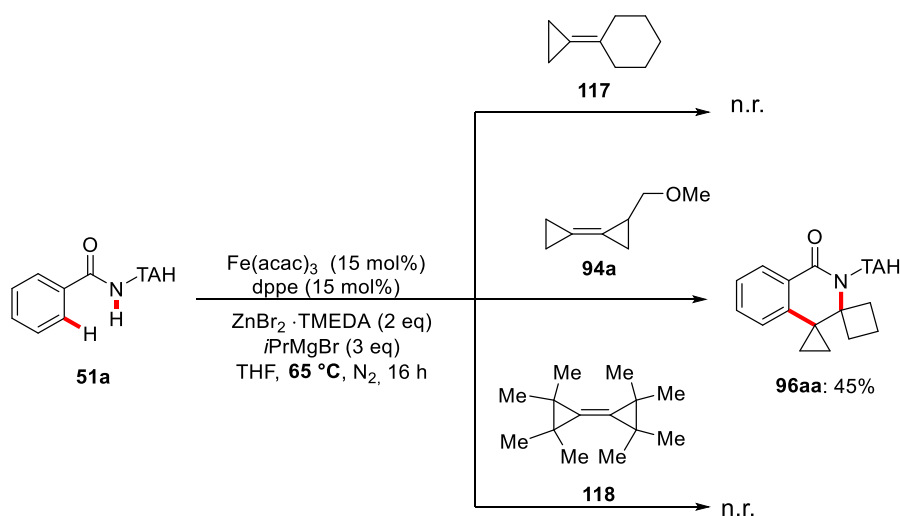
**Scheme 3.13** Proposed mechanism for the iron-catalyzed annulation with **91**.

### 3.3 Iron-Catalyzed C–H/C–C Activation with Bicyclopropylidenes

In recent years, the merger of C–H activation with challenging C–C cleavages has been developed for the construction of novel molecules. Despite considerable achievements, this approach was largely thus far restricted to precious metal catalysts,<sup>[83–84]</sup> activated vinylcyclopropanes,<sup>[24c, 85b–85d]</sup> as well as harsh oxidative conditions.<sup>[85a]</sup>

#### 3.3.1 Optimization Studies

A series of BCP derivatives were tested under the standard reaction conditions of the iron-catalyzed C–H oxidative annulation with allenes. To our delight, when substrate **94a** was used as the coupling partner, bispiro-fused product **96aa** was obtained in 45% yield (Scheme 3.14).



**Scheme 3.14** Test reactions with bicyclopropylidenes.

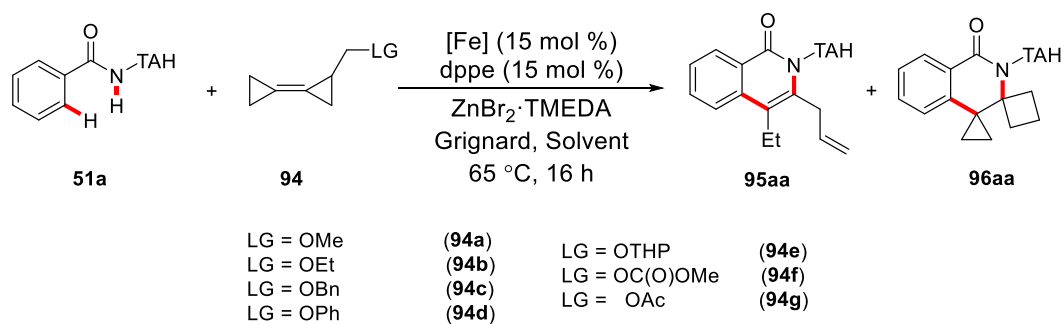
Thereafter, considerable efforts were devoted to improve the yield of the structurally interesting product (Table 3.11). We initiated our optimization by testing different iron catalysts, and  $\text{Fe}(\text{acac})_3$  delivered the best results among the tested catalysts (entries 1–4). In addition, various Grignard reagents are

### 3. Results and Discussion

probed, and *i*PrMgBr proved to be the best (entries 5–10). Other etheric solvents turned out to be less effective than THF (entries 11–15). Increasing the concentration of *i*PrMgBr did not facilitate the reaction (entries 16 and 17). Adding the BCP substrate **94a** dropwise instead of in one portion showed a comparable reactivity (entry 18). The yield dropped to 26% when the reaction was run at 80 °C, while further decreasing the temperature to 23 °C almost shut down the reaction (entries 19 and 20). As the use of acetate as the leaving group was mandatory to achieve reasonable conversion in the iron-catalyzed annulation of allenyl acetates, we reinvestigated the role of the leaving group. When acetate or carbonate was installed on the BCP, the isoquinolone **95aa** could be obtained as main product. In contrast, with alkoxy as the leaving group, product **96aa** was obtained (entries 21–26). The yield of product **95aa** decreased when FeCl<sub>2</sub> was used instead of Fe(acac)<sub>3</sub>, and a higher concentration of Grignard reagent was employed (entries 27–29). Interestingly, biomass-derived solvent 2-MeTHF also enabled the isoquinolone **95aa** transformation, while it proved to be inefficient for the reaction using methoxy as the leaving group (entries 15 and 30). Furthermore, the isoquinolone **95aa** synthesis worked efficiently even at room temperature (entry 31).

### 3. Results and Discussion

**Table 3.11** Optimizations of iron-catalyzed C–H/C–C activation.



Entry <sup>a</sup>	Catalyst	Grignard reagent (x M)	Solvent	LG	96aa [%]	95aa [%]
1	Fe(acac) <sub>3</sub>	<i>i</i> PrMgBr (3)	THF	OMe	25	---
2	FeCl <sub>3</sub>	<i>i</i> PrMgBr (3)	THF	OMe	25	---
3	Fe(dbm) <sub>3</sub>	<i>i</i> PrMgBr (3)	THF	OMe	21	---
4	Fe(acac) <sub>3</sub>	<i>i</i> PrMgBr (3)	THF	OMe	45	---
5	Fe(acac) <sub>3</sub>	MeMgBr (3)	THF	OMe	42	---
6	Fe(acac) <sub>3</sub>	<i>t</i> BuMgCl (2)	THF	OMe	40	---
7	Fe(acac) <sub>3</sub>	CyMgCl (2)	THF	OMe	24	---
8	Fe(acac) <sub>3</sub>	TMSCH <sub>2</sub> MgCl (2.5)	THF	OMe	---	---
9	Fe(acac) <sub>3</sub>	<i>i</i> PrMgCl (1)	THF	OMe	23	---
10	Fe(acac) <sub>3</sub>	cyclopropylMgBr (1)	THF	OMe	14	---
11 <sup>b</sup>	Fe(acac) <sub>3</sub>	<i>i</i> PrMgBr (3)	Et <sub>2</sub> O	OMe	21	---
12	Fe(acac) <sub>3</sub>	<i>i</i> PrMgBr (3)	DME	OMe	---	---
13	Fe(acac) <sub>3</sub>	<i>i</i> PrMgBr (3)	dioxane	OMe	---	---
14	Fe(acac) <sub>3</sub>	<i>i</i> PrMgBr (3)	( <i>n</i> Bu) <sub>2</sub> O	OMe	---	---

### 3. Results and Discussion

15	Fe(acac) <sub>3</sub>	<i>i</i> PrMgBr (3)	2-MeTHF	OMe	---	---
16 <sup>c</sup>	Fe(acac) <sub>3</sub>	<i>i</i> PrMgBr (3)	THF	OMe	26	---
17	Fe(acac) <sub>3</sub>	<i>i</i> PrMgBr (4.3)	THF	OMe	---	---
18 <sup>d</sup>	Fe(acac) <sub>3</sub>	<i>i</i> PrMgBr (3)	THF	OMe	40	---
19 <sup>e</sup>	Fe(acac) <sub>3</sub>	<i>i</i> PrMgBr (3)	THF	OMe	trace	---
20 <sup>f</sup>	Fe(acac) <sub>3</sub>	<i>i</i> PrMgBr (3)	THF	OMe	26	---
21	Fe(acac) <sub>3</sub>	<i>i</i> PrMgBr (3)	THF	OEt	35	---
22	Fe(acac) <sub>3</sub>	<i>i</i> PrMgBr (3)	THF	OBn	trace	---
23	Fe(acac) <sub>3</sub>	<i>i</i> PrMgBr (3)	THF	OPh	---	---
24	Fe(acac) <sub>3</sub>	<i>i</i> PrMgBr (3)	THF	<b>94e</b>	30	15
25	Fe(acac) <sub>3</sub>	<i>i</i> PrMgBr (3)	THF	<b>94f</b>	---	70
26	Fe(acac) <sub>3</sub>	<i>i</i> PrMgBr (3)	THF	OAc	---	80
27	FeCl <sub>2</sub>	<i>i</i> PrMgBr (3)	THF	OAc	---	53
28	Fe(acac) <sub>3</sub>	<i>i</i> PrMgBr (4.28)	THF	OAc	---	47
29 <sup>c</sup>	Fe(acac) <sub>3</sub>	<i>i</i> PrMgBr (3)	THF	OAc	---	53
30	Fe(acac) <sub>3</sub>	<i>i</i> PrMgBr (3)	2-MeTHF	OAc	---	70
31 <sup>e</sup>	Fe(acac) <sub>3</sub>	<i>i</i> PrMgBr (3)	2-MeTHF	OAc	---	64

<sup>[a]</sup> Reaction conditions: **51a** (0.30 mmol), **94** (0.90 mmol), [TM] (15 mol %), dppe (15 mol %), ZnBr<sub>2</sub>·TMEDA (0.60 mmol), Grignard reagent (0.90 mmol), THF (0.40 mL), 65 °C, 16 h; yields of isolated products. <sup>[b]</sup> at 40 °C. <sup>[c]</sup> 0.2 mL solvent was used. <sup>[d]</sup> dropwise addition of **94a** over 1 h. <sup>[e]</sup> at 23 °C. <sup>[f]</sup> at 80 °C.

### 3. Results and Discussion

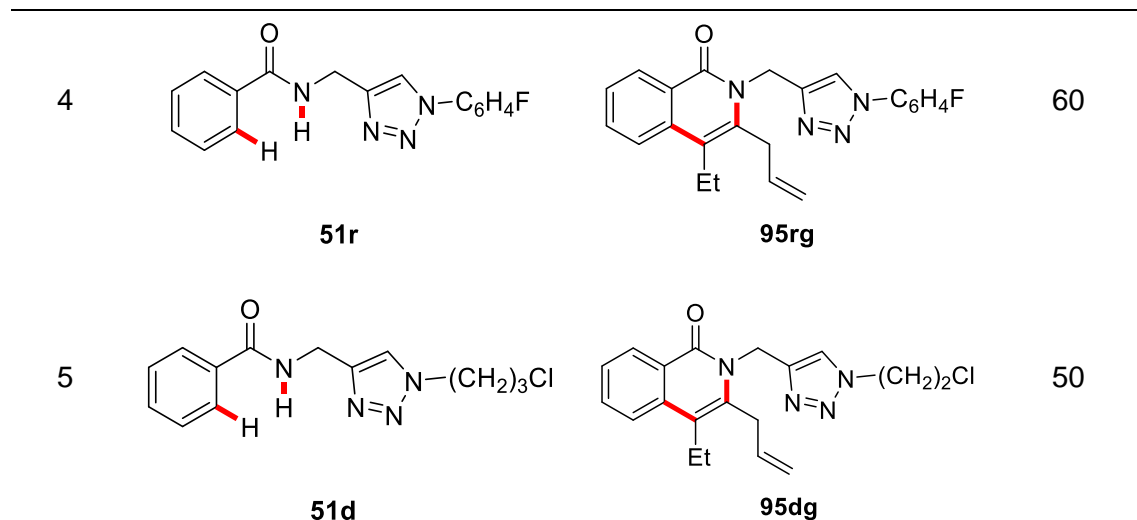
#### 3.3.2 Impact of the N-Substituent on the C–H/C–C Activation

The iron-catalyzed C–H/C–C activation with different TAH groups provided various isoquinolones in moderate to good yields (Table 3.12). Among them, methylene-tethered TAH triazoles delivered the desired isoquinolones **95** in good yields (entries 1–4), tolerating among others a reactive alkyl chloride **51d** without any cross-coupling products being observed (entry 5).

**Table 3.12** Impact of different TAH groups on the C–H/C–C activation.

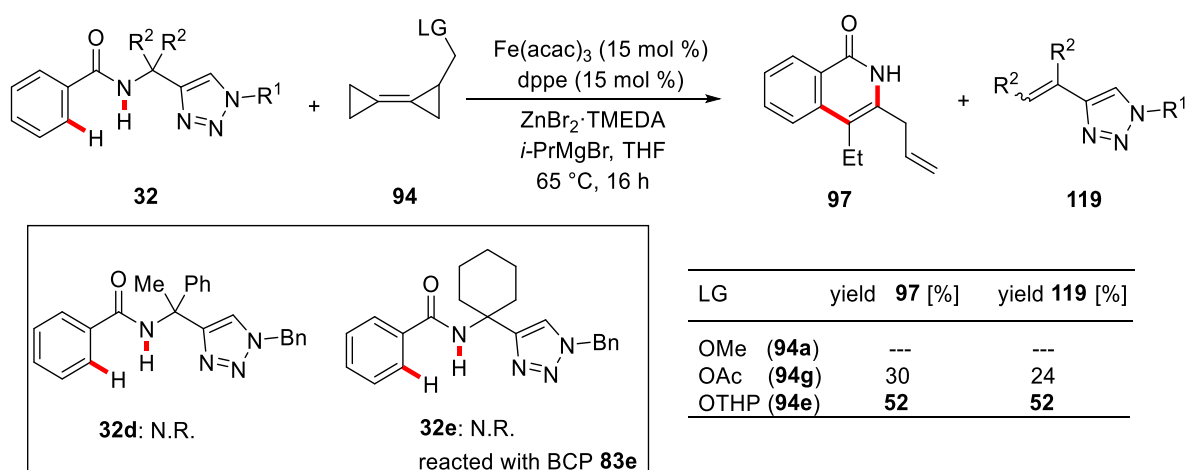
Entry	51	95	Yield [%]
1	<p><b>51a</b></p>	<p><b>95ag</b></p>	80
2	<p><b>51b</b></p>	<p><b>95bg</b></p>	68
3	<p><b>51c</b></p>	<p><b>95cg</b></p>	61

### 3. Results and Discussion



[a] Reaction conditions: **51** (0.30 mmol), **94g** (0.90 mmol), Fe(acac)<sub>3</sub> (15 mol %), dppe (15 mol %), ZnBr<sub>2</sub>·TMEDA (0.60 mmol), *i*-PrMgBr (3.0 M, 0.90 mmol), THF (0.40 mL), 65 °C, 16 h; yields of isolated products.

Notably, when TAM benzamide **32a** was used, the triazole group was directly removed *in situ*, leading to the products of free isoquinolone **97** and triazole substituted alkene **119** (Scheme 3.15). Employing tetrahydropyranyl as the leaving group on the BCP (**94e**), the yield of the free isoquinolone **97** was increased to 52%. While previous studies on iron-catalyzed C–H annulation always needed an additional step for TAM group removal, this finding provided an alternative way to synthesize the NH-free isoquinolone. However, no product



**Scheme 3.15** Impact of different TAM groups on the C–H/C–C activation.

### 3. Results and Discussion

formation was observed when other bulky groups were introduced on the TAM group (Scheme 3.15).

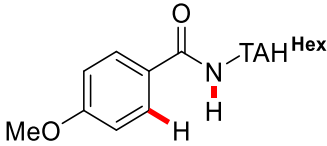
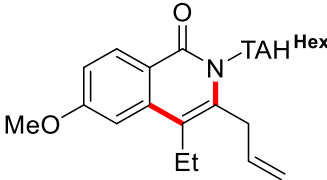
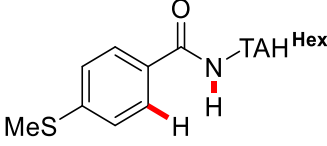
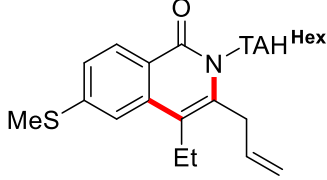
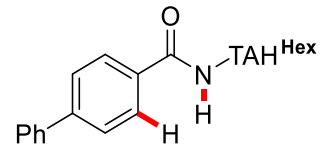
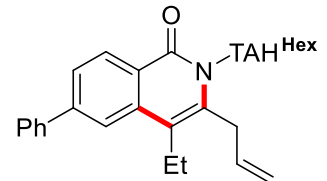
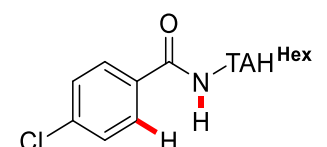
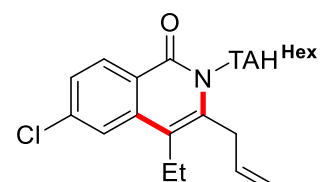
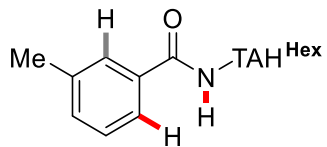
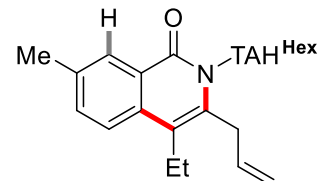
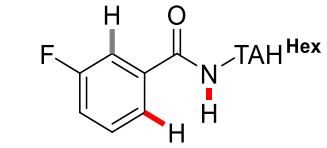
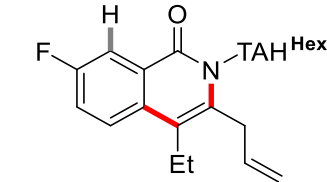
#### 3.3.3 Substrate Scope and Limitations

Next, the reactivity of various substituted TAH substrates and BCP acetates was investigated (Table 3.13). This transformation tolerated various functional groups, such as thioether (**51s**) and chloro (**51j**) (entries 1–6). For the *para*-methyl substituted TAH substrate **51e**, under the standard condition only 16% of the product **95eg** were obtained. By prolonging the reaction time and lowering the reaction temperature, the yield was improved to 60% (entry 2). *meta*-Substituted TAH substrates, such as methyl, chloro or bromo, were efficiently converted to the desired isoquinolones **95tg–95wg** with high chemo- and regio-selectivities (entries 7–10).

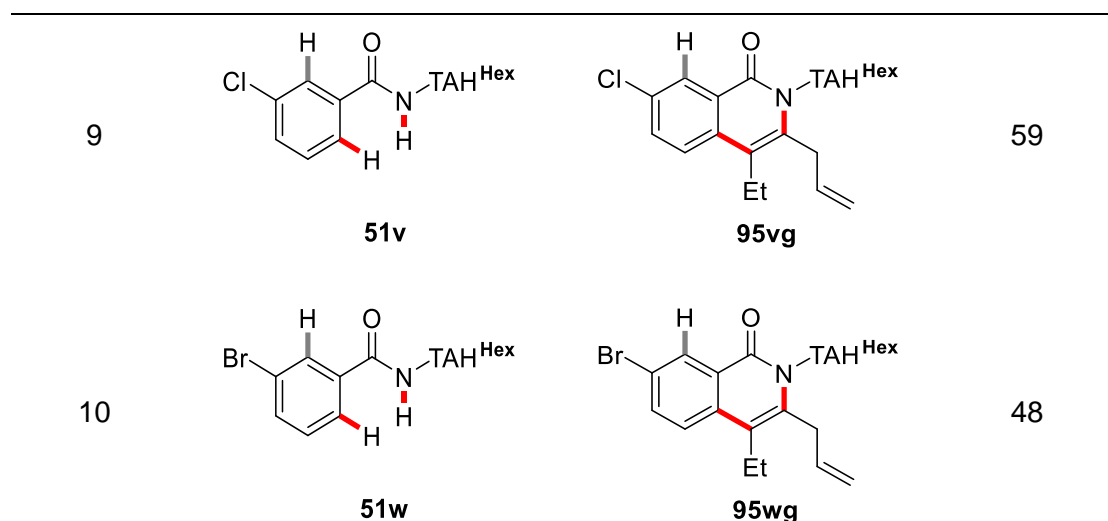
**Table 3.13** Substrate scope of TAH benzamide **51**.

Entry	51	95	Yield [%]
1	 <b>51a</b>	 <b>95ag</b>	80
2	 <b>51e</b>	 <b>95eg</b>	16(60) <sup>[b]</sup>

### 3. Results and Discussion

3	 <b>51g</b>	 <b>95gg</b>	78
4	 <b>51s</b>	 <b>95sg</b>	70
5	 <b>51f</b>	 <b>95fg</b>	61
6	 <b>51j</b>	 <b>95jg</b>	52
7	 <b>51t</b>	 <b>95tg</b>	64
8	 <b>51u</b>	 <b>95ug</b>	79

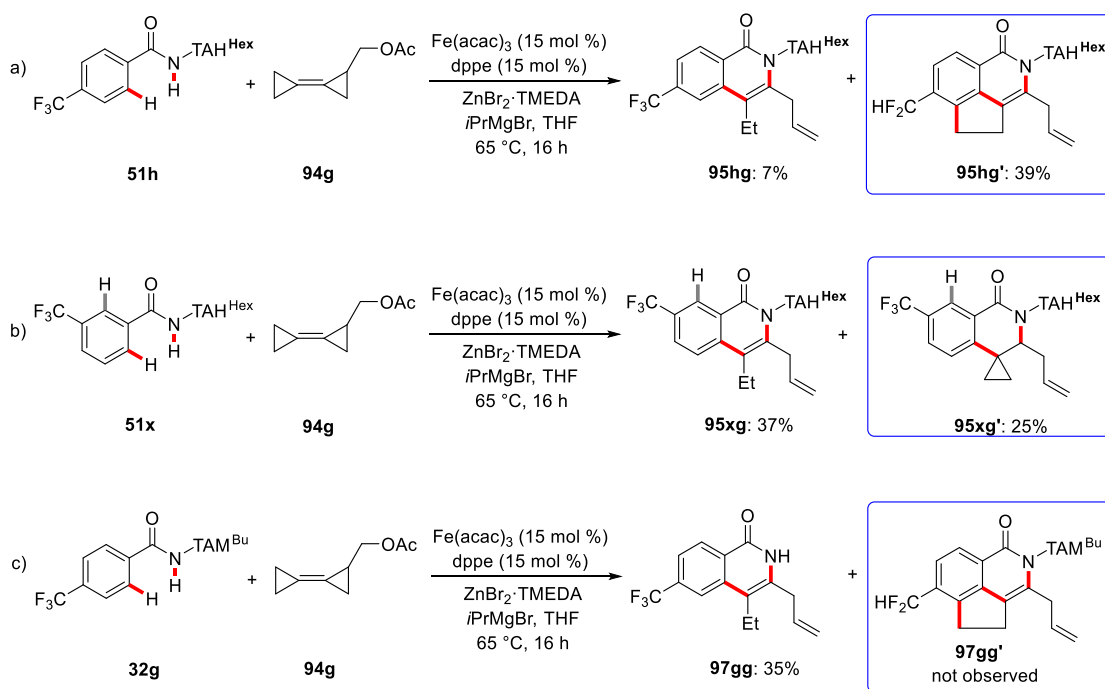
### 3. Results and Discussion



[a] Reaction conditions: **51** (0.30 mmol), **94g** (0.90 mmol), Fe(acac)<sub>3</sub> (15 mol %), dppe (15 mol %), ZnBr<sub>2</sub>·TMEDA (0.60 mmol), *i*PrMgBr (3.0 M, 0.90 mmol), THF (0.40 mL), 65 °C, 16 h; yields of isolated products.

A rare selective C–F/C–H activation could be induced when the *para*-CF<sub>3</sub> substituted TAH-substrate **51h** was used, providing the C–H/C–C/C–F/C–H functionalized product **95hg'** (Scheme 3.16a). Additionally, *meta*-CF<sub>3</sub> substituted TAH-substrate **51x** afforded the by-product **95xg'** with conservation of one cyclopropane ring (Scheme 3.16b). These findings strongly supported a  $\beta$ -O elimination or  $\beta$ -C elimination mechanism to be responsible for the ring opening of the cyclopropanes. For the *para*-CF<sub>3</sub> substituted TAM-substrate **32g**, the C–F/C–H functionalization product **97gg'** was here not observed (Scheme 3.16c), which is suggestive of the C–N bond cleavage taking place preferentially over the C–C cleavage of the second cyclopropane ring during the formation of the free isoquinolone products **97** (Scheme 3.21, pathway **C**).

### 3. Results and Discussion



**Scheme 3.16** Impact of CF<sub>3</sub>-substitution of benzamide.

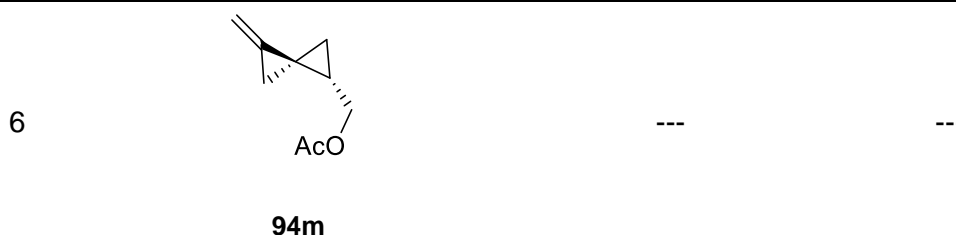
Pre-installed long alkyl chain or phenyl group at the  $\alpha$ -position of the BCP acetate significantly decreased the efficiency of the transformation (Table 3.14, entries 1 and 2). It is also worth to mention that the two cyclopropane rings of the BCP derivative are necessary for this C–H annulation reaction. The absence or replacement of one of them shut down the transformation (entries 3–6).

### 3. Results and Discussion

**Table 3.14** Substrate scope of BCP **94**.

Entry	<b>94</b>	<b>95</b>	Yield [%]
1	 <b>94h</b>	 <b>95ah</b>	61
2	 <b>94i</b>	 <b>95ai</b>	53
3	 <b>94j</b>	---	---
4	 <b>94k</b>	---	---
5	 <b>94l</b>	---	---

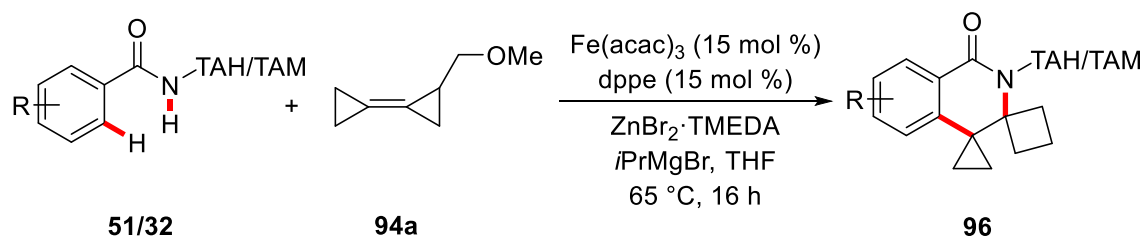
### 3. Results and Discussion

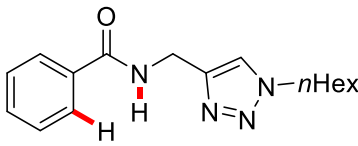
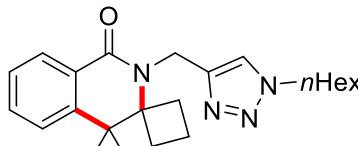
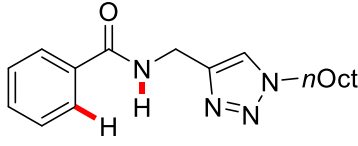
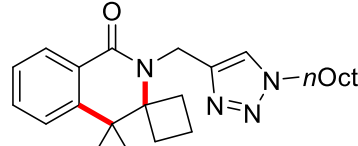


<sup>[a]</sup> Reaction conditions: **51a** (0.30 mmol), **94** (0.90 mmol), Fe(acac)<sub>3</sub> (15 mol %), dppe (15 mol %), ZnBr<sub>2</sub>·TMEDA (0.60 mmol), *i*PrMgBr (3.0 M, 0.90 mmol), THF (0.40 mL), 65 °C, 16 h; yields of isolated products.

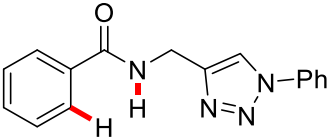
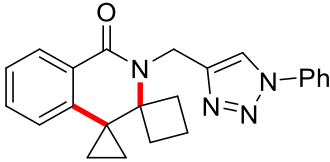
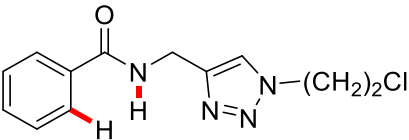
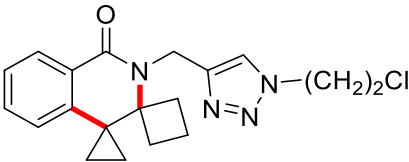
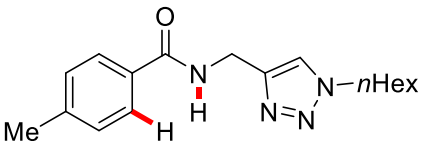
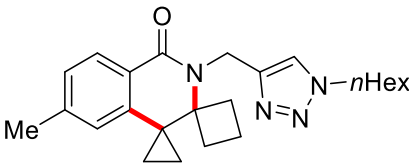
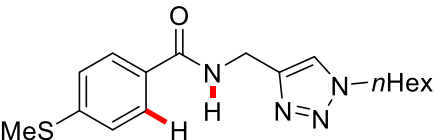
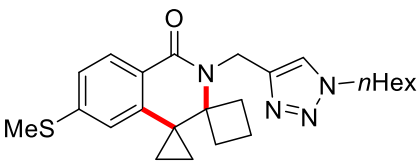
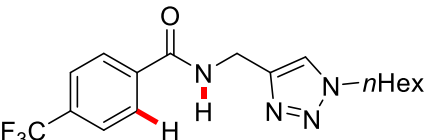
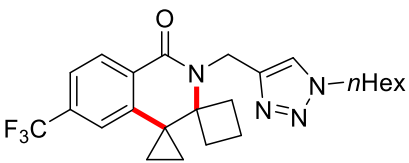
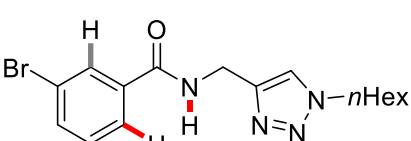
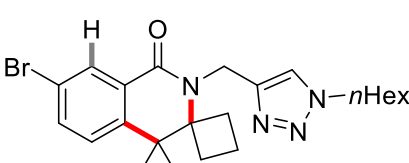
Efforts also have been made to extend the scope of the bispiro-fused product **96**. Unfortunately, BCPs bearing methoxy as the leaving group only afforded the corresponding products in low yields when reacted with different TAH substrates **51** (Table 3.15, entries 1–9). TAM substrates **32** were tested as well, however, no target product formation was observed (entries 10–12).

**Table 3.15** Substrate scope of bispiro-fused isoquinolone **96** formation.

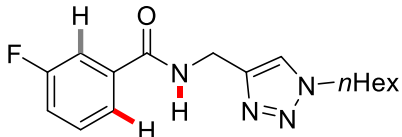
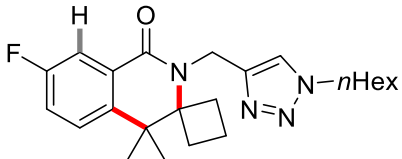
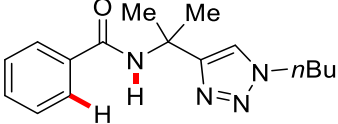
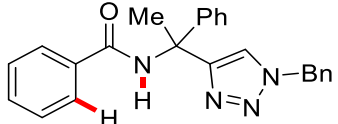
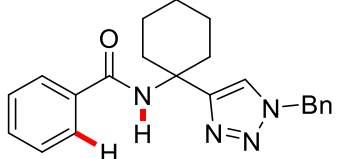


Entry	51/32	96	Yield [%]
1	 <p><b>51a</b></p>	 <p><b>96aa</b></p>	45
2	 <p><b>51b</b></p>	 <p><b>96ba</b></p>	35

### 3. Results and Discussion

3	 <b>51y</b>	 <b>96ya</b>	30
4	 <b>51d</b>	 <b>96da</b>	36
5	 <b>51e</b>	 <b>96ea</b>	32
6	 <b>51s</b>	 <b>96sa</b>	40
7	 <b>51h</b>	 <b>96ha</b>	28
8	 <b>51w</b>	 <b>96wa</b>	31

### 3. Results and Discussion

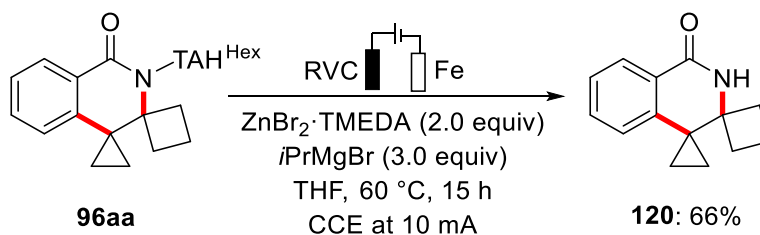
9	 <b>51u</b>	 <b>96ua</b>	29
10	 <b>32a</b>	---	---
11	 <b>32d</b>	---	---
12	 <b>32e</b>	---	---

<sup>[a]</sup> Reaction conditions: **51/32** (0.30 mmol), **88a** (0.90 mmol), Fe(acac)<sub>3</sub> (15 mol %), dppe (15 mol %), ZnBr<sub>2</sub>·TMEDA (0.60 mmol), *i*PrMgBr (3.0 M, 0.90 mmol), THF (0.40 mL), 65 °C, 16 h; yields of isolated products.

#### 3.3.4 Removal of TAH Group

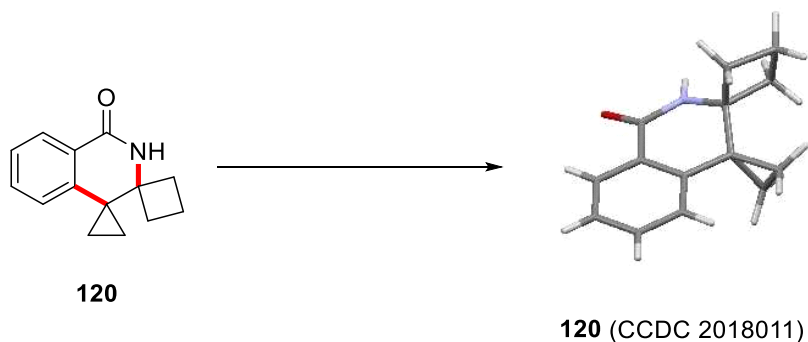
The TAH group of the bispiro-fused isoquinolone **96aa** was removed in an electro-oxidative fashion without breaking the strained rings (Scheme 3.17).

### 3. Results and Discussion



**Scheme 3.17** Traceless electrochemical removal of the TAH group.

Crystals suitable for X-ray diffraction were then grown by slow evaporation, unambiguously confirming the connectivity of product **120** (Scheme 3.18).



**Scheme 3.18** Molecular structure of **120** with thermal ellipsoids at 50% probability level. The crystal structure was measured and solved by Dr. Christopher Golz.

#### 3.3.5 Mechanistic Studies

In order to shed light on the reaction mechanism, experimental and Mössbauer spectroscopic studies were conducted.

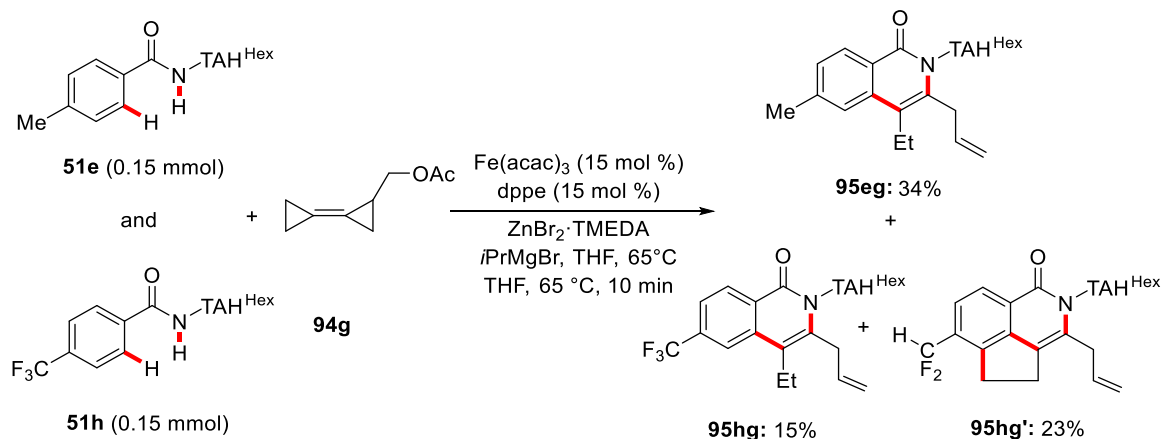
#### Experimental Studies

A comparable reactivity between electron-deficient benzamide **51h** and electron-rich benzamide **51e** was observed (Scheme 3.19a). A C–D/N–H functionalization with the isotopically labelled substrates [D]<sub>5</sub>-**51r** or [D]<sub>5</sub>-**51a**, either by independent reactions or an intermolecular KIE measurement in a one-pot fashion, showed a very minor kinetic isotope effect ( $k_H/k_D = 1.2$ ),

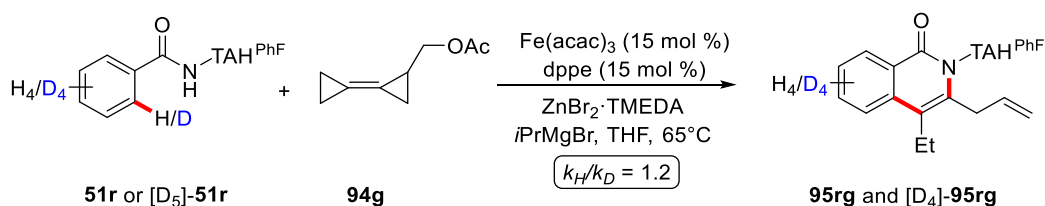
### 3. Results and Discussion

providing support for a facile C–H cleavage which is not the rate-determining step of the overall reaction (Scheme 3.19b and 3.19c).

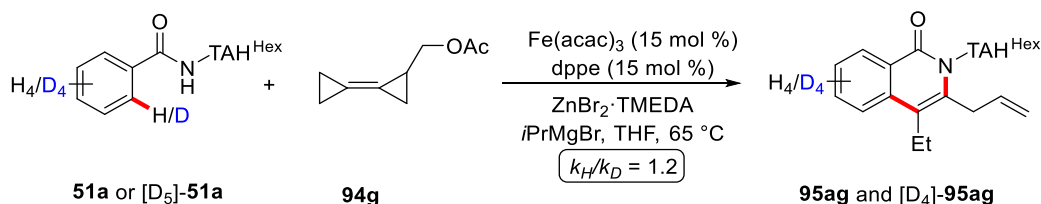
#### a) Competition Experiment



#### b) Intermolecular KIE (independent reactions)



#### c) Intermolecular KIE (one-pot)

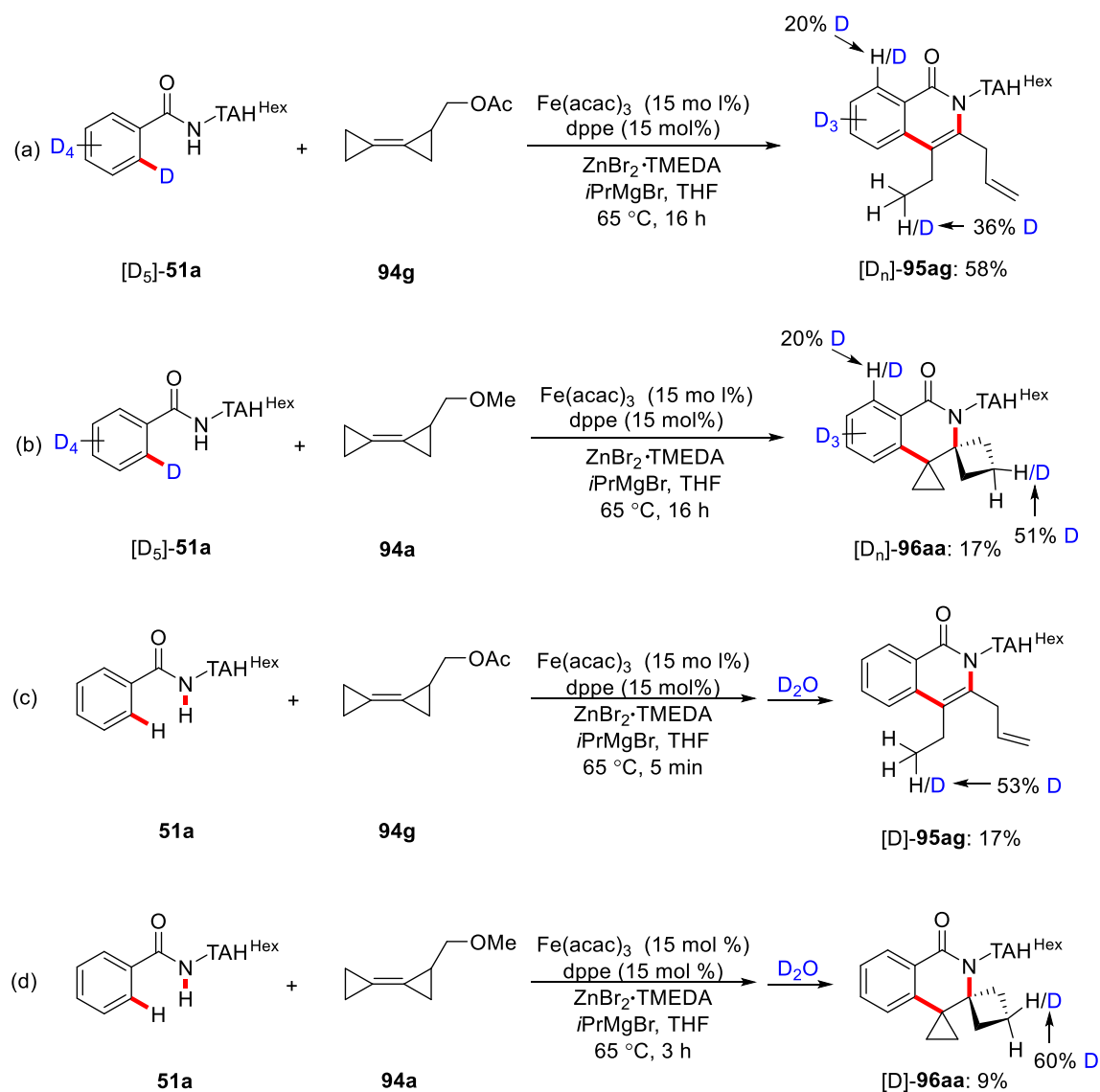


**Scheme 3.19** Competition reaction and KIE studies.

The deuterium-labelled substrate  $[\text{D}_5]\text{-51a}$  resulted in site selective deuterium incorporation of the product  $[\text{D}_n]\text{-95ag}$  or  $[\text{D}_n]\text{-96aa}$ , being indicative of a LLHT mechanism (Scheme 3.20a and 3.20b). Interestingly, deuterium incorporation was position-selective for the corresponding products (Scheme 3.20c and 3.20d), which indicates an iron-catalyzed C–C cleavage occurring during the catalytic reaction. The partial deuterium incorporation of the products  $[\text{D}]\text{-95ag}$  and  $[\text{D}]\text{-96aa}$  (Scheme 3.20c and 3.20d) indicates that intermediates **125** and

### 3. Results and Discussion

**126** could be the resting states for the corresponding pathways **A** and **B** (Scheme 3.21). In addition, diastereo-selective deuterium incorporation in the products  $[D_n]$ -**96aa** and  $[D]$ -**96aa** was observed, (Scheme 3.20b and 3.20d) which suggests a migratory insertion taking place for the formation of intermediate **126** (Scheme 3.21, pathway **B**).



**Scheme 3.20** Isotopically-labelled experiments.

### 3. Results and Discussion

#### Mössbauer spectroscopy studies

For further understanding the iron's oxidation and spin states in the reaction, detailed Mössbauer spectroscopic studies were conducted. In order to avoid the influence of iron-catalyzed  $\beta$ -H-elimination of Grignard reagent, MeMgBr was used instead of *i*PrMgBr for the Mössbauer measurement. Overall, the presence of high-spin iron(II) intermediates were support by our observations.<sup>[90]</sup> These studies were performed in collaboration with the research group of Prof. Dr. F. Meyer. After sample preparation, the data were recorded and interpreted by Dr. S. Demeshko.

**Table 3.16** Mössbauer parameters of reaction mixtures.

Entry	Reaction	Valence of Iron / Spin State	$\delta$ (mm·s <sup>-1</sup> )	$\Delta EQ$ (mm·s <sup>-1</sup> )	rel. int. (%)
1	<sup>57</sup> FeCl <sub>2</sub> + THF	+2 <sup>HS</sup>	1.26	3.05	100
2	Entry 1 + MeMgBr	+1.4 <sup>[91]</sup>	0.29	0.88	100
3	Entry 2 + ZnBr <sub>2</sub> ·TMEDA	+2 <sup>HS</sup>	1.01	2.69	69
		+2 <sup>HS</sup>	1.36	2.56	31
4	Entry 3 + dppe	+2 <sup>HS</sup>	0.92	1.42	23
		+2 <sup>HS</sup>	0.98	2.57	40
		+2 <sup>HS</sup>	1.24	2.68	37
5	Entry 4 + <b>51a</b>	+2 <sup>HS</sup>	0.89	2.05	30
		+2 <sup>HS</sup>	0.93	2.63	49
		+2 <sup>HS</sup>	1.02	3.07	21
6	Entry 5 + <b>94g</b>	+2 <sup>HS</sup>	0.95	2.22	33
		+2 <sup>HS</sup>	1.02	2.79	55
		+2 <sup>HS</sup>	1.05	3.13	12
7	Entry 4 + <b>32a</b> + <b>94g</b>	+2 <sup>HS</sup>	0.92	2.09	44
		+2 <sup>HS</sup>	0.95	2.66	36
		+2 <sup>HS</sup>	1.03	3.00	20

### 3. Results and Discussion

---

8	Entry 5 + <b>94a</b>	+2 <sup>HS</sup>	0.74	2.34	13
		+2 <sup>HS</sup>	1.02	2.63	65
		+2 <sup>HS</sup>	1.03	3.09	22

---

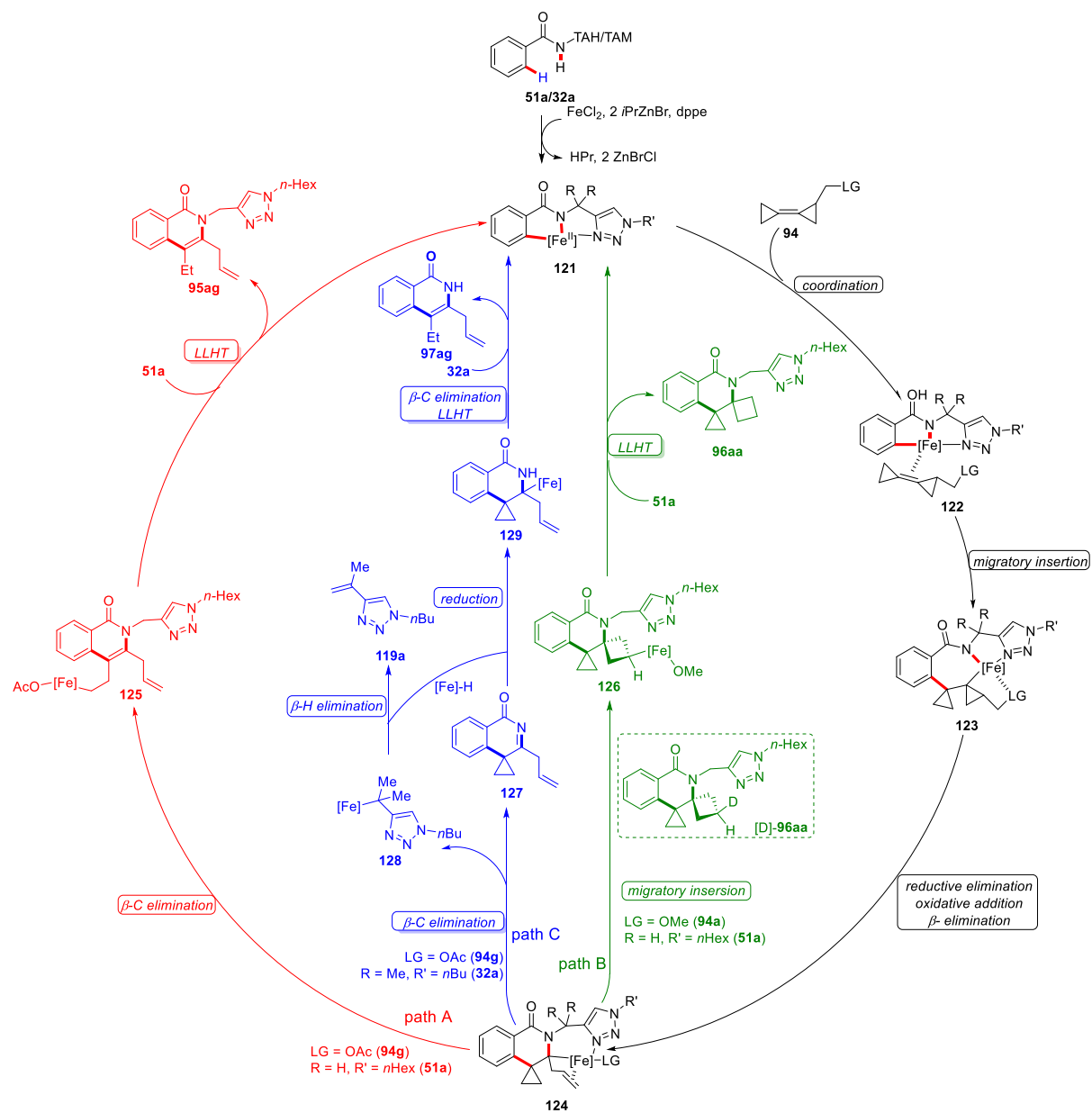
The data were recorded and interpreted by Dr. S. Demeshko.

#### 3.3.6 Proposed Mechanism

Based on experimental studies and previous findings,<sup>[94]</sup> we propose a novel iron-catalyzed C–H/C–C activation sequence, involving three pathways can lead to three different product formations (Scheme 3.21).

The catalytic cycle is initiated by a reversible C–H activation *via* LLHT to generate the cyclometalated iron species **121**, which can undergo coordination and migratory insertion to deliver complex **123**. After oxidation-induced reductive elimination<sup>[46, 94]</sup> and  $\beta$ -elimination of intermediate **123**, intermediate **124** is formed. From intermediate **124**, depending on the combination of leaving group and N-substituent, three pathways can lead to three different products. In pathway **A**, intermediate **124** undergoes  $\beta$ -C-elimination to give intermediate **125**, subsequent with proto-demetallation to yield product **95ag** and regenerate the active iron species **121**. In pathway **B**, migratory insertion of the alkene takes place to form the intermediate **126**. After proto-demetallation, product **96aa** is provided. Finally, in pathway **C**, a  $\beta$ -C-elimination occurs at the N–C bond which connects the directing group and benzamide moiety, thus forming the intermediates **127** and **128**. Intermediate **128** undergoes  $\beta$ -H-elimination to release the alkene **119a** and generate iron hydride species which reduces the intermediate **127** to generate intermediate **129**. After  $\beta$ -C-elimination and proto-demetallation, intermediate **129** yields the final product **97ag** and releases the active iron species **121**.

### 3. Results and Discussion



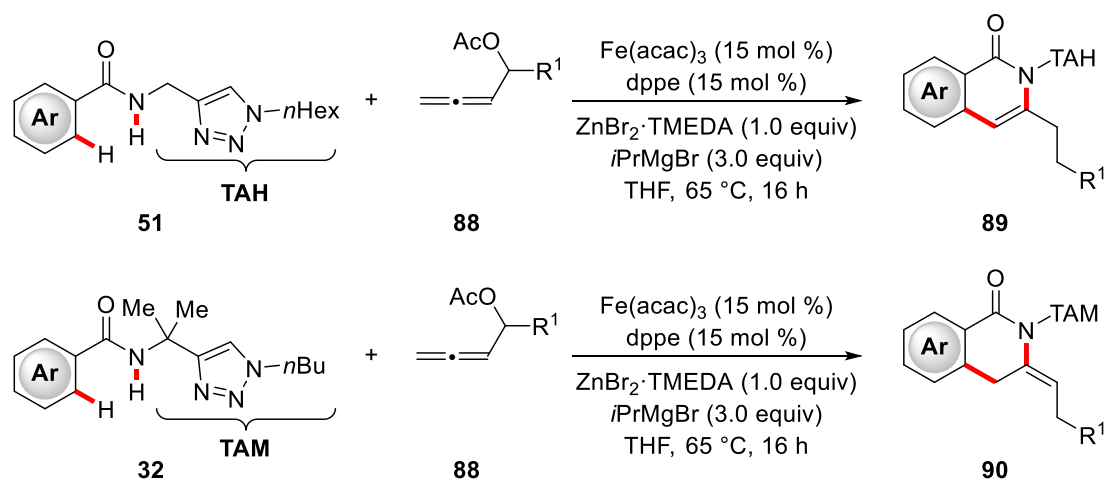
**Scheme 3.21** Proposed catalytic cycle for iron-catalyzed C-H/C-C activations.

### 4. Summary and Outlook

The last decades have witnessed considerable progress in iron-catalyzed C–H functionalizations for a sustainable and economically-efficient access to C–C and C–Het bonds. Despite considerable progress, several limitations in iron-catalyzed C–H annulation reactions need to be overcome. First, the types of viable coupling partners for this methodology are severely restricted, only alkynes were reported thus far. Next, an excess of DCIB as an external oxidant was required for an efficient annulation. In addition, a narrow substrate scope was presented in several cases. Then, the reaction mechanism was not fully elucidated. Last, efficient protocols for the removal of the TAH group are missing.

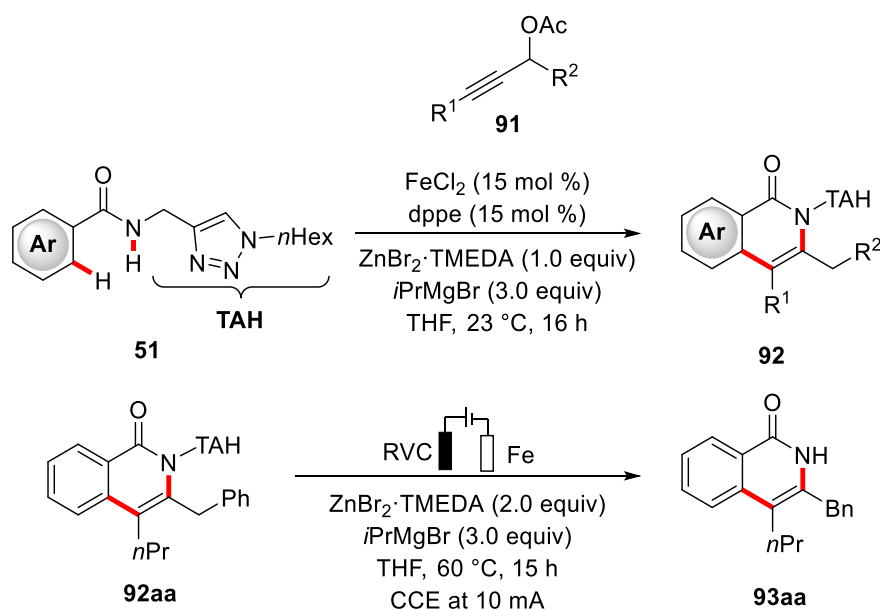
In the first project, iron-catalyzed C–H annulations with allenes **88** were disclosed (Scheme 4.1).<sup>[89]</sup> The notable achievements feature 1) a novel iron-catalyzed annulation reaction with allenes, 2) C–H activation at room temperature, 3) external-oxidant-free conditions, 4) not only TAH benzamides **51**, TAM benzamides **32** can be compatible for this novel transformation, and 5) detailed mechanistic insight into this 1,4-iron migration pathway for facile C–H activations.

## 4. Summary and Outlook



**Scheme 4.1** Iron-catalyzed C–H/N–H redox-neutral annulations with allenes **88**.

Within the second project, the synthesis of 3,4-disubstituted isoquinolones **92** through iron-catalyzed C–H annulations with propargyl acetates **91** was realized (Scheme 4.2).<sup>[93]</sup> Notably, the TAH group, whose removal proved to be difficult, can be tracelessly removed in an electrochemical fashion.

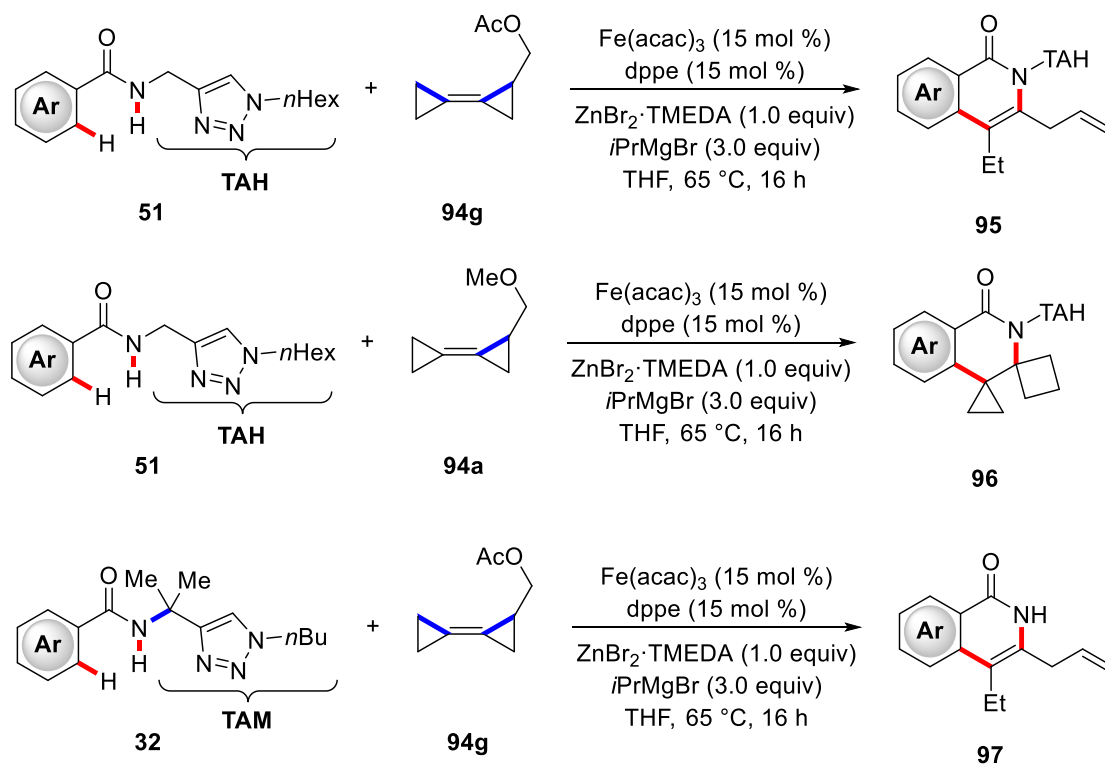


**Scheme 4.2** Iron-catalyzed C–H/N–H redox-neutral annulations with alkynes **91**.

In the third project, the merger of C–H activation and C–C cleavage by iron catalysis was achieved by the application of BCPs **94** (Scheme 4.3). Salient features of this novel transformation include 1) first iron-catalyzed C–H/C–C

## 4. Summary and Outlook

functionalizations, 2) the use of BCP derivatives **94** as coupling partners, 3) oxidant-free catalysis avoiding harsh conditions, 4) selective C–C cleavage enable divers product formation, and 5) a mono-selective C–F/C–H activation sequence of trifluoromethylarenes.



**Scheme 4.3** Iron-catalyzed C–H/C–C activation with BCPs **94**.

## 5. Experimental Part

### 5.1 General Remarks

All reactions involving moisture- or air-sensitive reagents or products were performed under an inert atmosphere of nitrogen using pre-dried glassware and standard Schlenk techniques. If not otherwise noted yields refer to isolated compounds, estimated to be >95% pure as determined by  $^1\text{H}$  NMR and GC analysis.

#### Vacuum

A Vacuubrand RZ 6 vacuum pump was used throughout the course of this thesis. The pressure was measured to be 0.7 mbar (uncorrected value).

#### Melting Points

Melting points were measured on a Stuart® Melting Point Apparatus SMP3 from Barloworld Scientific. Values are uncorrected.

#### Chromatography

Analytical thin layer chromatography (TLC) was performed on silica gel 60 F254 aluminum sheets from MERCK. Plates were either visualized under irradiation at 254 nm or 365 nm or developed by treatment with a potassium permanganate solution followed by careful warming. Chromatographic purification was accomplished by flash column chromatography on MERCK Geduran® silica gel, grade 60 (40–63  $\mu\text{m}$ , 70–230 mesh ASTM).

#### Gas Chromatography

Monitoring of reaction process *via* gas chromatography or coupled gas chromatography-mass spectrometry was performed using a 7890 GC-system with/without mass detector 5975C (Triple-Axis-Detector) or a 7890B GC-system coupled with a 5977A mass detector, both from Agilent Technologies®.

## 5. Experimental Part

### Infrared Spectroscopy

Infrared (IR) spectra were recorded using a Bruker® Alpha-P ATR spectrometer. Liquid samples were measured as film and solid samples neat. Spectra were recorded in the range from 4000 to 400  $\text{cm}^{-1}$ . Analysis of the spectral data were carried out using Opus 6. Absorption is given in wave numbers ( $\text{cm}^{-1}$ ).

### Nuclear Magnetic Resonance Spectroscopy

Nuclear magnetic resonance (NMR) spectra were recorded on Mercury Plus 300, VNMRs 300, Inova 500 and 600 from Varian®, or Avance 300, Avance III 300 and 400, Avance III HD 400 and 500 from Bruker®. Chemical shifts are reported in  $\delta$ -values in ppm relative to the residual proton peak or carbon peak of the deuterated solvent.

Solvent	$^1\text{H}$ NMR	$^{13}\text{C}$ NMR
$\text{CDCl}_3$	7.26	77.16
$\text{C}_6\text{D}_6$	7.16	128.06

The following abbreviations are used to describe the observed multiplicities: s (singlet), d (doublet), t (triplet), q (quartet), p (pentet), h (hexet), hept (heptet), m (multiplet) or analogous representations. The coupling constants  $J$  are reported in Hertz (Hz). Analysis of the recorded spectra was carried out using MestReNova 10 software.

### Mass Spectrometry

Electron ionization (EI) and EI high resolution mass spectra (HRMS) were measured on a time-of-flight mass spectrometer AccuTOF from JOEL. Electrospray ionization (ESI) mass spectra were recorded on an Io-Trap mass spectrometer LCQ from Finnigan, a quadrupole time-of-flight maXis from Bruker Daltonic or on a time-of-flight mass spectrometer microTOF from Bruker

## 5. Experimental Part

Daltonic. ESI-HRMS spectra were recorded on a Bruker Apex IV or Bruker Daltonic 7T, fourier transform ion cyclotron resonance (FTICR) mass spectrometer. The ratios of mass to charge ( $m/z$ ) are indicated, intensities relative to the base peak ( $I = 100$ ) are given in parentheses.

### Electrocatalysis

Electrocatalysis was conducted using an AXIOMET AX-3003P potentiostat in constant current mode.

### Mössbauer Spectroscopy

Mössbauer spectra were recorded with a  $^{57}\text{Co}$  source in a Rh matrix using an alternating constant acceleration *Wissel* Mössbauer spectrometer operated in the transmission mode and equipped with a *Janis* closed-cycle helium cryostat. Isomer shifts are given relative to iron metal at ambient temperature. Simulation of the experimental data was performed with the *Mfit* program<sup>[95]</sup> using *Lorentzian* line doublets.

### Solvents

Solvents for column chromatography were purified via distillation under reduced pressure prior to their use. All solvents for reactions involving moisture-sensitive reagents were dried, distilled and stored under inert atmosphere (Ar or  $\text{N}_2$ ) according to following standard procedures:

Purified by solvent purification system (SPS-800, M. Braun):  $\text{CH}_2\text{Cl}_2$ , toluene, tetrahydrofurane, dimethylformamide, diethylether.

Dried and distilled over sodium/benzophenone: 1,4-dioxane, DME, 2-MeTHF.

Dried and distilled over  $\text{CaH}_2$ : 1,2-dichloroethane

### Chemicals

Chemicals obtained from commercial sources with a purity  $>95\%$  were used as received without further purification. Stainless steel electrodes (Type 304, 10 mm  $\times$  15 mm  $\times$  0.25 mm; obtained from abcr, Germany) and RVC electrodes (5 mm  $\times$  10 mm  $\times$  6 mm, SIGRACELL® GFA 6 EA, obtained from SGL Carbon, Wiesbaden, Germany) were connected using stainless steel

## 5. Experimental Part

adapters. The following compounds were known from the literature and were synthesized according to the previously known methods:

TAH- and TAM- benzamides **51** and **32**,<sup>[45, 53, 61]</sup> allenyl acetates **88**,<sup>[96]</sup>  
<sup>57</sup>FeCl<sub>2</sub>,<sup>[97]</sup> propargyl acetates **91**,<sup>[98]</sup> cyclopropylidenecyclohexane **117**,<sup>[99]</sup>  
permethylated bicyclopropylidene **118**,<sup>[100]</sup> BCP derivatives **94a–94g**,<sup>[101]</sup>  
(Methylenecyclopropyl)methylacetate **94k–94l**,<sup>[102]</sup> 4-  
methylenespiropentylacetate **94m**.<sup>[103]</sup>

## 5. Experimental Part

### 5.2 General Procedures

#### General Procedure A (GPA): Iron-Catalyzed C–H/N–H Allene Annulation

To a stirred solution of **51/32** (0.30 mmol), ZnBr<sub>2</sub>·TMEDA (206 mg, 0.60 mmol) and dppe (17.9 mg, 15 mol %) in THF (0.20 mL), *i*PrMgBr (3.0 M in 2-MeTHF, 300 µL, 0.90 mmol) was added in one portion and the reaction mixture was stirred for 5 min at ambient temperature. Fe(acac)<sub>3</sub> (15.9 mg, 15 mol %) was added in a single portion. After stirring the solution for additional 5 min, allene **88** (0.90 mmol, 3.0 equiv) was added as a solution in THF (0.20 mL) in one portion. The mixture was placed in a pre-heated oil bath at 65 °C. After stirring for 16 h, sat. aqueous NH<sub>4</sub>Cl (2.0 mL) was added to the reaction mixture, which was then extracted with CH<sub>2</sub>Cl<sub>2</sub> (3 × 15 mL). The combined organic extracts were dried over Na<sub>2</sub>SO<sub>4</sub>, filtered and concentrated. The crude product was purified by column chromatography on silica gel to afford the desired product **89/90**.

#### General Procedure A' (GPA'): Iron-Catalyzed C–H/N–H Allene Annulation

To a stirred solution of **51/32** (0.30 mmol), ZnBr<sub>2</sub>·TMEDA (206 mg, 0.60 mmol) and dppe (17.9 mg, 15 mol %) in THF (0.20 mL), *i*PrMgBr (3.0 M in 2-MeTHF, 300 µL, 0.90 mmol) was added in one portion and the reaction mixture was stirred for 5 min at ambient temperature. Fe(acac)<sub>3</sub> (15.9 mg, 15 mol %), THF (0.20 mL), allene **88** (0.90 mmol, 3.0 equiv) was added to the mixture at the same time. The resulting mixture was placed in a pre-heated oil bath at 65 °C. After stirring for 16 h, sat. aqueous NH<sub>4</sub>Cl (2.0 mL) was added to the reaction mixture, which was then extracted with CH<sub>2</sub>Cl<sub>2</sub> (3 × 15 mL). The combined organic extracts were dried over Na<sub>2</sub>SO<sub>4</sub>, filtered and concentrated. The crude product was purified by column chromatography on silica gel to afford the desired product **89/90**.

## 5. Experimental Part

### General Procedure B (GPB): Iron-Catalyzed C–H/N–H Alkyne Annulation

To a stirred solution of **51** (0.30 mmol), ZnBr<sub>2</sub>·TMEDA (205 mg, 0.60 mmol) and dppe (17.9 mg, 15 mol %) in THF (0.40 mL), *i*PrMgBr (3.0 M in 2-MeTHF, 300 µL, 0.90 mmol) was added in one portion and the reaction mixture was stirred for 5 min at ambient temperature. Then, Fe(acac)<sub>2</sub> (5.7 mg, 15 mol %) was added in a single portion. After stirring the solution for additional 5 min, alkyne **91** (0.90 mmol, 3.0 equiv) was added as a solution in THF (0.40 mL). Then, the mixture was stirred at ambient temperature. After stirring for 16 h, sat. aqueous NH<sub>4</sub>Cl (3.0 mL) was added to the reaction mixture, which was extracted with CH<sub>2</sub>Cl<sub>2</sub> (3 × 15 mL). The combined organic extracts were dried over Na<sub>2</sub>SO<sub>4</sub>, filtered and concentrated under reduced pressure. The crude product was purified by column chromatography on silica gel to afford the desired product **92**.

### General Procedure C (GPC): Iron-Catalyzed C–H/C–C Activation

To a stirred solution of **51/32** (0.30 mmol), ZnBr<sub>2</sub>·TMEDA (206 mg, 0.60 mmol) and dppe (17.9 mg, 15 mol %) in THF (0.20 mL), *i*PrMgBr (3.0 M in 2-MeTHF, 300 µL, 0.90 mmol) was added in one portion and the reaction mixture was stirred for 5 min at ambient temperature. Fe(acac)<sub>3</sub> (15.9 mg, 15 mol %) was added in a single portion. After stirring the solution for additional 5 min, BCP **94** (0.90 mmol, 3.0 equiv) was added as a solution in THF (0.20 mL) in one portion. The mixture was placed in a pre-heated oil bath at 65 °C. After stirring for 16 h, sat. aqueous NH<sub>4</sub>Cl (2.0 mL) was added to the reaction mixture, which was then extracted with CH<sub>2</sub>Cl<sub>2</sub> (3 × 15 mL). The combined organic extracts were dried over Na<sub>2</sub>SO<sub>4</sub>, filtered and concentrated. The crude product was purified by column chromatography on silica gel to afford the desired product **95/96/97**.

## 5. Experimental Part

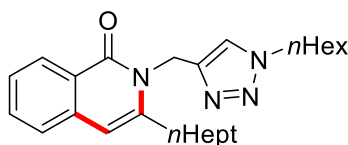
### General Procedure D (GPD): Electrochemical Removal of TAH Group

The electrochemical removal of the TAH group was carried out in an undivided cell with RVC anode (10 mm × 5 mm × 6 mm) and a steel cathode (20 mm × 10 mm × 0.25 mm). To a stirred solution of isoquinolone **92/96** (0.3 mmol) and ZnBr<sub>2</sub>·TMEDA (150 mg, 0.44 mmol) in THF (2.0 mL), *i*PrMgBr (3.0 M in 2-MeTHF, 220 μL, 0.66 mmol) was added in one portion. The electrocatalysis was performed at 60 °C with a constant current of 10.0 mA maintained for 15 h. Then, the mixture was allowed to cool to ambient temperature, and saturated aq. NH<sub>4</sub>Cl (3.0 mL) was added. The RVC anode was washed with CH<sub>2</sub>Cl<sub>2</sub> (3 × 10 mL) in an ultrasonic bath. The combined aqueous phases were extracted with CH<sub>2</sub>Cl<sub>2</sub> (3 × 15 mL), dried over Na<sub>2</sub>SO<sub>4</sub>, filtered and concentrated under reduced pressure. Purification by column chromatography (*n*hexane/EtOAc = 3/2) yielded **93/120**.

### 5.3 Iron-Catalyzed C–H/N–H Annulation with Allenes

#### 5.3.1 Analytical Data – Products with Different N-Substituted Triazolyl Moieties

##### 3-*n*-Heptyl-2-[(1-*n*-hexyl-1*H*-1,2,3-triazol-4-yl)methyl]isoquinolin-1(2*H*)-one(89aa)

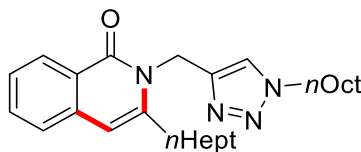


The general procedure **GPA** was followed using **51a** (85.9 mg, 0.30 mmol) and allene **88a** (164 mg, 0.90 mmol). Purification by column chromatography (*n*hexane/EtOAc = 4/1) yielded **89aa** (112 mg, 91%) as white solid.

**M.p.** = 76–78 °C. **<sup>1</sup>H NMR** (600 MHz, CDCl<sub>3</sub>): δ = 8.35 (d, *J* = 8.0 Hz, 1H), 7.70 (s, 1H), 7.60–7.56 (m, 1H), 7.43–7.38 (m, 2H), 6.34 (s, 1H), 5.38 (s, 2H), 4.24 (t, *J* = 7.3 Hz, 2H), 2.98 (t, *J* = 7.7 Hz, 2H), 1.86–1.80 (m, 2H), 1.71 (dt, *J* = 15.4, 7.7 Hz, 2H), 1.48 (dt, *J* = 15.4, 7.3 Hz, 2H), 1.40–1.34 (m, 2H), 1.32–1.23 (m, 10H), 0.89 (t, *J* = 6.9 Hz, 3H), 0.83 (t, *J* = 7.0 Hz, 3H). **<sup>13</sup>C NMR** (126 MHz, CDCl<sub>3</sub>): δ = 163.3 (C<sub>q</sub>), 144.1 (C<sub>q</sub>), 143.6 (C<sub>q</sub>), 136.9 (C<sub>q</sub>), 132.3 (CH), 127.7 (CH), 125.9 (CH), 125.4 (CH), 124.3 (C<sub>q</sub>), 123.8 (CH), 105.2 (CH), 50.5 (CH<sub>2</sub>), 39.2 (CH<sub>2</sub>), 33.2 (CH<sub>2</sub>), 31.9 (CH<sub>2</sub>), 31.3 (CH<sub>2</sub>), 30.3 (CH<sub>2</sub>), 29.4 (CH<sub>2</sub>), 29.3 (CH<sub>2</sub>), 28.9 (CH<sub>2</sub>), 26.3 (CH<sub>2</sub>), 22.8 (CH<sub>2</sub>), 22.6 (CH<sub>2</sub>), 14.3 (CH<sub>3</sub>), 14.1 (CH<sub>3</sub>). **IR** (ATR): 2926, 2853, 1643, 1618, 1593, 1413, 1052, 801, 756, 690 cm<sup>-1</sup>. **MS** (EI) *m/z* (relative intensity): 408 (70) [M]<sup>+</sup>, 337 (53), 324 (47), 295 (63), 242 (48), 172 (39), 159 (91), 43 (100). **HR-MS** (EI) *m/z* calcd for C<sub>25</sub>H<sub>36</sub>N<sub>4</sub>O [M]<sup>+</sup> 408.2889, found 408.2879.

## 5. Experimental Part

### 3-*n*-Heptyl-2-[(1-*n*-octyl-1*H*-1,2,3-triazol-4-yl)methyl]isoquinolin-1(2*H*)-one (89ba)

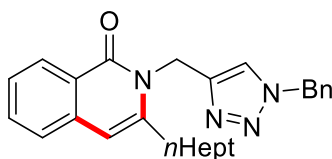


The general procedure **GPA** was followed using **51b** (94.3 mg, 0.30 mmol) and allene **88a** (164 mg, 0.90 mmol). Purification by column chromatography (*n*hexane/EtOAc = 3/1) yielded **89ba** (107 mg, 82%) as white solid.

**M.p.** = 56–57 °C. **<sup>1</sup>H NMR** (600 MHz, CDCl<sub>3</sub>): δ = 8.33 (dd, *J* = 8.1, 1.2 Hz, 1H), 7.70 (s, 1H), 7.56 (ddd, *J* = 8.1, 7.0, 1.3 Hz, 1H), 7.42–7.35 (m, 2H), 6.33 (s, 1H), 5.36 (s, 2H), 4.23 (t, *J* = 7.8 Hz, 2H), 2.96 (t, *J* = 7.8 Hz, 2H), 1.90–1.78 (m, 2H), 1.73–1.67 (m, 2H), 1.54–1.42 (m, 2H), 1.38–1.31 (m, 2H), 1.30–1.26 (m, 4H), 1.25–1.18 (m, 10H), 0.87 (t, *J* = 7.0 Hz, 3H), 0.83 (t, *J* = 7.1 Hz, 3H). **<sup>13</sup>C NMR** (126 MHz, CDCl<sub>3</sub>): δ = 163.2 (C<sub>q</sub>), 144.0 (C<sub>q</sub>), 143.6 (C<sub>q</sub>), 136.9 (C<sub>q</sub>), 132.3 (CH), 127.6 (CH), 125.9 (CH), 125.4 (CH), 124.2 (C<sub>q</sub>), 123.7 (CH), 105.1 (CH), 50.5 (CH<sub>2</sub>), 39.2 (CH<sub>2</sub>), 33.1 (CH<sub>2</sub>), 31.9 (CH<sub>2</sub>), 31.8 (CH<sub>2</sub>), 30.3 (CH<sub>2</sub>), 29.4 (CH<sub>2</sub>), 29.3 (CH<sub>2</sub>), 29.1 (CH<sub>2</sub>), 29.0 (CH<sub>2</sub>), 28.9 (CH<sub>2</sub>), 26.6 (CH<sub>2</sub>), 22.8 (CH<sub>2</sub>), 22.7 (CH<sub>2</sub>), 14.2 (CH<sub>3</sub>), 14.2 (CH<sub>3</sub>). **IR** (ATR): 2954, 2918, 2852, 1648, 1592, 1461, 1337, 1169, 1048, 723 cm<sup>-1</sup>. **MS** (EI) *m/z* (relative intensity): 436 (75) [M]<sup>+</sup>, 365 (47), 352 (40), 242 (43), 159 (100). **HR-MS** (EI) *m/z* calcd for C<sub>27</sub>H<sub>40</sub>N<sub>4</sub>O [M]<sup>+</sup> 436.3202, found 436.3208.

## 5. Experimental Part

### 2-[(1-Benzyl-1*H*-1,2,3-triazol-4-yl)methyl]-3-*n*-heptylisoquinolin-1(2*H*)-one (89ca)

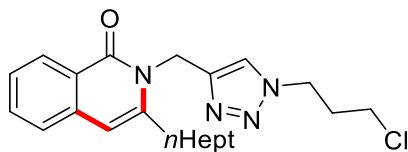


The general procedure **GPA** was followed using **51c** (87.7 mg, 0.30 mmol) and allene **88a** (164 mg, 0.90 mmol). Purification by column chromatography (*n*hexane/EtOAc = 3/1) yielded **89ca** (99.5 mg, 80%) as white solid.

**M.p.** = 96–97 °C. **<sup>1</sup>H NMR** (300 MHz, CDCl<sub>3</sub>):  $\delta$  = 8.32 (dd,  $J$  = 8.1, 1.3 Hz, 1H), 7.68 (s, 1H), 7.58 (ddd,  $J$  = 8.1, 7.1, 1.3 Hz, 1H), 7.46–7.39 (m, 2H), 7.39–7.32 (m, 3H), 7.30–7.25 (m, 2H), 6.34 (s, 1H), 5.43 (s, 2H), 5.36 (s, 2H), 2.98 (t,  $J$  = 7.8 Hz, 2H), 1.78–1.65 (m, 2H), 1.58–1.40 (m, 2H), 1.40–1.27 (m, 6H), 0.91 (t,  $J$  = 6.9 Hz, 3H). **<sup>13</sup>C NMR** (75 MHz, CDCl<sub>3</sub>):  $\delta$  = 163.4 (C<sub>q</sub>), 144.6 (C<sub>q</sub>), 143.6 (C<sub>q</sub>), 137.0 (C<sub>q</sub>), 134.6 (C<sub>q</sub>), 132.4 (CH), 129.2 (CH), 128.8 (CH), 128.2 (CH), 127.7 (CH), 126.0 (CH), 125.5 (CH), 124.2 (C<sub>q</sub>), 124.0 (CH), 105.2 (CH), 54.3 (CH<sub>2</sub>), 39.1 (CH<sub>2</sub>), 33.1 (CH<sub>2</sub>), 31.9 (CH<sub>2</sub>), 29.4 (CH<sub>2</sub>), 29.3 (CH<sub>2</sub>), 28.8 (CH<sub>2</sub>), 22.8 (CH<sub>2</sub>), 14.2 (CH<sub>3</sub>). **IR** (ATR): 2956, 2919, 2853, 1646, 1622, 1455, 1050, 728, 710, 693 cm<sup>-1</sup>. **MS** (EI)  $m/z$  (relative intensity): 414 (26) [M]<sup>+</sup>, 295 (26), 242 (15), 159 (30), 91(100). **HR-MS** (EI)  $m/z$  calcd for C<sub>26</sub>H<sub>30</sub>N<sub>4</sub>O [M]<sup>+</sup> 414.2420, found 414.2434.

## 5. Experimental Part

### 2-[[1-(2-Chloropropyl)-1*H*-1,2,3-triazol-4-yl]methyl]-3-heptylisoquinolin-1(2*H*)-one (**89da**)

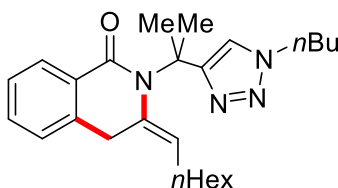


The general procedure **GPA** was followed using **51d** (83.6 mg, 0.30 mmol) and allene **88a** (164 mg, 0.90 mmol). Purification by column chromatography (*n*hexane/EtOAc = 3/1) yielded **89da** (82.8 mg, 69%) as white solid.

**M.p.** = 110–111 °C. **<sup>1</sup>H NMR** (300 MHz, CDCl<sub>3</sub>): δ = 8.32 (d, *J* = 8.0 Hz, 1H), 7.75 (s, 1H), 7.60–7.52 (m, 1H), 7.44–7.35 (m, 2H), 6.33 (s, 1H), 5.36 (s, 2H), 4.43 (t, *J* = 6.7 Hz, 2H), 3.47 (t, *J* = 6.1 Hz, 2H), 2.96 (t, *J* = 7.8 Hz, 2H), 2.38–2.18 (m, 2H), 1.78–1.64 (m, 2H), 1.51–1.43 (m, 2H), 1.39–1.32 (m, 2H), 1.31–1.26 (m, 4H), 0.87 (t, *J* = 6.8 Hz, 3H). **<sup>13</sup>C NMR** (75 MHz, CDCl<sub>3</sub>): δ = 163.4 (C<sub>q</sub>), 144.3 (C<sub>q</sub>), 143.6 (C<sub>q</sub>), 137.0 (C<sub>q</sub>), 132.5 (CH), 127.8 (CH), 126.1 (CH), 125.5 (CH), 124.6 (CH), 124.3 (C<sub>q</sub>), 105.3 (CH), 47.3 (CH<sub>2</sub>), 41.3 (CH<sub>2</sub>), 39.1 (CH<sub>2</sub>), 33.2 (CH<sub>2</sub>), 32.7 (CH<sub>2</sub>), 31.9 (CH<sub>2</sub>), 29.4 (CH<sub>2</sub>), 29.3 (CH<sub>2</sub>), 28.8 (CH<sub>2</sub>), 22.8 (CH<sub>2</sub>), 14.2 (CH<sub>3</sub>). **IR** (ATR): 2954, 2926, 2856, 1715, 1648, 1464, 1285, 1087, 799, 764 cm<sup>-1</sup>. **MS** (EI) *m/z* (relative intensity): 400 (57) [<sup>35</sup>Cl, M]<sup>+</sup>, 316 (37), 295 (86), 242 (66), 172 (46), 159 (100). **HR-MS** (ESI) *m/z* calcd for C<sub>22</sub>H<sub>30</sub><sup>35</sup>ClN<sub>4</sub>O [M+H]<sup>+</sup> 401.2103, found 401.2099.

## 5. Experimental Part

### (*E*)-2-[2-(1-*n*-Butyl-1*H*-1,2,3-triazol-4-yl)propan-2-yl]-3-heptylidene-3,4-dihydro-isoquinolin-1(2*H*)-one (**90aa**)

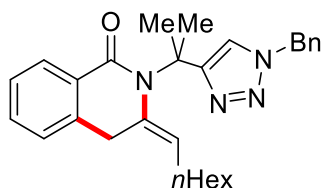


The general procedure **GPA** was followed using **32a** (85.9 mg, 0.30 mmol) and allene **88a** (164 mg, 0.90 mmol). Purification by column chromatography (*n*hexane/EtOAc = 3/1) yielded **90aa** (114 mg, 93%) as a colorless oil.

**<sup>1</sup>H NMR** (600 MHz, C<sub>6</sub>D<sub>6</sub>):  $\delta$  = 8.35 (dd,  $J$  = 7.6, 1.5 Hz, 1H), 7.49 (s, 1H), 7.05 (ddd,  $J$  = 7.5, 7.5, 1.5 Hz, 1H), 7.00 (ddd,  $J$  = 7.5, 7.5, 1.3 Hz, 1H), 6.84 (d,  $J$  = 7.2, 1H), 5.54 (t,  $J$  = 7.8, 1H), 3.69 (t,  $J$  = 7.3 Hz, 2H), 3.42 (s, 2H), 2.13 (s, 6H), 1.88 (dt,  $J$  = 7.3 Hz, 2H), 1.40–1.33 (m, 2H), 1.22–1.07 (m, 8H), 1.00–0.91 (m, 2H), 0.83 (t,  $J$  = 7.2 Hz, 3H), 0.63 (t,  $J$  = 7.4 Hz, 3H). **<sup>13</sup>C NMR** (126 MHz, C<sub>6</sub>D<sub>6</sub>):  $\delta$  = 164.7 (C<sub>q</sub>), 153.7 (C<sub>q</sub>), 139.0 (C<sub>q</sub>), 135.6 (C<sub>q</sub>), 131.6 (CH), 131.5 (C<sub>q</sub>), 129.1 (CH), 126.8 (CH), 126.4 (CH), 123.1 (CH), 121.9 (CH), 58.0 (C<sub>q</sub>), 49.7 (CH<sub>2</sub>), 32.9 (CH<sub>2</sub>), 32.5 (CH<sub>2</sub>), 32.1 (CH<sub>2</sub>), 30.2 (CH<sub>2</sub>), 30.0 (CH<sub>3</sub>), 29.5 (CH<sub>2</sub>), 27.6 (CH<sub>2</sub>), 23.1 (CH<sub>2</sub>), 20.1 (CH<sub>2</sub>), 14.5 (CH<sub>3</sub>), 13.7 (CH<sub>3</sub>). **IR** (ATR): 2956, 2927, 2856, 1649, 1457, 1375, 1323, 1169, 1046, 737 cm<sup>-1</sup>. **MS** (EI)  $m/z$  (relative intensity): 408 (6) [M]<sup>+</sup>, 323 (12), 243 (16), 172 (35), 166 (100), 172 (51), 57 (55). **HR-MS** (EI)  $m/z$  calcd for C<sub>25</sub>H<sub>36</sub>N<sub>4</sub>O [M]<sup>+</sup> 408.2889, found 408.2893.

## 5. Experimental Part

### ***E***-2-[2-(1-Benzyl-1*H*-1,2,3-triazol-4-yl)propan-2-yl]-3-hept-1-ylidene-3,4-dihydro-isoquinolin-1(2*H*)-one (**90ba**)

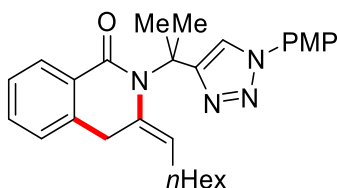


The general procedure **GPA** was followed using **32b** (96.1 mg, 0.30 mmol) and allene **88a** (164 mg, 0.90 mmol). Purification by column chromatography (*n*hexane/EtOAc = 3/1) yielded **90ba** (100 mg, 76%) as colorless oil.

**<sup>1</sup>H NMR** (600 MHz, C<sub>6</sub>D<sub>6</sub>):  $\delta$  = 8.34 (dd,  $J$  = 7.7, 1.5 Hz, 1H), 7.45 (s, 1H), 7.03 (ddd,  $J$  = 7.4, 7.4, 1.5 Hz, 1H), 7.01–6.96 (m, 4H), 6.90 (dd,  $J$  = 7.9, 1.6 Hz, 2H), 6.82 (d,  $J$  = 7.7 Hz, 1H), 5.51 (t,  $J$  = 7.7 Hz, 1H), 4.86 (s, 2H), 3.40 (s, 2H), 2.04 (s, 6H), 1.85 (dt,  $J$  = 7.2 Hz, 2H), 1.20–1.08 (m, 8H), 0.84 (t,  $J$  = 7.2 Hz, 3H). **<sup>13</sup>C NMR** (126 MHz, C<sub>6</sub>D<sub>6</sub>):  $\delta$  = 164.7 (C<sub>q</sub>), 154.4 (C<sub>q</sub>), 139.0 (C<sub>q</sub>), 136.1 (C<sub>q</sub>), 135.5 (C<sub>q</sub>), 131.5 (CH), 131.5 (C<sub>q</sub>), 129.1 (CH), 129.0 (CH), 128.4 (CH), 128.0 (CH), 126.9 (CH), 126.3 (CH), 123.1 (CH), 121.9 (CH), 58.0 (C<sub>q</sub>), 53.6 (CH<sub>2</sub>), 32.8 (CH<sub>2</sub>), 32.1 (CH<sub>2</sub>), 30.1 (CH<sub>2</sub>), 29.8 (CH<sub>3</sub>), 29.5 (CH<sub>2</sub>), 27.5 (CH<sub>2</sub>), 23.1 (CH<sub>2</sub>), 14.5 (CH<sub>3</sub>). **IR** (ATR): 2926, 2854, 1647, 1456, 1374, 1323, 1169, 1046, 733, 499 cm<sup>-1</sup>. **MS** (ESI)  $m/z$  (relative intensity): 907 (100) [2M+Na]<sup>+</sup>, 465 (47) [M+Na]<sup>+</sup>, 443 (48) [M+H]<sup>+</sup>, 200 (50). **HR-MS** (ESI)  $m/z$  calcd for C<sub>28</sub>H<sub>35</sub>N<sub>4</sub>O [M+H]<sup>+</sup> 443.2805, found 443.2803.

## 5. Experimental Part

### (*E*)-3-Hept-1-ylidene-2-[2-{1-(4-methoxyphenyl)-1*H*-1,2,3-triazol-4-yl}prop- an-2-yl]-3,4-dihydroisoquinolin-1(2*H*)-one (**90ca**)



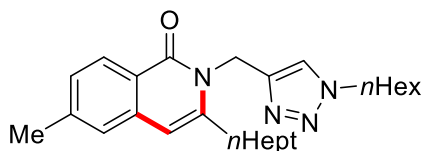
The general procedure **GPA** was followed using **32c** (101 mg, 0.30 mmol) and allene **88a** (164 mg, 0.90 mmol). Purification by column chromatography (*n*hexane/EtOAc = 3/1) yielded **90ca** (100 mg, 73%) as colorless oil.

**<sup>1</sup>H NMR** (300 MHz, C<sub>6</sub>D<sub>6</sub>):  $\delta$  = 8.39 (dd, *J* = 7.6, 1.7 Hz, 1H), 7.97 (s, 1H), 7.33 (d, *J* = 9.0 Hz, 2H), 7.10–6.94 (m, 2H), 6.90–6.78 (m, 1H), 6.64–6.49 (m, 2H), 5.55 (t, *J* = 8.1 Hz, 1H), 3.44 (s, 2H), 3.20 (s, 3H), 2.18 (s, 6H), 1.86 (t, *J* = 7.2 Hz, 2H), 1.23–1.05 (m, 8H), 0.83 (t, *J* = 6.9 Hz, 3H). **<sup>13</sup>C NMR** (75 MHz, C<sub>6</sub>D<sub>6</sub>):  $\delta$  = 164.9 (C<sub>q</sub>), 159.6 (C<sub>q</sub>), 154.5 (C<sub>q</sub>), 139.0 (C<sub>q</sub>), 135.5 (C<sub>q</sub>), 131.6 (CH), 131.4 (C<sub>q</sub>), 131.3 (C<sub>q</sub>), 129.2 (CH), 126.9 (CH), 126.4 (CH), 123.2 (CH), 122.1 (CH), 120.3 (CH), 114.7 (CH), 57.9 (C<sub>q</sub>), 55.0 (CH<sub>3</sub>), 32.7 (CH<sub>2</sub>), 32.0 (CH<sub>2</sub>), 30.0 (CH<sub>2</sub>), 29.7 (CH<sub>3</sub>), 29.4 (CH<sub>2</sub>), 27.5 (CH<sub>2</sub>), 23.0 (CH<sub>2</sub>), 14.3 (CH<sub>3</sub>). **IR** (ATR): 2928, 2855, 2167, 1648, 1516, 1252, 1172, 1038, 735, 499 cm<sup>-1</sup>. **MS** (EI) *m/z* (relative intensity): 458 (5) [M]<sup>+</sup>, 415 (13), 373 (12), 216 (41), 188 (100), 172 (51). **HR-MS** (EI) *m/z* calcd for C<sub>28</sub>H<sub>34</sub>N<sub>4</sub>O<sub>2</sub> [M]<sup>+</sup> 458.2682, found 458.2670.

## 5. Experimental Part

### 5.3.2 Analytical Data – Products 89

#### 3-*n*-Heptyl-2-[(1-*n*-hexyl-1*H*-1,2,3-triazol-4-yl)methyl]-6-methylisoquinolin-1(2*H*)-one (89ea)

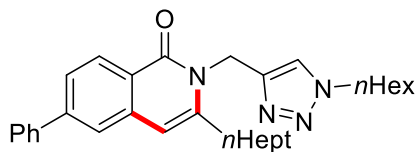


The general procedure **GPA** was followed using **51e** (90.1 mg, 0.30 mmol) and allene **88a** (164 mg, 0.90 mmol). Purification by column chromatography (*n*hexane/EtOAc = 3/1) yielded **89ea** (101 mg, 80%) as white solid.

**M. p.** = 71–72 °C. **<sup>1</sup>H NMR** (600 MHz, CDCl<sub>3</sub>): δ = 8.21 (d, *J* = 8.1 Hz, 1H), 7.68 (s, 1H), 7.20 (dd, *J* = 8.1, 1.7 Hz 1H), 7.18 (s, 1H), 6.26 (s, 1H), 5.35 (s, 2H), 4.40–4.08 (m, 2H), 3.03–2.82 (m, 2H), 2.41 (s, 3H), 1.90–1.75 (m, 2H), 1.71–1.65 (m, 2H), 1.48–1.42 (m, 2H), 1.38–1.32 (m, 2H), 1.31–1.26 (m, 4H), 1.26–1.22 (m, 6H), 0.87 (t, *J* = 7.0 Hz, 3H), 0.82 (t, *J* = 6.9 Hz, 3H). **<sup>13</sup>C NMR** (126 MHz, CDCl<sub>3</sub>): δ = 163.2 (C<sub>q</sub>), 144.2 (C<sub>q</sub>), 143.5 (C<sub>q</sub>), 142.8 (C<sub>q</sub>), 137.0 (C<sub>q</sub>), 127.6 (CH), 127.6 (CH), 125.0 (CH), 123.7 (CH), 122.0 (C<sub>q</sub>), 105.0 (CH), 50.4 (CH<sub>2</sub>), 39.1 (CH<sub>2</sub>), 33.1 (CH<sub>2</sub>), 31.9 (CH<sub>2</sub>), 31.2 (CH<sub>2</sub>), 30.2 (CH<sub>2</sub>), 29.4 (CH<sub>2</sub>), 29.3 (CH<sub>2</sub>), 28.9 (CH<sub>2</sub>), 26.3 (CH<sub>2</sub>), 22.8 (CH<sub>2</sub>), 22.5 (CH<sub>2</sub>), 21.9 (CH<sub>3</sub>), 14.2 (CH<sub>3</sub>), 14.0 (CH<sub>3</sub>). **IR** (ATR): 2927, 2856, 1649, 1625, 1601, 1264, 1046, 788, 735, 702 cm<sup>-1</sup>. **MS** (ESI) *m/z* (relative intensity): 445 (100) [M+Na]<sup>+</sup>, 423 (45) [M+H]<sup>+</sup>, 399 (5), 377 (15). **HR-MS** (ESI) *m/z* calcd for C<sub>26</sub>H<sub>39</sub>N<sub>4</sub>O [M+H]<sup>+</sup> 423.3118, found 423.3118.

## 5. Experimental Part

### 3-*n*-Heptyl-2-[(1-*n*-hexyl-1*H*-1,2,3-triazol-4-yl)methyl]-6-phenylisoquinolin-1(2*H*)-one (**89fa**)

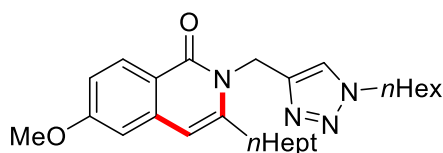


The general procedure **GPA** was followed using **51f** (109 mg, 0.30 mmol) and allene **88a** (164 mg, 0.90 mmol). Purification by column chromatography (*n*hexane/EtOAc = 3/1) yielded **89fa** (102 mg, 70%) as white solid.

**M.p.** = 95–96 °C. **<sup>1</sup>H NMR** (300 MHz, CDCl<sub>3</sub>): δ = 8.41 (d, *J* = 8.2 Hz, 1H), 7.72 (s, 1H), 7.69–7.60 (m, 4H), 7.52–7.37 (m, 3H), 6.41 (s, 1H), 5.40 (s, 2H), 4.26 (t, *J* = 7.5 Hz, 2H), 3.00 (t, *J* = 7.8 Hz, 2H), 1.90–1.83 (m, 2H), 1.77–1.70 (m, 2H), 1.55–1.46 (m, 2H), 1.41–1.35 (m, 2H), 1.34–1.24 (m, 10H), 0.90 (t, *J* = 7.2 Hz, 3H), 0.85 (t, *J* = 6.9 Hz, 3H). **<sup>13</sup>C NMR** (75 MHz, CDCl<sub>3</sub>): δ = 163.3 (C<sub>q</sub>), 145.2 (C<sub>q</sub>), 144.2 (C<sub>q</sub>), 144.1 (C<sub>q</sub>), 140.4 (C<sub>q</sub>), 137.4 (C<sub>q</sub>), 129.0 (CH), 128.4 (CH), 128.2 (CH), 127.5 (CH), 125.3 (CH), 123.9 (CH), 123.7 (CH), 123.2 (C<sub>q</sub>), 105.4 (CH), 50.5 (CH<sub>2</sub>), 39.1 (CH<sub>2</sub>), 33.2 (CH<sub>2</sub>), 31.9 (CH<sub>2</sub>), 31.2 (CH<sub>2</sub>), 30.3 (CH<sub>2</sub>), 29.4 (CH<sub>2</sub>), 29.3 (CH<sub>2</sub>), 28.8 (CH<sub>2</sub>), 26.3 (CH<sub>2</sub>), 22.8 (CH<sub>2</sub>), 22.5 (CH<sub>2</sub>), 14.2 (CH<sub>3</sub>), 14.0 (CH<sub>3</sub>). **IR** (ATR): 2925, 2855, 1647, 1622, 1598, 1422, 1044, 757, 697 cm<sup>-1</sup>. **MS** (EI) *m/z* (relative intensity): 484 (86) [M]<sup>+</sup>, 413 (36), 371 (57), 318 (50), 235 (61), 225 (44), 43 (100). **HR-MS** (ESI) *m/z* calcd C<sub>31</sub>H<sub>41</sub>N<sub>4</sub>O [M+H]<sup>+</sup> 485.3275, found 485.3267.

## 5. Experimental Part

### 3-*n*-Heptyl-2-[(1-*n*-hexyl-1*H*-1,2,3-triazol-4-yl)methyl]-6-methoxyisoquinolin-1(2*H*)-one (89ga)

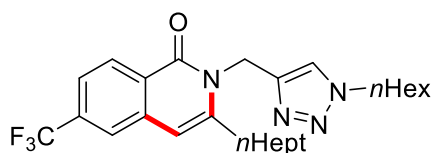


The general procedure **GPA** was followed using **51g** (94.9 mg, 0.30 mmol) and allene **88a** (164 mg, 0.90 mmol). Purification by column chromatography (*n*hexane/EtOAc = 3/1) yielded **89ga** (108 mg, 82%) as white solid.

**M.p.** = 62–63 °C. **<sup>1</sup>H NMR** (600 MHz, CDCl<sub>3</sub>): δ = 8.24 (d, *J* = 8.9 Hz, 1H), 7.69 (s, 1H), 6.97 (dd, *J* = 8.9, 2.5 Hz, 1H), 6.76 (d, *J* = 2.5 Hz, 1H), 6.26 (s, 1H), 5.34 (s, 2H), 4.23 (t, *J* = 7.5 Hz, 2H), 3.87 (s, 3H), 2.94 (t, *J* = 7.8 Hz, 2H), 1.86–1.79 (m, 2H), 1.73–1.65 (m, 2H), 1.50–1.43 (m, 2H), 1.39–1.33 (m, 2H), 1.32–1.27 (m, 4H), 1.27–1.22 (m, 6H), 0.88 (t, *J* = 6.9 Hz, 3H), 0.82 (t, *J* = 7.2 Hz, 3H). **<sup>13</sup>C NMR** (126 MHz, CDCl<sub>3</sub>): δ = 162.9 (C<sub>q</sub>), 162.8 (C<sub>q</sub>), 144.3 (C<sub>q</sub>), 144.2 (C<sub>q</sub>), 139.0 (C<sub>q</sub>), 129.7 (CH), 123.7 (CH), 118.2 (C<sub>q</sub>), 115.8 (CH), 106.0 (CH), 105.0 (CH), 55.6 (CH<sub>3</sub>), 50.5 (CH<sub>2</sub>), 39.0 (CH<sub>2</sub>), 33.2 (CH<sub>2</sub>), 31.9 (CH<sub>2</sub>), 31.3 (CH<sub>2</sub>), 30.3 (CH<sub>2</sub>), 29.4 (CH<sub>2</sub>), 29.3 (CH<sub>2</sub>), 28.9 (CH<sub>2</sub>), 26.3 (CH<sub>2</sub>), 22.8 (CH<sub>2</sub>), 22.5 (CH<sub>2</sub>), 14.3 (CH<sub>3</sub>), 14.1 (CH<sub>3</sub>). **IR** (ATR): 2953, 2925, 2855, 1648, 1619, 1596, 1250, 1168, 1028, 788 cm<sup>-1</sup>. **MS** (EI) *m/z* (relative intensity): 438 (96) [M]<sup>+</sup>, 367 (61), 325 (100), 272 (72), 202 (49), 189 (75). **HR-MS** (EI) *m/z* calcd for C<sub>26</sub>H<sub>38</sub>N<sub>4</sub>O<sub>2</sub> [M]<sup>+</sup> 438.2995, found 438.2996.

## 5. Experimental Part

### 3-*n*-Heptyl-2-[(1-*n*-hexyl-1*H*-1,2,3-triazol-4-yl)methyl]-6-(trifluoromethyl)-isoquinolin-1(2*H*)-one (**89ha**)

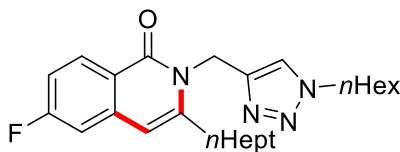


The general procedure **GPA** was followed using **51h** (106 mg, 0.30 mmol) and allene **88a** (164 mg, 0.90 mmol). Purification by column chromatography (*n*hexane/EtOAc = 3/1) yielded **89ha** (92.9 mg, 65%) as white solid.

**M.p.** = 114–116 °C. **<sup>1</sup>H NMR** (300 MHz, CDCl<sub>3</sub>): δ = 8.44 (dd, *J* = 8.4, 1.0 Hz, 1H), 7.74–7.68 (m, 2H), 7.58 (dd, *J* = 8.4, 1.7 Hz, 1H), 6.41 (s, 1H), 5.38 (s, 2H), 4.26 (t, *J* = 7.5 Hz, 2H), 3.03 (t, *J* = 7.8 Hz, 2H), 1.91–1.79 (m, 2H), 1.76–1.69 (m, 2H), 1.52–1.44 (m, 2H), 1.42–1.35 (m, 2H), 1.34–1.29 (m, 4H), 1.28–1.22 (m, 6H), 0.88 (t, *J* = 7.0 Hz, 3H), 0.84 (t, *J* = 7.0 Hz, 3H). **<sup>13</sup>C NMR** (75 MHz, CDCl<sub>3</sub>): δ = 162.6 (C<sub>q</sub>), 145.5 (C<sub>q</sub>), 143.6 (C<sub>q</sub>), 136.9 (C<sub>q</sub>), 134.0 (q, <sup>2</sup>*J*<sub>C-F</sub> = 32.4 Hz, C<sub>q</sub>), 128.9 (CH), 126.2 (C<sub>q</sub>), 123.9 (CH), 123.9 (q, <sup>1</sup>*J*<sub>C-F</sub> = 272.7 Hz, C<sub>q</sub>), 122.8 (q, <sup>3</sup>*J*<sub>C-F</sub> = 4.2 Hz, CH), 121.8 (q, <sup>3</sup>*J*<sub>C-F</sub> = 3.5 Hz, CH), 104.8 (CH), 50.5 (CH<sub>2</sub>), 39.3 (CH<sub>2</sub>), 33.2 (CH<sub>2</sub>), 31.9 (CH<sub>2</sub>), 31.2 (CH<sub>2</sub>), 30.2 (CH<sub>2</sub>), 29.3 (CH<sub>2</sub>), 29.3 (CH<sub>2</sub>), 28.7 (CH<sub>2</sub>), 26.2 (CH<sub>2</sub>), 22.8 (CH<sub>2</sub>), 22.5 (CH<sub>2</sub>), 14.2 (CH<sub>3</sub>), 14.0 (CH<sub>3</sub>). **<sup>19</sup>F NMR** (282 MHz, CDCl<sub>3</sub>): δ = –63.08 (s). **IR** (ATR): 2925, 2855, 1653, 1607, 1322, 1157, 1121, 1065, 796, 693 cm<sup>–1</sup>. **MS** (EI) *m/z* (relative intensity): 476 (73) [M]<sup>+</sup>, 405 (44), 392 (44), 227 (54), 167 (35), 138 (42), 43 (100). **HR-MS** (EI) *m/z* calcd for C<sub>26</sub>H<sub>35</sub>F<sub>3</sub>N<sub>4</sub>O [M]<sup>+</sup> 476.2763, found 476.2759.

## 5. Experimental Part

### 6-Fluoro-3-*n*-heptyl-2-[(1-*n*-hexyl-1*H*-1,2,3-triazol-4-yl)methyl]isoquinolin-1(2*H*)-one (**89ia**)

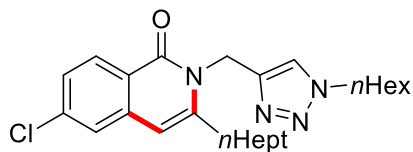


The general procedure **GPA** was followed using **51i** (91.3 mg, 0.30 mmol) and allene **88a** (164 mg, 0.90 mmol). Purification by column chromatography (*n*hexane/EtOAc = 3/1) yielded **89ia** (65.3 mg, 51%) as white solid.

**M.p.** = 57–58 °C. **<sup>1</sup>H NMR** (300 MHz, CDCl<sub>3</sub>): δ = 8.34 (dd, *J* = 8.9 Hz, 5.7 Hz, 1H), 7.70 (s, 1H), 7.15–6.95 (m, 2H), 6.28 (s, 1H), 5.35 (s, 2H), 4.25 (t, *J* = 7.4 Hz, 2H), 2.97 (t, *J* = 7.7 Hz, 2H), 1.95–1.77 (m, 2H), 1.77–1.61 (m, 2H), 1.53–1.42 (m, 2H), 1.40–1.34 (m, 2H), 1.32–1.23 (m, 10H), 0.83 (t, *J* = 7.5 Hz, 3H), 0.83 (t, *J* = 7.2 Hz, 3H). **<sup>13</sup>C NMR** (126 MHz, CDCl<sub>3</sub>): δ = 165.2 (d, <sup>1</sup>*J*<sub>C-F</sub> = 251.8 Hz, C<sub>q</sub>), 162.6 (C<sub>q</sub>), 145.2 (C<sub>q</sub>), 143.8 (C<sub>q</sub>), 139.1 (d, <sup>3</sup>*J*<sub>C-F</sub> = 10.5 Hz, C<sub>q</sub>), 130.9 (d, <sup>3</sup>*J*<sub>C-F</sub> = 10.1 Hz, CH), 123.7 (CH), 120.9 (d, <sup>4</sup>*J*<sub>C-F</sub> = 1.6 Hz, C<sub>q</sub>), 114.6 (d, <sup>2</sup>*J*<sub>C-F</sub> = 23.6 Hz, CH), 110.0 (d, <sup>2</sup>*J*<sub>C-F</sub> = 21.6 Hz, CH), 104.5 (CH), 50.5 (CH<sub>2</sub>), 39.1 (CH<sub>2</sub>), 33.2 (CH<sub>2</sub>), 31.9 (CH<sub>2</sub>), 31.2 (CH<sub>2</sub>), 30.3 (CH<sub>2</sub>), 29.4 (CH<sub>2</sub>), 29.3 (CH<sub>2</sub>), 28.8 (CH<sub>2</sub>), 26.3 (CH<sub>2</sub>), 22.8 (CH<sub>2</sub>), 22.5 (CH<sub>2</sub>), 14.3 (CH<sub>3</sub>), 14.0 (CH<sub>3</sub>). **<sup>19</sup>F NMR** (282 MHz, CDCl<sub>3</sub>): δ = -106.75 (ddd, *J* = 8.9, 8.9, 5.9 Hz). **IR** (ATR): 2927, 2857, 1645, 1623, 1604, 1446, 1249, 1154, 793, 474 cm<sup>-1</sup>. **MS** (ESI) *m/z* (relative intensity): 875 (100) [2M+Na]<sup>+</sup>, 449 (20) [M+Na]<sup>+</sup>, 427 (64) [M+H]<sup>+</sup>. **HR-MS** (ESI) *m/z* calcd for C<sub>25</sub>H<sub>36</sub>FN<sub>4</sub>O [M+H]<sup>+</sup> 427.2868, found 427.2869.

## 5. Experimental Part

### 6-Chloro-3-*n*-heptyl-2-[(1-*n*-hexyl-1*H*-1,2,3-triazol-4-yl)methyl]isoquinolin-1(2*H*)-one (**89ja**)

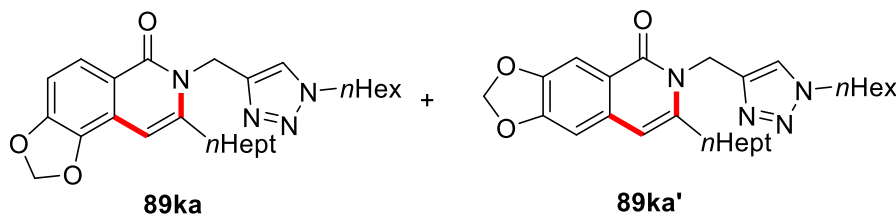


The general procedure **GPA** was followed using **51j** (96.2 mg, 0.30 mmol) and allene **88a** (164 mg, 0.90 mmol). Purification by column chromatography (*n*hexane/EtOAc = 3/1) yielded **89ja** (74.4 mg, 56%) as white solid.

**M.p.** = 58–59 °C. **<sup>1</sup>H NMR** (500 MHz, CDCl<sub>3</sub>): δ = 8.24 (d, *J* = 8.6 Hz, 1H), 7.69 (s, 1H), 7.38 (d, *J* = 2.0 Hz, 1H), 7.31 (dd, *J* = 8.6, 2.0 Hz, 1H), 6.25 (s, 1H), 5.34 (s, 2H), 4.24 (t, *J* = 7.4 Hz, 2H), 2.97 (t, *J* = 7.8 Hz, 2H), 1.87–1.79 (m, 2H), 1.74–1.64 (m, 2H), 1.50–1.42 (m, 2H), 1.39–1.33 (m, 2H), 1.31–1.27 (m, 4H), 1.27–1.22 (m, 6H), 0.87 (t, *J* = 7.0 Hz, 3H), 0.83 (t, *J* = 7.0 Hz, 3H). **<sup>13</sup>C NMR** (126 MHz, CDCl<sub>3</sub>): δ = 162.8 (C<sub>q</sub>), 145.3 (C<sub>q</sub>), 143.8 (C<sub>q</sub>), 138.8 (C<sub>q</sub>), 138.2 (C<sub>q</sub>), 129.6 (CH), 126.5 (CH), 124.6 (CH), 123.8 (CH), 122.5 (C<sub>q</sub>), 104.2 (CH), 50.5 (CH<sub>2</sub>), 39.1 (CH<sub>2</sub>), 33.1 (CH<sub>2</sub>), 31.8 (CH<sub>2</sub>), 31.2 (CH<sub>2</sub>), 30.2 (CH<sub>2</sub>), 29.3 (CH<sub>2</sub>), 29.2 (CH<sub>2</sub>), 28.7 (CH<sub>2</sub>), 26.2 (CH<sub>2</sub>), 22.7 (CH<sub>2</sub>), 22.5 (CH<sub>2</sub>), 14.2 (CH<sub>3</sub>), 13.0 (CH<sub>3</sub>). **IR** (ATR): 2954, 2927, 1717, 1650, 1593, 1464, 1286, 1049, 786 cm<sup>-1</sup>. **MS** (EI) *m/z* (relative intensity): 442 (72) [<sup>35</sup>Cl, M]<sup>+</sup>, 371 (49), 358 (45), 329 (41), 193 (57), 138 (60), 43 (100). **HR-MS** (EI) *m/z* calcd for C<sub>25</sub>H<sub>35</sub><sup>35</sup>ClN<sub>4</sub>O [M]<sup>+</sup> 442.2499, found 442.2499.

## 5. Experimental Part

**8-*n*-Heptyl-7-[(1-*n*-hexyl-1*H*-1,2,3-triazol-4-yl)methyl]-[1,3]dioxolo[4,5-*f*]isoquinolin-6(7*H*)-one (89ka)** and **7-*n*-Heptyl-6-[(1-*n*-hexyl-1*H*-1,2,3-triazol-4-yl)methyl]-[1,3]dioxolo[4,5-*g*]isoquinolin-5(6*H*)-one (89ka')**



The general procedure **GPA** was followed using **51k** (99.1 mg, 0.30 mmol) and allene **88a** (164 mg, 0.90 mmol). Purification by column chromatography (*n*hexane/EtOAc = 3/1) yielded **89ka** (49.6 mg, 36%) and **89ka'** (41.3 mg, 31%) as white solids.

**8-*n*-Heptyl-7-[(1-*n*-hexyl-1*H*-1,2,3-triazol-4-yl)methyl]-[1,3]dioxolo[4,5-*f*]isoquinolin-6(7*H*)-one (89ka):**

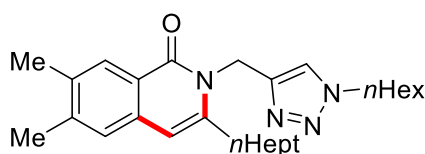
**M.p.** = 62–63 °C. **<sup>1</sup>H NMR** (600 MHz, CDCl<sub>3</sub>): δ = 7.96 (d, *J* = 8.5 Hz, 1H), 7.68 (s, 1H), 6.95 (d, *J* = 8.5 Hz, 1H), 6.31 (s, 1H), 6.11 (s, 2H), 5.33 (s, 2H), 4.24 (t, *J* = 7.3 Hz, 2H), 2.95 (t, *J* = 7.8 Hz, 2H), 1.87–1.82 (m, 2H), 1.73–1.67 (m, 2H), 1.51–1.44 (m, 2H), 1.39–1.34 (m, 2H), 1.31–1.25 (m, 10H), 0.88 (t, *J* = 6.9 Hz, 3H), 0.84 (t, *J* = 7.2 Hz, 3H). **<sup>13</sup>C NMR** (126 MHz, CDCl<sub>3</sub>): δ = 162.7 (C<sub>q</sub>), 149.5 (C<sub>q</sub>), 144.4 (C<sub>q</sub>), 144.2 (C<sub>q</sub>), 140.6 (C<sub>q</sub>), 123.7 (CH), 123.1 (CH), 121.4 (C<sub>q</sub>), 119.6 (C<sub>q</sub>), 108.2 (CH), 102.2 (CH<sub>2</sub>), 97.6 (CH), 50.5 (CH<sub>2</sub>), 39.1 (CH<sub>2</sub>), 33.4 (CH<sub>2</sub>), 31.9 (CH<sub>2</sub>), 31.3 (CH<sub>2</sub>), 30.3 (CH<sub>2</sub>), 29.4 (CH<sub>2</sub>), 29.3 (CH<sub>2</sub>), 28.8 (CH<sub>2</sub>), 26.3 (CH<sub>2</sub>), 22.8 (CH<sub>2</sub>), 22.6 (CH<sub>2</sub>), 14.3 (CH<sub>3</sub>), 14.1 (CH<sub>3</sub>). **IR** (ATR): 2954, 2921, 1602, 1589, 1477, 1425, 1243, 1036, 936, 749 cm<sup>-1</sup>. **MS** (EI) *m/z* (relative intensity): 452 (100) [M]<sup>+</sup>, 381 (45), 368 (40), 339 (57), 286 (71), 203 (98). **HR-MS** (EI) *m/z* calcd for C<sub>26</sub>H<sub>36</sub>N<sub>4</sub>O<sub>3</sub> [M]<sup>+</sup> 452.2787, found 452.2779.

## 5. Experimental Part

### 7-*n*-Heptyl-6-[(1-*n*-hexyl-1*H*-1,2,3-triazol-4-yl)methyl]-[1,3]dioxolo[4,5-*g*]isoquinolin-5(6*H*)-one (**89ka'**):

**M.p.** = 90–91 °C. **<sup>1</sup>H NMR** (300 MHz, CDCl<sub>3</sub>):  $\delta$  = 7.69 (s, 1H), 7.68 (s, 1H), 6.77 (s, 1H), 6.23 (s, 1H), 6.04 (s, 2H), 5.36 (s, 2H), 4.25 (t,  $J$  = 7.4 Hz, 2H), 2.94 (t,  $J$  = 7.8 Hz, 2H), 1.91–1.80 (m, 2H), 1.71–1.66 (m, 2H), 1.50–1.43 (m, 2H), 1.40–1.34 (m, 2H), 1.31–1.23 (m, 10H), 0.89 (t,  $J$  = 7.0 Hz, 3H), 0.84 (t,  $J$  = 7.2 Hz, 3H). **<sup>13</sup>C NMR** (126 MHz, CDCl<sub>3</sub>):  $\delta$  = 162.4 (C<sub>q</sub>), 152.0 (C<sub>q</sub>), 147.2 (C<sub>q</sub>), 144.1 (C<sub>q</sub>), 142.4 (C<sub>q</sub>), 134.4 (C<sub>q</sub>), 123.8 (CH), 119.6 (C<sub>q</sub>), 105.5 (CH), 105.1 (CH), 103.2 (CH), 101.6 (CH<sub>2</sub>), 50.5 (CH<sub>2</sub>), 39.3 (CH<sub>2</sub>), 33.1 (CH<sub>2</sub>), 32.0 (CH<sub>2</sub>), 31.3 (CH<sub>2</sub>), 30.3 (CH<sub>2</sub>), 29.5 (CH<sub>2</sub>), 29.4 (CH<sub>2</sub>), 29.0 (CH<sub>2</sub>), 26.4 (CH<sub>2</sub>), 22.8 (CH<sub>2</sub>), 22.6 (CH<sub>2</sub>), 14.3 (CH<sub>3</sub>), 14.1 (CH<sub>3</sub>). **IR** (ATR): 2954, 2924, 2857, 1649, 1597, 1478, 1427, 1247, 1037, 934 cm<sup>-1</sup>. **MS** (EI)  $m/z$  (relative intensity): 452 (100) [M]<sup>+</sup>, 339 (63), 286 (51), 203 (71). **HR-MS** (ESI)  $m/z$  calcd for C<sub>26</sub>H<sub>37</sub>N<sub>4</sub>O<sub>3</sub> [M+H]<sup>+</sup> 453.2860, found 453.2858.

### 3-*n*-Heptyl-2-[(1-*n*-hexyl-1*H*-1,2,3-triazol-4-yl)methyl]-6,7-dimethylisoquinolin-1(2*H*)-one (**89la**)



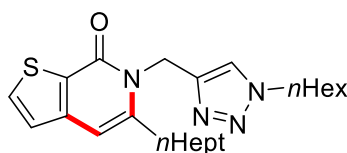
The general procedure **GPA** was followed using **89I** (94.3 mg, 0.30 mmol) and allene **88a** (164 mg, 0.90 mmol). Purification by column chromatography (*n*hexane/EtOAc = 4/1) yielded **89la** (90.4 mg, 69%) as white solid.

**M.p.** = 105–106 °C. **<sup>1</sup>H NMR** (600 MHz, CDCl<sub>3</sub>):  $\delta$  = 8.08 (s, 1H), 7.68 (s, 1H), 7.17 (s, 1H), 6.24 (s, 1H), 5.35 (s, 2H), 4.22 (t,  $J$  = 7.8 Hz, 2H), 2.92 (t,  $J$  = 7.8 Hz, 2H), 2.35 (s, 3H), 2.33 (s, 3H), 1.87–1.77 (m, 2H), 1.71–1.64 (m, 2H), 1.48–1.42 (m, 2H), 1.38–1.31 (m, 2H), 1.29–1.27 (m, 4H), 1.26–1.22 (m, 6H), 0.87 (t,  $J$  = 7.0 Hz, 3H), 0.82 (t,  $J$  = 7.2 Hz, 3H). **<sup>13</sup>C NMR** (126 MHz, CDCl<sub>3</sub>):  $\delta$  = 163.1 (C<sub>q</sub>), 144.3 (C<sub>q</sub>), 142.6 (C<sub>q</sub>), 142.2 (C<sub>q</sub>), 135.3 (C<sub>q</sub>), 135.2

## 5. Experimental Part

(C<sub>q</sub>), 127.6 (CH), 125.7 (CH), 123.7 (CH), 122.4 (C<sub>q</sub>), 104.8 (CH), 50.4 (CH<sub>2</sub>), 39.1 (CH<sub>2</sub>), 33.1 (CH<sub>2</sub>), 31.9 (CH<sub>2</sub>), 31.2 (CH<sub>2</sub>), 30.3 (CH<sub>2</sub>), 29.4 (CH<sub>2</sub>), 29.3 (CH<sub>2</sub>), 28.9 (CH<sub>2</sub>), 26.3 (CH<sub>2</sub>), 22.8 (CH<sub>2</sub>), 22.5 (CH<sub>2</sub>), 20.4 (CH<sub>3</sub>), 19.9 (CH<sub>3</sub>), 14.2 (CH<sub>3</sub>), 14.0 (CH<sub>3</sub>). **IR** (ATR): 2954, 2921, 2857, 1647, 1594, 1455, 1378, 1052, 897, 797 cm<sup>-1</sup>. **MS** (ESI) *m/z* (relative intensity): 896 (56) [2M+Na]<sup>+</sup>, 437 (100) [M+H]<sup>+</sup>. **HR-MS** (ESI) *m/z* calcd for C<sub>27</sub>H<sub>41</sub>N<sub>4</sub>O [M+H]<sup>+</sup> 437.3275, found 437.3271.

### 5-*n*-Heptyl-6-[(1-*n*-hexyl-1*H*-1,2,3-triazol-4-yl)methyl]thieno[2,3-*c*]pyridin-7(6*H*)-one (89ma)



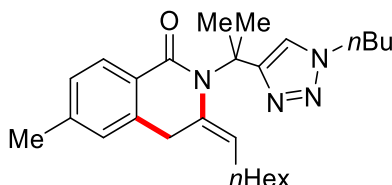
The general procedure **GPA** was followed using **51m** (87.7 mg, 0.30 mmol) and allene **88a** (164 mg, 0.90 mmol). Purification by column chromatography (*n*hexane/EtOAc = 4/1) yielded **89ma** (83.3 mg, 67%) as white solid.

**M.p.** = 94–95 °C. **<sup>1</sup>H NMR** (600 MHz, CDCl<sub>3</sub>): δ = 7.75 (s, 1H), 7.62 (d, *J* = 5.1 Hz, 1H), 7.10 (d, *J* = 5.1 Hz, 1H), 6.50 (s, 1H), 5.39 (s, 2H), 4.24 (t, *J* = 7.8 Hz, 2H), 3.00 (t, *J* = 3.0 Hz, 2H), 1.86–1.80 (m, 2H), 1.72–1.65 (m, 2H), 1.50–1.43 (m, 2H), 1.39–1.33 (m, 2H), 1.30–1.22 (m, 10H), 0.88 (t, *J* = 7.0 Hz, 3H), 0.85–0.81 (t, *J* = 7.2 Hz, 3H). **<sup>13</sup>C NMR** (126 MHz, CDCl<sub>3</sub>): δ = 159.4 (C<sub>q</sub>), 145.3 (C<sub>q</sub>), 145.1 (C<sub>q</sub>), 143.8 (C<sub>q</sub>), 133.3 (CH), 127.5 (C<sub>q</sub>), 124.0 (CH), 124.0 (CH), 102.5 (CH), 50.5 (CH<sub>2</sub>), 39.1 (CH<sub>2</sub>), 33.3 (CH<sub>2</sub>), 31.9 (CH<sub>2</sub>), 31.3 (CH<sub>2</sub>), 30.3 (CH<sub>2</sub>), 29.4 (CH<sub>2</sub>), 29.3 (CH<sub>2</sub>), 28.1 (CH<sub>2</sub>), 26.3 (CH<sub>2</sub>), 22.8 (CH<sub>2</sub>), 22.5 (CH<sub>2</sub>), 14.3 (CH<sub>3</sub>), 14.1 (CH<sub>3</sub>). **IR** (ATR): 3061, 2923, 2853, 1635, 1576, 1444, 1053, 805, 792, 657 cm<sup>-1</sup>. **MS** (ESI) *m/z* (relative intensity): 851 (100) [2M+Na]<sup>+</sup>, 437 (38) [M+Na]<sup>+</sup>, 415 (20) [M+H]<sup>+</sup>. **HR-MS** (ESI) *m/z* calcd for C<sub>23</sub>H<sub>35</sub>N<sub>4</sub>OS [M+H]<sup>+</sup> 415.2526, found 415.2525.

## 5. Experimental Part

### 5.3.3 Analytical Data – Products 90

#### (*E*)-2-[2-(1-*n*-Butyl-1*H*-1,2,3-triazol-4-yl)propan-2-yl]-3-heptylidene-6-methyl-3,4-dihydroisoquinolin-1(2*H*)-one (**90fa**)

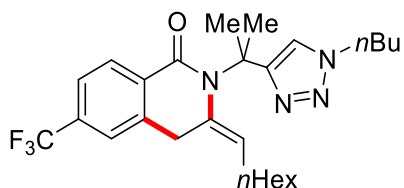


The general procedure **GPA** was followed using **32f** (90.1 mg, 0.30 mmol) and allene **88a** (164 mg, 0.90 mmol). Purification by column chromatography (*n*hexane/EtOAc = 3/1) yielded **90fa** (86.2 mg, 68%) as a colorless oil.

**<sup>1</sup>H NMR** (600 MHz, C<sub>6</sub>D<sub>6</sub>):  $\delta$  = 8.32 (d,  $J$  = 7.9 Hz, 1H), 7.50 (s, 1H), 6.81 (dd,  $J$  = 7.9, 1.7, 1H), 6.63 (s, 1H), 5.58 (t,  $J$  = 7.7 Hz, 1H), 3.65 (t,  $J$  = 7.3 Hz, 2H), 3.43 (s, 2H), 2.17 (s, 6H), 2.00 (s, 3H), 1.93 (dt,  $J$  = 7.4 Hz, 2H), 1.39–1.30 (m, 2H), 1.21–1.10 (m, 8H), 0.98–0.91 (m, 2H), 0.84 (t,  $J$  = 7.1 Hz, 3H), 0.62 (t,  $J$  = 7.4 Hz, 3H). **<sup>13</sup>C NMR** (126 MHz, C<sub>6</sub>D<sub>6</sub>):  $\delta$  = 164.9 (C<sub>q</sub>), 153.7 (C<sub>q</sub>), 141.8 (C<sub>q</sub>), 139.0 (C<sub>q</sub>), 135.8 (C<sub>q</sub>), 129.2 (CH), 129.0 (C<sub>q</sub>), 127.7 (CH), 127.0 (CH), 122.8 (CH), 122.0 (CH), 57.9 (C<sub>q</sub>), 49.6 (CH<sub>2</sub>), 32.9 (CH<sub>2</sub>), 32.5 (CH<sub>2</sub>), 32.1 (CH<sub>2</sub>), 30.2 (CH<sub>2</sub>), 30.1 (CH<sub>3</sub>), 29.5 (CH<sub>2</sub>), 27.6 (CH<sub>2</sub>), 23.2 (CH<sub>2</sub>), 21.5 (CH<sub>3</sub>), 20.1 (CH<sub>2</sub>), 14.5 (CH<sub>3</sub>), 13.6 (CH<sub>3</sub>). **IR** (ATR): 2957, 2930, 2871, 1648, 1457, 1378, 1163, 1046, 835, 498 cm<sup>-1</sup>. **MS** (ESI)  $m/z$  (relative intensity): 868 (100) [2M+Na]<sup>+</sup>, 445 (94) [M+Na]<sup>+</sup>, 423 (93) [M+H]<sup>+</sup>, 407 (100) [M+H]<sup>+</sup>. **HR-MS** (ESI)  $m/z$  calcd for C<sub>26</sub>H<sub>39</sub>N<sub>4</sub>O [M+H]<sup>+</sup> 423.3118, found 423.3114.

## 5. Experimental Part

### (*E*)-2-[2-(1-*n*-Butyl-1*H*-1,2,3-triazol-4-yl)propan-2-yl]-3-heptylidene-6-(trifluoro-methyl)-3,4-dihydroisoquinolin-1(2*H*)-one (**90ga**)

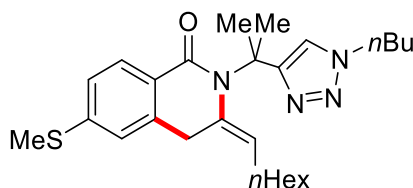


The general procedure **GPA** was followed using **32g** (106 mg, 0.30 mmol) and allene **88a** (164 mg, 0.90 mmol). Purification by column chromatography (*n*hexane/EtOAc = 3/1) yielded **90ga** (116 mg, 81%) as a colorless oil.

**<sup>1</sup>H NMR** (600 MHz, C<sub>6</sub>D<sub>6</sub>):  $\delta$  = 8.19 (d,  $J$  = 8.1 Hz, 1H), 7.35 (s, 1H), 7.15–7.11 (m, 1H), 7.09 (d,  $J$  = 1.7 Hz, 1H), 5.57 (t,  $J$  = 7.8 Hz, 1H), 3.66 (t,  $J$  = 7.3 Hz, 2H), 3.27 (s, 2H), 2.08 (s, 6H), 1.83 (dt,  $J$  = 7.4 Hz, 2H), 1.37–1.32 (m, 2H), 1.19–1.05 (m, 8H), 0.98–0.92 (m, 2H), 0.84 (t,  $J$  = 7.2 Hz, 3H), 0.63 (t,  $J$  = 7.4 Hz, 3H). **<sup>13</sup>C NMR** (126 MHz, C<sub>6</sub>D<sub>6</sub>):  $\delta$  = 163.4 (C<sub>q</sub>), 153.3 (C<sub>q</sub>), 139.8 (C<sub>q</sub>), 134.5 (C<sub>q</sub>), 134.4 (C<sub>q</sub>), 133.0 (q,  $^2J_{C-F}$  = 32.0 Hz, C<sub>q</sub>), 129.6 (CH), 128.3 (CH), 124.6 (q,  $^1J_{C-F}$  = 272.3 Hz, C<sub>q</sub>), 123.7 (q,  $^3J_{C-F}$  = 3.6 Hz, CH), 123.4 (q,  $^3J_{C-F}$  = 3.7 Hz, CH), 121.6 (CH), 58.2 (C<sub>q</sub>), 49.7 (CH<sub>2</sub>), 32.5 (CH<sub>2</sub>), 32.5 (CH<sub>2</sub>), 32.1 (CH<sub>2</sub>), 30.0 (CH<sub>2</sub>), 29.8 (CH<sub>3</sub>), 29.4 (CH<sub>2</sub>), 27.6 (CH<sub>2</sub>), 23.1 (CH<sub>2</sub>), 20.0 (CH<sub>2</sub>), 14.4 (CH<sub>3</sub>), 13.6 (CH<sub>3</sub>). **<sup>19</sup>F NMR** (282 MHz, C<sub>6</sub>D<sub>6</sub>):  $\delta$  = -62.50 (s). **IR** (ATR): 2930, 2858, 1652, 1458, 1431, 1324, 1166, 1126, 730, 418 cm<sup>-1</sup>. **MS** (ESI)  $m/z$  (relative intensity): 975 (75) [2M+Na]<sup>+</sup>, 953 (13) [2M+H]<sup>+</sup>, 499 (42) [M+Na]<sup>+</sup>, 477 (100) [M+H]<sup>+</sup>. **HR-MS** (ESI)  $m/z$  calcd for C<sub>26</sub>H<sub>36</sub>F<sub>3</sub>N<sub>4</sub>O [M+H]<sup>+</sup> 477.2836, found 477.2831.

## 5. Experimental Part

### (*E*)-2-[2-(1-*n*-Butyl-1*H*-1,2,3-triazol-4-yl)propan-2-yl]-3-heptylidene-6-(methylthio)-3,4-dihydroisoquinolin-1(2*H*)-one (**90ha**)

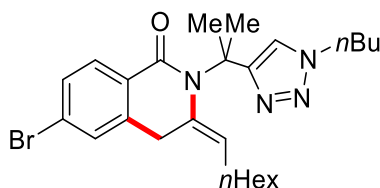


The general procedure **GPA** was followed using **32h** (99.7 mg, 0.30 mmol) and allene **88a** (164 mg, 0.90 mmol). Purification by column chromatography (*n*hexane/EtOAc = 3/1) yielded **90ha** (96.8 mg, 71%) as a colorless oil.

**<sup>1</sup>H NMR** (300 MHz, C<sub>6</sub>D<sub>6</sub>):  $\delta$  = 8.27 (d,  $J$  = 8.1, 1H), 7.46 (s, 1H), 6.83 (dd,  $J$  = 8.2, 2.0 Hz, 1H), 6.80 (s, 1H), 5.58 (t,  $J$  = 7.7 Hz, 1H), 3.65 (t,  $J$  = 7.3 Hz, 2H), 3.37 (s, 2H), 2.16 (s, 6H), 1.95–1.88 (m, 2H), 1.87 (s, 3H), 1.45–1.29 (m, 2H), 1.23–1.07 (m, 8H), 1.02–0.90 (m, 2H), 0.85 (t,  $J$  = 6.9 Hz, 3H), 0.63 (t,  $J$  = 7.3 Hz, 3H). **<sup>13</sup>C NMR** (126 MHz, C<sub>6</sub>D<sub>6</sub>):  $\delta$  = 164.7 (C<sub>q</sub>), 153.7 (C<sub>q</sub>), 143.9 (C<sub>q</sub>), 139.4 (C<sub>q</sub>), 135.4 (C<sub>q</sub>), 129.6 (CH), 128.4 (C<sub>q</sub>), 123.8 (CH), 123.4 (CH), 123.2 (CH), 121.9 (CH), 57.9 (C<sub>q</sub>), 49.7 (CH<sub>2</sub>), 32.9 (CH<sub>2</sub>), 32.4 (CH<sub>2</sub>), 32.1 (CH<sub>2</sub>), 30.2 (CH<sub>2</sub>), 30.0 (CH<sub>3</sub>), 29.5 (CH<sub>2</sub>), 27.6 (CH<sub>2</sub>), 23.2 (CH<sub>2</sub>), 20.1 (CH<sub>2</sub>), 14.7 (CH<sub>3</sub>), 14.5 (CH<sub>3</sub>), 13.6 (CH<sub>3</sub>). **IR** (ATR): 2956, 2927, 2856, 1645, 1593, 1323, 1164, 1046, 831, 677 cm<sup>-1</sup>. **MS** (ESI)  $m/z$  (relative intensity): 932 (100) [2M+Na]<sup>+</sup>, 910 (18) [2M+H]<sup>+</sup>, 477 (39) [M+Na]<sup>+</sup>, 455 (46) [M+H]<sup>+</sup>. **HR-MS** (ESI)  $m/z$  calcd for C<sub>26</sub>H<sub>39</sub>N<sub>4</sub>OS [M+H]<sup>+</sup> 455.2839, found 455.2837.

## 5. Experimental Part

### (*E*)-6-Bromo-2-[2-(1-*n*-butyl-1*H*-1,2,3-triazol-4-yl)propan-2-yl]-3-heptylidene-3,4-dihydro-isoquinolin-1(2*H*)-one (**90ia**)

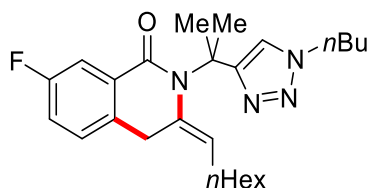


The general procedure **GPA** was followed using **32i** (110 mg, 0.30 mmol) and allene **88a** (164 mg, 0.90 mmol). Purification by column chromatography (*n*hexane/EtOAc = 3/1) yielded **90ia** (131 mg, 90%) as a colorless oil.

**<sup>1</sup>H NMR** (300 MHz, C<sub>6</sub>D<sub>6</sub>):  $\delta$  = 8.03 (d,  $J$  = 8.3 Hz, 1H), 7.38 (s, 1H), 7.06 (dd,  $J$  = 8.3, 2.0 Hz, 1H), 6.96 (s, 1H), 5.56 (t,  $J$  = 7.8 Hz, 1H), 3.64 (t,  $J$  = 7.3 Hz, 2H), 3.23 (s, 2H), 2.09 (s, 6H), 1.90–1.76 (m, 2H), 1.42–1.26 (m, 2H), 1.24–1.08 (m, 8H), 1.01–0.83 (m, 5H), 0.62 (t,  $J$  = 7.3 Hz, 3H). **<sup>13</sup>C NMR** (126 MHz, C<sub>6</sub>D<sub>6</sub>):  $\delta$  = 163.9 (C<sub>q</sub>), 153.4 (C<sub>q</sub>), 140.9 (C<sub>q</sub>), 134.8 (C<sub>q</sub>), 130.7 (CH), 130.3 (C<sub>q</sub>), 130.2 (CH), 129.4 (CH), 126.2 (C<sub>q</sub>), 123.8 (CH), 121.7 (CH), 58.1 (C<sub>q</sub>), 49.7 (CH<sub>2</sub>), 32.5 (CH<sub>2</sub>), 32.5 (CH<sub>2</sub>), 32.1 (CH<sub>2</sub>), 30.1 (CH<sub>2</sub>), 29.8 (CH<sub>3</sub>), 29.5 (CH<sub>2</sub>), 27.6 (CH<sub>2</sub>), 23.2 (CH<sub>2</sub>), 20.0 (CH<sub>2</sub>), 14.5 (CH<sub>3</sub>), 13.6 (CH<sub>3</sub>). **IR** (ATR): 2956, 2927, 2855, 1649, 1590, 1321, 1167, 1045, 766, 498 cm<sup>-1</sup>. **MS** (ESI)  $m/z$  (relative intensity): 509 (16) [<sup>79</sup>Br, 2M+Na]<sup>+</sup>, 487 (34) [<sup>79</sup>Br, M+H]<sup>+</sup>, 166 (100). **HR-MS** (ESI)  $m/z$  calcd for C<sub>25</sub>H<sub>36</sub><sup>79</sup>BrN<sub>4</sub>O [M+H]<sup>+</sup> 487.2067, found 487.2071.

## 5. Experimental Part

### (*E*)-2-[2-(1-*n*-Butyl-1*H*-1,2,3-triazol-4-yl)propan-2-yl]-7-fluoro-3-heptylidene-3,4-dihydro-isoquinolin-1(2*H*)-one (**90ja**)



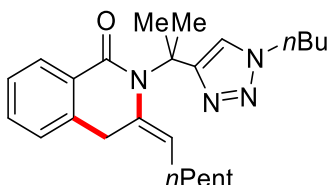
The general procedure **GPA** was followed using **32j** (91.3 mg, 0.30 mmol) and allene **88a** (164 mg, 0.90 mmol). Purification by column chromatography (*n*hexane/EtOAc = 3/1) yielded **90ja** (97.3 mg, 76%) as a colorless oil.

**<sup>1</sup>H NMR** (600 MHz, C<sub>6</sub>D<sub>6</sub>):  $\delta$  = 8.06 (dd,  $J$  = 9.3, 2.8 Hz, 1H), 7.43 (s, 1H), 6.72 (ddd,  $J$  = 8.3, 8.3, 2.8 Hz, 1H), 6.60 (dd,  $J$  = 8.3, 5.1 Hz, 1H), 5.55 (t,  $J$  = 7.8 Hz, 1H), 3.69 (t,  $J$  = 7.3 Hz, 2H), 3.32 (s, 2H), 2.09 (s, 6H), 1.87 (dt,  $J$  = 7.3 Hz, 2H), 1.41–1.33 (m, 2H), 1.21–1.06 (m, 8H), 1.00–0.90 (m, 2H), 0.84 (t,  $J$  = 7.2 Hz, 3H), 0.64 (t,  $J$  = 7.4 Hz, 3H). **<sup>13</sup>C NMR** (126 MHz, C<sub>6</sub>D<sub>6</sub>):  $\delta$  = 163.5 (d,  $^4J_{C-F}$  = 2.5 Hz, C<sub>q</sub>), 162.1 (d,  $^1J_{C-F}$  = 244.0 Hz, C<sub>q</sub>), 153.4 (C<sub>q</sub>), 135.2 (C<sub>q</sub>), 134.7 (d,  $^4J_{C-F}$  = 3.0 Hz, C<sub>q</sub>), 133.4 (d,  $^3J_{C-F}$  = 7.1 Hz, C<sub>q</sub>), 128.4 (CH), 123.6 (CH), 121.8 (CH), 118.5 (d,  $^2J_{C-F}$  = 22.0 Hz, CH), 115.4 (d,  $^2J_{C-F}$  = 23.0 Hz, CH), 58.2 (C<sub>q</sub>), 49.7 (CH<sub>2</sub>), 32.5 (CH<sub>2</sub>), 32.1 (CH<sub>2</sub>), 32.0 (CH<sub>2</sub>), 30.1 (CH<sub>2</sub>), 29.8 (CH<sub>3</sub>), 29.5 (CH<sub>2</sub>), 27.6 (CH<sub>2</sub>), 23.1 (CH<sub>2</sub>), 20.0 (CH<sub>2</sub>), 14.4 (CH<sub>3</sub>), 13.6 (CH<sub>3</sub>). **<sup>19</sup>F NMR** (282 MHz, C<sub>6</sub>D<sub>6</sub>):  $\delta$  = -115.37 (td,  $J$  = 8.6, 5.0 Hz). **IR** (ATR): 2955, 2928, 2858, 1713, 1684, 1606, 1484, 1347, 1280, 1151, 783 cm<sup>-1</sup>. **MS** (ESI)  $m/z$  (relative intensity): 875 (56) [2M+Na]<sup>+</sup>, 853 (11) [2M+H]<sup>+</sup>, 427 (100) [M+H]<sup>+</sup>, 166 (96).

## 5. Experimental Part

### 5.3.4 Analytical Data – Products of TAM Benzamide Annulation with Different Allene Acetates

#### (*E*)-2-[2-(1-*n*-Butyl-1*H*-1,2,3-triazol-4-yl)propan-2-yl]-3-hexylidene-3,4-dihydro-isoquinolin-1(2*H*)-one (**90ah**)



The general procedure **GPA** was followed using **32a** (85.9 mg, 0.30 mmol) and allene **88h** (151 mg, 0.90 mmol). Purification by column chromatography (*n*hexane/EtOAc = 3/1) yielded **90ah** (90.0 mg, 76%) as a colorless oil.

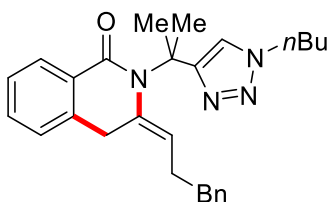
**<sup>1</sup>H NMR** (600 MHz, C<sub>6</sub>D<sub>6</sub>):  $\delta$  = 8.40 (dd,  $J$  = 7.6, 1.5 Hz, 1H), 7.47 (s, 1H), 7.03 (ddd,  $J$  = 7.4, 7.4, 1.6 Hz, 1H), 6.99 (ddd,  $J$  = 7.4, 7.4, 1.4 Hz, 1H), 6.82 (dd,  $J$  = 7.4, 1.0 Hz, 1H), 5.57 (t,  $J$  = 7.7 Hz, 1H), 3.65 (t,  $J$  = 7.3 Hz, 2H), 3.40 (s, 2H), 2.15 (s, 6H), 1.86 (dt,  $J$  = 7.5 Hz, 2H), 1.38–1.29 (m, 2H), 1.18–1.05 (m, 6H), 0.98–0.91 (m, 2H), 0.79 (t,  $J$  = 7.2 Hz, 3H), 0.62 (t,  $J$  = 7.4 Hz, 3H).

**<sup>13</sup>C NMR** (126 MHz, C<sub>6</sub>D<sub>6</sub>):  $\delta$  = 164.7 (C<sub>q</sub>), 153.6 (C<sub>q</sub>), 139.0 (C<sub>q</sub>), 135.5 (C<sub>q</sub>), 131.5 (CH), 131.5 (C<sub>q</sub>), 129.1 (CH), 126.9 (CH), 126.3 (CH), 123.1 (CH), 121.9 (CH), 58.0 (C<sub>q</sub>), 49.6 (CH<sub>2</sub>), 32.9 (CH<sub>2</sub>), 32.4 (CH<sub>2</sub>), 32.0 (CH<sub>2</sub>), 30.0 (CH<sub>2</sub>), 29.9 (CH<sub>3</sub>), 27.5 (CH<sub>2</sub>), 23.0 (CH<sub>2</sub>), 20.0 (CH<sub>2</sub>), 14.4 (CH<sub>3</sub>), 13.6 (CH<sub>3</sub>).

**IR** (ATR): 2927, 2861, 1647, 1457, 1372, 1319, 1168, 1045, 736 cm<sup>-1</sup>. **MS** (ESI)  $m/z$  (relative intensity): 811 (4) [2M+Na]<sup>+</sup>, 395 (22) [M+H]<sup>+</sup>, 166 (100). **HR-MS** (ESI)  $m/z$  calcd for C<sub>24</sub>H<sub>35</sub>N<sub>4</sub>O [M+H]<sup>+</sup> 395.2805, found 395.2800.

## 5. Experimental Part

### (*E*)-2-[2-(1-*n*-Butyl-1*H*-1,2,3-triazol-4-yl)propan-2-yl]-3-(3-phenylpropylidene)-3,4-dihydroisoquinolin-1(2*H*)-one (**90ai**)

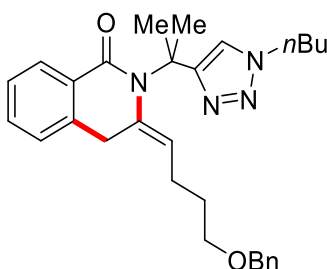


The general procedure **GPA** was followed using **32a** (85.9 mg, 0.30 mmol) and allene **88i** (182 mg, 0.90 mmol). Purification by column chromatography (*n*hexane/EtOAc = 3/1) yielded **90ai** (112 mg, 87%) as a colorless oil.

**<sup>1</sup>H NMR** (300 MHz, C<sub>6</sub>D<sub>6</sub>):  $\delta$  = 8.49–8.27 (m, 1H), 7.44 (s, 1H), 7.13–7.05 (m, 2H), 7.03–6.98 (m, 3H), 6.97–6.93 (m, 2H), 6.77–6.72 (m, 1H), 5.56 (t,  $J$  = 7.6 Hz, 1H), 3.66 (t,  $J$  = 7.3 Hz, 2H), 3.31 (s, 2H), 2.37 (t,  $J$  = 7.7 Hz, 2H), 2.18–2.12 (m, 2H), 2.10 (s, 6H), 1.46–1.24 (m, 2H), 1.02–0.86 (m, 2H), 0.62 (t,  $J$  = 7.3 Hz, 3H). **<sup>13</sup>C NMR** (75 MHz, C<sub>6</sub>D<sub>6</sub>):  $\delta$  = 164.7 (C<sub>q</sub>), 153.7 (C<sub>q</sub>), 141.7 (C<sub>q</sub>), 138.8 (C<sub>q</sub>), 136.0 (C<sub>q</sub>), 131.6 (CH), 131.3 (C<sub>q</sub>), 129.0 (CH), 128.7 (CH), 128.6 (CH), 126.8 (CH), 126.4 (CH), 126.3 (CH), 122.0 (CH), 121.8 (CH), 57.9 (C<sub>q</sub>), 49.5 (CH<sub>2</sub>), 36.1 (CH<sub>2</sub>), 32.6 (CH<sub>2</sub>), 32.3 (CH<sub>2</sub>), 29.8 (CH<sub>3</sub>), 29.3 (CH<sub>2</sub>), 19.9 (CH<sub>2</sub>), 13.5 (CH<sub>3</sub>). **IR** (ATR): 2931, 2866, 1648, 1456, 1373, 1321, 1167, 738, 699 cm<sup>-1</sup>. **MS** (ESI)  $m/z$  (relative intensity): 451 (78) [M+Na]<sup>+</sup>, 429 (100)[M+H]<sup>+</sup>. **HR-MS** (ESI)  $m/z$  calcd for C<sub>27</sub>H<sub>33</sub>N<sub>4</sub>O [M+H]<sup>+</sup> 429.2649, found 429.2650.

## 5. Experimental Part

### (*E*)-3-[4-(Benzyloxy)butylidene]-2-[2-(1-*n*-butyl-1*H*-1,2,3-triazol-4-yl)prop- an-2-yl]-3,4-dihydroisoquinolin-1(2*H*)-one (**90aj**)

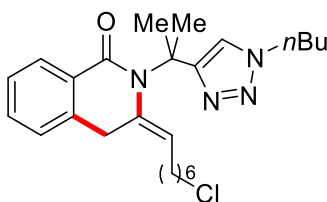


The general procedure **GPA** was followed using **32a** (85.9 mg, 0.30 mmol) and allene **88j** (222 mg, 0.90 mmol). Purification by column chromatography (*n*hexane/EtOAc = 3/1) yielded **90aj** (111 mg, 78%) as a colorless oil.

**<sup>1</sup>H NMR** (300 MHz, C<sub>6</sub>D<sub>6</sub>):  $\delta$  = 8.41–8.36 (m, 1H), 7.44 (s, 1H), 7.30–7.25 (m, 2H), 7.23–7.18 (m, 2H), 7.14–7.07 (m, 1H), 7.03–6.97 (m, 2H), 6.80–6.74 (m, 1H), 5.53 (t, *J* = 7.9 Hz, 1H), 4.22 (s, 2H), 3.66 (t, *J* = 7.3 Hz, 2H), 3.41 (s, 2H), 3.13 (t, *J* = 6.0 Hz, 2H), 2.12 (s, 6H), 2.04 (dt, *J* = 7.4 Hz, 2H), 1.48–1.29 (m, 4H), 1.04–0.85 (m, 2H), 0.62 (t, *J* = 7.3 Hz, 3H). **<sup>13</sup>C NMR** (75 MHz, C<sub>6</sub>D<sub>6</sub>):  $\delta$  = 164.8 (C<sub>q</sub>), 153.6 (C<sub>q</sub>), 139.5 (C<sub>q</sub>), 139.0 (C<sub>q</sub>), 136.1 (C<sub>q</sub>), 131.5 (CH), 131.4 (C<sub>q</sub>), 129.0 (CH), 128.6 (CH), 127.7 (CH), 127.6 (CH), 126.8 (CH), 126.5 (CH), 122.3 (CH), 121.9 (CH), 73.0 (CH<sub>2</sub>), 69.3 (CH<sub>2</sub>), 57.9 (C<sub>q</sub>), 49.5 (CH<sub>2</sub>), 32.5 (CH<sub>2</sub>), 32.3 (CH<sub>2</sub>), 30.0 (CH<sub>2</sub>), 29.8 (CH<sub>3</sub>), 23.9 (CH<sub>2</sub>), 19.9 (CH<sub>2</sub>), 13.5 (CH<sub>3</sub>). **IR** (ATR): 2930, 2863, 1648, 1456, 1371, 1320, 1102, 738, 697, 459 cm<sup>-1</sup>. **MS** (ESI) *m/z* (relative intensity): 495 (6) [M+Na]<sup>+</sup>, 473 (31) [M+H]<sup>+</sup>, 308 (10), 166 (100), 117 (19). **HR-MS** (ESI) *m/z* calcd for C<sub>29</sub>H<sub>37</sub>N<sub>4</sub>O<sub>2</sub> [M+H]<sup>+</sup> 473.2911, found 473.2911.

## 5. Experimental Part

### (*E*)-2-[2-(1-*n*-Butyl-1*H*-1,2,3-triazol-4-yl)propan-2-yl]-3-(7-chloroheptylidene)-3,4-dihydroisoquinolin-1(2*H*)-one (**90ak**)

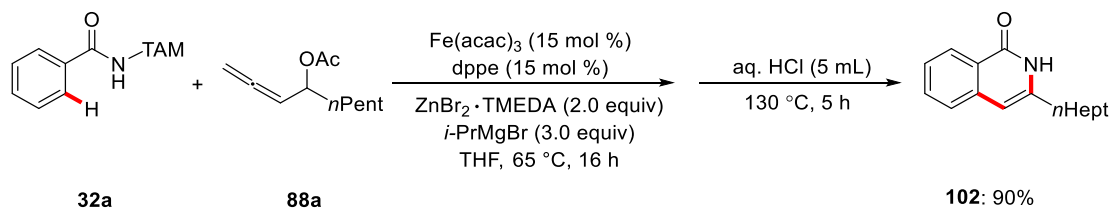


The general procedure **GPA** was followed using **32a** (85.9 mg, 0.30 mmol) and allene **88k** (195 mg, 0.90 mmol). Purification by column chromatography (*n*hexane/EtOAc = 3/1) yielded **90ak** (90.4 mg, 68%) as a colorless oil.

**<sup>1</sup>H NMR** (300 MHz, C<sub>6</sub>D<sub>6</sub>):  $\delta$  = 8.41–8.32 (m, 1H), 7.49 (s, 1H), 7.09–6.95 (m, 2H), 6.88–6.76 (m, 1H), 5.56 (t,  $J$  = 7.8 Hz, 1H), 3.67 (t,  $J$  = 7.3 Hz, 2H), 3.40 (s, 2H), 3.08 (t,  $J$  = 6.7 Hz, 2H), 2.13 (s, 6H), 1.83 (dt,  $J$  = 7.4 Hz, 2H), 1.42–1.27 (m, 4H), 1.09–0.86 (m, 8H), 0.63 (t,  $J$  = 7.3 Hz, 3H). **<sup>13</sup>C NMR** (126 MHz, C<sub>6</sub>D<sub>6</sub>):  $\delta$  = 164.7 (C<sub>q</sub>), 153.5 (C<sub>q</sub>), 139.0 (C<sub>q</sub>), 135.6 (C<sub>q</sub>), 131.6 (CH), 131.4 (C<sub>q</sub>), 129.1 (CH), 126.9 (CH), 126.3 (CH), 122.9 (CH), 122.0 (CH), 57.9 (C<sub>q</sub>), 49.7 (CH<sub>2</sub>), 45.1 (CH<sub>2</sub>), 32.9 (CH<sub>2</sub>), 32.9 (CH<sub>2</sub>), 32.5 (CH<sub>2</sub>), 29.9 (CH<sub>3</sub>), 29.8 (CH<sub>2</sub>), 28.8 (CH<sub>2</sub>), 27.3 (CH<sub>2</sub>), 27.0 (CH<sub>2</sub>), 20.0 (CH<sub>2</sub>), 13.7 (CH<sub>3</sub>). **IR** (ATR): 2931, 2857, 1601, 1457, 1374, 1323, 1306, 1046, 737 cm<sup>-1</sup>. **MS** (EI)  $m/z$  (relative intensity): 442 (6) [<sup>35</sup>Cl, M]<sup>+</sup>, 323 (15), 242 (13), 172 (39), 166 (100), 84 (38). **HR-MS** (ESI)  $m/z$  calcd for C<sub>25</sub>H<sub>35</sub>N<sub>4</sub>O<sup>35</sup>Cl [M+Na]<sup>+</sup> 465.2392, found 465.2380.

## 5. Experimental Part

### 5.3.5 Traceless Removal of TAM Group



To a stirred solution of benzamide **32a** (85.9 mg, 0.30 mmol),  $\text{ZnBr}_2 \cdot \text{TMEDA}$  (206 mg, 0.60 mmol),  $\text{dppe}$  (17.9 mg, 15 mol %) in THF (0.20 mL),  $i\text{-PrMgBr}$  (3.0 M in 2-MeTHF, 300  $\mu\text{L}$ , 0.90 mmol) was added in one portion and the reaction mixture was stirred for 5 min at ambient temperature. Then,  $\text{Fe}(\text{acac})_3$  (15.9 mg, 15 mol %) was added in a single portion. After stirring the solution for an additional 5 min, allene **88a** (164 mg, 0.90 mmol) was added as a solution in THF (0.20 mL) in one portion. After completion, the mixture was placed in a pre-heated oil bath at 65 °C, and stirred for 16 h. The reaction mixture was then transferred into a sealed tube using THF (2.0 mL). Conc. HCl (5.0 mL) was added, and the reaction mixture was placed in a pre-heated oil bath at 130 °C and stirred for 5 h. The mixture was allowed to cool to ambient temperature. The reaction mixture was extracted with  $\text{CH}_2\text{Cl}_2$  (3  $\times$  15 mL), and the combined organic layers were washed with sat. aqueous  $\text{NaHCO}_3$  (15 mL), dried over  $\text{Na}_2\text{SO}_4$ , filtered and concentrated. Purification by column chromatography (*n*hexane/EtOAc = 5/1) yielded **102** (65.7 mg, 90%) as a white solid.

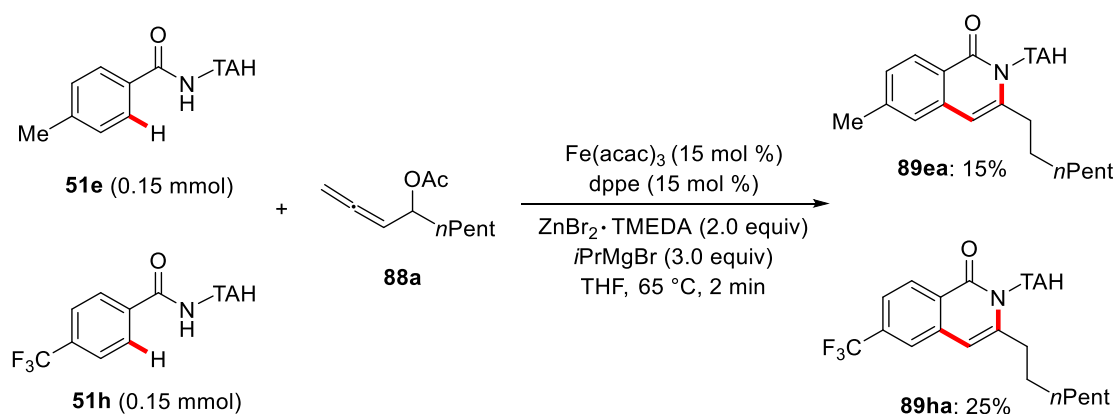
**M.p.** = 86–87 °C.  **$^1\text{H}$  NMR** (600 MHz,  $\text{CDCl}_3$ ):  $\delta$  = 10.82 (s, 1H), 8.39–8.36 (m, 1H), 7.62 (ddd,  $J$  = 8.1, 7.1, 1.4 Hz, 1H), 7.47 (d,  $J$  = 7.9 Hz, 1H), 7.42 (ddd,  $J$  = 8.1, 7.1, 1.1 Hz, 1H), 6.31 (s, 1H), 2.63 (t,  $J$  = 7.0 Hz, 2H), 1.75 (dt,  $J$  = 15.3, 7.6 Hz, 2H), 1.43–1.38 (m, 2H), 1.37–1.32 (m, 2H), 1.30–1.25 (m, 4H), 0.87 (t,  $J$  = 7.0 Hz, 3H).  **$^{13}\text{C}$  NMR** (126 MHz,  $\text{CDCl}_3$ ):  $\delta$  = 164.5 ( $\text{C}_\text{q}$ ), 142.0 ( $\text{C}_\text{q}$ ), 138.8 ( $\text{C}_\text{q}$ ), 132.6 (CH), 127.4 (CH), 125.8 (CH), 125.7 (CH), 124.5 ( $\text{C}_\text{q}$ ), 103.9 (CH), 33.7 ( $\text{CH}_2$ ), 31.9 ( $\text{CH}_2$ ), 29.3 ( $\text{CH}_2$ ), 29.2 ( $\text{CH}_2$ ), 28.6 ( $\text{CH}_2$ ), 22.9 ( $\text{CH}_2$ ), 14.3 ( $\text{CH}_3$ ). **IR** (ATR): 2926, 2855, 1642, 1607, 1555, 1465, 1346, 1044, 755,

## 5. Experimental Part

582  $\text{cm}^{-1}$ . **MS** (EI)  $m/z$  (relative intensity): 243 (42)  $[\text{M}]^+$ , 172 (29), 159 (100), 158 (18), 41 (33). **HR-MS** (EI)  $m/z$  calcd for  $\text{C}_{16}\text{H}_{21}\text{NO}$   $[\text{M}]^+$  243.1623, found 243.1623.

### 5.3.6 Mechanistic Studies

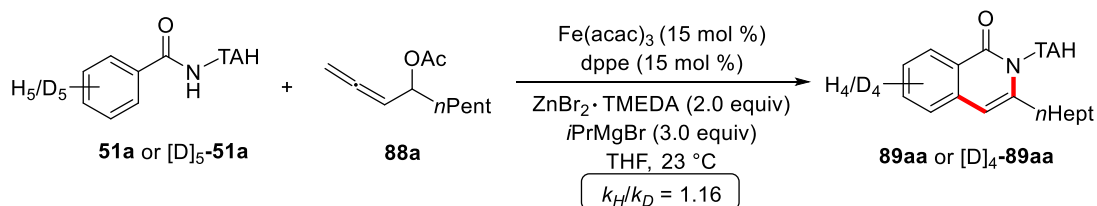
#### Intermolecular Competition Experiment



To a stirred solution of **51e** (45.1 mg, 0.15 mmol), **51h** (53.3 mg, 0.15 mmol),  $\text{ZnBr}_2 \cdot \text{TMEDA}$  (206 mg, 0.60 mmol),  $\text{dppe}$  (17.9 mg, 15 mol %) in THF (0.20 mL),  $i\text{PrMgBr}$  (3.0 M in 2-MeTHF, 300  $\mu\text{L}$ , 0.90 mmol) was added in one portion and the reaction mixture was stirred for 5 min at ambient temperature. Then,  $\text{Fe}(\text{acac})_3$  (15.9 mg, 15 mol %) was added in a single portion. After stirring the solution for additional 5 min, a solution of allene **88a** (164 mg, 0.90 mmol) in THF (0.20 mL) was added in one portion. The mixture was placed in a pre-heated oil bath at 65 °C. After stirring for 2 min, sat. aqueous  $\text{NH}_4\text{Cl}$  (2.0 mL) was added to the reaction mixture, which was extracted with  $\text{CH}_2\text{Cl}_2$  ( $3 \times 15$  mL). The combined organic extracts were dried over  $\text{Na}_2\text{SO}_4$ , filtered and concentrated. Purification by column chromatography ( $n\text{hexane}/\text{EtOAc} = 3/1$ ) yielded **89ea** (19.0 mg, 15%) and **89ha** (35.7 mg, 25%).

## 5. Experimental Part

### Kinetic Isotope Effect (KIE) Measurement



To a stirred solution of **51a** (172 mg, 0.60 mmol) or  $[D]_5$ -**51a** (175 mg, 0.60 mmol),  $ZnBr_2 \cdot TMEDA$  (412 mg, 1.20 mmol) and  $dppe$  (35.8 mg, 15 mol %) in THF (1.2 mL),  $iPrMgBr$  (3.0 M in THF, 600  $\mu$ L, 1.80 mmol) was added in one portion and the reaction mixture was stirred for 5 min at ambient temperature.  $Fe(acac)_3$  (31.8 mg, 15 mol %) was added in a single portion. After stirring the solution for additional 5 min, allene **88a** (328 mg, 1.80 mmol) was added as a solution in THF (1.2 mL) in one portion. An *in situ* IR spectrum was acquired every 30 s for 2 h.

The KIE was determined by measuring initial rates from the increase of the peak at  $1643\text{ cm}^{-1}$ , which corresponds to a C=O vibration of product **89aa**. The absolute peak area was measured from  $1659$  to  $1635\text{ cm}^{-1}$  with a one-point baseline at  $1659\text{ cm}^{-1}$ . A linear fit was employed to derive the initial rates.

## 5. Experimental Part

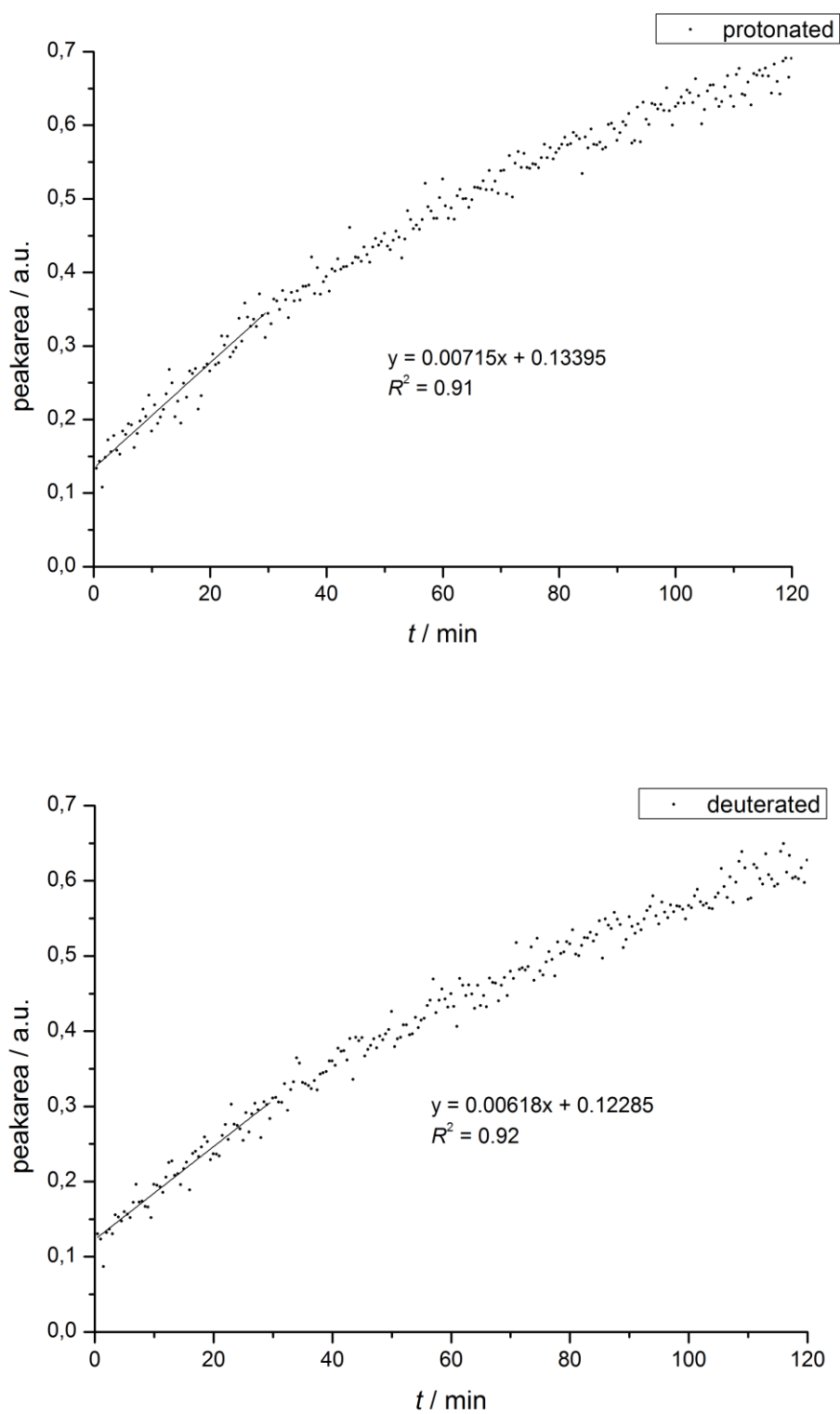
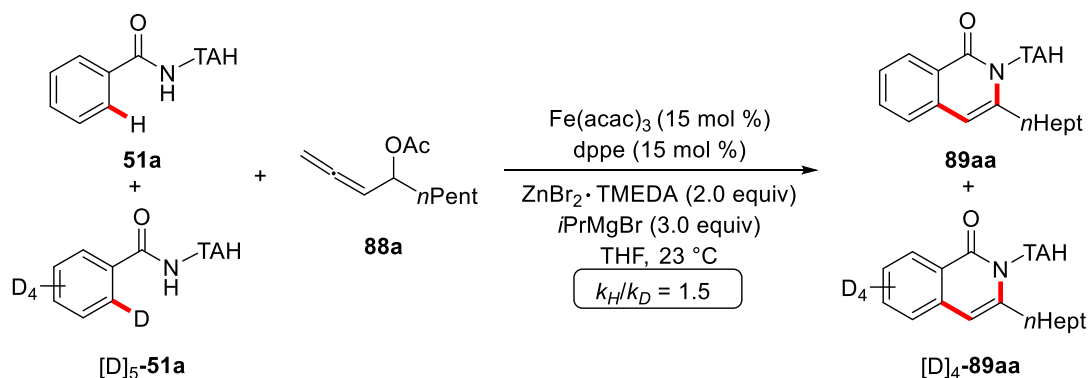


**Figure 5.1.** Plot of peak area at  $1643\text{ cm}^{-1}$  vs reaction time for **89aa** (top) and  $[D]_5$ -**89aa** (bottom).

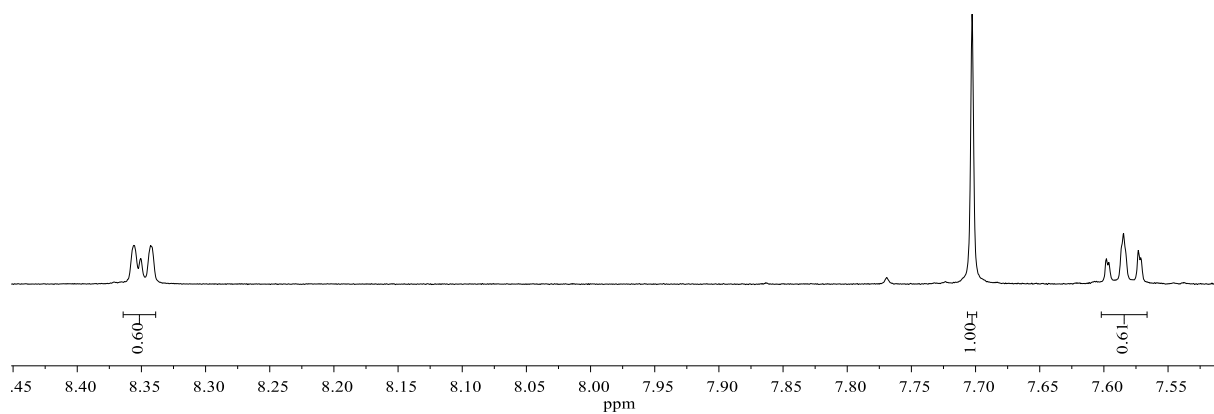
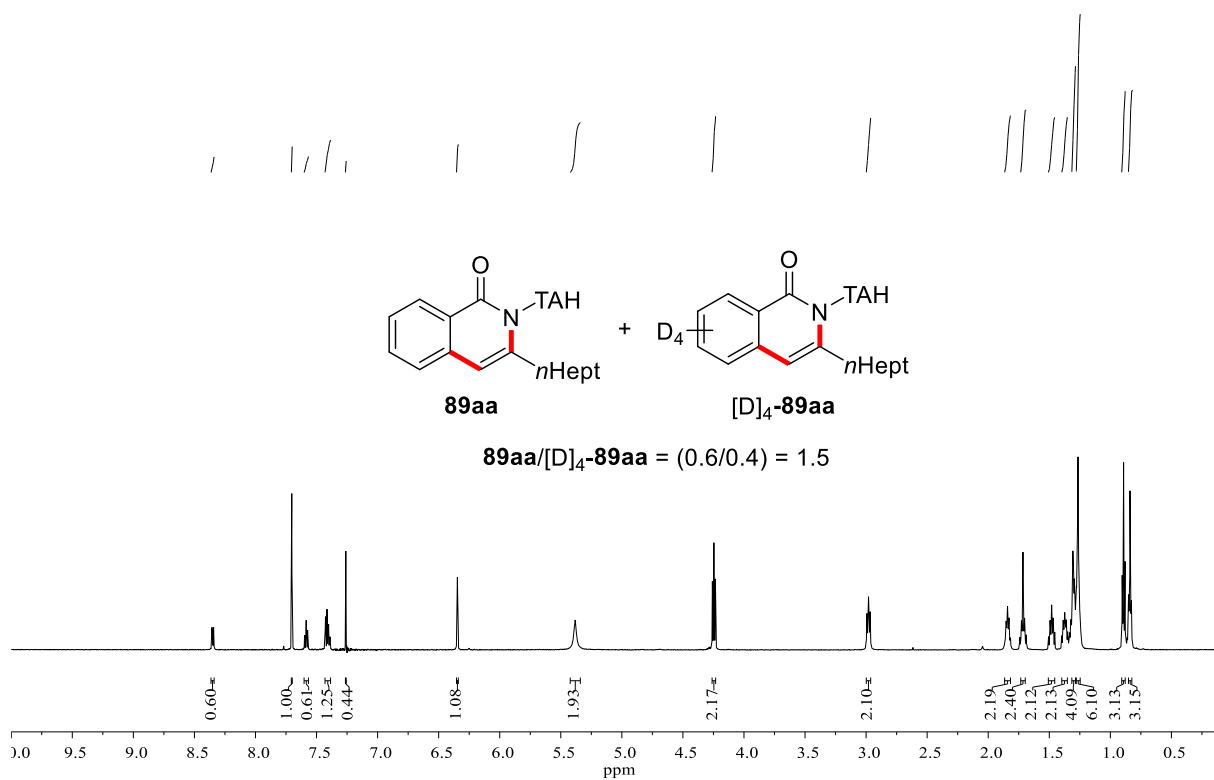
## 5. Experimental Part

### Intermolecular KIE Measurement



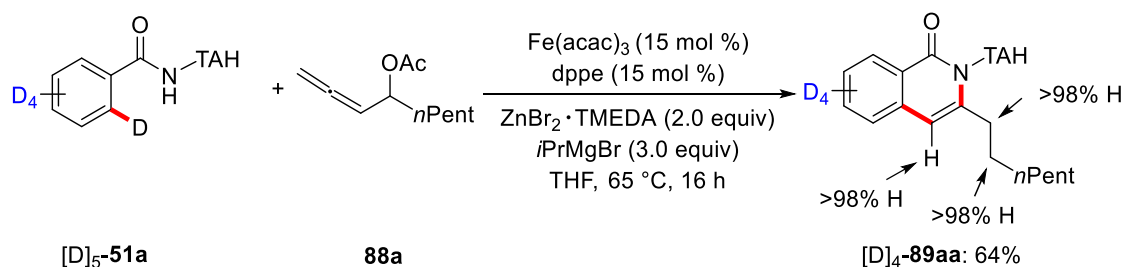
To a stirred solution of **51a** (43.0 mg, 0.15 mmol), **[D]<sub>5</sub>-51a** (43.7 mg, 0.15 mmol),  $\text{ZnBr}_2 \cdot \text{TMEDA}$  (206 mg, 0.60 mmol) and  $\text{dppe}$  (17.9 mg, 15 mol %) in THF (0.6 mL),  $i\text{PrMgBr}$  (3.0 M in THF, 300  $\mu\text{L}$ , 0.9 mmol) was added in one portion and the reaction mixture was stirred for 5 min at ambient temperature.  $\text{Fe}(\text{acac})_3$  (15.9 mg, 15 mol %) was added in a single portion. After stirring the solution for additional 5 min, allene **88a** (164 mg, 0.90 mmol) was added as a solution in THF (0.6 mL) in one portion. After stirring for 45 min, sat. aqueous  $\text{NH}_4\text{Cl}$  (2.0 mL) was added to the reaction mixture, which was then extracted with  $\text{CH}_2\text{Cl}_2$  ( $3 \times 15$  mL). The combined organic extracts were dried over  $\text{Na}_2\text{SO}_4$ , filtered and concentrated. The crude product was purified by column chromatography ( $n\text{hexane}/\text{EtOAc} = 3/1$ ). The mixture was analyzed by  $^1\text{H}$ -NMR spectroscopy to determine the ratio of **89aa**/**[D]<sub>4</sub>-89aa**.

## 5. Experimental Part



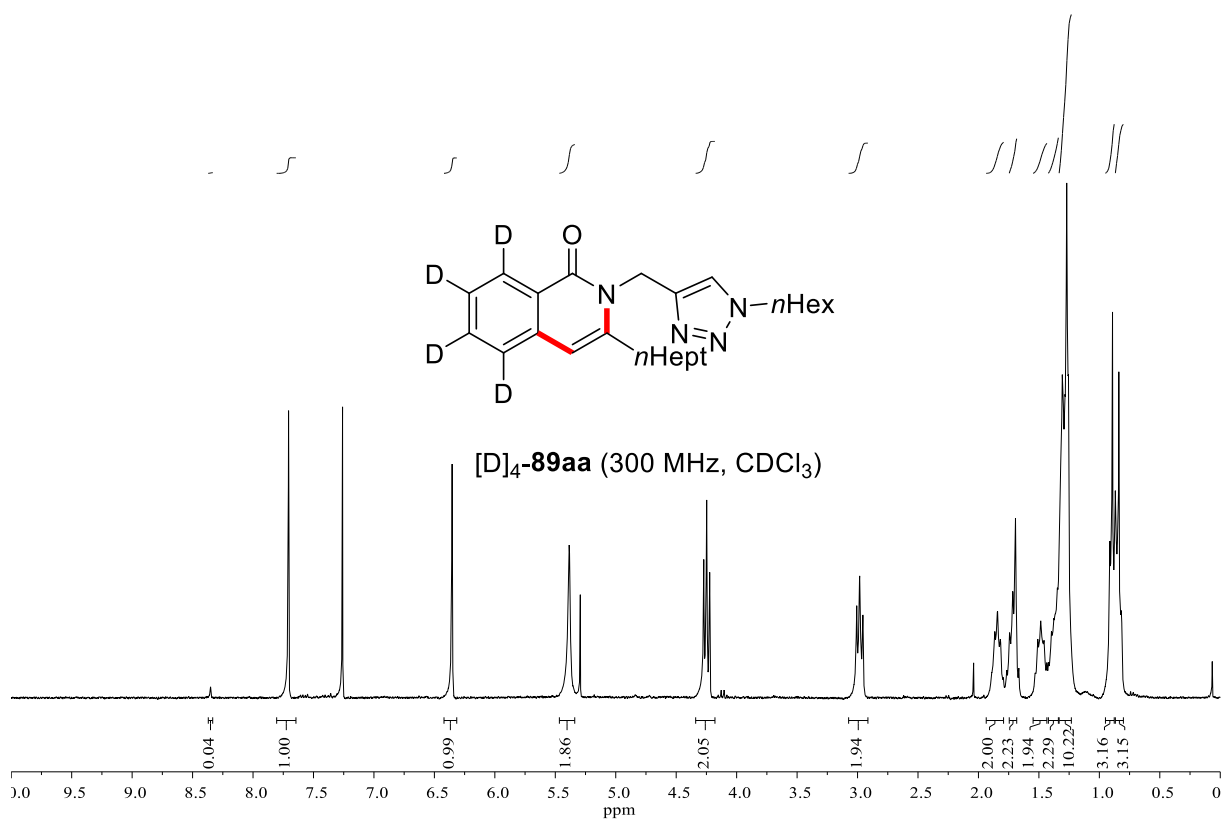
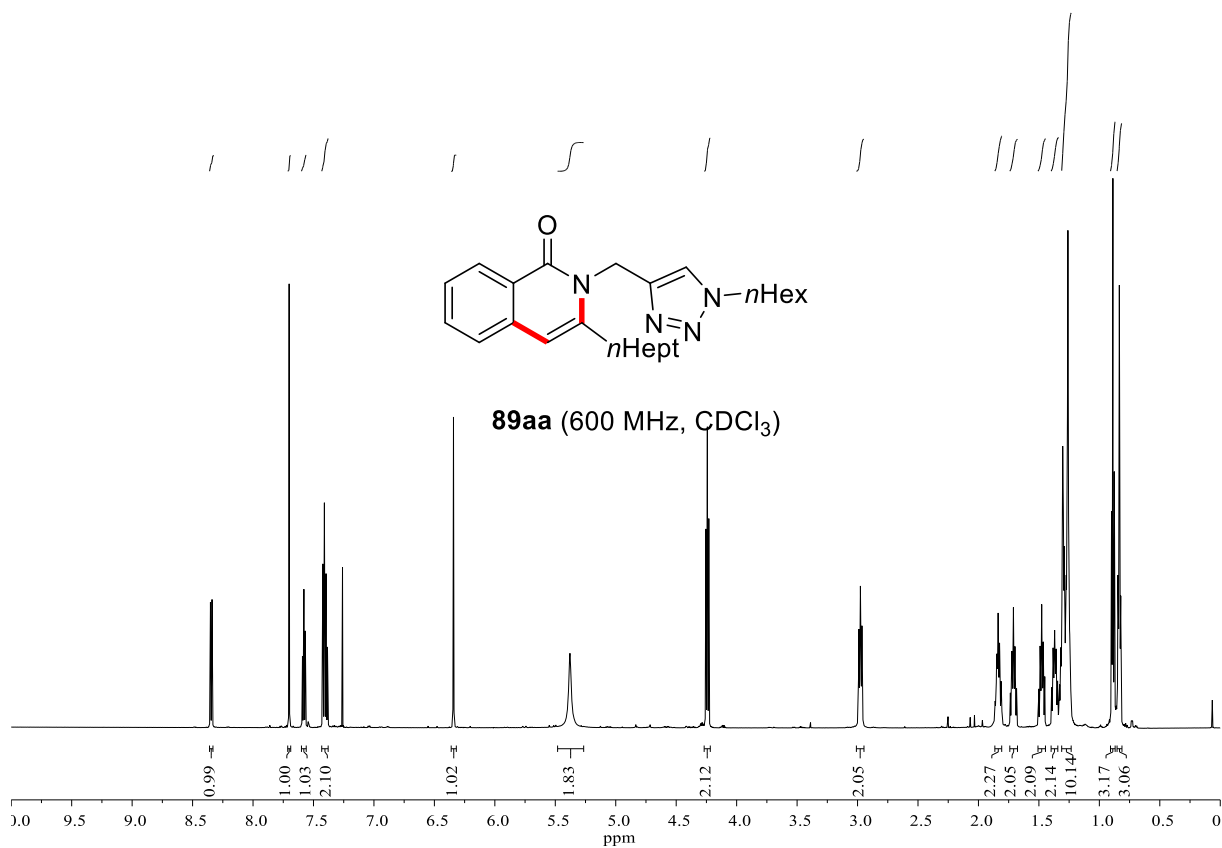
## 5. Experimental Part

### Experiments with Isotopically-labelled Substrates

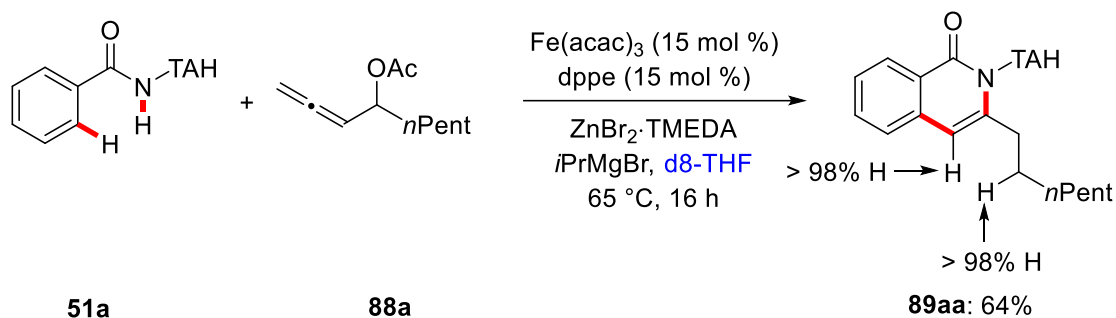


To a stirred solution of  $[D]_5\text{-51a}$  (87.4 mg, 0.30 mmol),  $\text{ZnBr}_2 \cdot \text{TMEDA}$  (206 mg, 0.60 mmol), dppe (17.9 mg, 15 mol %) in THF (0.20 mL),  $i\text{PrMgBr}$  (3.0 M in 2-MeTHF, 300  $\mu\text{L}$ , 0.90 mmol) was added in one portion and the reaction mixture was stirred for 5 min at ambient temperature. Then,  $\text{Fe(acac)}_3$  (15.9 mg, 15 mol %) was added in a single portion. After stirring the solution for additional 5 min, a solution of allene **88a** (164 mg, 0.90 mmol) in THF (0.20 mL) was added in one portion. The mixture was placed in a pre-heated oil bath at 65  $^\circ\text{C}$ . After stirring for 16 h, sat. aqueous  $\text{NH}_4\text{Cl}$  (2.0 mL) was added to the reaction mixture, which was extracted with  $\text{CH}_2\text{Cl}_2$  ( $3 \times 15$  mL). The combined organic extracts were dried over  $\text{Na}_2\text{SO}_4$ , filtered and concentrated. Purification by column chromatography ( $n\text{hexane}/\text{EtOAc} = 3/1$ ) yielded  $[D]_4\text{-89aa}$  (79.2 mg, 64%) as white solid. **HR-MS** (ESI)  $m/z$  calcd for  $\text{C}_{25}\text{H}_{33}\text{N}_4\text{OD}_4$   $[\text{M}+\text{H}]^+$  413.3213, found 413.3201.

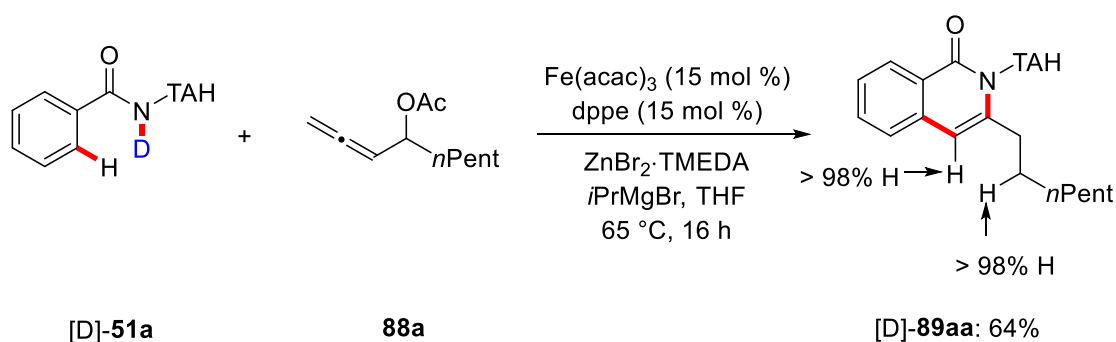
## 5. Experimental Part



## 5. Experimental Part



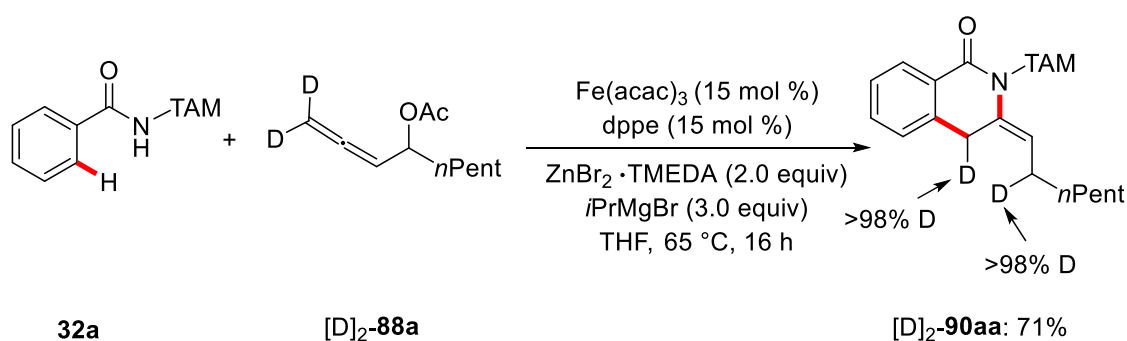
To a stirred solution of **51a** (85.9 mg, 0.30 mmol),  $\text{ZnBr}_2 \cdot \text{TMEDA}$  (206 mg, 0.60 mmol),  $\text{dppe}$  (17.9 mg, 15 mol %) in  $d_8\text{-THF}$  (0.20 mL),  $i\text{PrMgBr}$  (3.0 M in 2-MeTHF, 300  $\mu\text{L}$ , 0.90 mmol) was added in a single portion and the reaction mixture was stirred for 5 min at ambient temperature. Then,  $\text{Fe}(\text{acac})_3$  (15.9 mg, 15 mol %) was added in a single portion. After stirring the solution for additional 5 min, a solution of allene **88a** (166 mg, 0.90 mmol) in  $d_8\text{-THF}$  (0.20 mL) was added in one portion. The mixture was placed in a pre-heated oil bath at  $65^\circ\text{C}$ . After stirring for 16 h, sat. aqueous  $\text{NH}_4\text{Cl}$  (2.0 mL) was added to the reaction mixture, which was extracted with  $\text{CH}_2\text{Cl}_2$  ( $3 \times 15\text{ mL}$ ). The combined organic extracts were dried over  $\text{Na}_2\text{SO}_4$ , filtered and concentrated. The crude product was purified by column chromatography ( $n\text{hexane}/\text{EtOAc} = 3/1$ ) yielded **89aa** (76.4 mg, 64%).



To a stirred solution of **[D]-51a** (86.1 mg, 0.30 mmol),  $\text{ZnBr}_2 \cdot \text{TMEDA}$  (206 mg, 0.60 mmol),  $\text{dppe}$  (17.9 mg, 15 mol %) in  $\text{THF}$  (0.20 mL),  $i\text{PrMgBr}$  (3.0 M in 2-MeTHF, 300  $\mu\text{L}$ , 0.90 mmol) was added in a single portion and the reaction mixture was stirred for 5 min at ambient temperature. Then,  $\text{Fe}(\text{acac})_3$

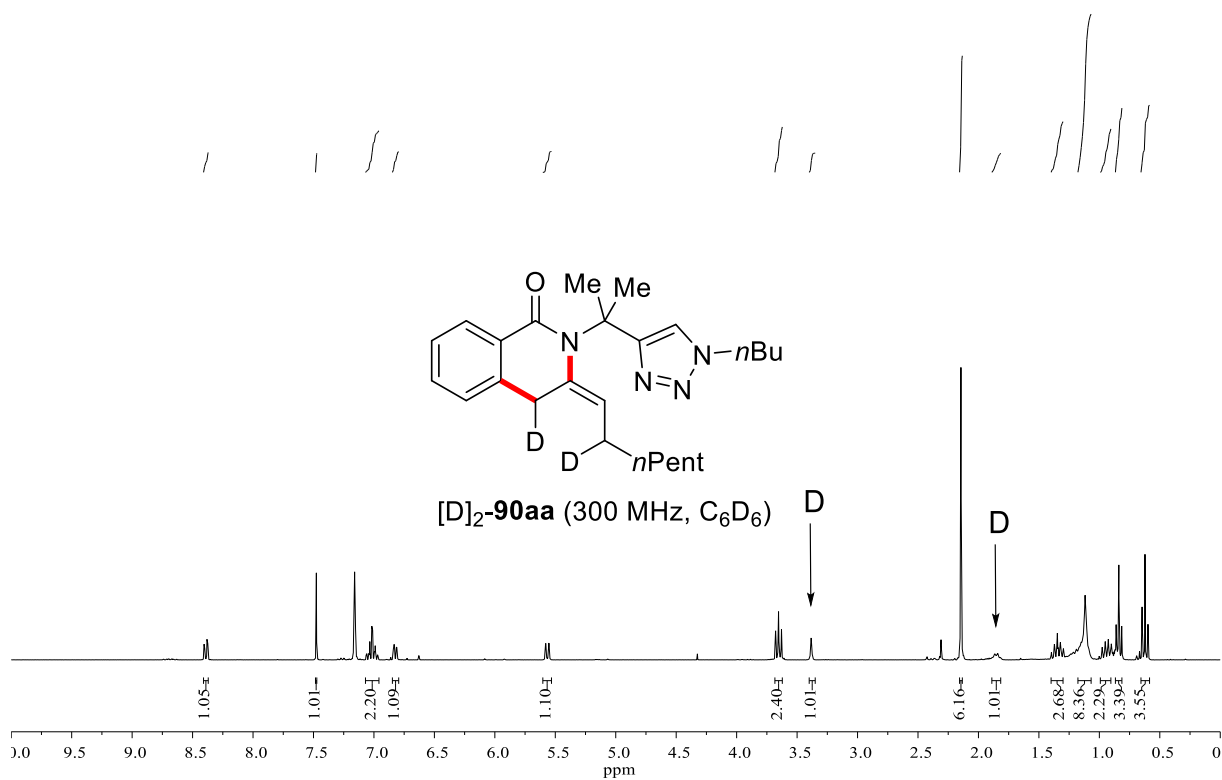
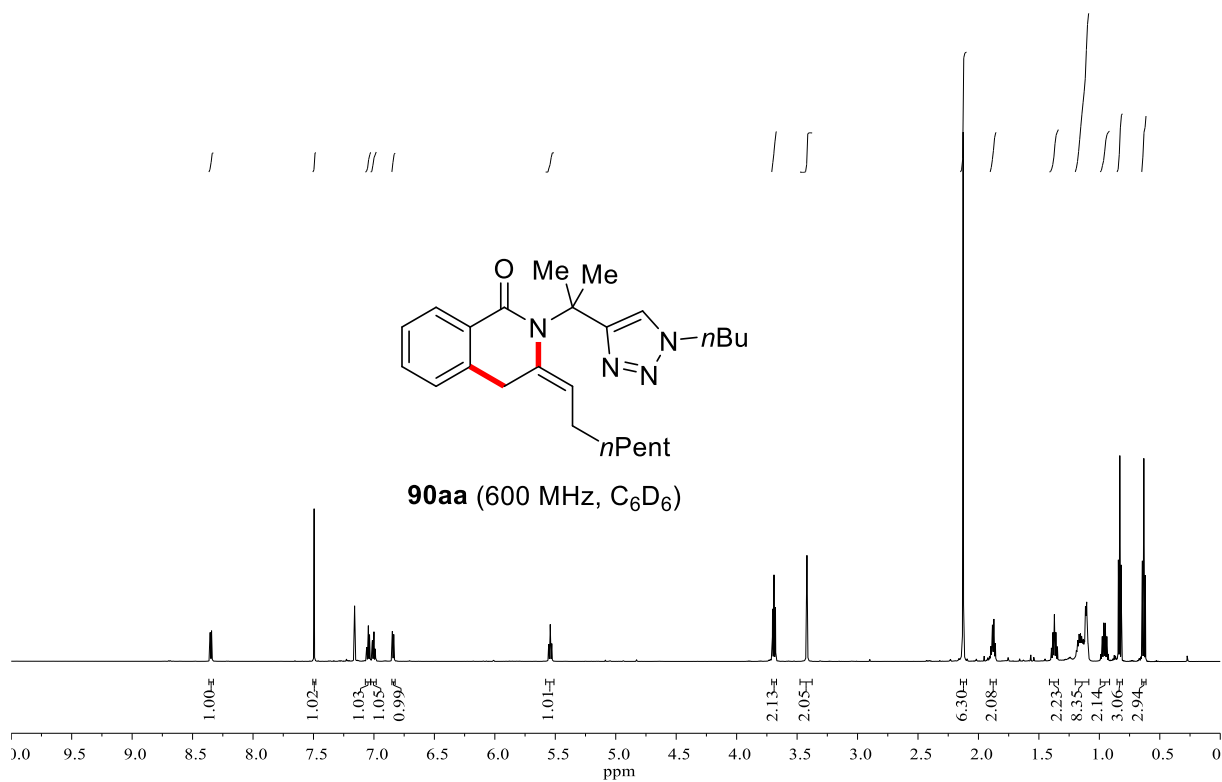
## 5. Experimental Part

(15.9 mg, 15 mol %) was added in a single portion. After stirring the solution for additional 5 min, a solution of allene **88a** (166 mg, 0.90 mmol) in THF (0.20 mL) was added in one portion. The mixture was placed in a pre-heated oil bath at 65 °C. After stirring for 16 h, sat. aqueous NH<sub>4</sub>Cl (2.0 mL) was added to the reaction mixture, which was extracted with CH<sub>2</sub>Cl<sub>2</sub> (3 × 15 mL). The combined organic extracts were dried over Na<sub>2</sub>SO<sub>4</sub>, filtered and concentrated. The crude product was purified by column chromatography (*n*hexane/EtOAc = 3/1) yielded [D]-**89aa** (76.4 mg, 64%).

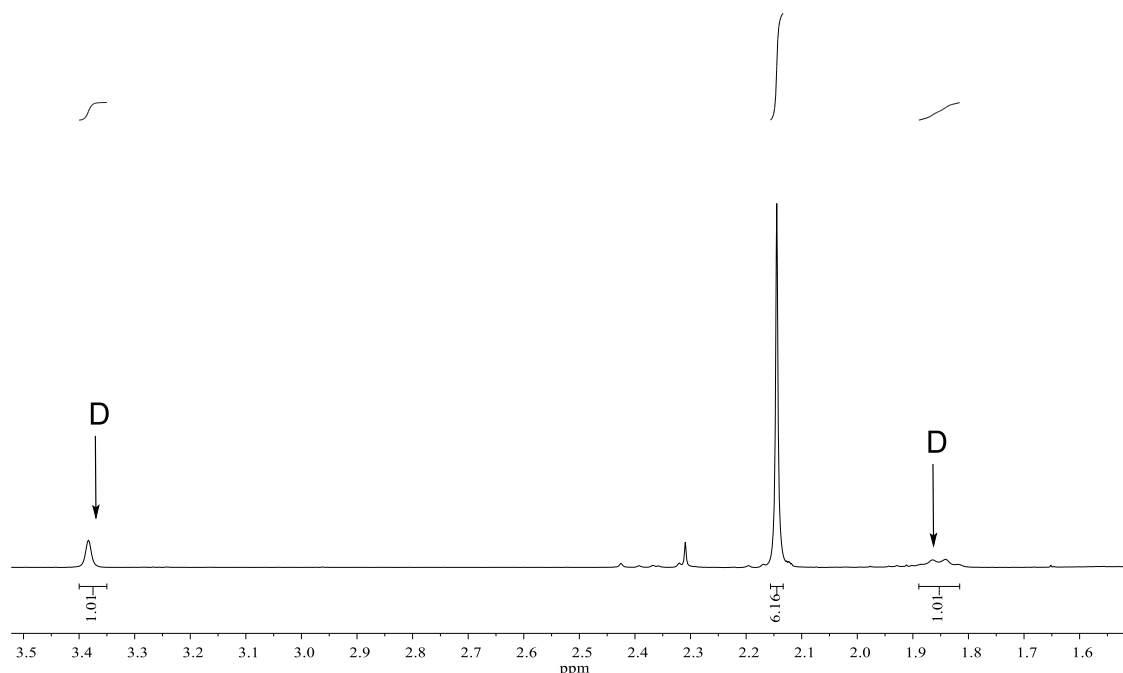


To a stirred solution of **32a** (85.9 mg, 0.30 mmol), ZnBr<sub>2</sub>·TMEDA (206 mg, 0.60 mmol), dppe (17.9 mg, 15 mol %) in THF (0.20 mL), *i*PrMgBr (3.0 M in 2-MeTHF, 300 μL, 0.90 mmol) was added in a single portion and the reaction mixture was stirred for 5 min at ambient temperature. Then, Fe(acac)<sub>3</sub> (15.9 mg, 15 mol %) was added in a single portion. After stirring the solution for additional 5 min, a solution of allene [D]<sub>2</sub>-**88a** (166 mg, 0.90 mmol) in THF (0.20 mL) was added in one portion. The mixture was placed in a pre-heated oil bath at 65 °C. After stirring for 16 h, sat. aqueous NH<sub>4</sub>Cl (2.0 mL) was added to the reaction mixture, which was extracted with CH<sub>2</sub>Cl<sub>2</sub> (3 × 15 mL). The combined organic extracts were dried over Na<sub>2</sub>SO<sub>4</sub>, filtered and concentrated. The crude product was purified by column chromatography (*n*hexane/EtOAc = 3/1) yielded [D]<sub>2</sub>-**90aa** (87.5 mg, 71%). **HR-MS** (ESI) *m/z* calcd for C<sub>25</sub>H<sub>35</sub>N<sub>4</sub>OD<sub>2</sub> [M+H]<sup>+</sup> 411.3087, found 411.3094.

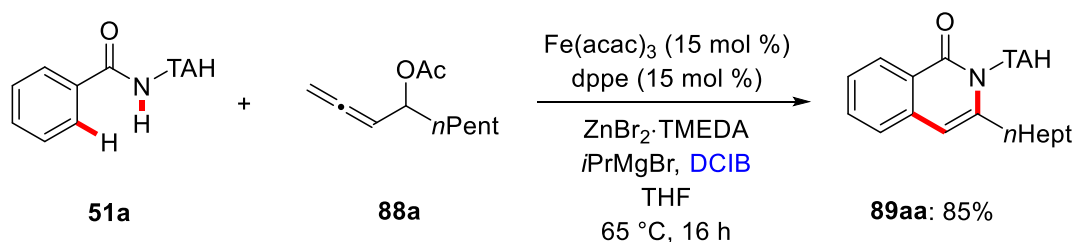
## 5. Experimental Part



## 5. Experimental Part



### Experiments with DCIB as Additive



To a stirred solution of **51a** (86.1 mg, 0.30 mmol),  $\text{ZnBr}_2\cdot\text{TMEDA}$  (206 mg, 0.60 mmol), dppe (17.9 mg, 15 mol %) in THF (0.20 mL),  $i\text{PrMgBr}$  (3.0 M in 2-MeTHF, 300  $\mu\text{L}$ , 0.90 mmol) was added in a single portion and the reaction mixture was stirred for 5 min at ambient temperature. Then,  $\text{Fe}(\text{acac})_3$  (15.9 mg, 15 mol %) was added in a single portion. After stirring the solution for additional 5 min, a solution of allene **88a** (166 mg, 0.90 mmol) and DCIB (76.2 mg, 0.60 mmol) in THF (0.20 mL) was added in one portion. The mixture was placed in a pre-heated oil bath at 65  $^\circ\text{C}$ . After stirring for 16 h, sat. aqueous  $\text{NH}_4\text{Cl}$  (2.0 mL) was added to the reaction mixture, which was extracted with  $\text{CH}_2\text{Cl}_2$  (3  $\times$  15 mL). The combined organic extracts were dried over  $\text{Na}_2\text{SO}_4$ ,

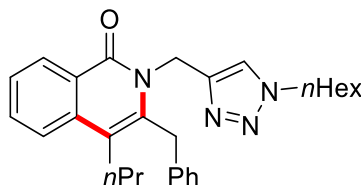
## 5. Experimental Part

filtered and concentrated. The crude product was purified by column chromatography (*n*hexane/EtOAc = 3/1) yielded **89aa** (101 mg, 85%).

### 5.4 Iron-Catalyzed C–H/N–H Annulation with Propargyl Acetates

#### 5.4.1 Analytical Data – Products 92

##### 3-Benzyl-2-[(1-*n*-hexyl-1*H*-1,2,3-triazol-4-yl)methyl]-4-*n*propylisoquinolin-1(2*H*)-one (**92aa**)



The general procedure **GPB** was followed using **51a** (85.9 mg, 0.30 mmol) and alkyne **88a** (130 mg, 0.60 mmol). Purification by column chromatography (*n*hexane/EtOAc = 3/2) yielded **92aa** (79.5 mg, 60%) as a white solid.

**M.p.** = 97–98 °C. **<sup>1</sup>H NMR** (600 MHz, CDCl<sub>3</sub>): δ = 8.49 (d, *J* = 8.0 Hz, 1H), 7.74–7.68 (m, 3H), 7.48 (t, *J* = 7.3 Hz, 1H), 7.33 (t, *J* = 7.7 Hz, 2H), 7.28–7.24 (m, 3H), 5.19 (br s, 2H), 4.61 (s, 2H), 4.26 (t, *J* = 7.3 Hz, 2H), 2.77–2.71 (m, 2H), 1.89–1.82 (m, 2H), 1.61–1.53 (m, 2H), 1.32–1.23 (m, 6H), 0.99 (t, *J* = 7.3 Hz, 3H), 0.84 (t, *J* = 6.7 Hz, 3H). **<sup>13</sup>C NMR** (126 MHz, CDCl<sub>3</sub>): δ = 162.7 (C<sub>q</sub>), 144.2 (C<sub>q</sub>), 137.4 (C<sub>q</sub>), 137.1 (C<sub>q</sub>), 136.7 (C<sub>q</sub>), 132.4 (CH), 129.1 (CH), 128.3 (CH), 128.0 (CH), 126.9 (CH), 126.2 (CH), 125.3 (C<sub>q</sub>), 124.0 (CH), 123.1 (CH), 116.4 (C<sub>q</sub>), 50.5 (CH<sub>2</sub>), 40.0 (CH<sub>2</sub>), 35.0 (CH<sub>2</sub>), 31.3 (CH<sub>2</sub>), 30.4 (CH<sub>2</sub>), 30.3 (CH<sub>2</sub>), 26.3 (CH<sub>2</sub>), 23.6 (CH<sub>2</sub>), 22.6 (CH<sub>2</sub>), 14.6 (CH<sub>3</sub>), 14.1 (CH<sub>3</sub>). **IR** (ATR): 3122, 2952, 2931, 1650, 1610, 1313, 1063, 776, 732, 715 cm<sup>-1</sup>. **MS** (EI) *m/z* (relative intensity): 442 (72) [M]<sup>+</sup>, 329 (32), 276 (86), 248 (100),

## 5. Experimental Part

242 (47), 112 (64). **HR-MS** (EI)  $m/z$  calcd for  $C_{28}H_{34}N_4O$   $[M]^+$  442.2733, found 442.2722.

### 5.4.2 Traceless Removal of TAH Group

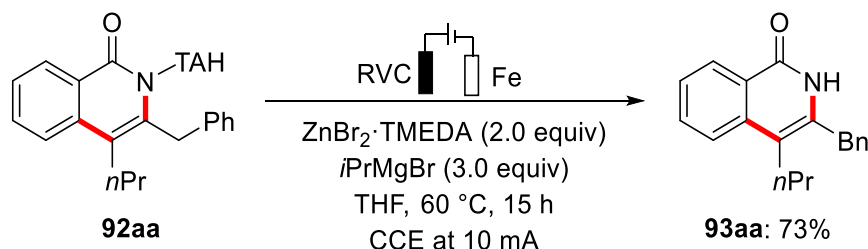


**Figure 5.2** Traceless removal of TAH group.

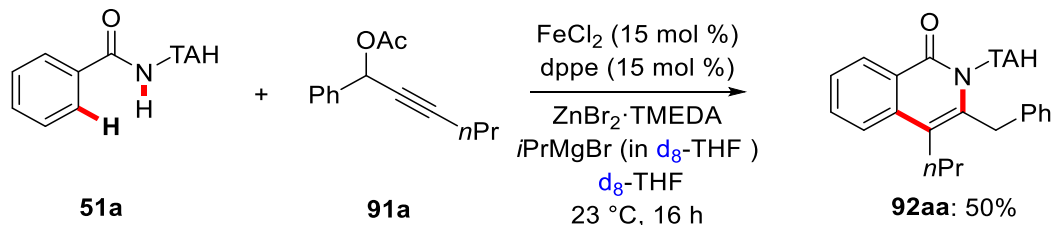
The general procedure **GPD** was followed using **92aa** (97.0 mg, 0.22 mmol). Purification by column chromatography ( $n$ hexane/EtOAc = 3/2) yielded **93aa** (54.0 mg, 73%) as a white solid.

**M.p.** = 194–196 °C.  **$^1H$  NMR** (300 MHz,  $CDCl_3$ ):  $\delta$  = 9.92 (s, 1H), 8.44 (d,  $J$  = 7.9 Hz, 1H), 7.72 (dd,  $J$  = 4.3, 2.0 Hz, 2H), 7.48 (ddd,  $J$  = 8.1, 5.4, 2.8 Hz, 1H), 7.38–7.18 (m, 5H), 4.08 (s, 2H), 2.81 (t,  $J$  = 8.1, 2H), 1.65–1.54 (m, 2H), 1.06 (t,  $J$  = 7.3 Hz, 3H).  **$^{13}C$  NMR** (126 MHz,  $CDCl_3$ ):  $\delta$  = 163.2 ( $C_q$ ), 138.3 ( $C_q$ ), 137.1 ( $C_q$ ), 135.5 ( $C_q$ ), 132.6 (CH), 129.1 (CH), 128.9 (CH), 128.0 (CH), 127.3 (CH), 125.9 (CH), 125.6 ( $C_q$ ), 123.3 (CH), 114.2 ( $C_q$ ), 36.8 ( $CH_2$ ), 29.0 ( $CH_2$ ), 23.5 ( $CH_2$ ), 14.4 ( $CH_3$ ). **IR** (ATR): 3022, 2954, 2871, 2031, 1653, 1630, 1606, 758, 709, 511  $cm^{-1}$ . **MS** (ESI)  $m/z$  (relative intensity): 168 (100), 278 (67)  $[M+H]^+$ , 577 (25)  $[2M+Na]^+$ . **HR-MS** (ESI)  $m/z$  calcd for  $C_{19}H_{19}NO$   $[M+H]^+$  278.1539, found 278.1538.

## 5. Experimental Part

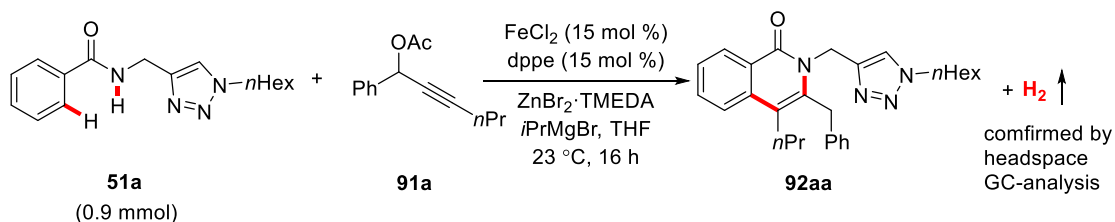
### 5.4.3 Mechanistic Studys

#### Reaction Using Deuterium-Labelled Solvent



To a stirred solution of **51a** (85.9 mg, 0.3 mmol),  $ZnBr_2 \cdot TMEDA$  (205 mg, 0.60 mmol) and dppe (17.9 mg, 15 mol %) in  $d_8$ -THF (0.4 mL),  $iPrMgBr$  (0.5 M in  $d_8$ -THF, 1.8 mL, 0.90 mmol) was added in one portion and the reaction mixture was stirred for 5 min at ambient temperature. Then,  $FeCl_2$  (5.7 mg, 15 mol %) was added in a single portion. After stirring for additional 5 min, a solution of alkyne **91a** (130 mg, 0.60 mmol) in  $d_8$ -THF (0.40 mL) was added in one portion. The reaction mixture was stirred at ambient temperature. After 16 h, sat. aqueous  $NH_4Cl$  (3.0 mL) was added and the reaction mixture was extracted with  $CH_2Cl_2$  ( $3 \times 15$  mL). The combined organic extracts were dried over  $Na_2SO_4$ , filtered and concentrated. Purification by column chromatography ( $n$ hexane/ $EtOAc$  = 3/2) yielded the annulated isoquinolone **92aa** (86.8 mg, 50%) as a white solid.

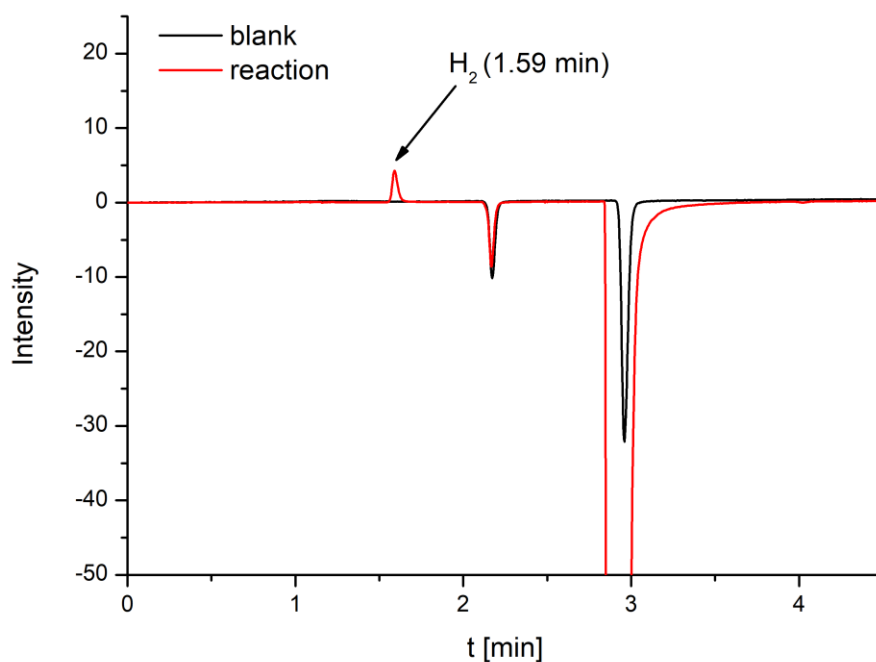
#### GC-Headspace Detection of $H_2$ for Standard Reaction



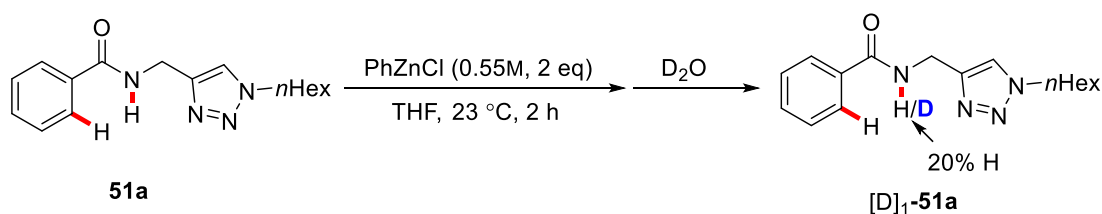
To a stirred solution of **51a** (0.9 mmol),  $ZnBr_2 \cdot TMEDA$  (2.0 equiv) and dppe (15 mol %) in THF (1.2 mL),  $iPrMgBr$  (3.0 M in 2-MeTHF, 3.0 equiv) was added in one portion and the reaction mixture was stirred for 5 min at ambient temperature. Then,  $FeCl_2$  (15 mol %) was added in a single portion. After

## 5. Experimental Part

stirring the solution for additional 5 min, alkyne **91a** (2.70 mmol, 3.0 equiv) was added as a solution in THF (1.2 mL). Then, the mixture was stirred at ambient temperature. After stirring for 16 h, the gas of headspace was injected to GC-  
Ms.

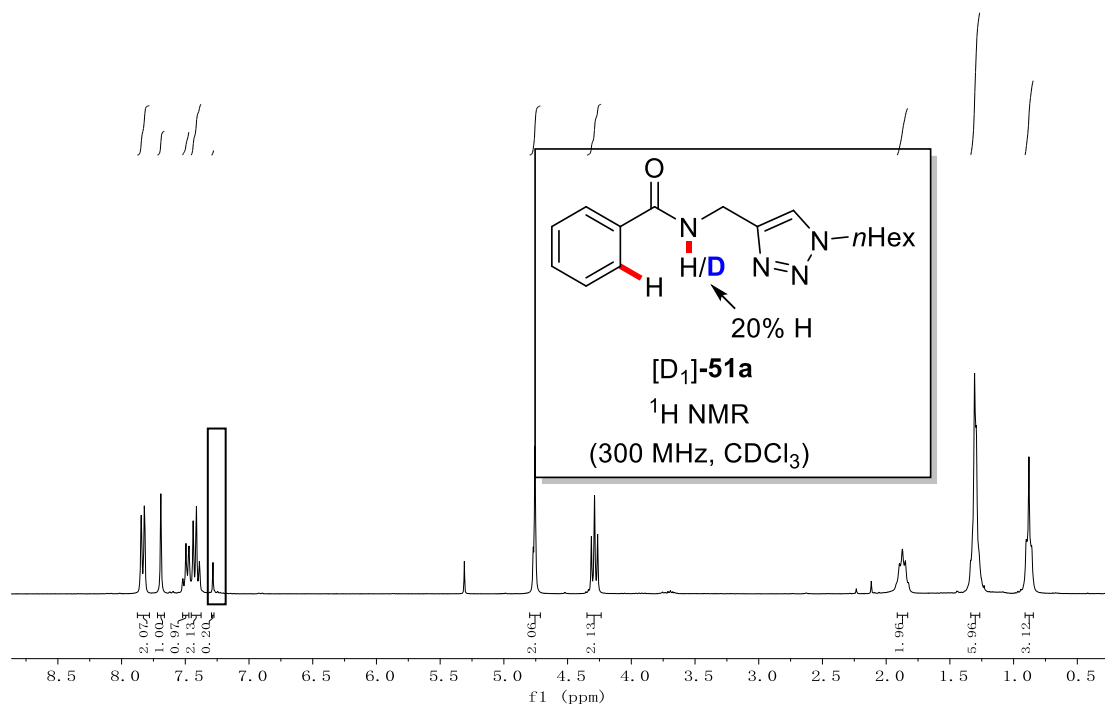


### Deprotonation of Substrate **51a** by PhZnCl

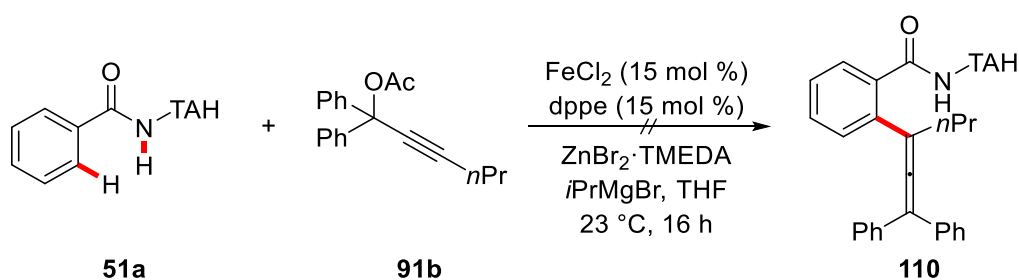


To a Schlenk tube charged with **51a** (85.9 mg, 0.30 mmol), PhZnCl (0.55 M in THF, 1.1 mL, 2.0 equiv) was added in one portion and the reaction mixture was stirred at ambient temperature. After 2 h, D<sub>2</sub>O (2.0 mL) was added and the mixture was extracted with CH<sub>2</sub>Cl<sub>2</sub> (3 × 15 mL). The combined organic extracts were dried over Na<sub>2</sub>SO<sub>4</sub>, filtered and concentrated under reduced pressure. Deuterium contents were determined by <sup>1</sup>H NMR spectroscopic analysis.

## 5. Experimental Part



### Reaction Using Propargyl Acetate **91b**



To a stirred solution of **51a** (85.9 mg, 0.30 mmol), ZnBr<sub>2</sub>·TMEDA (205 mg, 0.60 mmol) and dppe (17.9 mg, 15 mol %) in THF (0.40 mL), *i*PrMgBr (3.0 M in THF, 300  $\mu$ L, 0.90 mmol) was added in oneportion and the reaction mixture was stirred for 5 min at ambient temperature. Then, FeCl<sub>2</sub> (5.7 mg, 15 mol %) was added in a single portion. After stirring the solution for additional 5 min, alkyne **91b** (175 mg, 0.60 mmol) was added as a solution in THF (0.40 mL). Then, the mixture was stirred at ambient temperature. After stirring for 16 h, sat. aqueous NH<sub>4</sub>Cl (3.0 mL) was added and the reaction mixture was extracted with CH<sub>2</sub>Cl<sub>2</sub> (3  $\times$  15 mL). The combined organic extracts were dried over

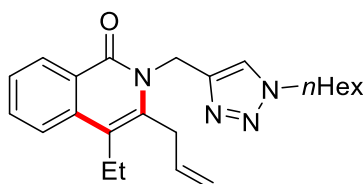
## 5. Experimental Part

Na<sub>2</sub>SO<sub>4</sub>, filtered and concentrated. Product **110** was not observed by <sup>1</sup>H NMR spectroscopic analysis.

### 5.5 Iron-Catalyzed C–H/C–C Activations

#### 5.5.1 Analytical Data – Products with Different N-Substituted Triazolyl Moieties

**3-Allyl-2-[(1-*n*-hexyl-1*H*-1,2,3-triazol-4-yl)methyl]-4-*n*-propylisoquinolin-1(2*H*)-one (95ag):**

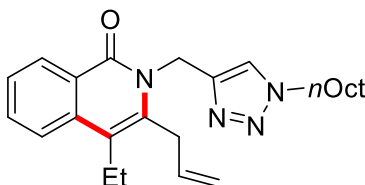


The general procedure **GPC** was followed using **51a** (85.9 mg, 0.30 mmol) and BCP **94g** (137 mg, 0.90 mmol). Purification by column chromatography (*n*hexane/EtOAc = 3/2) yielded **95ag** (90.8 mg, 80%) as colourless oil.

**<sup>1</sup>H NMR** (300 MHz, CDCl<sub>3</sub>):  $\delta$  = 8.44 (d, *J* = 7.8 Hz, 1H), 7.74 (s, 1H), 7.70–7.56 (m, 2H), 7.49–7.37 (m, 1H), 6.18–6.05 (m, 1H), 5.32 (s, 2H), 5.20 (dd, *J* = 10.3, 1.5 Hz, 1H), 5.02 (dd, *J* = 17.3, 1.5 Hz, 1H), 4.24 (t, *J* = 7.5 Hz, 2H), 3.89 (s, 2H), 2.71 (q, *J* = 7.5 Hz, 2H), 1.87–1.78 (m, 2H), 1.30–1.21 (m, 6H), 1.15 (t, *J* = 7.5 Hz, 3H), 0.81 (t, *J* = 6.9 Hz, 3H). **<sup>13</sup>C NMR** (126 MHz, CDCl<sub>3</sub>):  $\delta$  = 162.6 (C<sub>q</sub>), 144.4 (C<sub>q</sub>), 136.4 (C<sub>q</sub>), 136.4 (C<sub>q</sub>), 134.2 (CH), 132.3 (CH), 128.2 (CH), 126.0 (CH), 125.1 (C<sub>q</sub>), 124.0 (CH), 122.8 (CH), 117.1 (CH<sub>2</sub>), 117.1 (C<sub>q</sub>), 50.5 (CH<sub>2</sub>), 40.0 (CH<sub>2</sub>), 33.1 (CH<sub>2</sub>), 31.3 (CH<sub>2</sub>), 30.3 (CH<sub>2</sub>), 26.3 (CH<sub>2</sub>), 22.5 (CH<sub>2</sub>), 21.1 (CH<sub>2</sub>), 14.7 (CH<sub>3</sub>), 14.1 (CH<sub>3</sub>). **IR** (ATR): 2925, 2855, 1642, 1592, 1337, 1183, 1047, 968, 773, 678 cm<sup>-1</sup>. **MS** (ESI) *m/z* (relative intensity): 379 (100) [M+H]<sup>+</sup>, 401 (21) [M+Na]<sup>+</sup>, 757 (36) [2M+H]<sup>+</sup>, 779 (50) [2M+Na]<sup>+</sup>. **HR-MS** (ESI) *m/z* calcd for C<sub>23</sub>H<sub>31</sub>N<sub>4</sub>O [M+H]<sup>+</sup> 379.2492, found 379.2492.

## 5. Experimental Part

### 3-Allyl-2-[(1-octyl-1*H*-1,2,3-triazol-4-yl)methyl]-4-ethylisoquinolin-1(2*H*)-one (**95bg**):

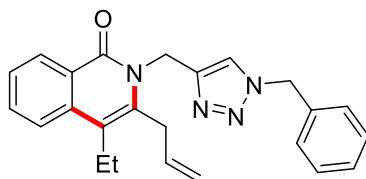


The general procedure **GPC** was followed using **51b** (98.6 mg, 0.30 mmol) and BCP **94g** (137 mg, 0.90 mmol). Purification by column chromatography (*n*hexane/EtOAc = 3/2) yielded **95bg** (82.9 mg, 68%) as colourless oil.

**<sup>1</sup>H NMR** (400 MHz, CDCl<sub>3</sub>):  $\delta$  = 8.44 (d,  $J$  = 7.8 Hz, 1H), 7.74 (s, 1H), 7.68–7.60 (m, 2H), 7.43 (d,  $J$  = 8.1 Hz, 1H), 6.11 (ddt,  $J$  = 17.3, 10.3, 4.7 Hz, 1H), 5.32 (s, 2H), 5.20 (dd,  $J$  = 10.3, 1.5 Hz, 1H), 5.02 (dd,  $J$  = 17.3, 1.5 Hz, 1H), 4.22 (t,  $J$  = 7.4 Hz, 2H), 3.90 (s, 2H), 2.71 (q,  $J$  = 7.5 Hz, 2H), 1.82 (t,  $J$  = 7.4 Hz, 2H), 1.28–1.18 (m, 10H), 1.15 (t,  $J$  = 7.5 Hz, 3H), 0.81 (d,  $J$  = 7.1 Hz, 3H). **<sup>13</sup>C NMR** (101 MHz, CDCl<sub>3</sub>):  $\delta$  = 162.8 (C<sub>q</sub>), 144.5 (C<sub>q</sub>), 136.6 (C<sub>q</sub>), 136.5 (C<sub>q</sub>), 134.3 (CH), 132.5 (CH), 128.3 (CH), 126.1 (CH), 125.2 (C<sub>q</sub>), 124.2 (CH), 122.9 (CH), 117.2 (CH<sub>2</sub>), 117.2 (C<sub>q</sub>), 50.5 (CH<sub>2</sub>), 39.9 (CH<sub>2</sub>), 33.0 (CH<sub>2</sub>), 31.8 (CH<sub>2</sub>), 30.3 (CH<sub>2</sub>), 29.1 (CH<sub>2</sub>), 29.0 (CH<sub>2</sub>), 26.6 (CH<sub>2</sub>), 22.7 (CH<sub>2</sub>), 21.0 (CH<sub>2</sub>), 14.6 (CH<sub>3</sub>), 14.2 (CH<sub>3</sub>). **IR** (ATR): 2926, 2855, 1643, 1592, 1428, 1336, 1047, 916, 773, 700 cm<sup>-1</sup>. **MS** (ESI)  $m/z$  (relative intensity): 407 (100) [M+H]<sup>+</sup>, 429 (21) [M+Na]<sup>+</sup>, 769 (50) [2M+H]<sup>+</sup>, 835 (54) [2M+Na]<sup>+</sup>. **HR-MS** (ESI)  $m/z$  calcd for C<sub>25</sub>H<sub>35</sub>N<sub>4</sub>O [M+H]<sup>+</sup> 407.2805, found 407.2805.

## 5. Experimental Part

### 3-Allyl-2-[(1-benzyl-1*H*-1,2,3-triazol-4-yl)methyl]-4-ethylisoquinolin-1(2*H*)-one (**95cg**):

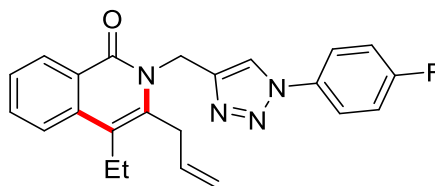


The general procedure **GPC** was followed using **51c** (87.7 mg, 0.30 mmol) and BCP **94g** (137 mg, 0.90 mmol). Purification by column chromatography (*n*hexane/EtOAc = 3/2) yielded **95cg** (70.4 mg, 61%) as colourless oil.

**<sup>1</sup>H NMR** (400 MHz, CDCl<sub>3</sub>):  $\delta$  = 8.41 (dd,  $J$  = 8.0, 0.7 Hz, 1H), 7.72 (s, 1H), 7.68–7.61 (m, 2H), 7.41 (ddd,  $J$  = 8.1, 6.4, 1.8 Hz, 1H), 7.32–7.27 (m, 3H), 7.24–7.21 (m, 2H), 6.16–6.06 (m, 1H), 5.41 (s, 2H), 5.30 (s, 2H), 5.19 (dd,  $J$  = 10.3, 1.3 Hz, 1H), 5.01 (dd,  $J$  = 17.3, 1.3 Hz, 1H), 3.89 (s, 2H), 2.70 (q,  $J$  = 7.5 Hz, 2H), 1.15 (t,  $J$  = 7.5 Hz, 3H). **<sup>13</sup>C NMR** (101 MHz, CDCl<sub>3</sub>):  $\delta$  = 162.7 (C<sub>q</sub>), 144.9 (C<sub>q</sub>), 136.5 (C<sub>q</sub>), 136.3 (C<sub>q</sub>), 134.6 (C<sub>q</sub>), 134.2 (CH), 132.4 (CH), 129.1 (CH), 128.8 (CH), 128.3 (CH), 128.2 (CH), 126.0 (CH), 125.1 (C<sub>q</sub>), 124.2 (CH), 122.9 (CH), 117.1 (CH<sub>2</sub>), 117.1 (C<sub>q</sub>), 54.2 (CH<sub>2</sub>), 39.8 (CH<sub>2</sub>), 33.0 (CH<sub>2</sub>), 20.9 (CH<sub>2</sub>), 14.6 (CH<sub>3</sub>). **IR** (ATR): 2958, 2928, 1642, 1602, 1472, 1433, 1302, 1033, 812, 778 cm<sup>-1</sup>. **MS** (ESI)  $m/z$  (relative intensity): 385 (100) [M+H]<sup>+</sup>, 407 (23) [M+Na]<sup>+</sup>, 769 (35) [2M+H]<sup>+</sup>, 791 (48) [2M+Na]<sup>+</sup>. **HR-MS** (ESI)  $m/z$  calcd for C<sub>24</sub>H<sub>25</sub>N<sub>4</sub>O [M+H]<sup>+</sup> 385.2023, found 385.2022.

## 5. Experimental Part

### 3-Allyl-4-ethyl-2-[[1-(4-fluorophenyl)-1*H*-1,2,3-triazol-4-yl]methyl]isoquinolin-1(2*H*)-one (95rg):

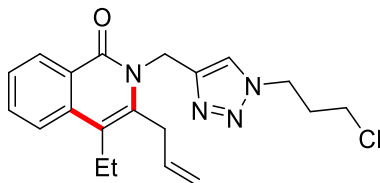


The general procedure **GPC** was followed using **51r** (88.9 mg, 0.30 mmol) and BCP **94g** (137 mg, 0.90 mmol). Purification by column chromatography (*n*hexane/EtOAc = 3/2) yielded **95rg** (69.9 mg, 60%) as a white solid.

**M.p.** = 138–139 °C. **<sup>1</sup>H NMR** (400 MHz, CDCl<sub>3</sub>): δ = 8.46 (ddd, *J* = 8.1, 1.4, 0.7 Hz, 1H), 8.21 (s, 1H), 7.73–7.65 (m, 4H), 7.46 (ddd, *J* = 8.1, 6.4, 1.8 Hz, 1H), 7.19–7.12 (m, 2H), 6.17 (ddt, *J* = 17.3, 10.3, 4.7 Hz, 1H), 5.42 (s, 2H), 5.26 (dd, *J* = 10.3, 1.3 Hz, 1H), 5.08 (dd, *J* = 17.3, 1.3 Hz, 1H), 3.95 (s, 2H), 2.74 (q, *J* = 7.5 Hz, 2H), 1.18 (t, *J* = 7.5 Hz, 3H). **<sup>13</sup>C NMR** (101 MHz, CDCl<sub>3</sub>): δ = 162.9 (C<sub>q</sub>), 162.5 (d, <sup>1</sup>*J*<sub>C-F</sub> = 249.1 Hz, C<sub>q</sub>), 145.4 (C<sub>q</sub>), 136.6 (C<sub>q</sub>), 136.3 (C<sub>q</sub>), 134.2 (CH), 133.4 (d, <sup>4</sup>*J*<sub>C-F</sub> = 3.3 Hz, C<sub>q</sub>), 132.6 (CH), 128.3 (CH), 126.2 (CH), 125.2 (C<sub>q</sub>), 123.0 (CH), 122.8 (CH), 122.6 (d, <sup>3</sup>*J*<sub>C-F</sub> = 8.6 Hz, CH), 117.4 (C<sub>q</sub>), 117.4 (CH<sub>2</sub>), 116.8 (d, <sup>2</sup>*J*<sub>C-F</sub> = 23.3 Hz, CH), 39.9 (CH<sub>2</sub>), 33.1 (CH<sub>2</sub>), 21.0 (CH<sub>2</sub>), 14.6 (CH<sub>3</sub>). **<sup>19</sup>F NMR** (377 MHz, CDCl<sub>3</sub>): δ = −112.25 (tt, *J* = 8.4, 4.6 Hz). **IR** (ATR): 3081, 2969, 2930, 1639, 1598, 1431, 1313, 1232, 1042, 837 cm<sup>−1</sup>. **MS** (ESI) *m/z* (relative intensity): 389 (100) [M+H]<sup>+</sup>, 777 (24) [2M+H]<sup>+</sup>, 799 (35) [2M+Na]<sup>+</sup>. **HR-MS** (ESI) *m/z* calcd for C<sub>23</sub>H<sub>22</sub>N<sub>4</sub>OF [M+H]<sup>+</sup> 389.1772, found 389.1774.

## 5. Experimental Part

### 3-Allyl-2-([1-(3-chloropropyl)-1*H*-1,2,3-triazol-4-yl]methyl)-4-ethylisoquinolin-1(2*H*)-one (**95dg**):

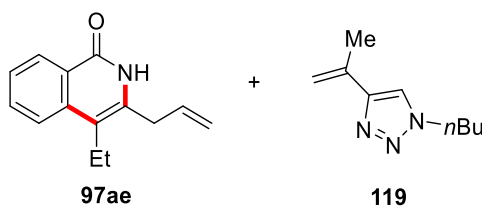


The general procedure **GPC** was followed using **51d** (86.3 mg, 0.30 mmol) and BCP **94g** (137 mg, 0.90 mmol). Purification by column chromatography (*n*hexane/EtOAc = 3/2) yielded **95dg** (55.7 mg, 50%) as colourless oil.

**<sup>1</sup>H NMR** (400 MHz, CDCl<sub>3</sub>):  $\delta$  = 8.45 (d,  $J$  = 8.1 Hz, 1H), 7.81 (s, 1H), 7.71–7.63 (m, 2H), 7.45 (d,  $J$  = 8.1 Hz, 1H), 6.13 (ddt,  $J$  = 17.3, 10.3, 4.7 Hz, 1H), 5.33 (s, 2H), 5.23 (dd,  $J$  = 10.3, 1.9 Hz, 1H), 5.04 (dd,  $J$  = 17.3, 1.9 Hz, 1H), 4.45 (t,  $J$  = 6.7 Hz, 2H), 3.90 (s, 2H), 3.50 (t,  $J$  = 6.1 Hz, 2H), 2.73 (q,  $J$  = 7.5 Hz, 2H), 2.33 (q,  $J$  = 6.7 Hz, 2H), 1.17 (t,  $J$  = 7.5 Hz, 3H). **<sup>13</sup>C NMR** (101 MHz, CDCl<sub>3</sub>):  $\delta$  = 162.7 (C<sub>q</sub>), 144.6 (C<sub>q</sub>), 136.5 (C<sub>q</sub>), 136.3 (C<sub>q</sub>), 134.2 (CH), 132.5 (CH), 128.3 (CH), 126.1 (CH), 125.1 (C<sub>q</sub>), 124.8 (CH), 122.9 (CH), 117.2 (C<sub>q</sub>), 117.2 (CH<sub>2</sub>), 47.2 (CH<sub>2</sub>), 41.3 (CH<sub>2</sub>), 39.8 (CH<sub>2</sub>), 33.0 (CH<sub>2</sub>), 32.6 (CH<sub>2</sub>), 21.0 (CH<sub>2</sub>), 14.6 (CH<sub>3</sub>). **IR** (ATR): 2965, 1710, 1611, 1590, 1428, 1338, 1221, 1047, 774, 700 cm<sup>-1</sup>. **MS** (ESI)  $m/z$  (relative intensity): 371 (100) [<sup>35</sup>Cl, M+H]<sup>+</sup>, 763 (67) [<sup>35</sup>Cl, 2M+Na]<sup>+</sup>. **HR-MS** (ESI)  $m/z$  calcd for C<sub>20</sub>H<sub>24</sub>N<sub>4</sub>O<sup>35</sup>Cl [M+H]<sup>+</sup> 371.1633, found 371.1629.

## 5. Experimental Part

### 3-Allyl-4-ethylisoquinolin-1(2*H*)-one (**97ae**) and 1-Butyl-4-(prop-1-en-2-yl)-1*H*-1,2,3-triazole (**119**):



The general procedure **GPC** was followed using **32a** (85.9 mg, 0.30 mmol) and BCP **94e** (177 mg, 0.90 mmol). Purification by column chromatography (*n*hexane/EtOAc/DCM = 3/1/1) yielded **97ae** (33.2 mg, 52%) as a white solid and **119** (25.7 mg, 52%) as colourless oil.

#### 3-Allyl-4-ethylisoquinolin-1(2*H*)-one (**97ae**):

**M.p.** = 109–110 °C. **<sup>1</sup>H NMR** (400 MHz, CDCl<sub>3</sub>): δ = 9.55 (s, 1H), 8.43 (dd, *J* = 8.0, 1.0 Hz, 1H), 7.72–7.67 (m, 2H), 7.45 (ddd, *J* = 8.1, 5.6, 2.6 Hz, 1H), 5.91 (ddt, *J* = 16.7, 10.0, 6.5 Hz, 1H), 5.34–5.12 (m, 2H), 3.42 (d, *J* = 6.5 Hz, 2H), 2.76 (q, *J* = 7.5 Hz, 2H), 1.19 (t, *J* = 7.5 Hz, 3H). **<sup>13</sup>C NMR** (101 MHz, CDCl<sub>3</sub>): δ = 163.1 (C<sub>q</sub>), 138.1 (C<sub>q</sub>), 133.9 (C<sub>q</sub>), 133.4 (CH), 132.8 (CH), 128.1 (CH), 126.0 (CH), 125.4 (C<sub>q</sub>), 123.1 (CH), 119.2 (CH<sub>2</sub>), 115.5 (C<sub>q</sub>), 35.3 (CH<sub>2</sub>), 19.8 (CH<sub>2</sub>), 14.8 (CH<sub>3</sub>). **IR** (ATR): 2965, 2932, 1726, 1654, 1607, 1552, 1469, 1355, 914, 773 cm<sup>-1</sup>. **MS** (ESI) *m/z* (relative intensity): 214 (100) [M+H]<sup>+</sup>, 256 (64), 321 (77), 449 (54) [2M+Na]<sup>+</sup>. **HR-MS** (ESI) *m/z* calcd for C<sub>14</sub>H<sub>16</sub>NO [M+H]<sup>+</sup> 214.1226, found 214.1227.

#### 1-Butyl-4-(prop-1-en-2-yl)-1*H*-1,2,3-triazole (**119**):

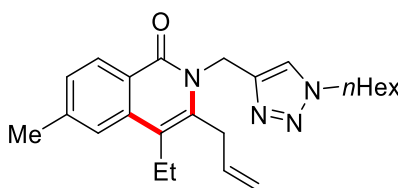
**<sup>1</sup>H NMR** (400 MHz, CDCl<sub>3</sub>): δ = 7.47 (s, 1H), 5.69 (s, 1H), 5.09 (s, 1H), 4.34 (t, *J* = 7.2 Hz, 2H), 2.14 (d, *J* = 1.2 Hz, 3H), 1.89 (p, *J* = 7.4 Hz, 2H), 1.37 (h, *J* = 7.4 Hz, 2H), 0.96 (t, *J* = 7.4 Hz, 3H). **<sup>13</sup>C NMR** (101 MHz, CDCl<sub>3</sub>): δ = 148.9 (C<sub>q</sub>), 133.9 (C<sub>q</sub>), 119.5 (CH), 112.4 (CH<sub>2</sub>), 50.1 (CH<sub>2</sub>), 32.5 (CH<sub>2</sub>), 20.8 (CH<sub>3</sub>), 19.9 (CH<sub>2</sub>), 13.6 (CH<sub>3</sub>). **IR** (ATR): 3124, 2959, 2933, 2873, 1640, 1456, 1228,

## 5. Experimental Part

1127, 1046, 892,  $\text{cm}^{-1}$ . **MS** (ESI)  $m/z$  (relative intensity): 166 (100)  $[\text{M}+\text{H}]^+$ , 188 (54)  $[\text{M}+\text{Na}]^+$ . **HR-MS** (ESI)  $m/z$  calcd for  $\text{C}_9\text{H}_{16}\text{N}_3$   $[\text{M}+\text{H}]^+$  166.1339, found 166.1341.

### 5.5.2 Analytical Data – Isoquinolone 95

**3-Allyl-4-ethyl-2-[(1-hexyl-1*H*-1,2,3-triazol-4-yl)methyl]-6-methyisoquinolin-1(2*H*)-one (95eg):**

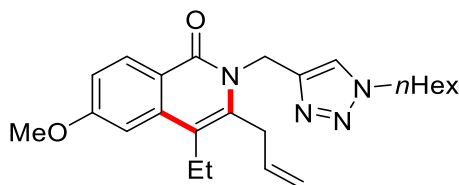


The general procedure **GPC** was followed using **51e** (90.1 mg, 0.30 mmol) and BCP **94g** (137 mg, 0.90 mmol). Purification by column chromatography (*n*hexane/EtOAc = 3/2) yielded **95eg** (70.7 mg, 60%) as colourless oil.

**$^1\text{H}$  NMR** (300 MHz,  $\text{CDCl}_3$ ):  $\delta$  = 8.36 (d,  $J$  = 8.2 Hz, 1H), 7.77 (s, 1H), 7.47 (s, 1H), 7.37–7.26 (m, 1H), 6.15 (ddt,  $J$  = 17.3, 10.3, 4.6 Hz, 1H), 5.34 (s, 2H), 5.23 (dd,  $J$  = 10.3, 1.6 Hz, 1H), 5.05 (dd,  $J$  = 17.3, 1.6 Hz, 1H), 4.27 (t,  $J$  = 7.4 Hz, 2H), 3.91 (d,  $J$  = 4.6 Hz, 2H), 2.73 (q,  $J$  = 7.5 Hz, 2H), 2.51 (s, 3H), 2.03–1.72 (m, 2H), 1.33–1.22 (m, 6H), 1.18 (t,  $J$  = 7.5 Hz, 3H), 0.85 (t,  $J$  = 7.0 Hz, 3H).  **$^{13}\text{C}$  NMR** (75 MHz,  $\text{CDCl}_3$ ):  $\delta$  = 162.7 ( $\text{C}_\text{q}$ ), 144.6 ( $\text{C}_\text{q}$ ), 142.8 ( $\text{C}_\text{q}$ ), 136.6 ( $\text{C}_\text{q}$ ), 136.4 ( $\text{C}_\text{q}$ ), 134.3 (CH), 128.3 (CH), 127.7 (CH), 124.1 (CH), 123.0 ( $\text{C}_\text{q}$ ), 122.7 (CH), 117.1 ( $\text{CH}_2$ ), 116.9 ( $\text{C}_\text{q}$ ), 50.4 ( $\text{CH}_2$ ), 39.8 ( $\text{CH}_2$ ), 33.0 ( $\text{CH}_2$ ), 31.2 ( $\text{CH}_2$ ), 30.2 ( $\text{CH}_2$ ), 26.2 ( $\text{CH}_2$ ), 22.5 ( $\text{CH}_2$ ), 22.3 ( $\text{CH}_3$ ), 20.9 ( $\text{CH}_2$ ), 14.6 ( $\text{CH}_3$ ), 14.0 ( $\text{CH}_3$ ). **IR** (ATR): 2958, 2928, 1642, 1602, 1472, 1433, 1302, 1033, 812, 778  $\text{cm}^{-1}$ . **MS** (ESI)  $m/z$  (relative intensity): 393 (71)  $[\text{M}+\text{H}]^+$ , 415 (100)  $[\text{M}+\text{Na}]^+$ , 807 (48)  $[2\text{M}+\text{Na}]^+$ . **HR-MS** (ESI)  $m/z$  calcd for  $\text{C}_{24}\text{H}_{33}\text{N}_4\text{O}$   $[\text{M}+\text{H}]^+$  393.2649, found 393.2650.

## 5. Experimental Part

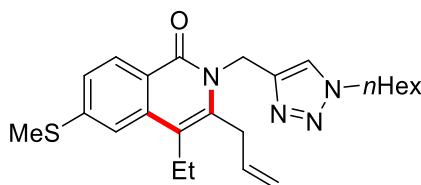
### 3-Allyl-4-ethyl-2-[(1-hexyl-1*H*-1,2,3-triazol-4-yl)methyl]-6-methoxyisoquinolin-1(2*H*)-one (**95gg**):



The general procedure **GPC** was followed using **51g** (94.9 mg, 0.30 mmol) and BCP **94g** (137 mg, 0.90 mmol). Purification by column chromatography (*n*hexane/EtOAc = 3/2) yielded **95gg** (95.6 mg, 78%) as colourless oil.

**<sup>1</sup>H NMR** (400 MHz, CDCl<sub>3</sub>):  $\delta$  = 8.39–8.35 (m, 1H), 7.74 (s, 1H), 7.04–7.00 (m, 2H), 6.11 (ddt,  $J$  = 17.3, 10.4, 4.6 Hz, 1H), 5.30 (s, 2H), 5.21 (d,  $J$  = 10.4 Hz, 1H), 5.02 (d,  $J$  = 17.3 Hz, 1H), 4.24 (t,  $J$  = 7.3 Hz, 2H), 3.90 (s, 3H), 3.88 (s, 2H), 2.67 (q,  $J$  = 7.5 Hz, 2H), 1.84 (q,  $J$  = 7.2 Hz, 2H), 1.28–1.22 (m, 6H), 1.16 (t,  $J$  = 7.5 Hz, 3H), 0.81 (t,  $J$  = 6.7 Hz, 3H). **<sup>13</sup>C NMR** (101 MHz, CDCl<sub>3</sub>):  $\delta$  = 163.0 (C<sub>q</sub>), 162.4 (C<sub>q</sub>), 144.6 (C<sub>q</sub>), 138.5 (C<sub>q</sub>), 137.2 (C<sub>q</sub>), 134.2 (CH), 130.4 (CH), 124.1 (CH), 119.2 (C<sub>q</sub>), 117.1 (CH<sub>2</sub>), 116.7 (C<sub>q</sub>), 114.8 (CH), 104.8 (CH), 55.5 (CH<sub>3</sub>), 50.5 (CH<sub>2</sub>), 39.7 (CH<sub>2</sub>), 33.1 (CH<sub>2</sub>), 31.2 (CH<sub>2</sub>), 30.2 (CH<sub>2</sub>), 26.2 (CH<sub>2</sub>), 22.5 (CH<sub>2</sub>), 21.1 (CH<sub>2</sub>), 14.4 (CH<sub>3</sub>), 14.0 (CH<sub>3</sub>). **IR** (ATR): 2956, 2929, 1642, 1612, 1491, 1464, 1235, 1215, 1035, 790 cm<sup>-1</sup>. **MS** (ESI)  $m/z$  (relative intensity): 409 (67) [M+H]<sup>+</sup>, 431 (100) [M+Na]<sup>+</sup>, 839 (48) [2M+Na]<sup>+</sup>. **HR-MS** (ESI)  $m/z$  calcd for C<sub>24</sub>H<sub>33</sub>N<sub>4</sub>O<sub>2</sub> [M+H]<sup>+</sup> 409.2598, found 409.2602.

### 3-Allyl-4-ethyl-2-[(1-hexyl-1*H*-1,2,3-triazol-4-yl)methyl]-6-(methylthio)isoquinolin-1(2*H*)-one (**95sg**):

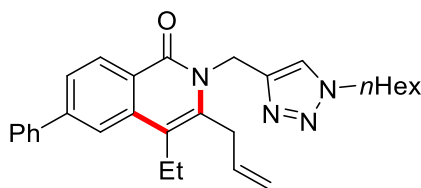


The general procedure **GPC** was followed using **51s** (99.8 mg, 0.30 mmol) and BCP **94g** (137 mg, 0.90 mmol). Purification by column chromatography (*n*hexane/EtOAc = 3/2) yielded **95sg** (89.2 mg, 70%) as colourless oil.

## 5. Experimental Part

**<sup>1</sup>H NMR** (400 MHz, CDCl<sub>3</sub>):  $\delta$  = 8.33 (d,  $J$  = 8.5 Hz, 1H), 7.74 (s, 1H), 7.42 (d,  $J$  = 1.8 Hz, 1H), 7.29 (dd,  $J$  = 8.5, 1.8 Hz, 1H), 6.12 (ddt,  $J$  = 17.3, 10.3, 4.6 Hz, 1H), 5.30 (s, 2H), 5.22 (dd,  $J$  = 10.3, 1.4 Hz, 1H), 5.03 (dd,  $J$  = 17.3, 1.4 Hz, 1H), 4.25 (t,  $J$  = 7.4 Hz, 2H), 3.89 (s, 2H), 2.69 (q,  $J$  = 7.5 Hz, 2H), 2.55 (s, 3H), 1.89–1.78 (m, 2H), 1.30–1.24 (m, 6H), 1.16 (t,  $J$  = 7.5 Hz, 3H), 0.83 ( $J$  = 6.9 Hz, 3H). **<sup>13</sup>C NMR** (101 MHz, CDCl<sub>3</sub>):  $\delta$  = 162.5 (C<sub>q</sub>), 144.7 (C<sub>q</sub>), 144.4 (C<sub>q</sub>), 137.4 (C<sub>q</sub>), 136.8 (C<sub>q</sub>), 134.1 (CH), 128.6 (CH), 124.1 (CH), 123.8 (CH), 122.1 (C<sub>q</sub>), 118.5 (CH), 117.2 (CH<sub>2</sub>), 116.4 (C<sub>q</sub>), 50.4 (CH<sub>2</sub>), 39.8 (CH<sub>2</sub>), 33.0 (CH<sub>2</sub>), 31.2 (CH<sub>2</sub>), 30.2 (CH<sub>2</sub>), 26.2 (CH<sub>2</sub>), 22.4 (CH<sub>2</sub>), 20.9 (CH<sub>2</sub>), 15.2 (CH<sub>3</sub>), 14.5 (CH<sub>3</sub>), 14.0 (CH<sub>3</sub>). **IR** (ATR): 2957, 2927, 2870, 1638, 1583, 1428, 1324, 1182, 1047, 790 cm<sup>-1</sup>. **MS** (ESI)  $m/z$  (relative intensity): 425 (100) [M+H]<sup>+</sup>, 447 (50) [M+Na]<sup>+</sup>. **HR-MS** (ESI)  $m/z$  calcd for C<sub>24</sub>H<sub>33</sub>N<sub>4</sub>OS [M+H]<sup>+</sup> 425.2370, found 425.2379.

### 3-Allyl-4-ethyl-2-[(1-hexyl-1*H*-1,2,3-triazol-4-yl)methyl]-6-phenylisoquinolin-1(2*H*)-one (**95fg**):



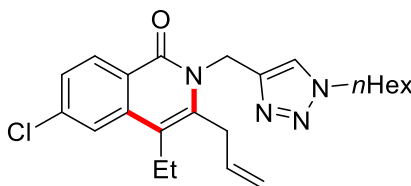
The general procedure **GPC** was followed using **51f** (109 mg, 0.30 mmol) and BCP **94g** (137 mg, 0.90 mmol). Purification by column chromatography (*n*hexane/EtOAc = 3/2) yielded **95fg** (83.2 mg, 61%) as colourless oil.

**<sup>1</sup>H NMR** (400 MHz, CDCl<sub>3</sub>):  $\delta$  = 8.53 (d,  $J$  = 8.3 Hz, 1H), 7.86 (s, 1H), 7.78 (s, 1H), 7.72–7.64 (m, 3H), 7.52–7.46 (m, 2H), 7.41 (dd,  $J$  = 7.3, 7.3 Hz, 1H), 6.15 (ddd,  $J$  = 17.8, 10.1, 4.9 Hz, 1H), 5.37 (s, 2H), 5.25 (d,  $J$  = 10.4 Hz, 1H), 5.07 (d,  $J$  = 17.3 Hz, 1H), 4.27 (t,  $J$  = 7.4 Hz, 2H), 3.94 (s, 2H), 2.80 (q,  $J$  = 7.5 Hz, 2H), 1.85 (q,  $J$  = 7.2 Hz, 2H), 1.42–1.25 (m, 6H), 1.22 (t,  $J$  = 7.5 Hz, 3H), 0.85 (t,  $J$  = 6.7 Hz, 3H). **<sup>13</sup>C NMR** (101 MHz, CDCl<sub>3</sub>):  $\delta$  = 162.7 (C<sub>q</sub>), 145.3 (C<sub>q</sub>), 144.5 (C<sub>q</sub>), 140.9 (C<sub>q</sub>), 136.9 (C<sub>q</sub>), 136.9 (C<sub>q</sub>), 134.2 (CH), 129.1 (CH), 129.0 (CH), 128.2 (CH), 127.7 (CH), 125.5 (CH), 124.1 (CH), 124.1 (C<sub>q</sub>), 121.3 (CH), 117.2 (CH<sub>2</sub>), 117.2 (C<sub>q</sub>), 50.5 (CH<sub>2</sub>), 39.9 (CH<sub>2</sub>), 33.1 (CH<sub>2</sub>), 31.2 (CH<sub>2</sub>), 30.2

## 5. Experimental Part

(CH<sub>2</sub>), 26.3 (CH<sub>2</sub>), 22.5 (CH<sub>2</sub>), 21.0 (CH<sub>2</sub>), 14.7 (CH<sub>3</sub>), 14.0 (CH<sub>3</sub>). **IR** (ATR): 2929, 2870, 1642, 1615, 1591, 1451, 1429, 1328, 1047, 790 cm<sup>-1</sup>. **MS** (ESI) *m/z* (relative intensity): 455 (100) [M+H]<sup>+</sup>, 477 (29) [M+Na]<sup>+</sup>, 909 (33) [2M+H]<sup>+</sup>, 931 (60) [2M+Na]<sup>+</sup>. **HR-MS** (ESI) *m/z* calcd for C<sub>29</sub>H<sub>35</sub>N<sub>4</sub>O [M+H]<sup>+</sup> 455.2805, found 455,2798.

### 3-Allyl-6-chloro-4-ethyl-2-[(1-hexyl-1*H*-1,2,3-triazol-4-yl)methyl]isoquinolin-1(2*H*)-one (**95jg**):

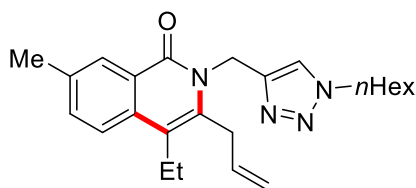


The general procedure **GPC** was followed using **51j** (96.2 mg, 0.30 mmol) and BCP **94g** (137 mg, 0.90 mmol). Purification by column chromatography (*n*hexane/EtOAc = 3/2) yielded **95jg** (64.4 mg, 52%) as colourless oil.

**<sup>1</sup>H NMR** (400 MHz, CDCl<sub>3</sub>): δ = 8.38 (d, *J* = 8.6 Hz, 1H), 7.75 (s, 1H), 7.64 (s, 1H), 7.39 (d, *J* = 8.6 Hz, 1H), 6.12 (ddt, *J* = 17.4, 10.3, 4.9 Hz, 1H), 5.31 (s, 2H), 5.24 (d, *J* = 10.3 Hz, 1H), 5.03 (d, *J* = 17.4 Hz, 1H), 4.26 (t, *J* = 7.3 Hz, 2H), 3.92 (s, 2H), 2.68 (q, *J* = 7.4 Hz, 2H), 1.85 (t, *J* = 7.2 Hz, 2H), 1.29–1.22(m, 6H), 1.17 (t, *J* = 7.4 Hz, 3H), 0.84 (t, *J* = 6.4 Hz, 3H). **<sup>13</sup>C NMR** (101 MHz, CDCl<sub>3</sub>): δ = 162.2 (C<sub>q</sub>), 144.2 (C<sub>q</sub>), 139.2 (C<sub>q</sub>), 138.1 (C<sub>q</sub>), 137.9 (C<sub>q</sub>), 133.9 (CH), 130.2 (CH), 126.6 (CH), 124.2 (CH), 123.5 (C<sub>q</sub>), 122.5 (CH), 117.4 (CH<sub>2</sub>), 116.3 (C<sub>q</sub>), 50.5 (CH<sub>2</sub>), 40.0 (CH<sub>2</sub>), 33.1 (CH<sub>2</sub>), 31.2 (CH<sub>2</sub>), 30.2 (CH<sub>2</sub>), 26.3 (CH<sub>2</sub>), 22.5 (CH<sub>2</sub>), 21.0 (CH<sub>2</sub>), 14.5 (CH<sub>3</sub>), 14.0 (CH<sub>3</sub>). **IR** (ATR): 2957, 2929, 1644, 1474, 1429, 1378, 1326, 1173, 1047, 790 cm<sup>-1</sup>. **MS** (ESI) *m/z* (relative intensity): 413 (100) [<sup>35</sup>Cl, M+H]<sup>+</sup>, 435 (35) [<sup>35</sup>Cl, M+Na]<sup>+</sup>, 847 (53) [<sup>35</sup>Cl, 2M+Na]<sup>+</sup>. **HR-MS** (ESI) *m/z* calcd for C<sub>23</sub>H<sub>30</sub>N<sub>4</sub>O<sup>35</sup>Cl [M+H]<sup>+</sup> 413.2103, found 413.2101.

## 5. Experimental Part

### 3-Allyl-4-ethyl-2-[(1-hexyl-1*H*-1,2,3-triazol-4-yl)methyl]-7-methylisoquinolin-1(2*H*)-one (**95tg**):

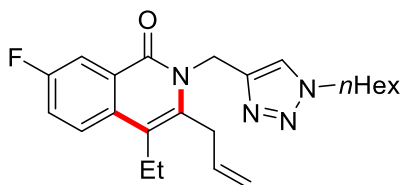


The general procedure **GPC** was followed using **51t** (90.1 mg, 0.30 mmol) and BCP **94g** (137 mg, 0.90 mmol). Purification by column chromatography (*n*hexane/EtOAc = 3/2) yielded **95tg** (75.0 mg, 64%) as colourless oil.

**<sup>1</sup>H NMR** (400 MHz, CDCl<sub>3</sub>):  $\delta$  = 8.25 (d,  $J$  = 2.5 Hz, 1H), 7.75 (s, 1H), 7.58 (d,  $J$  = 8.4 Hz, 1H), 7.47 (d,  $J$  = 8.4 Hz, 1H), 6.12 (ddt,  $J$  = 17.3, 10.3, 4.6 Hz, 1H), 5.33 (s, 2H), 5.20 (dd,  $J$  = 10.3, 1.7 Hz, 1H), 5.02 (dd,  $J$  = 17.3, 1.7 Hz, 1H), 4.23 (t,  $J$  = 7.4 Hz, 2H), 3.87 (s, 2H), 2.70 (q,  $J$  = 7.5 Hz, 2H), 2.46 (s, 3H), 1.83 (p,  $J$  = 7.3 Hz, 2H), 1.31–1.20 (m, 6H), 1.14 (t,  $J$  = 7.5 Hz, 3H), 0.83 (t,  $J$  = 6.8 Hz, 3H). **<sup>13</sup>C NMR** (101 MHz, CDCl<sub>3</sub>):  $\delta$  = 162.7 (C<sub>q</sub>), 144.5 (C<sub>q</sub>), 136.0 (C<sub>q</sub>), 135.3 (C<sub>q</sub>), 134.4 (CH), 134.2 (C<sub>q</sub>), 133.9 (CH), 127.8 (CH), 125.1 (C<sub>q</sub>), 124.1 (CH), 122.9 (CH), 117.1 (CH<sub>2</sub>), 117.0 (C<sub>q</sub>), 50.4 (CH<sub>2</sub>), 39.9 (CH<sub>2</sub>), 32.8 (CH<sub>2</sub>), 31.1 (CH<sub>2</sub>), 30.2 (CH<sub>2</sub>), 26.2 (CH<sub>2</sub>), 22.4 (CH<sub>2</sub>), 21.3 (CH<sub>3</sub>), 21.0 (CH<sub>2</sub>), 14.6 (CH<sub>3</sub>), 14.0 (CH<sub>3</sub>). **IR** (ATR): 2960, 2929, 1644, 1596, 1504, 1458, 1429, 1340, 1300, 823 cm<sup>-1</sup>. **MS** (ESI)  $m/z$  (relative intensity): 393 (64) [M+H]<sup>+</sup>, 415 (100) [M+Na]<sup>+</sup>. **HR-MS** (ESI)  $m/z$  calcd for C<sub>24</sub>H<sub>33</sub>N<sub>4</sub>O [M+H]<sup>+</sup> 393.2649, found 393.2652.

## 5. Experimental Part

**3-Allyl-4-ethyl-7-fluoro-2-[(1-hexyl-1*H*-1,2,3-triazol-4-yl)methyl]isoquinolin-1(2*H*)-one (95ug):**

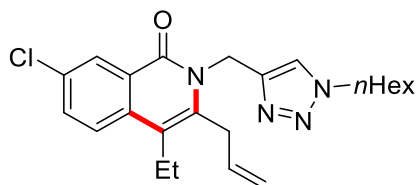


The general procedure **GPC** was followed using **51u** (91.3 mg, 0.30 mmol) and BCP **94g** (137 mg, 0.90 mmol). Purification by column chromatography (*n*hexane/EtOAc = 3/2) yielded **95ug** (94.0 mg, 79%) as light yellow oil.

**<sup>1</sup>H NMR** (600 MHz, CDCl<sub>3</sub>):  $\delta$  = 8.09 (dd,  $J$  = 9.3, 2.9 Hz, 1H), 7.76 (s, 1H), 7.69 (dd,  $J$  = 9.0, 5.0 Hz, 1H), 7.40 (ddd,  $J$  = 9.0, 8.0, 2.9 Hz, 1H), 6.14 (ddt,  $J$  = 17.3, 10.3, 4.7 Hz, 1H), 5.33 (s, 2H), 5.24 (dd,  $J$  = 10.3, 1.8 Hz, 1H), 5.04 (dd,  $J$  = 17.3, 1.8 Hz, 1H), 4.26 (t,  $J$  = 7.4 Hz, 2H), 3.92 (s, 2H), 2.72 (q,  $J$  = 7.6 Hz, 2H), 1.86 (p,  $J$  = 7.2 Hz, 2H), 1.30–1.24 (m, 6H), 1.17 (t,  $J$  = 7.6 Hz, 3H), 0.84 (t,  $J$  = 7.0 Hz, 3H). **<sup>13</sup>C NMR** (151 MHz, CDCl<sub>3</sub>):  $\delta$  = 162.0 (d,  $^4J_{C-F}$  = 3.5 Hz, C<sub>q</sub>), 161.1 (d,  $^1J_{C-F}$  = 246.9 Hz, C<sub>q</sub>), 144.2 (C<sub>q</sub>), 135.7 (d,  $^4J_{C-F}$  = 2.5 Hz, C<sub>q</sub>), 134.2 (CH), 133.2 (d,  $^4J_{C-F}$  = 2.1 Hz, C<sub>q</sub>), 126.8 (d,  $^3J_{C-F}$  = 7.7 Hz, C<sub>q</sub>), 125.5 (d,  $^3J_{C-F}$  = 7.7 Hz, CH), 124.2 (CH), 121.2 (d,  $^2J_{C-F}$  = 23.3 Hz, CH), 117.3 (CH<sub>2</sub>), 116.8 (C<sub>q</sub>), 113.2 (d,  $^2J_{C-F}$  = 22.4 Hz, CH), 50.5 (CH<sub>2</sub>), 40.1 (CH<sub>2</sub>), 32.9 (CH<sub>2</sub>), 31.2 (CH<sub>2</sub>), 30.3 (CH<sub>2</sub>), 26.3 (CH<sub>2</sub>), 22.5 (CH<sub>2</sub>), 21.2 (CH<sub>2</sub>), 14.6 (CH<sub>3</sub>), 14.0 (CH<sub>3</sub>). **<sup>19</sup>F NMR** (377 MHz, CDCl<sub>3</sub>):  $\delta$  = -114.75 (td,  $J$  = 8.6, 5.0 Hz). **IR** (ATR): 2957, 2929, 1644, 1597, 1499, 1431, 1351, 1048, 827, 724 cm<sup>-1</sup>. **MS** (ESI)  $m/z$  (relative intensity): 397 (53) [M+H]<sup>+</sup>, 419 (100) [M+Na]<sup>+</sup>, 815 (47) [2M+Na]<sup>+</sup>. **HR-MS** (ESI)  $m/z$  calcd for C<sub>23</sub>H<sub>30</sub>FN<sub>4</sub>O [M+H]<sup>+</sup> 397.2398, found 397.2400.

## 5. Experimental Part

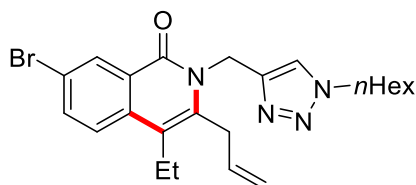
### 3-Allyl-7-chloro-4-ethyl-2-[(1-hexyl-1*H*-1,2,3-triazol-4-yl)methyl]isoquinolin-1(2*H*)-one (95vg):



The general procedure **GPC** was followed using **51v** (96.2 mg, 0.30 mmol) and BCP **94g** (137 mg, 0.90 mmol). Purification by column chromatography (*n*hexane/EtOAc = 3/2) yielded **95vg** (73.1 mg, 59%) as light yellow oil.

**<sup>1</sup>H NMR** (300 MHz, CDCl<sub>3</sub>):  $\delta$  = 8.44 (dd,  $J$  = 2.1, 0.7 Hz, 1H), 7.78 (s, 1H), 7.70–7.52 (m, 2H), 6.15 (ddt,  $J$  = 17.3, 10.2, 4.6 Hz, 1H), 5.34 (s, 2H), 5.26 (dd,  $J$  = 10.2, 1.7 Hz, 1H), 5.05 (dd,  $J$  = 17.3, 1.7 Hz, 1H), 4.28 (t,  $J$  = 7.4 Hz, 2H), 3.94 (s, 2H), 2.72 (q,  $J$  = 7.5 Hz, 2H), 1.87 (p,  $J$  = 7.3 Hz, 2H), 1.37–1.24 (m, 6H), 1.17 (t,  $J$  = 7.5 Hz, 3H), 0.86 (t,  $J$  = 6.7 Hz, 3H). **<sup>13</sup>C NMR** (126 MHz, CDCl<sub>3</sub>):  $\delta$  = 161.7 (C<sub>q</sub>), 144.1 (C<sub>q</sub>), 136.9 (C<sub>q</sub>), 134.9 (C<sub>q</sub>), 134.0 (CH), 132.8 (CH), 132.1 (C<sub>q</sub>), 127.7 (CH), 126.3 (C<sub>q</sub>), 124.7 (CH), 124.2 (CH), 117.3 (CH<sub>2</sub>), 116.7 (C<sub>q</sub>), 50.5 (CH<sub>2</sub>), 40.1 (CH<sub>2</sub>), 33.0 (CH<sub>2</sub>), 31.2 (CH<sub>2</sub>), 30.2 (CH<sub>2</sub>), 26.2 (CH<sub>2</sub>), 22.5 (CH<sub>2</sub>), 21.0 (CH<sub>2</sub>), 14.6 (CH<sub>3</sub>), 14.0 (CH<sub>3</sub>). **IR** (ATR): 2956, 2928, 1642, 1591, 1461, 1337, 1293, 1047, 910, 824 cm<sup>-1</sup>. **MS** (ESI)  $m/z$  (relative intensity): 413 (57) [<sup>35</sup>Cl, M+H]<sup>+</sup>, 435 (100) [<sup>35</sup>Cl, M+Na]<sup>+</sup>. **HR-MS** (ESI)  $m/z$  calcd for C<sub>23</sub>H<sub>30</sub><sup>35</sup>ClN<sub>4</sub>O [M+H]<sup>+</sup> 413.2103, found 413.2104.

### 3-Allyl-7-bromo-4-ethyl-2-[(1-hexyl-1*H*-1,2,3-triazol-4-yl)methyl]isoquinolin-1(2*H*)-one : (95wg):



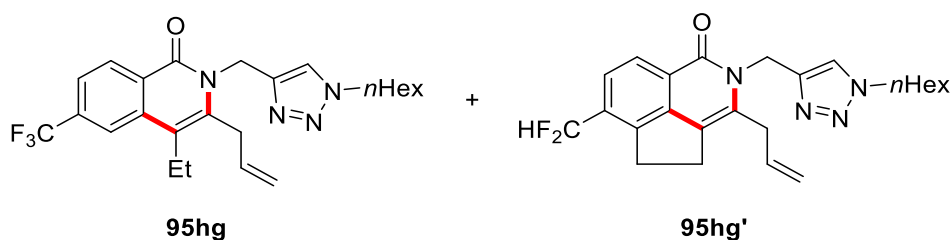
The general procedure **GPC** was followed using **51w** (110 mg, 0.30 mmol) and BCP **94g** (137 mg, 0.90 mmol). Purification by column chromatography (*n*hexane/EtOAc = 3/2) yielded **95wg** (65.8 mg, 48%) as colourless oil.

## 5. Experimental Part

**<sup>1</sup>H NMR** (600 MHz, CDCl<sub>3</sub>):  $\delta$  = 8.59 (d,  $J$  = 2.2 Hz, 1H), 7.76 (s, 1H), 7.73 (dd,  $J$  = 8.7, 2.2 Hz, 1H), 7.55 (d,  $J$  = 8.7 Hz, 1H), 6.13 (ddt,  $J$  = 17.3, 10.4, 4.7 Hz, 1H), 5.32 (s, 2H), 5.24 (dd,  $J$  = 10.4, 1.2 Hz, 1H), 5.03 (dd,  $J$  = 17.3, 1.2 Hz, 1H), 4.26 (t,  $J$  = 7.4 Hz, 2H), 3.92 (s, 2H), 2.70 (q,  $J$  = 7.5 Hz, 2H), 1.85 (qd,  $J$  = 7.9, 7.2, 4.0 Hz, 2H), 1.30–1.25 (m, 6H), 1.15 (t,  $J$  = 7.5 Hz, 3H), 0.85 (t,  $J$  = 7.0 Hz, 3H). **<sup>13</sup>C NMR** (75 MHz, CDCl<sub>3</sub>):  $\delta$  = 161.6 (C<sub>q</sub>), 144.1 (C<sub>q</sub>), 137.1 (C<sub>q</sub>), 135.6 (CH), 135.3 (C<sub>q</sub>), 134.0 (CH), 130.9 (CH), 126.6 (C<sub>q</sub>), 124.9 (CH), 124.2 (CH), 120.0 (C<sub>q</sub>), 117.3 (CH<sub>2</sub>), 116.8 (C<sub>q</sub>), 50.5 (CH<sub>2</sub>), 40.1 (CH<sub>2</sub>), 33.0 (CH<sub>2</sub>), 31.2 (CH<sub>2</sub>), 30.3 (CH<sub>2</sub>), 26.3 (CH<sub>2</sub>), 22.5 (CH<sub>2</sub>), 21.0 (CH<sub>2</sub>), 14.6 (CH<sub>3</sub>), 14.0 (CH<sub>3</sub>). **IR** (ATR): 2956, 2928, 1644, 1588, 1478, 1336, 1293, 1048, 930, 824 cm<sup>-1</sup>. **MS** (ESI)  $m/z$  (relative intensity): 457 (67) [<sup>79</sup>Br, M+H]<sup>+</sup>, 481 (100), 937 (50). **HR-MS** (ESI)  $m/z$  calcd for C<sub>23</sub>H<sub>30</sub><sup>79</sup>BrN<sub>4</sub>O [M+H]<sup>+</sup> 457.1598, found 457.1598.

### 5.5.3 Analytical Data – Impact of CF<sub>3</sub>-Substitution of Benzamide

**3-Allyl-4-ethyl-2-[(1-hexyl-1*H*-1,2,3-triazol-4-yl)methyl]-6-(trifluoromethyl)-isoquinolin-1(2*H*)-one (95hg)** and **3-Allyl-6-(difluoromethyl)-2-[(1-hexyl-1*H*-1,2,3-triazol-4-yl)methyl]-4,5-dihydrocyclopenta[de]isoquinolin-1(2*H*)-one (95hg')**:



The general procedure **GPC** was followed using **51h** (106 mg, 0.30 mmol) and BCP **94g** (137 mg, 0.90 mmol). Purification by column chromatography (*n*hexane/EtOAc = 3/2 to 1/1) yielded **95hg** (9.4 mg, 7%) as a white solid. and **95hg'** (49.8 mg, 39%) as yellow oil.

## 5. Experimental Part

### 3-Allyl-4-ethyl-2-[(1-hexyl-1*H*-1,2,3-triazol-4-yl)methyl]-6-(trifluoromethyl)-isoquinolin-1(2*H*)-one (95hg):

**M.p.** = 96–97 °C. **<sup>1</sup>H NMR** (400 MHz, CDCl<sub>3</sub>): δ = 8.55 (dd, *J* = 8.3, 1.0 Hz, 1H), 7.92 (s, 1H), 7.74 (s, 1H), 7.63 (dd, *J* = 8.3, 1.6 Hz, 1H), 6.13 (ddt, *J* = 17.3, 10.3, 4.7 Hz, 1H), 5.33 (s, 2H), 5.24 (dd, *J* = 10.3, 1.4 Hz, 1H), 5.02 (dd, *J* = 17.3, 1.4 Hz, 1H), 4.25 (t, *J* = 7.4 Hz, 2H), 3.95 (s, 2H), 2.74 (q, *J* = 7.5 Hz, 2H), 1.83 (q, *J* = 7.3 Hz, 2H), 1.27–1.22 (m, 6H), 1.17 (t, *J* = 7.5 Hz, 3H), 0.83 (t, *J* = 6.9 Hz, 3H). **<sup>13</sup>C NMR** (101 MHz, CDCl<sub>3</sub>): δ = 162.0 (C<sub>q</sub>), 144.0 (C<sub>q</sub>), 138.3 (C<sub>q</sub>), 136.6 (C<sub>q</sub>), 134.1 (d, <sup>2</sup>*J*<sub>C-F</sub> = 32.3 Hz, C<sub>q</sub>), 133.9 (CH), 129.5 (CH), 127.3 (C<sub>q</sub>), 124.2 (CH), 124.1 (d, <sup>1</sup>*J*<sub>C-F</sub> = 273.0 Hz, C<sub>q</sub>), 122.1 (d, <sup>3</sup>*J*<sub>C-F</sub> = 3.4 Hz, CH), 120.3 (d, <sup>3</sup>*J*<sub>C-F</sub> = 4.2 Hz, CH), 117.5 (CH<sub>2</sub>), 117.0 (C<sub>q</sub>), 50.5 (CH<sub>2</sub>), 40.1 (CH<sub>2</sub>), 33.1 (CH<sub>2</sub>), 31.2 (CH<sub>2</sub>), 30.3 (CH<sub>2</sub>), 26.3 (CH<sub>2</sub>), 22.5 (CH<sub>2</sub>), 21.0 (CH<sub>2</sub>), 14.6 (CH<sub>3</sub>), 14.0 (CH<sub>3</sub>). **<sup>19</sup>F NMR** (376 MHz, CDCl<sub>3</sub>): δ = –62.89 (s). **IR** (ATR): 2959, 2931, 2860, 1650, 1597, 1433, 1313, 1130, 1074, 797 cm<sup>–1</sup>. **MS** (ESI) *m/z* (relative intensity): 447 (86) [M+H]<sup>+</sup>, 469 (100) [M+Na]<sup>+</sup>. **HR-MS** (ESI) *m/z* calcd for C<sub>24</sub>H<sub>30</sub>F<sub>3</sub>N<sub>4</sub>O [M+H]<sup>+</sup> 447.2366, found 447.2367.

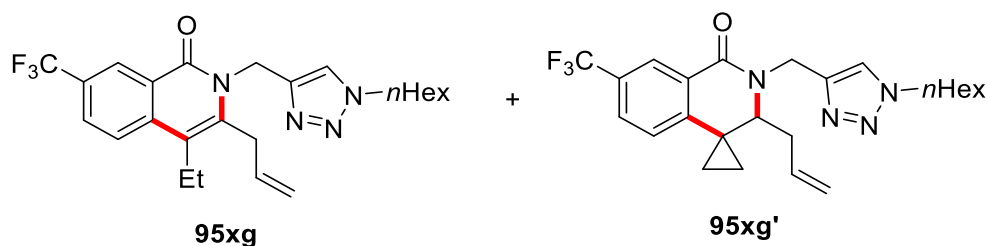
### 3-Allyl-6-(difluoromethyl)-2-[(1-hexyl-1*H*-1,2,3-triazol-4-yl)methyl]-4,5-dihydrocyclopenta[de]isoquinolin-1(2*H*)-one (95hg'):

**<sup>1</sup>H NMR** (400 MHz, CDCl<sub>3</sub>): δ = 8.05 (d, *J* = 8.2 Hz, 1H), 7.72 (s, 1H), 7.45 (d, *J* = 8.2 Hz, 1H), 6.75 (t, *J* = 55.6 Hz, 1H), 6.05 (ddt, *J* = 17.3, 10.3, 5.1 Hz, 1H), 5.34 (s, 2H), 5.20 (dq, *J* = 10.3, 1.6 Hz, 1H), 5.08 (dq, *J* = 17.3, 1.6 Hz, 1H), 4.25 (t, *J* = 7.3 Hz, 2H), 3.80 (s, 2H), 3.40–3.34 (m, 2H), 3.15–3.05 (m, 2H), 1.84 (p, *J* = 7.4 Hz, 2H), 1.29–1.24 (m, 6H), 0.83 (t, *J* = 6.9 Hz, 3H). **<sup>13</sup>C NMR** (101 MHz, CDCl<sub>3</sub>): δ = 162.3 (C<sub>q</sub>), 144.3 (C<sub>q</sub>), 144.0 (C<sub>q</sub>), 142.0 (t, <sup>3</sup>*J*<sub>C-F</sub> = 4.5 Hz, C<sub>q</sub>), 134.7 (C<sub>q</sub>), 133.3 (CH), 132.3 (t, <sup>2</sup>*J*<sub>C-F</sub> = 22.5 Hz, C<sub>q</sub>), 124.4 (CH), 124.2 (t, <sup>3</sup>*J*<sub>C-F</sub> = 6.5 Hz, CH), 123.9 (CH), 123.2 (C<sub>q</sub>), 121.8 (C<sub>q</sub>), 117.2 (CH<sub>2</sub>), 114.2 (t, <sup>1</sup>*J*<sub>C-F</sub> = 239.0 Hz, CH), 50.5 (CH<sub>2</sub>), 39.5 (CH<sub>2</sub>), 34.5 (CH<sub>2</sub>), 31.2 (CH<sub>2</sub>),

## 5. Experimental Part

30.2 (CH<sub>2</sub>), 29.7 (CH<sub>2</sub>), 27.5 (CH<sub>2</sub>), 26.2 (CH<sub>2</sub>), 22.5 (CH<sub>2</sub>), 14.0 (CH<sub>3</sub>). **<sup>19</sup>F NMR** (377 MHz, CDCl<sub>3</sub>):  $\delta$  = -112.87 (d,  $J$  = 55.5 Hz). **IR** (ATR): 2955, 2928, 2857, 1664, 1619, 1428, 1371, 1103, 1027, 784 cm<sup>-1</sup>. **MS** (ESI)  $m/z$  (relative intensity): 427 (100) [M+H]<sup>+</sup>, 449 (67) [M+Na]<sup>+</sup>. **HR-MS** (ESI)  $m/z$  calcd for C<sub>24</sub>H<sub>28</sub>F<sub>2</sub>N<sub>4</sub>ONa [M+Na]<sup>+</sup> 449.2123, found 449.2117.

**3-Allyl-4-ethyl-2-[(1-hexyl-1*H*-1,2,3-triazol-4-yl)methyl]-7-(trifluoromethyl)-isoquinolin-1(2*H*)-one (95xg)** and **3'-Allyl-2'-[(1-hexyl-1*H*-1,2,3-triazol-4-yl)methyl]-7'-(trifluoromethyl)-2',3'-dihydro-1'*H*-spiro(cyclopropane-1,4'-isoquinolin)-1'-one (95xg')**:



The general procedure **GPC** was followed using **51x** (106 mg, 0.30 mmol) and BCP **94g** (137 mg, 0.90 mmol). Purification by column chromatography (*n*hexane/EtOAc = 3/2) yielded **95xg** (49.6 mg, 37%) as colourless oil and **95xg'** (33.5 mg, 25%) as yellow oil.

**3-Allyl-4-ethyl-2-[(1-hexyl-1*H*-1,2,3-triazol-4-yl)methyl]-7-(trifluoromethyl)-isoquinolin-1(2*H*)-one (95xg)**:

**<sup>1</sup>H NMR** (400 MHz, CDCl<sub>3</sub>):  $\delta$  = 8.75 (s, 1H), 7.89–7.75 (m, 3H), 6.15 (ddt,  $J$  = 17.3, 10.2, 2.9 Hz, 1H), 5.35 (s, 2H), 5.26 (dd,  $J$  = 10.2, 1.5 Hz, 1H), 5.05 (dd,  $J$  = 17.3, 1.5 Hz, 1H), 4.27 (t,  $J$  = 6.9 Hz, 2H), 3.98 (s, 2H), 2.81–2.70 (m, 2H), 1.93–1.81 (m, 2H), 1.31–1.25 (m, 6H), 1.18 (t,  $J$  = 7.6 Hz, 3H), 0.85 (t,  $J$  = 6.7 Hz, 3H). **<sup>13</sup>C NMR** (75 MHz, CDCl<sub>3</sub>):  $\delta$  = 162.2 (C<sub>q</sub>), 143.9 (C<sub>q</sub>), 139.2 (C<sub>q</sub>), 139.0 (C<sub>q</sub>), 133.8 (CH), 128.3 (q, <sup>3</sup> $J_{C-F}$  = 3.4 Hz, CH), 127.9 (q, <sup>2</sup> $J_{C-F}$  = 33.5

## 5. Experimental Part

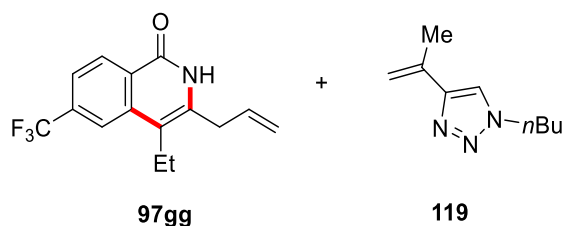
Hz, C<sub>q</sub>), 126.6 (q,  $^1J_{C-F}$  = 249.3 Hz, C<sub>q</sub>), 126.0 (q,  $^3J_{C-F}$  = 4.1 Hz, CH), 124.9 (C<sub>q</sub>), 124.3 (CH), 123.9 (CH), 117.5 (CH<sub>2</sub>), 116.7 (C<sub>q</sub>), 50.5 (CH<sub>2</sub>), 40.1 (CH<sub>2</sub>), 33.2 (CH<sub>2</sub>), 31.2 (CH<sub>2</sub>), 30.3 (CH<sub>2</sub>), 26.3 (CH<sub>2</sub>), 22.5 (CH<sub>2</sub>), 21.1 (CH<sub>2</sub>), 14.5 (CH<sub>3</sub>), 14.0 (CH<sub>3</sub>). **<sup>19</sup>F NMR** (282 MHz, CDCl<sub>3</sub>):  $\delta$  = -62.35 (s). **IR** (ATR): 2958, 2930, 1652, 1598, 1554, 1323, 1292, 1163, 1126, 840 cm<sup>-1</sup>. **MS** (ESI) *m/z* (relative intensity): 447 (57) [M+H]<sup>+</sup>, 469 (100) [M+Na]<sup>+</sup>. **HR-MS** (ESI) *m/z* calcd for C<sub>24</sub>H<sub>30</sub>F<sub>3</sub>N<sub>4</sub>O [M+H]<sup>+</sup> 447.2366, found 447.2368.

**3'-Allyl-2'-[(1-hexyl-1*H*-1,2,3-triazol-4-yl)methyl]-7'-(trifluoromethyl)-2',3'-dihydro-1'*H*-spiro(cyclopropane-1,4'-isoquinolin)-1'-one (95xg'):**

**<sup>1</sup>H NMR** (600 MHz, CDCl<sub>3</sub>):  $\delta$  = 8.31 (d, *J* = 2.1 Hz, 1H), 7.65–7.60 (m, 2H), 6.93 (d, *J* = 8.1 Hz, 1H), 5.71 (ddt, *J* = 16.8, 10.2, 7.4 Hz, 1H), 5.36 (d, *J* = 14.9 Hz, 1H), 4.98–4.94 (m, 2H), 4.29 (td, *J* = 7.2, 2.7 Hz, 2H), 4.19 (d, *J* = 14.9 Hz, 1H), 3.19 (t, *J* = 6.7 Hz, 1H), 2.38–2.33 (m, 2H), 1.85 (t, *J* = 7.2 Hz, 2H), 1.55 (ddd, *J* = 9.6, 6.3, 6.0 Hz, 1H), 1.27–1.22 (m, 6H), 1.00 (ddd, *J* = 9.8, 6.8, 6.0 Hz, 1H), 0.83 (t, *J* = 7.0 Hz, 3H), 0.68 (ddd, *J* = 9.6, 6.3, 4.4 Hz, 1H), 0.35 (ddd, *J* = 9.8, 6.8, 4.4 Hz, 1H). **<sup>13</sup>C NMR** (101 MHz, CDCl<sub>3</sub>):  $\delta$  = 162.6 (C<sub>q</sub>), 145.1 (C<sub>q</sub>), 144.3 (C<sub>q</sub>), 133.8 (CH), 130.9 (C<sub>q</sub>), 129.2 (C<sub>q</sub>), 129.0 (q,  $^3J_{C-F}$  = 3.0 Hz, CH), 125.4 (q,  $^3J_{C-F}$  = 3.9 Hz, CH), 124.0 (q,  $^1J_{C-F}$  = 271.7 Hz, C<sub>q</sub>), 123.1 (CH), 122.5 (CH), 118.6 (CH<sub>2</sub>), 64.6 (CH), 50.5 (CH<sub>2</sub>), 42.0 (CH<sub>2</sub>), 38.4 (CH<sub>2</sub>), 31.2 (CH<sub>2</sub>), 30.3 (CH<sub>2</sub>), 26.2 (CH<sub>2</sub>), 23.4 (C<sub>q</sub>), 22.5 (CH<sub>2</sub>), 19.8 (CH<sub>2</sub>), 14.0 (CH<sub>3</sub>), 10.1 (CH<sub>2</sub>). **<sup>19</sup>F NMR** (565 MHz, CDCl<sub>3</sub>):  $\delta$  = -62.58 (s). **IR** (ATR): 2929, 2860, 1649, 1617, 1469, 1331, 1252, 1160, 1129, 922 cm<sup>-1</sup>. **MS** (ESI) *m/z* (relative intensity): 447 (45) [M+H]<sup>+</sup>, 469 (100) [M+Na]<sup>+</sup>. **HR-MS** (ESI) *m/z* calcd for C<sub>24</sub>H<sub>30</sub>F<sub>3</sub>N<sub>4</sub>O [M+H]<sup>+</sup> 447.2366, found 447.2370.

## 5. Experimental Part

### 3-Allyl-4-ethyl-6-(trifluoromethyl)isoquinolin-1(2H)-one (**97gg**) and 1-Butyl-4-(prop-1-en-2-yl)-1H-1,2,3-triazole (**119**):



The procedure was followed using **32g** (106 mg, 0.30 mmol) and BCP **94g** (137 mg, 0.90 mmol). Purification by column chromatography (*n*hexane/EtOAc/DCM = 3/1/1) yielded **97gg** (27.2 mg, 32%) as a white solid and **119** (16.4 mg, 33%) as colourless oil.

### 3-Allyl-4-ethyl-6-(trifluoromethyl)isoquinolin-1(2H)-one (**97gg**):

**M.p.** = 97–98 °C. **<sup>1</sup>H NMR** (400 MHz, CDCl<sub>3</sub>):  $\delta$  = 9.76 (s, 1H), 8.62–8.43 (m, 1H), 7.98 (s, 1H), 7.75–7.58 (m, 1H), 5.96 (ddt,  $J$  = 16.7, 10.1, 6.5 Hz, 1H), 5.37–5.28 (m, 2H), 3.49 (dt,  $J$  = 6.5, 1.8 Hz, 2H), 2.82 (q,  $J$  = 7.6 Hz, 2H), 1.25 (t,  $J$  = 7.6 Hz, 3H). **<sup>13</sup>C NMR** (126 MHz, CDCl<sub>3</sub>):  $\delta$  = 162.1 (C<sub>q</sub>), 138.1 (C<sub>q</sub>), 135.5 (C<sub>q</sub>), 134.4 (d,  $^2J_{C-F}$  = 32.0 Hz, C<sub>q</sub>), 132.8 (CH), 129.2 (CH), 127.8 (C<sub>q</sub>), 124.1 (d,  $^1J_{C-F}$  = 272.8 Hz, C<sub>q</sub>), 122.1 (d,  $^3J_{C-F}$  = 3.9 Hz, CH), 120.5 (d,  $^3J_{C-F}$  = 4.5 Hz, CH), 119.9 (CH<sub>2</sub>), 115.0 (C<sub>q</sub>), 35.3 (CH<sub>2</sub>), 19.8 (CH<sub>2</sub>), 14.8 (CH<sub>3</sub>). **<sup>19</sup>F NMR** (377 MHz, CDCl<sub>3</sub>):  $\delta$  = –62.90 (s). **IR** (ATR): 2963, 2923, 2851, 1651, 1626, 1459, 1300, 1179, 1119, 842 cm<sup>-1</sup>. **MS** (ESI)  $m/z$  (relative intensity): 282 (86) [M+H]<sup>+</sup>, 304 (100). **HR-MS** (ESI)  $m/z$  calcd for C<sub>15</sub>H<sub>15</sub>F<sub>3</sub>N<sub>4</sub>O [M+H]<sup>+</sup> 282.1100, found 282.1101.

### 1-Butyl-4-(prop-1-en-2-yl)-1H-1,2,3-triazole (**119**):

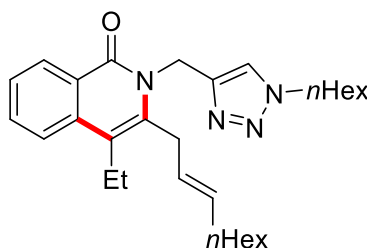
**<sup>1</sup>H NMR** (400 MHz, CDCl<sub>3</sub>):  $\delta$  = 7.47 (s, 1H), 5.69 (s, 1H), 5.09 (s, 1H), 4.34 (t,  $J$  = 7.2 Hz, 2H), 2.14 (d,  $J$  = 1.2 Hz, 3H), 1.89 (p,  $J$  = 7.4 Hz, 2H), 1.37 (h,  $J$  = 7.4 Hz, 2H), 0.96 (t,  $J$  = 7.4 Hz, 3H). **<sup>13</sup>C NMR** (101 MHz, CDCl<sub>3</sub>):  $\delta$  = 148.9 (C<sub>q</sub>), 133.9 (C<sub>q</sub>), 119.5 (CH), 112.4 (CH<sub>2</sub>), 50.1 (CH<sub>2</sub>), 32.5 (CH<sub>2</sub>), 20.8 (CH<sub>3</sub>),

## 5. Experimental Part

19.9 (CH<sub>2</sub>), 13.6 (CH<sub>3</sub>). **IR** (ATR): 3124, 2959, 2933, 2873, 1640, 1456, 1228, 1127, 1046, 892, cm<sup>-1</sup>. **MS** (ESI) *m/z* (relative intensity): 166 (100) [M+H]<sup>+</sup>, 188 (54) [M+Na]<sup>+</sup>. **HR-MS** (ESI) *m/z* calcd for C<sub>9</sub>H<sub>16</sub>N<sub>3</sub> [M+H]<sup>+</sup> 166.1339, found 166.1341.

### 5.5.4 Analytical Data – Substrate Scope with BCP 94

**(*E*)-4-Ethyl-2-[(1-hexyl-1*H*-1,2,3-triazol-4-yl)methyl]-3-(non-2-en-1-yl)isoquinolin-1(2*H*)-one (95ah):**

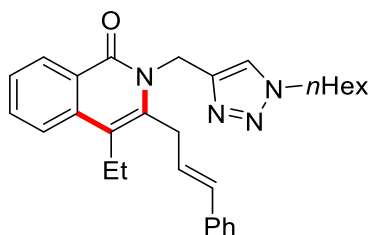


The general procedure **GPC** was followed using **51a** (85.9 mg, 0.30 mmol) and BCP **94h** (213 mg, 0.90 mmol). Purification by column chromatography (*n*hexane/EtOAc = 3/2) yielded **95ah** (84.8 mg, 61%) as colourless oil.

**<sup>1</sup>H NMR** (400 MHz, CDCl<sub>3</sub>): δ = 8.46 (d, *J* = 7.5 Hz, 1H), 7.75 (s, 1H), 7.70–7.63 (m, 2H), 7.44 (ddd, *J* = 8.1, 6.5, 1.7 Hz, 1H), 5.74–5.63 (m, 1H), 5.50–5.40 (m, 1H), 5.37 (s, 2H), 4.25 (t, *J* = 7.4 Hz, 2H), 3.83 (s, 2H), 2.74 (q, *J* = 7.5 Hz, 2H), 2.03 (q, *J* = 6.7 Hz, 2H), 1.84 (p, *J* = 7.2 Hz, 2H), 1.29–1.22 (m, 14H), 1.17 (t, *J* = 7.5 Hz, 3H), 0.87–0.81 (m, 6H). **<sup>13</sup>C NMR** (101 MHz, CDCl<sub>3</sub>): δ = 162.8 (C<sub>q</sub>), 144.6 (C<sub>q</sub>), 137.5 (C<sub>q</sub>), 136.6 (C<sub>q</sub>), 133.5 (CH), 132.4 (CH), 128.3 (CH), 125.9 (CH), 125.5 (CH), 125.1 (C<sub>q</sub>), 124.1 (CH), 122.9 (CH), 116.7 (C<sub>q</sub>), 50.4 (CH<sub>2</sub>), 39.9 (CH<sub>2</sub>), 32.7 (CH<sub>2</sub>), 32.0 (CH<sub>2</sub>), 31.8 (CH<sub>2</sub>), 31.2 (CH<sub>2</sub>), 30.2 (CH<sub>2</sub>), 29.3 (CH<sub>2</sub>), 28.9 (CH<sub>2</sub>), 26.2 (CH<sub>2</sub>), 22.7 (CH<sub>2</sub>), 22.5 (CH<sub>2</sub>), 20.9 (CH<sub>2</sub>), 14.6 (CH<sub>3</sub>), 14.2 (CH<sub>3</sub>), 14.0 (CH<sub>3</sub>). **IR** (ATR): 2955, 2926, 2856, 1643, 1592, 1460, 1337, 1047, 968, 773 cm<sup>-1</sup>. **MS** (ESI) *m/z* (relative intensity): 469 (100), 495 (17) [M+Na]<sup>+</sup>. **HR-MS** (ESI) *m/z* calcd for C<sub>29</sub>H<sub>43</sub>N<sub>4</sub>O [M+H]<sup>+</sup> 463.3431, found 463.3426.

## 5. Experimental Part

### 3-Cinnamyl-4-ethyl-2-[(1-hexyl-1*H*-1,2,3-triazol-4-yl)methyl]isoquinolin-1(2*H*)-one (**95ai**):



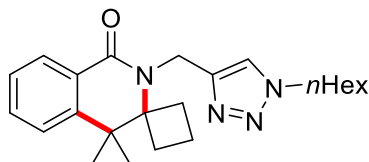
The general procedure **GPC** was followed using **51a** (85.9 mg, 0.30 mmol) and BCP **94i** (205 mg, 0.90 mmol). Purification by column chromatography (*n*hexane/EtOAc = 3/2) yielded **95ai** (72.3 mg, 53%) as colourless oil.

**<sup>1</sup>H NMR** (400 MHz, CDCl<sub>3</sub>):  $\delta$  = 8.50 (d,  $J$  = 6.6 Hz, 1H), 7.78 (s, 1H), 7.74–7.68 (m, 2H), 7.49 (ddd,  $J$  = 8.1, 6.6, 1.6 Hz, 1H), 7.39–7.27 (m, 4H), 7.24–7.18 (m, 1H), 6.50 (dt,  $J$  = 16.1, 4.9 Hz, 1H), 6.37 (d,  $J$  = 16.1 Hz, 1H), 5.40 (s, 2H), 4.25 (t,  $J$  = 7.4 Hz, 2H), 4.10 (s, 2H), 2.80 (q,  $J$  = 7.5 Hz, 2H), 1.91–1.80 (m, 2H), 1.34–1.24 (m, 6H), 1.21 (t,  $J$  = 7.5 Hz, 3H), 0.85 (t,  $J$  = 7.6 Hz, 3H). **<sup>13</sup>C NMR** (101 MHz, CDCl<sub>3</sub>):  $\delta$  = 162.8 (C<sub>q</sub>), 144.4 (C<sub>q</sub>), 136.9 (C<sub>q</sub>), 136.7 (C<sub>q</sub>), 136.5 (C<sub>q</sub>), 132.5 (CH), 131.9 (CH), 128.7 (CH), 128.3 (CH), 127.6 (CH), 126.3 (CH), 126.2 (CH), 125.8 (CH), 125.3 (C<sub>q</sub>), 124.1 (CH), 123.0 (CH), 117.2 (C<sub>q</sub>), 50.5 (CH<sub>2</sub>), 40.0 (CH<sub>2</sub>), 32.3 (CH<sub>2</sub>), 31.2 (CH<sub>2</sub>), 30.2 (CH<sub>2</sub>), 26.2 (CH<sub>2</sub>), 22.5 (CH<sub>2</sub>), 21.1 (CH<sub>2</sub>), 14.6 (CH<sub>3</sub>), 14.0 (CH<sub>3</sub>). **IR** (ATR): 2929, 2869, 1641, 1591, 1459, 1336, 1219, 1048, 773 cm<sup>-1</sup>. **MS** (ESI)  $m/z$  (relative intensity): 455 (100) [M+H]<sup>+</sup>, 477 (77) [M+Na]<sup>+</sup>, 931 (62) [2M+Na]<sup>+</sup>. **HR-MS** (ESI)  $m/z$  calcd for C<sub>29</sub>H<sub>35</sub>N<sub>4</sub>O [M+H]<sup>+</sup> 455.2805, found 455.2803.

## 5. Experimental Part

### 5.5.5 Analytical Data – Bispiro-Fused Isoquinolone 96

2'-[(1-Hexyl-1*H*-1,2,3-triazol-4-yl)methyl]dispiro(cyclobutane-1,3'-isoquinoline-4',1''-cyclopropan)-1'(2'*H*)-one (**96aa**):

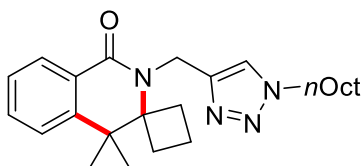


The general procedure **GPC** was followed using **51a** (85.9 mg, 0.30 mmol) and BCP **94a** (112 mg, 0.90 mmol). Purification by column chromatography (*n*hexane/EtOAc = 1/2) yielded **96aa** (51 mg, 45%) as colourless oil.

**<sup>1</sup>H NMR** (600 MHz, CDCl<sub>3</sub>):  $\delta$  = 8.02 (dd, *J* = 7.7, 1.5 Hz, 1H), 7.60 (s, 1H), 7.38 (td, *J* = 7.7, 7.5 Hz, 1H), 7.27 (dd, *J* = 7.8, 7.6 Hz, 1H), 6.98 (dd, *J* = 7.8, 1.1 Hz, 1H), 5.02 (s, 2H), 4.27 (t, *J* = 7.2 Hz, 2H), 2.49 (d, *J* = 11.1 Hz, 2H), 1.86–1.82 (m, 4H), 1.77 (dt, *J* = 11.5, 9.1 Hz, 1H), 1.56 (dt, *J* = 11.5, 9.1 Hz, 1H), 1.26–1.23 (m, 6H), 1.05–1.01 (m, 2H), 0.99–0.93 (m, 2H), 0.82 (t, *J* = 6.8 Hz, 3H). **<sup>13</sup>C NMR** (126 MHz, CDCl<sub>3</sub>):  $\delta$  = 164.6 (C<sub>q</sub>), 146.0 (C<sub>q</sub>), 141.4 (C<sub>q</sub>), 132.2 (CH), 130.3 (C<sub>q</sub>), 128.3 (CH), 126.4 (CH), 123.1 (CH), 122.2 (CH), 63.3 (C<sub>q</sub>), 50.5 (CH<sub>2</sub>), 38.2 (CH<sub>2</sub>), 31.3 (CH<sub>2</sub>), 30.3 (CH<sub>2</sub>), 30.1 (CH<sub>2</sub>), 26.3 (CH<sub>2</sub>), 25.8 (C<sub>q</sub>), 22.6 (CH<sub>2</sub>), 14.6 (CH<sub>2</sub>), 14.1 (CH<sub>3</sub>), 10.3 (CH<sub>2</sub>). **IR** (ATR): 2954, 2931, 2858, 1640, 1603, 1461, 1394, 1276, 1045, 757 cm<sup>-1</sup>. **MS** (ESI) *m/z* (relative intensity): 379 (100) [M+H]<sup>+</sup>, 757 (36) [2M+H]<sup>+</sup>, 779 (29) [2M+Na]<sup>+</sup>. **HR-MS** (ESI) *m/z* calcd for C<sub>23</sub>H<sub>31</sub>N<sub>4</sub>O [M+H]<sup>+</sup> 379.2492, found 379.2490.

## 5. Experimental Part

**2'-[(1-Octyl-1*H*-1,2,3-triazol-4-yl)methyl]dispiro(cyclobutane-1,3'-isoquinoline-4',1''-cyclopropan)-1'(2'*H*)-one (96ba):**

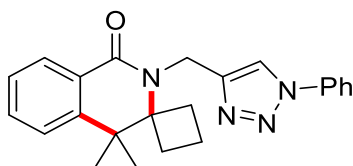


The general procedure **GPC** was followed using **51b** (98.6 mg, 0.30 mmol) and BCP **94a** (112 mg, 0.90 mmol). Purification by column chromatography (*n*hexane/EtOAc = 1/2) yielded **96ba** (42.6 mg, 35%) as colourless oil.

**<sup>1</sup>H NMR** (600 MHz, CDCl<sub>3</sub>):  $\delta$  = 8.03 (dd,  $J$  = 7.7, 1.5 Hz, 1 H), 7.61 (s, 1H), 7.40 (dd,  $J$  = 7.7, 7.6 Hz, 1H), 7.28 (dd,  $J$  = 7.8, 7.5 Hz, 1H), 7.00 (dd,  $J$  = 7.8, 1.2 Hz, 1H), 5.03 (s, 2H), 4.28 (t,  $J$  = 7.2 Hz, 2H), 2.56–2.45 (m, 2H), 1.88–1.83 (m, 4H), 1.80–1.75 (m, 1H), 1.58 (dt,  $J$  = 11.6, 9.1 Hz, 1H), 1.26–1.20 (m, 10H), 1.06–1.03 (m, 2H), 1.00–0.94 (m, 2H), 0.83 (t,  $J$  = 7.0 Hz, 3H). **<sup>13</sup>C NMR** (151 MHz, CDCl<sub>3</sub>):  $\delta$  = 164.8 (C<sub>q</sub>), 146.1 (C<sub>q</sub>), 141.5 (C<sub>q</sub>), 132.3 (CH), 130.4 (C<sub>q</sub>), 128.4 (CH), 126.5 (CH), 123.2 (CH), 122.3 (CH), 63.3 (C<sub>q</sub>), 50.5 (CH<sub>2</sub>), 38.2 (CH<sub>2</sub>), 31.8 (CH<sub>2</sub>), 30.3 (CH<sub>2</sub>), 29.9 (CH<sub>2</sub>), 29.2 (CH<sub>2</sub>), 29.1 (CH<sub>2</sub>), 26.6 (CH<sub>2</sub>), 25.8 (C<sub>q</sub>), 22.7 (CH<sub>2</sub>), 14.6 (CH<sub>2</sub>), 14.2 (CH<sub>3</sub>), 10.2 (CH<sub>2</sub>). **IR** (ATR): 2925, 2854, 1642, 1604, 1462, 1395, 1329, 1276, 1047, 769 cm<sup>-1</sup>. **MS** (ESI)  $m/z$  (relative intensity): 407 (59) [M+H]<sup>+</sup>, 429 (100) [M+Na]<sup>+</sup>, 835 (24) [2M+Na]<sup>+</sup>. **HR-MS** (ESI)  $m/z$  calcd for C<sub>25</sub>H<sub>35</sub>N<sub>4</sub>O [M+H]<sup>+</sup> 407.2805, found 407.2809.

## 5. Experimental Part

**2'-[(1-Phenyl-1*H*-1,2,3-triazol-4-yl)methyl]dispiro(cyclobutane-1,3'-isoquinoline-4',1''-cyclopropan)-1'(2'*H*)-one (96ya):**

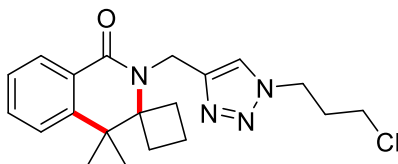


The general procedure **GPC** was followed using **51y** (83.5 mg, 0.30 mmol) and BCP **94a** (112 mg, 0.90 mmol). Purification by column chromatography (*n*hexane/EtOAc = 1/2) yielded **96ya** (33.3 mg, 30%) as colourless oil.

**<sup>1</sup>H NMR** (400 MHz, CDCl<sub>3</sub>):  $\delta$  = 8.13 (s, 1H), 8.06 (ddd,  $J$  = 7.7, 1.5, 0.5 Hz, 1H), 7.77–7.73 (m, 2H), 7.52–7.48 (m, 2H), 7.45–7.39 (m, 2H), 7.31 (dd,  $J$  = 7.6, 7.3 Hz, 1H), 7.03 (dd,  $J$  = 8.1, 1.1 Hz, 1H), 5.13 (s, 2H), 2.58 (d,  $J$  = 11.3 Hz, 2H), 1.96–1.91 (m, 2H), 1.89–1.83 (m, 1H), 1.65–1.60 (m, 1H), 1.15–1.07 (m, 2H), 1.06–0.98 (m, 2H). **<sup>13</sup>C NMR** (101 MHz, CDCl<sub>3</sub>):  $\delta$  = 164.9 (C<sub>q</sub>), 146.8 (C<sub>q</sub>), 141.5 (C<sub>q</sub>), 137.2 (C<sub>q</sub>), 132.4 (CH), 130.4 (C<sub>q</sub>), 129.8 (CH), 128.8 (CH), 128.4 (CH), 126.6 (CH), 122.4 (CH), 121.6 (CH), 120.5 (CH), 63.4 (C<sub>q</sub>), 38.2 (CH<sub>2</sub>), 30.1 (CH<sub>2</sub>), 25.8 (C<sub>q</sub>), 14.6 (CH<sub>2</sub>), 10.3 (CH<sub>2</sub>). **IR** (ATR): 2923, 2853, 1639, 1601, 1502, 1434, 1395, 1280, 1041, 758 cm<sup>-1</sup>. **MS** (ESI)  $m/z$  (relative intensity): 371 (48) [M+H]<sup>+</sup>, 393 (100) [M+Na]<sup>+</sup>, 763 (29) [2M+Na]<sup>+</sup>. **HR-MS** (ESI)  $m/z$  calcd for C<sub>23</sub>H<sub>23</sub>N<sub>4</sub>O [M+H]<sup>+</sup> 371.1866, found 371.1861.

## 5. Experimental Part

**2'-{[1-(3-Chloropropyl)-1*H*-1,2,3-triazol-4-yl]methyl}dispiro(cyclobutane-1,3'-isoquinoline-4',1''-cyclopropan)-1'(2'*H*)-one (96da):**

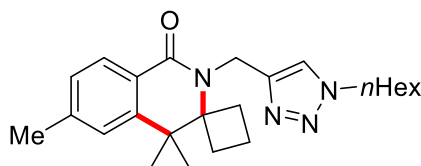


The general procedure **GPC** was followed using **51d** (86.3 mg, 0.30 mmol) and BCP **94a** (112 mg, 0.90 mmol). Purification by column chromatography (*n*hexane/EtOAc = 1/2) yielded **96da** (40.0 mg, 36%) as colourless oil.

**<sup>1</sup>H NMR** (500 MHz, CDCl<sub>3</sub>):  $\delta$  = 8.05 (ddd, *J* = 7.7, 1.5, 0.5 Hz, 1H), 7.69 (s, 1H), 7.42 (dd, *J* = 7.7, 7.6 Hz, 1H), 7.31 (dd, *J* = 7.8, 7.6 Hz, 1H), 7.02 (ddd, *J* = 7.8, 1.2, 0.5 Hz, 1H), 5.05 (s, 2H), 4.51 (t, *J* = 6.7 Hz, 2H), 3.52–3.48 (m, 2H), 2.51 (d, *J* = 11.2 Hz, 2H), 2.40–2.34 (m, 2H), 1.94–1.87 (m, 2H), 1.84–1.77 (m, 1H), 1.66–1.60 (m, 1H), 1.11–1.05 (m, 2H), 1.05–0.96 (m, 2H). **<sup>13</sup>C NMR** (126 MHz, CDCl<sub>3</sub>):  $\delta$  = 164.8 (C<sub>q</sub>), 146.3 (C<sub>q</sub>), 141.5 (C<sub>q</sub>), 132.4 (CH), 130.3 (C<sub>q</sub>), 128.4 (CH), 126.6 (CH), 123.9 (CH), 122.3 (CH), 63.3 (C<sub>q</sub>), 47.2 (CH<sub>2</sub>), 41.2 (CH<sub>2</sub>), 38.2 (CH<sub>2</sub>), 32.7 (CH<sub>2</sub>), 30.0 (CH<sub>2</sub>), 25.7 (C<sub>q</sub>), 14.6 (CH<sub>2</sub>), 10.2 (CH<sub>2</sub>). **IR** (ATR): 2948, 1639, 1604, 1461, 1406, 1298, 1152, 1044, 758, 557 cm<sup>-1</sup>. **MS** (ESI) *m/z* (relative intensity): 371 (40) [<sup>35</sup>Cl, M+H]<sup>+</sup>, 393 (100) [<sup>35</sup>Cl, M+Na]<sup>+</sup>, 763 (13) [<sup>35</sup>Cl, 2M+Na]<sup>+</sup>. **HR-MS** (ESI) *m/z* calcd for C<sub>20</sub>H<sub>24</sub><sup>35</sup>ClN<sub>4</sub>O [M+H]<sup>+</sup> 371.1633, found 371.1635.

## 5. Experimental Part

### 2'-[(1-Hexyl-1*H*-1,2,3-triazol-4-yl)methyl]-6'-methyldispiro(cyclobutane-1,3'-isoquinoline-4',1''-cyclopropan)-1'(2'*H*)-one (**96ea**):

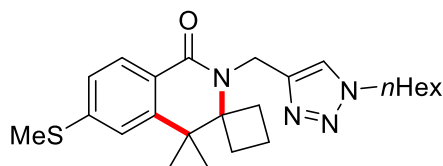


The general procedure **GPC** was followed using **51e** (90.1 mg, 0.30 mmol) and BCP **94a** (112 mg, 0.90 mmol). Purification by column chromatography (*n*hexane/EtOAc = 1/2) yielded **96ea** (37.6 mg, 32%) as colourless oil.

**<sup>1</sup>H NMR** (600 MHz, CDCl<sub>3</sub>):  $\delta$  = 7.60 (s, 1H), 7.22 (d,  $J$  = 7.6 Hz, 1H), 7.08 (d,  $J$  = 7.6 Hz, 1H), 6.86 (s, 1H), 4.99 (s, 2H), 4.28 (t,  $J$  = 7.2 Hz, 2H), 2.67 (s, 3H), 2.61–2.33 (m, 2H), 1.87–1.78 (m, 4H), 1.75 (ddd,  $J$  = 11.5, 7.3, 2.4 Hz, 1H), 1.56 (dt,  $J$  = 11.5, 9.0 Hz, 1H), 1.29–1.22 (m, 6H), 0.99–0.80 (m, 7H). **<sup>13</sup>C NMR** (101Mz, CDCl<sub>3</sub>):  $\delta$  = 165.3 (C<sub>q</sub>), 146.4 (C<sub>q</sub>), 142.0 (C<sub>q</sub>), 140.4 (C<sub>q</sub>), 131.0 (CH), 130.6 (CH), 129.2 (C<sub>q</sub>), 123.1 (CH), 120.6 (CH), 62.7 (C<sub>q</sub>), 50.5 (CH<sub>2</sub>), 37.9 (CH<sub>2</sub>), 31.3 (CH<sub>2</sub>), 30.3 (CH<sub>2</sub>), 29.9 (CH<sub>2</sub>), 26.7 (CH<sub>2</sub>), 26.3 (C<sub>q</sub>), 22.6 (CH<sub>2</sub>), 22.3 (CH<sub>3</sub>), 14.7 (CH<sub>2</sub>), 14.1 (CH<sub>3</sub>), 10.0 (CH<sub>2</sub>). **IR** (ATR): 2954, 2929, 2857, 1636, 1469, 1389, 1277, 1045, 778, 705 cm<sup>-1</sup>. **MS** (ESI)  $m/z$  (relative intensity): 393 (100) [M+H]<sup>+</sup>, 4415 (95) [M+Na]<sup>+</sup>. **HR-MS** (ESI)  $m/z$  calcd for C<sub>24</sub>H<sub>33</sub>N<sub>4</sub>O [M+H]<sup>+</sup> 393.2649, found 393.2653.

## 5. Experimental Part

**2'-[(1-Hexyl-1*H*-1,2,3-triazol-4-yl)methyl]-6'-(methylthio)dispiro(cyclobutane-1,3'-isoquinoline-4',1''-cyclopropan)-1'(2'*H*)-one (96sa):**

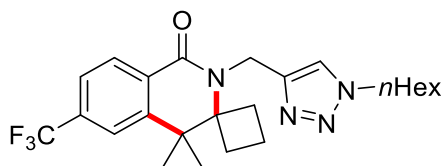


The general procedure **GPC** was followed using **51s** (99.8 mg, 0.30 mmol) and BCP **94a** (112 mg, 0.90 mmol). Purification by column chromatography (*n*hexane/EtOAc = 1/2) yielded **96sa** (50.8 mg, 40%) as colourless oil.

**<sup>1</sup>H NMR** (400 MHz, CDCl<sub>3</sub>): δ = 7.93 (d, *J* = 8.2 Hz, 1H), 7.60 (s, 1H), 7.10 (dd, *J* = 8.2, 1.8 Hz, 1H), 6.82 (s, 1H), 5.00 (s, 2H), 4.27 (t, *J* = 7.2 Hz, 2H), 2.50–2.44 (m, 5H), 1.88–1.82 (m, 4H), 1.79–1.73 (m, 1H), 1.56 (dt, *J* = 11.5, 9.0 Hz, 1H), 1.28–1.22 (m, 6H), 1.06–1.02 (m, 2H), 0.99–0.92 (m, 2H), 0.83 (t, *J* = 7.0 Hz, 3H). **<sup>13</sup>C NMR** (101 MHz, CDCl<sub>3</sub>): δ = 164.5 (C<sub>q</sub>), 146.1 (C<sub>q</sub>), 144.2 (C<sub>q</sub>), 142.0 (C<sub>q</sub>), 128.9 (CH), 127.0 (CH), 123.1 (C<sub>q</sub>), 123.0 (CH), 119.4 (CH), 63.2 (C<sub>q</sub>), 50.5 (CH<sub>2</sub>), 38.1 (CH<sub>2</sub>), 31.2 (CH<sub>2</sub>), 30.3 (CH<sub>2</sub>), 30.0 (CH<sub>2</sub>), 26.2 (CH<sub>2</sub>), 25.9 (C<sub>q</sub>), 22.5 (CH<sub>2</sub>), 15.1 (CH<sub>3</sub>), 14.5 (CH<sub>2</sub>), 14.0 (CH<sub>3</sub>), 10.2 (CH<sub>2</sub>). **IR** (ATR): 2854, 2928, 2857, 1638, 1594, 1435, 1422, 1384, 1046, 784 cm<sup>-1</sup>. **MS** (ESI) *m/z* (relative intensity): 425 (100) [M+H]<sup>+</sup>, 447 (60) [M+Na]<sup>+</sup>. **HR-MS** (ESI) *m/z* calcd for C<sub>24</sub>H<sub>33</sub>N<sub>4</sub>OS [M+H]<sup>+</sup> 425.2370, found 425.2374.

## 5. Experimental Part

**2'-[(1-Hexyl-1*H*-1,2,3-triazol-4-yl)methyl]-6'-(trifluoromethyl)dispiro(cyclobutane-1,3'-isoquinoline-4',1''-cyclopropan)-1'(2'*H*)-one (96ha):**

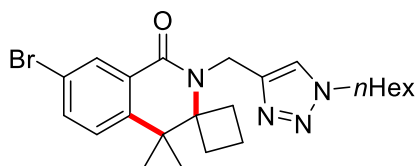


The general procedure **GPC** was followed using **51h** (106 mg, 0.30 mmol) and BCP **94a** (112 mg, 0.90 mmol). Purification by column chromatography (*n*hexane/EtOAc = 1/2) yielded **96ha** (37.5 mg, 28%) as colourless oil.

**<sup>1</sup>H NMR** (600 MHz, CDCl<sub>3</sub>):  $\delta$  = 8.14 (dd,  $J$  = 8.0, 0.7 Hz, 1H), 7.61 (s, 1H), 7.54 (ddd,  $J$  = 8.0, 1.7, 0.8 Hz, 1H), 7.23 (d,  $J$  = 1.6 Hz, 1H), 5.03 (s, 2H), 4.29 (t,  $J$  = 7.2 Hz, 2H), 2.54 (d,  $J$  = 11.9 Hz, 2H), 1.88–1.83 (m, 4H), 1.83–1.7 (m, 1H), 1.60 (dt,  $J$  = 11.6, 9.1 Hz, 1H), 1.32–1.23 (m, 6H), 1.15–1.10 (m, 2H), 1.08–0.99 (m, 2H), 0.83 (t,  $J$  = 7.0 Hz, 3H). **<sup>13</sup>C NMR** (151 MHz, CDCl<sub>3</sub>):  $\delta$  = 163.6 (C<sub>q</sub>), 145.6 (C<sub>q</sub>), 142.6 (C<sub>q</sub>), 133.9 (q,  $^2J_{C-F}$  = 32.3 Hz, C<sub>q</sub>), 133.5 (C<sub>q</sub>), 129.0 (CH), 123.9 (q,  $^1J_{C-F}$  = 272.8 Hz, C<sub>q</sub>), 123.4 (q,  $^3J_{C-F}$  = 3.9 Hz, CH), 123.0 (CH), 119.5 (q,  $^3J_{C-F}$  = 3.9 Hz, CH), 63.3 (C<sub>q</sub>), 50.5 (CH<sub>2</sub>), 38.3 (CH<sub>2</sub>), 31.2 (CH<sub>2</sub>), 30.3 (CH<sub>2</sub>), 30.0 (CH<sub>2</sub>), 26.3 (CH<sub>2</sub>), 25.9 (C<sub>q</sub>), 22.5 (CH<sub>2</sub>), 14.5 (CH<sub>2</sub>), 14.0 (CH<sub>3</sub>), 10.6 (CH<sub>2</sub>). **<sup>19</sup>F NMR** (565 MHz, CDCl<sub>3</sub>):  $\delta$  = –62.89 (s). **IR** (ATR): 2954, 2933, 1646, 1443, 1295, 1443, 1295, 1167, 1128, 1048 cm<sup>–1</sup>. **MS** (ESI)  $m/z$  (relative intensity): 447 (45) [M+H]<sup>+</sup>, 469 (100) [M+Na]<sup>+</sup>. **HR-MS** (ESI)  $m/z$  calcd for C<sub>24</sub>H<sub>30</sub>F<sub>3</sub>N<sub>4</sub>O [M+H]<sup>+</sup> 447.2366, found 447.2371.

## 5. Experimental Part

**7'-Bromo-2'-[(1-hexyl-1*H*-1,2,3-triazol-4-yl)methyl]dispiro(cyclobutane-1,3'-isoquinoline-4',1''-cyclopropan)-1'(2'*H*)-one (96wa):**

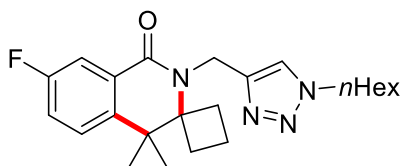


The general procedure **GPC** was followed using **51w** (110 mg, 0.30 mmol) and BCP **94a** (112 mg, 0.90 mmol). Purification by column chromatography (*n*hexane/EtOAc = 1/2) yielded **96wa** (42.3 mg, 31%) as colourless oil.

**<sup>1</sup>H NMR** (500 MHz, CDCl<sub>3</sub>): δ = 8.15 (d, *J* = 2.2 Hz, 1H), 7.60 (s, 1H), 7.50 (d, *J* = 8.3 Hz, 1H), 6.87 (d, *J* = 8.3 Hz, 1H), 5.00 (s, 2H), 4.28 (t, *J* = 7.2 Hz, 2H), 2.50 (d, *J* = 11.8 Hz, 2H), 1.88–1.83 (m, 4H), 1.80–1.74 (m, 1H), 1.57 (dt, *J* = 11.5, 9.1 Hz, 1H), 1.28–1.23 (m, 6H), 1.09–1.04 (m, 2H), 0.97–0.91 (m, 2H), 0.83 (t, *J* = 6.9 Hz, 3H). **<sup>13</sup>C NMR** (126 MHz, CDCl<sub>3</sub>): δ = 163.5 (C<sub>q</sub>), 145.7 (C<sub>q</sub>), 140.6 (C<sub>q</sub>), 135.1 (CH), 132.2 (C<sub>q</sub>), 131.3 (CH), 124.3 (CH), 123.18 (CH), 120.3 (C<sub>q</sub>), 63.2 (C<sub>q</sub>), 50.5 (CH<sub>2</sub>), 38.3 (CH<sub>2</sub>), 31.2 (CH<sub>2</sub>), 30.3 (CH<sub>2</sub>), 30.0 (CH<sub>2</sub>), 26.2 (CH<sub>2</sub>), 25.6 (C<sub>q</sub>), 22.5 (CH<sub>2</sub>), 14.5 (CH<sub>2</sub>), 14.0 (CH<sub>3</sub>), 10.4 (CH<sub>2</sub>). **IR** (ATR): 2954, 2930, 1642, 1425, 1374, 1320, 1249, 1132, 1047, 789 cm<sup>-1</sup>. **MS** (ESI) *m/z* (relative intensity): 457 (47) [<sup>79</sup>Br, M+H]<sup>+</sup>, 479 (100) [<sup>79</sup>Br, M+Na]<sup>+</sup>. **HR-MS** (ESI) *m/z* calcd for C<sub>23</sub>H<sub>30</sub><sup>79</sup>BrN<sub>4</sub>O [M+H]<sup>+</sup> 457.1598, found 457.1597.

## 5. Experimental Part

### 7'-Fluoro-2'-[(1-hexyl-1*H*-1,2,3-triazol-4-yl)methyl]dispiro(cyclobutane-1,3'-isoquinoline-4',1''-cyclopropan)-1'(2'*H*)-one (**96ua**):



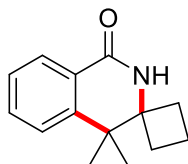
The general procedure **GPC** was followed using **51u** (91.3 mg, 0.30 mmol) and BCP **94a** (112 mg, 0.90 mmol). Purification by column chromatography (*n*hexane/EtOAc = 1/2) yielded **96ua** (34.5 mg, 29%) as colourless oil.

**<sup>1</sup>H NMR** (400 MHz, CDCl<sub>3</sub>):  $\delta$  = 7.75 (dd,  $J$  = 9.1, 2.8 Hz, 1H), 7.65 (s, 1H), 7.12 (dd,  $J$  = 8.4, 2.8 Hz, 1H), 7.00 (dd,  $J$  = 8.5, 4.9 Hz, 1H), 5.05 (s, 2H), 4.32 (t,  $J$  = 7.2 Hz, 2H), 2.61–2.48 (m, 2H), 1.92–1.86 (m, 4H), 1.82–1.76 (m, 1H), 1.61 (dt,  $J$  = 11.4, 9.1 Hz, 1H), 1.34–1.24 (m, 6H), 1.12–1.06 (m, 2H), 1.01–0.94 (m, 2H), 0.87 (t,  $J$  = 6.9 Hz, 3H). **<sup>13</sup>C NMR** (101 MHz, CDCl<sub>3</sub>):  $\delta$  = 163.7 (d,  $^4J_{C-F}$  = 2.6 Hz, C<sub>q</sub>), 161.6 (d,  $^1J_{C-F}$  = 245.1 Hz, C<sub>q</sub>), 145.7 (C<sub>q</sub>), 137.2 (d,  $^4J_{C-F}$  = 3.0 Hz, C<sub>q</sub>), 132.3 (d,  $^3J_{C-F}$  = 7.4 Hz, CH), 124.3 (d,  $^3J_{C-F}$  = 7.6 Hz, C<sub>q</sub>), 123.1 (CH), 119.1 (d,  $^2J_{C-F}$  = 21.9 Hz, CH), 115.1 (d,  $^2J_{C-F}$  = 23.2 Hz, CH), 63.4 (C<sub>q</sub>), 50.5 (CH<sub>2</sub>), 38.3 (CH<sub>2</sub>), 31.2 (CH<sub>2</sub>), 30.3 (CH<sub>2</sub>), 29.9 (CH<sub>2</sub>), 26.2 (CH<sub>2</sub>), 25.3 (C<sub>q</sub>), 22.5 (CH<sub>2</sub>), 14.5 (CH<sub>2</sub>), 14.0 (CH<sub>3</sub>), 10.2 (CH<sub>2</sub>). **<sup>19</sup>F NMR** (377 MHz, CDCl<sub>3</sub>):  $\delta$  = –115.76 (td,  $J$  = 8.8, 5.0 Hz). **IR** (ATR): 2955, 2931, 2858, 1642, 1588, 1443, 1382, 1265, 1047, 825 cm<sup>–1</sup>. **MS** (ESI)  $m/z$  (relative intensity): 397 (44) [M+H]<sup>+</sup>, 419 (100) [M+Na]<sup>+</sup>, 815 (20) [2M+Na]<sup>+</sup>. **HR-MS** (ESI)  $m/z$  calcd for C<sub>23</sub>H<sub>30</sub>FN<sub>4</sub>O [M+H]<sup>+</sup> 397.2398, found 397.2402.

## 5. Experimental Part

### 5.5.6 Removal of TAH Group

**Dispiro(cyclobutane-1,3'-isoquinoline-4',1''-cyclopropan)-1'(2'*H*)-one (120):**



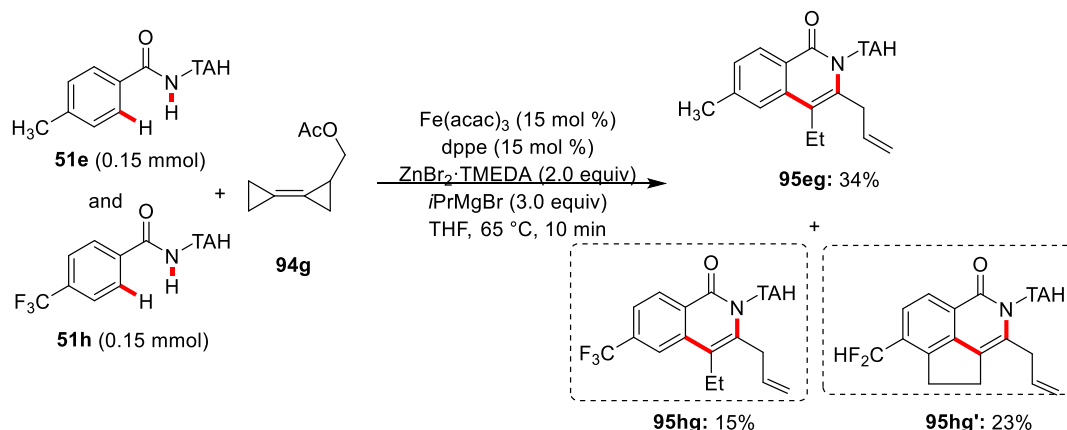
The general procedure **GPD** was followed using **96aa** (114 mg, 0.30 mmol). Purification by column chromatography (*n*hexane/EtOAc = 1/2) yielded **120** (42.2 mg, 66%) as a white solid.

**M.p.** = 188–189 °C. **<sup>1</sup>H NMR** (400 MHz, CDCl<sub>3</sub>): δ = 8.09 (dd, *J* = 7.7, 1.6 Hz, 1H), 7.47 (dd, *J* = 7.7, 7.6 Hz, 1H), 7.33 (dd, *J* = 7.8, 7.5 Hz, 1H), 7.02 (dd, *J* = 7.8, 1.3 Hz, 1H), 6.41 (s, 1H), 2.18–2.10 (m, 2H), 2.03–1.94 (m, 3H), 1.76–1.66 (m, 1H), 1.19–1.13 (m, 2H), 1.07–1.00 (m, 2H). **<sup>13</sup>C NMR** (101 MHz, CDCl<sub>3</sub>): δ = 165.6 (C<sub>q</sub>), 141.8 (C<sub>q</sub>), 132.8 (CH), 129.7 (C<sub>q</sub>), 128.2 (CH), 126.4 (CH), 122.4 (CH), 59.2 (C<sub>q</sub>), 32.5 (CH<sub>2</sub>), 25.5 (C<sub>q</sub>), 13.9 (CH<sub>2</sub>), 10.6 (CH<sub>2</sub>). **IR** (ATR): 2954, 2930, 2857, 1665, 1605, 1465, 1439, 1382, 1052, 759 cm<sup>-1</sup>. **MS** (ESI) *m/z* (relative intensity): 214 (100) [M+H]<sup>+</sup>, 256 (78) [M+Na]<sup>+</sup>, 449 (48) [2M+Na]<sup>+</sup>. **HR-MS** (ESI) *m/z* calcd for C<sub>14</sub>H<sub>16</sub>NO [M+H]<sup>+</sup> 214.1226, found 214.1227.

## 5. Experimental Part

### 5.5.7 Mechanistic Studies

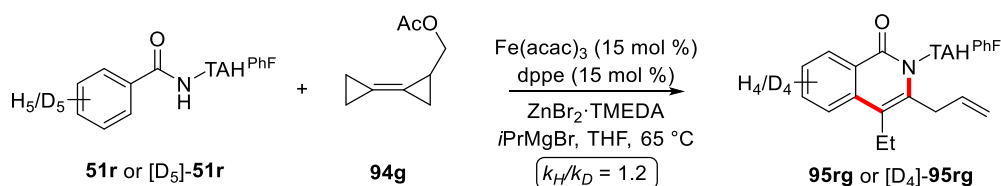
#### Competition Experiments



To a stirred solution of **51e** (45.1 mg, 0.15 mmol), **51h** (53.2 mg, 0.15 mmol),  $\text{ZnBr}_2 \cdot \text{TMEDA}$  (205 mg, 0.60 mmol) and  $\text{dppe}$  (17.9 mg, 15 mol %) in THF (0.20 mL),  $i\text{PrMgBr}$  (3.0 M in 2-MeTHF, 300  $\mu\text{L}$ , 0.90 mmol) was added in one portion and the reaction mixture was stirred for 5 min at ambient temperature. Then,  $\text{Fe}(\text{acac})_3$  (15.9 mg, 15 mol %) was added. After stirring for additional 5 min, a solution of BCP **94g** (137 mg, 0.90 mmol) in THF (0.20 mL) was added in one portion. The reaction mixture was stirred at 65 °C. After 10 min, sat. aqueous  $\text{NH}_4\text{Cl}$  (3.0 mL) was added and the aqueous phase was extracted with  $\text{CH}_2\text{Cl}_2$  (3  $\times$  15 mL). The combined organic phases were dried over  $\text{Na}_2\text{SO}_4$ , filtered and concentrated. Purification by column chromatography ( $n\text{hexane}/\text{EtOAc}$  = 3/1 to 3/2) yielded **95eg** (19.9 mg, 34%), **95hg** (10.2 mg, 15%) and **95hg'** (15.4 mg, 23%).

## 5. Experimental Part

### Intermolecular Kinetic Isotope Effect (KIE) Study



To a stirred solution of **51r** (29.6 mg, 0.10 mmol) or  $[\text{D}_5]\text{-51r}$  (30.1 mg, 0.10 mmol),  $\text{ZnBr}_2\cdot\text{TMEDA}$  (68.3 mg, 0.20 mmol) and dppe (5.98 mg, 15 mol %) in THF (0.1 mL),  $i\text{PrMgBr}$  (3.0 M in 2-MeTHF, 0.30 mmol) was added in one portion and the reaction mixture was stirred for 5 min at ambient temperature. Then,  $\text{Fe}(\text{acac})_3$  (5.29 mg, 15 mol %) in THF (0.1 mL) was added in a single portion. After stirring for additional 5 min, BCP **94g** (30.8 mg, 0.2 mmol) was added in one portion. The reaction mixture was stirred at 65 °C. After the times indicated below, sat. aqueous  $\text{NH}_4\text{Cl}$  (3.0 mL) was added and the aqueous phase was extracted with  $\text{CH}_2\text{Cl}_2$  ( $3 \times 15$  mL). The combined organic phases were dried over  $\text{Na}_2\text{SO}_4$ , filtered and concentrated. 1,3,5-Triisopropylbenzene (10.2 mg, 0.05 mmol) was added into the reaction mixture then diluted with  $\text{CDCl}_3$  (0.7 mL). The yields of product were determined *via*  $^1\text{H}$  NMR using 1,3,5-Triisopropylbenzene (10.2 mg, 0.05 mmol) as the standard.

Time [min]	1	3	5	7	9	11	13
<b>95rg</b> [%]	0.0	4.0	6.0	8.0	11.0	13.0	15.0
$[\text{D}_4]\text{-95rg}$ [%]	1.0	3.0	5.0	7.0	10.0	11.0	13.0

## 5. Experimental Part

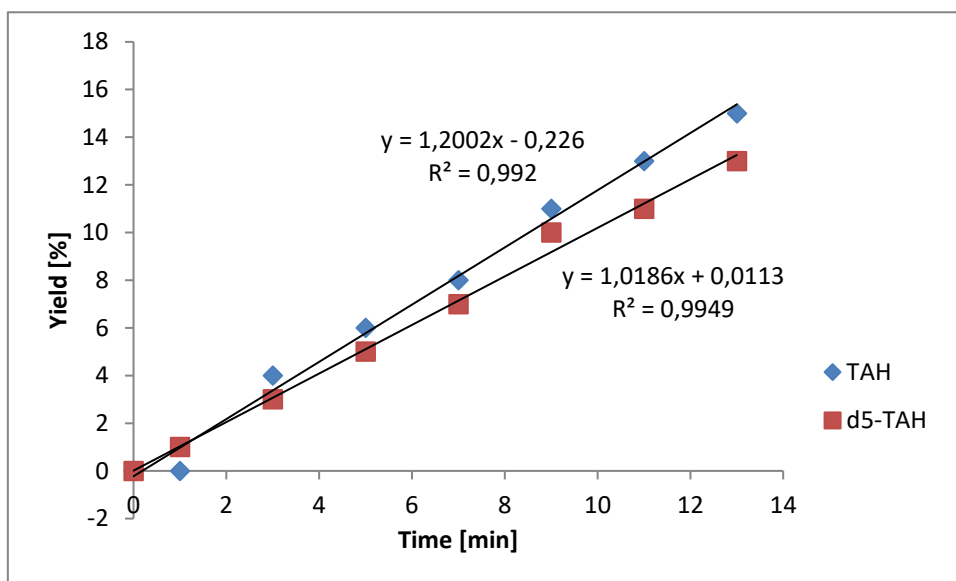
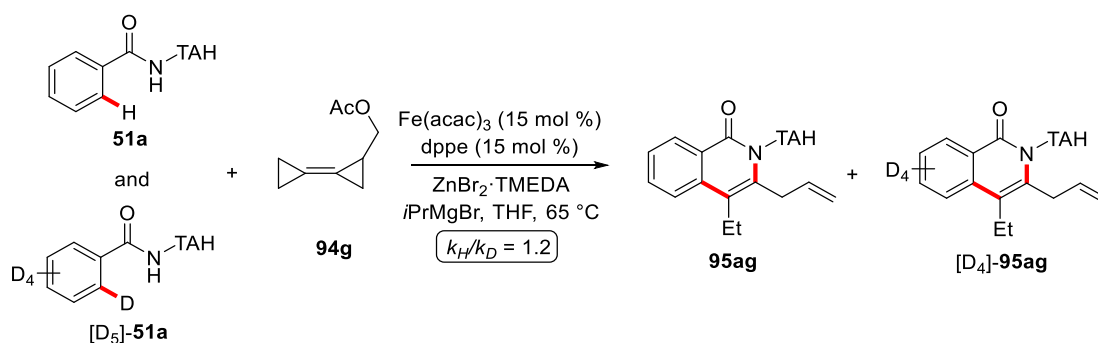


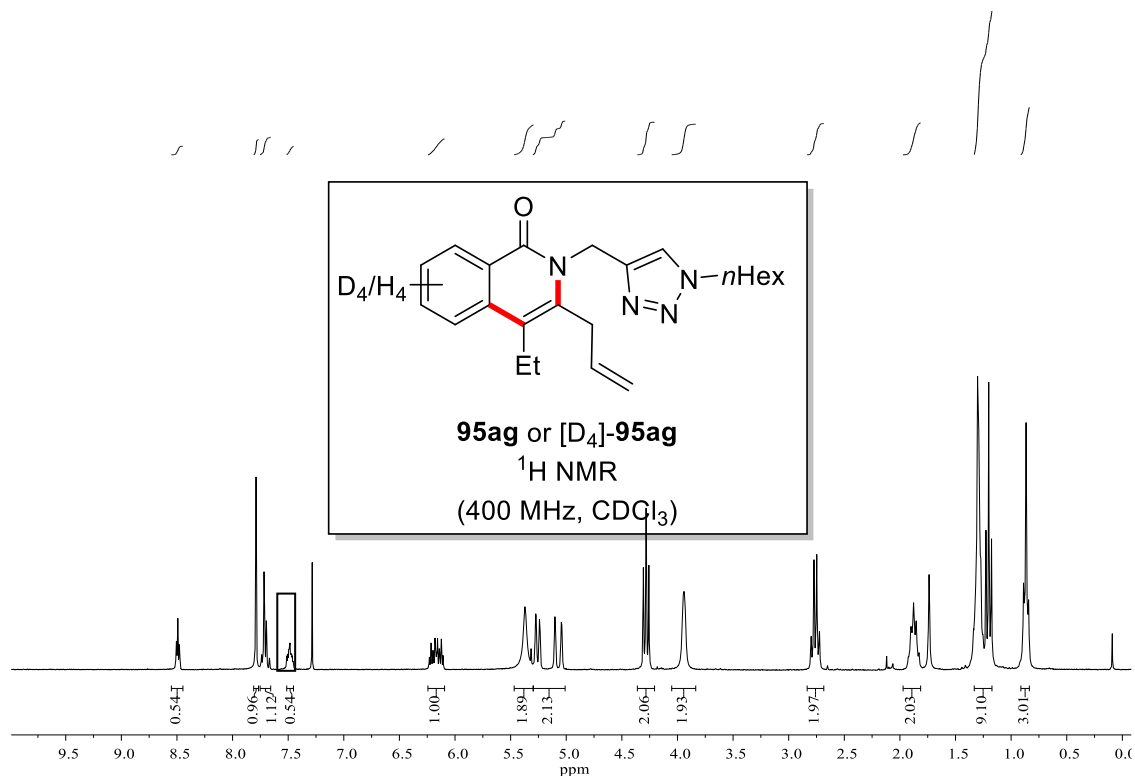
**Figure 5.3** Initial rates for the reaction of **51r** or [**D**<sub>5</sub>]-**51r** with **94g**.



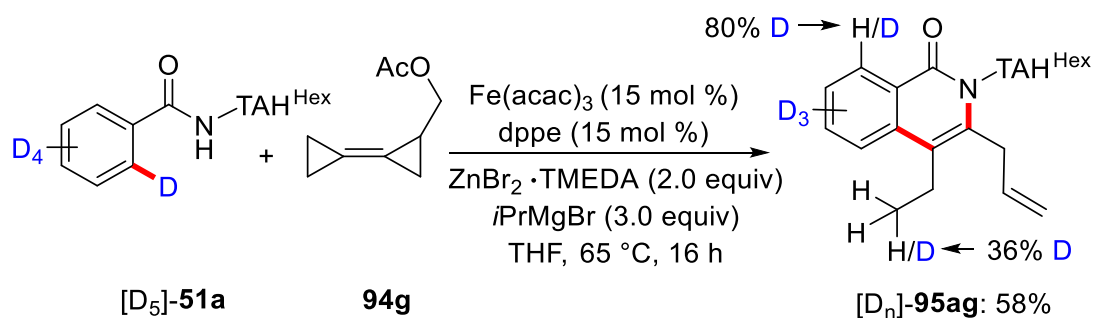
To a stirred solution of **51a** (43.0 mg, 0.15 mmol), [**D**<sub>5</sub>]-**51a** (43.7 mg, 0.15 mmol)  $\text{ZnBr}_2 \cdot \text{TMEDA}$  (205 mg, 0.60 mmol) and  $\text{dppe}$  (17.9 mg, 15 mol %) in THF (0.20 mL),  $i\text{PrMgBr}$  (3.0 M in 2-MeTHF, 300  $\mu\text{L}$ , 0.90 mmol) was added in one portion and the reaction mixture was stirred for 5 min at ambient temperature. Then,  $\text{Fe}(\text{acac})_3$  (15.9 mg, 15 mol %) was added. After stirring for additional 5 min, a solution of BCP **94g** (137 mg, 0.90 mmol) in THF (0.2 mL) was added in one portion. After stirring 10 min at 65 °C, sat. aqueous  $\text{NH}_4\text{Cl}$  (3.0 mL) was added and aqueous phase was extracted with  $\text{CH}_2\text{Cl}_2$  ( $3 \times 15$  mL). The combined organic phases were dried over  $\text{Na}_2\text{SO}_4$ , filtered and concentrated under reduced pressure. Purification by column

## 5. Experimental Part

chromatography (*n*hexane/EtOAc = 3/2) afforded a mixture of both products. The ratio of **95ag** to [D<sub>4</sub>]-**95ag** was determined by <sup>1</sup>H NMR spectroscopic analysis.



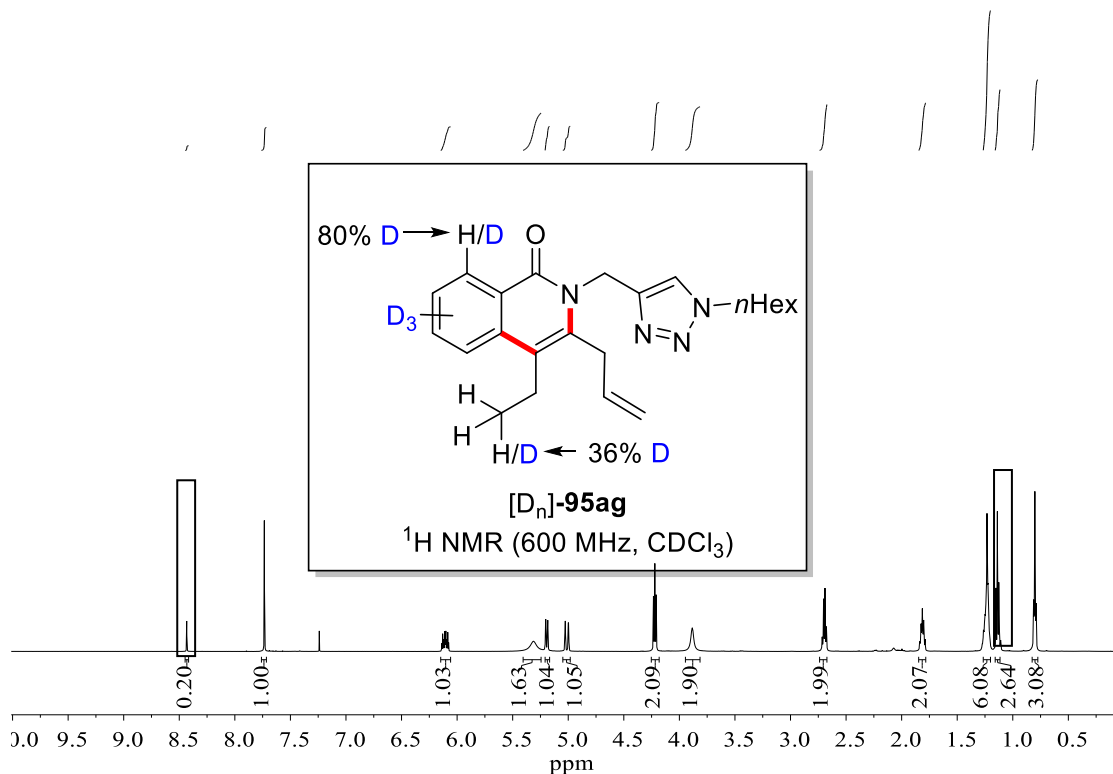
## Isotopically-labelled Experiments



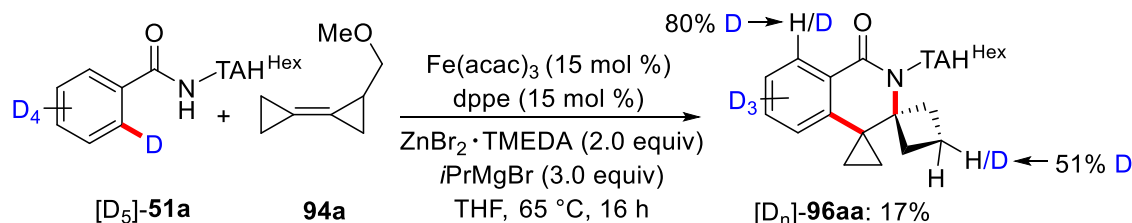
To a stirred solution of [D<sub>5</sub>]-**51a** (87.4 mg, 0.30 mmol), ZnBr<sub>2</sub>·TMEDA (205 mg, 0.60 mmol), dppe (17.9 mg, 15 mol %) in THF (0.20 mL), *i*PrMgBr (3.0 M in 2-MeTHF, 300 μL, 0.90 mmol) was added in one portion and the reaction mixture was stirred for 5 min at ambient temperature. Then, Fe(acac)<sub>3</sub> (15.9 mg, 15 mol %) was added. After stirring the solution for additional 5 min, a solution of BCP **94g** (137 mg, 0.90 mmol) in THF (0.20 mL) was added in one portion.

## 5. Experimental Part

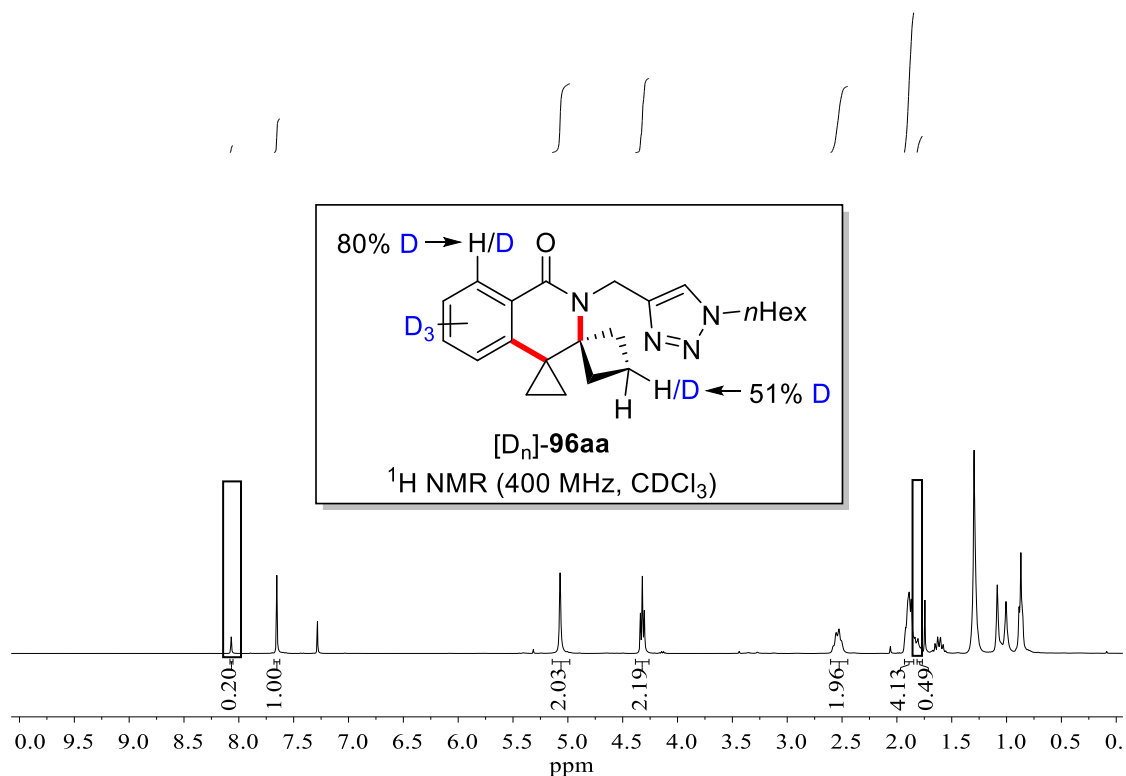
The mixture was placed in a pre-heated oil bath at 65 °C. After stirring for 16 h, sat. aqueous  $\text{NH}_4\text{Cl}$  (2.0 mL) was added to the reaction mixture and the aqueous phase was extracted with  $\text{CH}_2\text{Cl}_2$  ( $3 \times 15$  mL). The combined organic phases were dried over  $\text{Na}_2\text{SO}_4$ , filtered and concentrated. Purification by column chromatography (*n*hexane/EtOAc = 3/2) yielded **[D<sub>n</sub>]-95ag** (66.6 mg, 58%) as colourless oil.



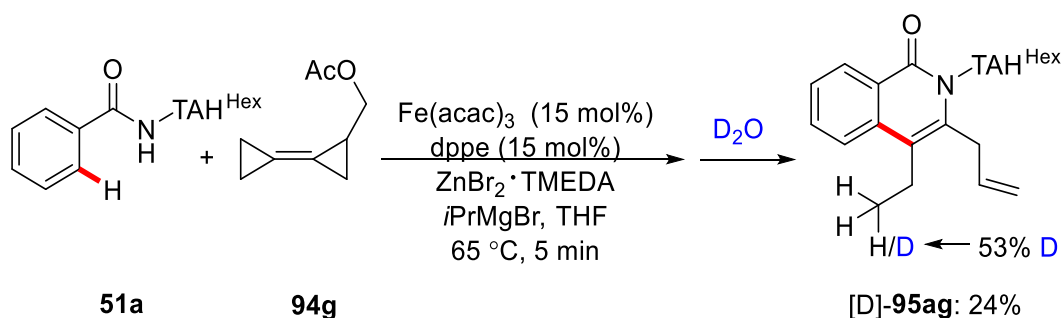
## 5. Experimental Part



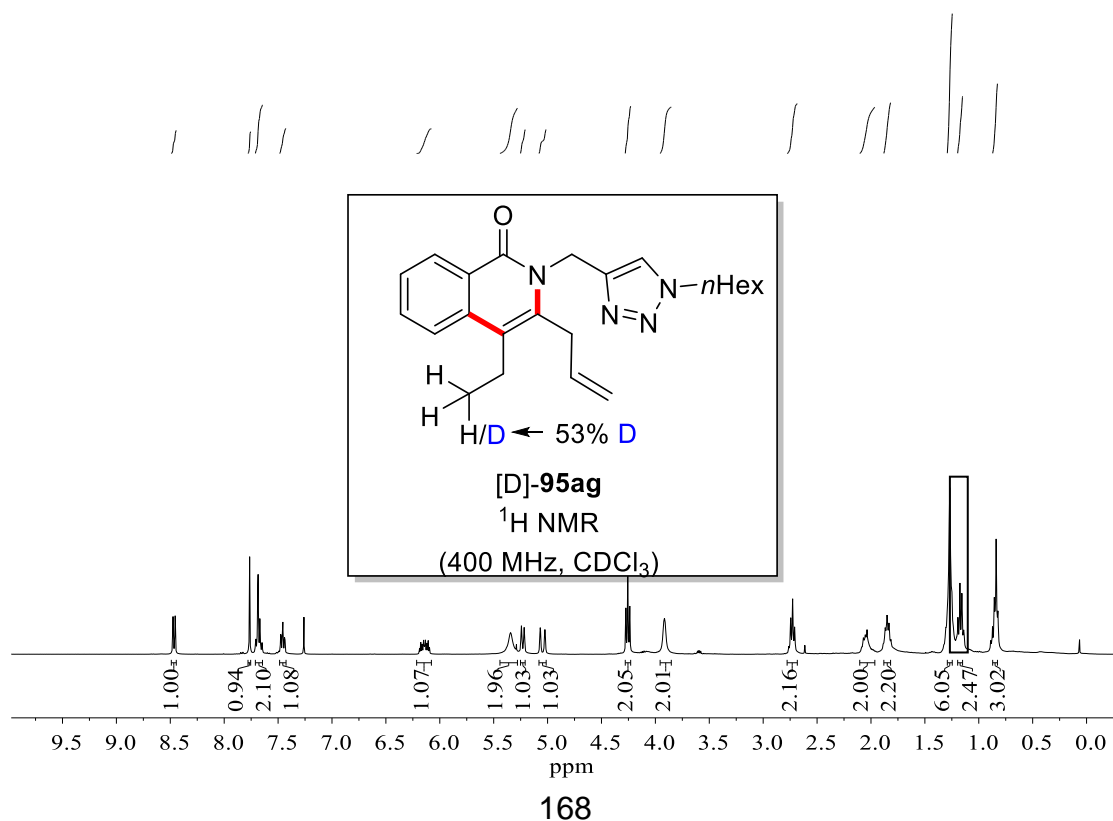
To a stirred solution of  $[D_5]\text{-51a}$  (87.4 mg, 0.30 mmol),  $\text{ZnBr}_2 \cdot \text{TMEDA}$  (205 mg, 0.60 mmol),  $\text{dppe}$  (17.9 mg, 15 mol %) in THF (0.20 mL),  $i\text{PrMgBr}$  (3.0 M in 2-MeTHF, 300  $\mu\text{L}$ , 0.90 mmol) was added in one portion and the reaction mixture was stirred for 5 min at ambient temperature. Then,  $\text{Fe}(\text{acac})_3$  (15.9 mg, 15 mol %) was added. After stirring the solution for additional 5 min, a solution of BCP **94a** (137 mg, 0.90 mmol) in THF (0.20 mL) was added in one portion. The mixture was placed in a pre-heated oil bath at 65 °C. After stirring for 16 h, sat. aqueous  $\text{NH}_4\text{Cl}$  (2.0 mL) was added to the reaction mixture and the aqueous phase was extracted with  $\text{CH}_2\text{Cl}_2$  ( $3 \times 15$  mL). The combined organic phases were dried over  $\text{Na}_2\text{SO}_4$ , filtered and concentrated. Purification by column chromatography ( $n\text{hexane}/\text{EtOAc} = 1/2$ ) yielded  $[D_n]\text{-96aa}$  (19.5 mg, 17%) as colourless oil.



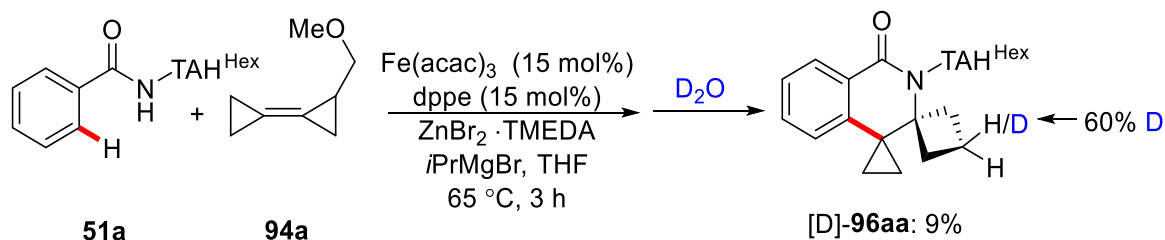
## 5. Experimental Part



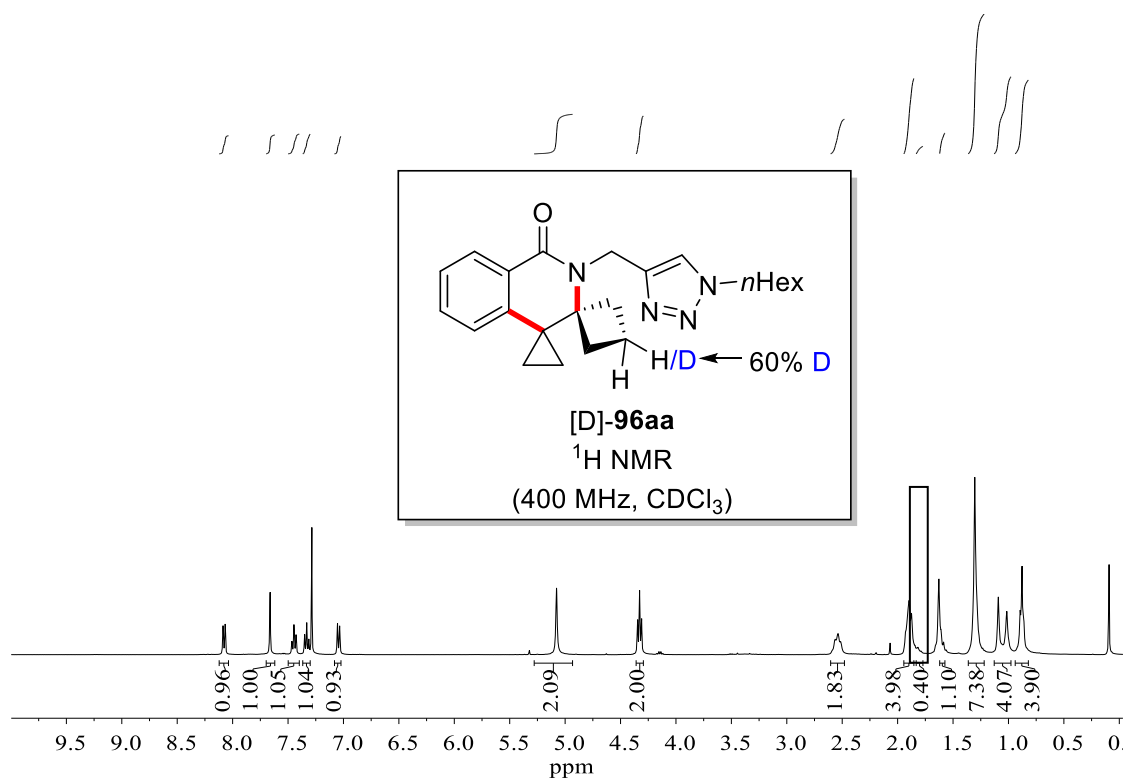
To a stirred solution of **51a** (85.9 mg, 0.3 mmol),  $\text{ZnBr}_2 \cdot \text{TMEDA}$  (205 mg, 0.60 mmol) and  $\text{dppe}$  (17.9 mg, 15 mol %) in THF (0.2 mL),  $i\text{PrMgBr}$  (3.0 M in 2-MeTHF, 300  $\mu\text{L}$ , 0.90 mmol) was added in one portion and the reaction mixture was stirred for 5 min at ambient temperature. Then,  $\text{Fe}(\text{acac})_3$  (15.9 mg, 15 mol %) was added. After stirring for additional 5 min, a solution of BCP **94g** (137 mg, 0.90 mmol) in THF (0.20 mL) was added in one portion. The reaction mixture was stirred at 65 °C. After 5 min,  $\text{D}_2\text{O}$  (2.0 mL) was added and the aqueous phase was extracted with  $\text{CH}_2\text{Cl}_2$  ( $3 \times 15 \text{ mL}$ ). The combined organic phases were dried over  $\text{Na}_2\text{SO}_4$ , filtered and concentrated. Purification by column chromatography ( $n\text{hexane}/\text{EtOAc} = 3/2$ ) yielded **[D]-95ag** (27 mg, 24%) The amount of deuterium incorporation was determined by  $^1\text{H}$  NMR.



## 5. Experimental Part



To a stirred solution of **51a** (85.9 mg, 0.3 mmol),  $\text{ZnBr}_2 \cdot \text{TMEDA}$  (205 mg, 0.60 mmol) and dppe (17.9 mg, 15 mol %) in THF (0.2 mL),  $i\text{PrMgBr}$  (3.0 M in 2-MeTHF, 300  $\mu\text{L}$ , 0.90 mmol) was added in one portion and the reaction mixture was stirred for 5 min at ambient temperature. Then,  $\text{Fe(acac)}_3$  (15.9 mg, 15 mol %) was added. After stirring for additional 5 min, a solution of BCP **94a** (112 mg, 0.90 mmol) in THF (0.20 mL) was added in one portion. The reaction mixture was stirred at 65  $^\circ\text{C}$ . After 3 h,  $\text{D}_2\text{O}$  (2.0 mL) was added and the aqueous phase was extracted with  $\text{CH}_2\text{Cl}_2$  ( $3 \times 15 \text{ mL}$ ). The combined organic phases were dried over  $\text{Na}_2\text{SO}_4$ , filtered and concentrated. Purification by column chromatography ( $n\text{hexane}/\text{EtOAc} = 1/2$ ) yielded **[D]-96aa** (10.2 mg, 9%) The position of deuterium incorporation was determined by  $^1\text{H}$  NMR.



## 5. Experimental Part

### 5.6 Mössbauer Measurement

After sample preparation, the spectra were recorded and interpreted by Dr. S. Demeshko.

**Table 5.1** Mössbauer parameters of reaction mixtures.

Entry	Reaction	Valence of Iron/ Spin State	$\delta$ (mm s <sup>-1</sup> )	$\Delta E_Q$ (mm s <sup>-1</sup> )	rel. int. (%)
1	<sup>57</sup> FeCl <sub>2</sub> + THF	+2 <sup>HS</sup>	1.26	3.05	100
2	Entry 1 + MeMgBr	+1.4 <sup>[91]</sup>	0.29	0.88	100
3	Entry 2 + ZnBr <sub>2</sub> ·TMEDA	+2 <sup>HS</sup> +2 <sup>HS</sup>	1.01 1.36	2.69 2.56	69 31
4	Entry 3 + dppe	+2 <sup>HS</sup> +2 <sup>HS</sup>	0.92 0.98 1.24	1.42 2.57 2.68	23 40 37
5	Entry 4 + <b>51a</b>	n.a. +2 <sup>HS</sup> +2 <sup>HS</sup>	0.26 1.14 1.00	1.01 2.45 3.17	43 36 21
6 <sup>[a]</sup>	Entry 4 + <b>51a</b>	+2 <sup>HS</sup> +2 <sup>HS</sup>	0.89 0.93 1.02	2.05 2.63 3.07	30 49 21
7	Entry 5 + <b>88a</b>	n.a. +2 <sup>HS</sup> +2 <sup>HS</sup>	0.24 0.68 1.12	1.43 1.94 2.60	28 29 43
8	Entry 5 + <b>91a</b>	+2 <sup>HS</sup> +2 <sup>HS</sup>	1.00 0.95	2.94 2.29	48 52

## 5. Experimental Part

9	Entry 6 + <b>94g</b>	+2 <sup>HS</sup>	0.95	2.22	33
		+2 <sup>HS</sup>	1.02	2.79	55
		+2 <sup>HS</sup>	1.05	3.13	12
10 <sup>[a]</sup>	Entry 4 + <b>32a</b> + <b>94g</b>	+2 <sup>HS</sup>	0.92	2.09	44
		+2 <sup>HS</sup>	0.95	2.66	36
		+2 <sup>HS</sup>	1.03	3.00	20
11	Entry 6 + <b>94a</b>	+2 <sup>HS</sup>	0.74	2.34	13
		+2 <sup>HS</sup>	1.02	2.63	65
		+2 <sup>HS</sup>	1.03	3.09	22

<sup>[a]</sup> used MeMgBr (3 equiv), ZnBr<sub>2</sub>·TMEDA (2 equiv). n.a. = not assign.

### Sample Preparation for Mössbauer Measurements

#### Entry 1. <sup>57</sup>FeCl<sub>2</sub> + THF

Inside a nitrogen-filled glovebox, a suspension of <sup>57</sup>FeCl<sub>2</sub> (3.2 mg, 25 μmol) in THF (0.80 mL) was stirred at ambient temperature for 5 min. Then, the solution was filtered and added into a sample holder. The sample holder was taken out of the glovebox and frozen in liquid nitrogen immediately.

#### Entry 2. <sup>57</sup>FeCl<sub>2</sub> + MeMgBr + THF

Inside a nitrogen-filled glovebox, a suspension of MeMgBr (3.0 M in Et<sub>2</sub>O, 75 μL, 9.0 equiv) in THF (17 μL) was stirred at ambient temperature for 5 min. Then, <sup>57</sup>FeCl<sub>2</sub> (3.2 mg, 25 μmol) was added. After stirring for additional 5 min, the solution was diluted to 5.0 mL by adding THF, 0.80 mL of the solution was filtered and added into a sample holder. The sample holder was taken out of the glovebox and frozen in liquid nitrogen immediately.

## 5. Experimental Part

### Entry 3. $^{57}\text{FeCl}_2$ + MeMgBr + $\text{ZnBr}_2\cdot\text{TMEDA}$ + THF

Inside a nitrogen-filled glovebox, to a stirred solution of  $\text{ZnBr}_2\cdot\text{TMEDA}$  (51.6 mg, 6.0 equiv) in THF (17  $\mu\text{L}$ ), MeMgBr (3.0 M in  $\text{Et}_2\text{O}$ , 75  $\mu\text{L}$ , 9.0 equiv) was added in one portion and the reaction mixture was stirred for 5 min at ambient temperature. Then,  $^{57}\text{FeCl}_2$  (3.2 mg, 25  $\mu\text{mol}$ ) was added. After stirring for additional 5 min, the solution was diluted to 5.0 mL by adding THF, 0.80 mL of the solution was filtered and added into a sample holder. The sample holder was taken out of the glovebox and frozen in liquid nitrogen immediately.

### Entry 4. $^{57}\text{FeCl}_2$ + MeMgBr + $\text{ZnBr}_2\cdot\text{TMEDA}$ + dppe + THF

Inside a nitrogen-filled glovebox, to a stirred solution of  $\text{ZnBr}_2\cdot\text{TMEDA}$  (51.6 mg, 6.0 equiv) and dppe (10.0 mg, 1.0 equiv) in THF (17  $\mu\text{L}$ ), MeMgBr (3.0 M in  $\text{Et}_2\text{O}$ , 75  $\mu\text{L}$ , 9.0 equiv) was added in one portion and the reaction mixture was stirred for 5 min at ambient temperature. Then,  $^{57}\text{FeCl}_2$  (3.2 mg, 25  $\mu\text{mol}$ ) was added. After stirring for additional 5 min, the solution was diluted to 5.0 mL by adding THF, 0.80 mL of the solution was filtered and added into a sample holder. The sample holder was taken out of the glovebox and frozen in liquid nitrogen immediately.

### Entry 5. $^{57}\text{FeCl}_2$ + MeMgBr (9 equiv) + $\text{ZnBr}_2\cdot\text{TMEDA}$ (3 equiv) + dppe + TAH-substrate (**51a**) + THF

Inside a nitrogen-filled glovebox, to a stirred solution of **51a** (7.2 mg, 1.0 equiv),  $\text{ZnBr}_2\cdot\text{TMEDA}$  (51.6 mg, 6.0 equiv) and dppe (10.0 mg, 1.0 equiv) in THF (17  $\mu\text{L}$ ), MeMgBr (3.0 M in  $\text{Et}_2\text{O}$ , 75  $\mu\text{L}$ , 9.0 equiv) was added in one portion and the reaction mixture was stirred for 5 min at ambient temperature. Then,  $^{57}\text{FeCl}_2$  (3.2 mg, 25  $\mu\text{mol}$ ) was added. After stirring for additional 5 min, the solution was diluted to 5.0 mL by adding THF, 0.80 mL of the solution was filtered and added into a sample holder. The sample holder was taken out of the glovebox and frozen in liquid nitrogen immediately.

## 5. Experimental Part

### **Entry 6. $^{57}\text{FeCl}_2$ + MeMgBr + ZnBr<sub>2</sub>·TMEDA + dppe + TAH-substrate (51a) + THF**

Inside a nitrogen-filled glovebox, to a stirred solution of **51a** (7.2 mg, 1.0 equiv), ZnBr<sub>2</sub>·TMEDA (17.2 mg, 2.0 equiv) and dppe (10.0 mg, 1.0 equiv) in THF (17  $\mu\text{L}$ ), MeMgBr (3.0 M in Et<sub>2</sub>O, 25  $\mu\text{L}$ , 3.0 equiv) was added in one portion and the reaction mixture was stirred for 5 min at ambient temperature. Then,  $^{57}\text{FeCl}_2$  (3.2 mg, 25  $\mu\text{mol}$ ) was added. After stirring for additional 5 min, the solution was diluted to 5.0 mL by adding THF, 0.80 mL of the solution was filtered and added into a sample holder. The sample holder was taken out of the glovebox and frozen in liquid nitrogen immediately.

### **Entry 7. $^{57}\text{FeCl}_2$ + MeMgBr + ZnBr<sub>2</sub>·TMEDA + dppe + TAH-substrate (51a) + allene (88a) + THF**

Inside a nitrogen-filled glovebox, to a stirred solution of **51a** (7.2 mg, 1.0 equiv), ZnBr<sub>2</sub>·TMEDA (51.6 mg, 6.0 equiv) and dppe (10.0 mg, 1.0 equiv) in THF (17  $\mu\text{L}$ ), MeMgBr (3.0 M in Et<sub>2</sub>O, 75  $\mu\text{L}$ , 9.0 equiv) was added in one portion and the reaction mixture was stirred for 5 min at ambient temperature. Then,  $^{57}\text{FeCl}_2$  (3.2 mg, 25  $\mu\text{mol}$ ) was added. After stirring for additional 5 min, allene **88a** (13.6 mg, 3.0 equiv) was added as a solution in THF (17  $\mu\text{L}$ ). After stirring for additional 5 min, the solution was diluted to 5.0 mL by adding THF, 0.80 mL of the solution was filtered and added into a sample holder. The sample holder was taken out of the glovebox and frozen in liquid nitrogen immediately.

### **Entry 8. $^{57}\text{FeCl}_2$ + MeMgBr + ZnBr<sub>2</sub>·TMEDA + dppe + TAH-substrate (51a) + alkyne (91a) + THF**

Inside a nitrogen-filled glovebox, to a stirred solution of **51a** (7.2 mg, 1.0 equiv), ZnBr<sub>2</sub>·TMEDA (51.6 mg, 6.0 equiv) and dppe (10.0 mg, 1.0 equiv) in THF (17  $\mu\text{L}$ ), MeMgBr (3.0 M in Et<sub>2</sub>O, 75  $\mu\text{L}$ , 9.0 equiv) was added in one portion and the reaction mixture was stirred for 5 min at ambient temperature. Then,

## 5. Experimental Part

$^{57}\text{FeCl}_2$  (3.2 mg, 25  $\mu\text{mol}$ ) was added. After stirring for additional 5 min, alkyne **91a** (16.2 mg, 3.0 equiv) was added as a solution in THF (17  $\mu\text{L}$ ). After stirring for additional 5 min, the solution was diluted to 5.0 mL by adding THF, 0.80 mL of the solution was filtered and added into a sample holder. The sample holder was taken out of the glovebox and frozen in liquid nitrogen immediately.

### **Entry 9. $^{57}\text{FeCl}_2$ + MeMgBr + ZnBr $_2$ ·TMEDA + dppe + TAH-substrate (51a) + BCP (94g)+ THF**

Inside a nitrogen-filled glovebox, to a stirred solution of **51a** (7.2 mg, 1.0 equiv), ZnBr $_2$ ·TMEDA (17.2 mg, 2.0 equiv) and dppe (10.0 mg, 1.0 equiv) in THF (17  $\mu\text{L}$ ), MeMgBr (3.0 M in Et $_2$ O, 25  $\mu\text{L}$ , 3.0 equiv) was added in one portion and the reaction mixture was stirred for 5 min at ambient temperature. Then,  $^{57}\text{FeCl}_2$  (3.2 mg, 25  $\mu\text{mol}$ ) was added. After stirring for additional 5 min, BCP **94g** (11.4 mg, 3.0 equiv) was added as a solution in THF (17  $\mu\text{L}$ ). After stirring for additional 5 min, the solution was diluted to 5.0 mL by adding THF, 0.80 mL of the solution was filtered and added into a sample holder. The sample holder was taken out of the glovebox and frozen in liquid nitrogen immediately.

### **Entry 10. $^{57}\text{FeCl}_2$ + MeMgBr + ZnBr $_2$ ·TMEDA + dppe + TAM-substrate (32a) + BCP (94g)+ THF**

Inside a nitrogen-filled glovebox, to a stirred solution of **32a** (7.2 mg, 1.0 equiv), ZnBr $_2$ ·TMEDA (17.2 mg, 2.0 equiv) and dppe (10.0 mg, 1.0 equiv) in THF (17  $\mu\text{L}$ ), MeMgBr (3.0 M in Et $_2$ O, 25  $\mu\text{L}$ , 3.0 equiv) was added in one portion and the reaction mixture was stirred for 5 min at ambient temperature. Then,  $^{57}\text{FeCl}_2$  (3.2 mg, 25  $\mu\text{mol}$ ) was added. After stirring for additional 5 min, BCP **94g** (11.4 mg, 3.0 equiv) was added as a solution in THF (17  $\mu\text{L}$ ). After stirring for additional 5 min, the solution was diluted to 5.0 mL by adding THF, 0.80 mL of the solution was filtered and added into a sample holder. The sample holder was taken out of the glovebox and frozen in liquid nitrogen immediately.

## 5. Experimental Part

### Entry 11. $^{57}\text{FeCl}_2$ + MeMgBr + ZnBr<sub>2</sub>·TMEDA + dppe + TAH-substrate (**51a**) + BCP (**94a**)+ THF

Inside a nitrogen-filled glovebox, to a stirred solution of **51a** (7.2 mg, 1.0 equiv), ZnBr<sub>2</sub>·TMEDA (17.2 mg, 2.0 equiv) and dppe (10.0 mg, 1.0 equiv) in THF (17  $\mu\text{L}$ ), MeMgBr (3.0 M in Et<sub>2</sub>O, 25  $\mu\text{L}$ , 3.0 equiv) was added in one portion and the reaction mixture was stirred for 5 min at ambient temperature. Then,  $^{57}\text{FeCl}_2$  (3.2 mg, 25  $\mu\text{mol}$ ) was added. After stirring for additional 5 min, BCP **94a** (9.3 mg, 3.0 equiv) was added as a solution in THF (17  $\mu\text{L}$ ). After stirring for additional 20 min, the solution was diluted to 5.0 mL by adding THF, 0.80 mL of the solution was filtered and added into a sample holder. The sample holder was taken out of the glovebox and frozen in liquid nitrogen immediately.

## 5.7 X-Ray Crystallographic Analysis

The crystal structures of **89la** and **120** were measured and solved by Dr. Christopher Golz (*Prof. Dr. Manuel Alcarazo* research group).

### 5.7.1 Data Analysis for Crystal Structure of **89la**

The crystal was kept at 99.98 K during data collection. Using Olex2,<sup>[104]</sup> the structure was solved with the XT<sup>[105]</sup> structure solution program using Intrinsic Phasing and refined with the XL<sup>[106]</sup> refinement package using Least Squares minimisation.

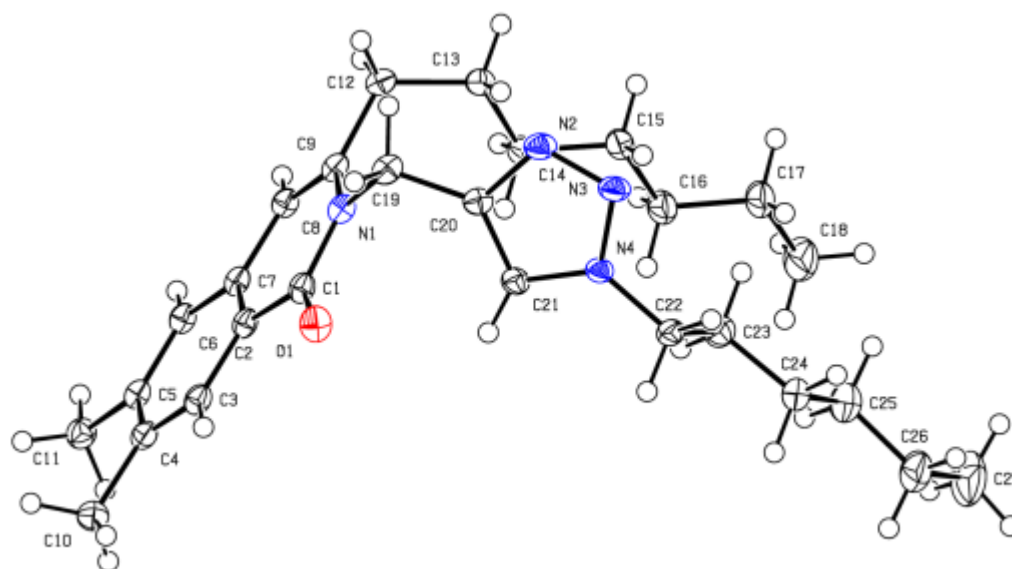


**Figure 5.4** Molecular structure of **89la** with thermal ellipsoids at 50% probability level.

**Crystal Data** for  $C_{27}H_{40}N_4O$  ( $M=436.63$  g/mol) triclinic, space group P-1 (no. 2),  $a = 5.6131(13)$  Å,  $b = 8.0980(19)$  Å,  $c = 27.986(7)$  Å,  $\alpha = 87.340(7)^\circ$ ,  $\beta = 87.040(7)^\circ$ ,  $\gamma = 84.035(7)^\circ$ ,  $V = 1262.5(5)$  Å<sup>3</sup>,  $Z = 2$ ,  $T = 99.98$  K,  $\mu(\text{MoK}\alpha) = 0.071$  mm<sup>-1</sup>,  $D_{\text{calc}} = 1.149$  g/cm<sup>3</sup>, 15862 reflections measured ( $4.376^\circ \leq 2\theta \leq 63.042^\circ$ ), 8285 unique ( $R_{\text{int}} = 0.0437$ ,  $R_{\text{sigma}} = 0.0624$ ) which

## 5. Experimental Part

were used in all calculations. The final  $R_1$  was 0.0547 ( $I > 2\sigma(I)$ ) and  $wR_2$  was 0.1521 (all data).

**Table 5.2** Crystal data and structure refinement for **89Ia**.

Compound	<b>89Ia</b>
Identification code	mo_0230_CG_0m
Empirical formula	$C_{27}H_{40}N_4O$
Formula weight	436.63
Temperature/K	99.98
Crystal system	triclinic
Space group	P-1
$a/\text{\AA}$	5.6131(13)
$b/\text{\AA}$	8.0980(19)
$c/\text{\AA}$	27.986(7)
$\alpha/^\circ$	87.340(7)
$\beta/^\circ$	87.040(7)
$\gamma/^\circ$	84.035(7)
Volume/ $\text{\AA}^3$	1262.5(5)
Z	2
$\rho_{\text{calc}}/\text{g cm}^{-3}$	1.149
$\mu/\text{mm}^{-1}$	0.071
F(000)	476.0
Crystal size/ $\text{mm}^3$	$0.714 \times 0.391 \times 0.052$
Radiation	MoK $\alpha$ ( $\lambda = 0.71073$ )
$2\theta$ range for data collection/ $^\circ$	4.376 to 63.042
Index ranges	$-8 \leq h \leq 8, -11 \leq k \leq 9, -41 \leq l \leq 41$
Reflections collected	15862
Independent reflections	8285 [ $R_{\text{int}} = 0.0437, R_{\text{sigma}} = 0.0624$ ]
Data/restraints/parameters	8285/0/293
Goodness-of-fit on $F^2$	1.031
Final R indexes [ $I \geq 2\sigma(I)$ ]	$R_1 = 0.0547, wR_2 = 0.1421$
Final R indexes [all data]	$R_1 = 0.0688, wR_2 = 0.1521$
Largest diff. peak/hole / $e \text{\AA}^{-3}$	0.52/-0.26

## 5. Experimental Part

**Table 5.3** Bond Lengths [Å] for **89Ia**.

Atom	Atom	Length/Å	Atom	Atom	Length/Å
O1	C1	1.2339(13)	C6	C7	1.4127(15)
N1	C1	1.3951(14)	C7	C8	1.4337(15)
N1	C9	1.4023(14)	C8	C9	1.3534(15)
N1	C19	1.4703(14)	C9	C12	1.5123(15)
N2	N3	1.3207(14)	C12	C13	1.5332(16)
N2	C20	1.3605(14)	C13	C14	1.5216(16)
N3	N4	1.3428(12)	C14	C15	1.5224(16)
N4	C21	1.3522(13)	C15	C16	1.5187(17)
N4	C22	1.4588(14)	C16	C17	1.5173(18)
C1	C2	1.4588(15)	C17	C18	1.522(2)
C2	C3	1.4095(15)	C19	C20	1.4957(15)
C2	C7	1.4036(15)	C20	C21	1.3724(15)
C3	C4	1.3820(16)	C22	C23	1.5185(17)
C4	C5	1.4213(16)	C23	C24	1.5230(17)
C4	C10	1.5062(15)	C24	C25	1.5201(19)
C5	C6	1.3861(15)	C25	C26	1.518(2)
C5	C11	1.5071(16)	C26	C27	1.523(2)

## 5. Experimental Part

**Table 5.4** Bond Angles [°] for **89la**.

Atom	Atom	Atom	Angle/°	Atom	Atom	Atom	Angle/°
C1	N1	C9	123.33(9)	C2	C7	C8	118.76(10)
C1	N1	C19	114.38(9)	C6	C7	C8	122.78(10)
C9	N1	C19	122.19(9)	C9	C8	C7	121.64(10)
N3	N2	C20	108.88(9)	N1	C9	C12	120.19(10)
N2	N3	N4	107.19(9)	C8	C9	N1	119.25(10)
N3	N4	C21	110.88(9)	C8	C9	C12	120.53(10)
N3	N4	C22	119.81(9)	C9	C12	C13	117.73(9)
C21	N4	C22	129.30(9)	C14	C13	C12	114.42(9)
O1	C1	N1	119.83(10)	C13	C14	C15	112.60(9)
O1	C1	C2	123.75(10)	C16	C15	C14	113.68(10)
N1	C1	C2	116.42(9)	C17	C16	C15	113.71(11)
C3	C2	C1	119.47(10)	C16	C17	C18	112.98(12)
C7	C2	C1	120.36(10)	N1	C19	C20	113.87(9)
C7	C2	C3	120.17(10)	N2	C20	C19	119.61(9)
C4	C3	C2	121.04(10)	N2	C20	C21	108.30(10)
C3	C4	C5	119.16(10)	C21	C20	C19	132.09(10)
C3	C4	C10	120.39(10)	N4	C21	C20	104.74(9)
C5	C4	C10	120.45(10)	N4	C22	C23	113.18(9)
C4	C5	C11	120.17(10)	C22	C23	C24	110.42(10)
C6	C5	C4	119.88(10)	C25	C24	C23	114.16(11)
C6	C5	C11	119.95(10)	C26	C25	C24	112.80(13)
C5	C6	C7	121.27(10)	C25	C26	C27	113.65(16)
C2	C7	C6	118.46(10)				

## 5. Experimental Part

### 5.7.2 Data Analysis for Crystal Structure of **120**

The crystal was kept at 100.0 K during data collection. Using Olex2,<sup>[104]</sup> the structure was solved with the XT<sup>[105]</sup> structure solution program using Intrinsic Phasing and refined with the XL<sup>[106]</sup> refinement package using Least Squares minimisation.

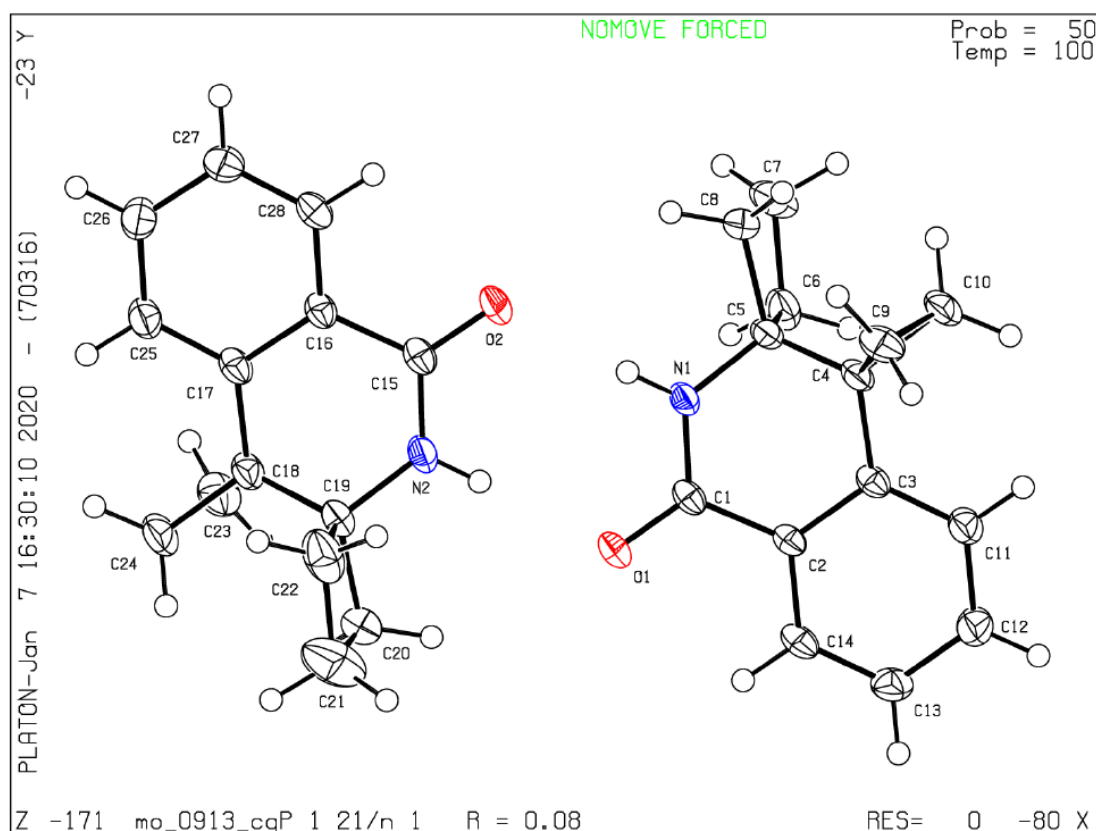


**Figure 5.5** Molecular structure of **120** with thermal ellipsoids at 50% probability level.

**Crystal Data** for  $C_{14}H_{15}NO$  ( $M = 213.27$  g/mol): monoclinic, space group  $P2_1/n$  (no. 14),  $a = 13.9071(8)$  Å,  $b = 9.5864(5)$  Å,  $c = 16.9660(10)$  Å,  $\beta = 100.194(2)^\circ$ ,  $V = 2226.2(2)$  Å<sup>3</sup>,  $Z = 8$ ,  $T = 100.0$  K,  $\mu(\text{MoK}\alpha) = 0.080$  mm<sup>-1</sup>,  $D_{\text{calc}} = 1.273$  g/cm<sup>3</sup>, 67587 reflections measured ( $4.168^\circ \leq 2\theta \leq 54.268^\circ$ ), 4911 unique ( $R_{\text{int}} = 0.0438$ ,  $R_{\text{sigma}} = 0.0190$ ) which were used in all calculations. The final  $R_1$  was 0.0774 ( $I > 2\sigma(I)$ ) and  $wR_2$  was 0.2170 (all data).

## 5. Experimental Part

**Table 5.5** Crystal data and structure refinement for **120**.

CCDC code	2018011
Empirical formula	$\text{C}_{14}\text{H}_{15}\text{NO}$
Formula weight	213.27
Temperature/K	100.0
Crystal system	monoclinic
Space group	$P2_1/n$
$a/\text{\AA}$	13.9071(8)
$b/\text{\AA}$	9.5864(5)
$c/\text{\AA}$	16.9660(10)
$\alpha/^\circ$	90
$\beta/^\circ$	100.194(2)
$\gamma/^\circ$	90
Volume/ $\text{\AA}^3$	2226.2(2)
Z	8
$\rho_{\text{calc}}/\text{g/cm}^3$	1.273
$\mu/\text{mm}^{-1}$	0.080
F(000)	912.0
Crystal size/ $\text{mm}^3$	$0.247 \times 0.182 \times 0.168$

## 5. Experimental Part

Radiation	MoK $\alpha$ ( $\lambda = 0.71073$ )
2 $\Theta$ range for data collection/°	4.168 to 54.268
Index ranges	$-17 \leq h \leq 17$ , $-12 \leq k \leq 12$ , $-21 \leq l \leq 21$
Reflections collected	67587
Independent reflections	4911 [ $R_{\text{int}} = 0.0438$ , $R_{\text{sigma}} = 0.0190$ ]
Data/restraints/parameters	4911/0/289
Goodness-of-fit on $F^2$	1.087
Final R indexes [ $I \geq 2\sigma(I)$ ]	$R_1 = 0.0774$ , $wR_2 = 0.2080$
Final R indexes [all data]	$R_1 = 0.0866$ , $wR_2 = 0.2170$
Largest diff. peak/hole / e $\text{\AA}^{-3}$	0.57/-0.34

## 5. Experimental Part

**Table 5.6** Bond Lengths [Å] for **120**.

Atom	Atom	Length/Å	Atom	Atom	Length/Å
O1	C1	1.244(2)	O2	C15	1.245(2)
N1	C1	1.339(2)	N2	C15	1.336(3)
N1	C5	1.456(2)	N2	C19	1.456(2)
C1	C2	1.486(3)	C15	C16	1.489(3)
C2	C3	1.407(3)	C16	C17	1.405(3)
C2	C14	1.402(3)	C16	C28	1.394(3)
C3	C4	1.500(3)	C17	C18	1.498(3)
C3	C11	1.395(3)	C17	C25	1.393(3)
C4	C5	1.515(3)	C18	C19	1.510(3)
C4	C9	1.513(3)	C18	C23	1.519(3)
C4	C10	1.504(3)	C18	C24	1.500(3)
C5	C6	1.564(3)	C19	C20	1.566(3)
C5	C8	1.550(3)	C19	C22	1.551(3)
C6	C7	1.533(3)	C20	C21	1.510(4)
C7	C8	1.538(4)	C21	C22	1.543(4)
C9	C10	1.500(3)	C23	C24	1.503(4)
C11	C12	1.392(3)	C25	C26	1.389(3)

## 5. Experimental Part

C12 C13	1.394(3)	C26 C27	1.399(3)
C13 C14	1.383(3)	C27 C28	1.386(3)

**Table 5.7** Bond Angles [°] for **120**.

Atom Atom Atom	Angle/°	Atom Atom Atom	Angle/°
C1 N1 C5	124.01(17)	C15 N2 C19	124.42(18)
O1 C1 N1	122.03(18)	O2 C15 N2	122.13(19)
O1 C1 C2	121.65(17)	O2 C15 C16	121.22(18)
N1 C1 C2	116.32(16)	N2 C15 C16	116.64(17)
C3 C2 C1	120.44(17)	C17 C16 C15	120.48(18)
C14 C2 C1	119.28(17)	C28 C16 C15	118.78(17)
C14 C2 C3	120.20(18)	C28 C16 C17	120.67(19)
C2 C3 C4	117.86(17)	C16 C17 C18	118.04(18)
C11 C3 C2	118.41(18)	C25 C17 C16	118.01(19)
C11 C3 C4	123.65(17)	C25 C17 C18	123.78(18)
C3 C4 C5	111.78(16)	C17 C18 C19	112.54(17)
C3 C4 C9	116.87(18)	C17 C18 C23	116.04(19)
C3 C4 C10	120.92(17)	C17 C18 C24	121.00(18)
C9 C4 C5	119.69(18)	C19 C18 C23	119.80(19)
C10 C4 C5	118.90(17)	C24 C18 C19	118.23(19)

## 5. Experimental Part

C10	C4	C9	59.62(14)	C24	C18	C23	59.73(16)
N1	C5	C4	108.55(16)	N2	C19	C18	109.74(18)
N1	C5	C6	114.59(17)	N2	C19	C20	111.50(18)
N1	C5	C8	112.46(17)	N2	C19	C22	114.33(19)
C4	C5	C6	113.59(17)	C18	C19	C20	116.56(18)
C4	C5	C8	118.06(17)	C18	C19	C22	114.25(19)
C8	C5	C6	88.71(17)	C22	C19	C20	89.32(19)
C7	C6	C5	89.68(18)	C21	C20	C19	89.4(2)
C6	C7	C8	90.31(17)	C20	C21	C22	91.7(2)
C7	C8	C5	89.99(18)	C21	C22	C19	88.7(2)
C10	C9	C4	59.90(13)	C24	C23	C18	59.54(15)
C9	C10	C4	60.48(14)	C18	C24	C23	60.74(15)
C12	C11	C3	120.95(19)	C26	C25	C17	121.29(19)
C11	C12	C13	120.5(2)	C25	C26	C27	120.4(2)
C14	C13	C12	119.26(19)	C28	C27	C26	118.9(2)
C13	C14	C2	120.72(18)	C27	C28	C16	120.77(18)

## 6. References

- [1] a) J.-R. Pouliot, F. Grenier, J. T. Blaskovits, S. Beaupre, M. Leclerc, *Chem. Rev.* **2016**, *116*, 14225–14274; b) A. Paun, N. D. Hadade, C. C. Paraschivescu, M. Matache, *Mater. Chem. C* **2016**, *4*, 8596–8610; c) D. J. Schipper, K. Fagnou, *Chem. Mater.* **2011**, *23*, 1594–1600; d) V. Maman, *Mini-Reviews in Organic Chemistry* **2008**, *5*, 303–312.
- [2] a) S. J. Kalita, F. Cheng, Y.-Y. Huang, *Adv. Synth. Catal.* **2020**, *362*, 2778–2800; b) E. R. Welin, A. Ngamnithiporn, M. Klatte, G. Lapointe, G. M. Pototschnig, M. S. J. McDermott, D. Conklin, C. D. Gilmore, P. M. Tadross, C. K. Haley, K. Negoro, E. Glibstrup, C. U. Grünanger, K. M. Allan, S. C. Virgil, D. J. Slamon, B. M. Stoltz, *Science* **2019**, *363*, 270–275; c) R. Rossi, F. Bellina, M. Lessi, C. Manzini, G. Marianetti, L. A. Perego, *Curr. Org. Chem.* **2015**, *19*, 1302–1409; d) J. Yamaguchi, A. D. Yamaguchi, K. Itami, *Angew. Chem. Int. Ed.* **2012**, *51*, 8960–9009; e) K. C. Nicolaou, C. R. H. Hale, C. Nilewski, H. A. Ioannidou, *Chem. Soc. Rev.* **2012**, *41*, 5185–5238.
- [3] a) S. D. Friis, M. J. Johansson, L. Ackermann, *Nat. Chem.* **2020**, *12*, 511–519; b) T. Cernak, K. D. Dykstra, S. Tyagarajan, P. Vachal, S. W. Krska, *Chem. Soc. Rev.* **2016**, *45*, 546–576; c) M. Seki, *Org. Process Res. Dev.* **2016**, *20*, 867–877; d) L. Ackermann, *Org. Process Res. Dev.* **2015**, *19*, 260–269.
- [4] a) P. Ruiz-Castillo, S. L. Buchwald, *Chem. Rev.* **2016**, *116*, 12564–12649; b) A. V. Bhatia, H. J. Federsel, Q. Chen, *Org. Process Res. Dev.* **2014**, *18*, 179–179; c) N. Miyaura, A. Suzuki, *Chem. Rev.* **1995**, *95*, 2457–2483; d) J.-P. Corbet, G. Mignani, *Chem. Rev.* **2006**, *106*, 2651–2710.
- [5] a) A. Biffis, P. Centomo, A. D. Zotto, M. Zecca, *Chem. Rev.* **2018**, *118*, 2249–229; b) C. C. C. J. Seechurn, M. O. Kitching, T. J. Colacot, V. Snieckus, *Angew. Chem. Int. Ed.* **2012**, *51*, 5062–5085.

## 6. References

- [6] a) P. T. Anastas, M. M. Kirchhoff, *Acc. Chem. Res.* **2002**, *35*, 686–694; b) P. T. Anastas, J. C. Warner, *Green chemistry: theory and practice*, Oxford University Press, Oxford, **1998**.
- [7] a) X. Zhang, M. Fevre, G. O. Jones, R. M. Waymouth, *Chem. Rev.* **2018**, *118*, 839–885; b) F. E. Celik, B. Peters, M.-O. Coppens, A. McCormick, R. F. Hicks, J. Ekerdt, *ACS Catal.* **2017**, *7*, 8628–8640.
- [8] a) L. Ackermann, R. Vicente, A. R. Kapdi, *Angew. Chem. Int. Ed.* **2009**, *48*, 9792–9826; b) R. G. Bergman, *Nature* **2007**, *446*, 391–393.
- [9] a) S. Rej, Y. Ano, N. Chatani, *Chem. Rev.* **2020**, *120*, 1788–1887; b) S. Rej, N. Chatani, *Angew. Chem. Int. Ed.* **2019**, *58*, 8304–8329; c) J. Kalepu, P. Gandeepan, L. Ackermann, L. Pilarski, *Chem. Sci.* **2018**, *9*, 4203–4216; d) J. He, M. Wasa, K. S. L. Chan, Q. Shao, J.-Q. Yu, *Chem. Rev.* **2017**, *117*, 8754–8786; e) P. H. Dixneuf, H. Doucet, *C–H Bond Activation and Catalytic Functionalization I*, Springer, Cham, **2016**; f) J. F. Hartwig, M. A. Larsen, *ACS Cent. Sci.* **2016**, *2*, 281–292; g) O. Daugulis, J. Roane, L. D. Tran, *Acc. Chem. Res.* **2015**, *48*, 1053–1064; h) A. D. Giuseppe, R. Castarlenas, L. A. Oroac, *C. R. Chimie* **2015**, *18*, 713–741; i) G. Rouquet, N. Chatani, *Angew. Chem. Int. Ed.* **2013**, *52*, 11726–11743; j) S. R. Neufeldt, M. S. Sanford, *Acc. Chem. Res.* **2012**, *45*, 936–946; k) L. McMurray, F. O'Hara, M. J. Gaunt, *Chem. Soc. Rev.* **2011**, *40*, 1885–1898; l) T. W. Lyons, M. S. Sanford, *Chem. Rev.* **2010**, *110*, 1147–1169; m) O. Daugulis, H.-Q. Do, D. Shabashov, *Acc. Chem. Res.* **2009**, *42*, 1074–1086.
- [10] a) R. A. Periana, G. Bhalla, W. J. Tenn III, K. J. H. Young, X. Y. Liu, O. Mironov, C. Jones, V. R. Ziatdinov, *J. Mol. Catal. A: Chem.* **2004**, *220*, 7–25; b) A. S. Goldman, K. I. Goldberg, *ACS Symposium Series 885, Activation and Functionalization of C–H Bonds*, **2004**, 1–43; c) B. A. Arndtsen, R. G. Bergman, T. A. Mobley, T. H. Peterson, *Acc. Chem. Res.* **1995**, *28*, 154–162.

## 6. References

- [11] a) The Nobel prize in Chemistry **2010** – Press Release [https://www.nobelprize.org/nobel\\_prizes/chemistry/laureates/2010/press.html](https://www.nobelprize.org/nobel_prizes/chemistry/laureates/2010/press.html) (accessed on 18.08.2020); b) A. Suzuki, *Angew. Chem. Int. Ed.* **2011**, *50*, 6722–6737; c) E.-i. Negishi, *Angew. Chem. Int. Ed.* **2011**, *50*, 6738–6764.
- [12] S. J. Blanksby, G. B. Ellison, *Acc. Chem. Res.* **2003**, *36*, 255–263.
- [13] a) L. N. Lewis, J. F. Smith, *J. Am. Chem. Soc.* **1986**, *108*, 2728–2735; b) P. Hong, B.-R. Cho, H. Yamazaki, *Chem. Lett.* **1979**, *50*, 339–342.
- [14] a) H. M. L. Davies, D. Morton, *ACS Cent. Sci.* **2017**, *3*, 936–943; b) J. R. Hummel, J. A. Boerth, J. A. Ellman, *Chem. Rev.* **2017**, *117*, 9163–9227; c) T. Gensch, M. N. Hopkinson, F. Glorius, *Chem. Soc. Rev.* **2016**, *45*, 2900–2936; d) P. Gandeepan, C.-H. Cheng, *Chem. Asian J.* **2015**, *10*, 824–838.
- [15] I. V. Seregin, V. Gevorgyan, *Chem. Soc. Rev.* **2007**, *36*, 1173–1193.
- [16] N. Kuhl, M. N. Hopkinson, J. Wencel-Delord, F. Glorius, *Angew. Chem. Int. Ed.* **2012**, *51*, 10236–10254.
- [17] a) C. Sambriago, D. Schönbauer, R. Blicke, T. Dao-Huy, G. Pototschnig, P. Schaaf, T. Wiesinger, M. F. Zia, J. Wencel-Delord, T. Besset, B. U. W. Maes, M. Schnürch, *Chem. Soc. Rev.* **2018**, *47*, 6603–6743; b) Y. Kuninobu, H. Ida, M. Nishi, M. Kanai, *Nat. Chem.* **2015**, *7*, 712–717; c) F. Zhang, D. R. Spring, *Chem. Soc. Rev.* **2014**, *43*, 6906–6919; d) L. Ackermann, *Top. Organomet. Chem.* **2007**, *24*, 35–60.
- [18] S. D. Sarkar, W. Liu, S. I. Kozhushkov, L. Ackermann, *Adv. Synth. Catal.* **2014**, *356*, 1461–1479.
- [19] W. Ma, P. Gandeepan, J. Li, L. Ackermann, *Org. Chem. Front.* **2017**, *4*, 1435–1467.
- [20] P. Gandeepan, L. Ackermann, *Chem* **2018**, *4*, 199–222.
- [21] a) L. Ackermann, *Chem. Rev.* **2011**, *111*, 1315–1345; b) D. Balcells, E. Clot, O. Eisenstein, *Chem. Rev.* **2010**, *110*, 749–823.

## 6. References

- [22] D. Lapointe, K. Fagnou, *Chem. Lett.* **2010**, 39, 1118–1126.
- [23] a) Y. Boutadla, D. L. Davies, S. A. Macgregor, A. I. Poblador-Bahamonde, *Dalton Trans.* **2009**, 5887–5893; b) Y. Boutadla, D. L. Davies, S. A. Macgregor, A. I. Poblador-Bahamonde, *Dalton Trans.* **2009**, 5820–5831.
- [24] a) K. Naksomboon, J. Poater, F. M. Bickelhaupt, M. A. Fernandez-Ibanez, *J. Am. Chem. Soc.* **2019**, 141, 6719–6725; b) E. Tan, O. Quinonero, M. E. de Orbe, A. M. Echavarren, *ACS Catal.* **2018**, 8, 2166–2172; c) Y.-F. Liang, V. Müller, W. Liu, A. Münch, D. Stalke, L. Ackermann, *Angew. Chem. Int. Ed.* **2017**, 56, 9415–9419; d) D. Zell, M. Bursch, V. Müller, S. Grimme, L. Ackermann, *Angew. Chem. Int. Ed.* **2017**, 56, 10378–10382; e) H. Wang, M. Moselage, M. J. González, L. Ackermann, *ACS Catal.* **2016**, 6, 2705–2709; f) D. Santrač, S. Cella, W. Wang, L. Ackermann, *Eur. J. Org. Chem.* **2016**, 5429–5436; g) R. Mei, J. Loup, L. Ackermann, *ACS Catal.* **2016**, 6, 793–797; h) W. Ma, R. Mei, G. Tenti, L. Ackermann, *Chem. Eur. J.* **2014**, 20, 15248–15251.
- [25] J. Oxgaard, W. J. Tenn, R. J. Nielsen, R. A. Periana, W. A. Goddard, *Organometallics* **2007**, 26, 1565–1567.
- [26] L. Wang, B. P. Carrow, *ACS Catal.* **2019**, 9, 6821–6836.
- [27] a) <http://www.infomine.com/investment/metal-prices/>; b) <https://mineralprices.com/>.
- [28] J. W. Morgan, E. Anders, *Proc. Natl. Acad. Sci. USA* **1980**, 77, 6973–6977.
- [29] a) P. B. Tchounwou, C. G. Yedjou, A. K. Patlolla, D. J. Sutton, in *Molecular, clinical, and environmental toxicology* (Ed.: A. Luch), Springer, Basel, **2009**, 133–164; b) S. H. Gilani, Y. Alibhai, *J. Toxicol. Environ. Health* **1990**, 30, 23–31.
- [30] a) P. Gandeepan, T. Müller, D. Zell, G. Cera, S. Warratz, L. Ackermann, *Chem. Rev.* **2019**, 119, 2192–2452; b) L. Ackermann, T. B. Gunnoe, L. G. Habgood, *Catalytic Hydroarylation of Carbon-Carbon Multiple Bonds*, Wiley-VCH:

## 6. References

- Weinheim, **2018**; c) Y. Hu, B. Zhou, C. Wang, *Acc. Chem. Res.* **2018**, *51*, 816–827; d) Y. Kommagalla, N. Chatani, *Coord. Chem. Rev.* **2017**, *350*, 117–135; e) M. Moselage, J. Li, L. Ackermann, *ACS Catal.* **2016**, *6*, 498–525; f) J. Yamaguchi, K. Muto, K. Itami, *Top. Curr. Chem.* **2016**, *374*, 157–189; g) L. C. M. Castro, N. Chatani, *Chem. Lett.* **2015**, *44*, 410–421; h) E. P. Jackson, H. A. Malik, G. J. Sormunen, R. D. Baxter, P. Liu, H. Wang, A.-R. Shareef, J. Montgomery, *Acc. Chem. Res.* **2015**, *48*, 1736–1745; i) K. Gao, N. Yoshikai, *Acc. Chem. Res.* **2014**, *47*, 1208–1219; j) A. A. Kulkarni, O. Daugulis, *Synthesis* **2009**, (24), 4087–4109.
- [31] a) R. Shang, L. Ilies, E. Nakamura, *Chem. Rev.* **2017**, *117*, 9086–9139; b) G. Cera, L. Ackermann, *Top. Curr. Chem.* **2016**, *374*, 191–224.
- [32] K. S. Egorova, V. P. Ananikov, *Angew. Chem. Int. Ed.* **2016**, *55*, 12150–12162.
- [33] a) E. Bisz, M. Szostak, *ChemSusChem* **2017**, *10*, 3964–3981; b) A. Fürstner, *ACS Cent. Sci.* **2016**, *2*, 778–789; c) I. Bauer, H.-J. Knölker, *Chem. Rev.* **2015**, *115*, 3170–3387; d) K. Schröder, K. Junge, B. Bitterlich, M. Beller, *Top. Organomet. Chem.* **2011**, *33*, 83–109; e) C.-L. Sun, B.-J. Li, Z.-J. Shi, *Chem. Rev.* **2011**, *111*, 1293–1314; f) A. A. O. Sarhan, C. Bolm, *Chem. Soc. Rev.* **2009**, *38*, 2730–2744; g) S. Enthaler, K. Junge, M. Beller, *Angew. Chem. Int. Ed.* **2008**, *47*, 3317–3321; h) A. Correa, O. G. Mancheno, C. Bolm, *Chem. Soc. Rev.* **2008**, *37*, 1108–1117; i) C. Bolm, J. Legros, J. L. Paih, L. Zani, *Chem. Rev.* **2004**, *104*, 6217–6254.
- [34] a) E. McNeill, T. Ritter, *Acc. Chem. Res.* **2015**, *48*, 2330–2343; b) A. Fürstner, R. Martin, K. Majima, *J. Am. Chem. Soc.* **2005**, *127*, 12236–12237.
- [35] A. Guðmundsson, J.-E. Bäckvall, *Molecules* **2020**, *25*, 1349.
- [36] E. Nakamura, N. Yoshikai, *J. Org. Chem.* **2010**, *75*, 6061–6067.
- [37] G. Hata, H. Kondo, A. Miyake, *J. Am. Chem. Soc.* **1968**, *90*, 2278–2281.

## 6. References

- [38] a) M. V. Baker, L. D. Field, *J. Am. Chem. Soc.* **1987**, *109*, 2825–2826; b) J. W. Rathke, E. L. Muetterties, *J. Am. Chem. Soc.* **1975**, *97*, 3272–3273; c) H. H. Karsch, H.-F. Klein, H. Schmidbaur, *Angew. Chem. Int. Ed.* **1975**, *14*, 637–638.
- [39] a) S. Camadanli, R. Beck, U. Flörke, H.-F. Klein, *Organometallics* **2009**, *28*, 2300–2310; b) H.-F. Klein, S. Camadanli, R. Beck, D. Leukel, U. Flörke, *Angew. Chem. Int. Ed.* **2005**, *44*, 975–977.
- [40] W. D. Jones, G. P. Foster, J. M. Putinas, *J. Am. Chem. Soc.* **1987**, *109*, 5047–5048.
- [41] E. Nakamura, Two stories of iron - <https://chemistrycommunity.nature.com/posts/46018-two-stories-of-iron> (consulted on 17.09.2020).
- [42] J. Norinder, A. Matsumoto, N. Yoshikai, E. Nakamura, *J. Am. Chem. Soc.* **2008**, *130*, 5858–5859.
- [43] a) W. Xu, N. Yoshikai, *ChemSusChem* **2019**, *12*, 3049–3053; b) R. Shang, L. Ilies, E. Nakamura, *J. Am. Chem. Soc.* **2016**, *138*, 10132–10135; c) J. J. Sirois, R. Davis, B. DeBoef, *Org. Lett.* **2014**, *16*, 868–871; d) S. Asako, J. Norinder, L. Ilies, N. Yoshikai, E. Nakamura, *Adv. Synth. Catal.* **2014**, *356*, 1481–1485; e) L. Ilies, M. Kobayashi, A. Matsumoto, N. Yoshikai, E. Nakamura, *Adv. Synth. Catal.* **2012**, *354*, 593–596; f) L. Ilies, E. Konno, Q. Chen, E. Nakamura, *Asian J. Org. Chem.* **2012**, *1*, 142–145; g) L. Ilies, S. Asako, E. Nakamura, *J. Am. Chem. Soc.* **2011**, *133*, 7672–7675; h) N. Yoshikai, S. Asako, T. Yamakawa, L. Ilies, E. Nakamura, *Chem. Asian J.* **2011**, *6*, 3059–3065; i) N. Yoshikai, A. Matsumoto, J. Norinder, E. Nakamura, *Synlett* **2010**, (2), 313–316; j) N. Yoshikai, A. Matsumoto, J. Norinder, E. Nakamura, *Angew. Chem. Int. Ed.* **2009**, *48*, 2925–2928.
- [44] R. Shang, L. Ilies, A. Matsumoto, E. Nakamura, *J. Am. Chem. Soc.* **2013**, *135*, 6030–6032.

## 6. References

- [45] Q. Gu, H. H. A. Mamari, K. Graczyk, E. Diers, L. Ackermann, *Angew. Chem. Int. Ed.* **2014**, *53*, 3868–3871.
- [46] C. Zhu, M. Stangier, J. C. A. Oliveira, L. Massignan, L. Ackermann, *Chem. Eur. J.* **2019**, *25*, 16382–16389.
- [47] R. Shang, L. Ilies, S. Asako, E. Nakamura, *J. Am. Chem. Soc.* **2014**, *136*, 14349–14352.
- [48] L. Ilies, S. Ichikawa, S. Asako, T. Matsubara, E. Nakamura, *Adv. Synth. Catal.* **2015**, *357*, 2175–2179.
- [49] R. Shang, L. Ilies, E. Nakamura, *J. Am. Chem. Soc.* **2015**, *137*, 7660–7663.
- [50] a) Z. Shen, G. Cera, T. Haven, L. Ackermann, *Org. Lett.* **2017**, *19*, 3795–3798; b) K. Graczyk, T. Haven, L. Ackermann, *Chem. Eur. J.* **2015**, *21*, 8812–8815.
- [51] a) G. Cera, T. Haven, L. Ackermann, *Angew. Chem. Int. Ed.* **2016**, *55*, 1484–1488; b) E. R. Fruchey, B. M. Monks, S. P. Cook, *J. Am. Chem. Soc.* **2014**, *136*, 13130–13133; c) L. Ilies, T. Matsubara, S. Ichikawa, S. Asako, E. Nakamura, *J. Am. Chem. Soc.* **2014**, *136*, 13126–13129; d) B. M. Monks, E. R. Fruchey, S. P. Cook, *Angew. Chem. Int. Ed.* **2014**, *53*, 11065–11069.
- [52] S. Asako, L. Ilies, E. Nakamura, *J. Am. Chem. Soc.* **2013**, *135*, 17755–17757.
- [53] G. Cera, T. Haven, L. Ackermann, *Chem. Eur. J.* **2017**, *23*, 3577–3582.
- [54] a) B. Plietker, A. Dieskau, K. Möws, A. Jatsch, *Angew. Chem. Int. Ed.* **2007**, *47*, 198–201; b) B. Plietker, *Angew. Chem. Int. Ed.* **2006**, *45*, 1469–1473.
- [55] S. Ito, Y. Fujiwara, E. Nakamura, M. Nakamura, *Org. Lett.* **2009**, *11*, 4306–4309.
- [56] a) M. D. Greenhalgh, A. S. Jones, S. P. Thomas, *ChemCatChem* **2015**, *7*, 190–222; b) B. D. Sherry, A. Fürstner, *Acc. Chem. Res.* **2008**, *41*, 1500–1511.
- [57] A. Matsumoto, L. Ilies, E. Nakamura, *J. Am. Chem. Soc.* **2011**, *133*, 6557–6559.

## 6. References

- [58] L. Ilies, A. Matsumoto, M. Kobayashi, N. Yoshikai, E. Nakamura, *Synlett* **2012**, 23, 2381–2384.
- [59] L. Adak, N. Yoshikai, *Tetrahedron* **2012**, 68, 5167–5171.
- [60] T. Matsubara, L. Ilies, E. Nakamura, *Chem. Asian J.* **2016**, 11, 380–384.
- [61] G. Cera, T. Haven, L. Ackermann, *Chem. Commun.* **2017**, 53, 6460–6463.
- [62] M. M. Bagga, P. L. Pauson, F. J. Preston, R. I. Reed, *Chem. Commun.* **1965**, 543–544.
- [63] T. Jia, C. Zhao, R. He, H. Chen, C. Wang, *Angew. Chem. Int. Ed.* **2016**, 55, 5268–5271.
- [64] a) S. Yu, S. Ma, *Angew. Chem. Int. Ed.* **2012**, 51, 3074–3112; b) P. Rivera-Fuentes, F. Diederich, *Angew. Chem. Int. Ed.* **2012**, 51, 2818–2828.
- [65] J. Ye, S. Ma, *Acc. Chem. Res.* **2014**, 47, 989–1000.
- [66] a) A. Ahlers, T. de Haro, B. Gabor, A. Fürstner, *Angew. Chem. Int. Ed.* **2016**, 55, 1406–1411; b) P. Rivera-Fuentes, F. Diederich, *Angew. Chem. Int. Ed.* **2012**, 51, 2818–2828.
- [67] a) Z. Dong, Z. Ren, S. J. Thompson, Y. Xu, G. Dong, *Chem. Rev.* **2017**, 117, 9333–9403; b) G. E. M. Crisenza, J. F. Bower, *Chem. Lett.* **2016**, 45, 2–9; c) S. Pan, T. Shibata, *ACS Catal.* **2013**, 3, 704–712; d) D. A. Colby, R. G. Bergman, J. A. Ellman, *Chem. Rev.* **2010**, 110, 624–655.
- [68] a) Z.-J. Jia, C. Merten, R. Gontla, C. G. Daniliuc, A. P. Antonchick, H. Waldmann, *Angew. Chem. Int. Ed.* **2017**, 56, 2429–2434; b) S. Nakanowatari, L. Ackermann, *Chem. Eur. J.* **2015**, 21, 16246–16251; c) X.-F. Xia, Y.-Q. Wang, L.-L. Zhang, X.-R. Song, X.-Y. Liu, Y.-M. Liang, *Chem. Eur. J.* **2014**, 20, 5087–5091; d) B. Ye, N. Cramer, *J. Am. Chem. Soc.* **2013**, 135, 636–639; e) R. Zeng, J. Ye, C. Fu, S. Ma, *Adv. Synth. Catal.* **2013**, 355, 1963–1970; f) R. Zeng, C. Fu, S. Ma, *J. Am. Chem. Soc.* **2012**, 134, 9597–9600; g) Y. J. Zhang, E. Skucas, M. J. Krische, *Org. Lett.* **2009**, 11, 4248–4250.

## 6. References

- [69] a) A. Brandi, S. Cicchi, F. M. Cordero, A. Goti, *Chem. Rev.* **2014**, *114*, 7317–7420; b) H. Pellissier, *Tetrahedron* **2010**, *66*, 8341–8375; c) A. Goti, M. F. Cordero, A. Brandi, *Top. Curr. Chem.* **2005**, *178*, 1–97; d) A. Brandi, S. Cicchi, F. M. Cordero, A. Goti, *Chem. Rev.* **2003**, *103*, 1213–1270; e) A. de Meijere, S. I. Kozhushkov, *Eur. J. Org. Chem.* **2000**, 3809–3822; f) A. de Meijere, S. I. Kozhushkov, A. F. Khlebnikov, *Top. Curr. Chem.* **2000**, *207*, 89–147; g) A. de Meijere, S. I. Kozhushkov, A. F. Khlebnikov, *Russ. J. Org. Chem.* **1996**, *32*, 1555–1575.
- [70] a) M. Schinkel, J. Wallbaum, S. I. Kozhushkov, I. Marek, L. Ackermann, *Org. Lett.* **2013**, *15*, 4482–4484; b) L. Ackermann, S. I. Kozhushkov, D. S. Yufit, *Eur. J. Org. Chem.* **2012**, 12068–12077; c) S. I. Kozhushkov, D. S. Yufit, L. Ackermann, *Org. Lett.* **2008**, *10*, 3409–3412.
- [71] a) Y. Cohen, A. Cohen, I. Marek, *Chem. Rev.* **2020**, doi: 10.1021/acs.chemrev.0c00167; b) P. H. Chen, B. A. Billett, T. Tsukamoto, G. Dong, *ACS Catal.* **2017**, *7*, 1340–1360; c) D. S. Kim, W. J. Park, C. H. Jun, *Chem. Rev.* **2017**, *117*, 8977–9015; d) L. Souillart, N. Cramer, *Chem. Rev.* **2015**, *115*, 9410–9464; e) T. Xu, A. Dermenci, G. Dong, *Top. Curr. Chem.* **2014**, *346*, 233–257; f) K. Ruhland, *Eur. J. Org. Chem.* **2012**, 2683–2706; g) M. Murakami, T. Matsuda, *Chem. Commun.* **2011**, *47*, 1100–1105.
- [72] M. Murakami, Y. Ito, *Top. Organomet. Chem.* **1999**, *3*, 97–127.
- [73] Z. Nairoukh, M. Cormier, I. Marek, *Nat. Rev. Chem.* **2017**, *1*, 0035.
- [74] a) K. Korvorapun, M. Moselage, J. Struwe, T. Rogge, A. M. Messinis, L. Ackermann, *Angew. Chem. Int. Ed.* **2020**, doi: 10.1002/anie.202007144; b) N. Y. P. Kumar, T. Rogge, S. R. Yetra, A. Bechtoldt, E. Clot, L. Ackermann, *Chem. Eur. J.* **2017**, *23*, 17449–17453; c) N. Y. P. Kumar; A. Bechtoldt, K. Raghuvanshi, L. Ackermann, *Angew. Chem. Int. Ed.* **2016**, *55*, 6929–6932; d) M. P. Drapeau, L. J. Gooßen, *Chem. Eur. J.* **2016**, *22*, 18654–18677; e) X.-Y. Shi, X.-F. Dong, J. Fan, K.-Y. Liu, L.-F. Wei, C.-J. Li, *Sci. China Chem.* **2015**,

## 6. References

- 58, 1286–1292; f) X.-Y. Shi, K.-Y. Liu, J. Fan, X.-F. Dong, J.-F. Wei, C.-J. Li, *Chem. Eur. J.* **2014**, *20*, 1–5; g) W. I. Dzik, P. P. Lange, L. J. Gooßen, *Chem. Sci.* **2012**, *3*, 2671–2678; h) J. Cornella, M. Righi, I. Larrosa, *Angew. Chem. Int. Ed.* **2011**, *50*, 9429–9432; i) L. J. Gooßen, N. Rodriguez, K. Gooßen, *Angew. Chem. Int. Ed.* **2008**, *47*, 3100–3120.
- [75] a) A. Dermenci, G. Dong, *Sci. China Chem.* **2013**, *56*, 685–701; b) Q. Shuai, L. Yang, X. Guo, O. Baslé, C.-J. Li, *J. Am. Chem. Soc.* **2010**, *132*, 12212–12213; c) X. Guo, J. Wang, C.-J. Li, *J. Am. Chem. Soc.* **2009**, *131*, 15092–15093; d) P. Fristrup, M. Kreis, A. Palmelund, P.-O. Norrby, R. Madsen, *J. Am. Chem. Soc.* **2008**, *130*, 5206–5215; e) J. Tsuji, K. Ohno, *Tetrahedron Lett.* **1965**, *44*, 3969–3971; f) H. E. Eschinazi, H. Pines, *J. Org. Chem.* **1959**, *24*, 1369–1369.
- [76] a) C. L. Ladd, D. S. Roman, A. B. Charette, *Tetrahedron* **2013**, *69*, 4479–4487; b) D. A. Colby, A. S. Tsai, R. G. Bergman, A. J. Ellman, *Acc. Chem. Res.* **2012**, *45*, 814–825; c) S. Rousseaux, B. Liégault, K. Fagnou, *Chem. Sci.* **2012**, *3*, 244–248.
- [77] R. D. Bach, O. Dmitrenko, *J. Am. Chem. Soc.* **2004**, *126*, 4444–4452.
- [78] a) G. Fumagalli, S. Stanton, J. F. Bower, *Chem. Rev.* **2017**, *117*, 9404–9432; b) I. Marek, A. Masarwa, P. O. Delaye, M. Leibeling, *Angew. Chem. Int. Ed.* **2015**, *54*, 414–429.
- [79] a) R. A. Periana, R. G. Bergman, *J. Am. Chem. Soc.* **1986**, *108*, 7346–7355; b) R. A. Periana, R. G. Bergman, *J. Am. Chem. Soc.* **1984**, *106*, 7272–7273.
- [80] a) X. Zhou, S. Yu, L. Kong, X. Li, *ACS Catal.* **2016**, *6*, 647–651; b) X. Zhou, S. Yu, Z. Qi, L. Kong, X. Li, *J. Org. Chem.* **2016**, *81*, 4869–4875; c) A. Masarwa, M. Weber, R. Sarpong, *J. Am. Chem. Soc.* **2015**, *137*, 6327–6334; d) T. Matsuda, I. Yuihara, *Chem. Commun.* **2015**, *51*, 7393–7396; e) A. Vasseur, P. Perrin, O. Eisenstein, I. Marek, *Chem. Sci.* **2015**, *6*, 2770–2776; f) A. Masarwa, D. Didier, T. Zabrodski, M. Schinkel, L. Ackermann, I. Marek, *Nature* **2014**, *505*,

## 6. References

- 199–203; g) D. Rosa, A. Orellana, *Chem. Commun.* **2012**, 48, 1922–1924; h) Z. Chai, T. J. Rainey, *J. Am. Chem. Soc.* **2012**, 134, 3615–3618; i) D. Crépin, J. Dawick, C. Aïssa, *Angew. Chem. Int. Ed.* **2010**, 49, 620–623; j) T. Seiser, O. A. Roth, N. Cramer, *Angew. Chem. Int. Ed.* **2009**, 48, 6320–6323; k) M. Shigeno, T. Yamamoto, M. Murakami, *Chem. Eur. J.* **2009**, 15, 12929–12931; l) C. Aïssa, A. Fürstner, *J. Am. Chem. Soc.* **2007**, 129, 14836–14837; m) T. Matsuda, M. Shigeno, M. Murakami, *J. Am. Chem. Soc.* **2007**, 129, 12086–12087.
- [81] A. D. Aloise, M. E. Layton, M. D. Shair, *J. Am. Chem. Soc.* **2000**, 122, 12610–12611.
- [82] A. Schweinitz, A. Chtchemelinine, A. Orellana, *Org. Lett.* **2011**, 13, 232–235.
- [83] a) Q. Li, X. Yuan, B. Li, B. Wang, *Chem. Commun.* **2020**, 56, 1835–1838; b) Q. Wang, L. Shi, S. Liu, C. Zhi, L.-R. Fu, X.-Q. Hao, M.-P. Song, *RSC Adv.* **2020**, 10, 10883–10887; c) Q. Wang, C.-L. Zhi, P.-P. Lu, S. Liu, X. Zhu, X. Q. Hao, M.-P. Song, *Adv. Synth. Catal.* **2019**, 361, 1253–1258; d) Z. Hu, X.-Q. Hu, G. Zhang, L. J. Gooßen, *Org. Lett.* **2019**, 21, 6770–6773; e) Y.-Q. Zhu, Y.-X. Niu, L.-W. Hui, J.-L. He, K. Zhu, *Adv. Synth. Catal.* **2019**, 361, 2897–2903; f) J.-Q. Wu, Z.-P. Qiu, S.-S. Zhang, J.-G. Liu, Y.-X. Lao, L.-Q. Gu, Z.-S. Huang, J. Li, H. Wang, *Chem. Commun.* **2015**, 51, 77–80; g) J.-Q. Wu, Z.-P. Qiu, S.-S. Zhang, J.-G. Liu, Y.-X. Lao, L.-Q. Gu, Z.-S. Huang, J. Li, H. Wang, *Chem. Commun.* **2015**, 51, 77–80.
- [84] S. Cui, Y. Zhang, Q. Wu, *Chem. Sci.* **2013**, 4, 3421–3426.
- [85] a) M. Li, F. Y. Kwong, *Angew. Chem. Int. Ed.* **2018**, 57, 6512–6515; b) Q. Lu, F. J. R. Klauck, F. Glorius, *Chem. Sci.* **2017**, 8, 3379–3383; c) T. H. Meyer, W. Liu, M. Feldt, A. Wuttke, R. A. Mata, L. Ackermann, *Chem. Eur. J.* **2017**, 23, 5443–5447; d) D. Zell, Q. Bu, M. Feldt, L. Ackermann, *Angew. Chem. Int. Ed.* **2016**, 55, 7408–7412.

## 6. References

- [86] a) S. Guo, D. I. AbuSalim, S. P. Cook, *J. Am. Chem. Soc.* **2018**, *140*, 12378–12382; b) N. Yoshikai, *Isr. J. Chem.* **2017**, *57*, 1117–1130; c) R. P. Yu, D. Hesk, N. Rivera, I. Pelczar, P. J. Chirik, *Nature* **2016**, *529*, 195–199; d) T. J. Osberger, D. C. Rogness, J. T. Kohrt, A. F. Stepan, M. C. White, *Nature* **2016**, *537*, 214–219; e) C. Bornschein, S. Werkmeister, B. Wendt, H. Jiao, E. Alberico, W. Baumann, H. Junge, K. Junge, M. Beller, *Nat. Commun.* **2014**, *5*, 4111; f) R. V. Jagadeesh, A.-E. Surkus, H. Junge, M.-M. Pohl, J. Radnik, J. Rabeah, H. Huan, V. Schuenemann, A. Brueckner, M. Beller, *Science* **2013**, *342*, 1073–1076.
- [87] P. Gandeepan, N. Kaplaneris, S. Santoro, L. Vaccaro, L. Ackermann, *ACS Sustainable Chem. Eng.* **2019**, *7*, 8023–8040.
- [88] a) S. Tang, O. Eisenstein, Y. Nakao, S. Sakaki, *Organometallics* **2017**, *36*, 2761–2771; b) O. Eisenstein, J. Milani, R. N. Perutz, *Chem. Rev.* **2017**, *117*, 8710–8753; c) J. Loup, D. Zell, J. C. A. Oliveira, H. Keil, D. Stalke, L. Ackermann, *Angew. Chem. Int. Ed.* **2017**, *56*, 14197–14201.
- [89] J. Mo, T. Müller, J. C. A. Oliveira, L. Ackermann, *Angew. Chem. Int. Ed.* **2018**, *57*, 7719–7723.
- [90] a) P. Gütllich, E. Bill, A. X. Trautwein, *Mössbauer Spectroscopy and Transition Metal Chemistry*, Springer, Heidelberg, **2011**; b) P. Gütllich, *Z. Anorg. Allg. Chem.* **2012**, *638*, 15–43.
- [91] S. B. Munoz III, S. L. Daifuku, W. W. Brennessel, M. L. Neidig, *J. Am. Chem. Soc.* **2016**, *138*, 7492–7495.
- [92] a) M. Callingham, B. M. Partridge, W. Lewis, H. W. Lam, *Angew. Chem. Int. Ed.* **2017**, *56*, 16352–16356; b) B. M. Partridge, M. Callingham, W. Lewis, H. W. Lam, *Angew. Chem. Int. Ed.* **2017**, *56*, 7227–7232; c) S. E. Korkis, D. J. Burns, H. W. Lam, *J. Am. Chem. Soc.* **2016**, *138*, 12252–12257; d) D. J. Burns, H. W. Lam, *Angew. Chem. Int. Ed.* **2014**, *53*, 9931–9935; e) J. Yan, N. Yoshikai, *Org. Chem. Front.* **2017**, *4*, 1972–1975; f) J. Yan, N. Yoshikai, *ACS*

## 6. References

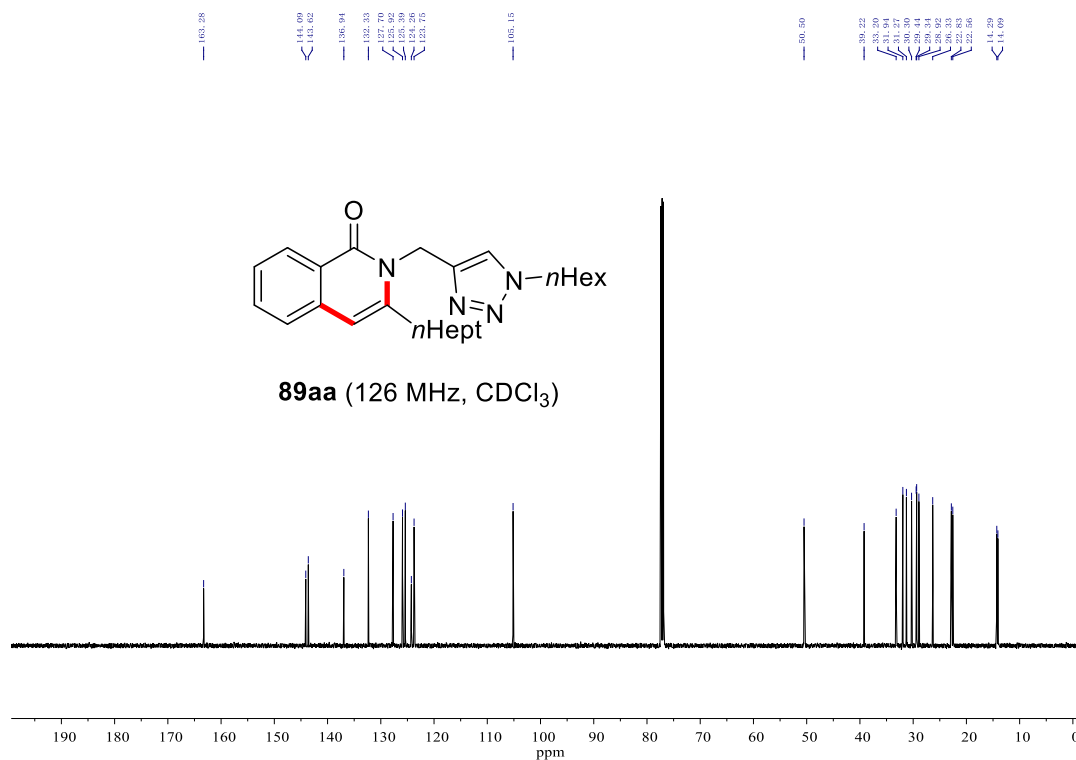
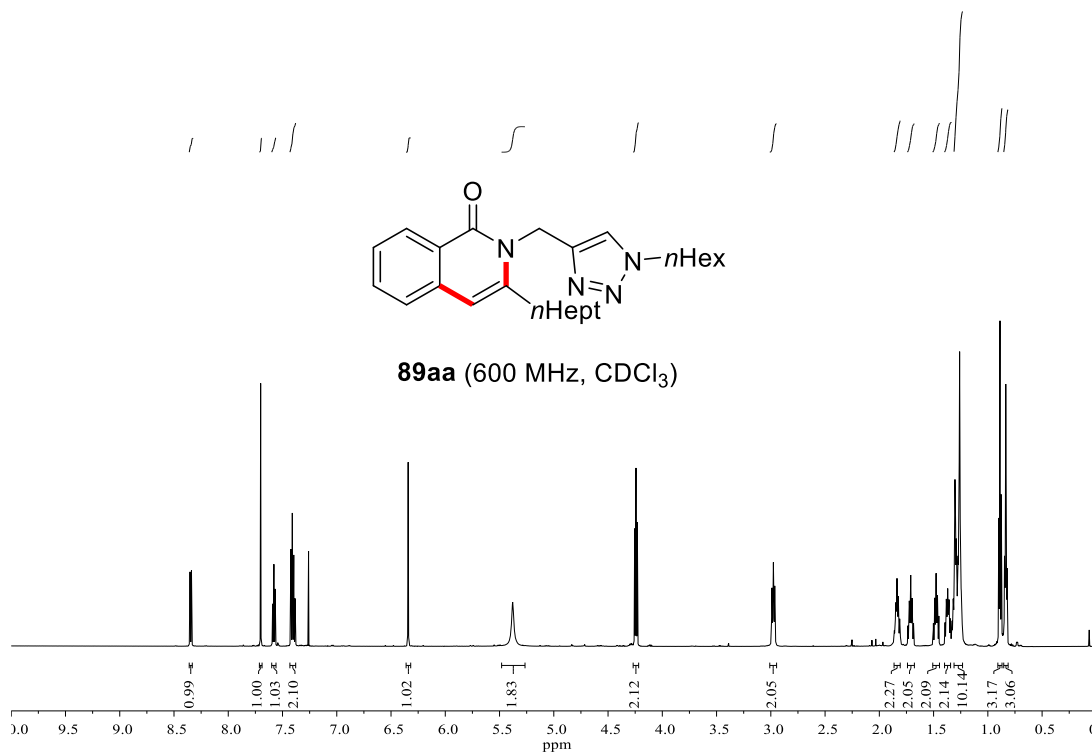
- Catal.* **2016**, *6*, 3738–3742; g) B.-H. Tan, J. Dong, N. Yoshikai, *Angew. Chem. Int. Ed.* **2012**, *51*, 9610–9614; h) B. Zhou, H. Sato, L. Ilies, E. Nakamura, *ACS Catal.* **2018**, *8*, 8–11.
- [93] J. Mo, T. Müller, J. C. A. Oliveira, S. Demeshko, F. Meyer, L. Ackermann, *Angew. Chem. Int. Ed.* **2019**, *58*, 12874–12878.
- [94] T. E. Boddie, S. H. Carpenter, T. M. Baker, J. C. DeMuth, G. Cera, W. W. Brennessel, L. Ackermann, M. L. Neidig, *J. Am. Chem. Soc.* **2019**, *141*, 12338–12345.
- [95] E. Bill, E. Mfit Program; Max-Planck Institute for Chemical Energy Conversion: Mülheim/Ruhr, Germany, **2008**.
- [96] a) W. Li, Z. Lin, L. Chen, X. Tian, Y. Wenig, S.-H. Huang, R. Hong, *Tetrahedron Lett.* **2016**, *57*, 603–606; b) H. Luo, S. Ma, *Eur. J. Org. Chem.* **2013**, 3041–3048; c) L. Zhang, X. Li, Y. Liu, D. Zhang, *Chem. Commun.* **2015**, *51*, 6633–6636; d) Q. Li, C. Fu, S. Ma, *Angew. Chem. Int. Ed.* **2012**, *51*, 11783–11786.
- [97] G. Winter, D. W. Thompson, J. R. Loehe, *Inorg. Synth.* **2007**, *14*, 99–104.
- [98] T. Schwier, M. Rubin, V. Gevorgyan, *Org. Lett.* **2004**, *6*, 1999–2001.
- [99] T. Kippo, K. Hamaoka, I. Ryu, *J. Am. Chem. Soc.* **2013**, *135*, 632–635.
- [100] Anderson H. W. (**1972**) PhD Thesis, Massachusetts Institute of Technology, Cambridge, Massachusetts.
- [101] a) A. de Meijere, S. I. Kozhushkov, T. Späth, *Org. Synth.* **2002**, *78*, 142; b) A. de Meijere, S. I. Kozhushkov, N. S. Zefirov, *Synthesis* **1993**, (7), 681–683; c) K. A. Lukin, S. I. Kozhushkov, A. A. Andrievsky, B. I. Ugrak, N. S. Zefirov, *J. Org. Chem.* **1991**, *56*, 6176–6179.
- [102] H.-P. Guan, M. B. Ksebati, Y.-C. Cheng, J. C. Drach, E. R. Kern, J. Zemlicka, *J. Org. Chem.* **2000**, *65*, 1280–1290.
- [103] K. Miyazawa, D. S. Yufit, J. A. K. Howard, A. de Meijere, *Eur. J. Org. Chem.* **2000**, 4109–4117.

## 6. References

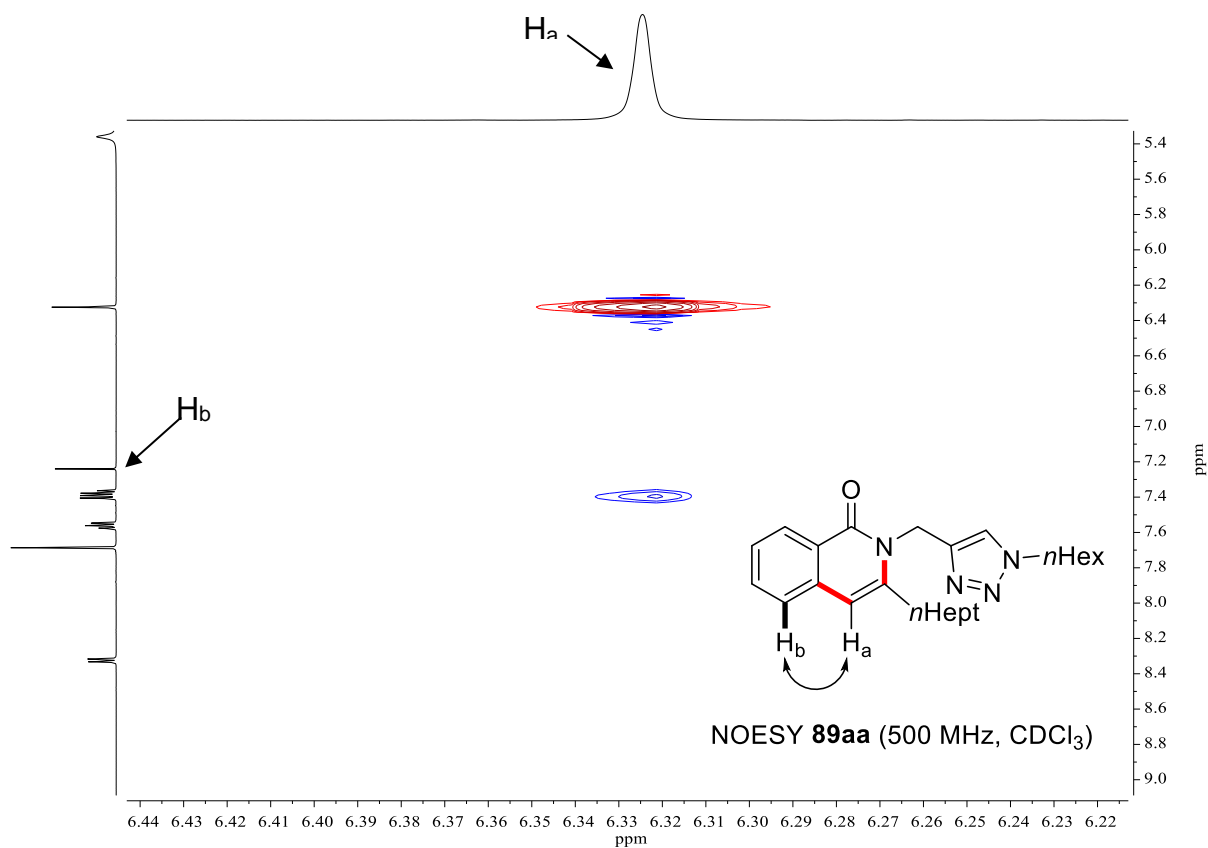
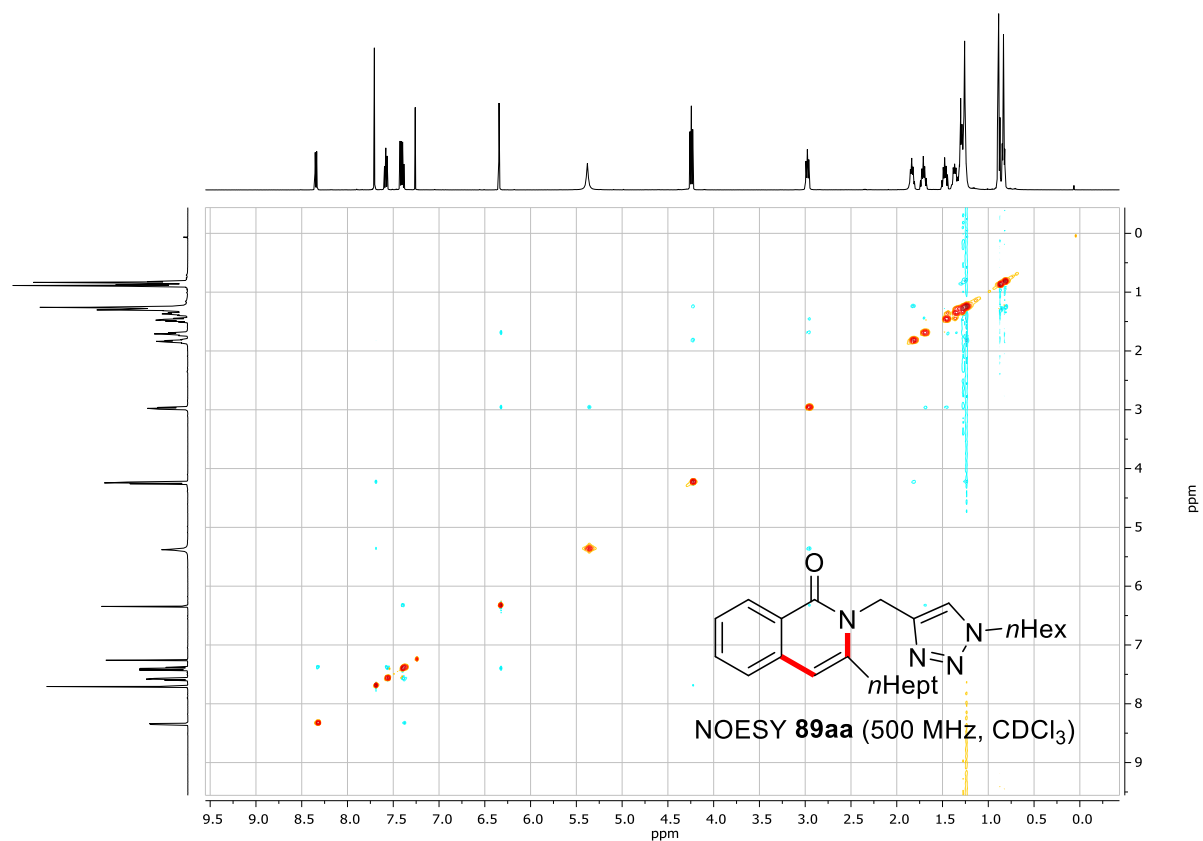
- [104] O. V. Dolomanov, L. J. Bourhis, R. J. Gildea, J. A. K. Howard, H. Puschmann, *J. Appl. Cryst.* **2009**, 42, 339–341.
- [105] G. M. Sheldrick, *Acta Cryst.* **2015**, A71, 3–8.
- [106] G. M. Sheldrick, *Acta Cryst.* **2008**, A64, 112–122.

# NMR Spectra

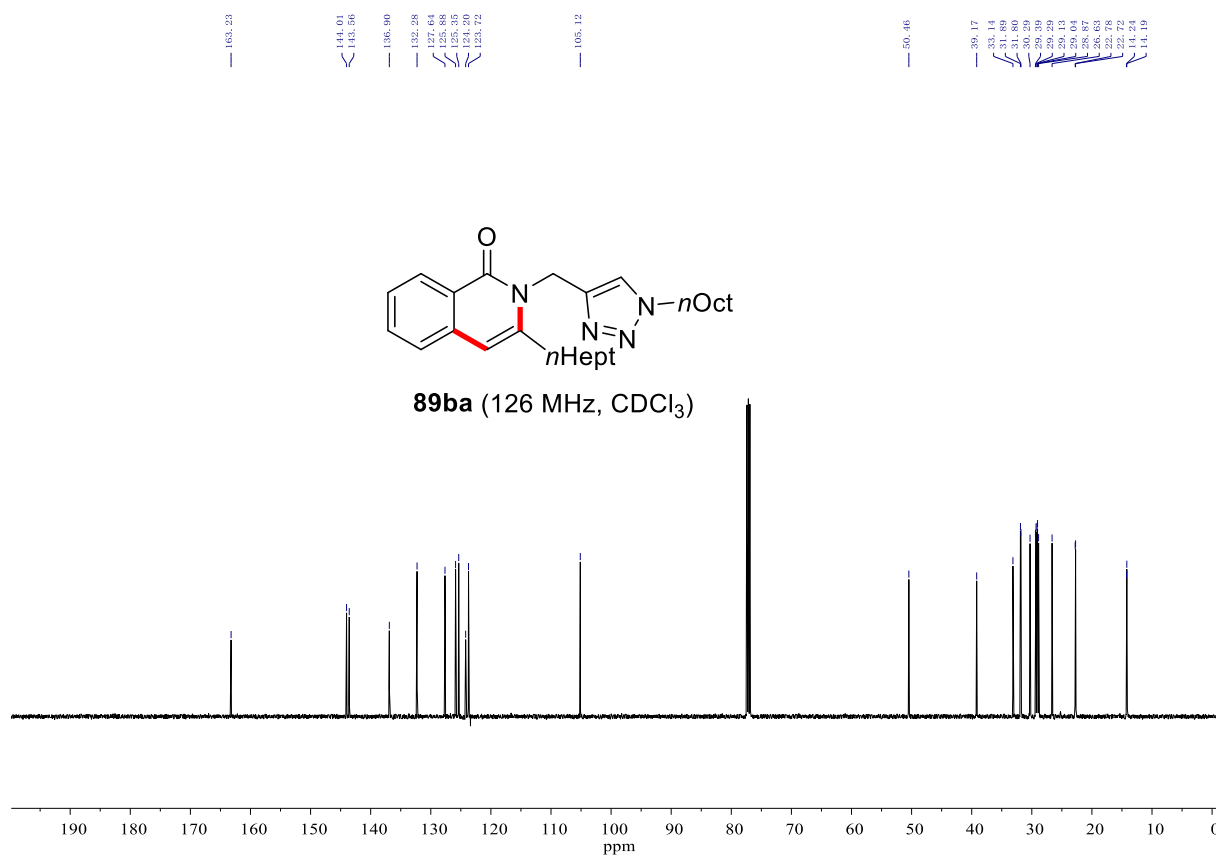
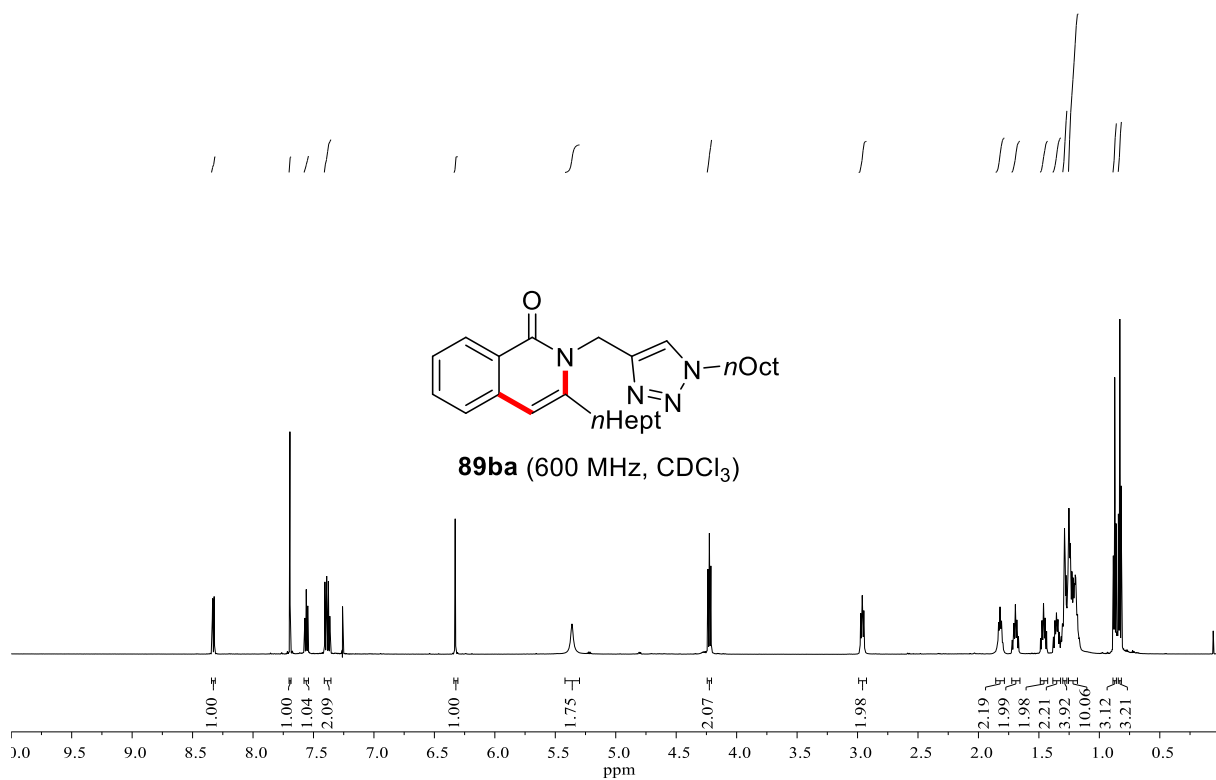
## NMR Spectra



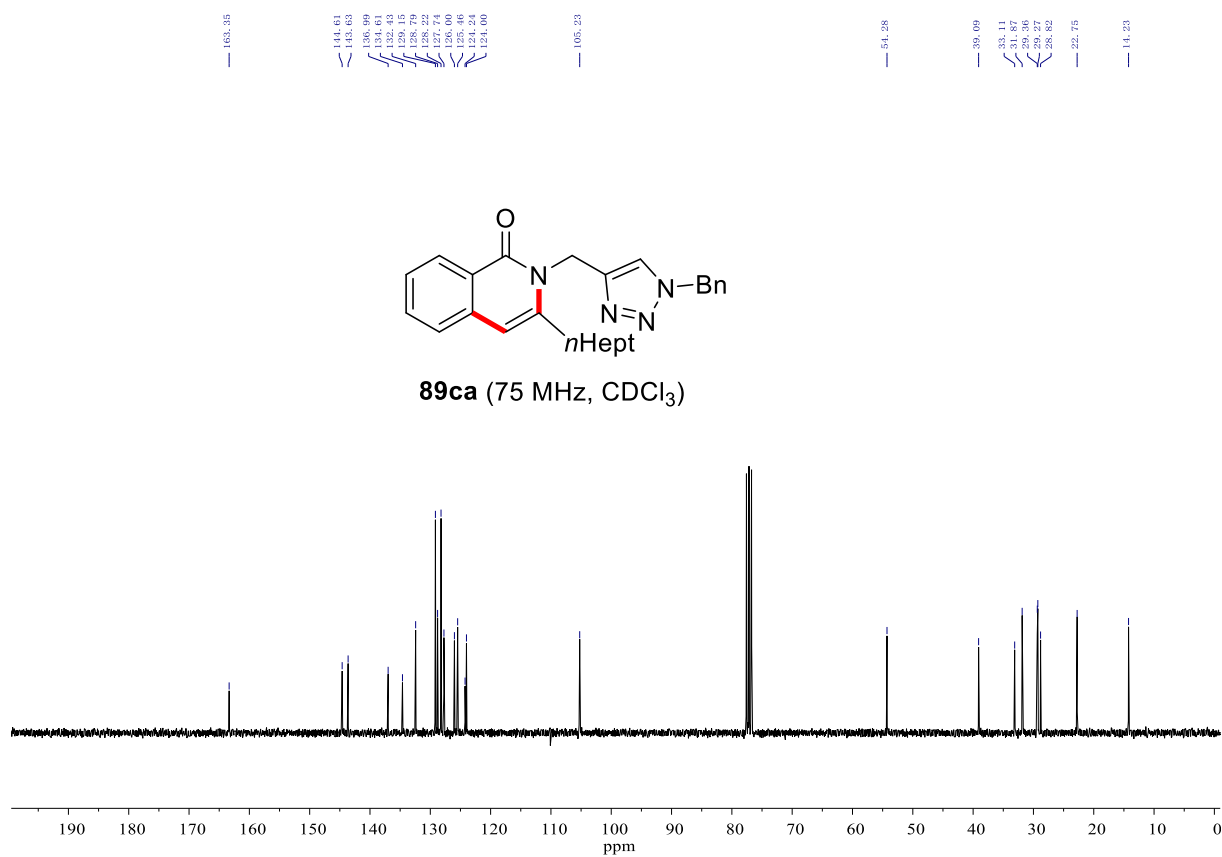
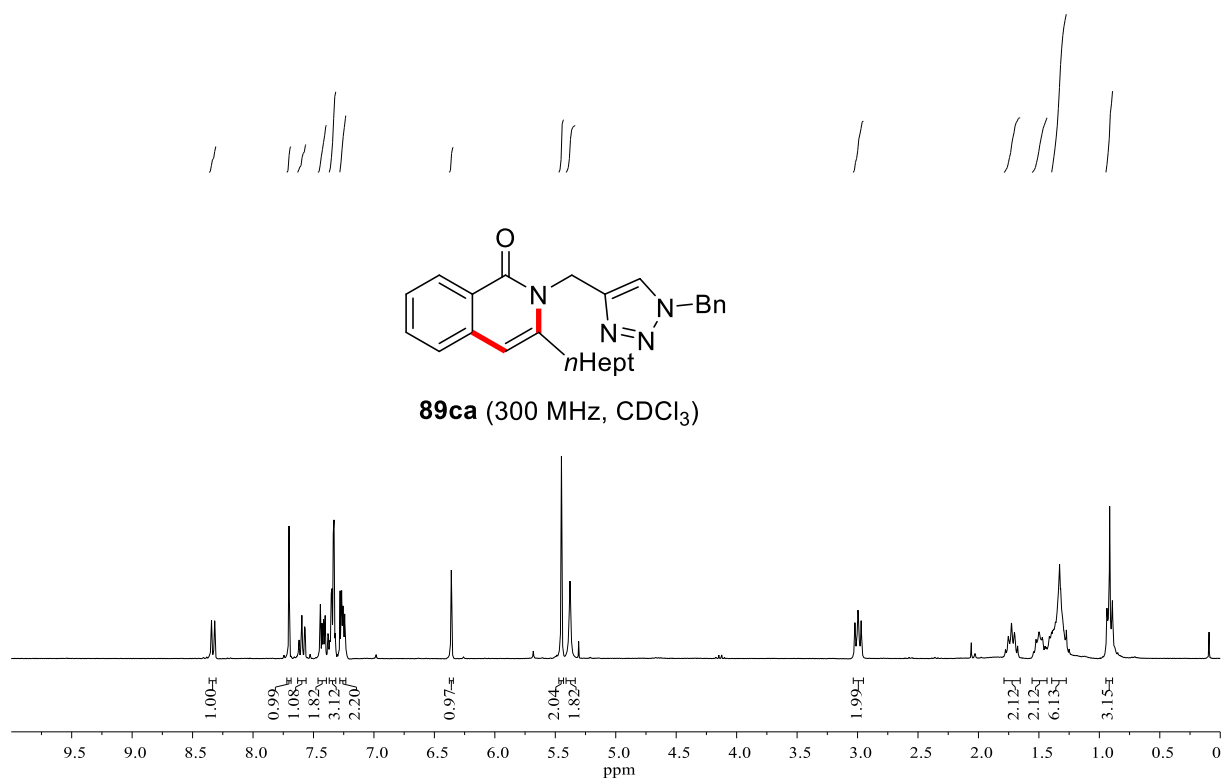
# NMR Spectra



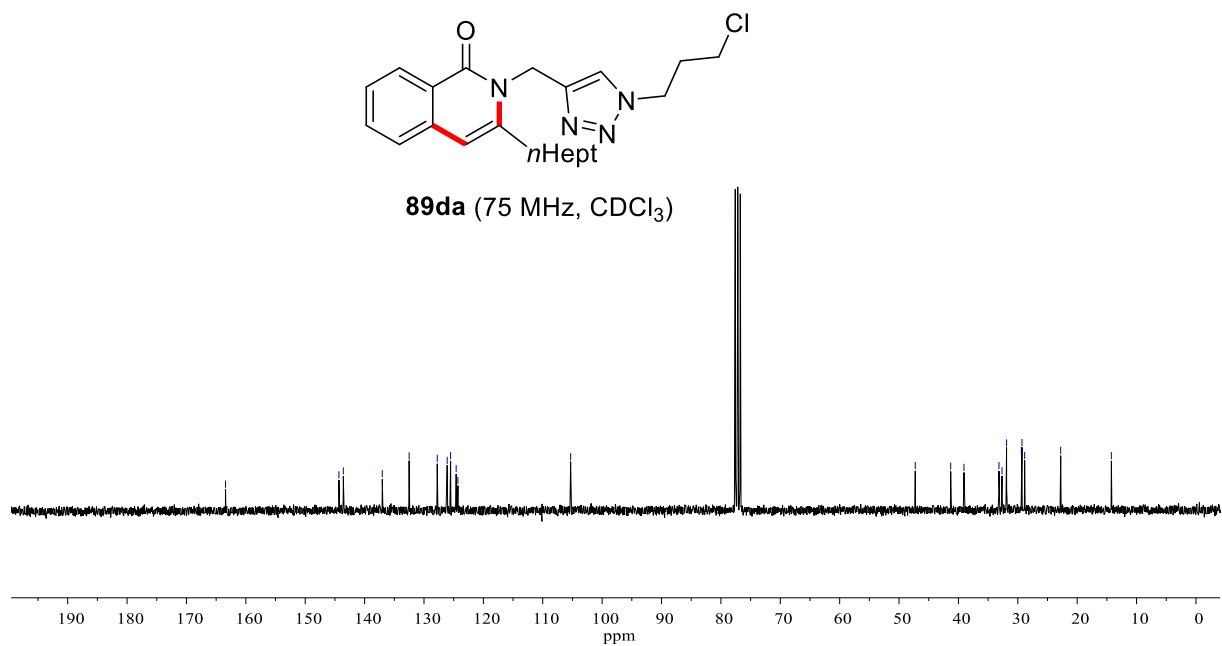
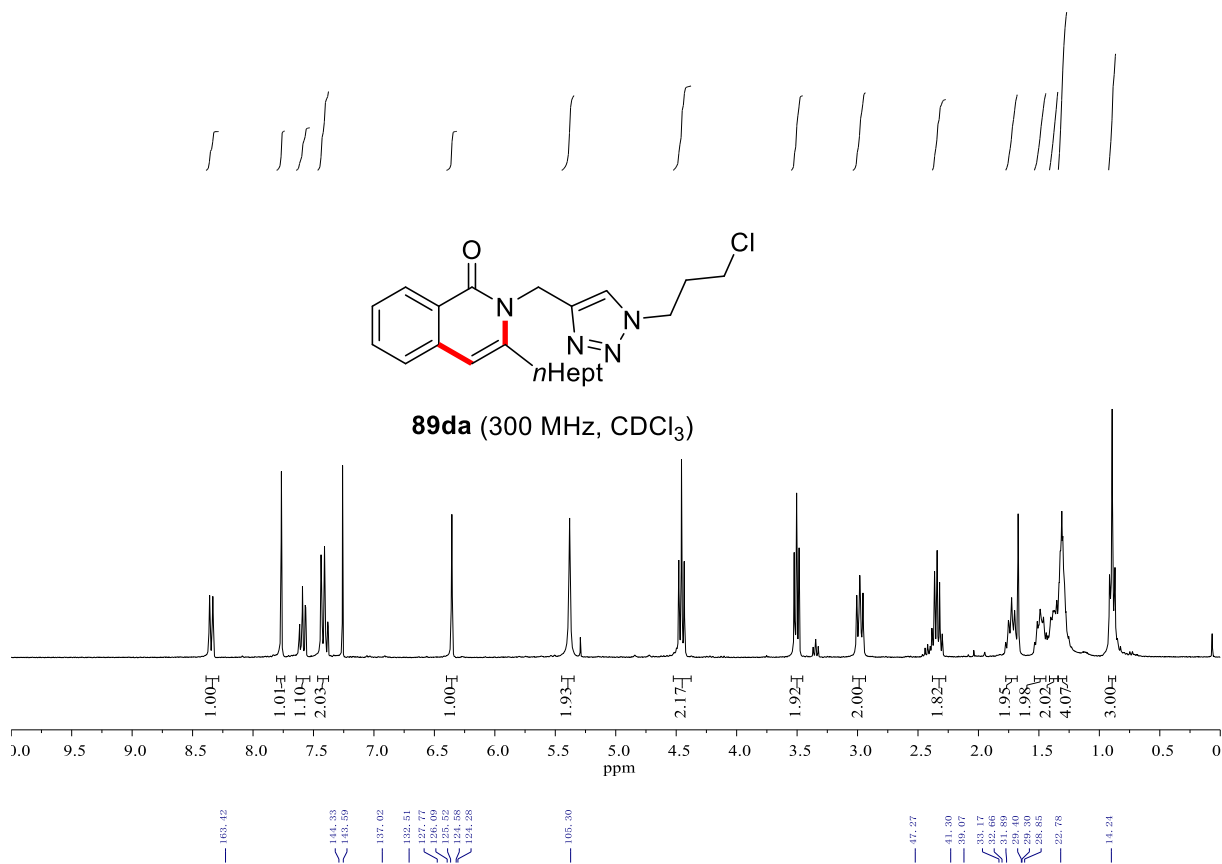
# NMR Spectra



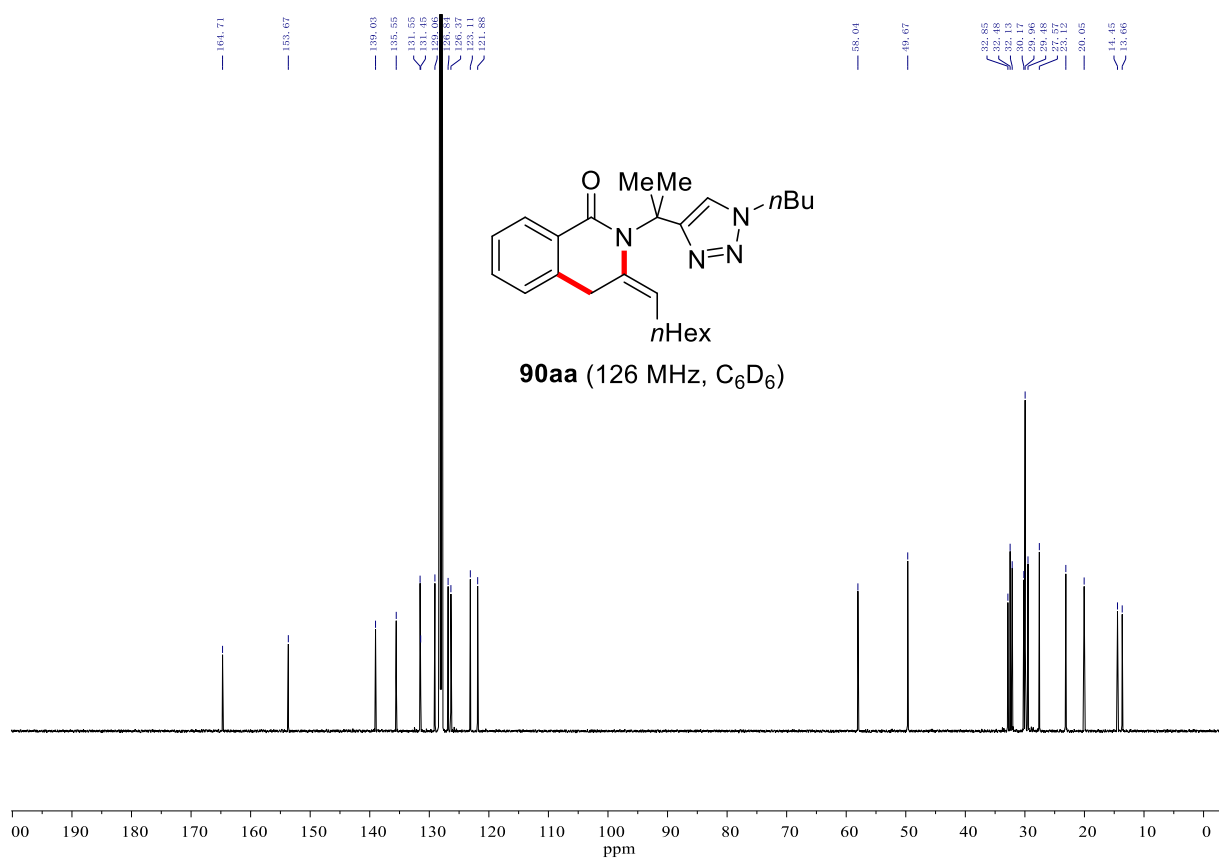
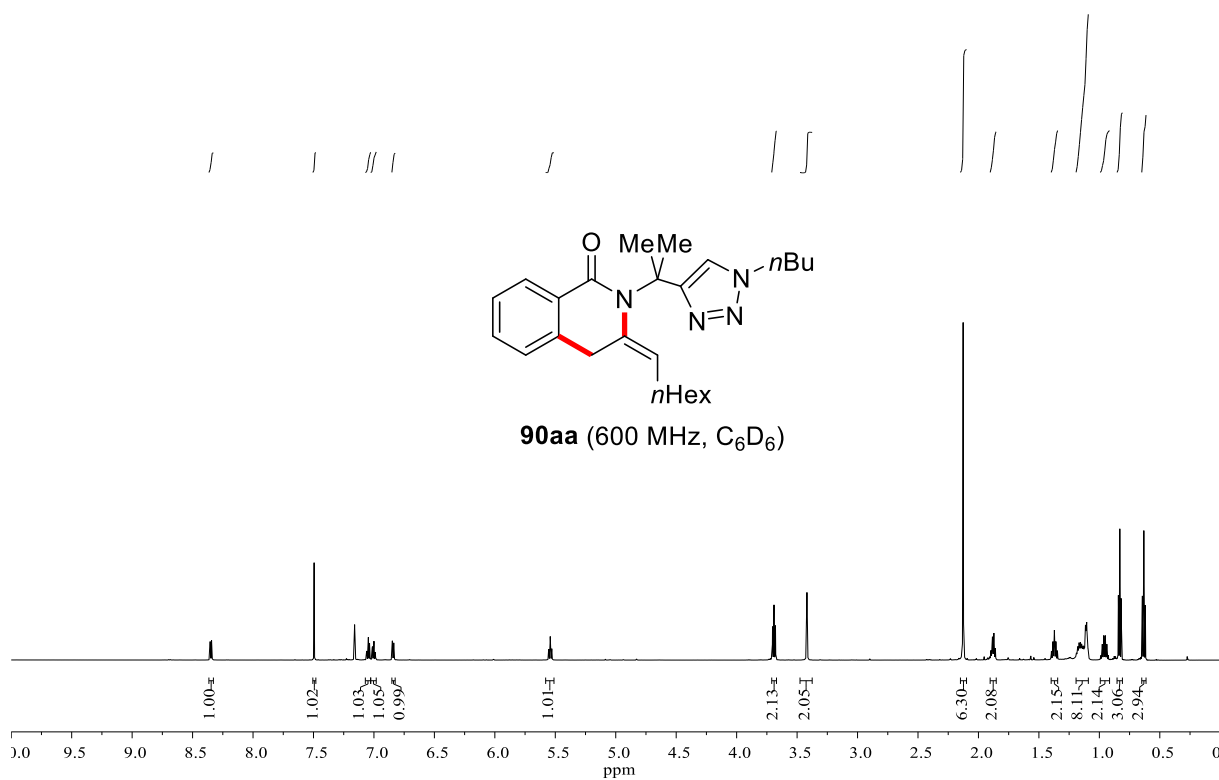
# NMR Spectra



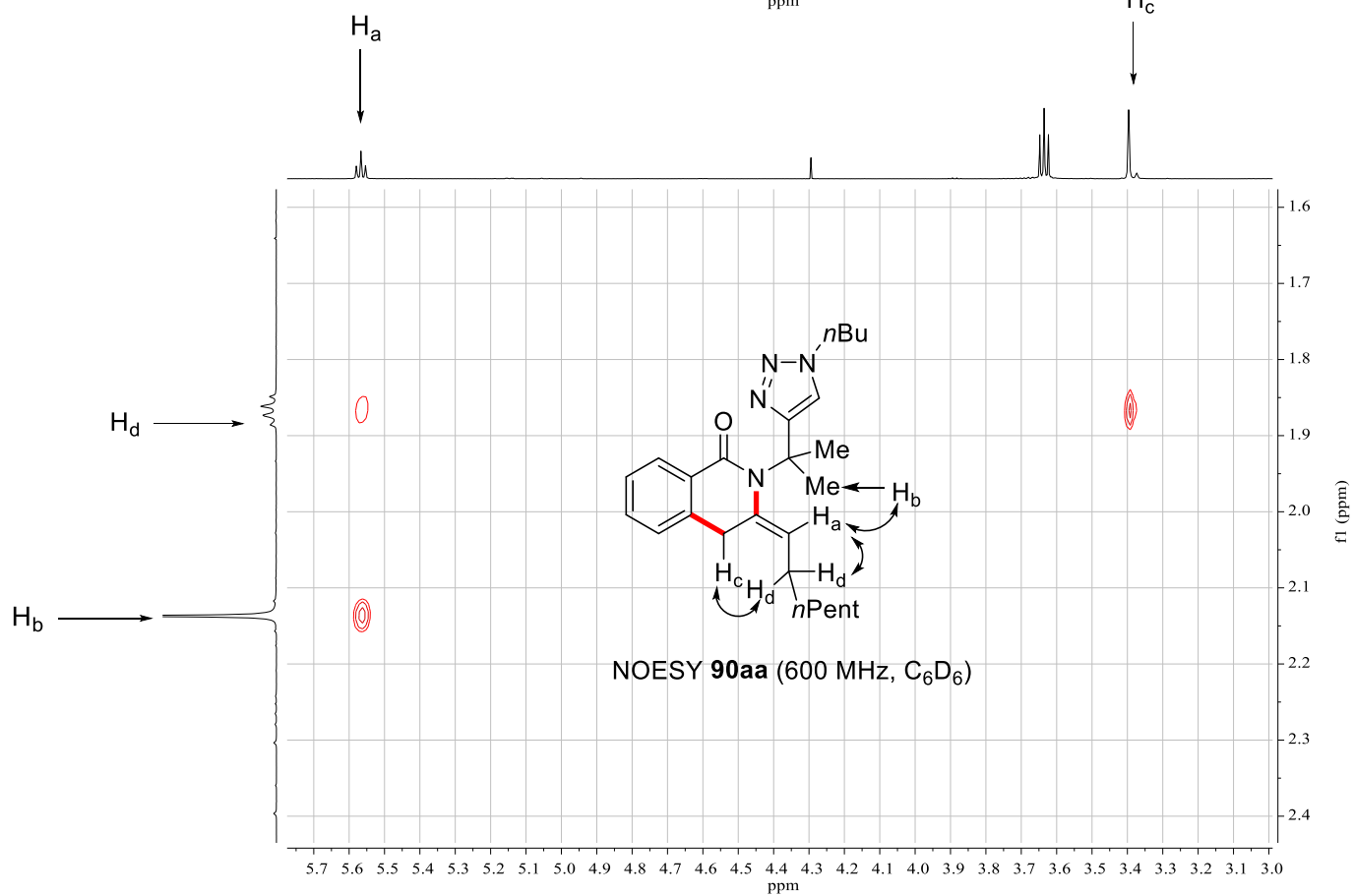
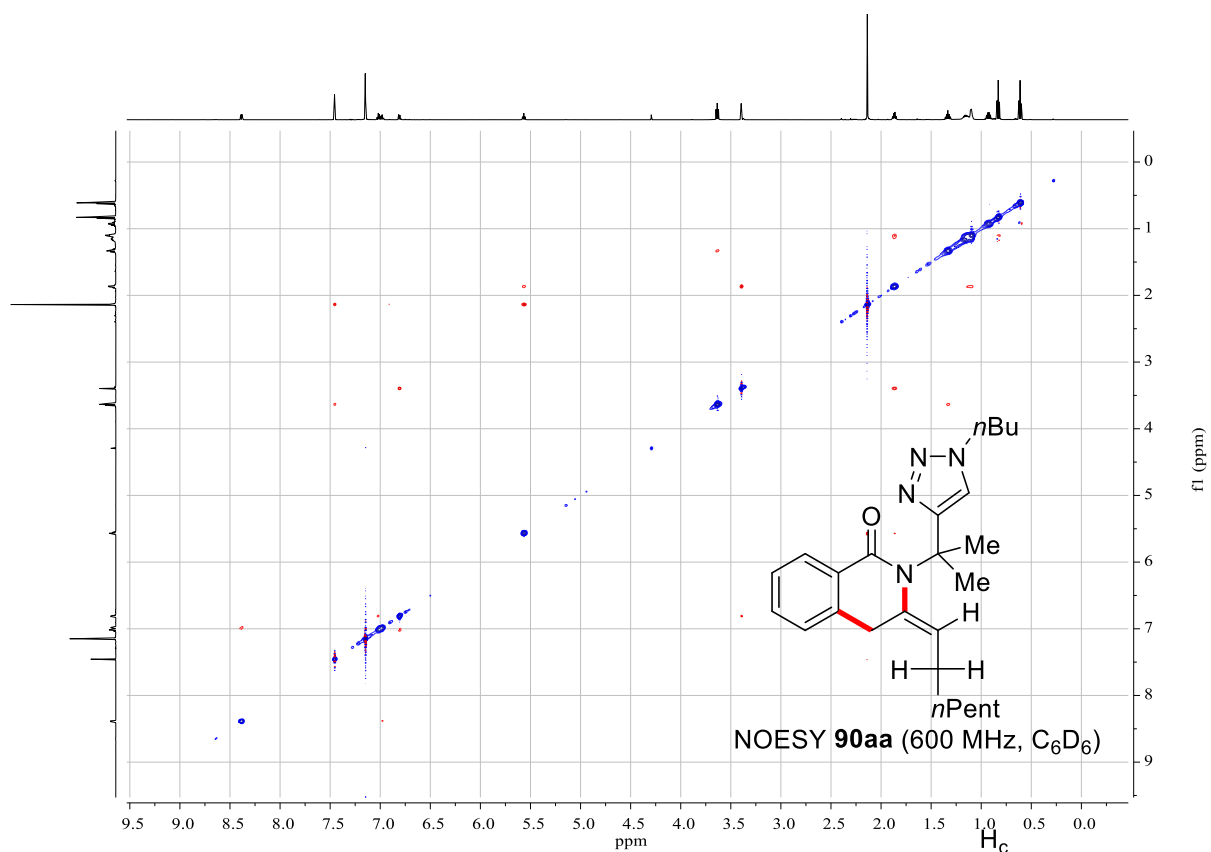
# NMR Spectra



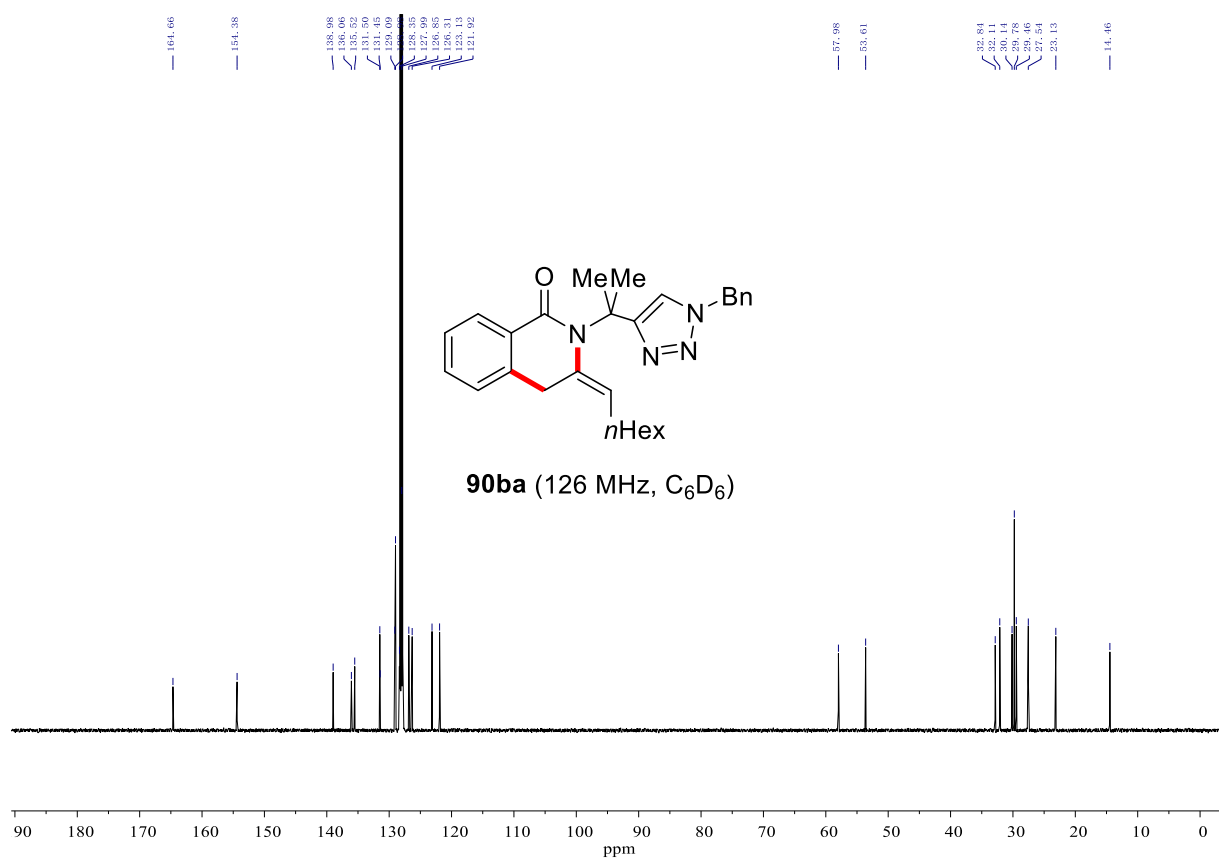
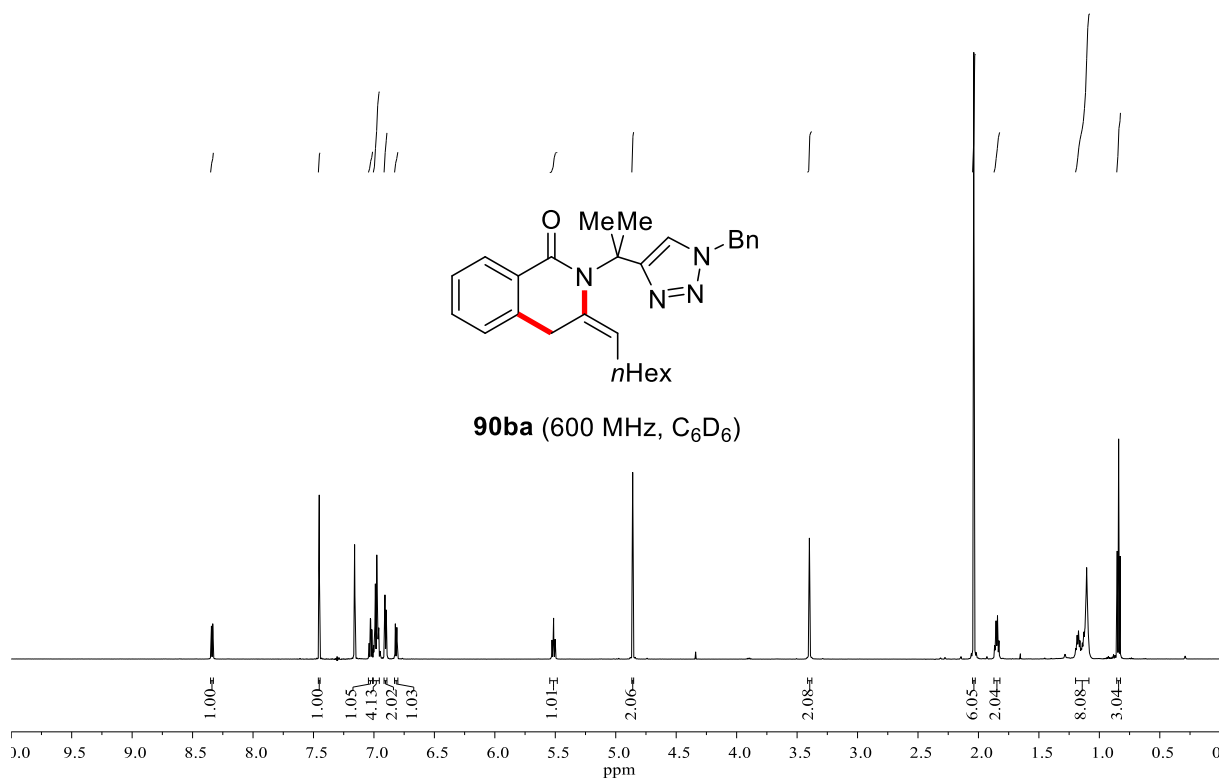
# NMR Spectra



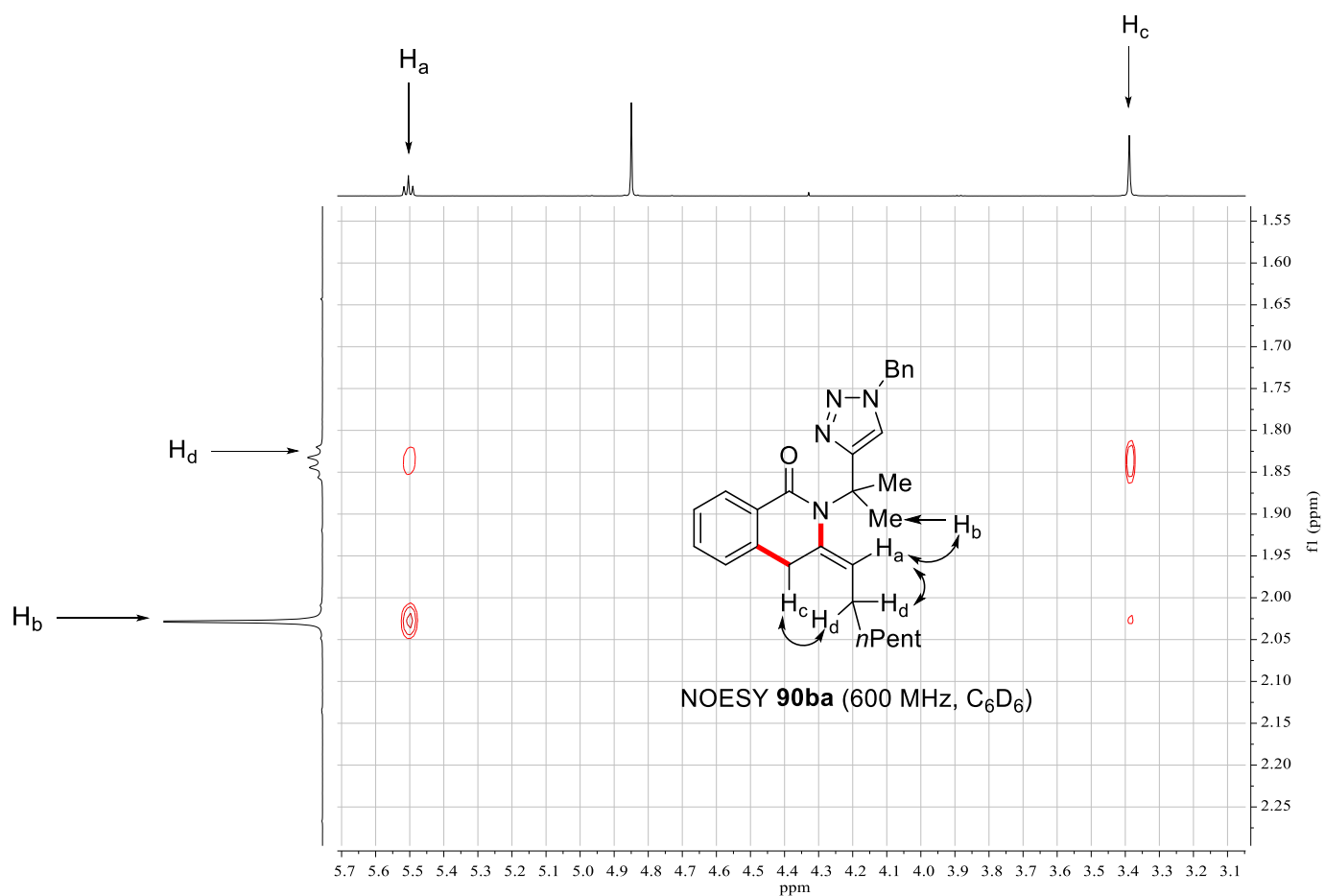
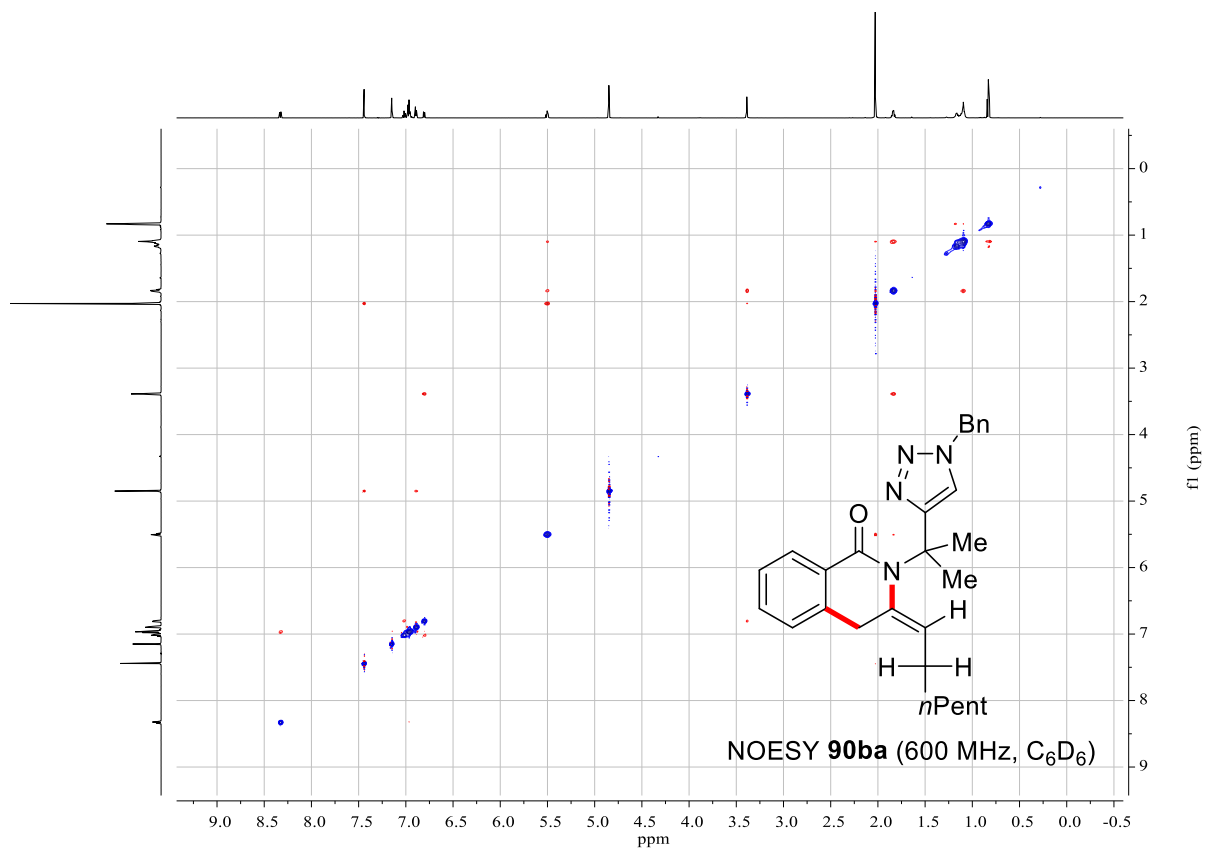
# NMR Spectra



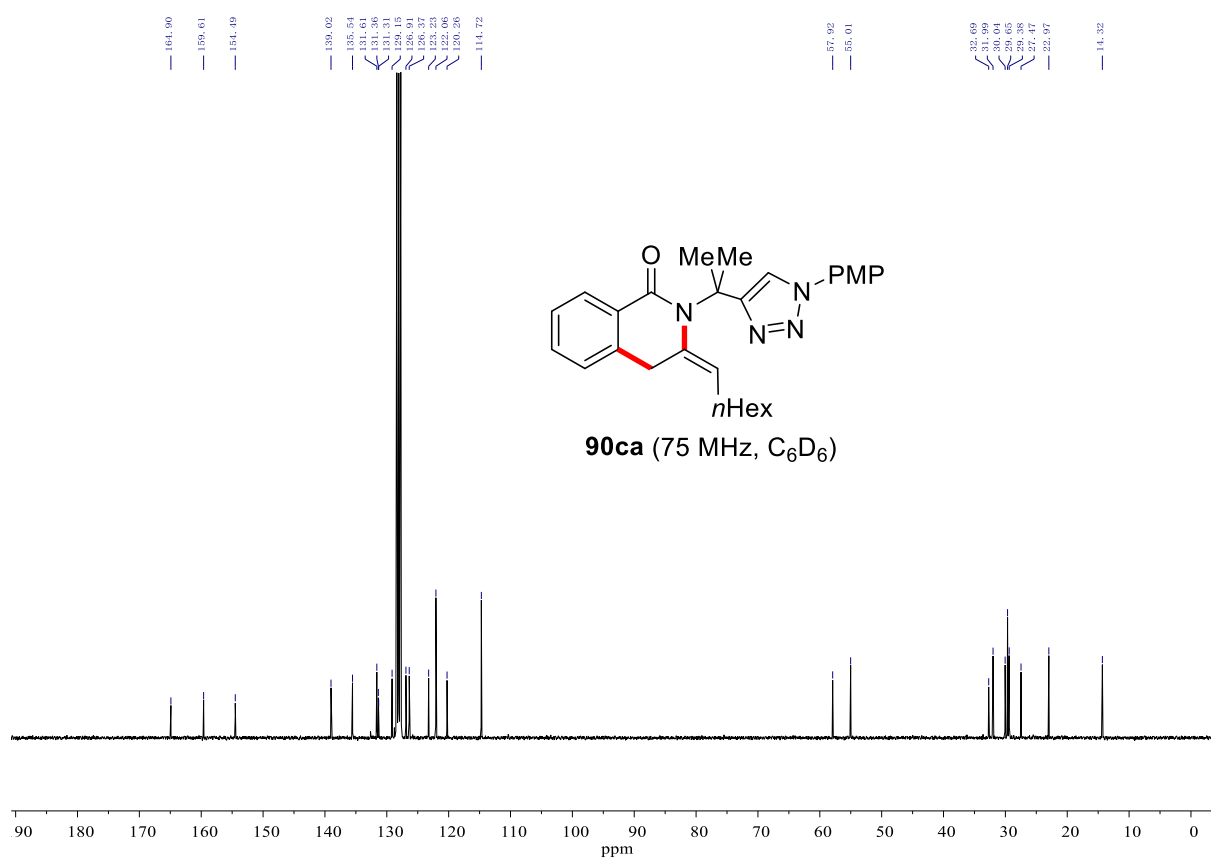
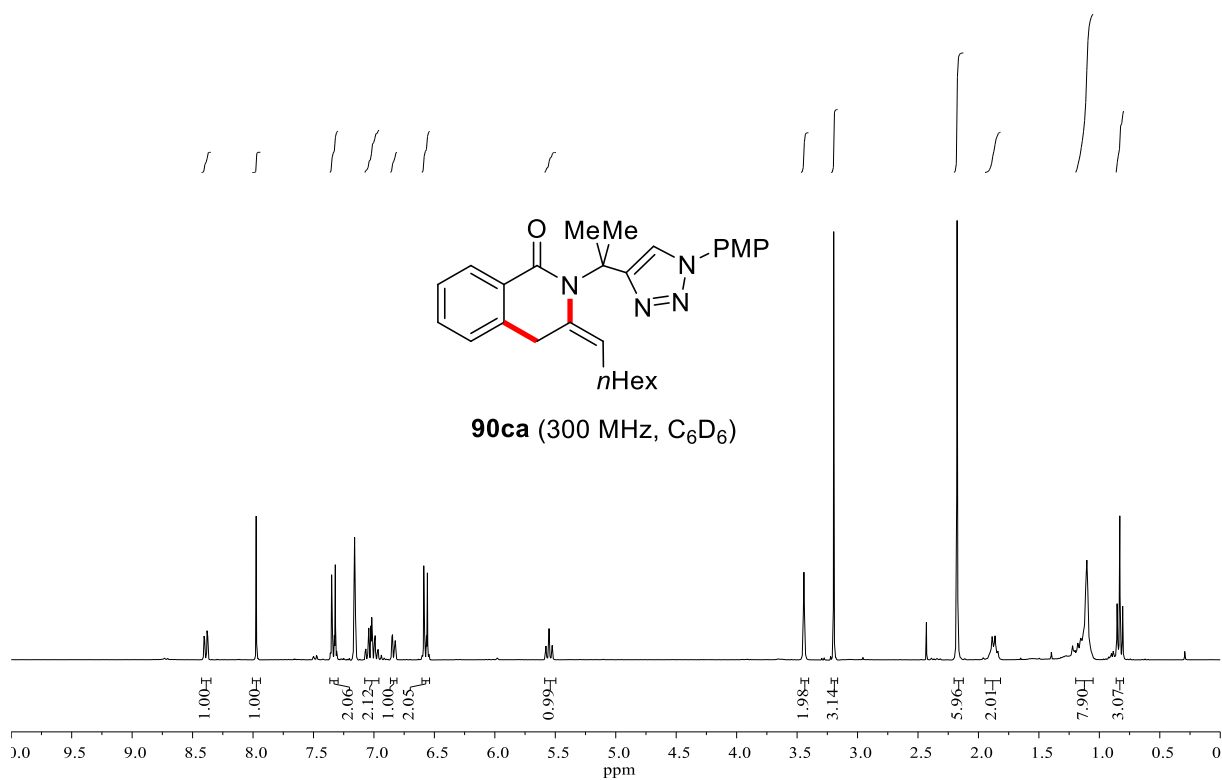
# NMR Spectra



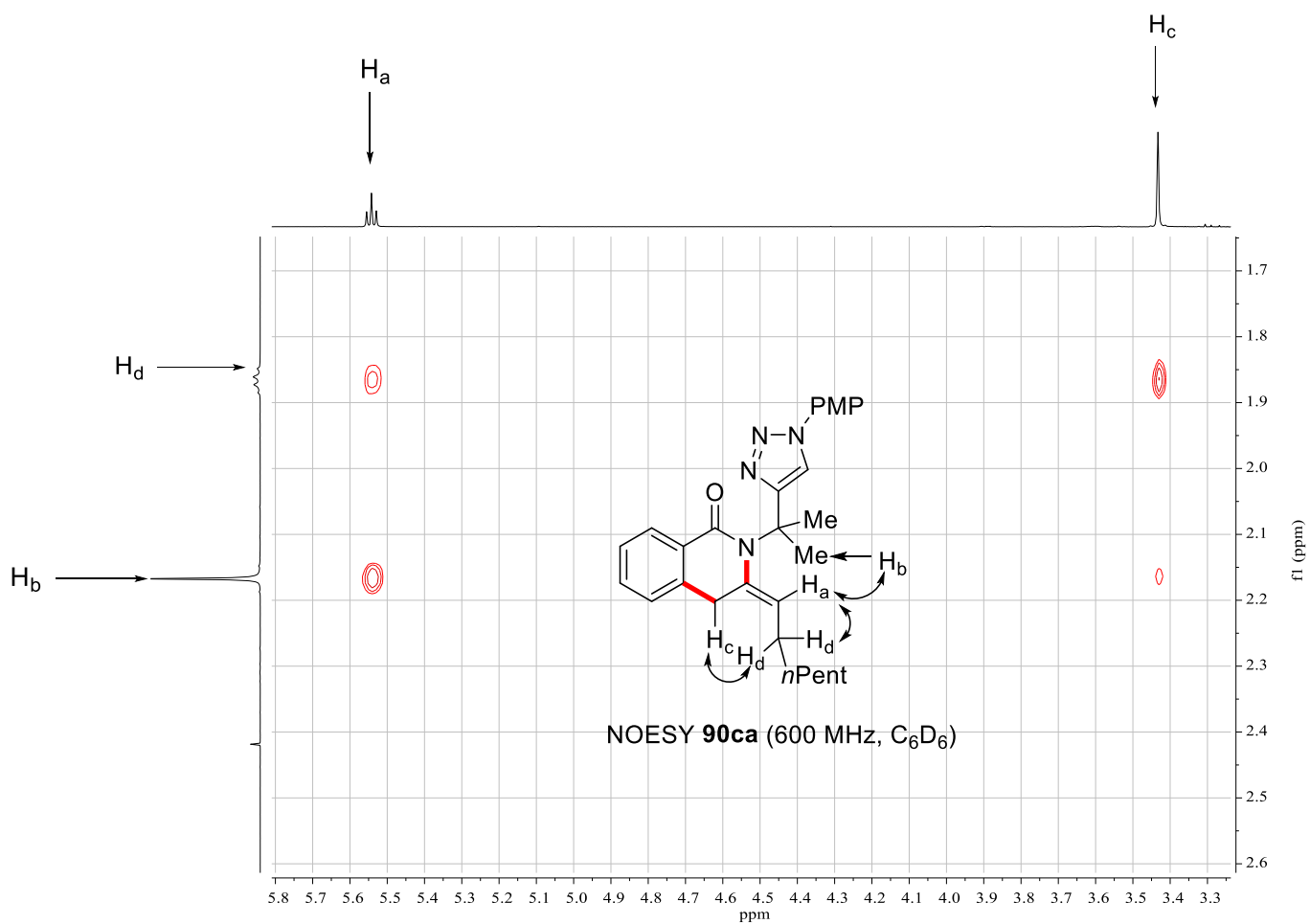
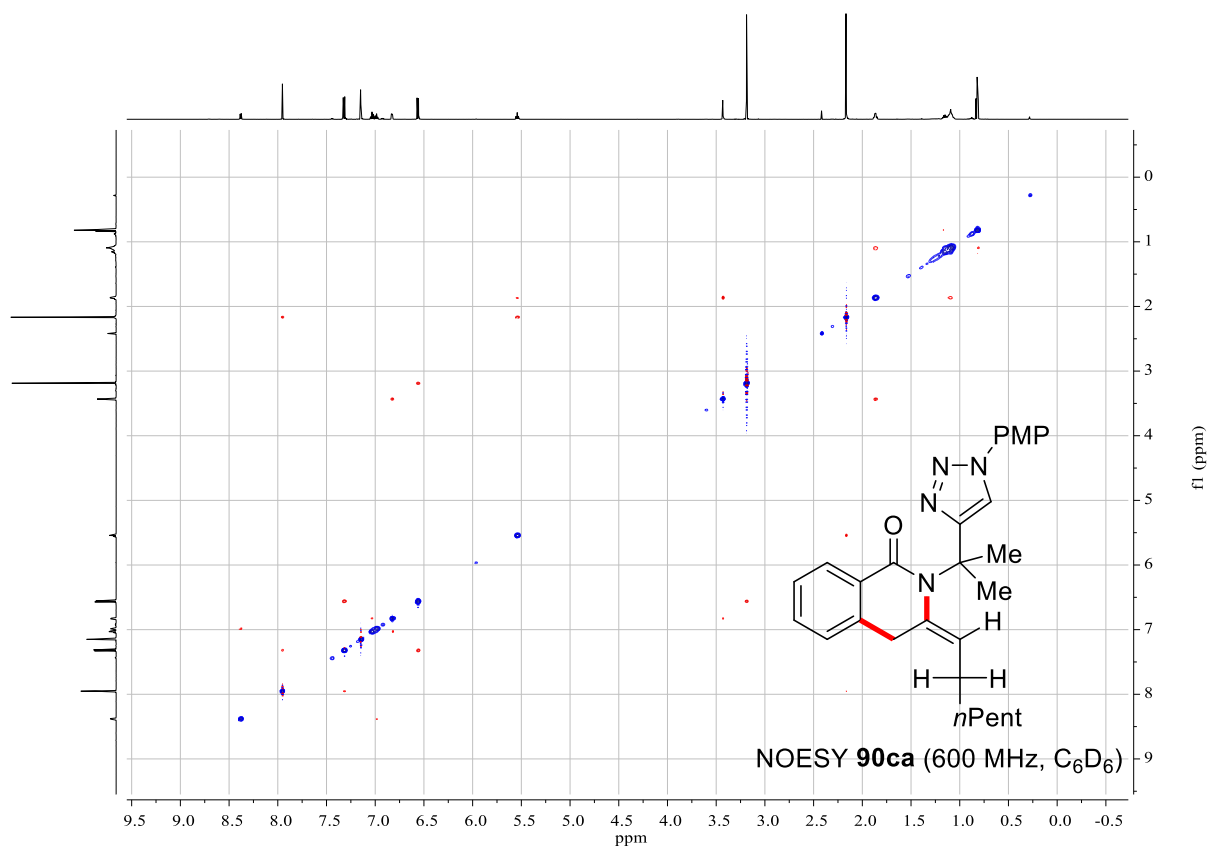
# NMR Spectra



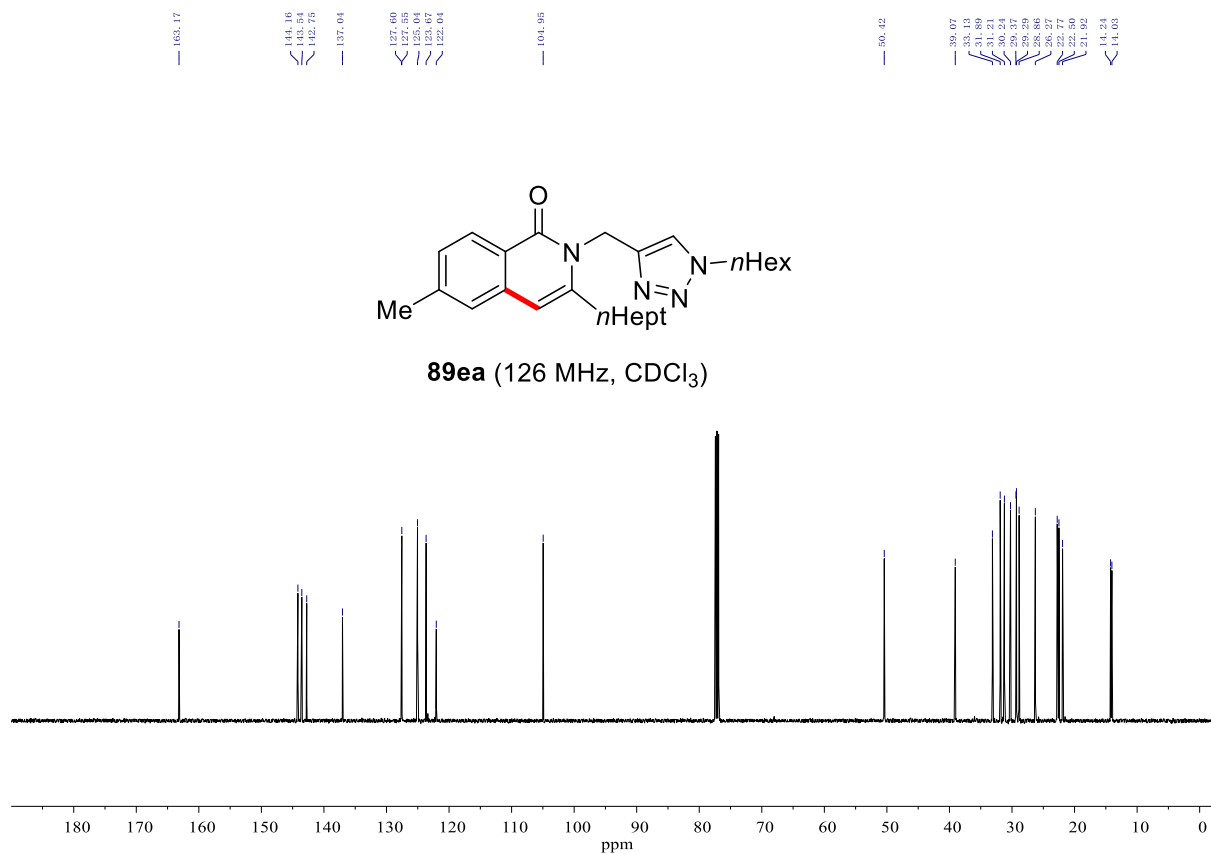
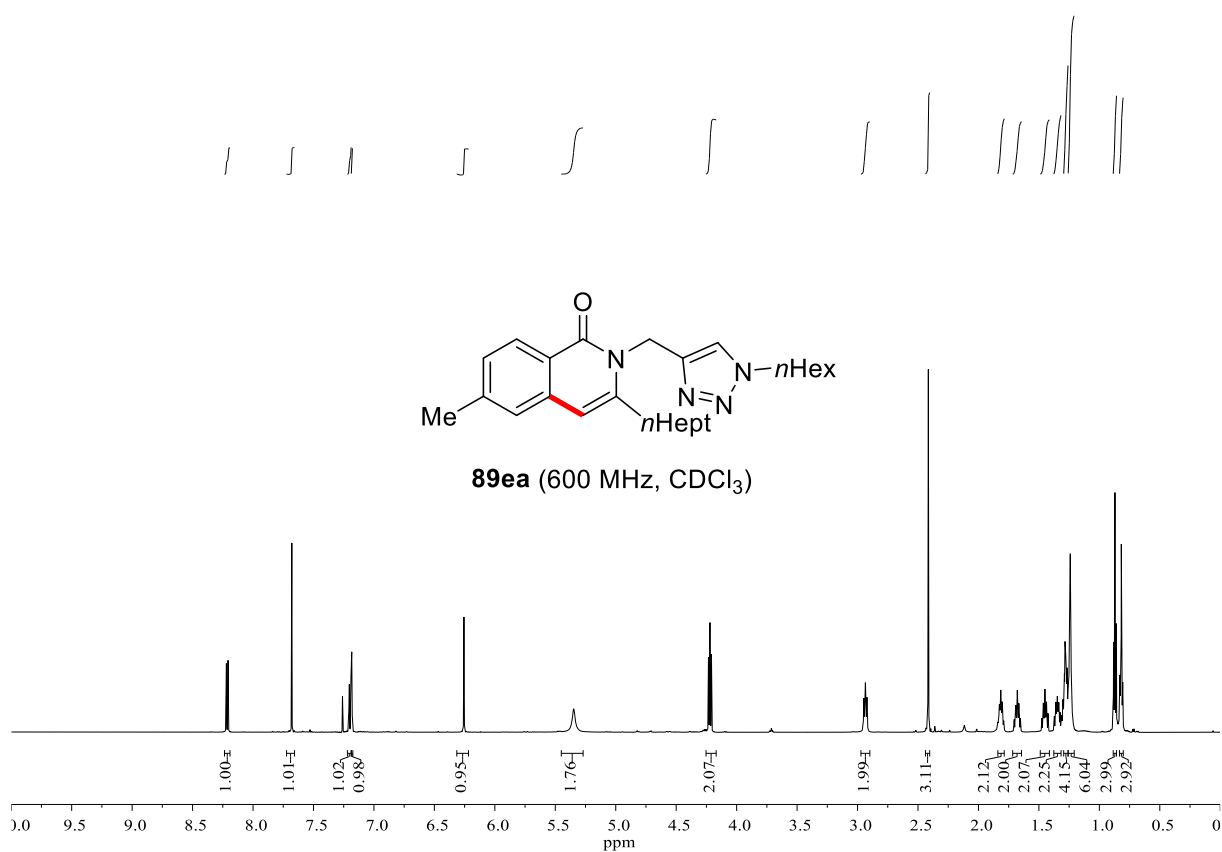
# NMR Spectra



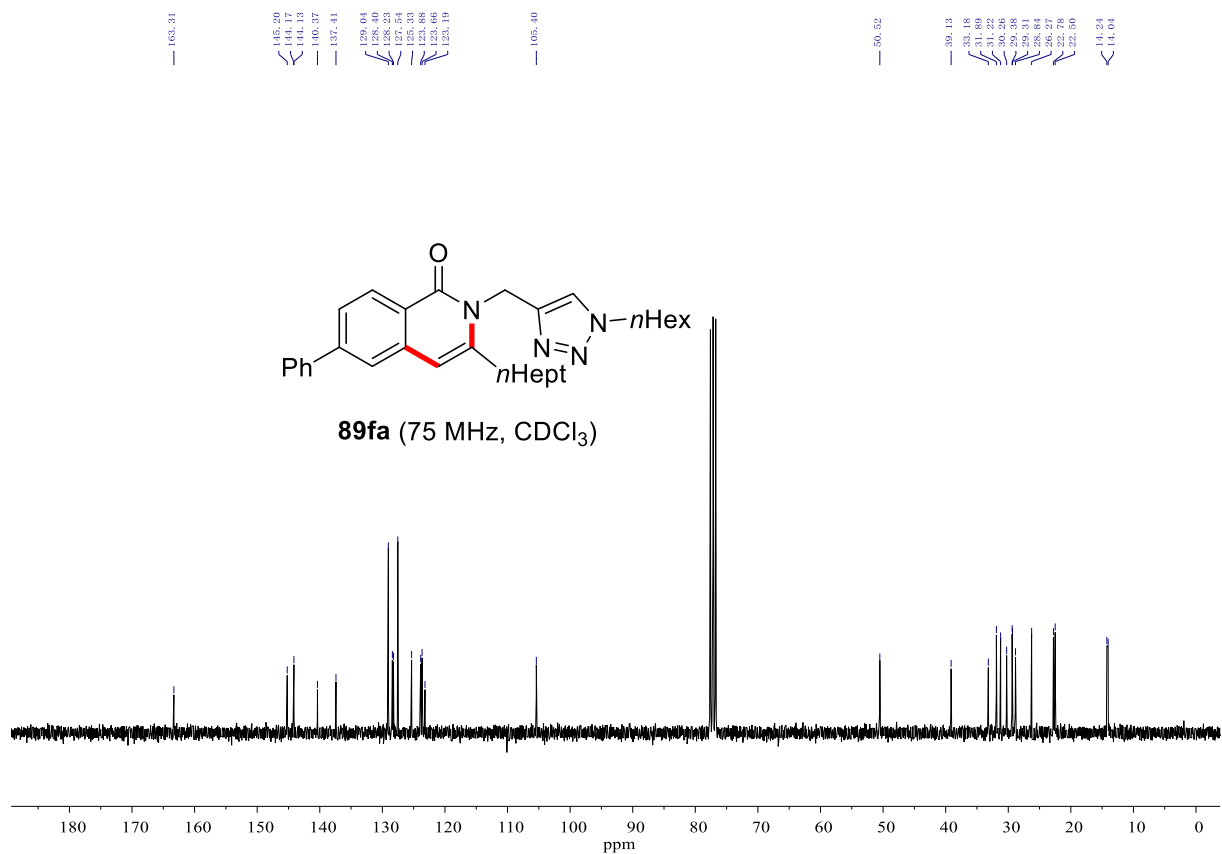
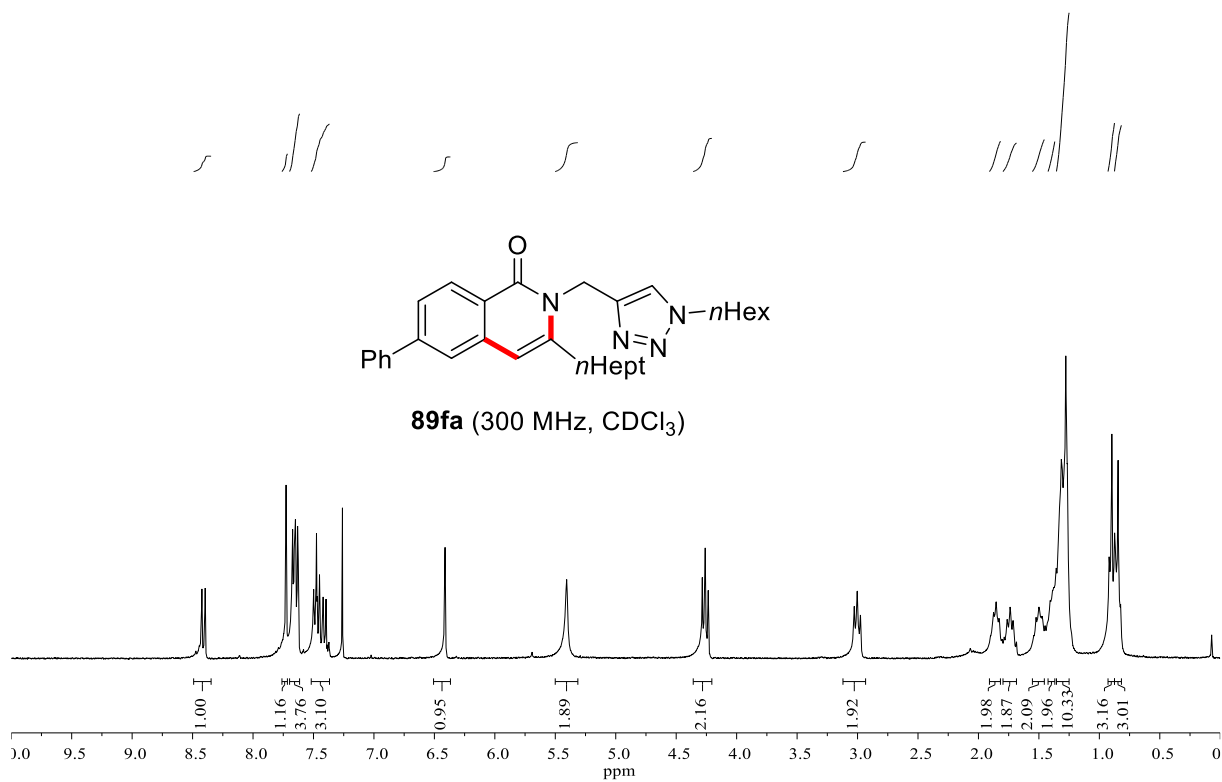
# NMR Spectra



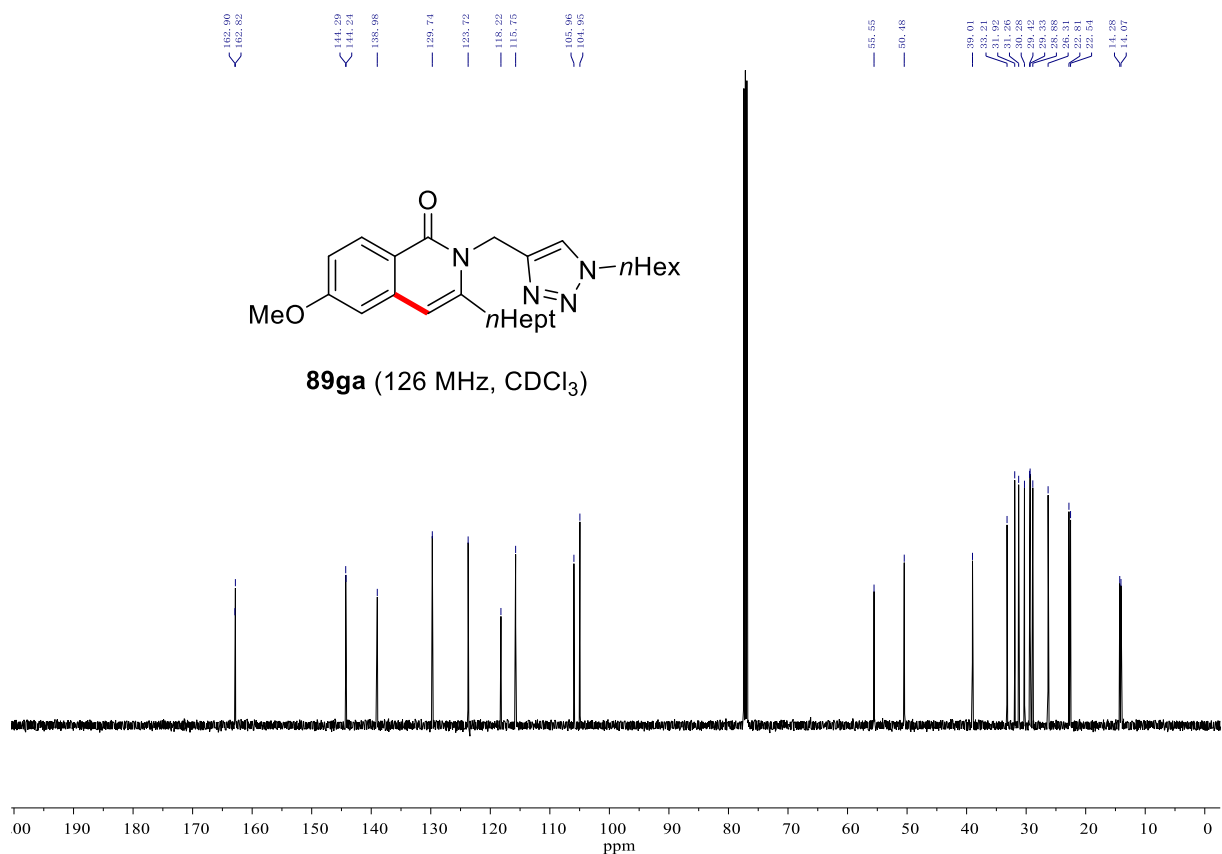
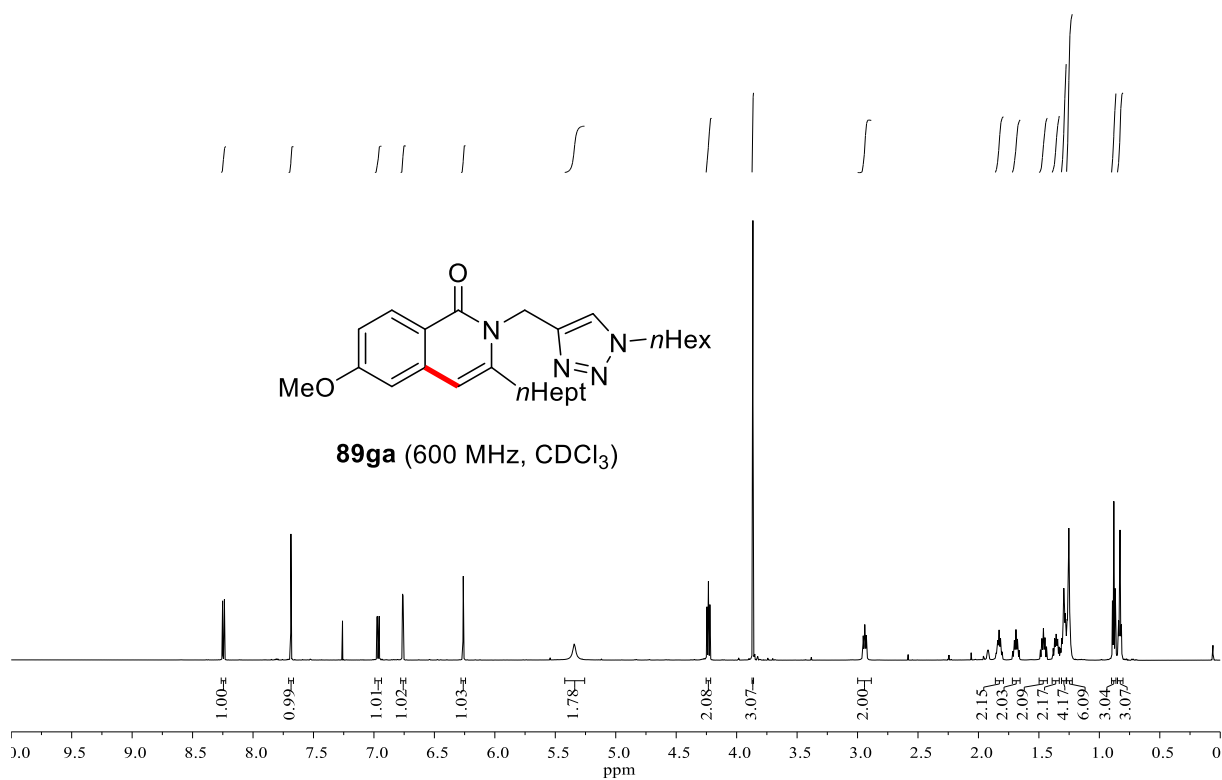
# NMR Spectra



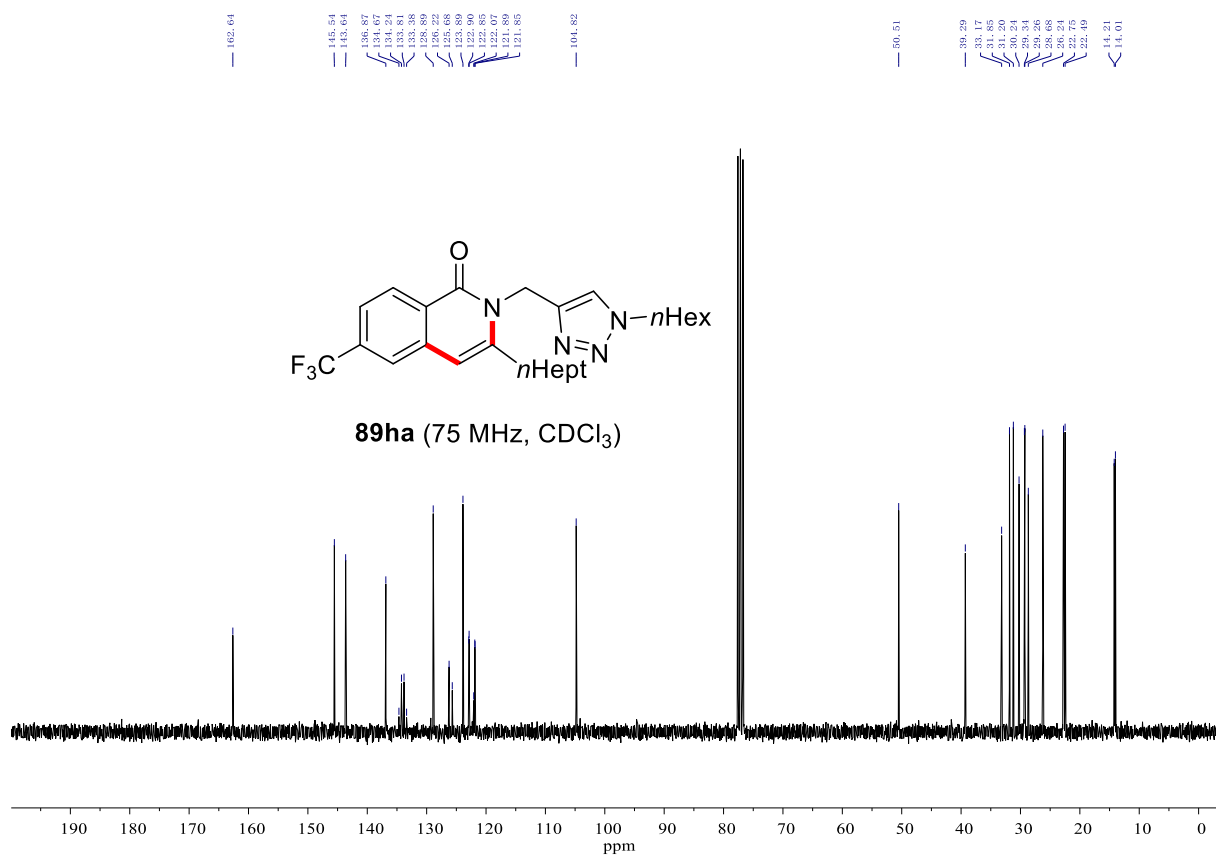
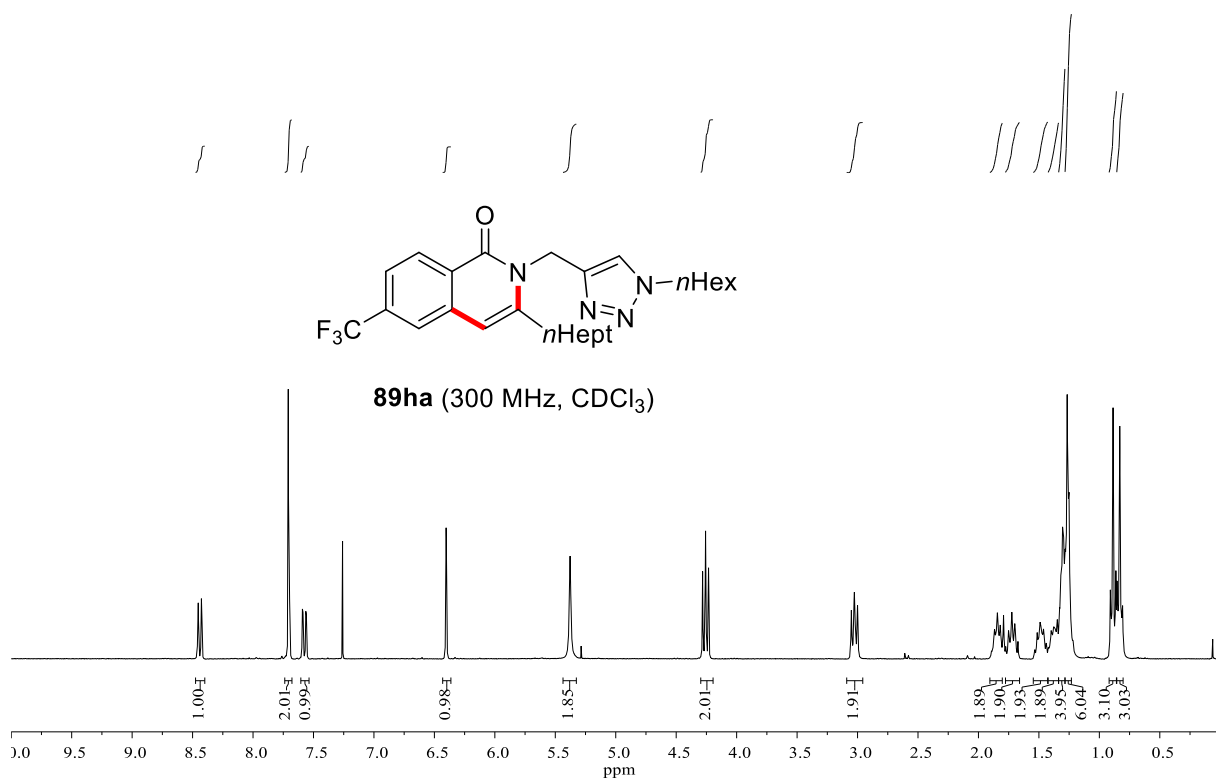
# NMR Spectra



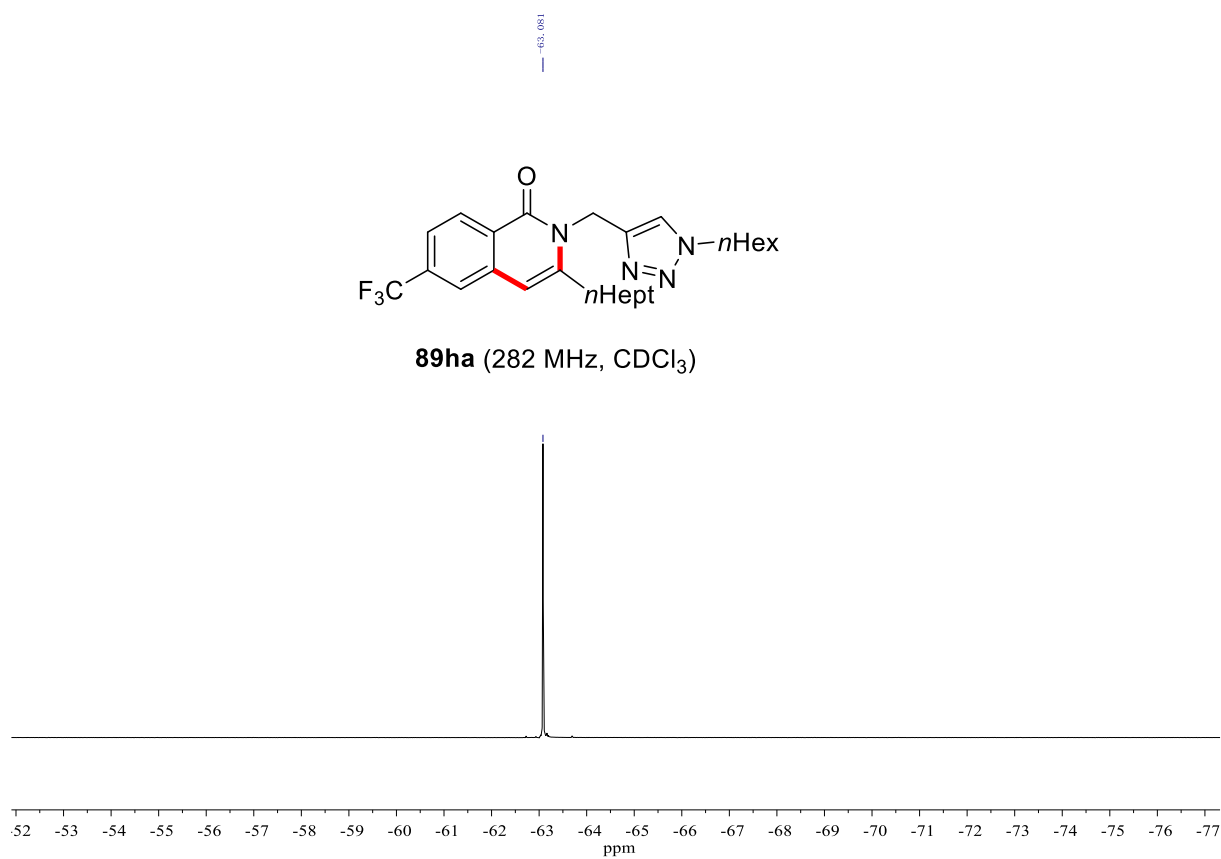
# NMR Spectra



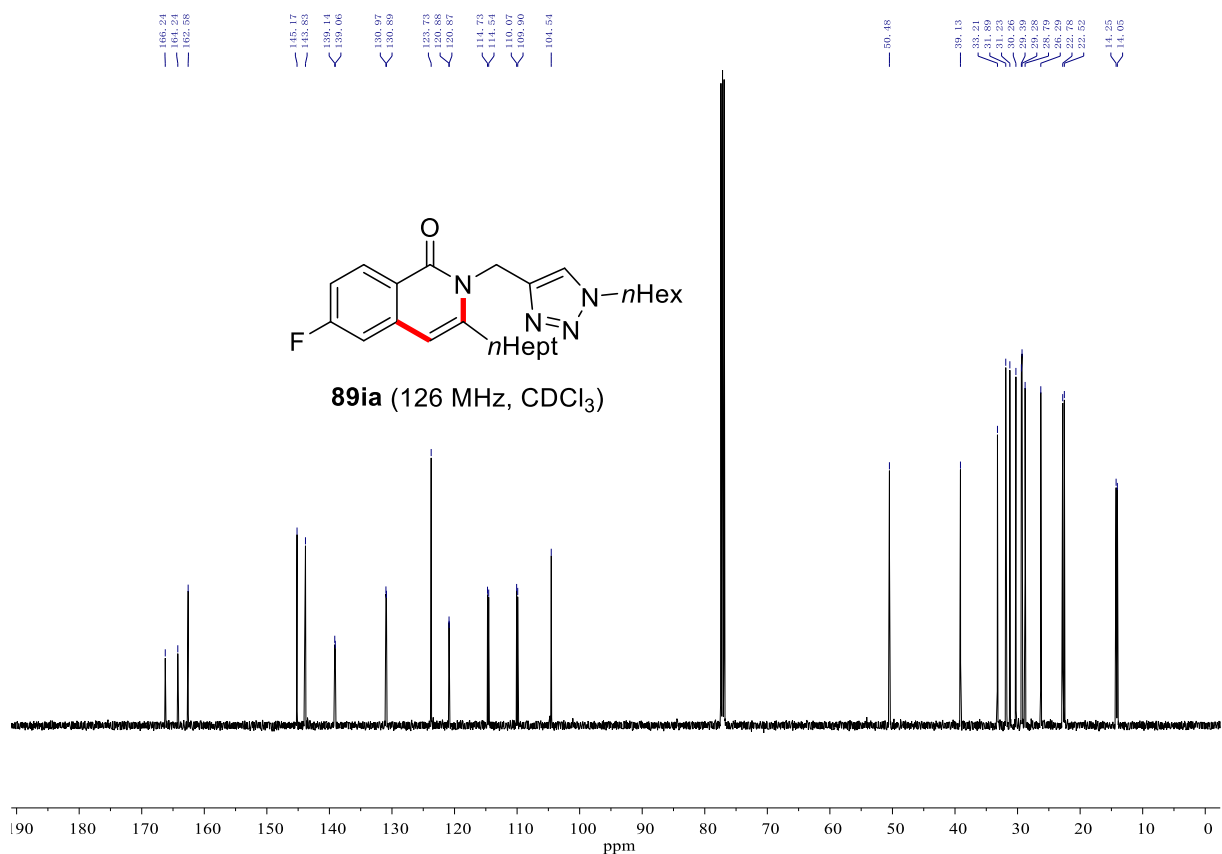
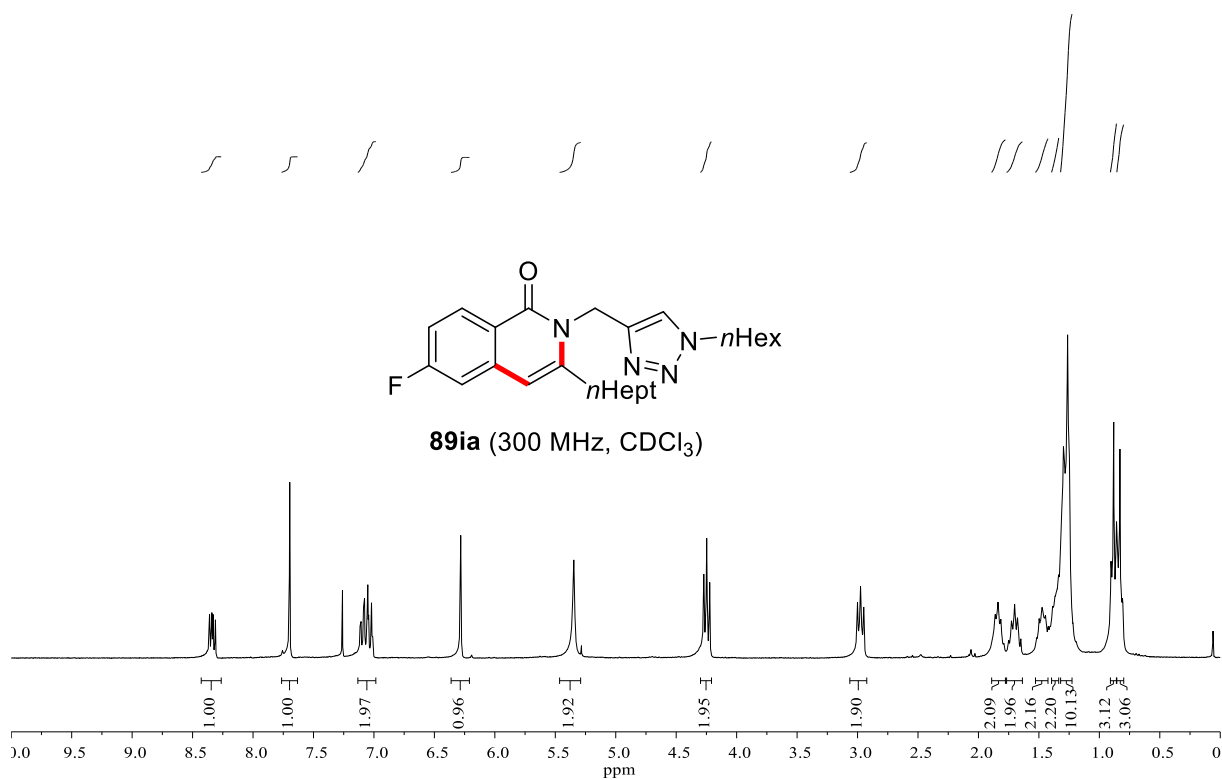
# NMR Spectra



# NMR Spectra

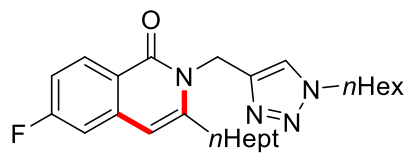


# NMR Spectra

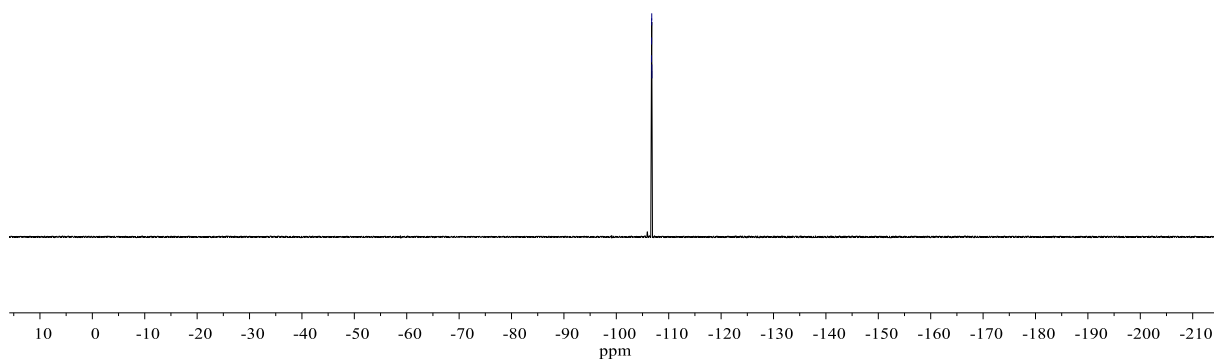


## NMR Spectra

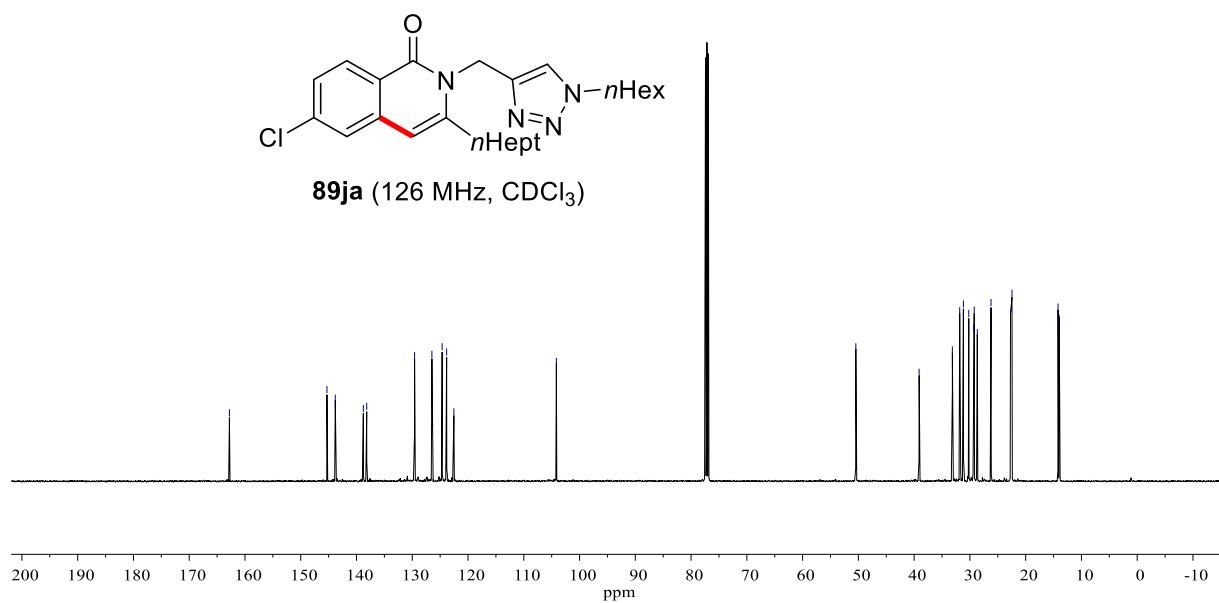
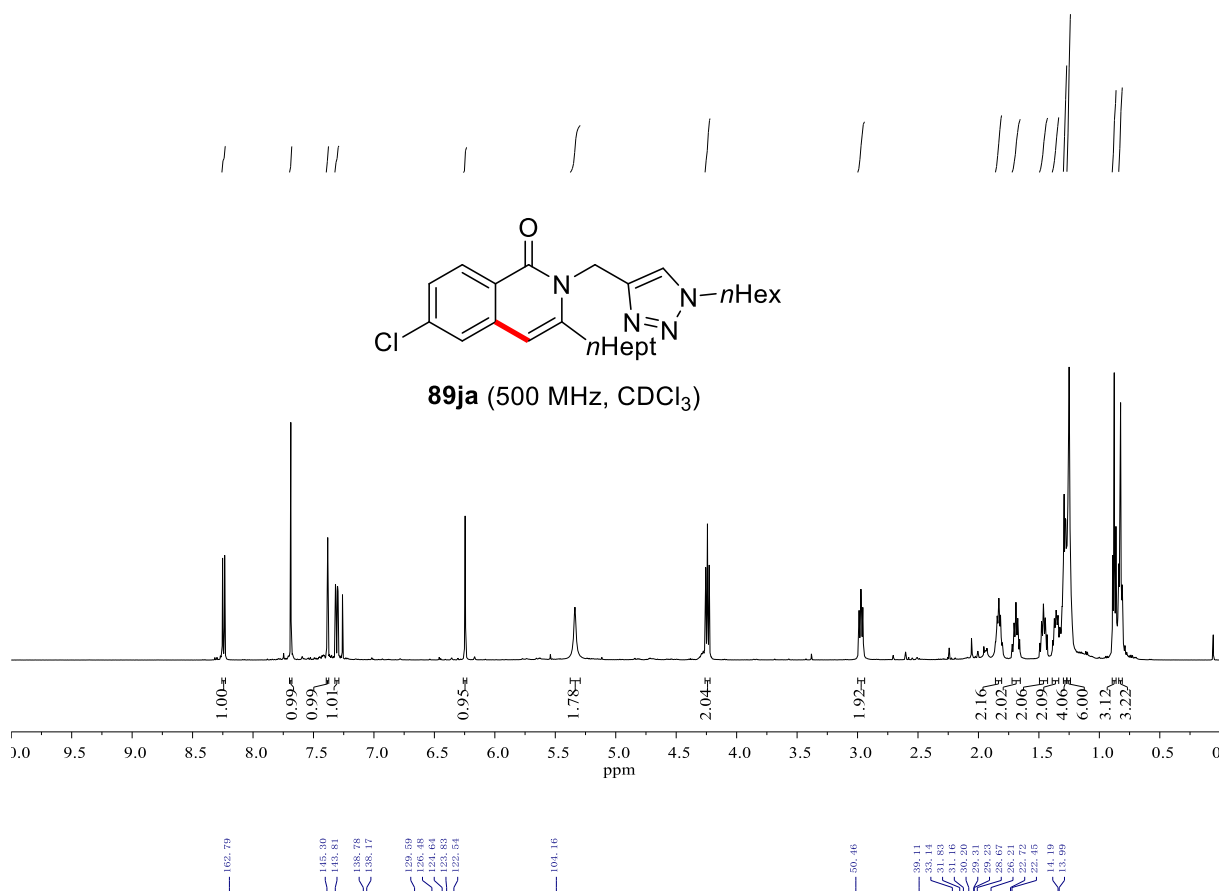
-106.71  
-106.73  
-106.74  
-106.76  
-106.77  
-106.79



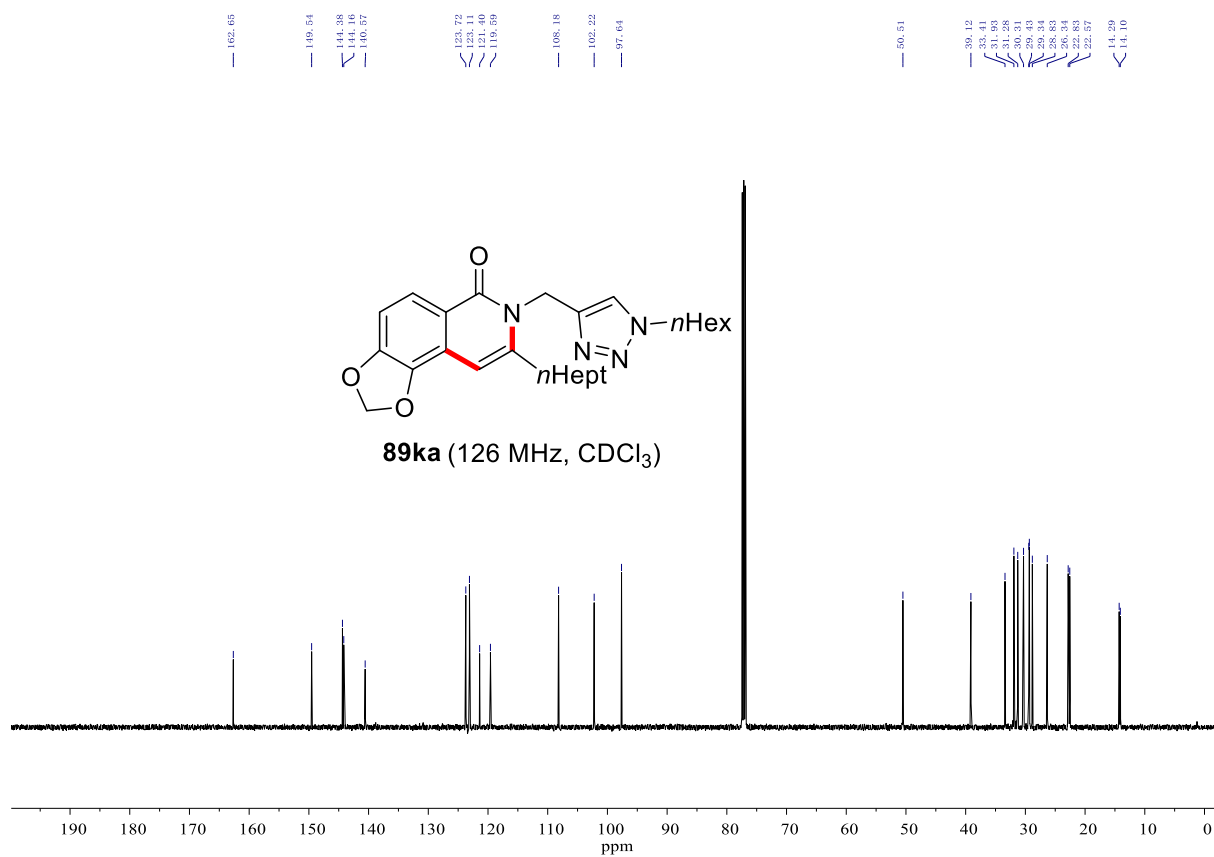
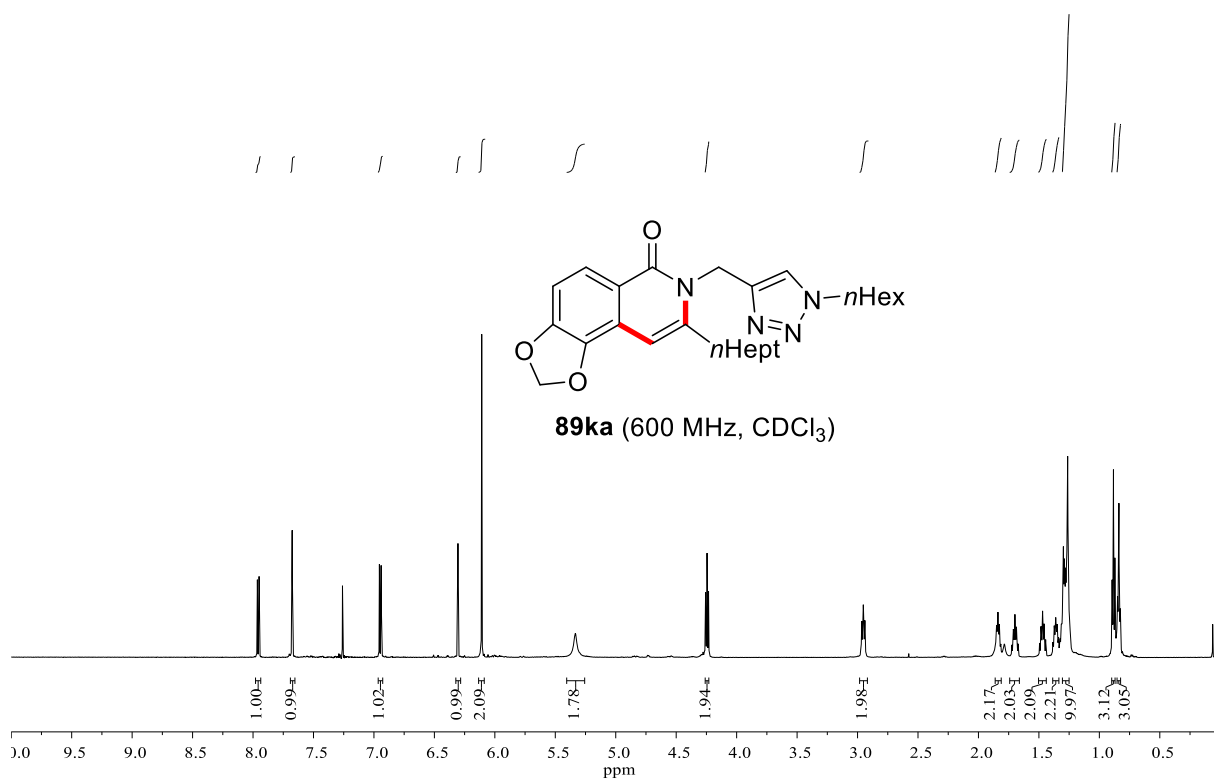
**89ia** (282 MHz, CDCl<sub>3</sub>)



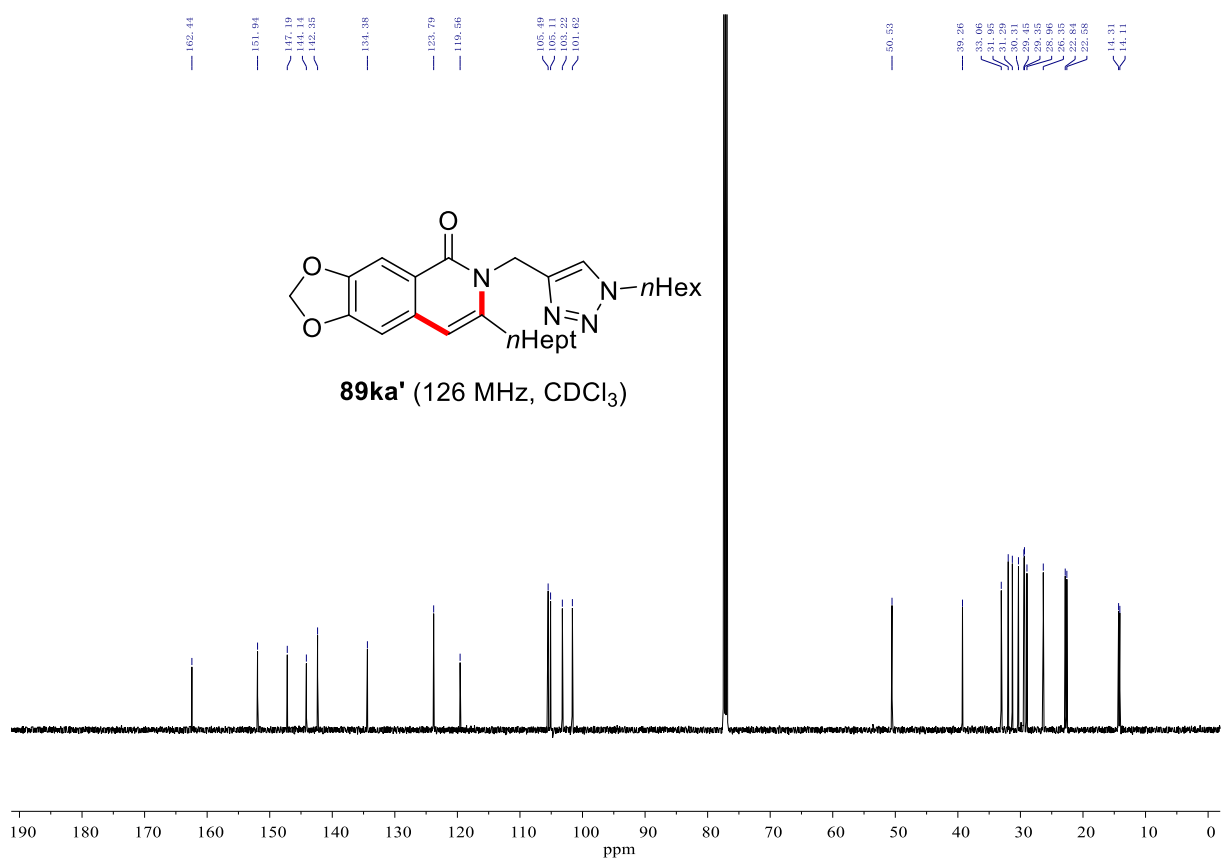
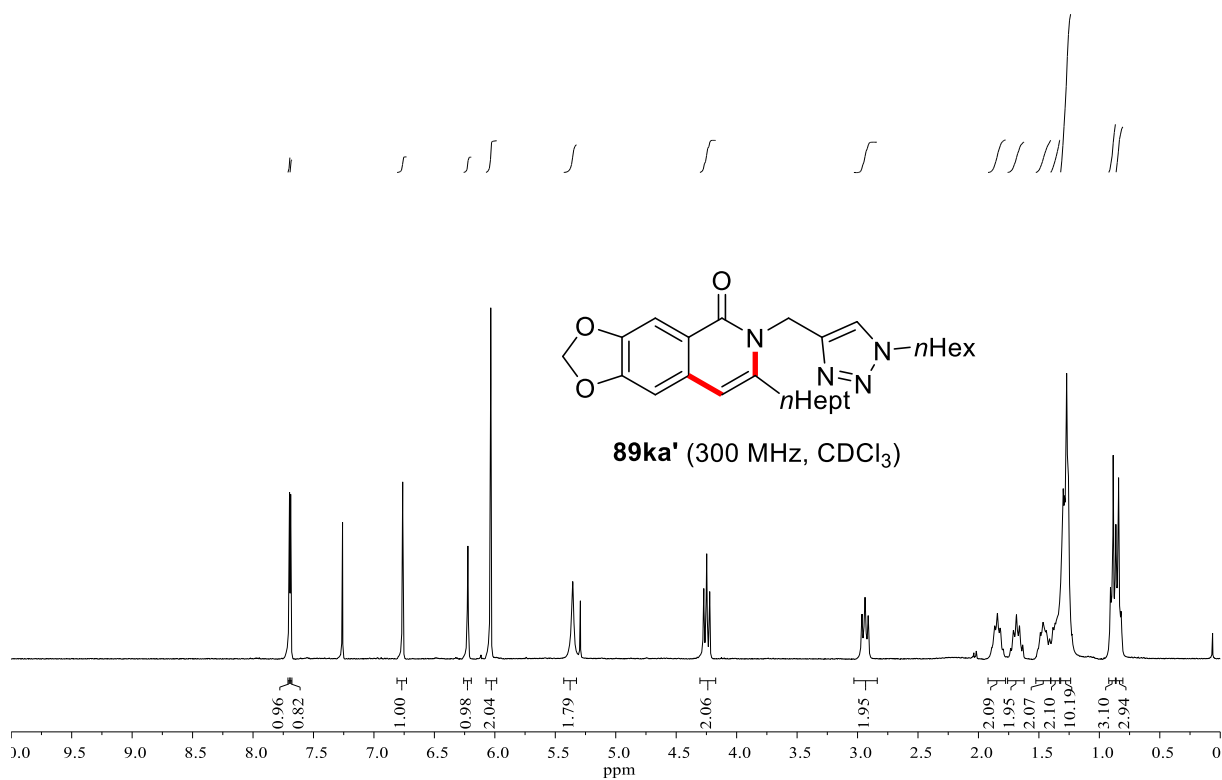
# NMR Spectra



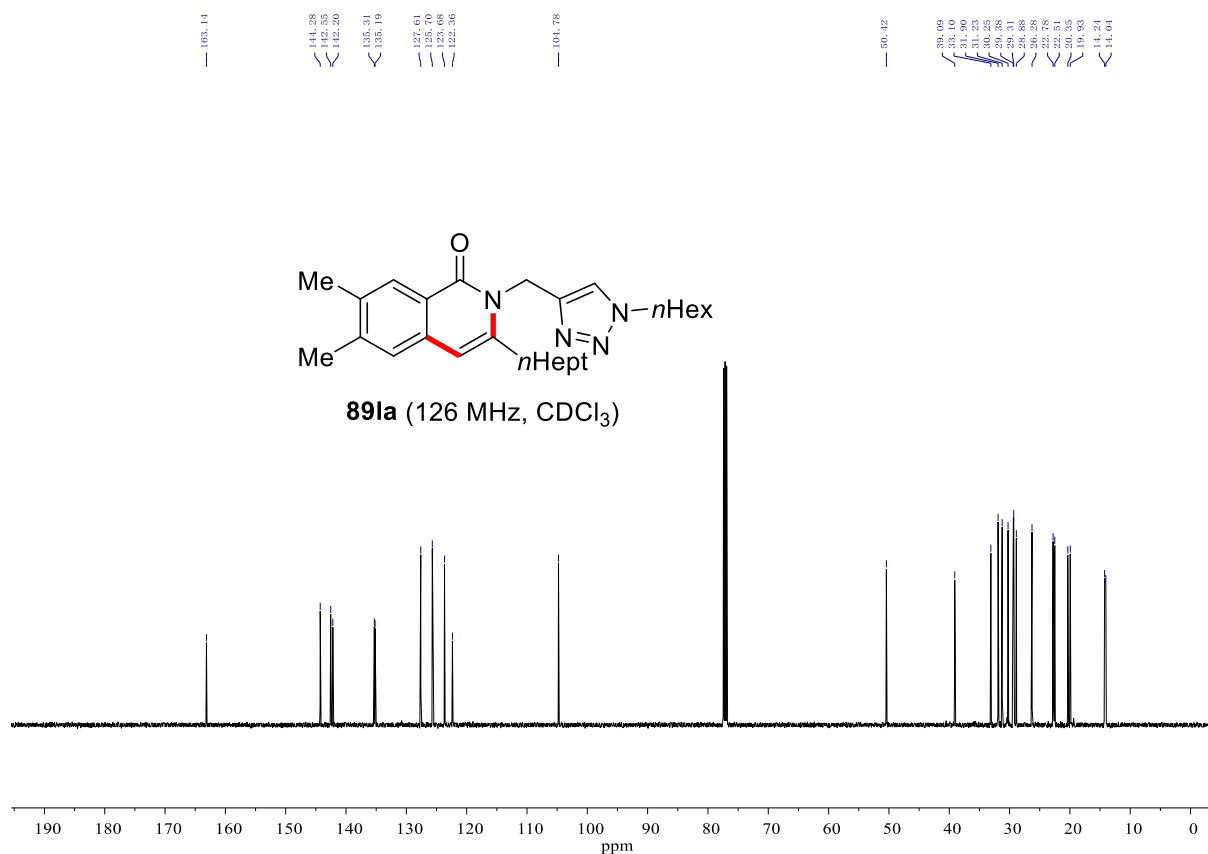
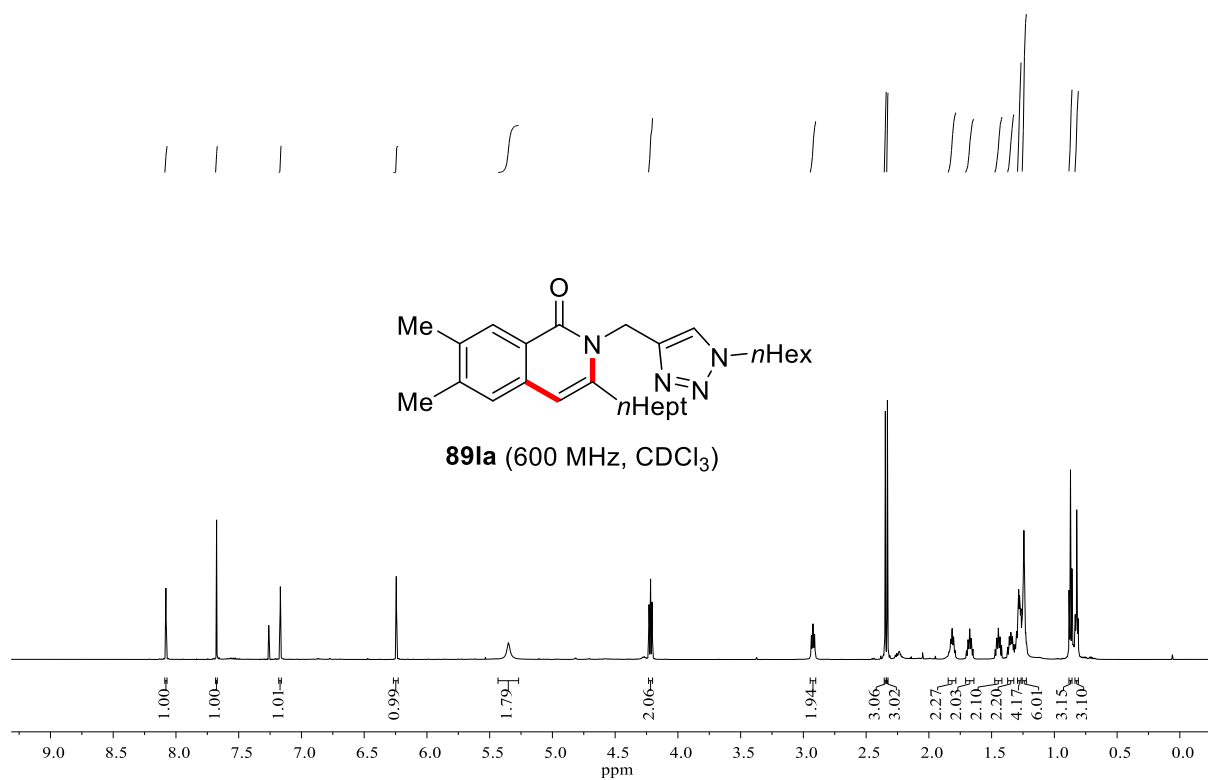
# NMR Spectra



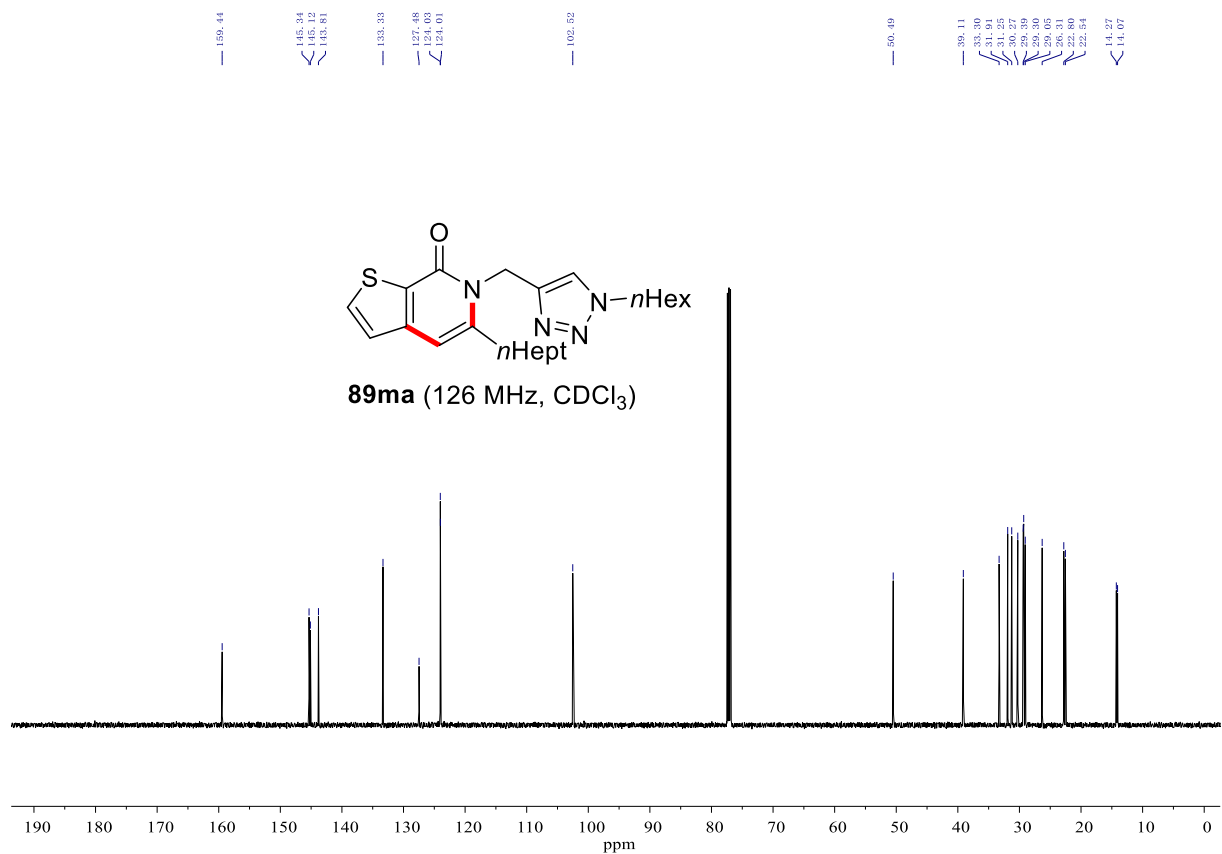
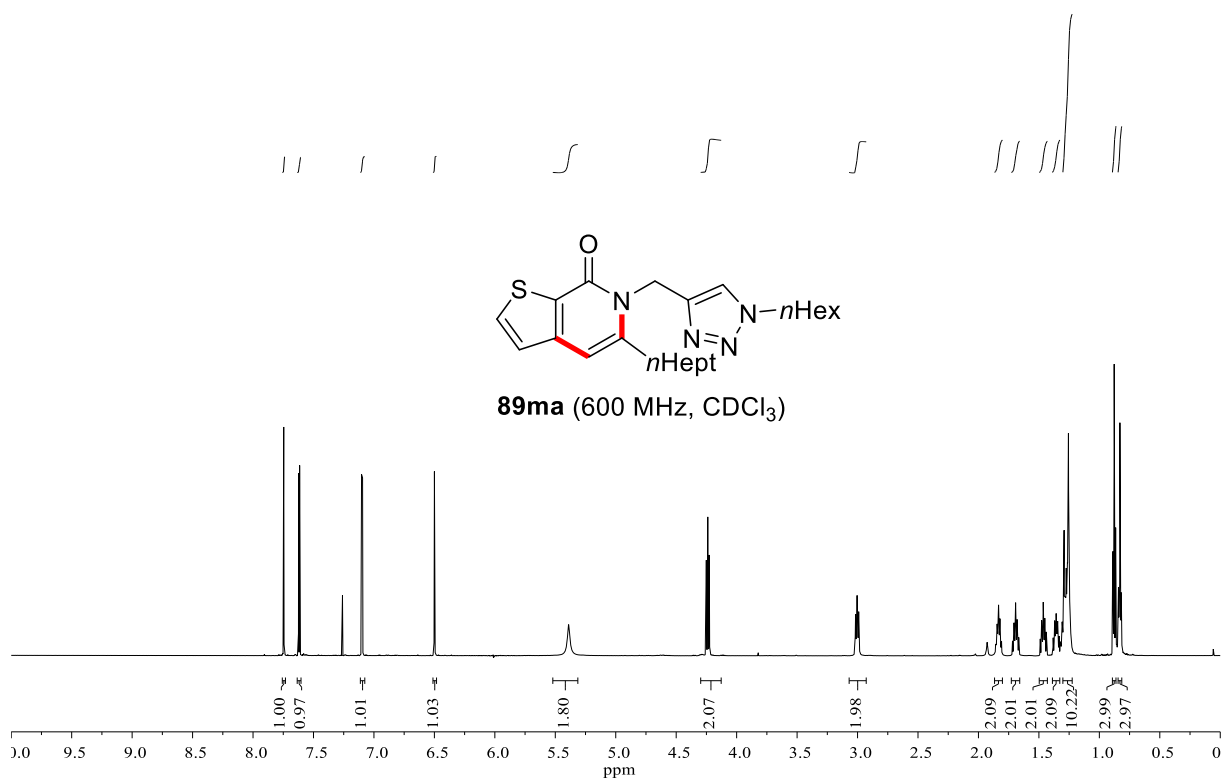
# NMR Spectra



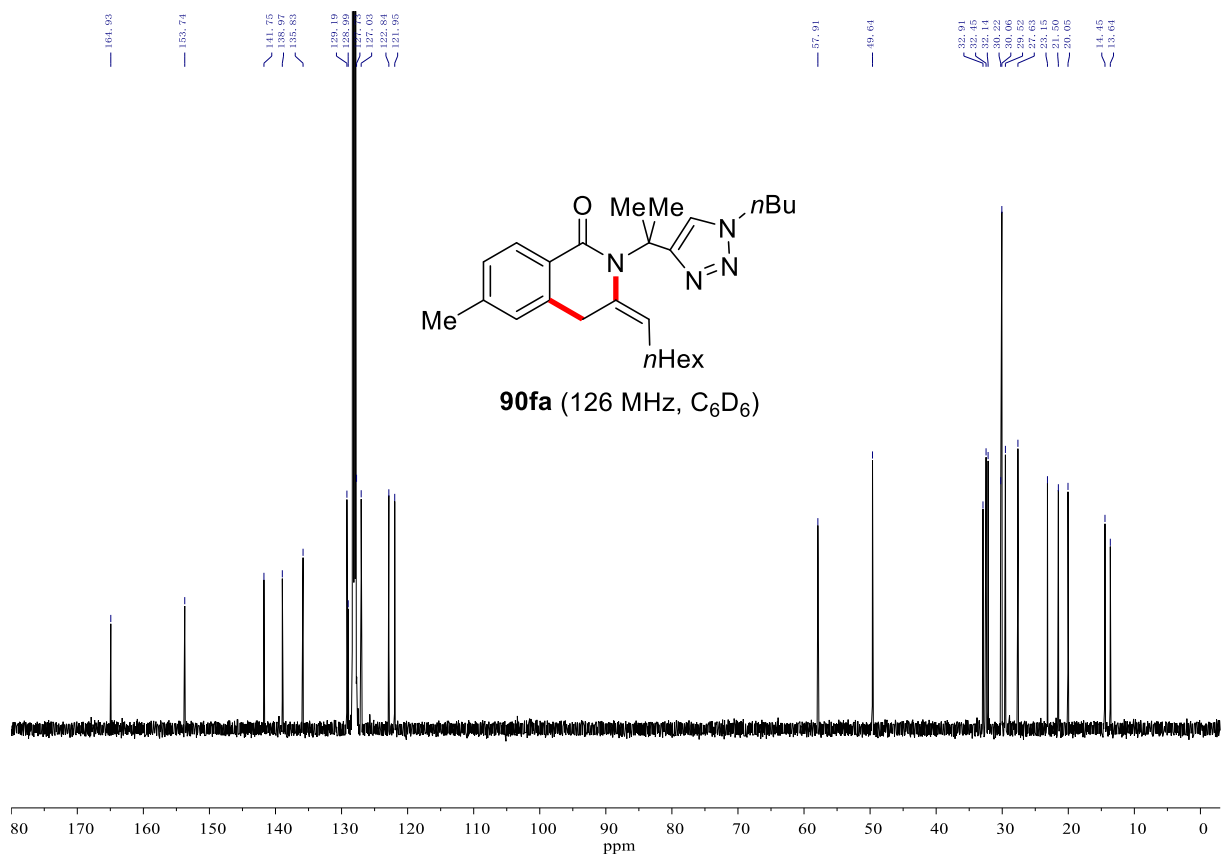
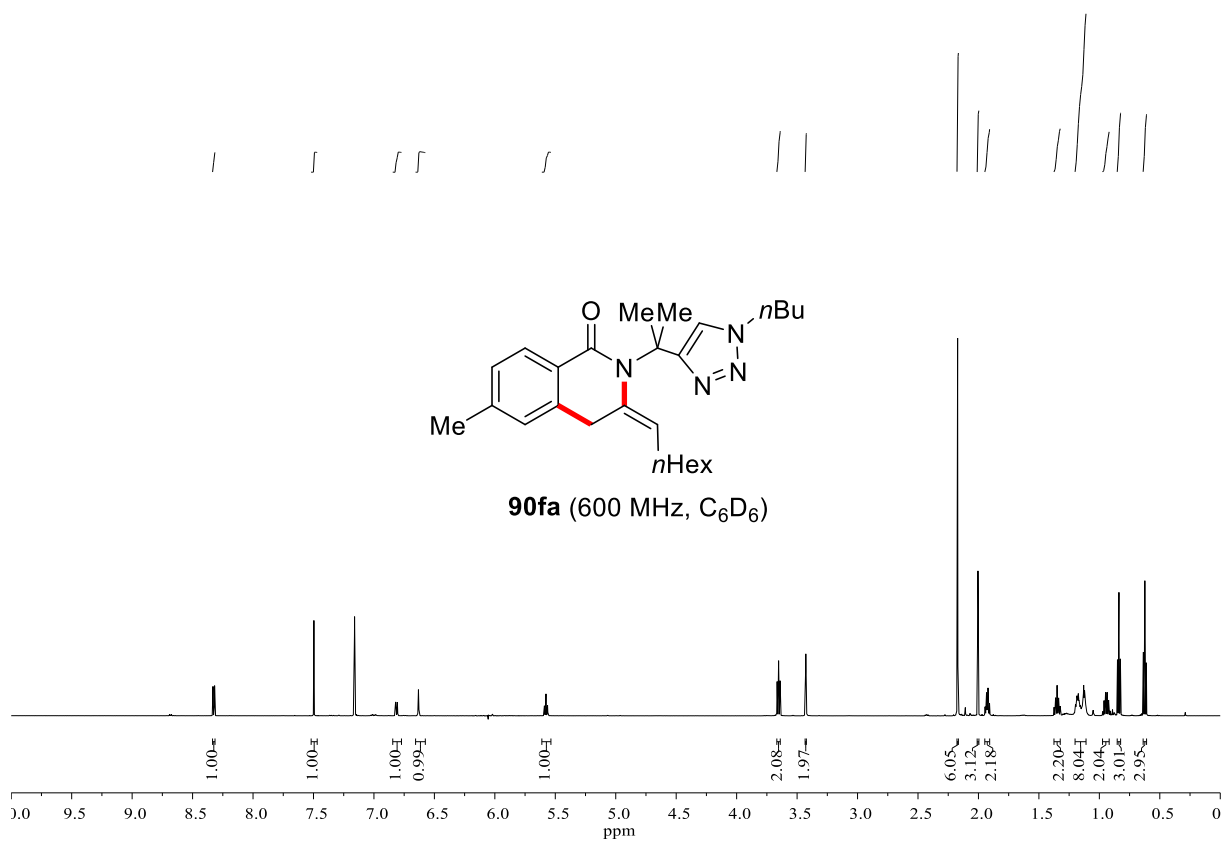
# NMR Spectra



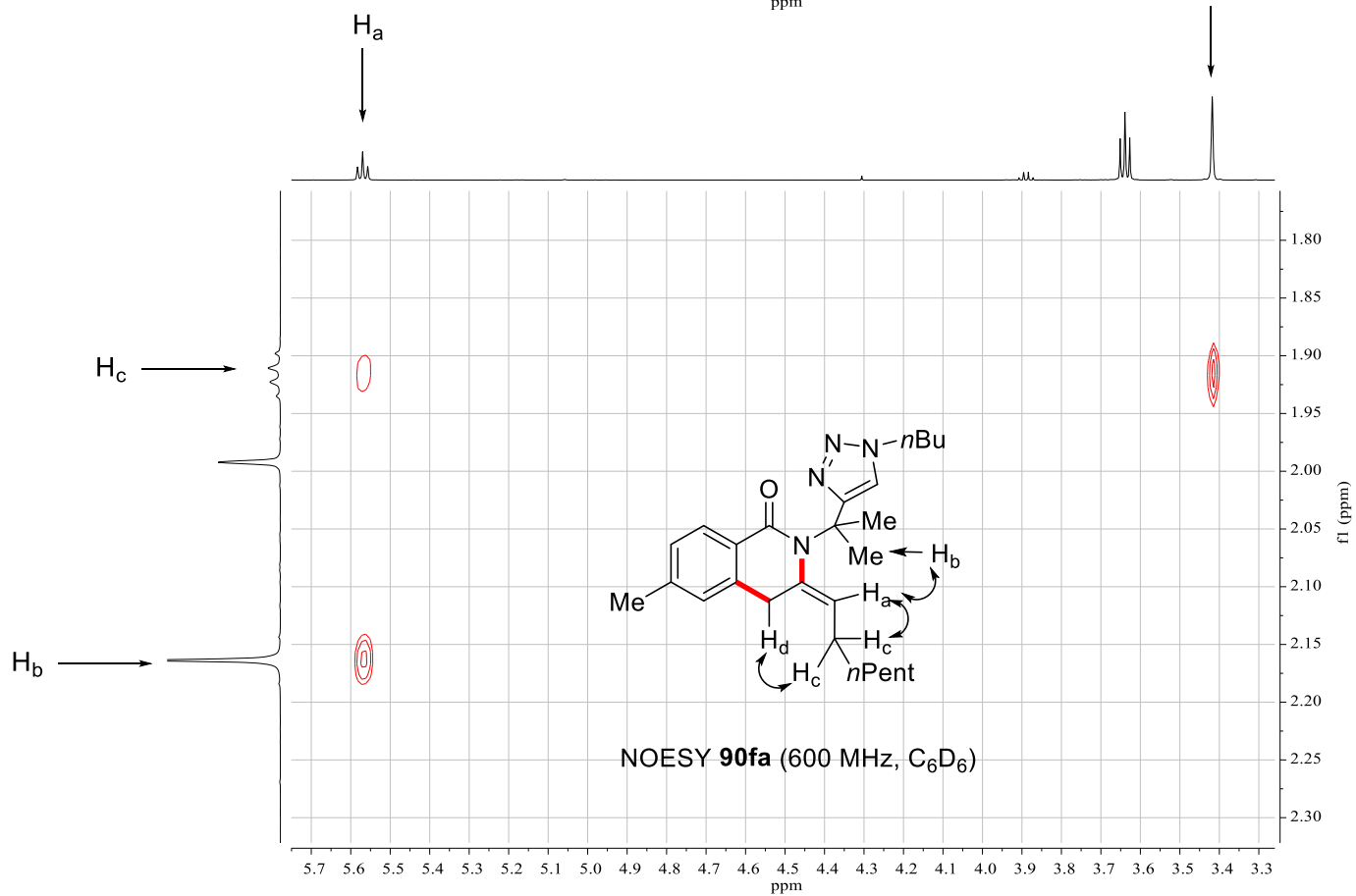
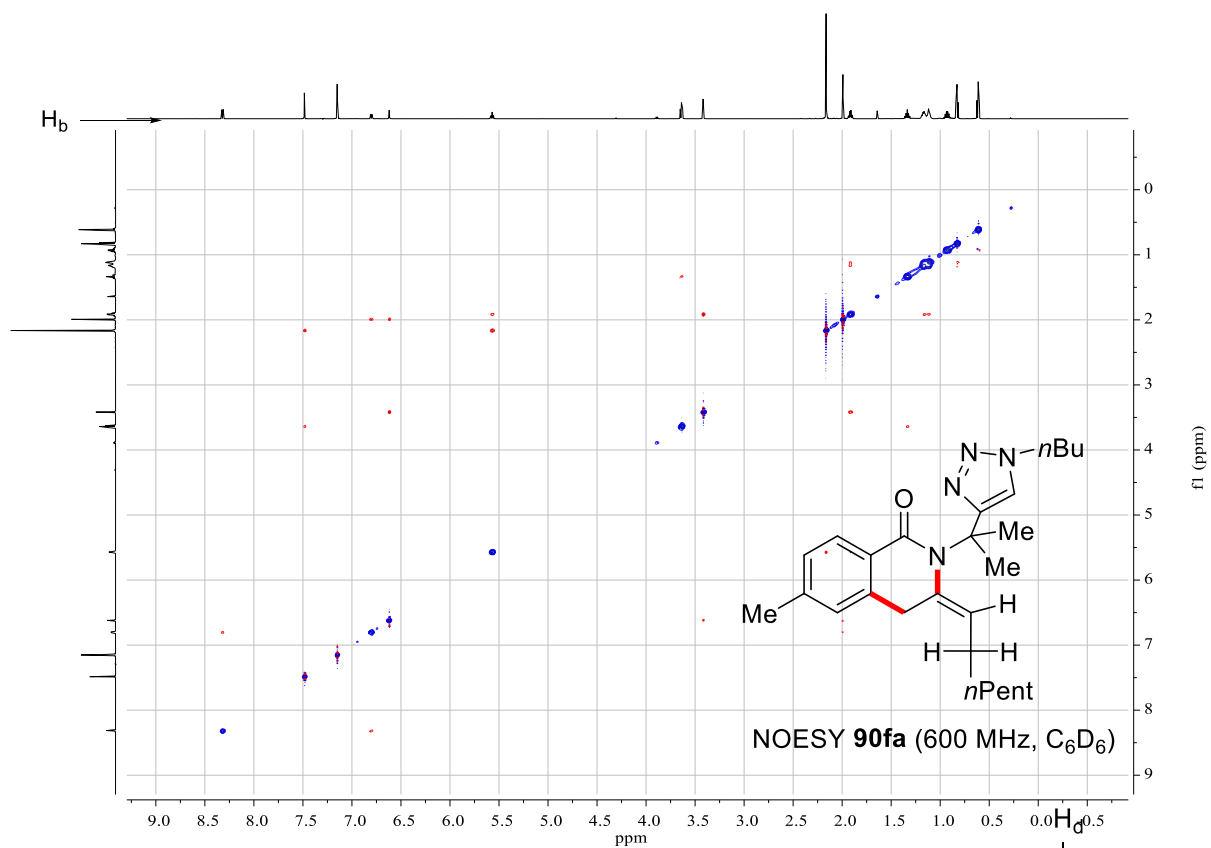
# NMR Spectra



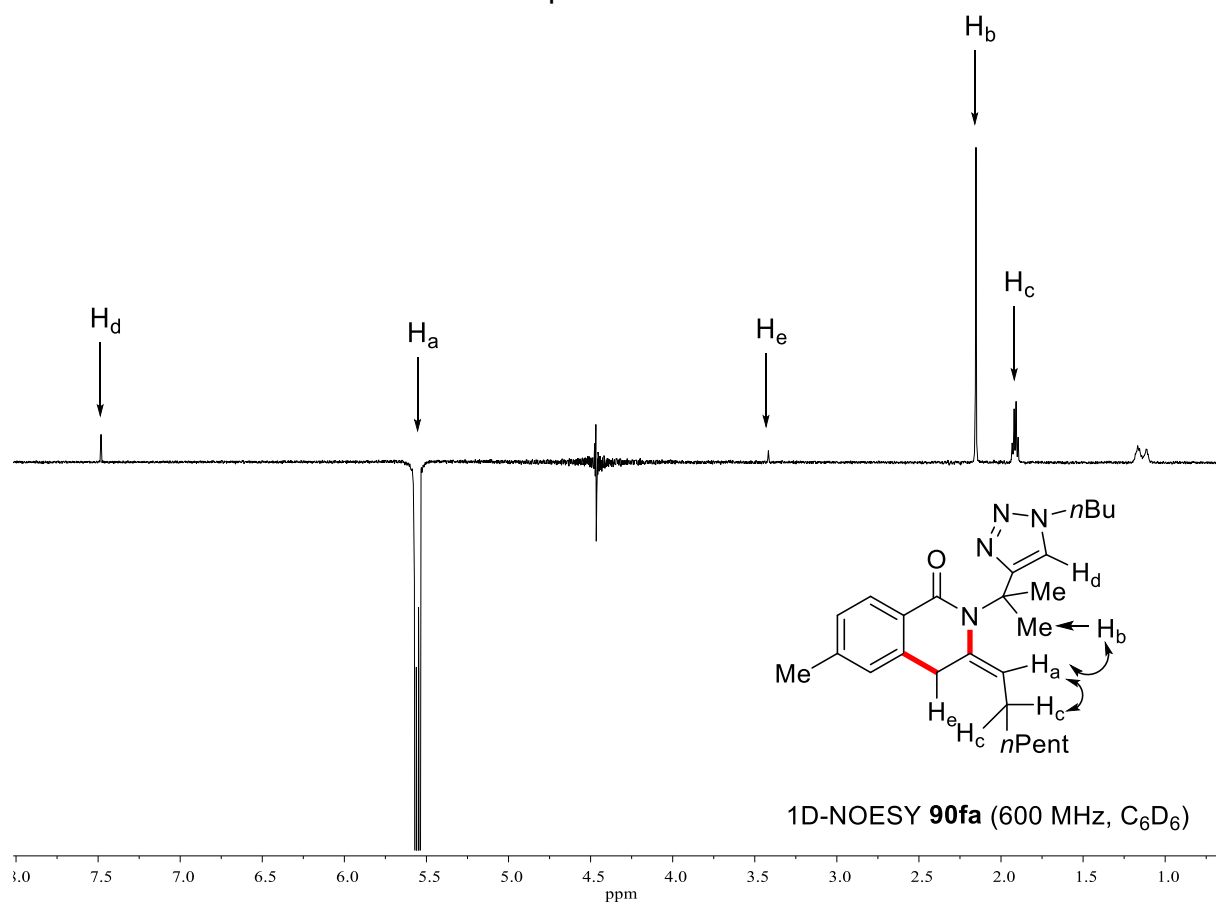
# NMR Spectra



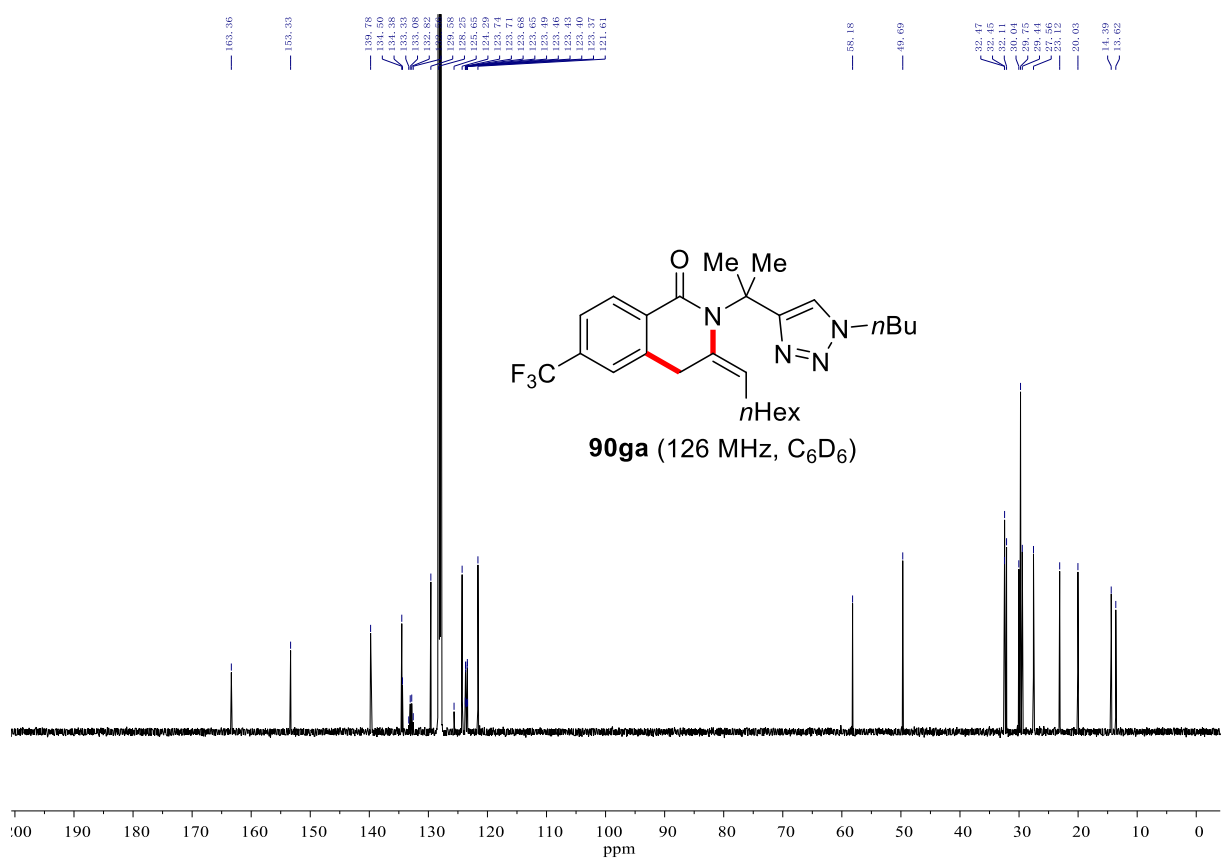
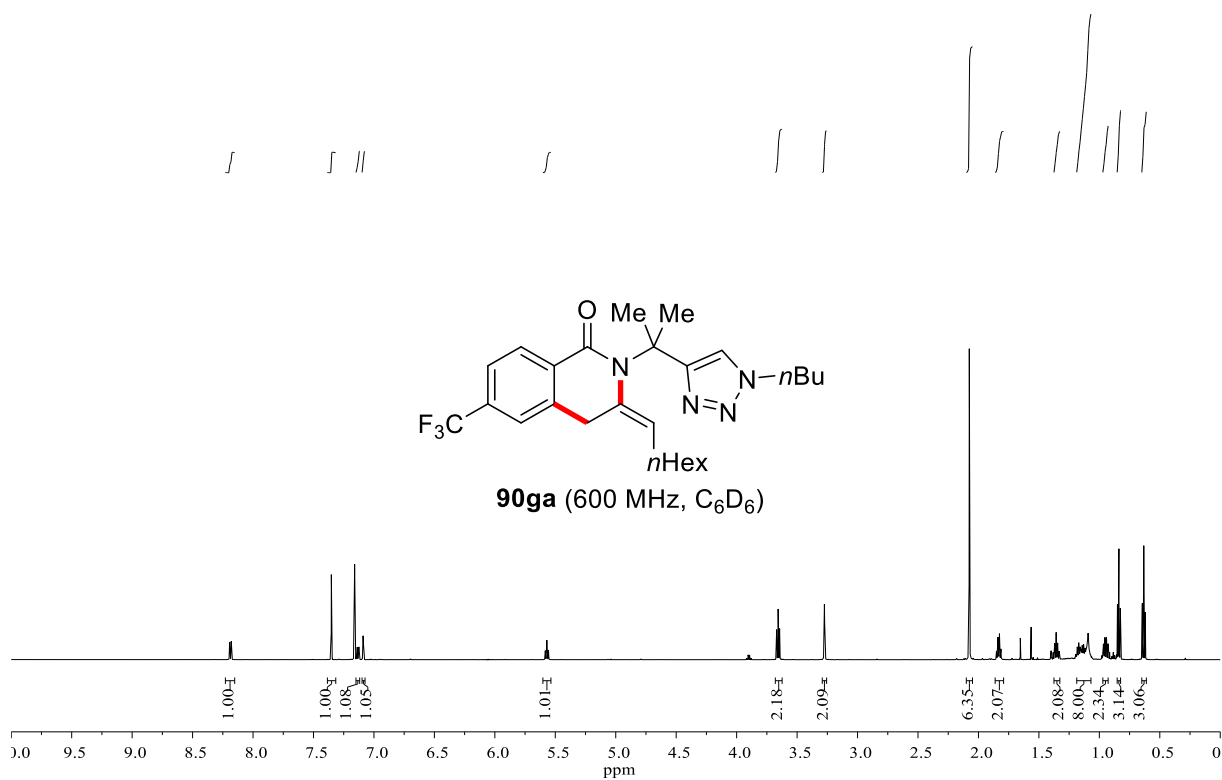
# NMR Spectra



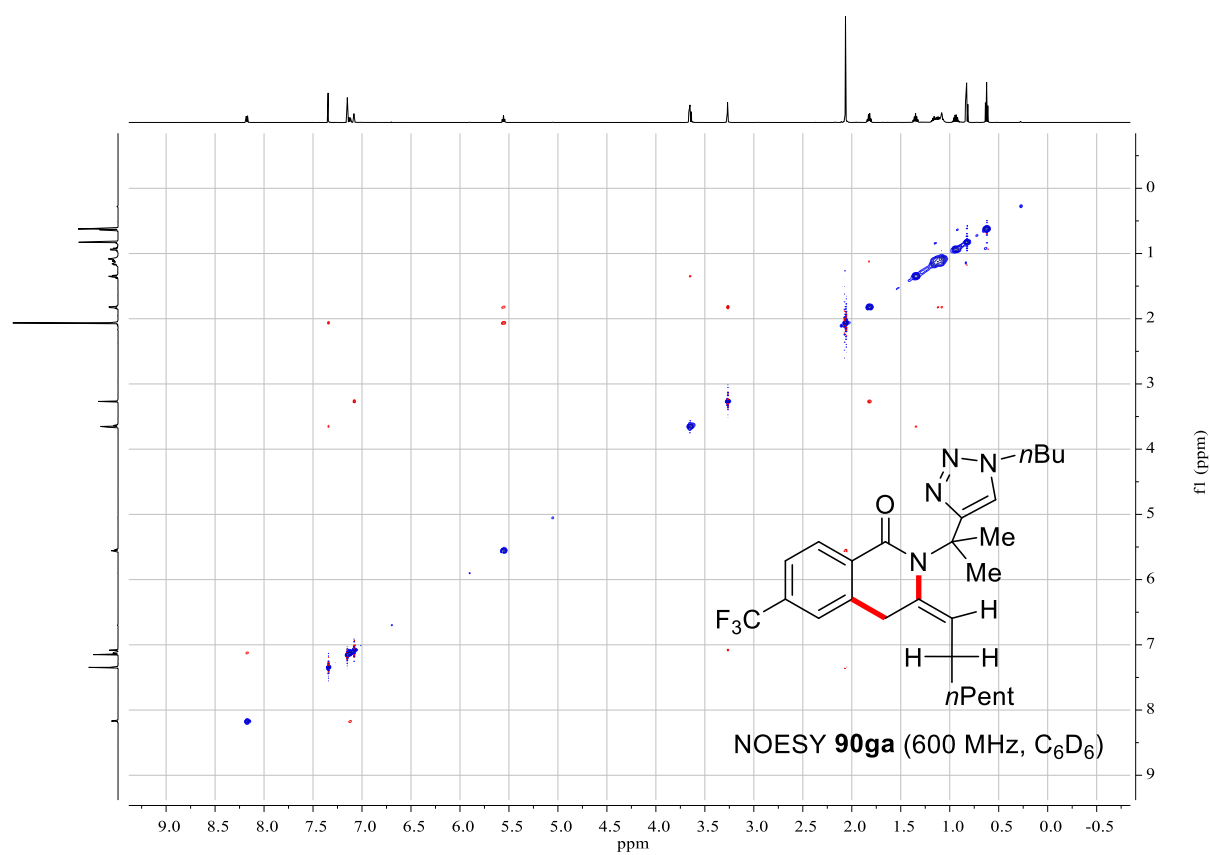
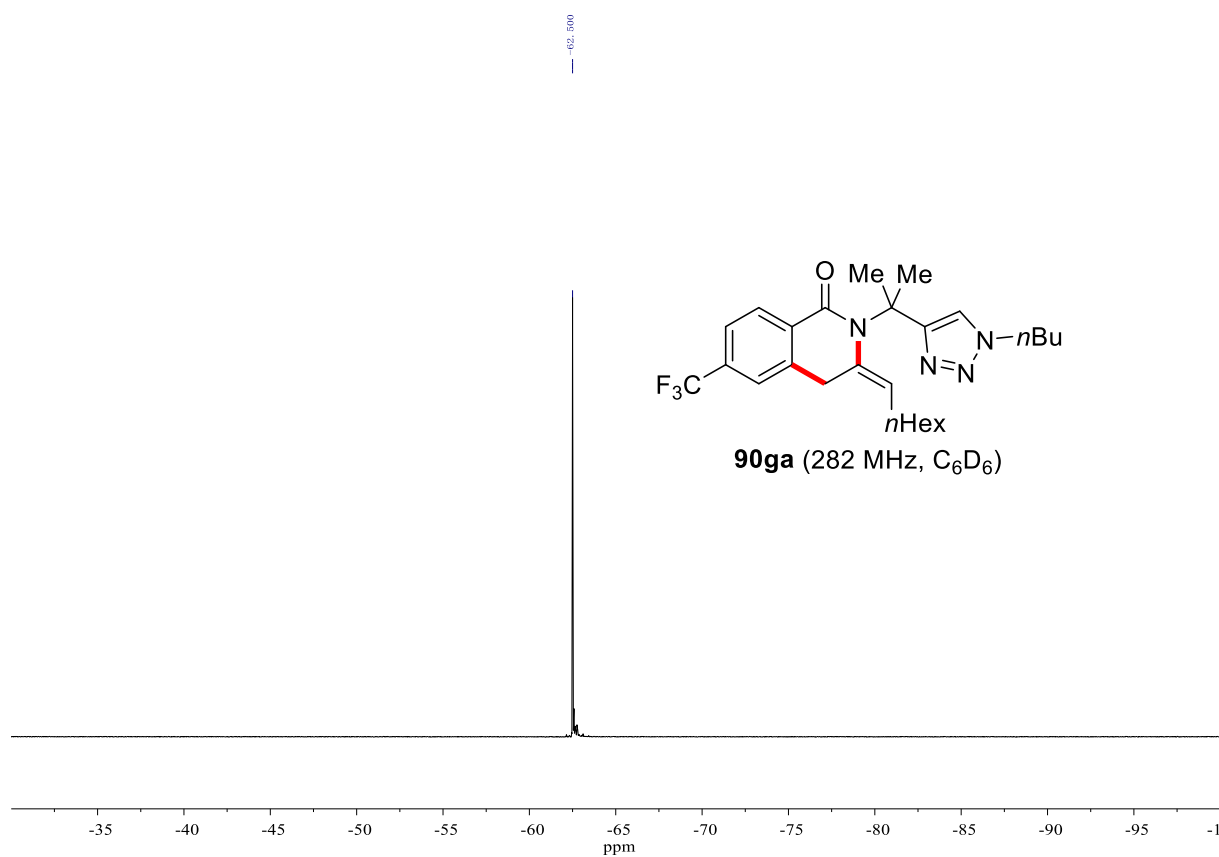
# NMR Spectra



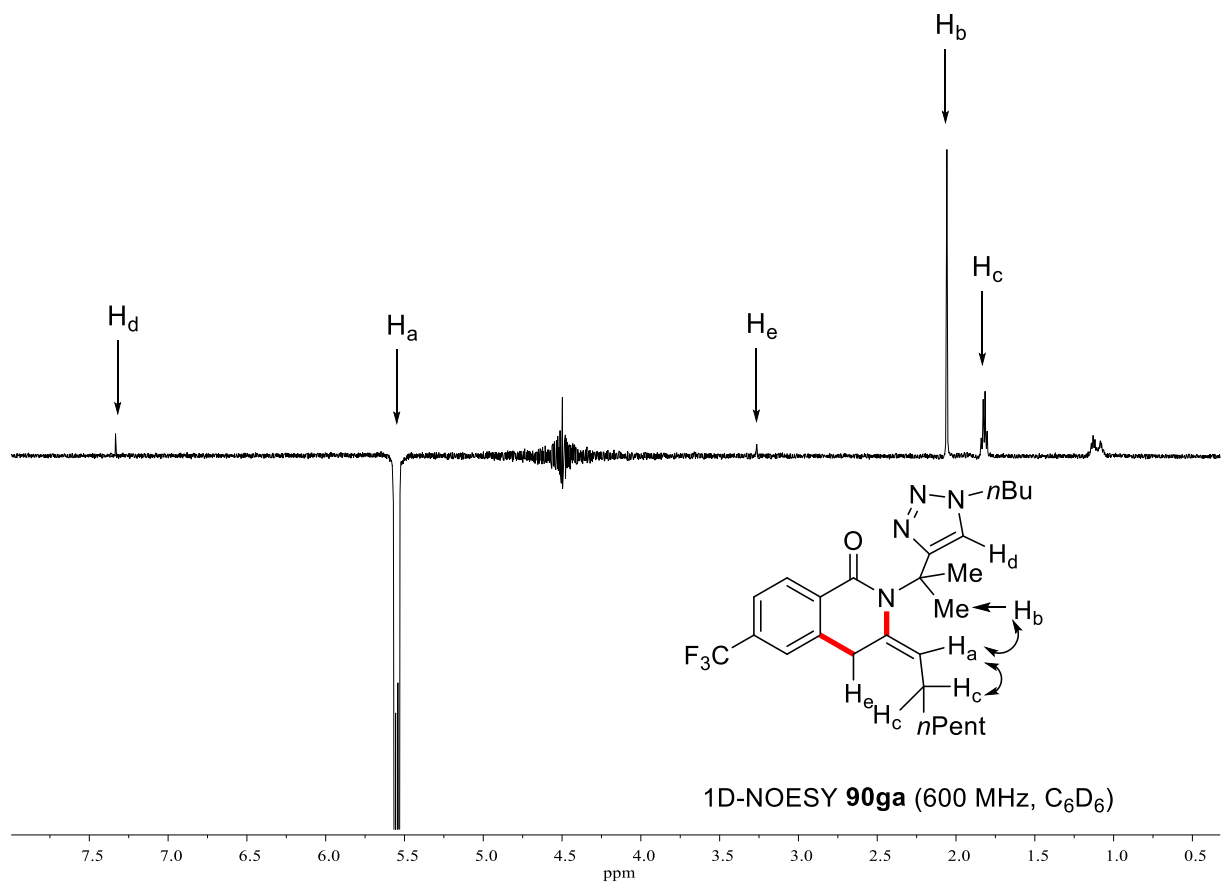
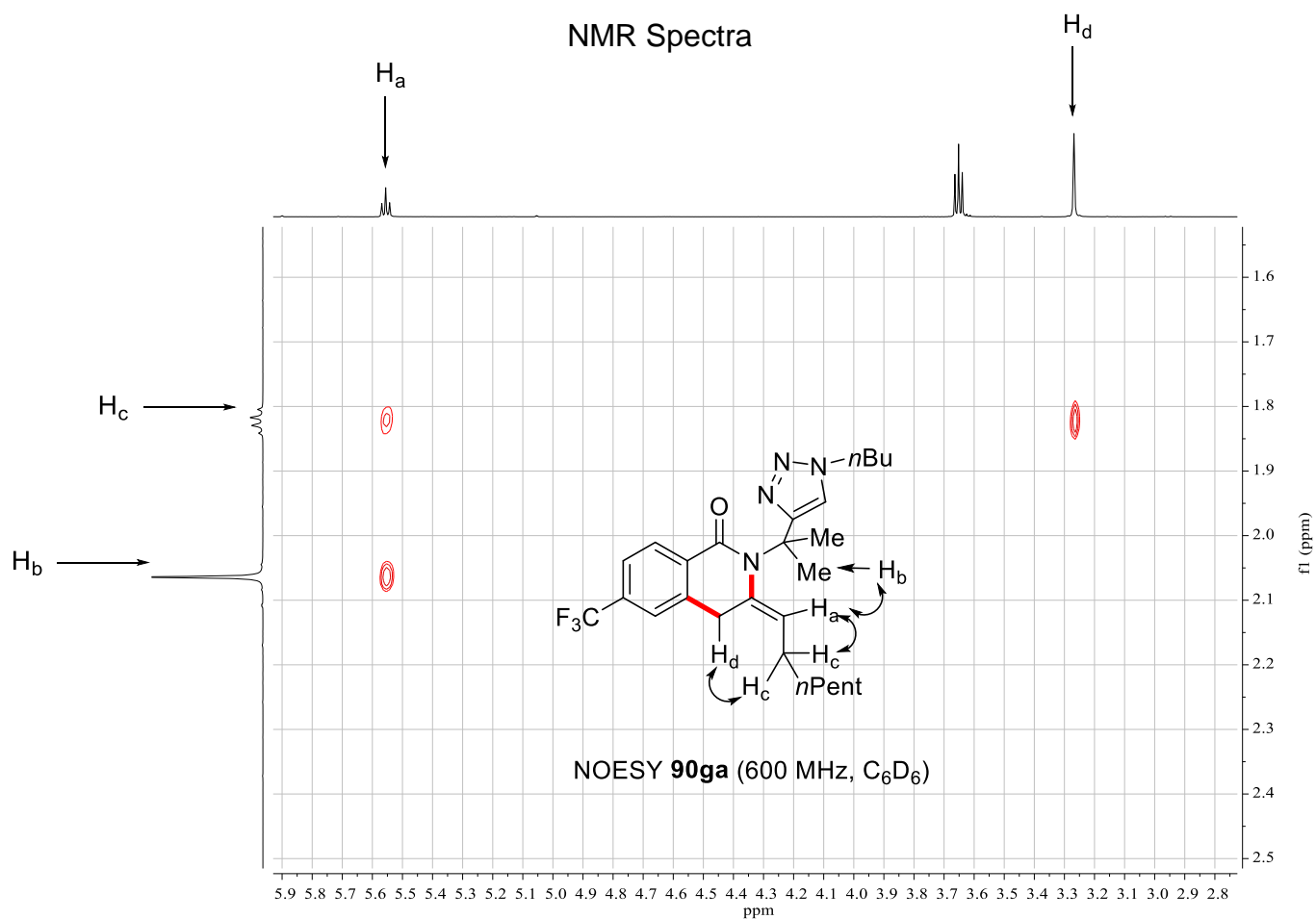
# NMR Spectra



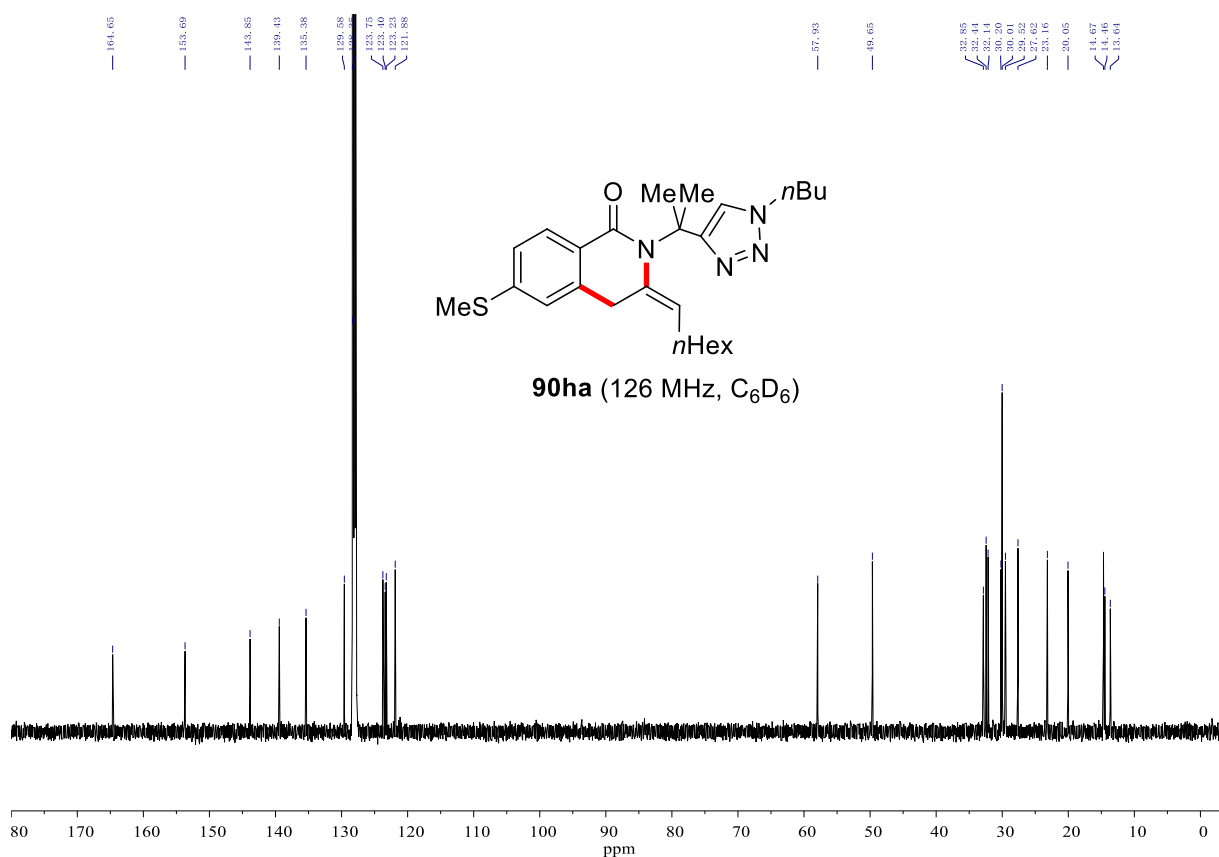
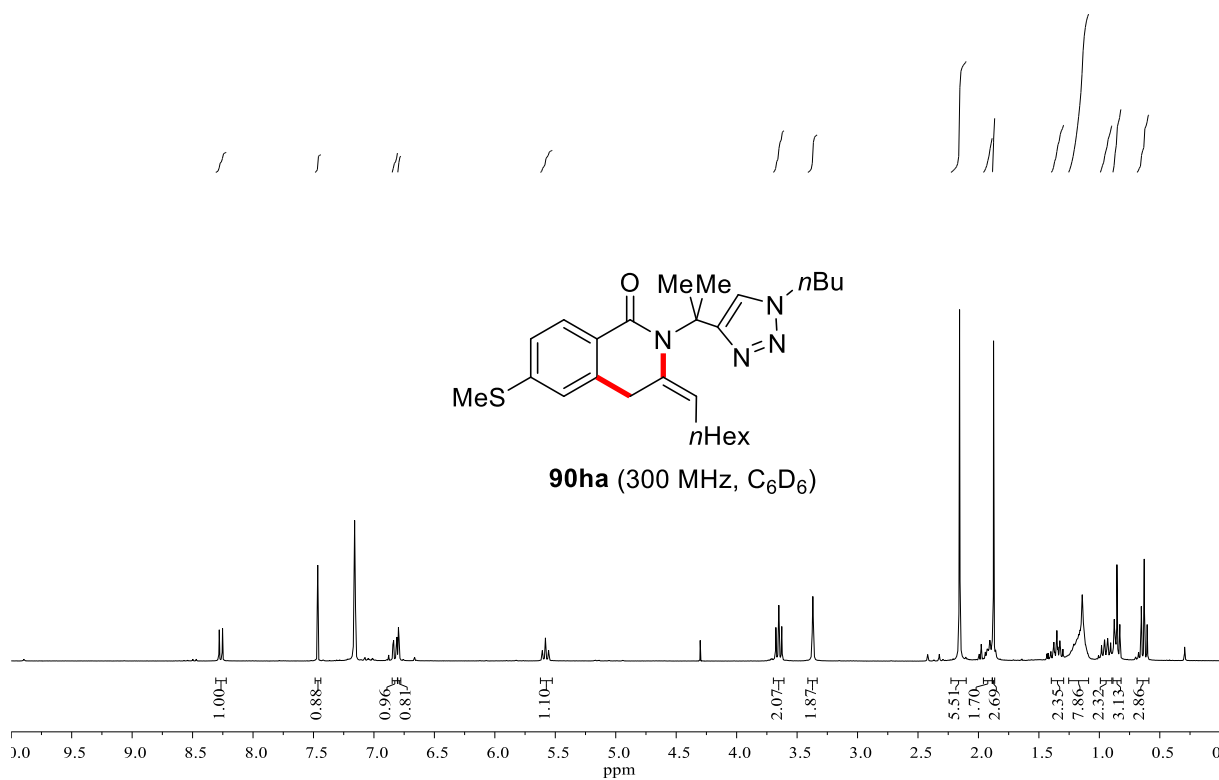
# NMR Spectra



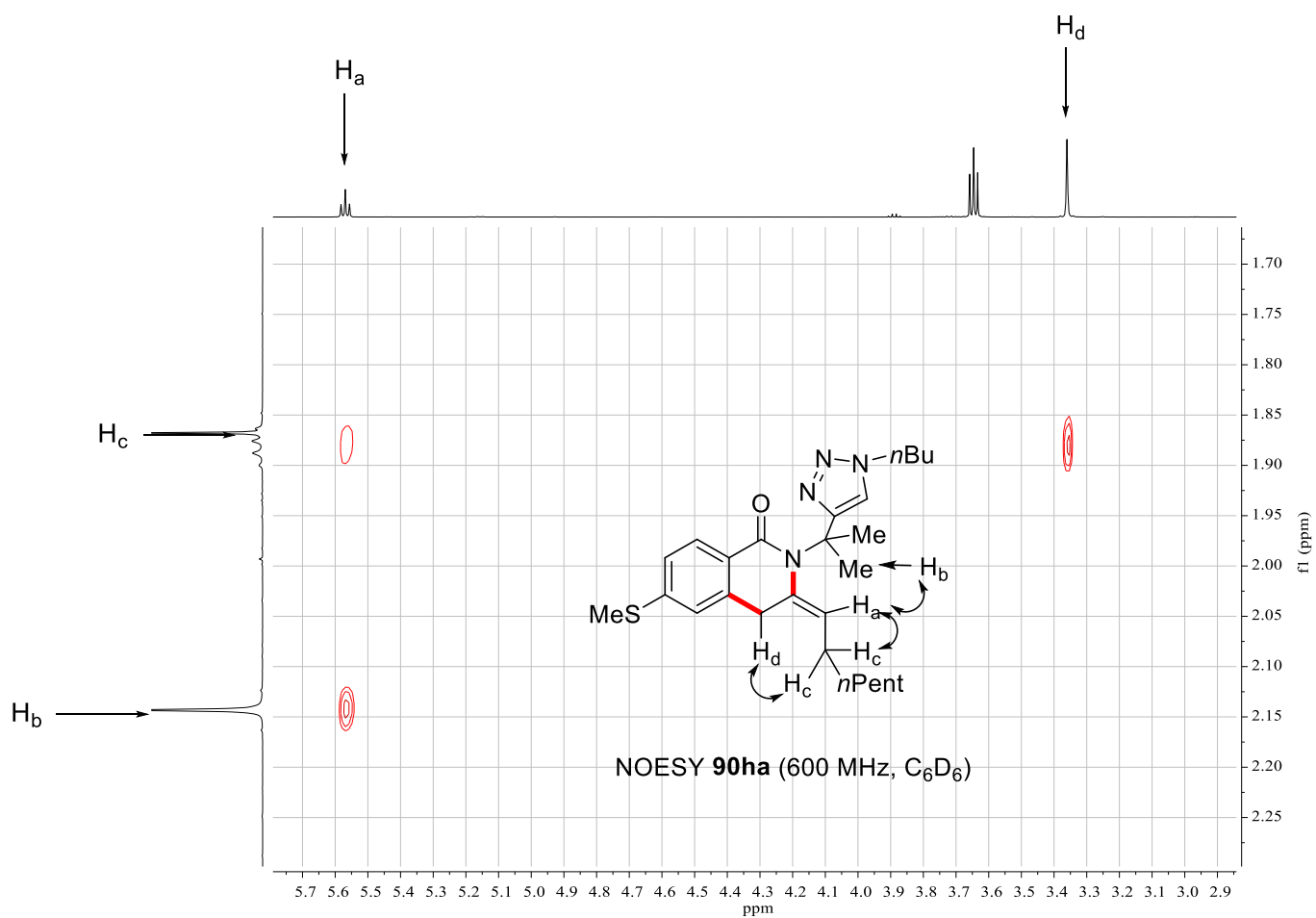
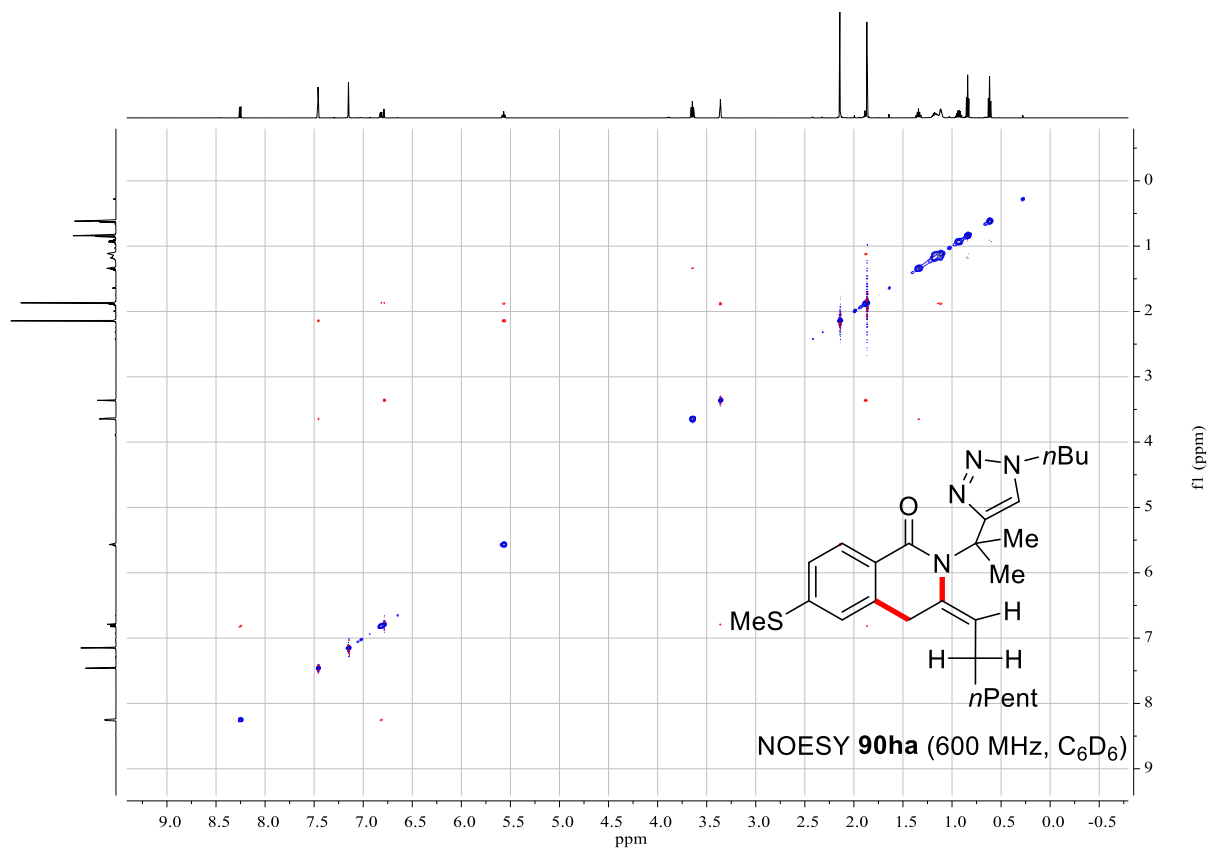
# NMR Spectra



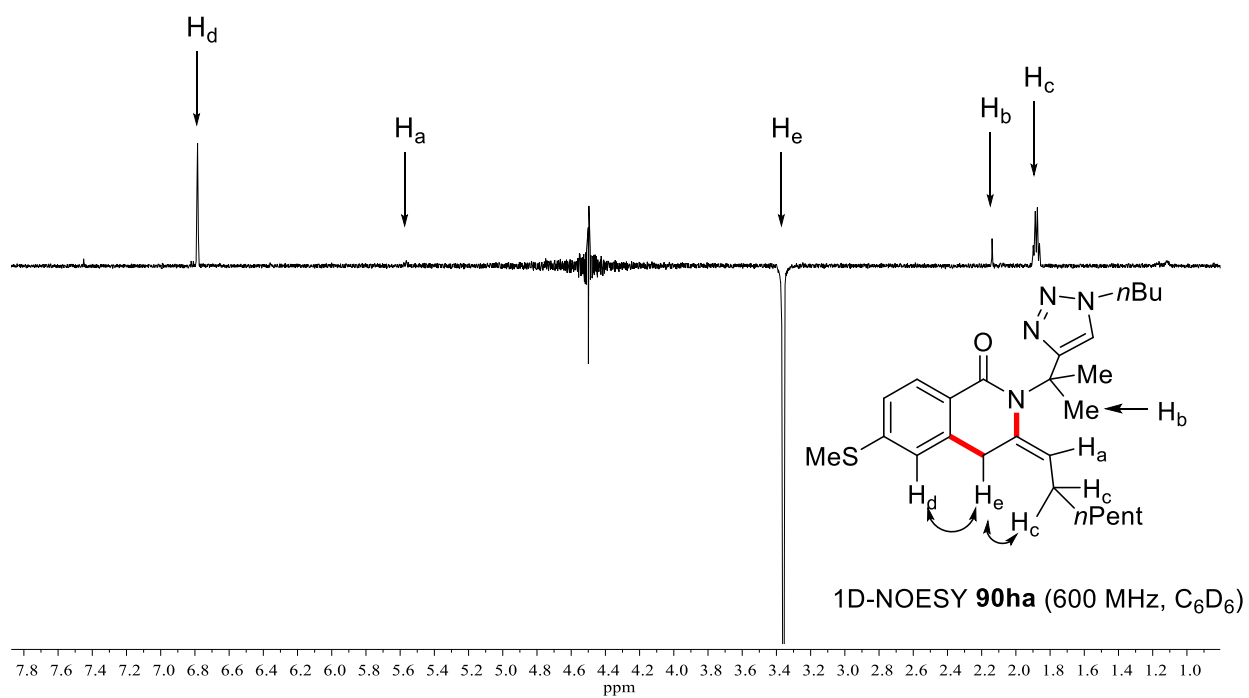
# NMR Spectra



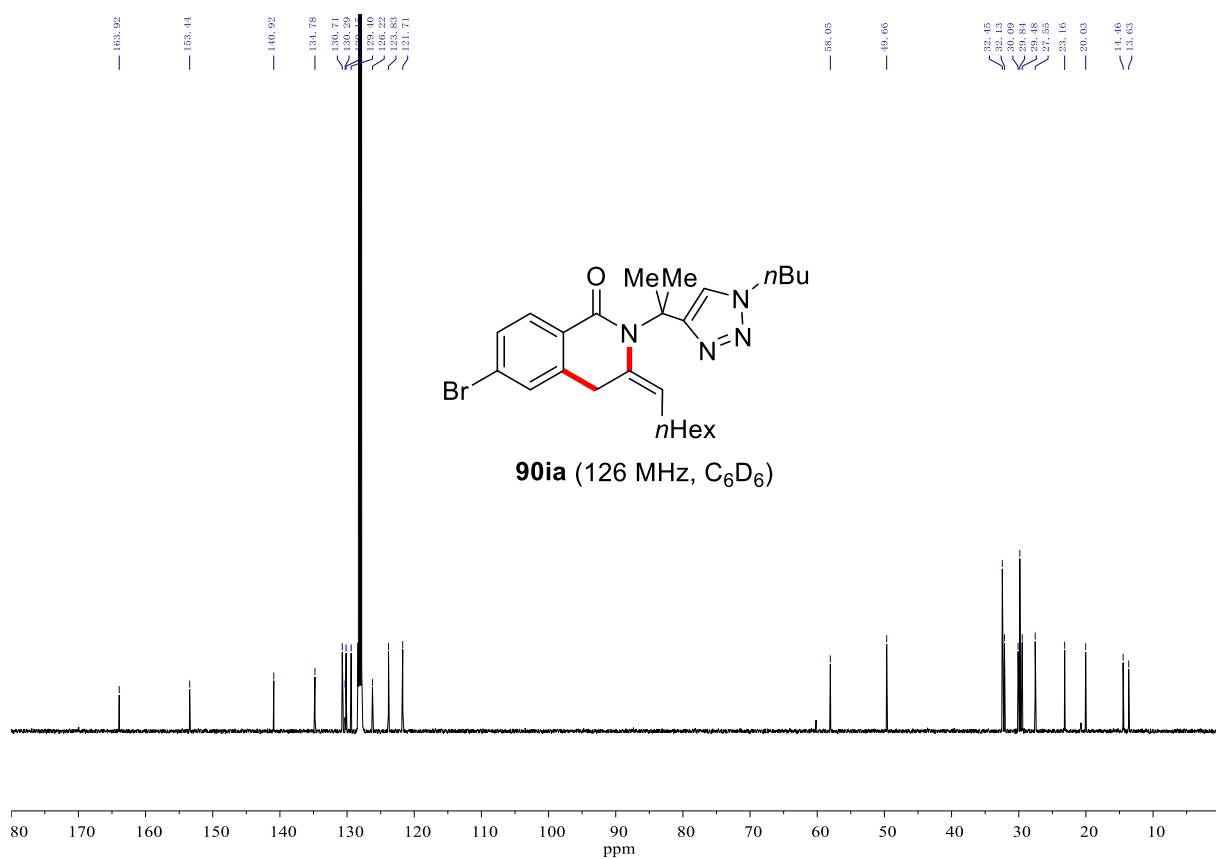
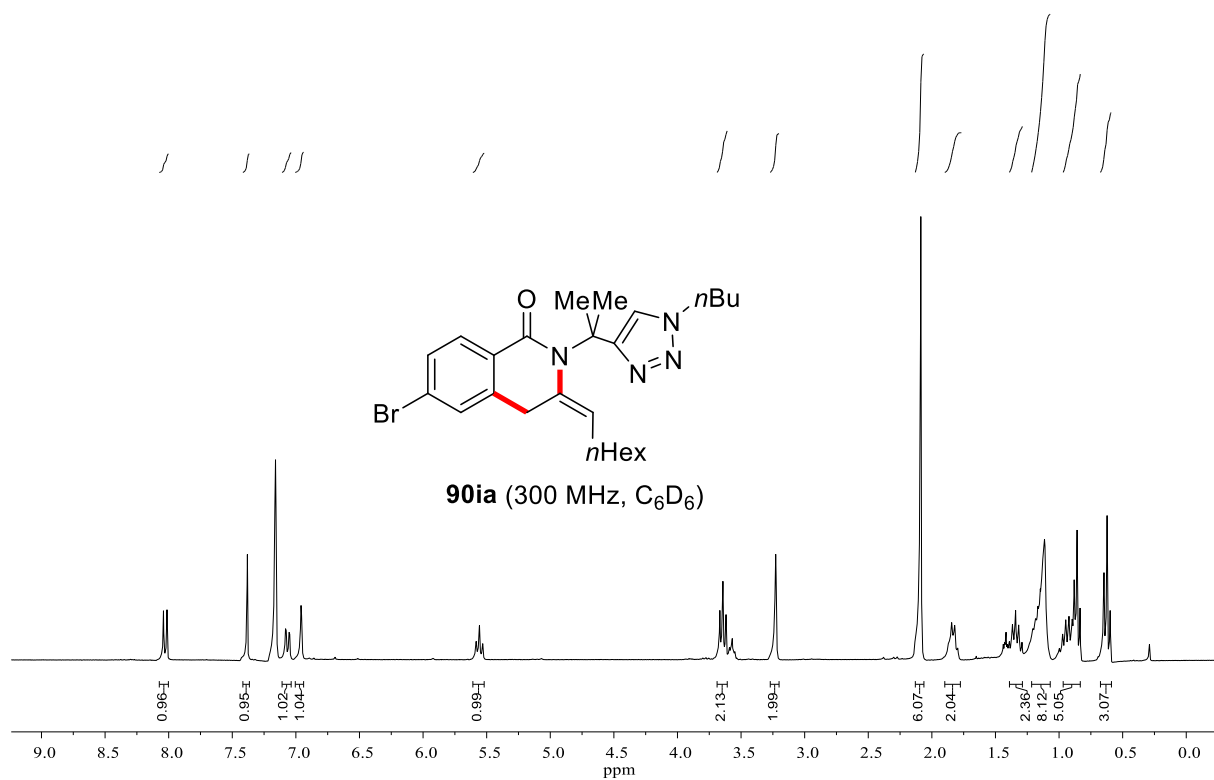
# NMR Spectra



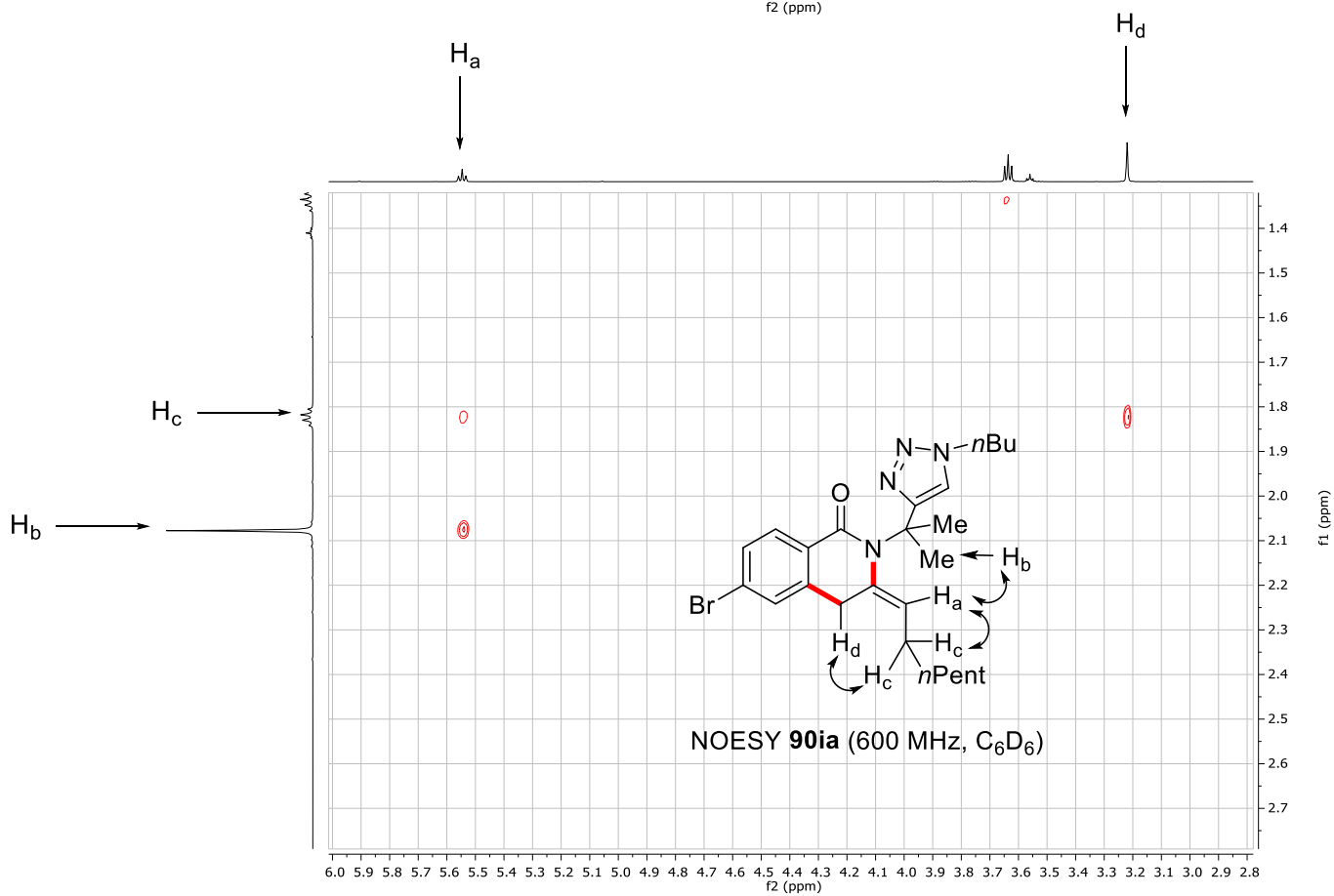
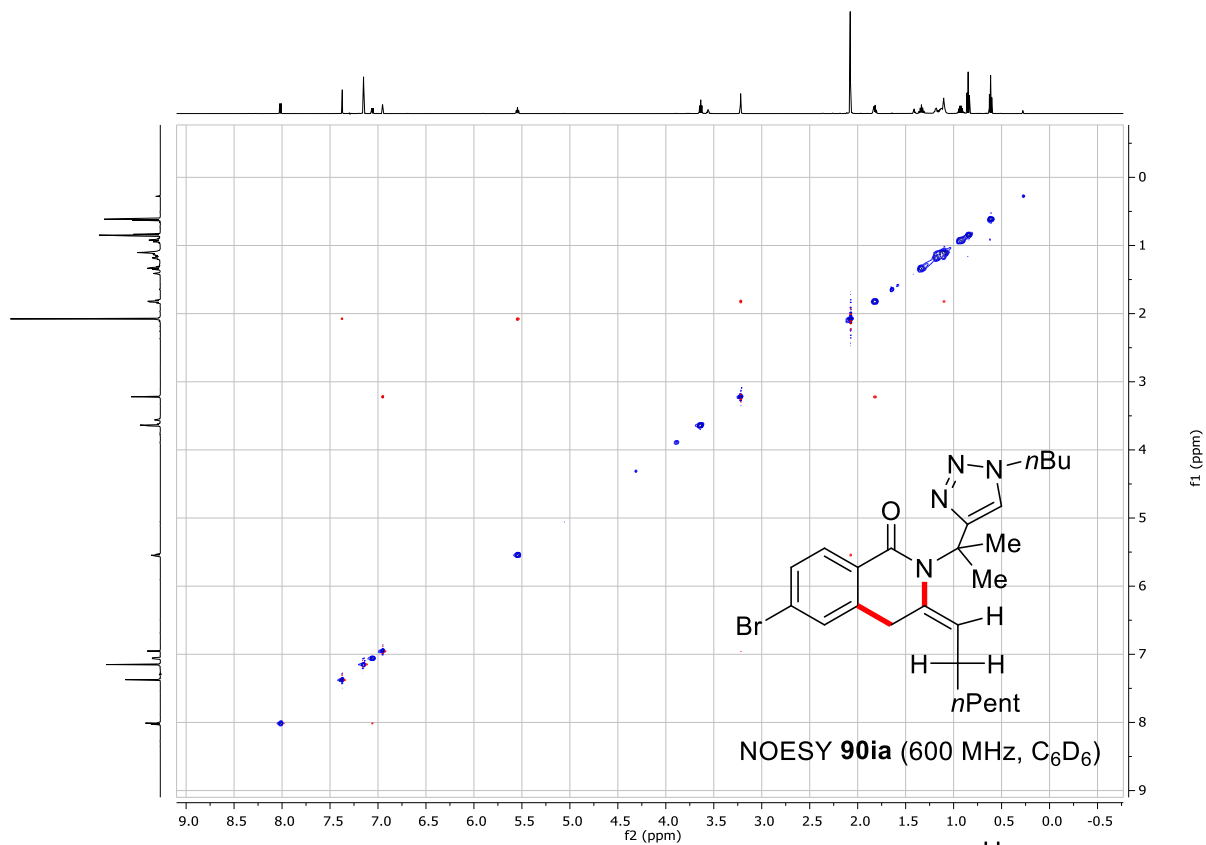
# NMR Spectra



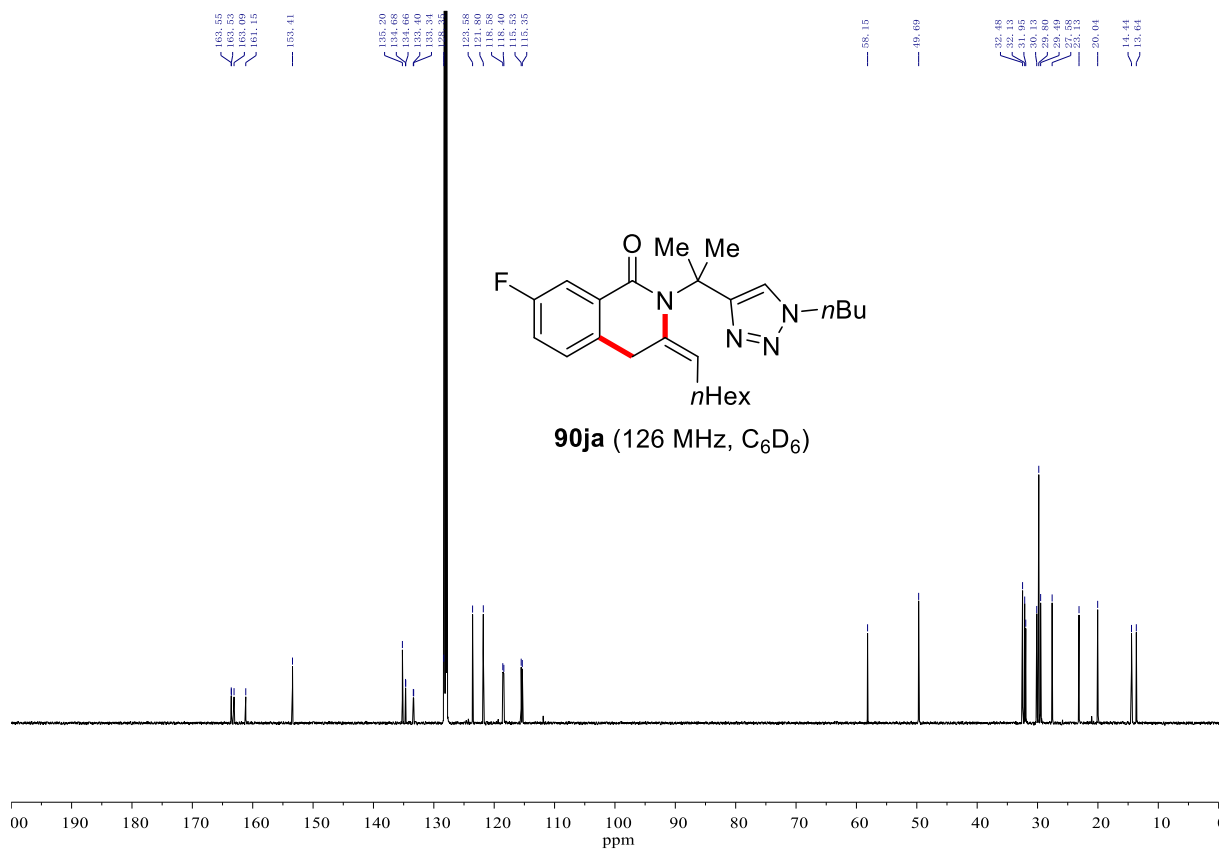
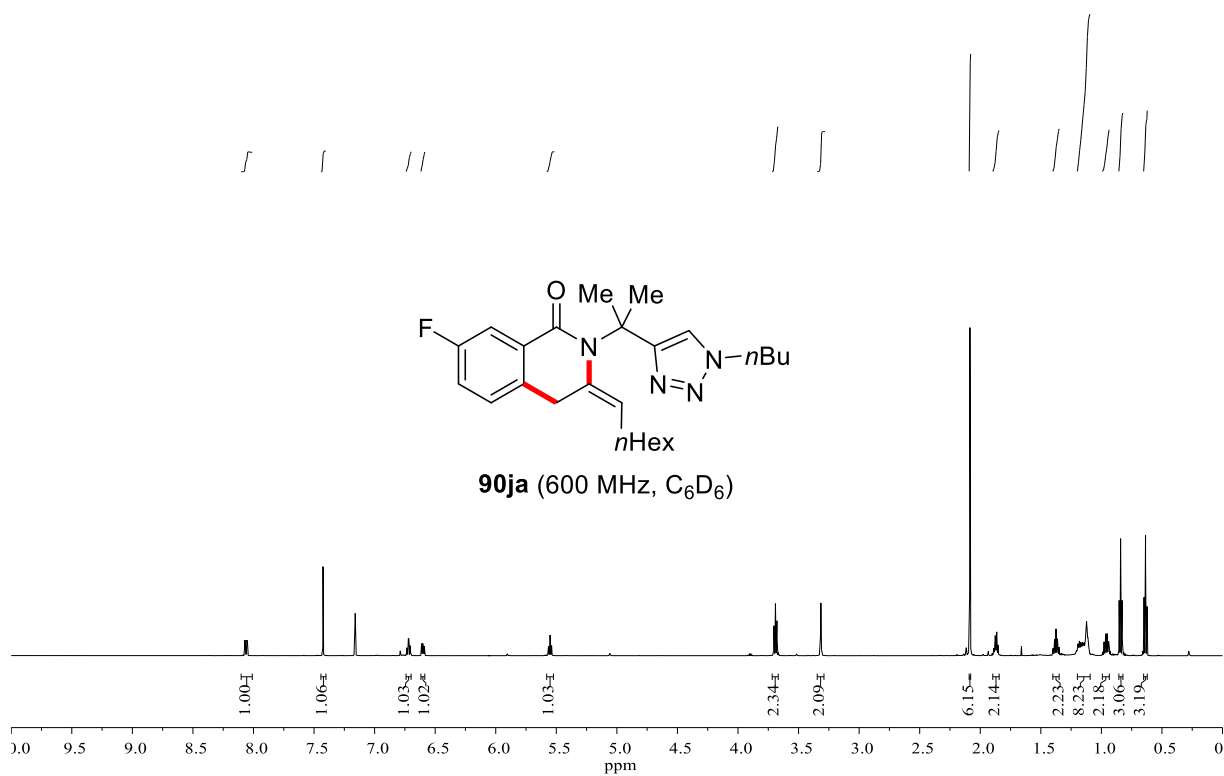
# NMR Spectra



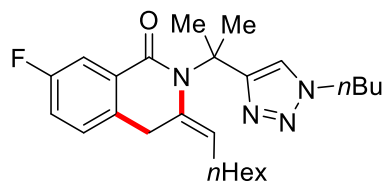
# NMR Spectra



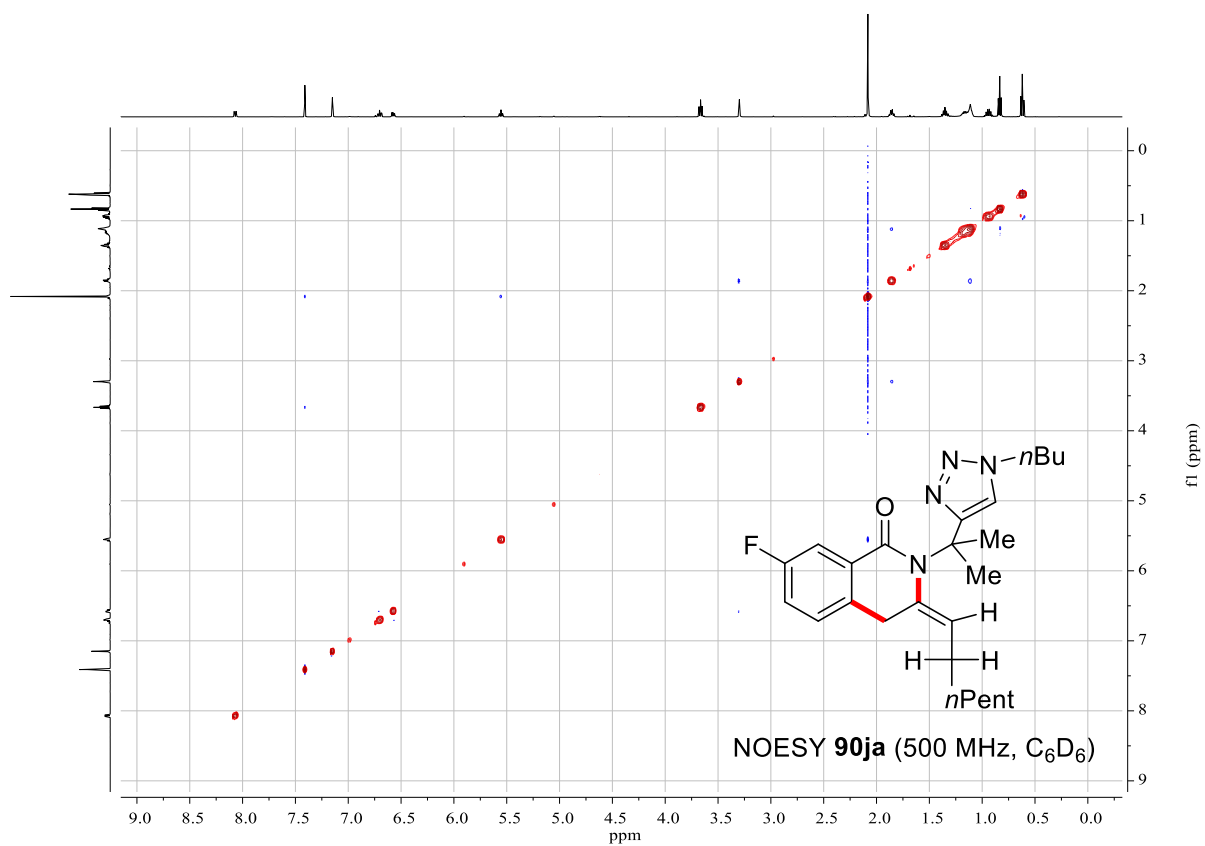
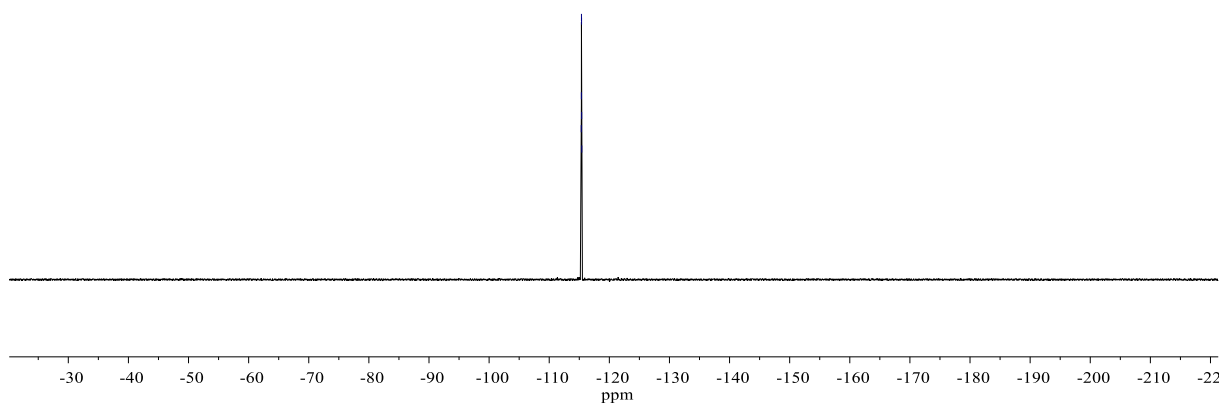
# NMR Spectra



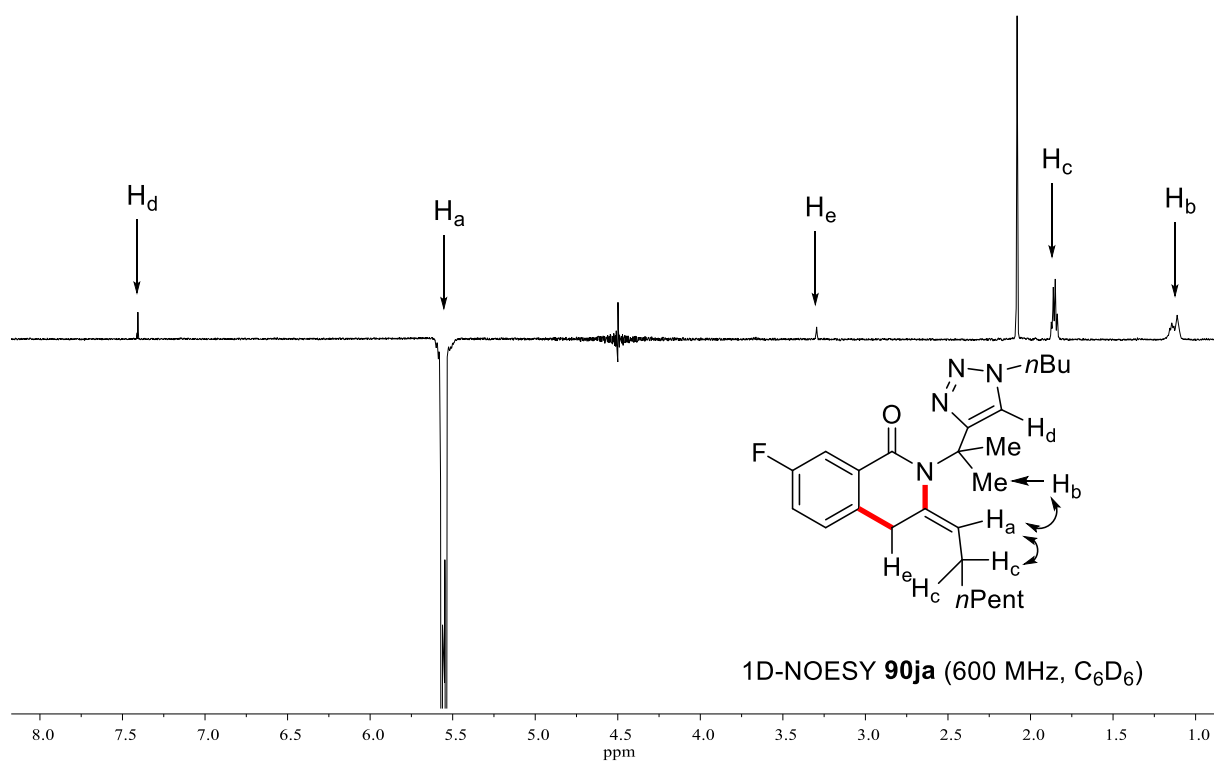
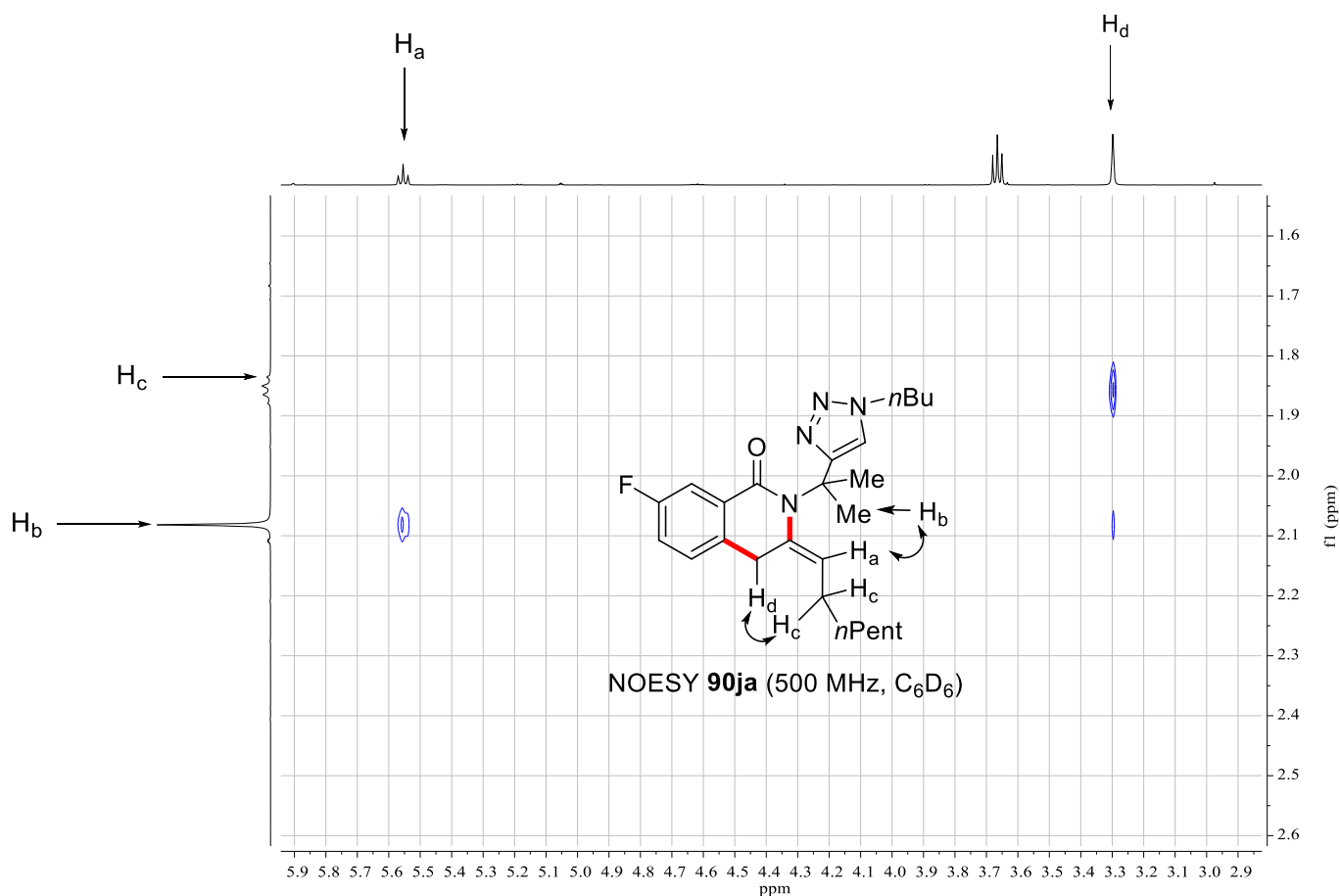
# NMR Spectra



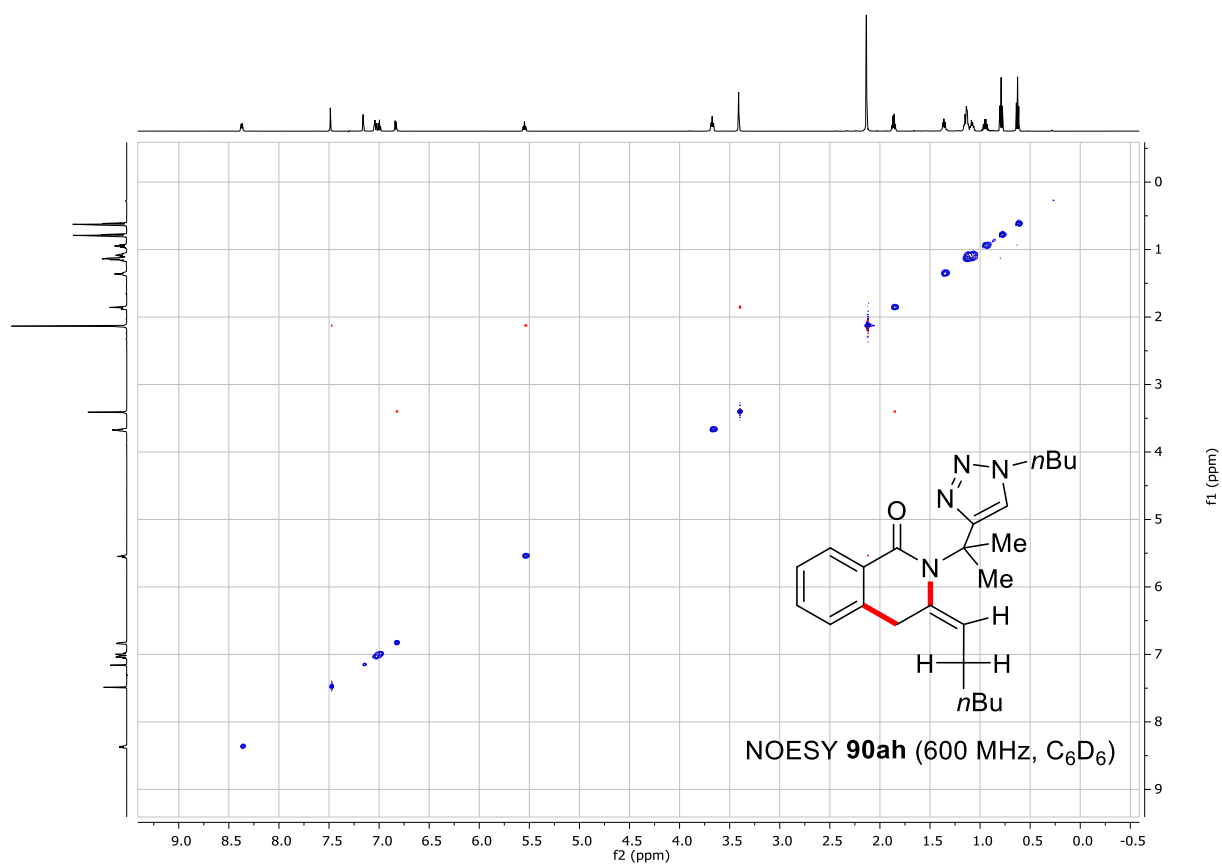
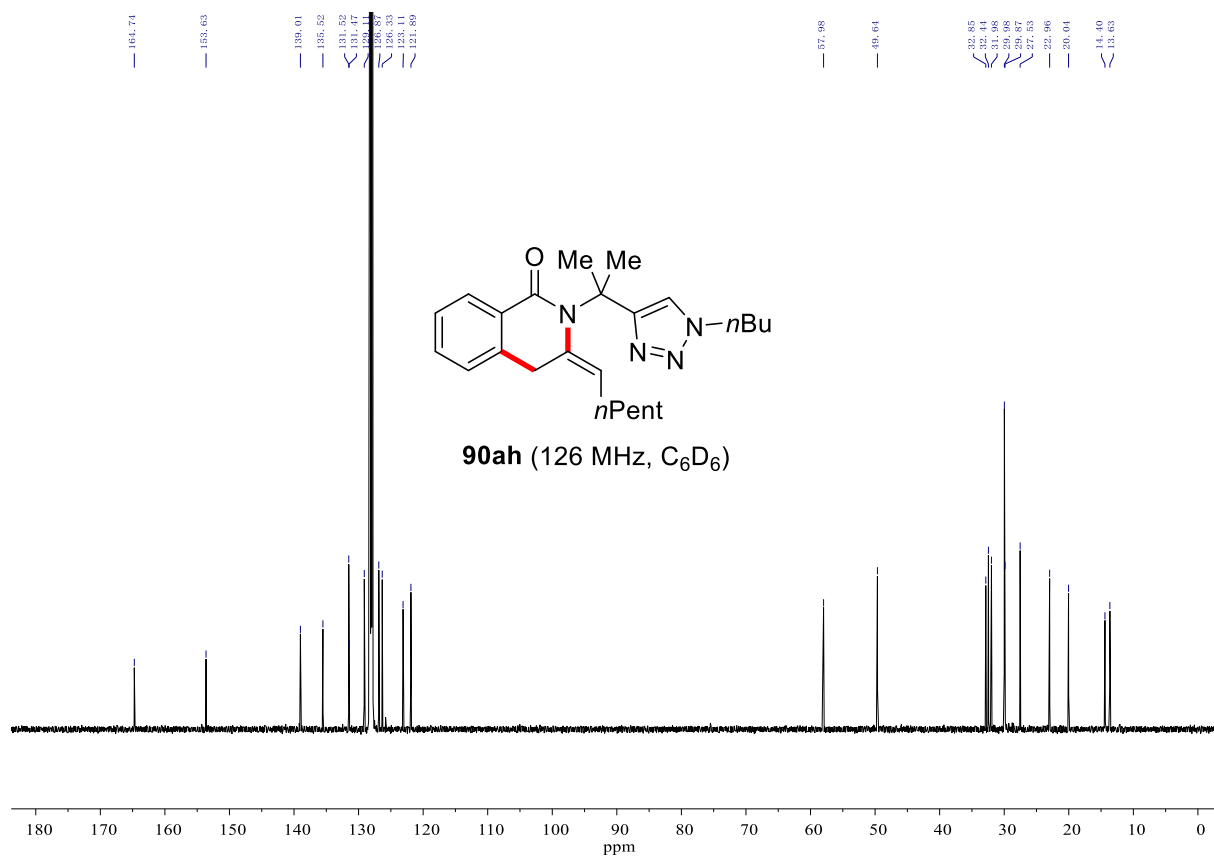
**90ja** (282 MHz, C<sub>6</sub>D<sub>6</sub>)



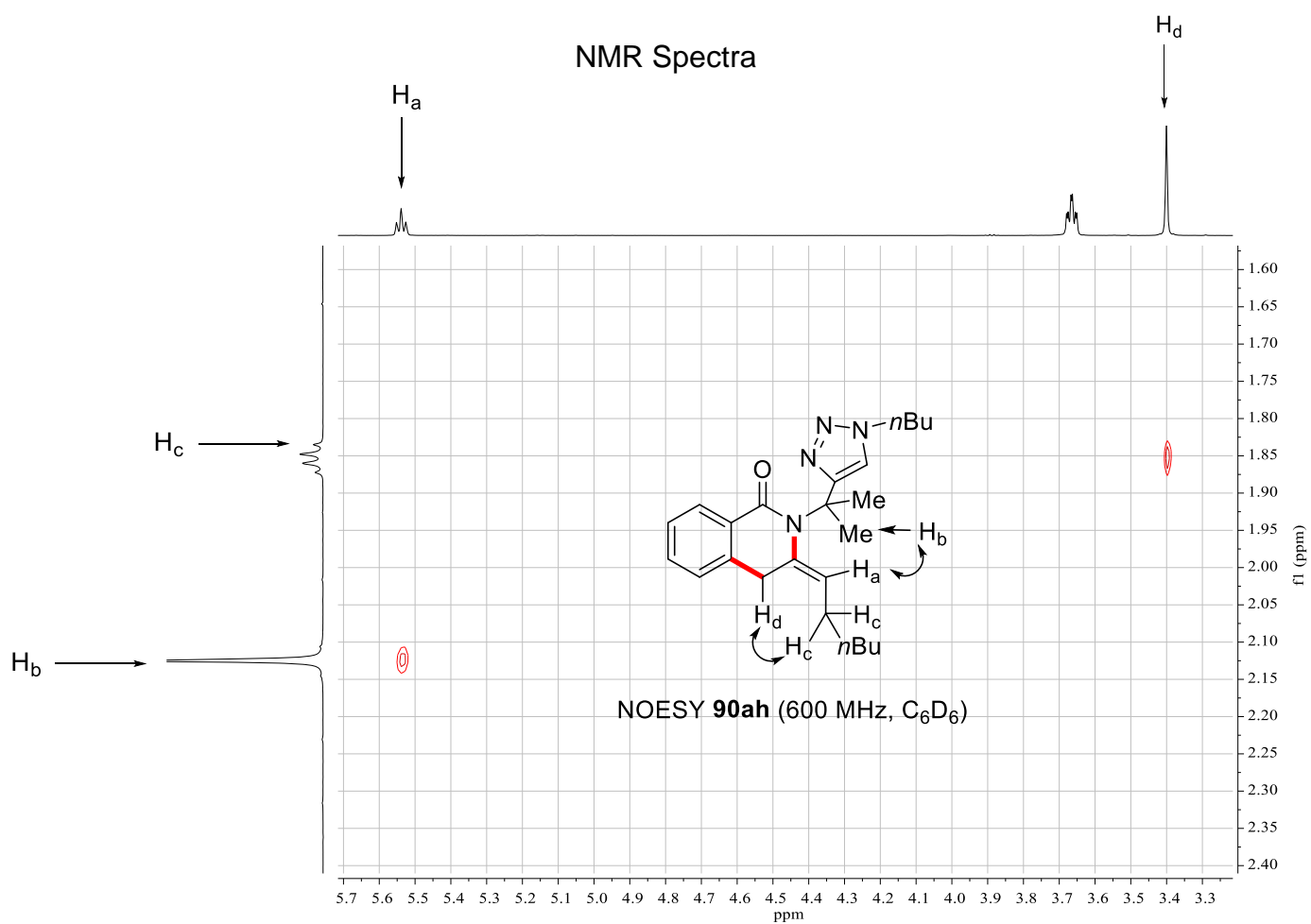
# NMR Spectra



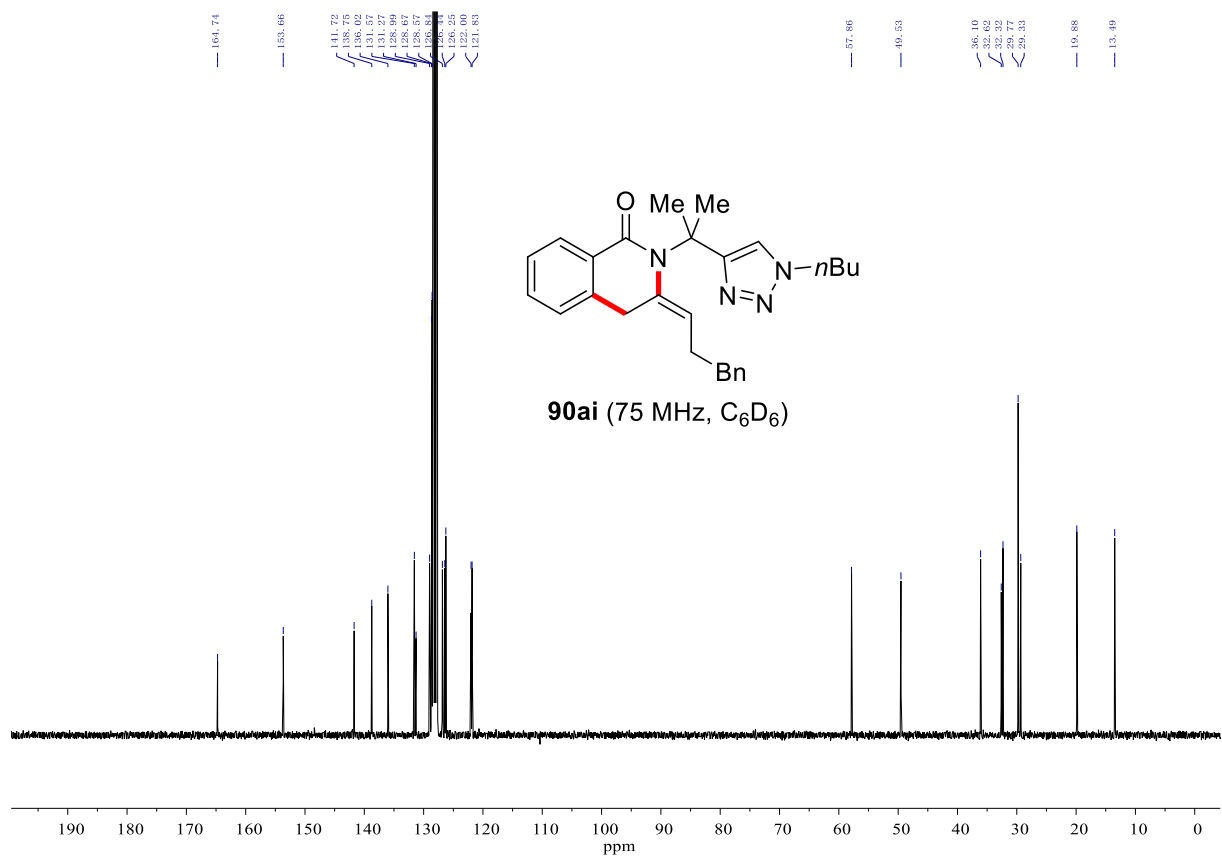
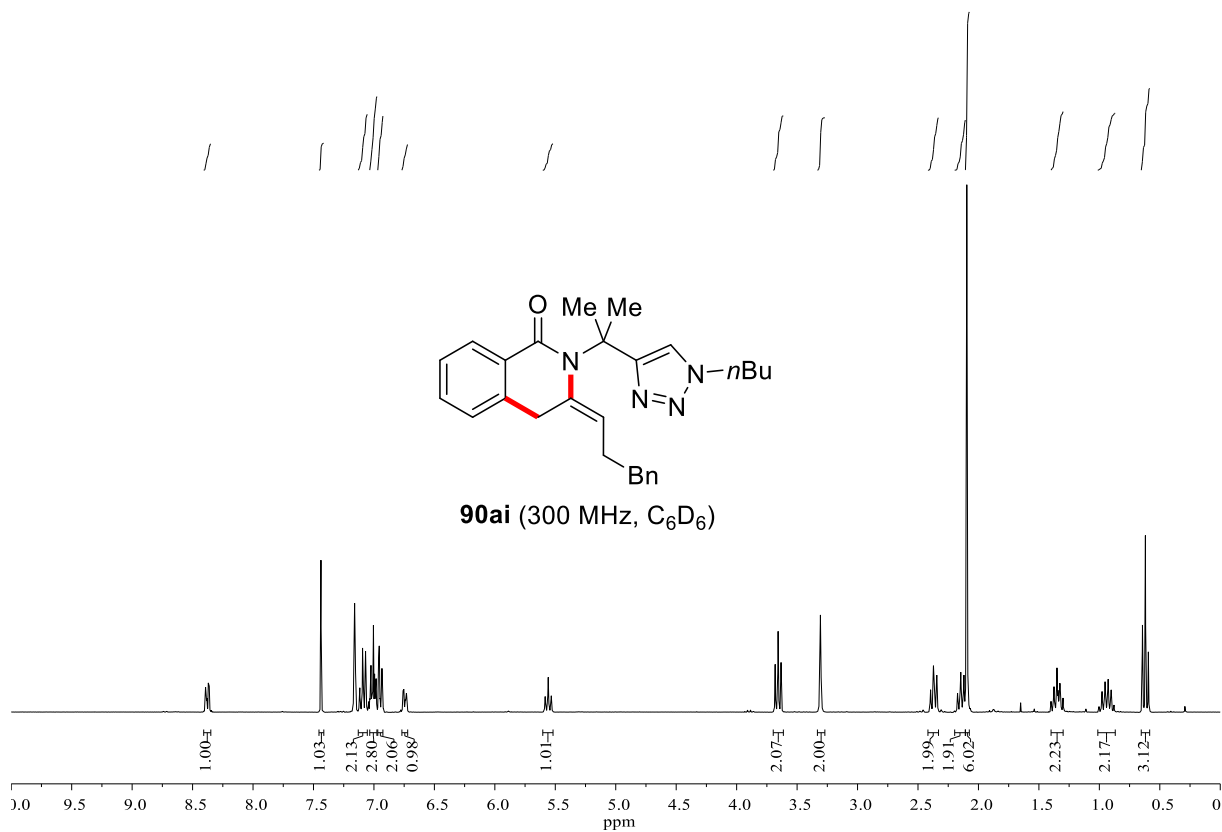
# NMR Spectra



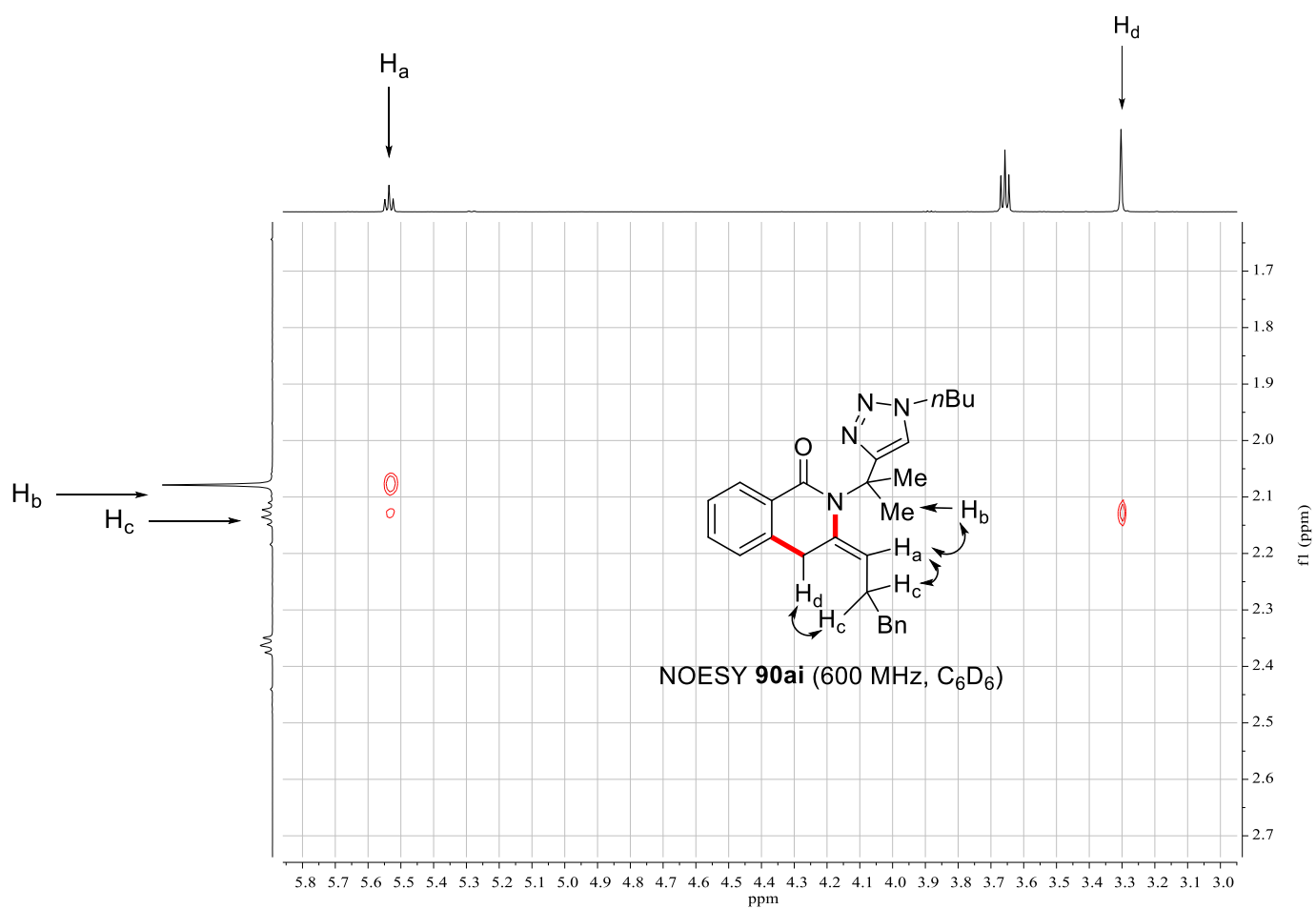
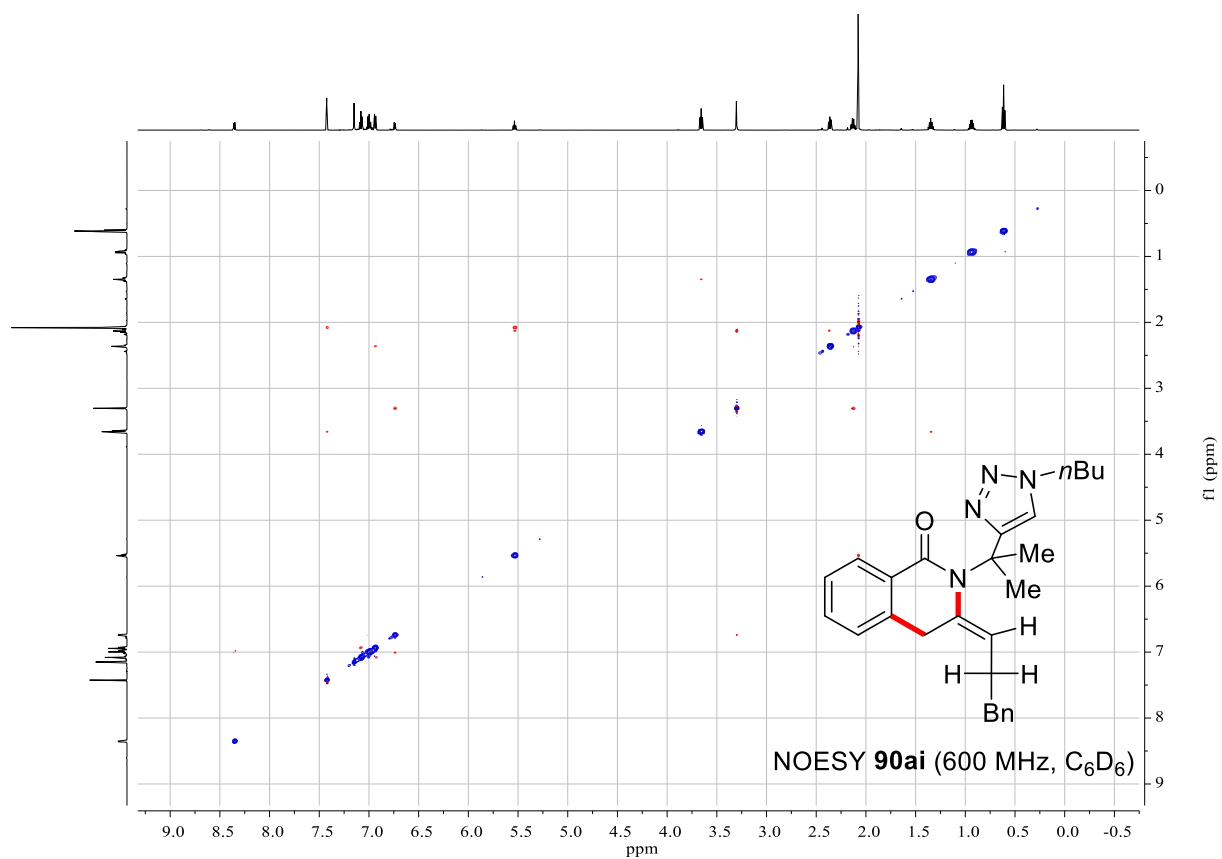
# NMR Spectra



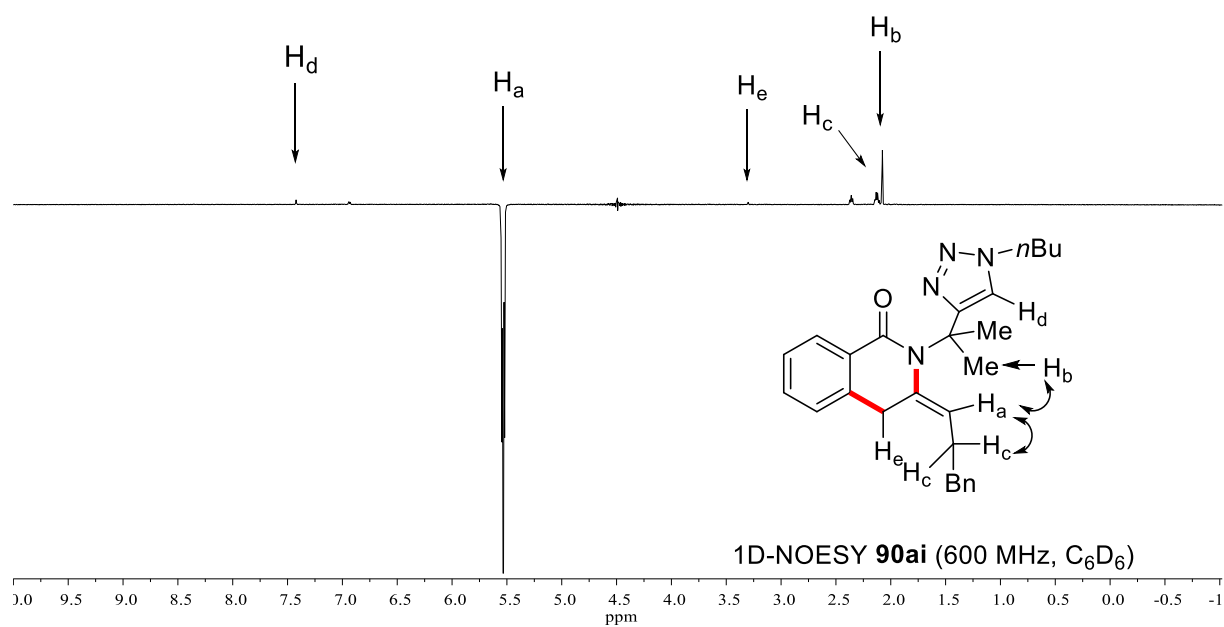
# NMR Spectra



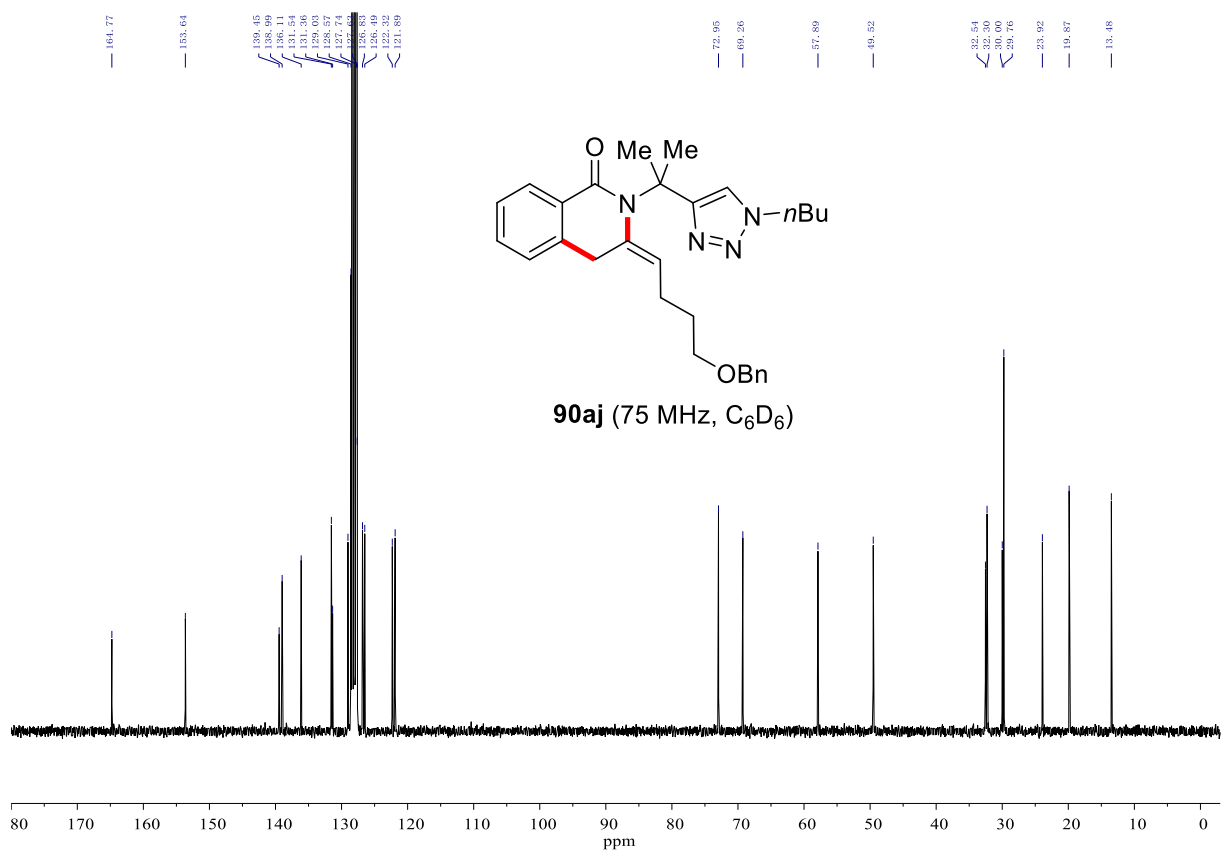
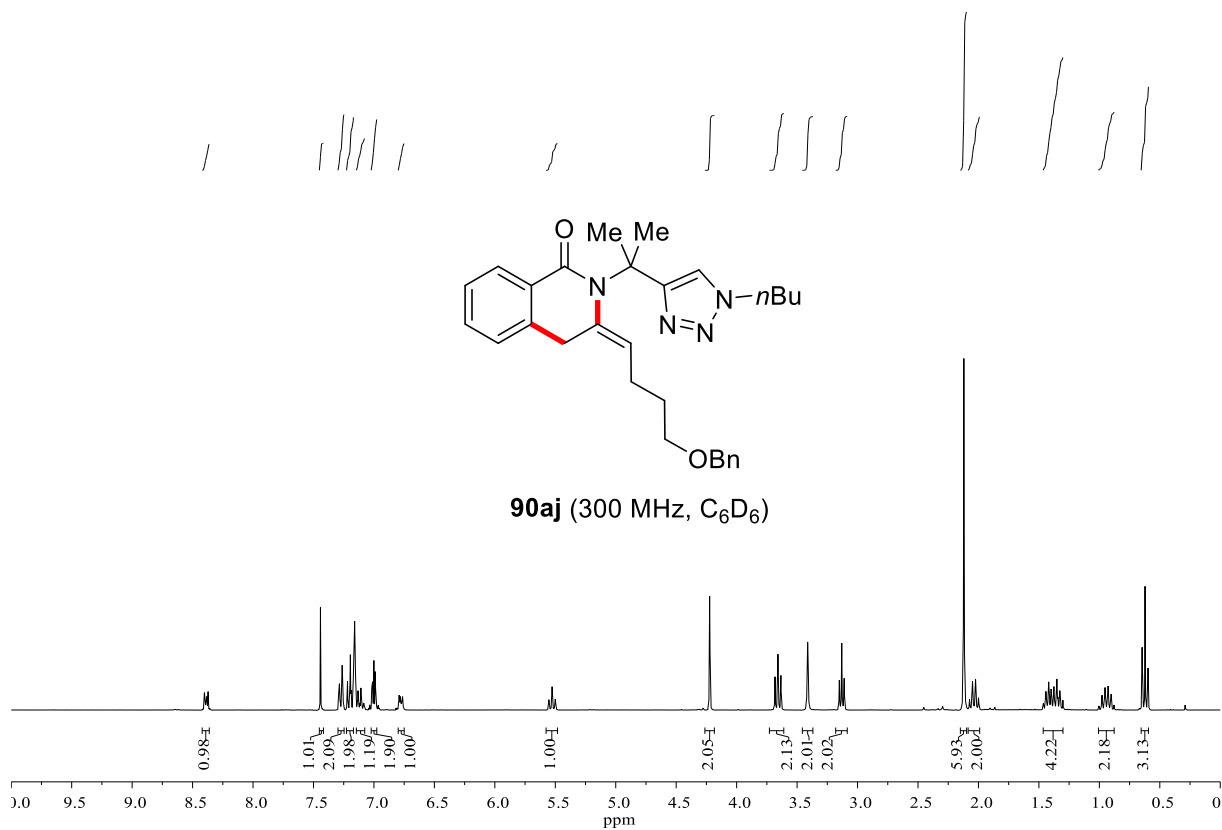
# NMR Spectra



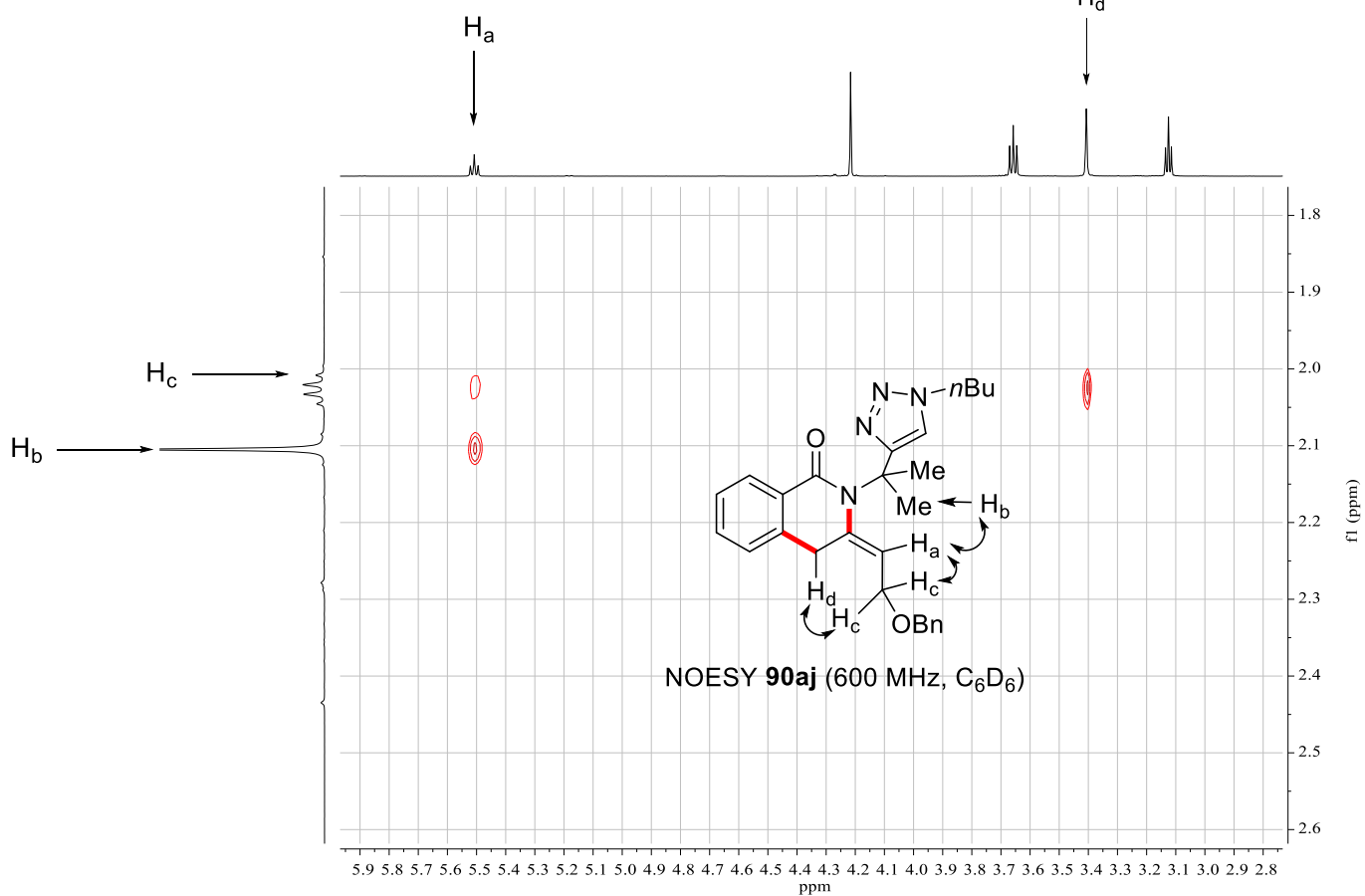
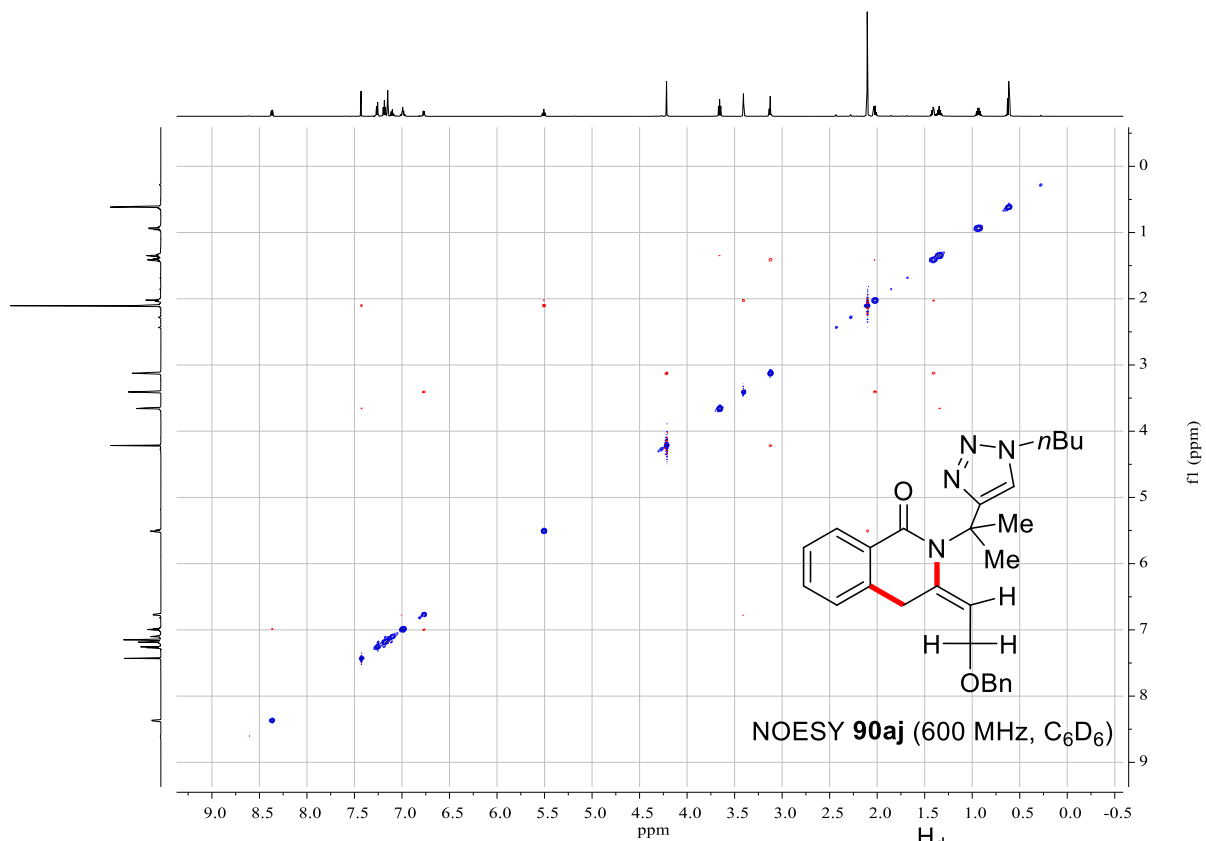
# NMR Spectra



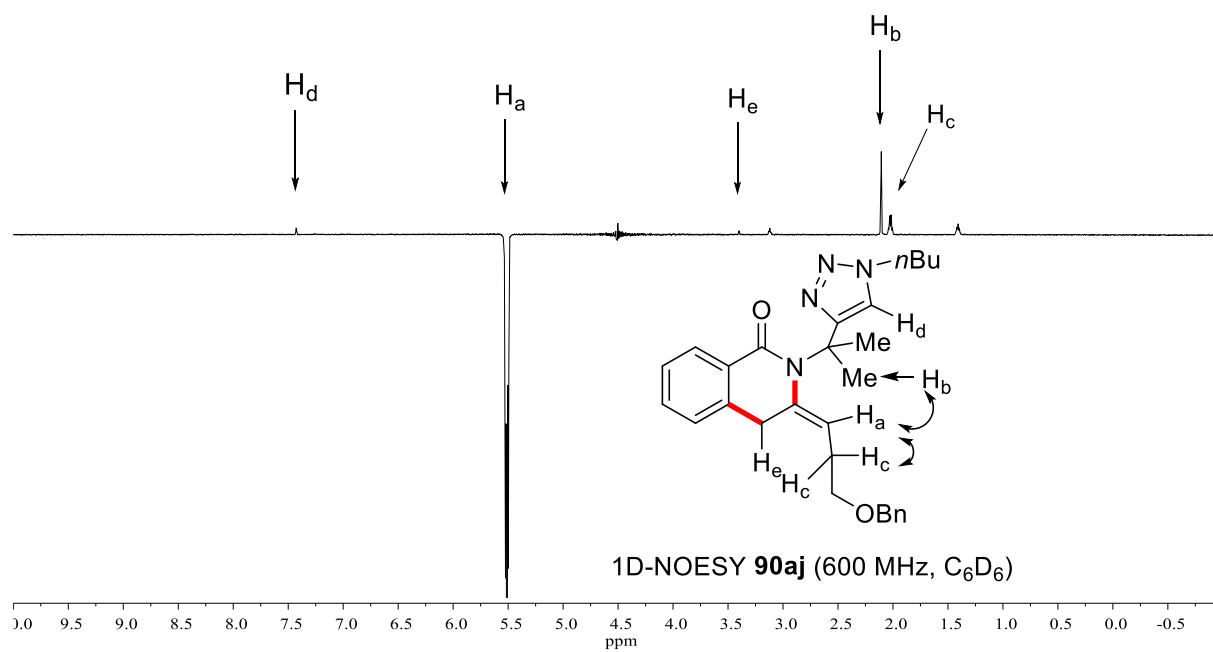
# NMR Spectra



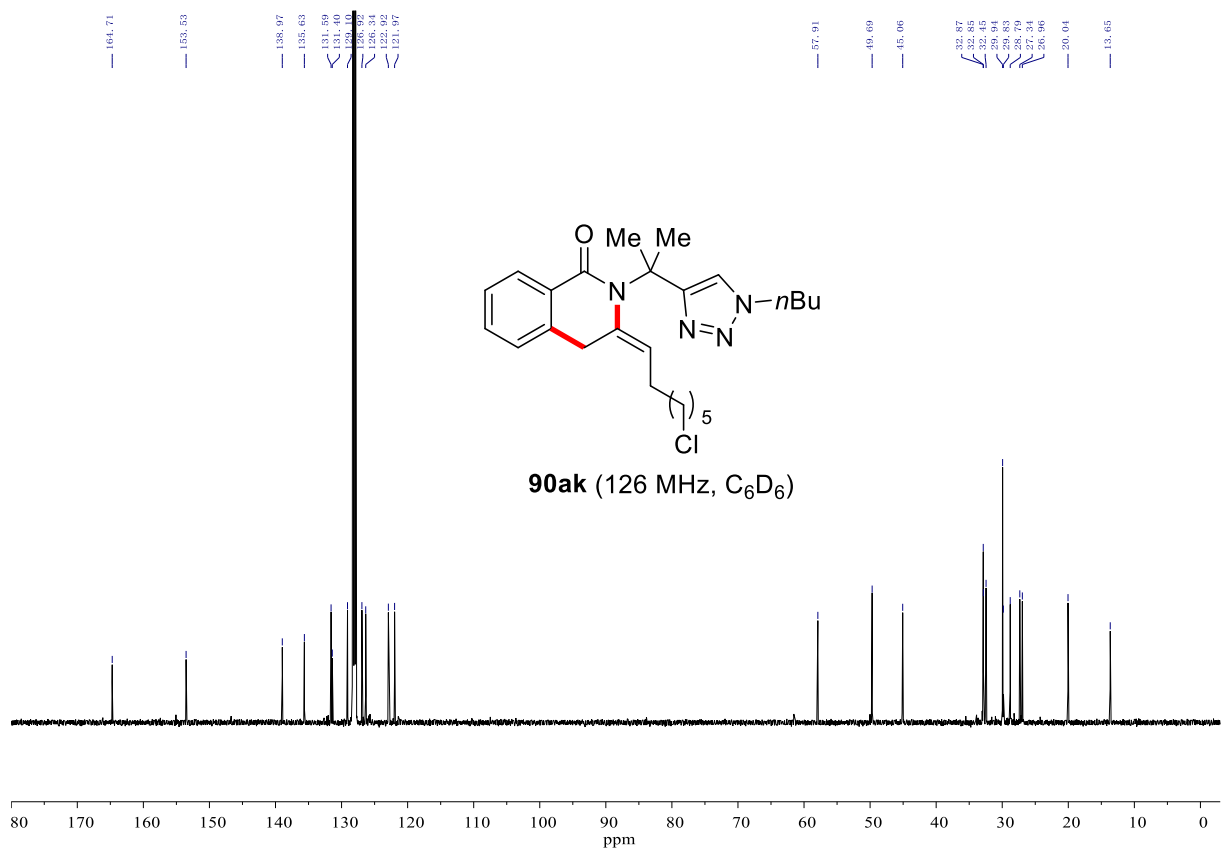
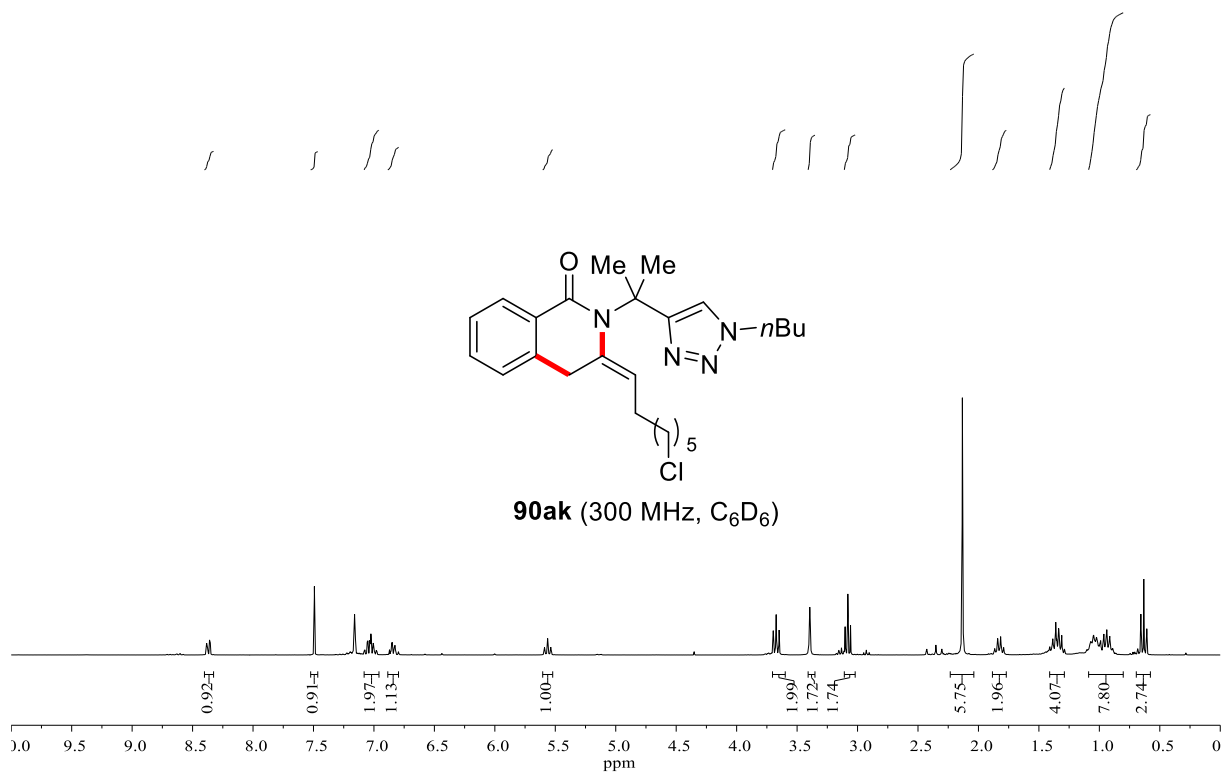
# NMR Spectra



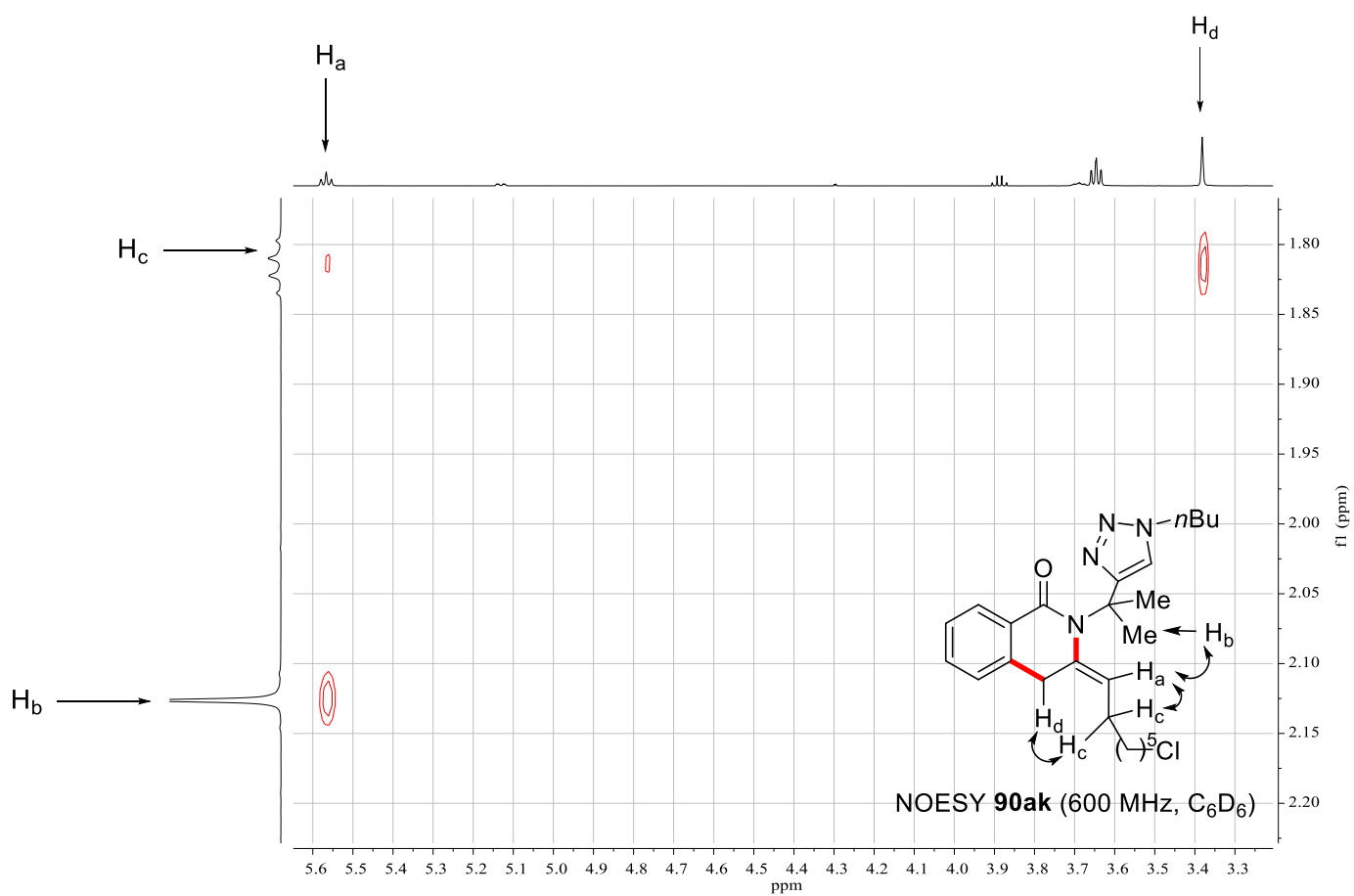
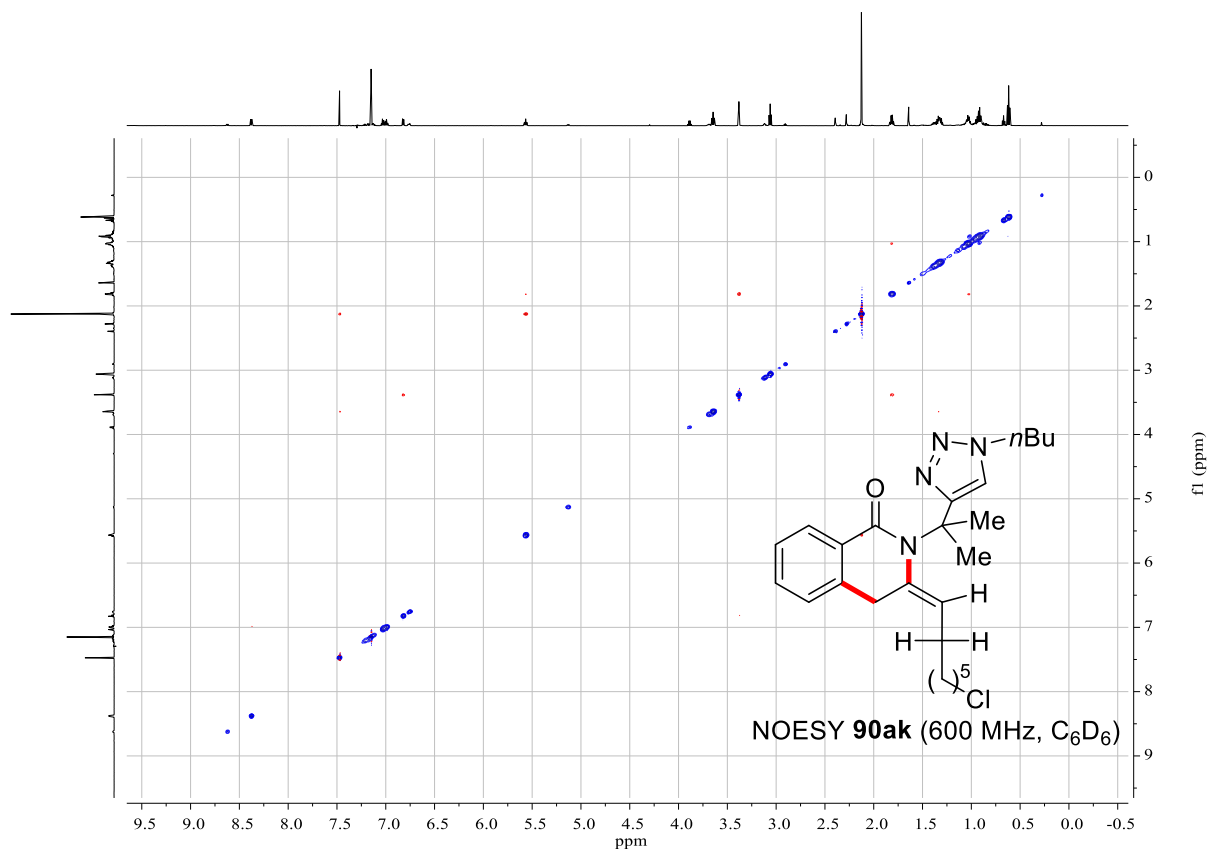
# NMR Spectra



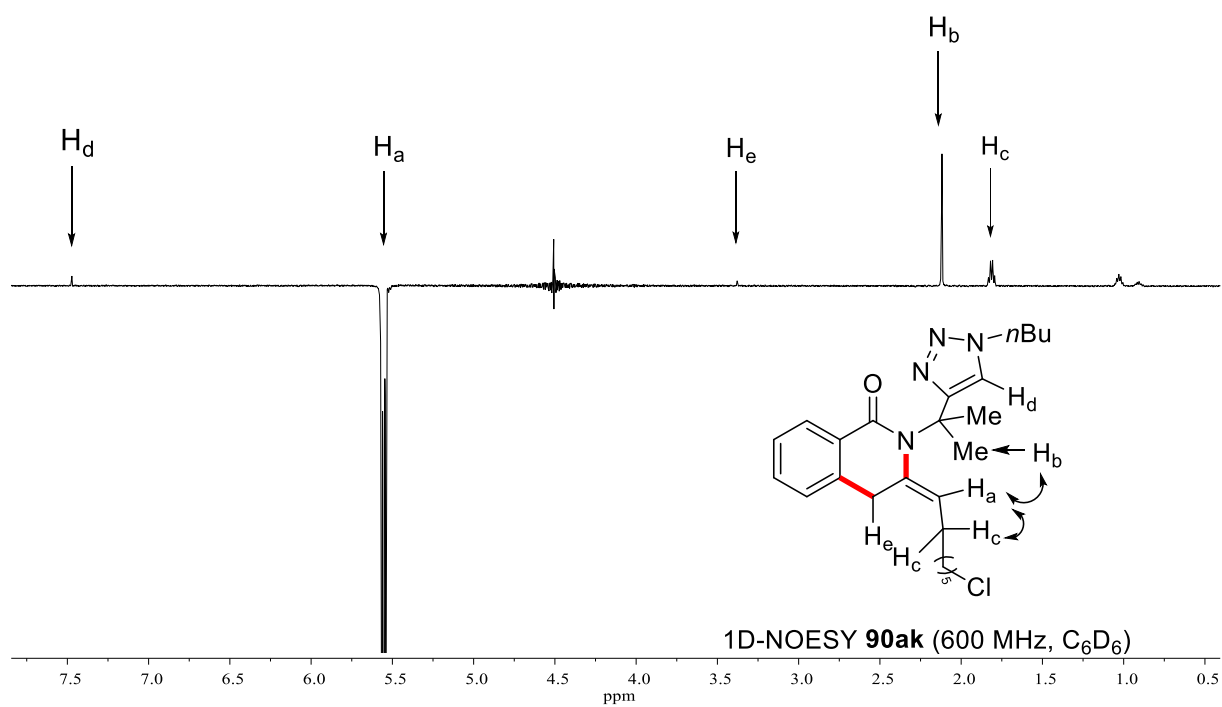
# NMR Spectra



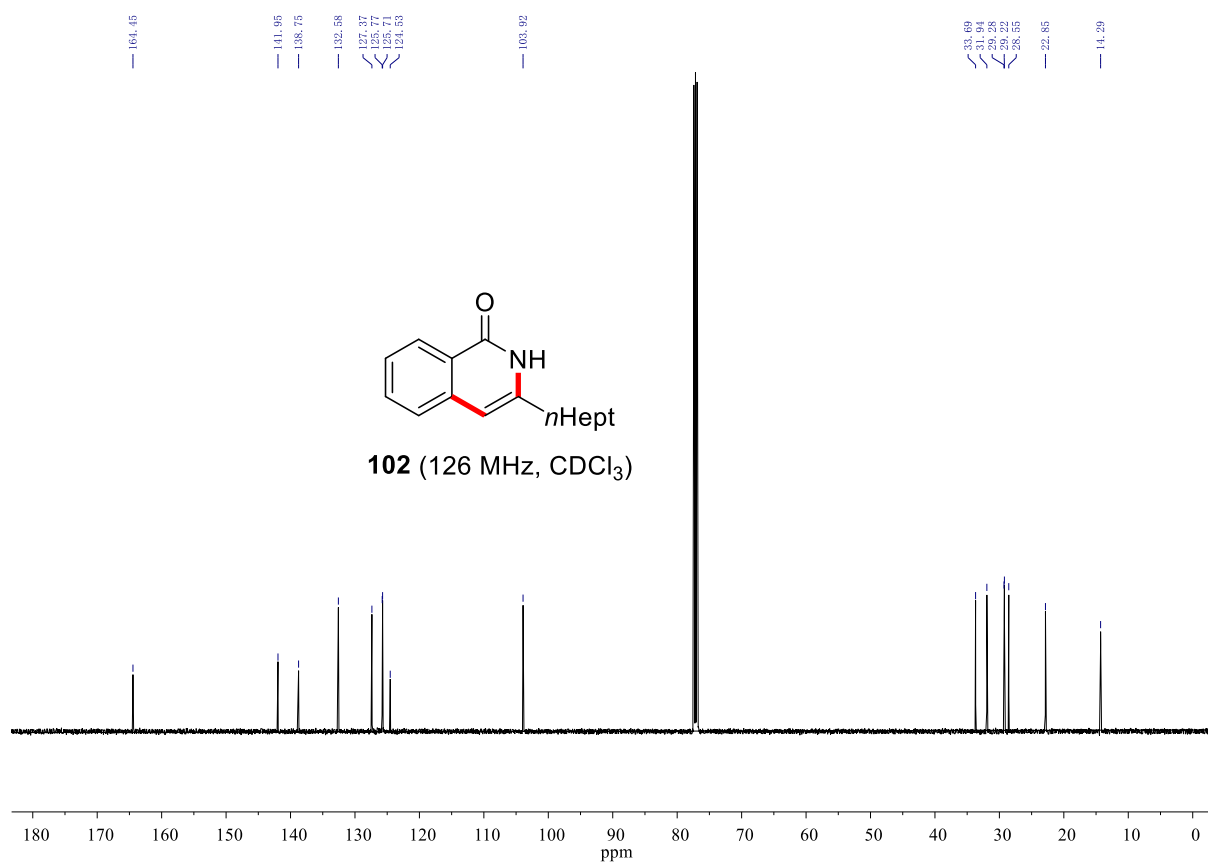
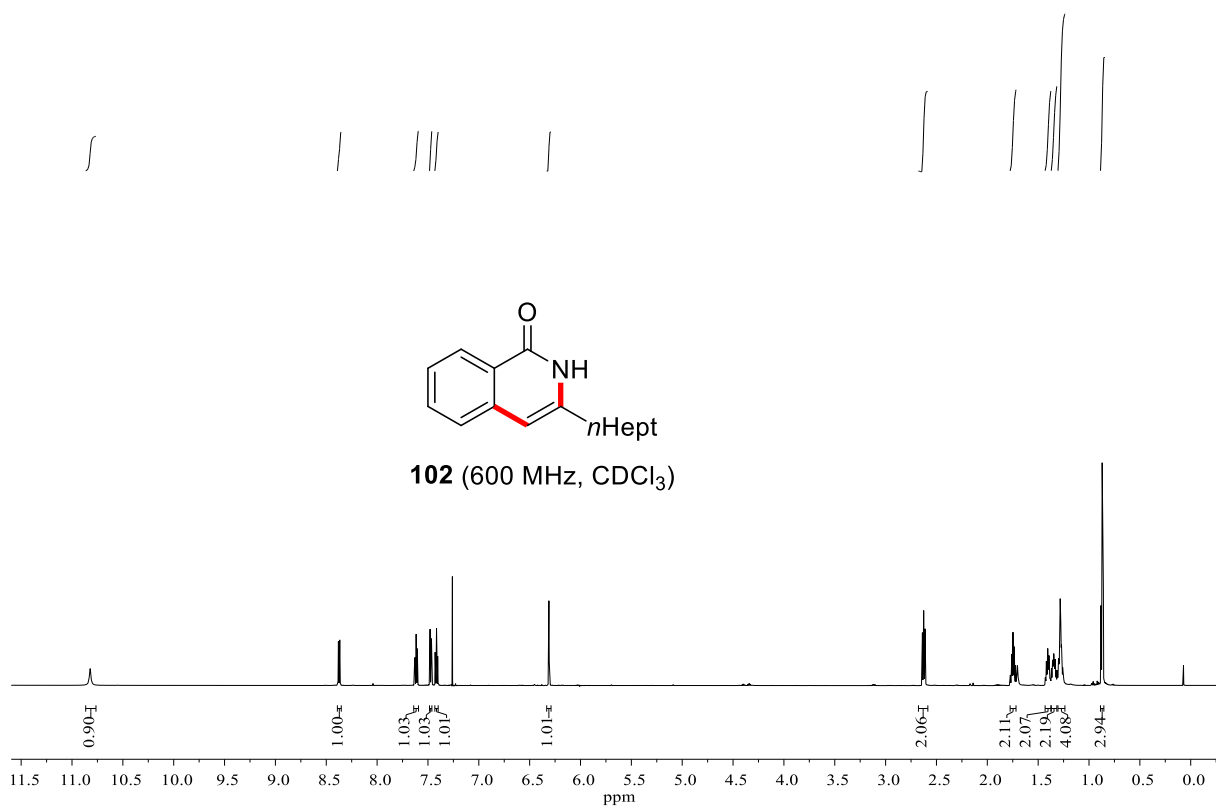
# NMR Spectra



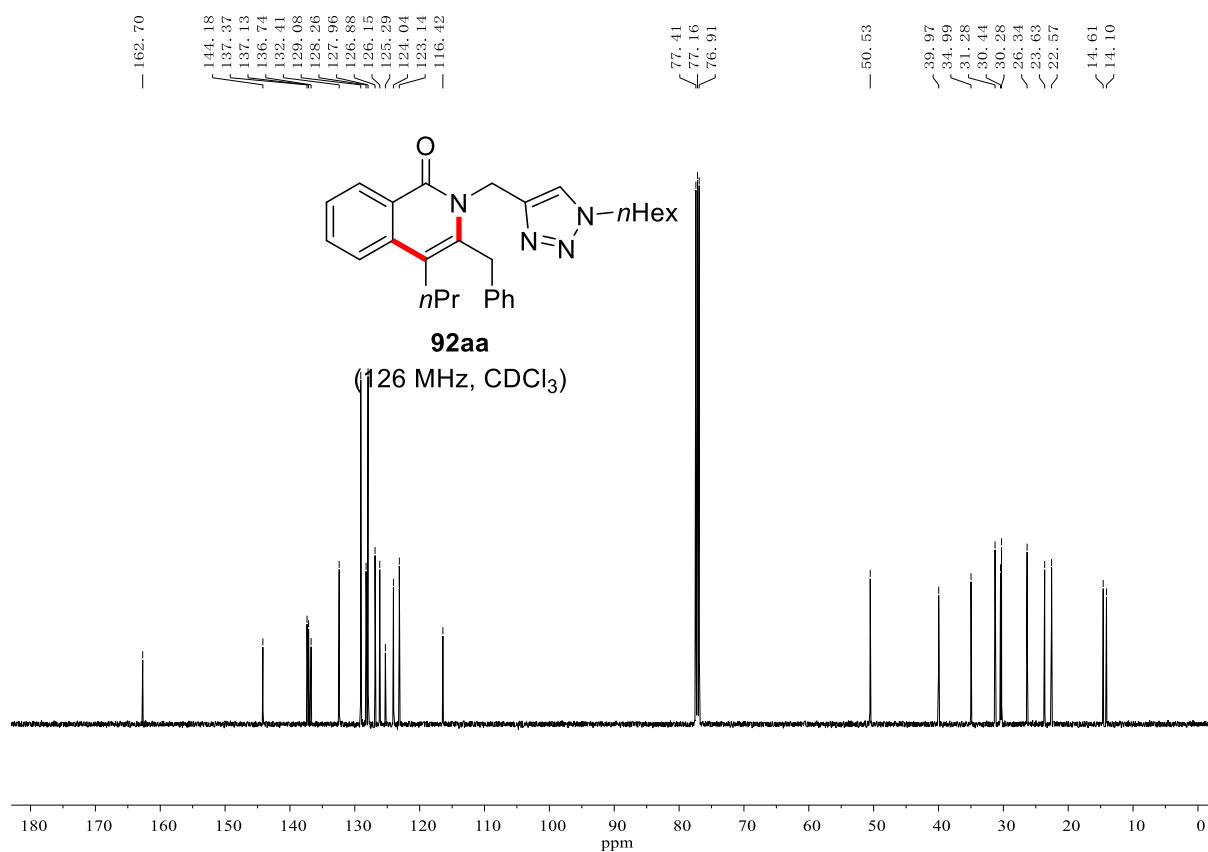
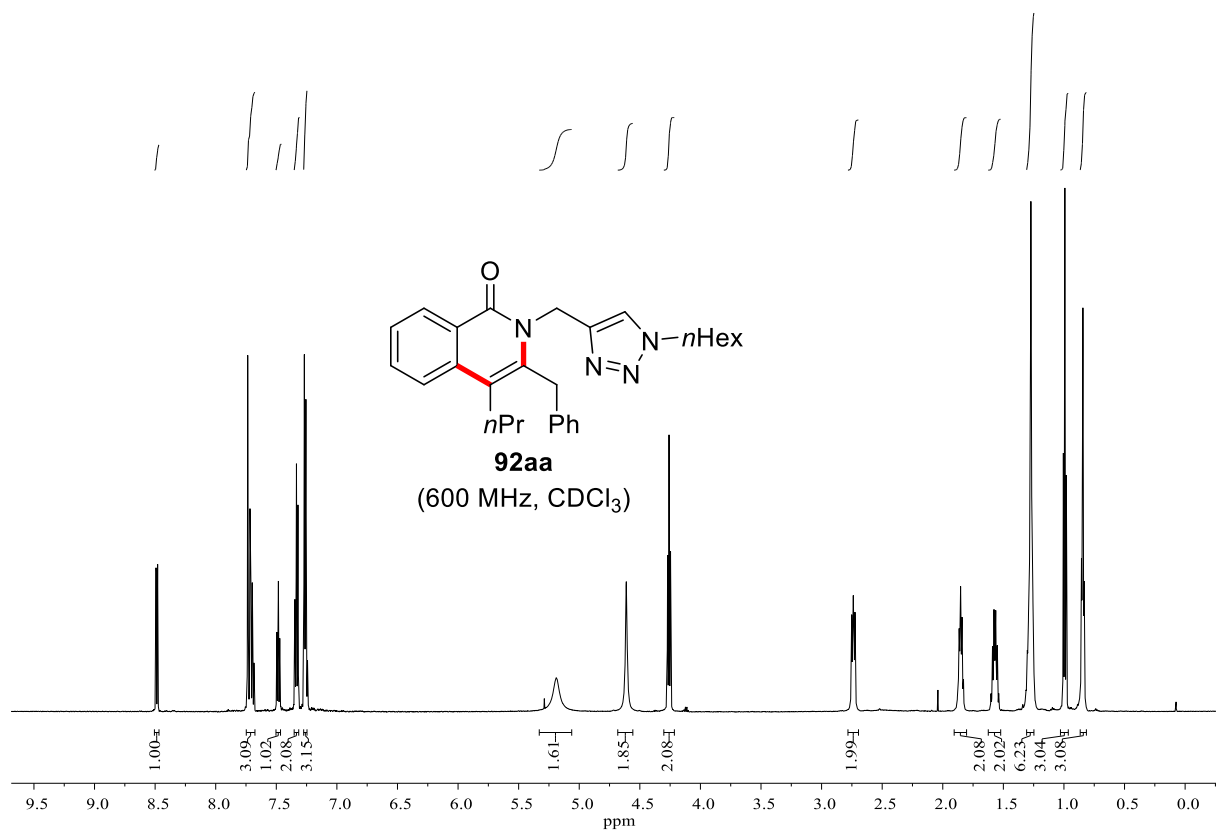
# NMR Spectra



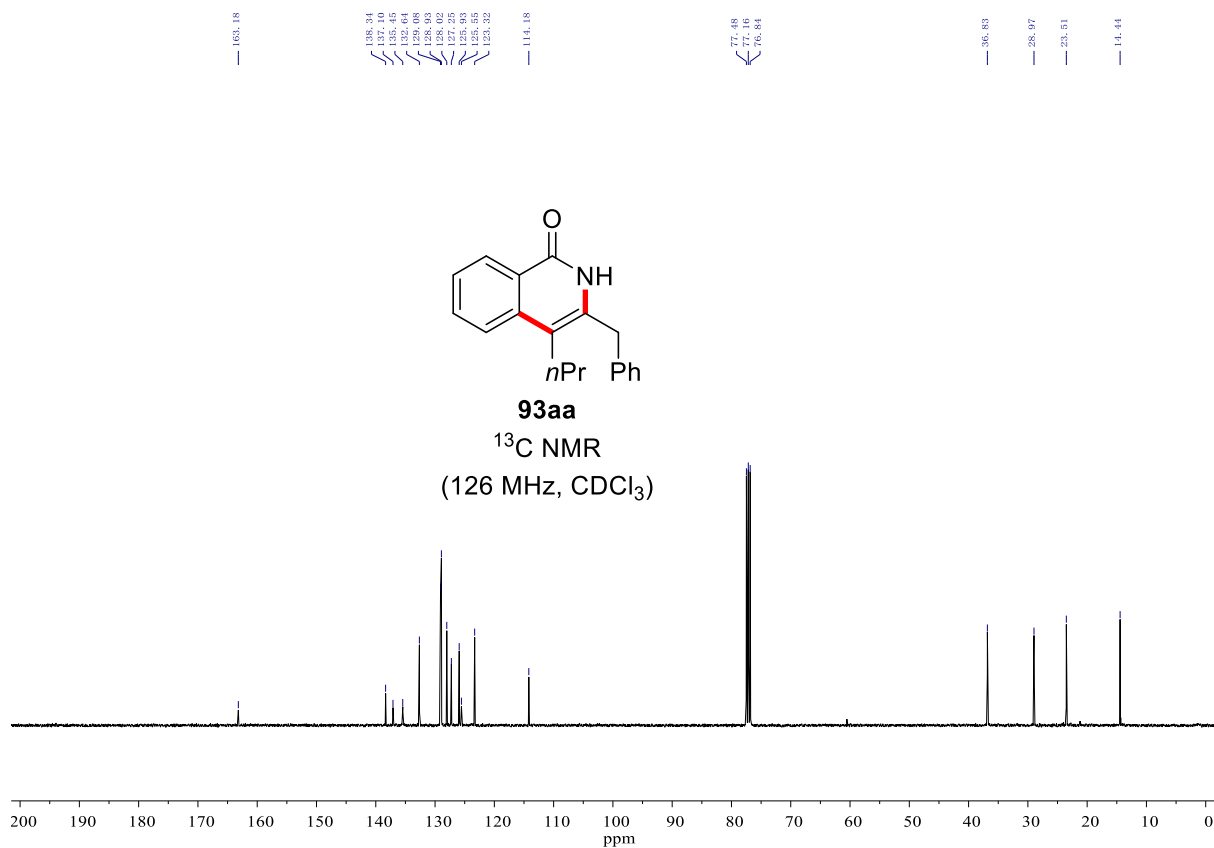
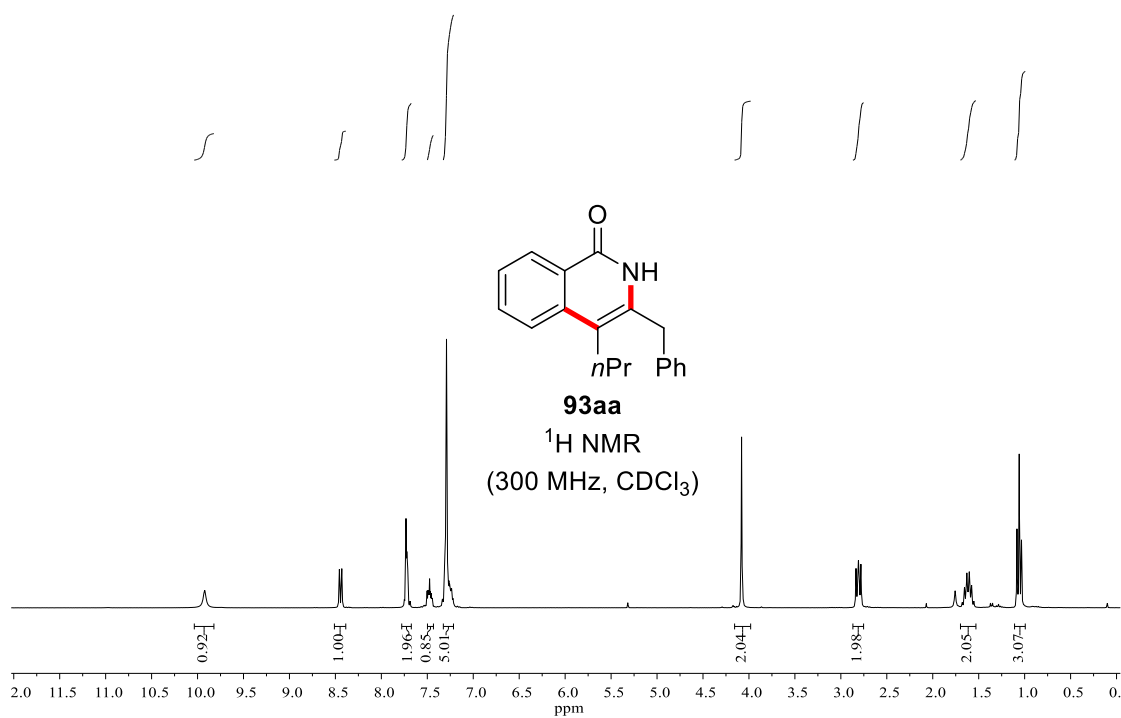
# NMR Spectra



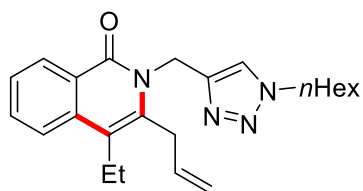
# NMR Spectra



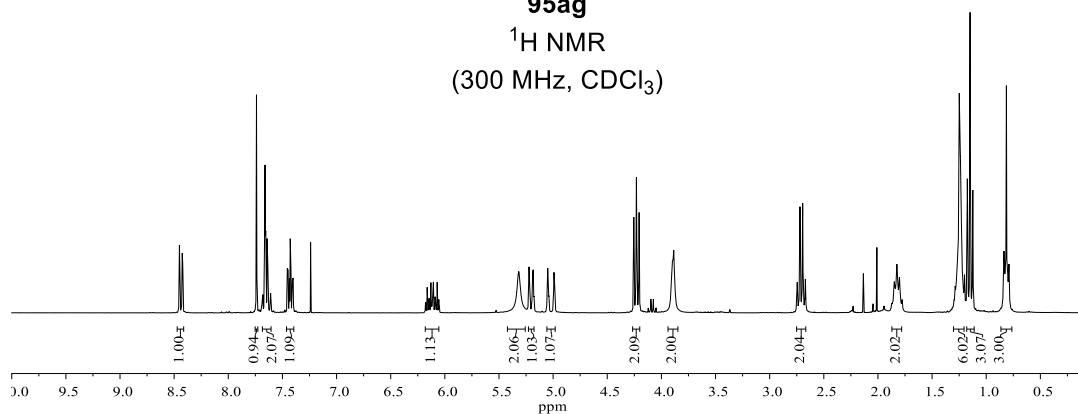
# NMR Spectra



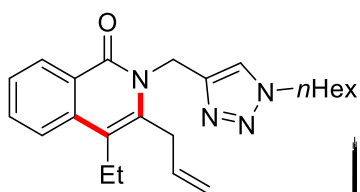
# NMR Spectra



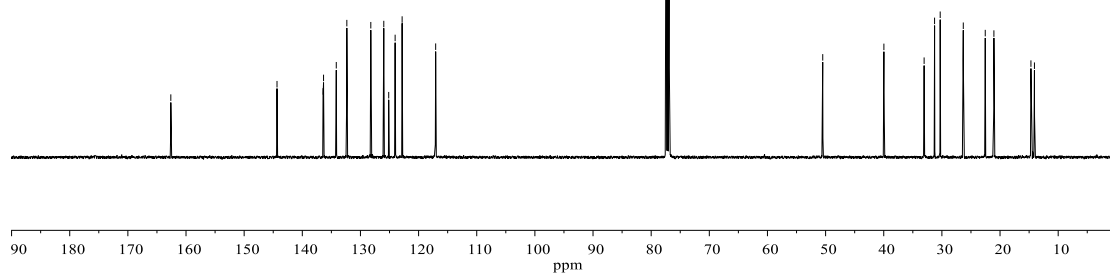
**95ag**  
 $^1\text{H}$  NMR  
 (300 MHz,  $\text{CDCl}_3$ )



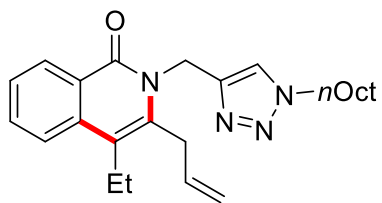
162.61  
 144.35  
 136.43  
 136.35  
 134.16  
 132.34  
 128.22  
 128.99  
 125.14  
 124.01  
 122.83  
 117.09  
 117.06  
 77.41  
 77.16  
 76.91  
 50.49  
 39.97  
 33.06  
 31.26  
 30.29  
 26.32  
 22.54  
 21.05  
 14.69  
 14.08



**95ag**  
 $^{13}\text{C}$  NMR  
 (126 MHz,  $\text{CDCl}_3$ )

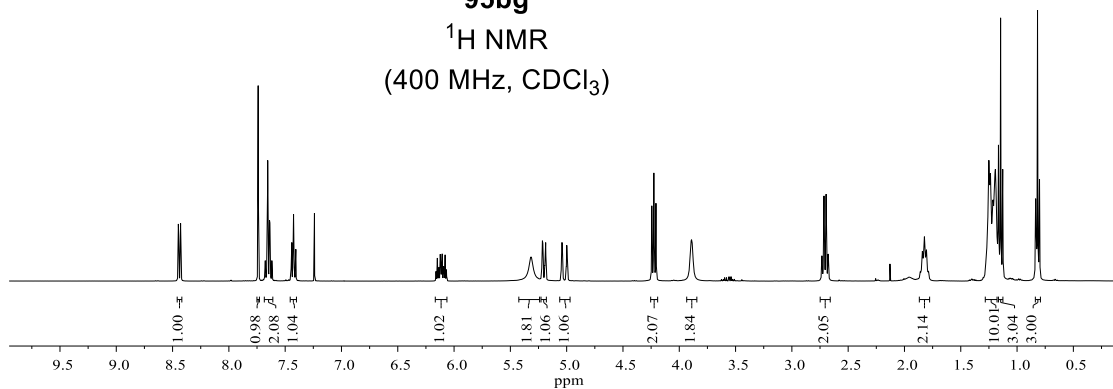


# NMR Spectra

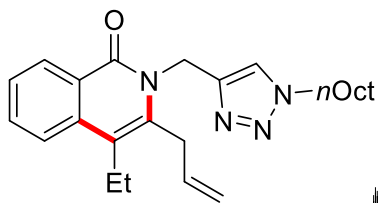


**95bg**

<sup>1</sup>H NMR  
(400 MHz, CDCl<sub>3</sub>)

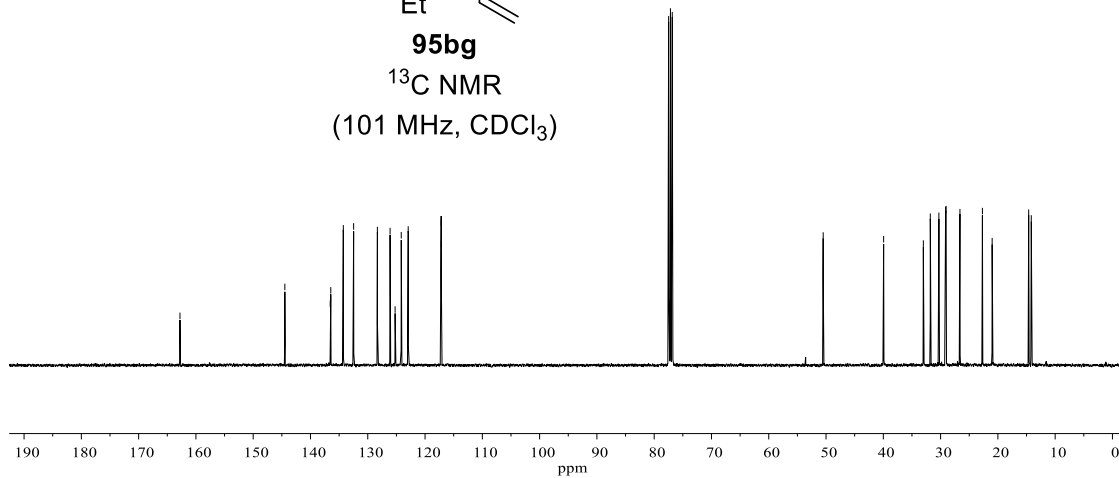


162.79  
144.48  
136.55  
136.46  
134.27  
132.47  
128.32  
126.11  
125.23  
124.15  
122.94  
117.19  
117.17  
77.48  
77.16  
76.84  
50.50  
39.94  
33.01  
31.80  
30.30  
29.12  
29.04  
26.62  
22.70  
21.00  
14.62  
14.17

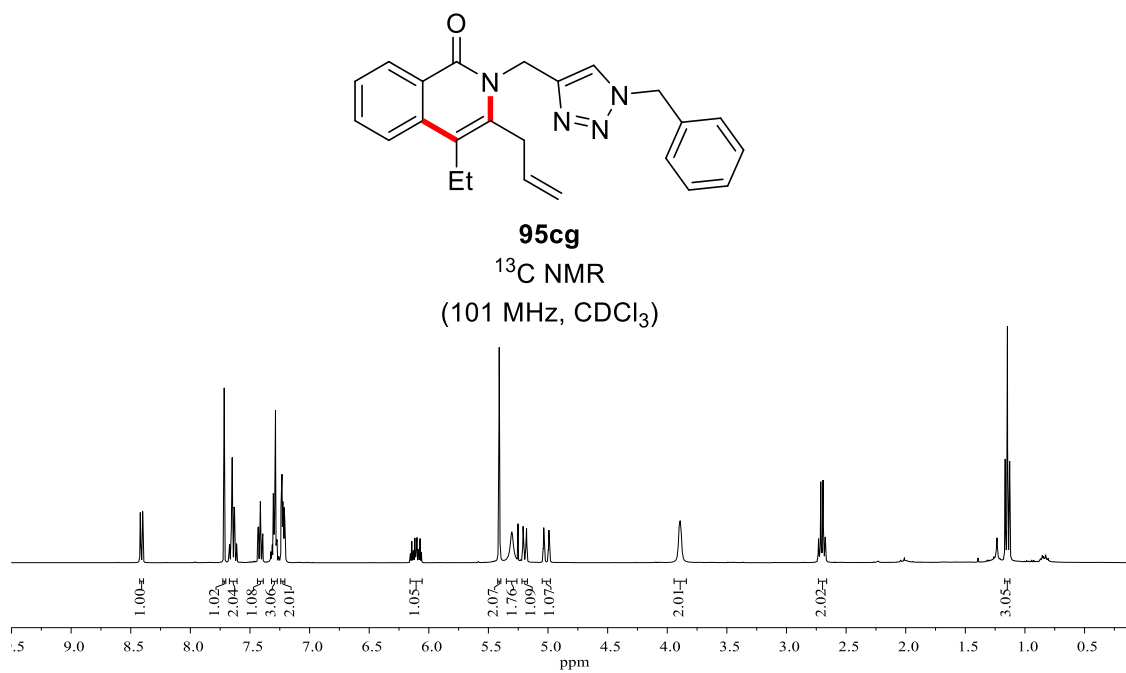
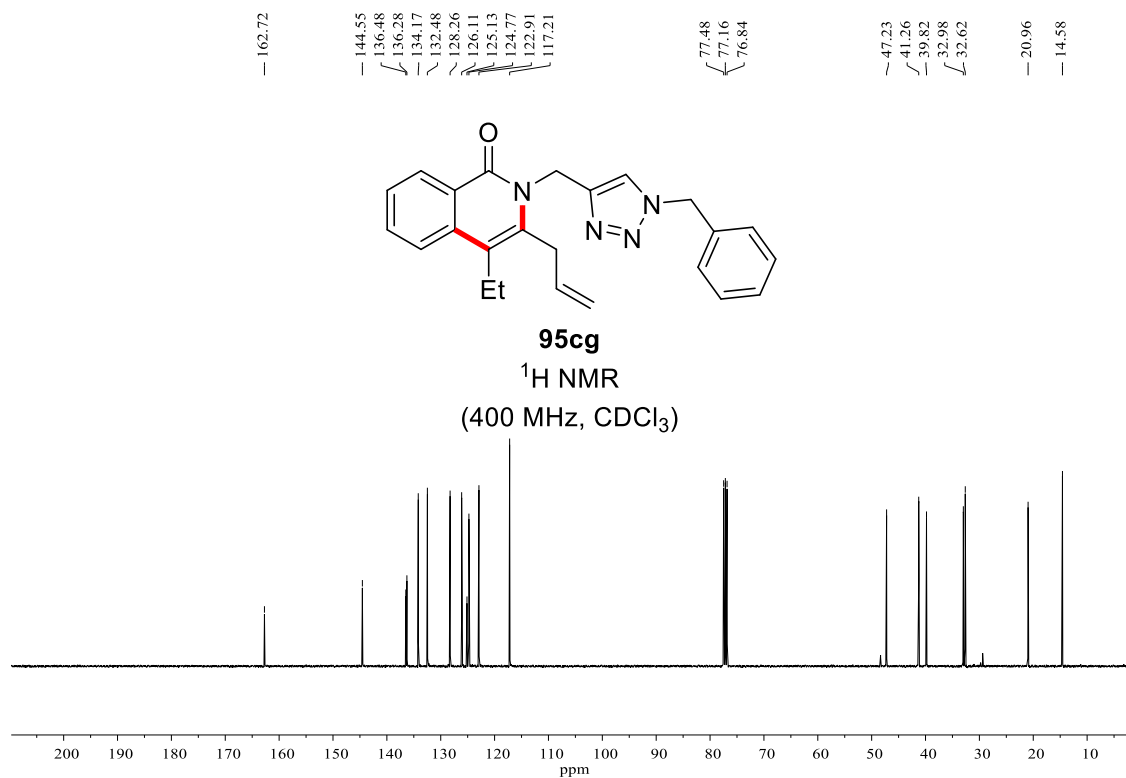


**95bg**

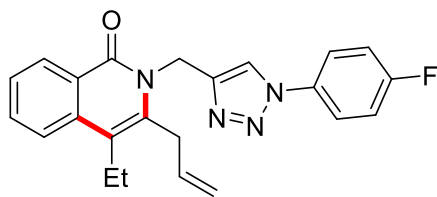
<sup>13</sup>C NMR  
(101 MHz, CDCl<sub>3</sub>)



# NMR Spectra

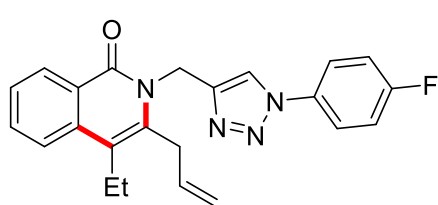
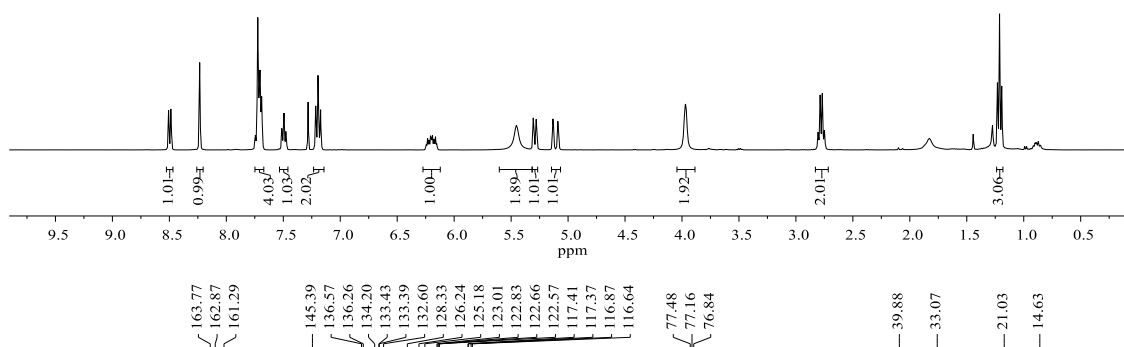


# NMR Spectra



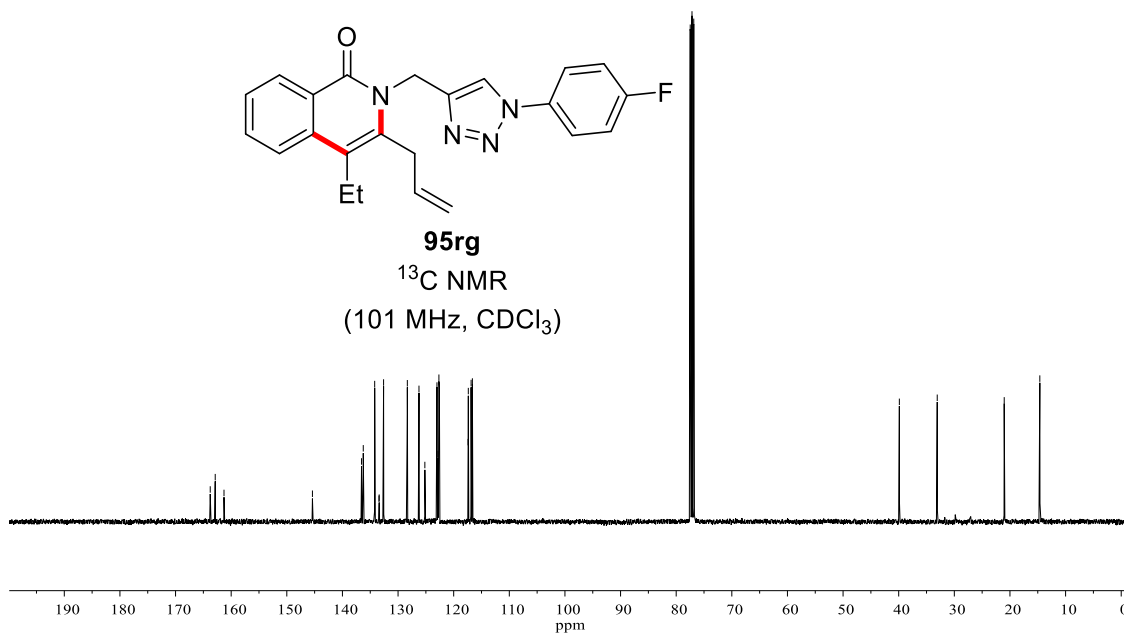
**95rg**

$^1\text{H}$  NMR  
(400 MHz,  $\text{CDCl}_3$ )

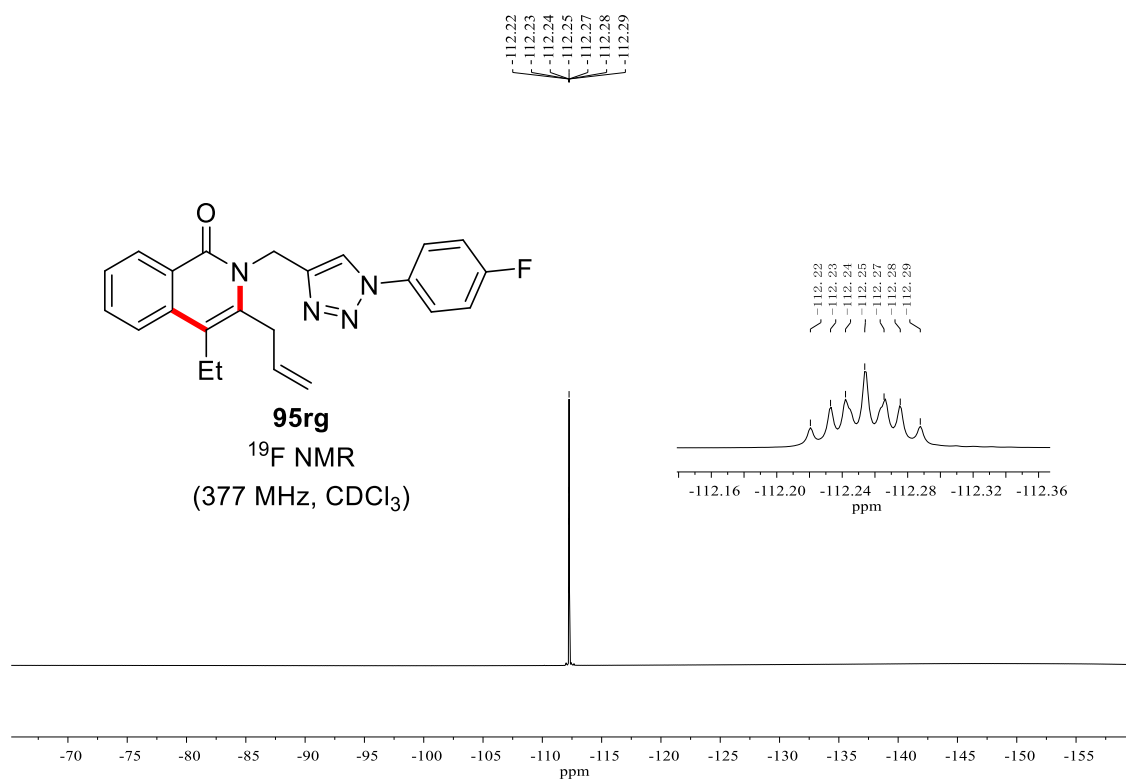


**95rg**

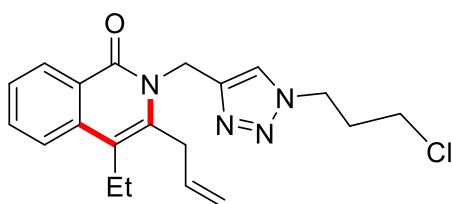
$^{13}\text{C}$  NMR  
(101 MHz,  $\text{CDCl}_3$ )



# NMR Spectra

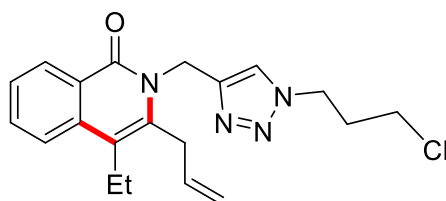
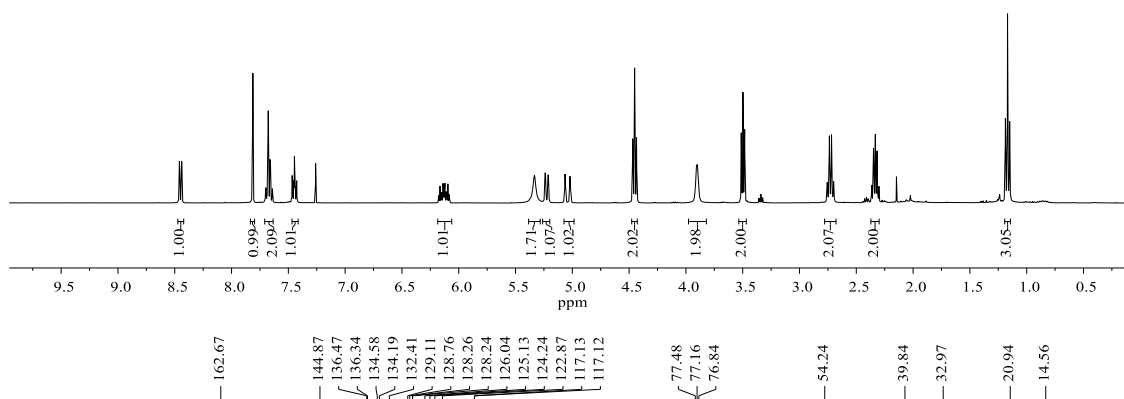


# NMR Spectra



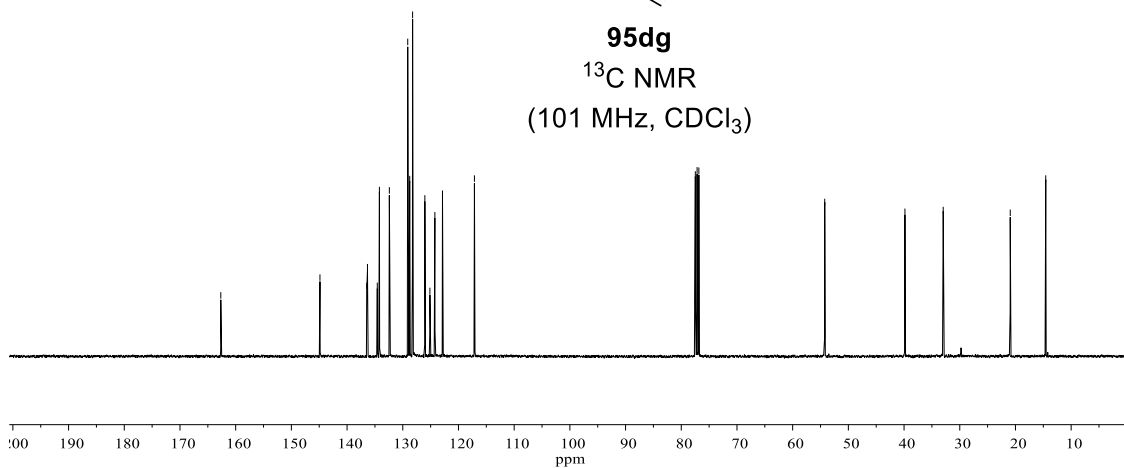
**95dg**

$^1\text{H}$  NMR  
(400 MHz,  $\text{CDCl}_3$ )

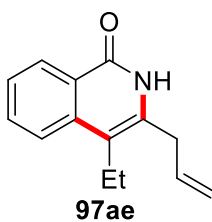


**95dg**

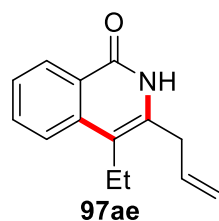
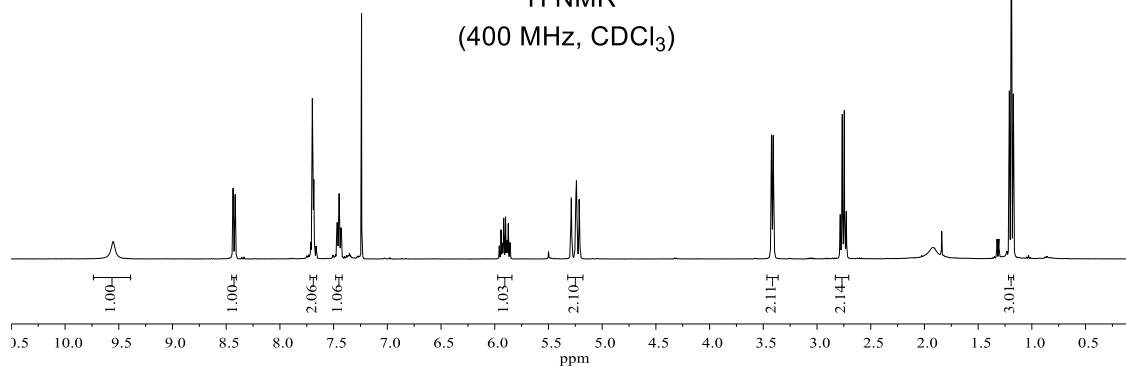
$^{13}\text{C}$  NMR  
(101 MHz,  $\text{CDCl}_3$ )



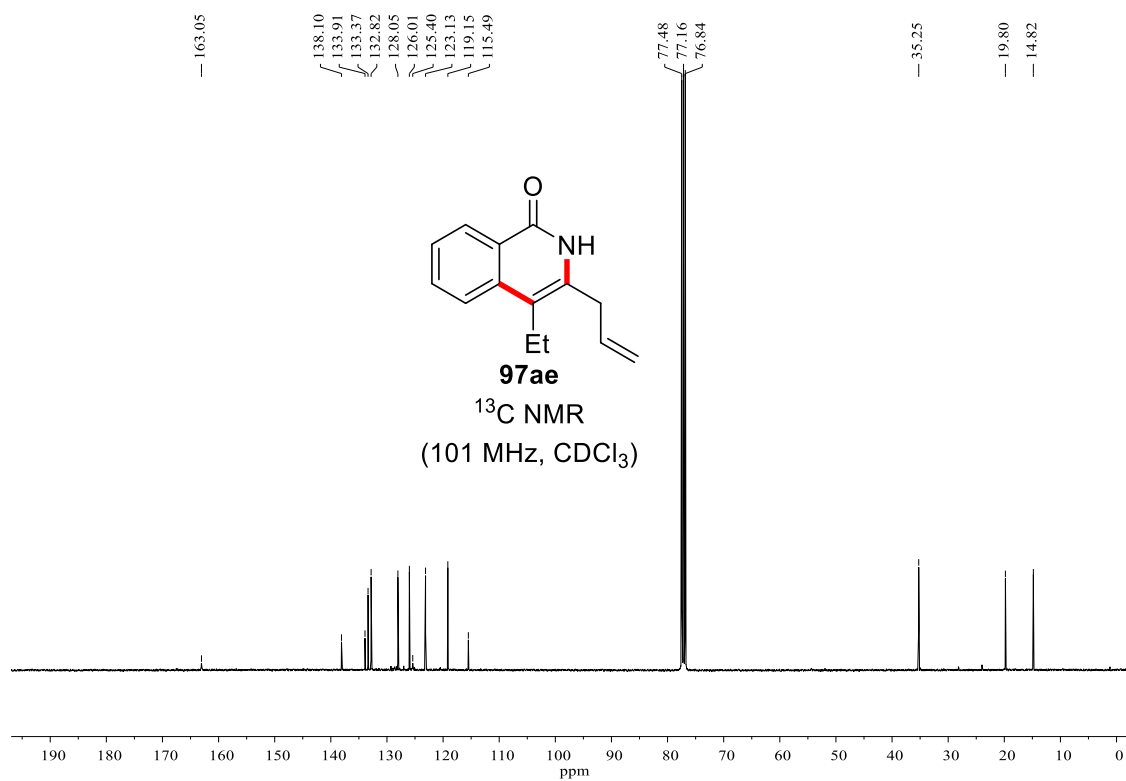
# NMR Spectra



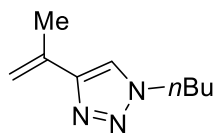
$^1\text{H}$  NMR  
(400 MHz,  $\text{CDCl}_3$ )



$^{13}\text{C}$  NMR  
(101 MHz,  $\text{CDCl}_3$ )

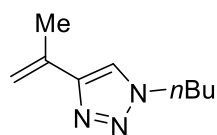
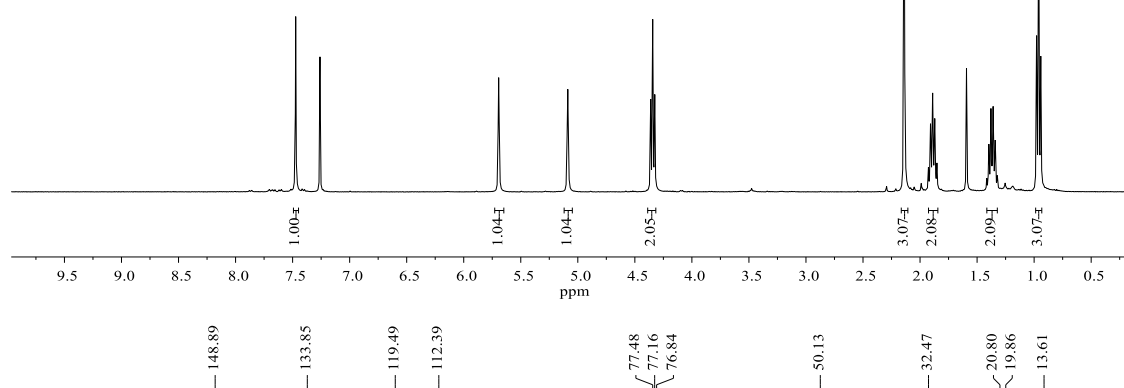


# NMR Spectra



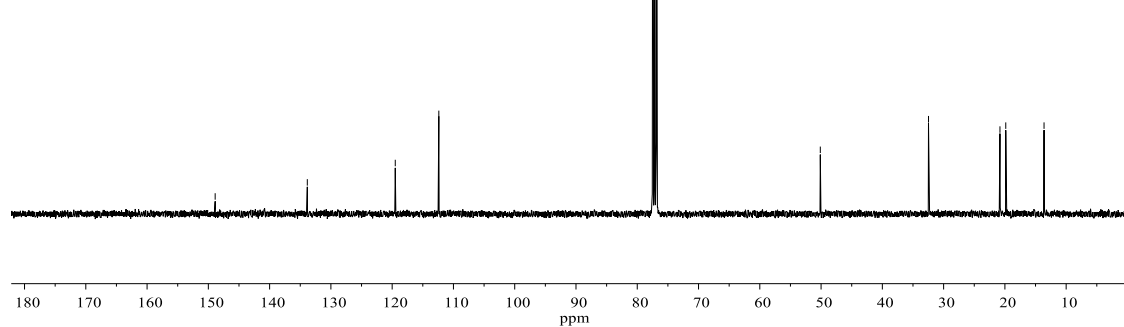
**119**

<sup>1</sup>H NMR  
(400 MHz, CDCl<sub>3</sub>)

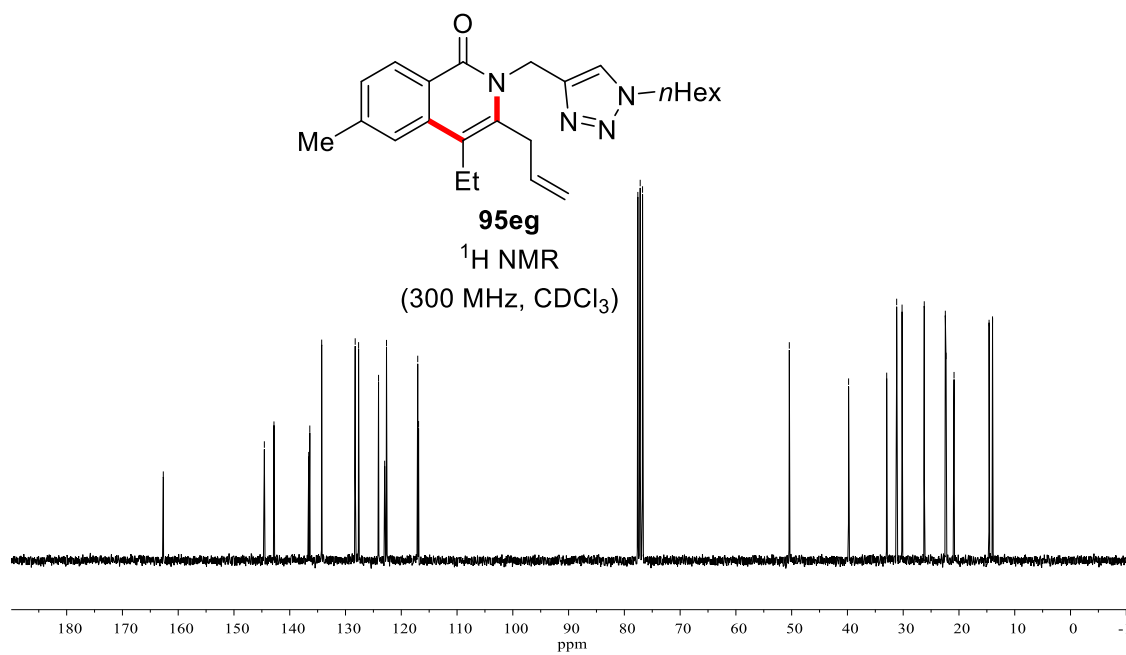
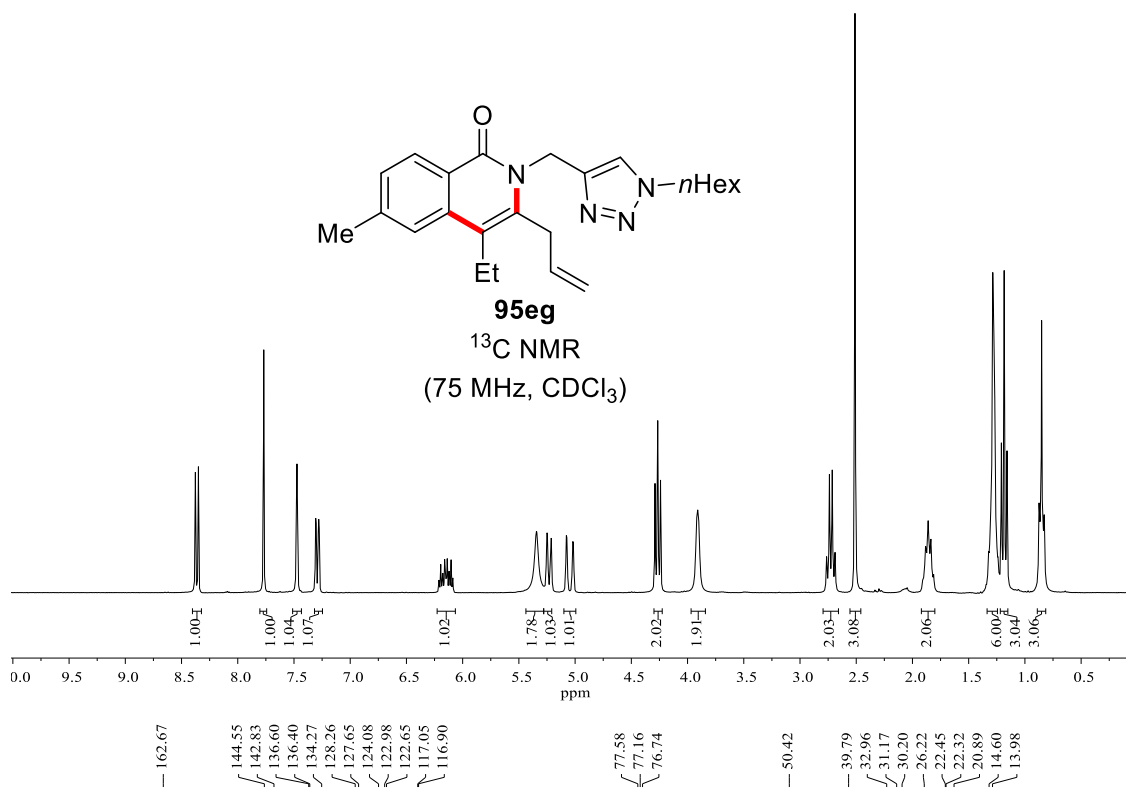


**119**

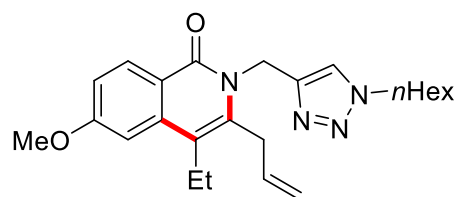
<sup>13</sup>C NMR  
(101 MHz, CDCl<sub>3</sub>)



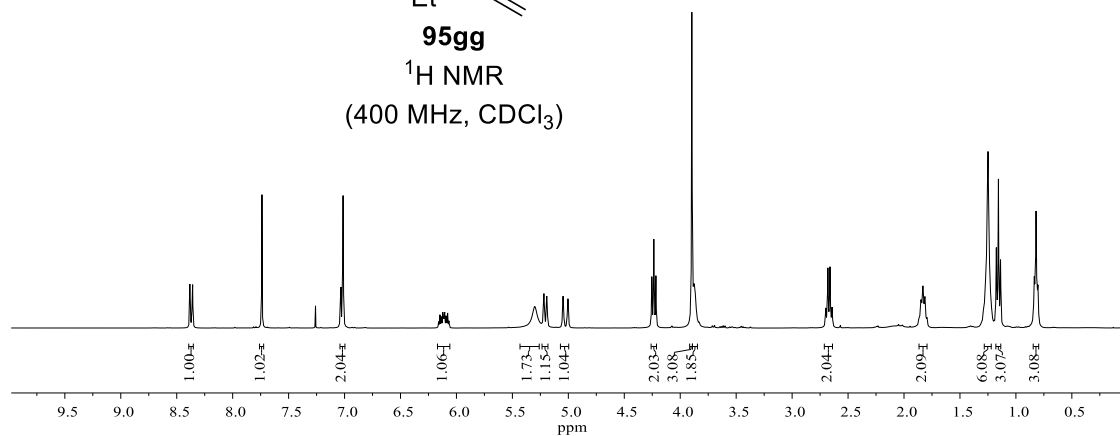
# NMR Spectra



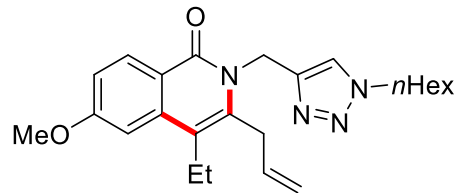
# NMR Spectra



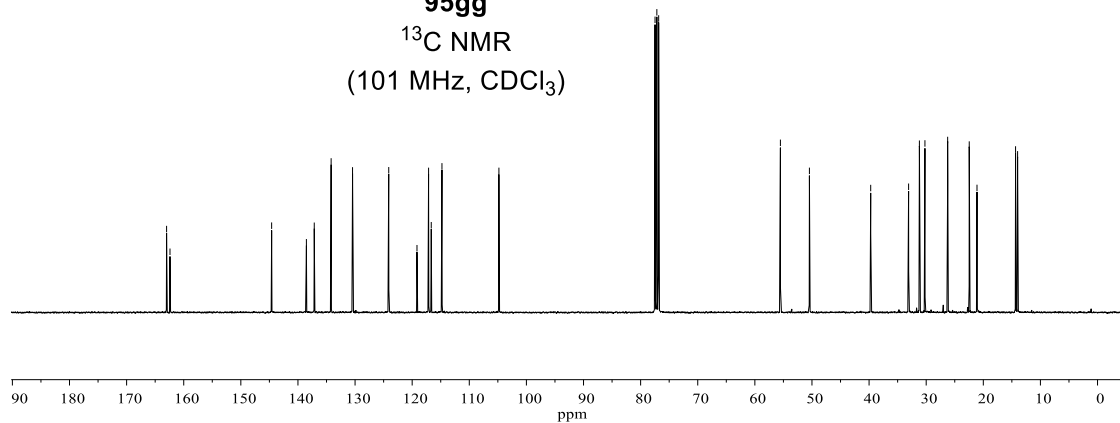
**95gg**  
 $^1\text{H}$  NMR  
 (400 MHz,  $\text{CDCl}_3$ )



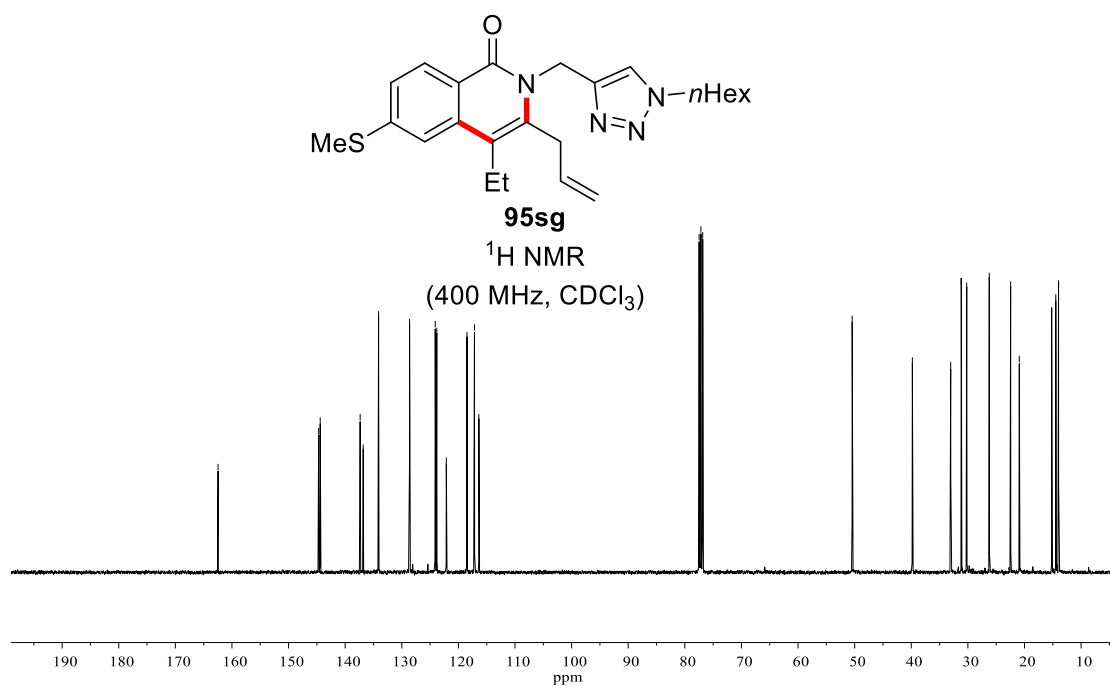
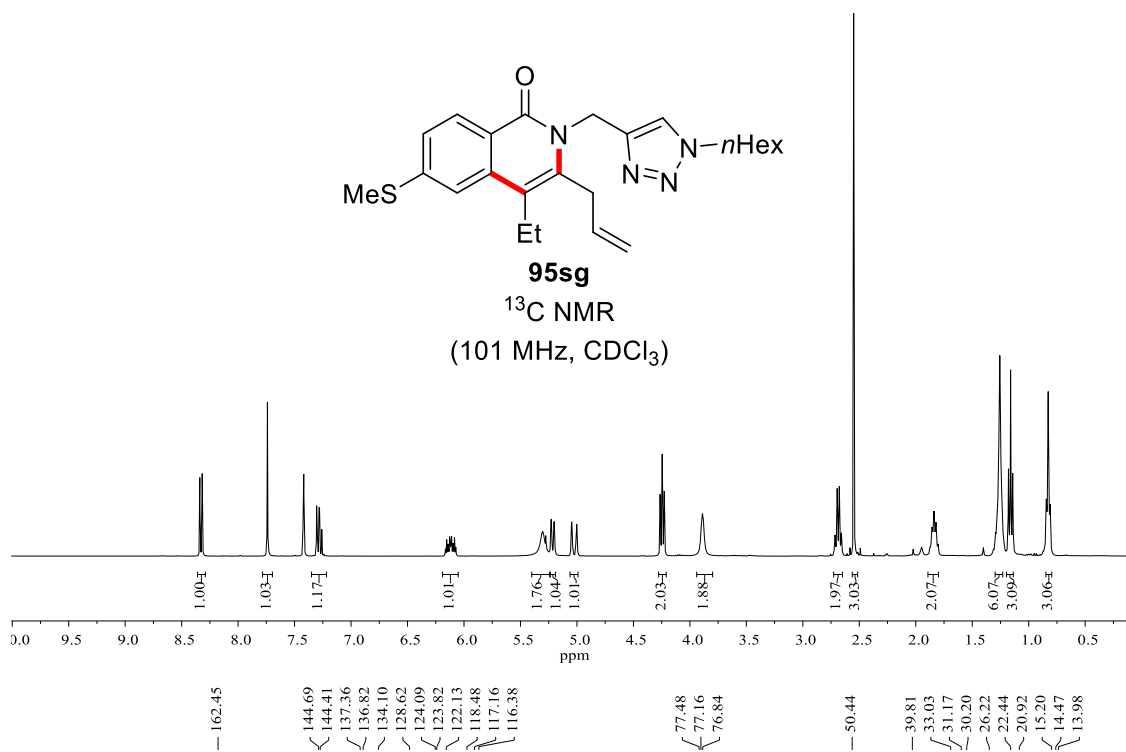
163.00  
 162.40  
 144.61  
 138.52  
 137.15  
 134.19  
 130.44  
 124.10  
 119.16  
 117.13  
 116.66  
 114.78  
 104.81  
 77.48  
 77.16  
 76.84  
 55.53  
 50.45  
 39.71  
 33.08  
 31.19  
 30.22  
 26.24  
 22.46  
 21.10  
 14.35  
 14.00



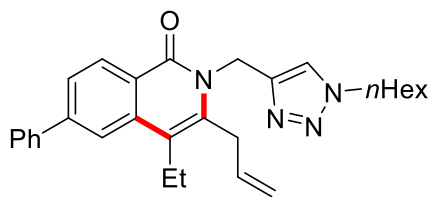
**95gg**  
 $^{13}\text{C}$  NMR  
 (101 MHz,  $\text{CDCl}_3$ )



# NMR Spectra

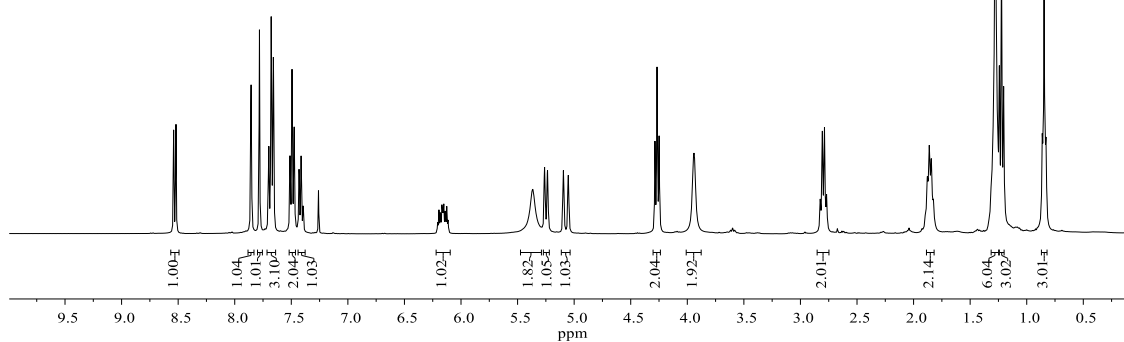


# NMR Spectra

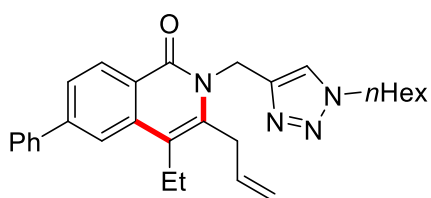


**95fg**

$^1\text{H}$  NMR  
(400 MHz,  $\text{CDCl}_3$ )

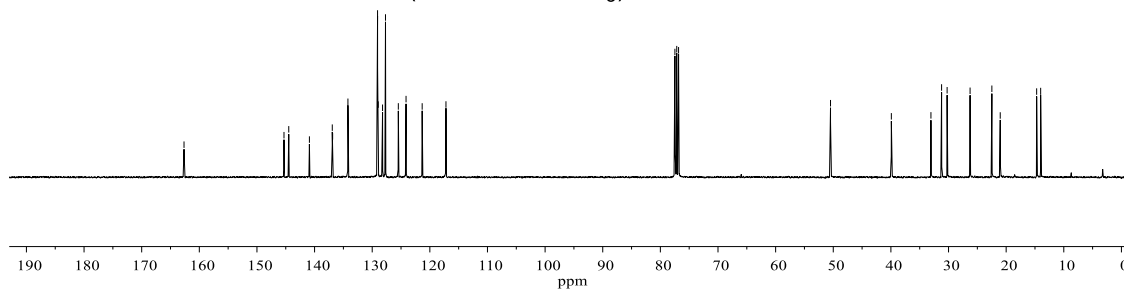


$^1\text{H}$  NMR peak list (ppm): 162.65, 145.31, 144.48, 140.90, 136.93, 136.87, 134.21, 129.07, 128.95, 128.21, 127.69, 125.47, 124.13, 124.11, 121.33, 117.23, 117.20, 77.48, 77.16, 76.84, 50.48, 39.92, 33.05, 31.20, 30.24, 26.26, 22.48, 21.03, 14.71, 14.01.

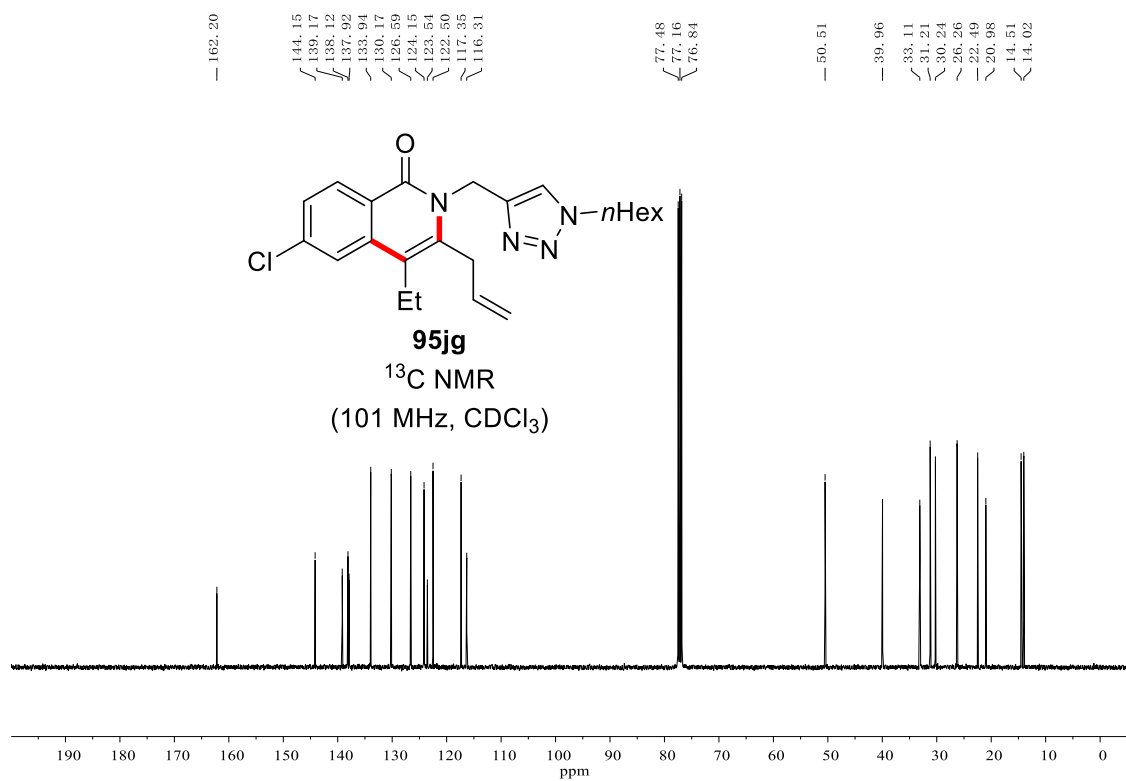
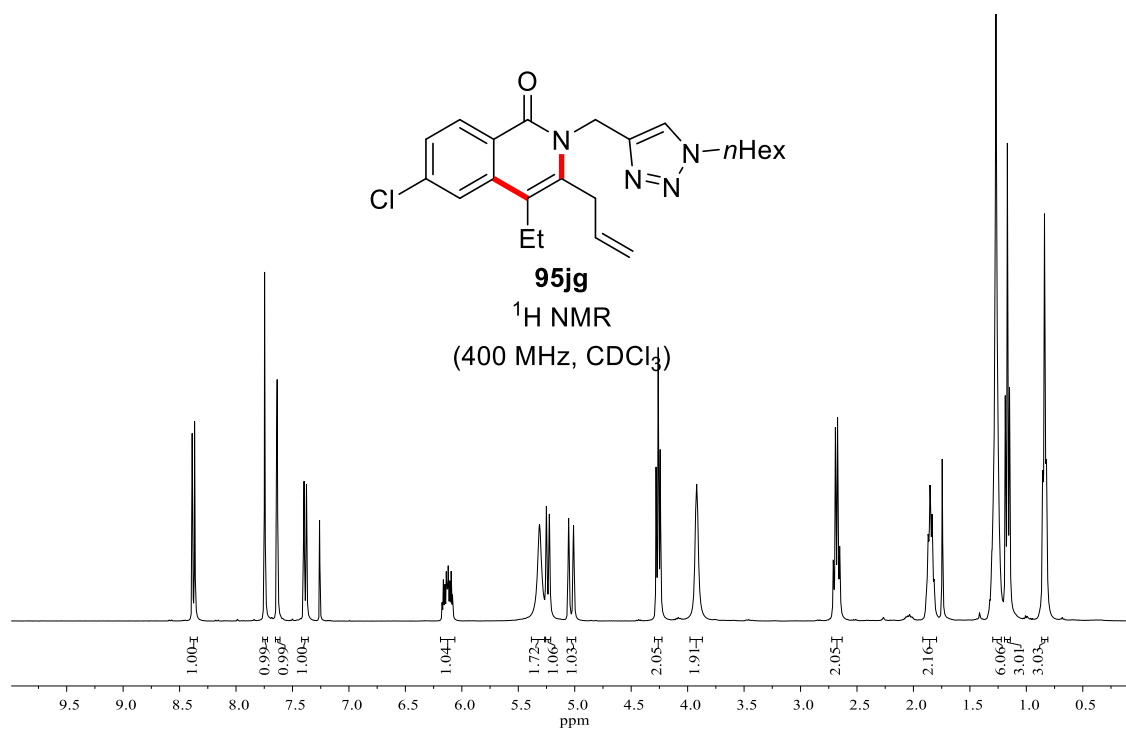


**95fg**

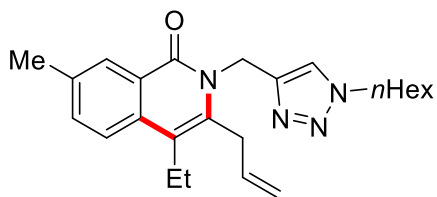
$^{13}\text{C}$  NMR  
(101 MHz,  $\text{CDCl}_3$ )



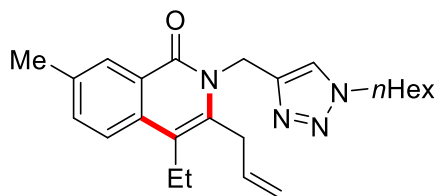
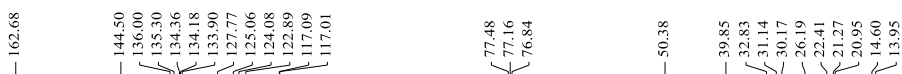
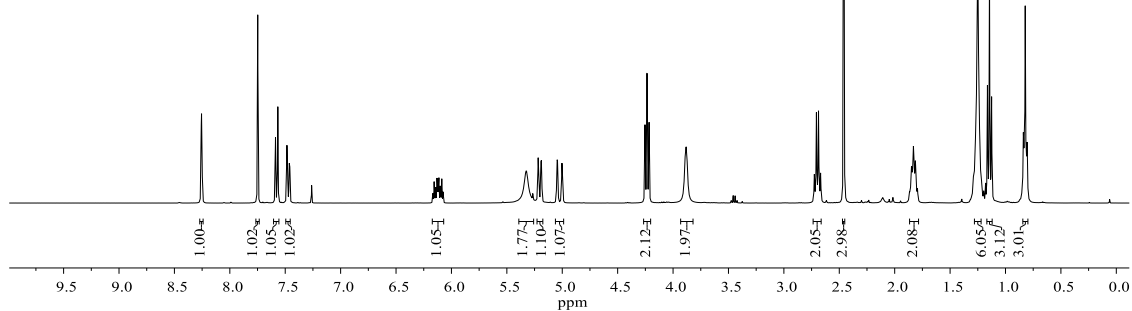
# NMR Spectra



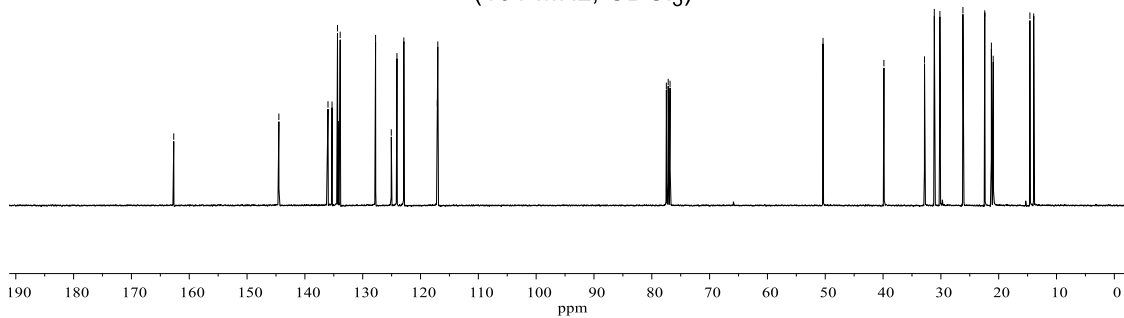
# NMR Spectra



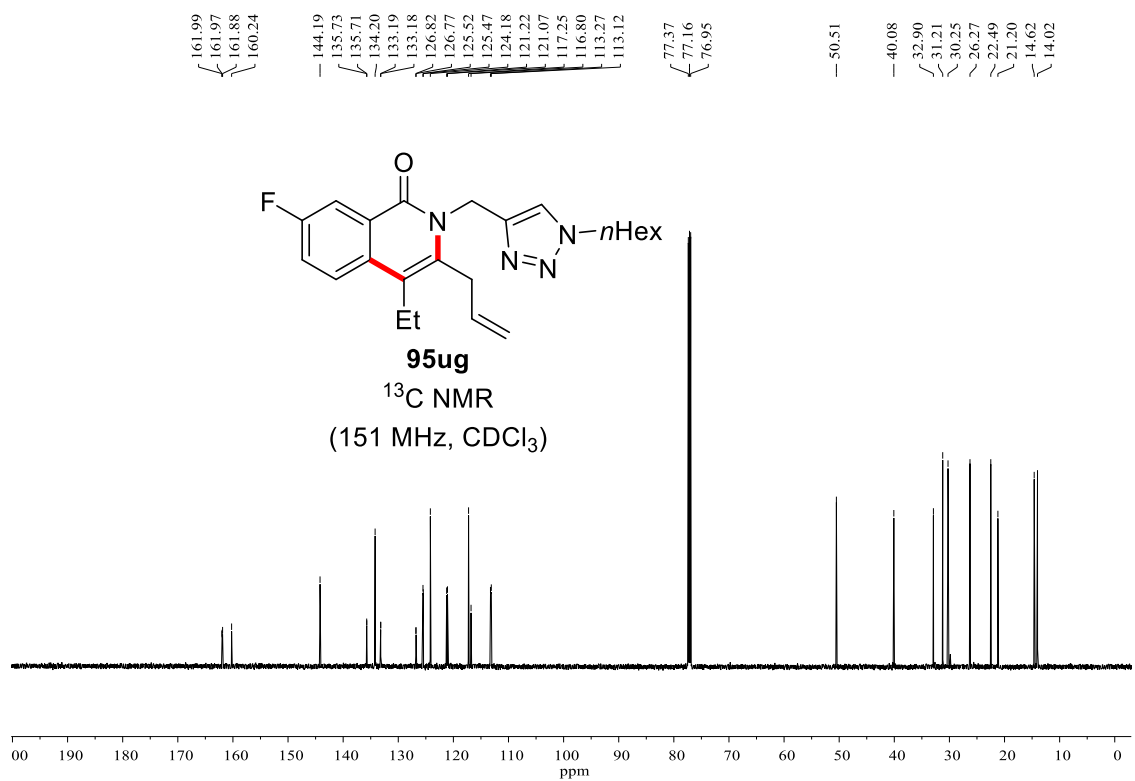
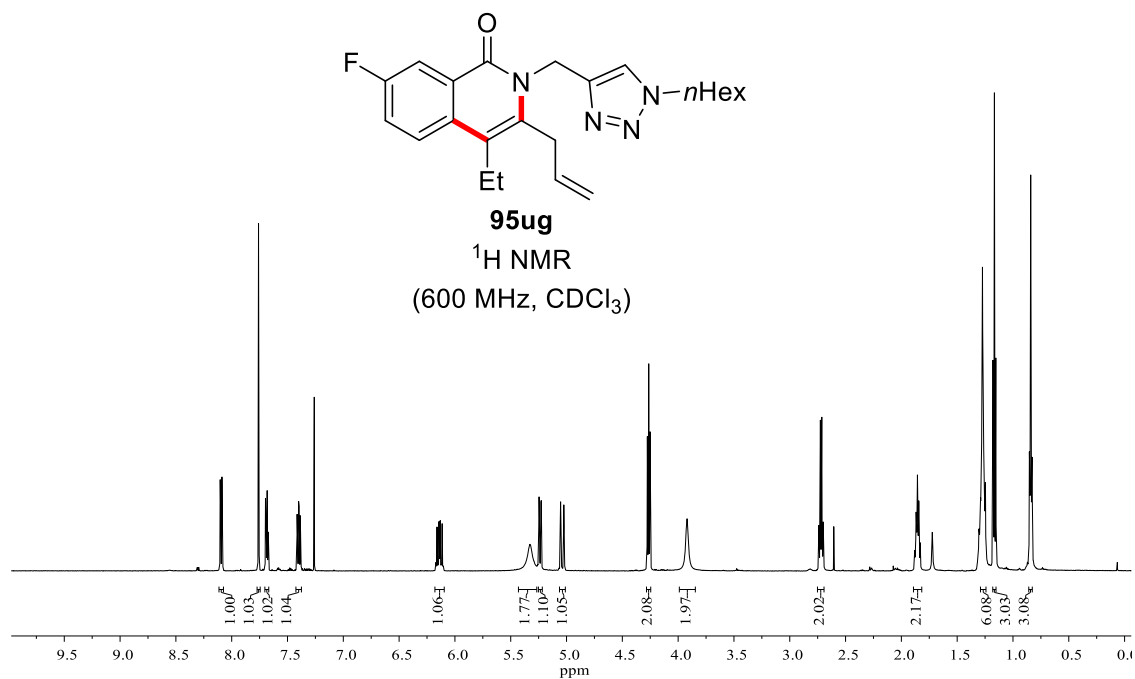
**95tg**  
 $^1\text{H}$  NMR  
 (400 MHz,  $\text{CDCl}_3$ )



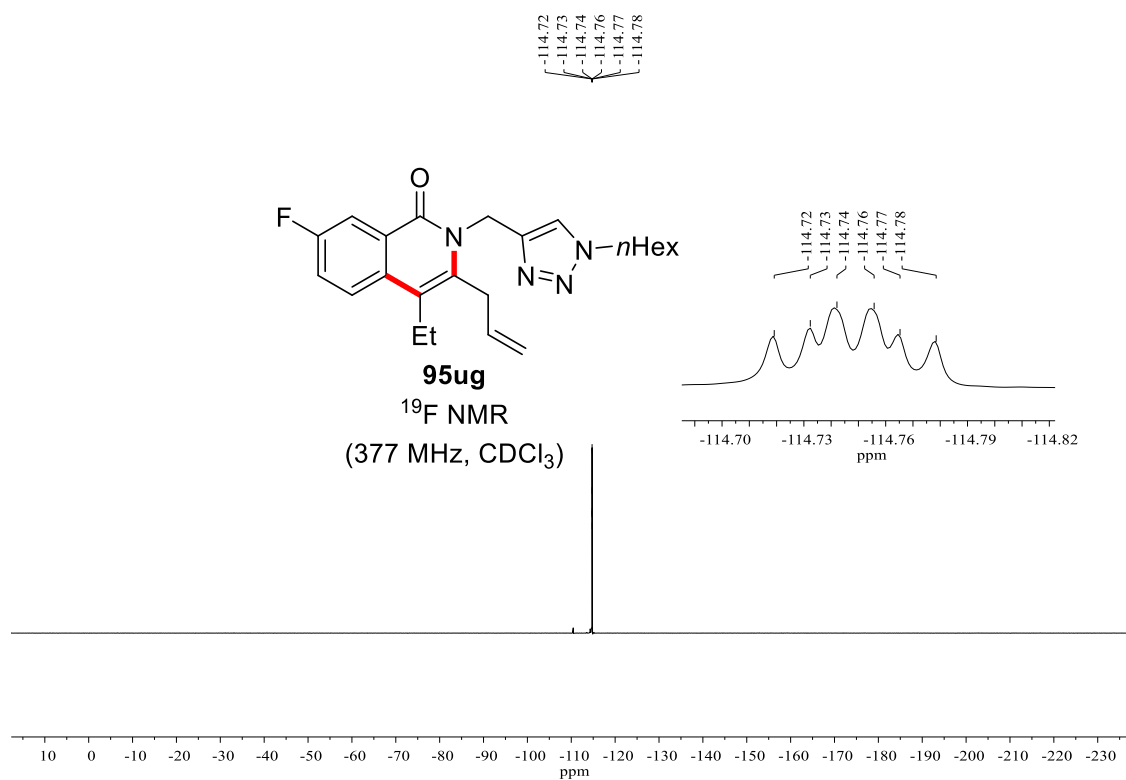
**95tg**  
 $^{13}\text{C}$  NMR  
 (101 MHz,  $\text{CDCl}_3$ )



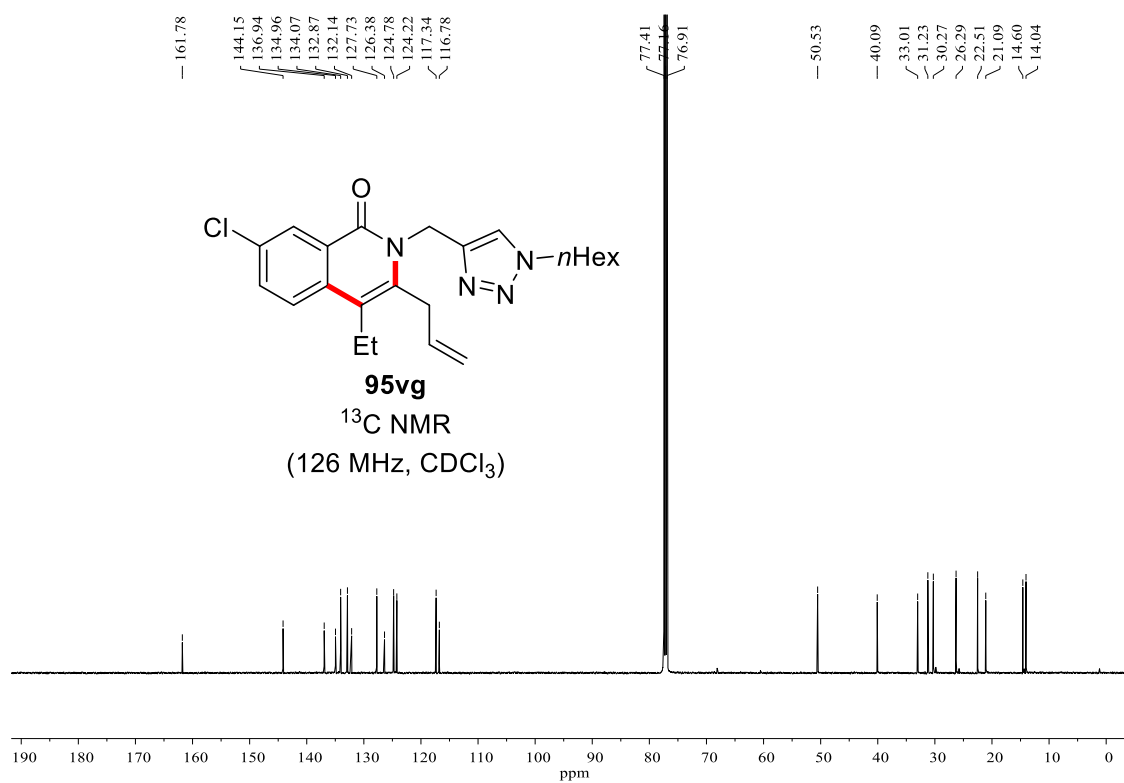
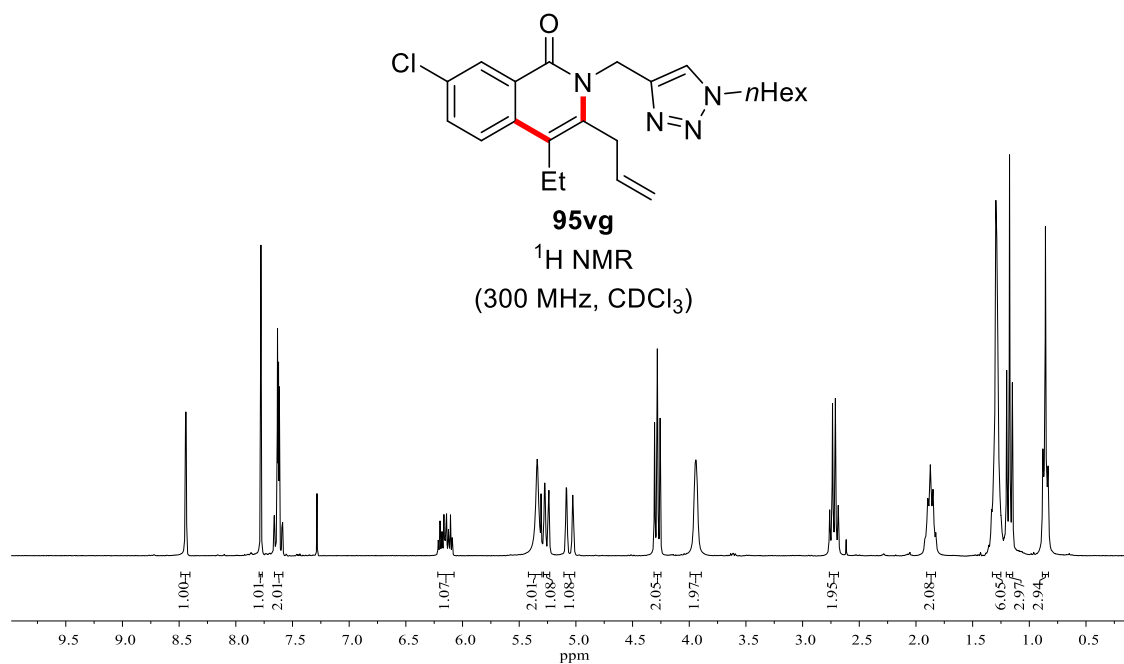
# NMR Spectra



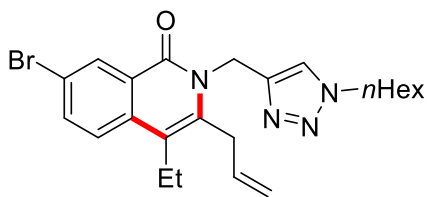
# NMR Spectra



# NMR Spectra



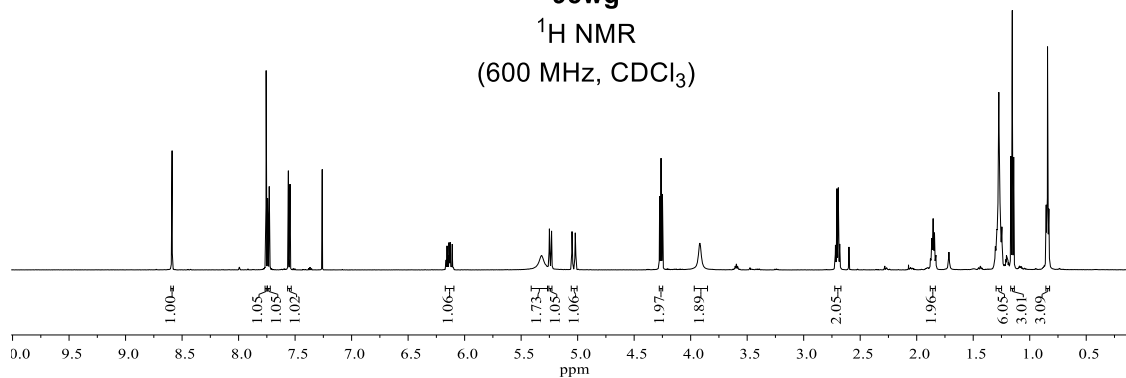
# NMR Spectra



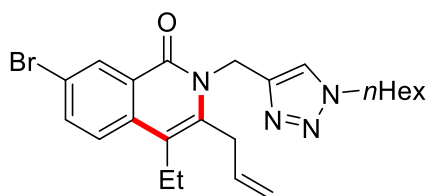
**95wg**

<sup>1</sup>H NMR

(600 MHz, CDCl<sub>3</sub>)



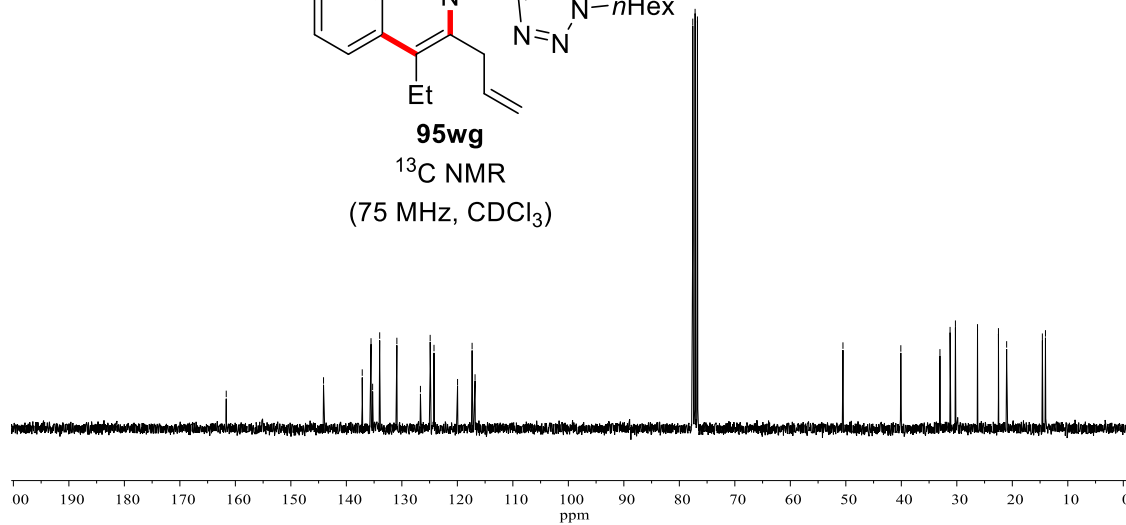
161.64, 144.11, 137.14, 135.56, 135.27, 133.99, 130.90, 126.65, 124.90, 124.21, 119.96, 117.34, 116.81, 77.58, 77.16, 76.74, 50.52, 40.09, 33.04, 31.21, 30.25, 26.27, 22.50, 21.02, 14.58, 14.03



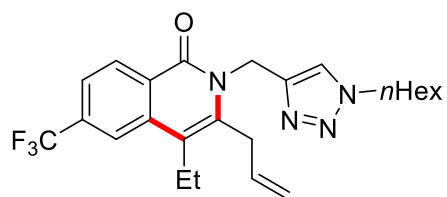
**95wg**

<sup>13</sup>C NMR

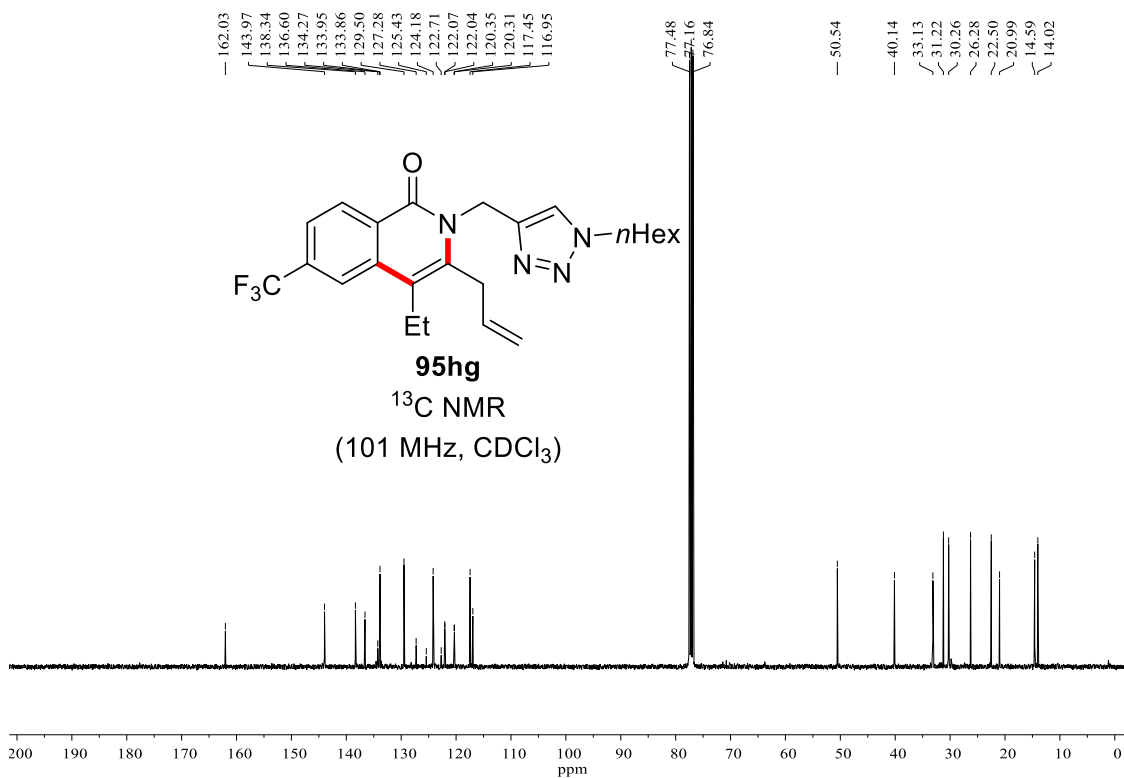
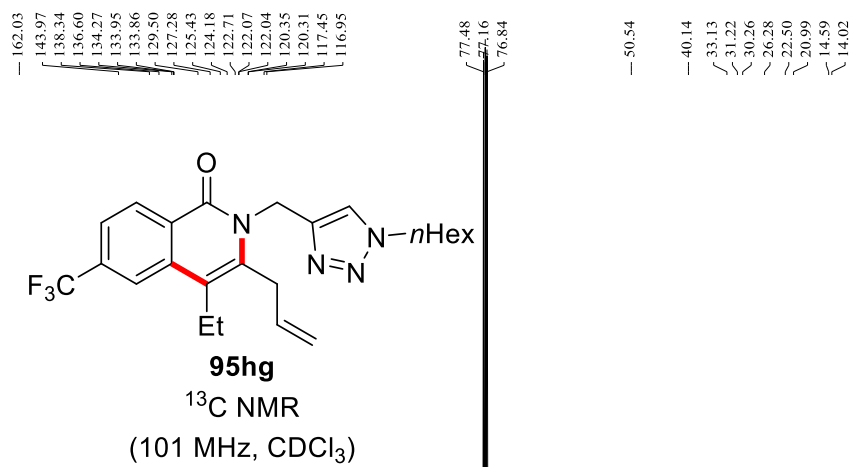
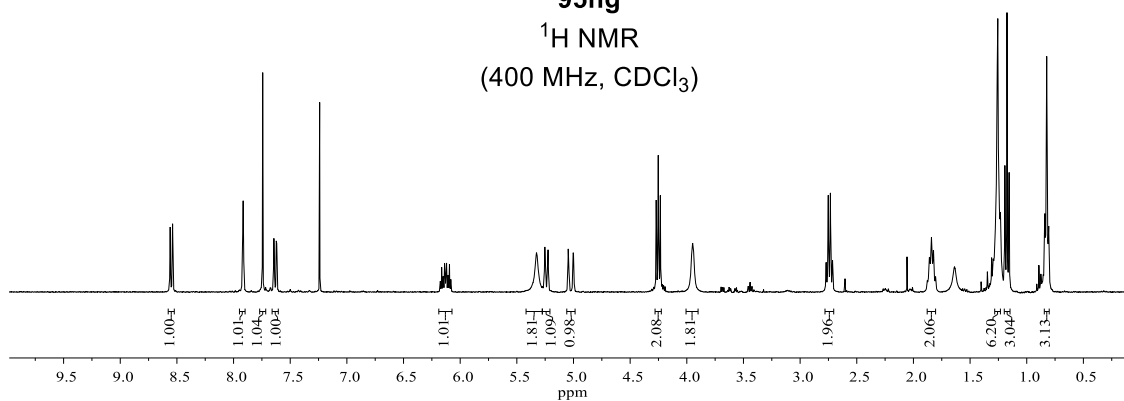
(75 MHz, CDCl<sub>3</sub>)



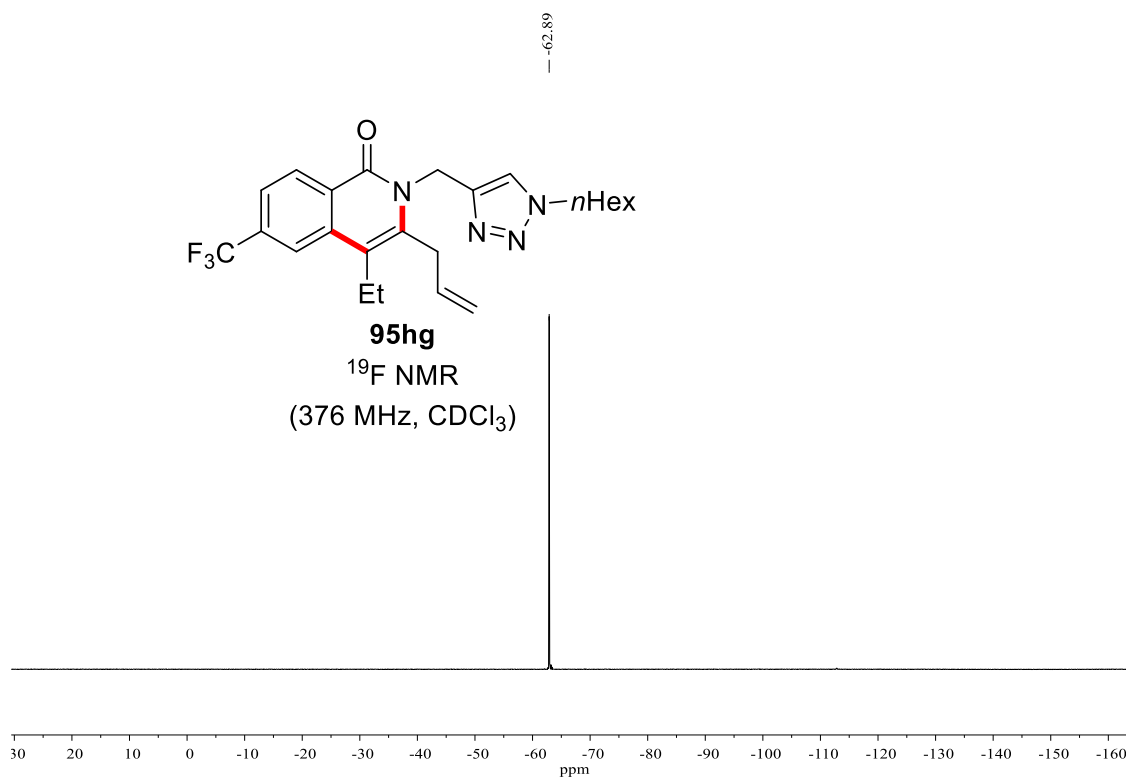
# NMR Spectra



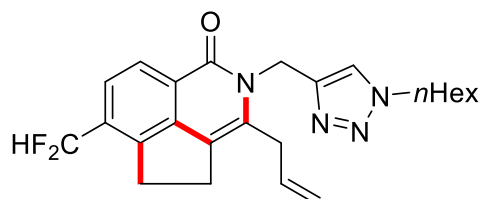
**95hg**  
 $^1\text{H}$  NMR  
 (400 MHz,  $\text{CDCl}_3$ )



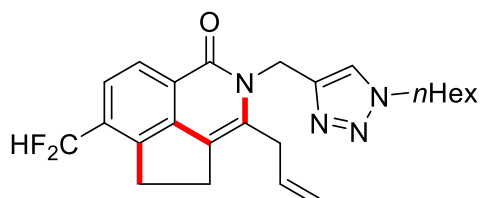
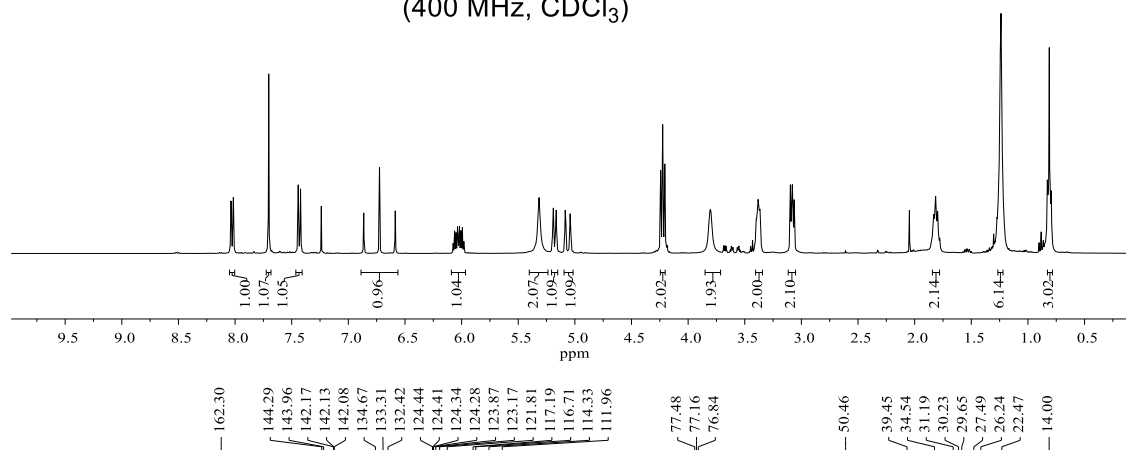
# NMR Spectra



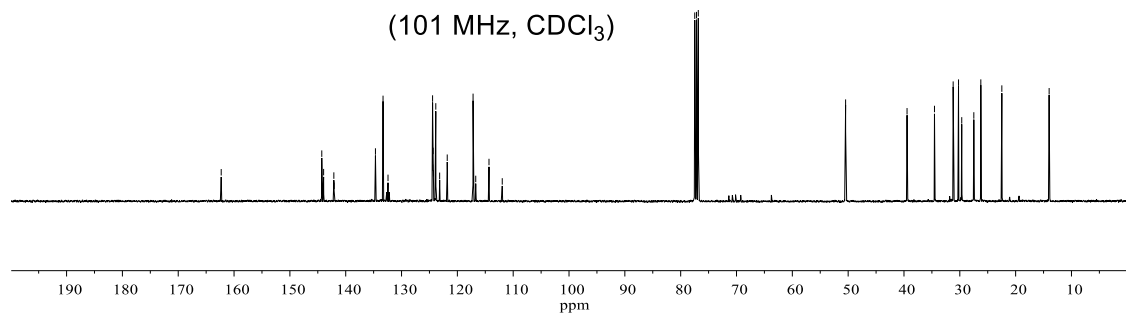
# NMR Spectra



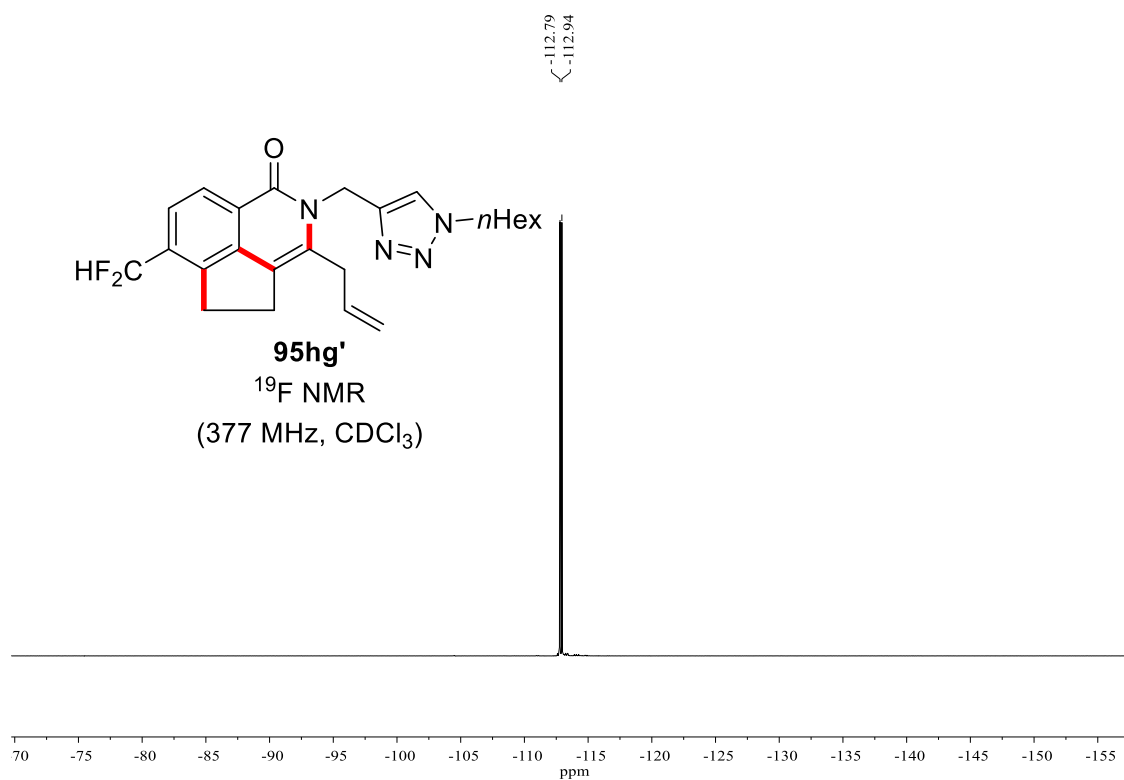
**95hg'**  
<sup>1</sup>H NMR  
 (400 MHz, CDCl<sub>3</sub>)



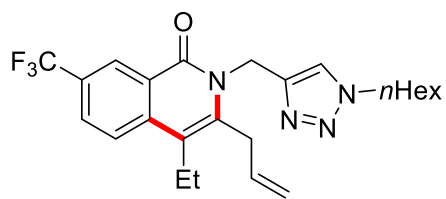
**95hg'**  
<sup>13</sup>C NMR  
 (101 MHz, CDCl<sub>3</sub>)



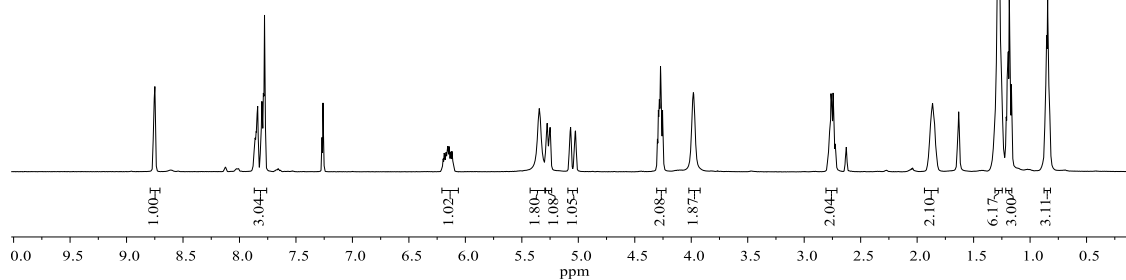
# NMR Spectra



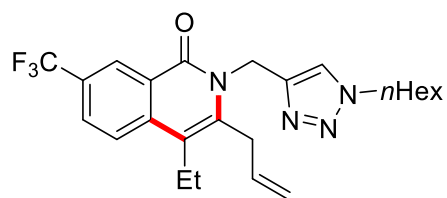
# NMR Spectra



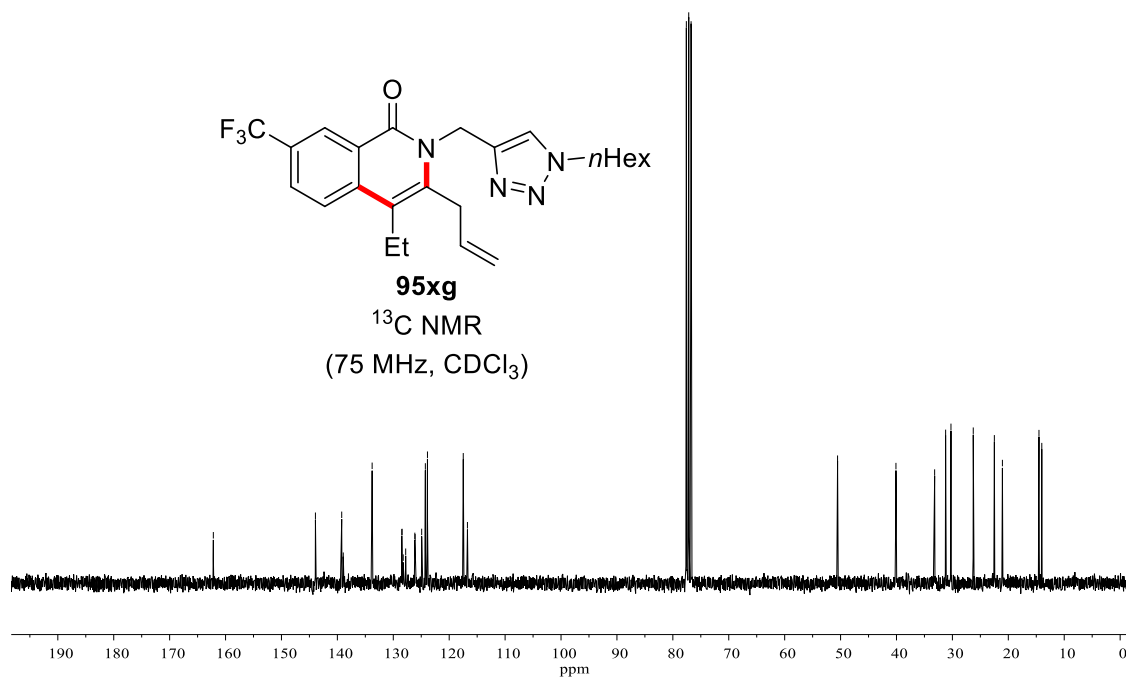
**95xg**  
 $^1\text{H}$  NMR  
 (400 MHz,  $\text{CDCl}_3$ )



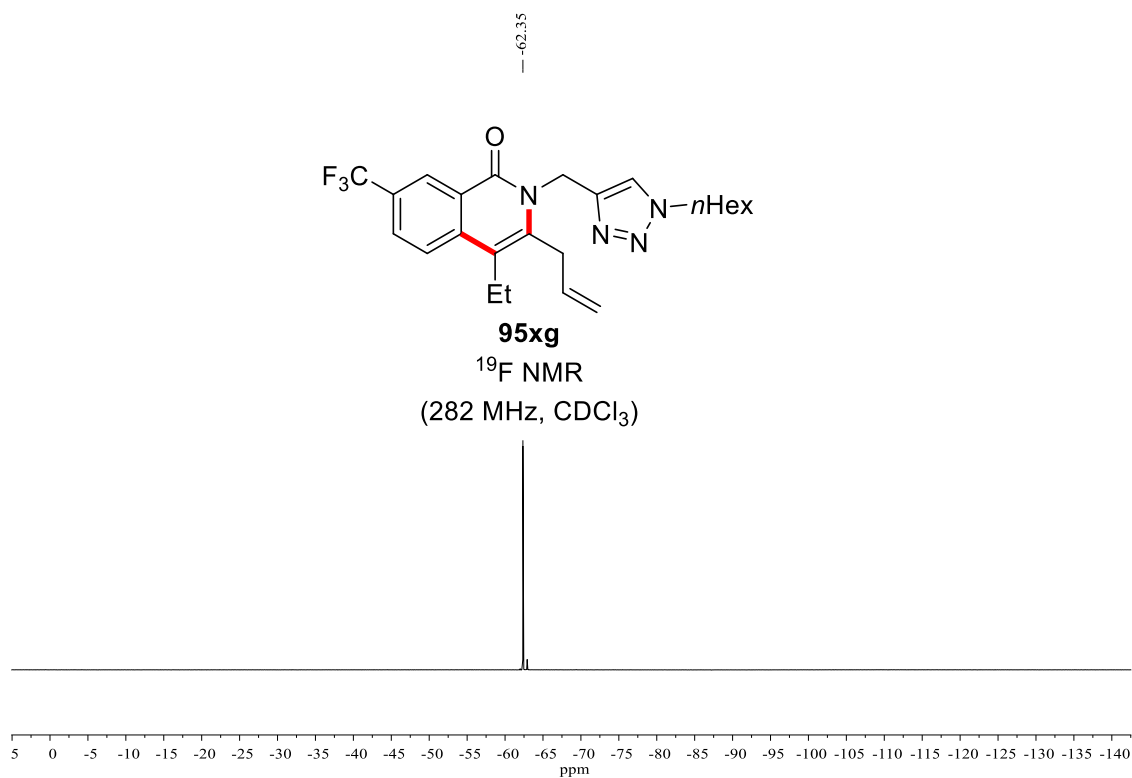
162.18  
 143.92  
 139.22  
 138.95  
 133.78  
 128.48  
 128.43  
 128.23  
 127.78  
 126.15  
 126.09  
 124.92  
 124.26  
 123.89  
 117.49  
 116.74  
 77.58  
 77.16  
 76.74  
 50.54  
 40.10  
 33.18  
 31.21  
 30.26  
 26.27  
 22.50  
 21.06  
 14.52  
 14.01



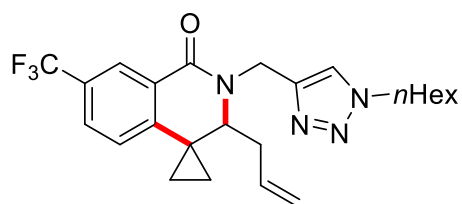
**95xg**  
 $^{13}\text{C}$  NMR  
 (75 MHz,  $\text{CDCl}_3$ )



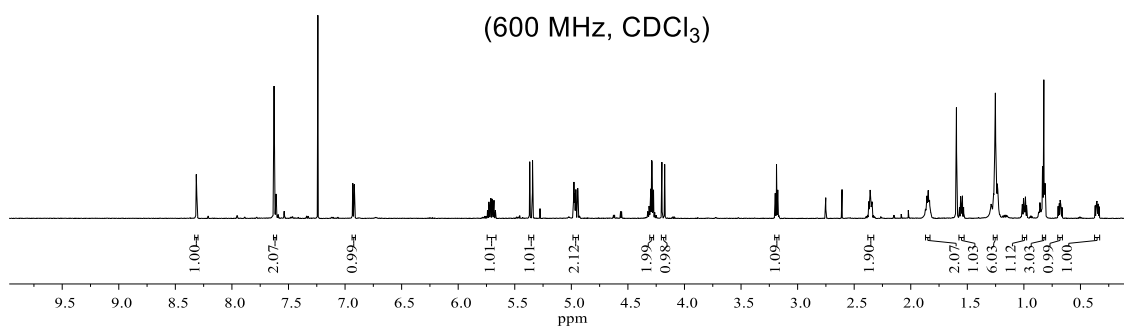
# NMR Spectra



# NMR Spectra

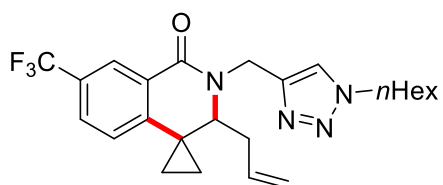


**95xg'**  
<sup>1</sup>H NMR  
 (600 MHz, CDCl<sub>3</sub>)

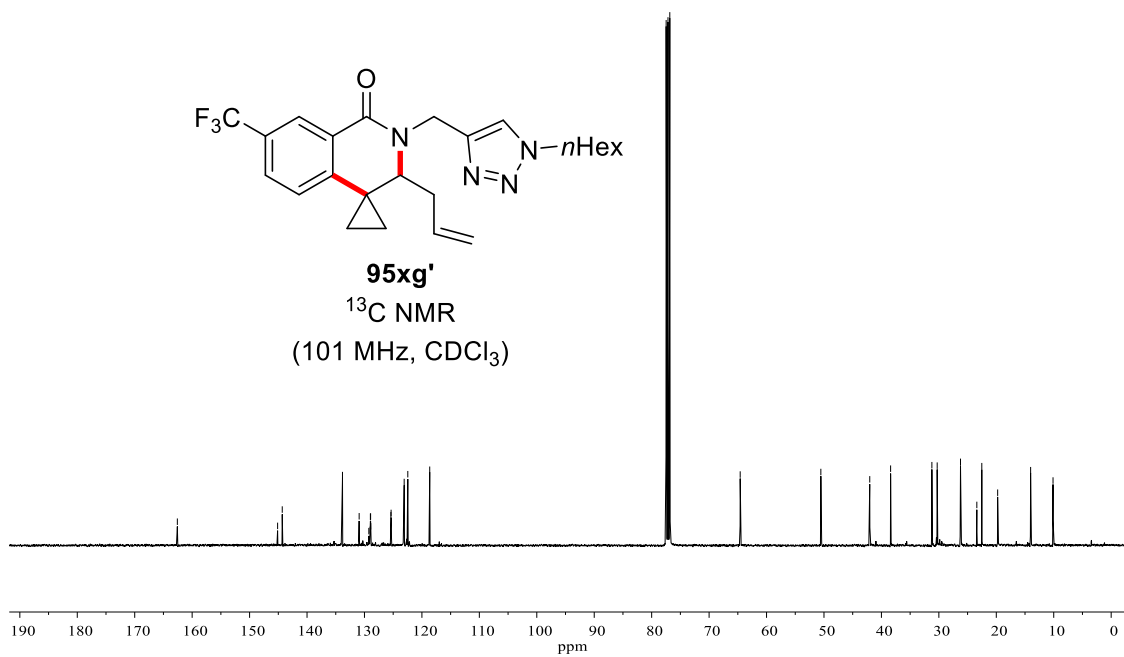


Chemical shift values (ppm) for <sup>13</sup>C NMR:

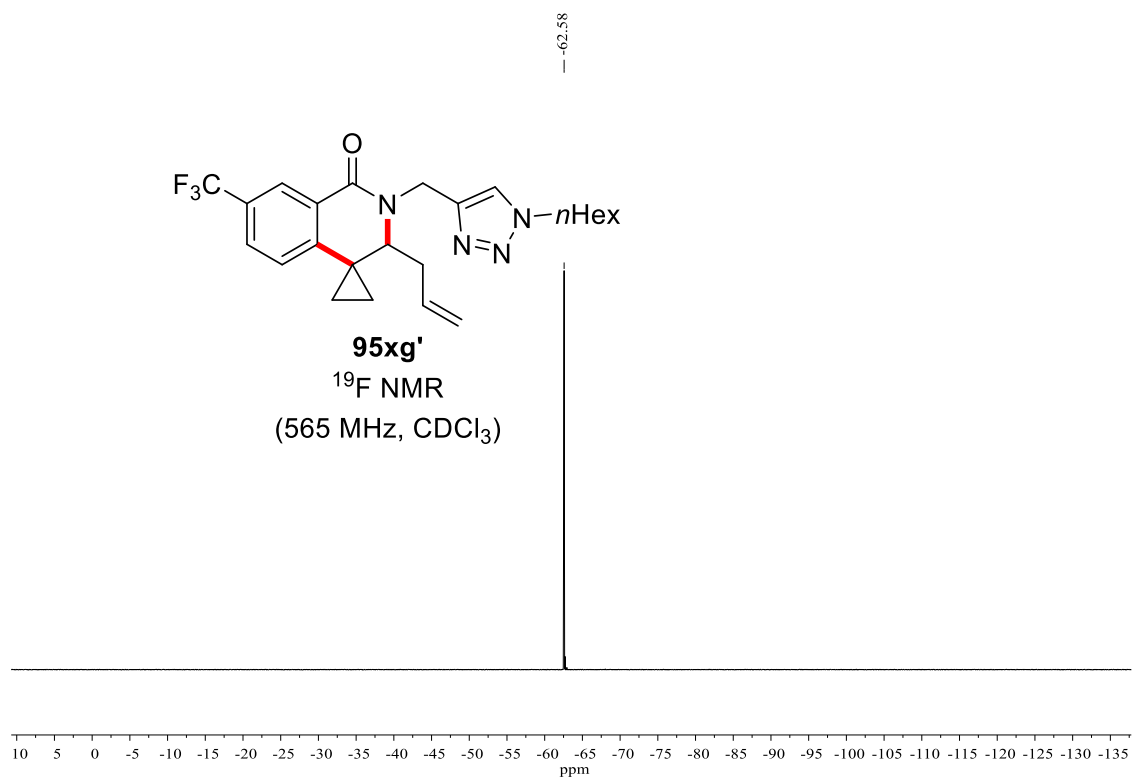
162.58	145.12	144.32	133.83	130.93	129.24	129.01	128.97	128.93	128.91	125.44	125.40	125.36	123.09	122.46	118.64
77.48	77.16	76.84	64.59	50.54	42.03	38.40	31.21	30.29	26.23	23.39	22.52	19.76	14.02	10.12	



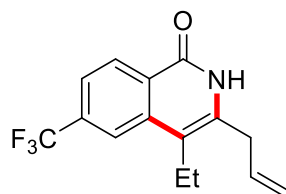
**95xg'**  
<sup>13</sup>C NMR  
 (101 MHz, CDCl<sub>3</sub>)



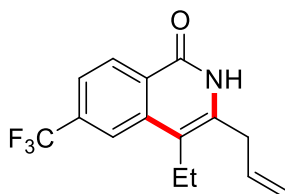
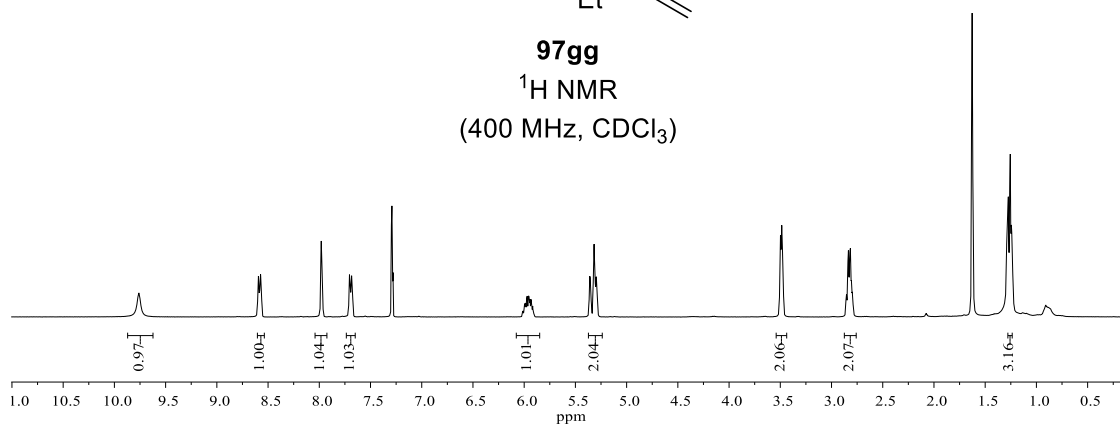
# NMR Spectra



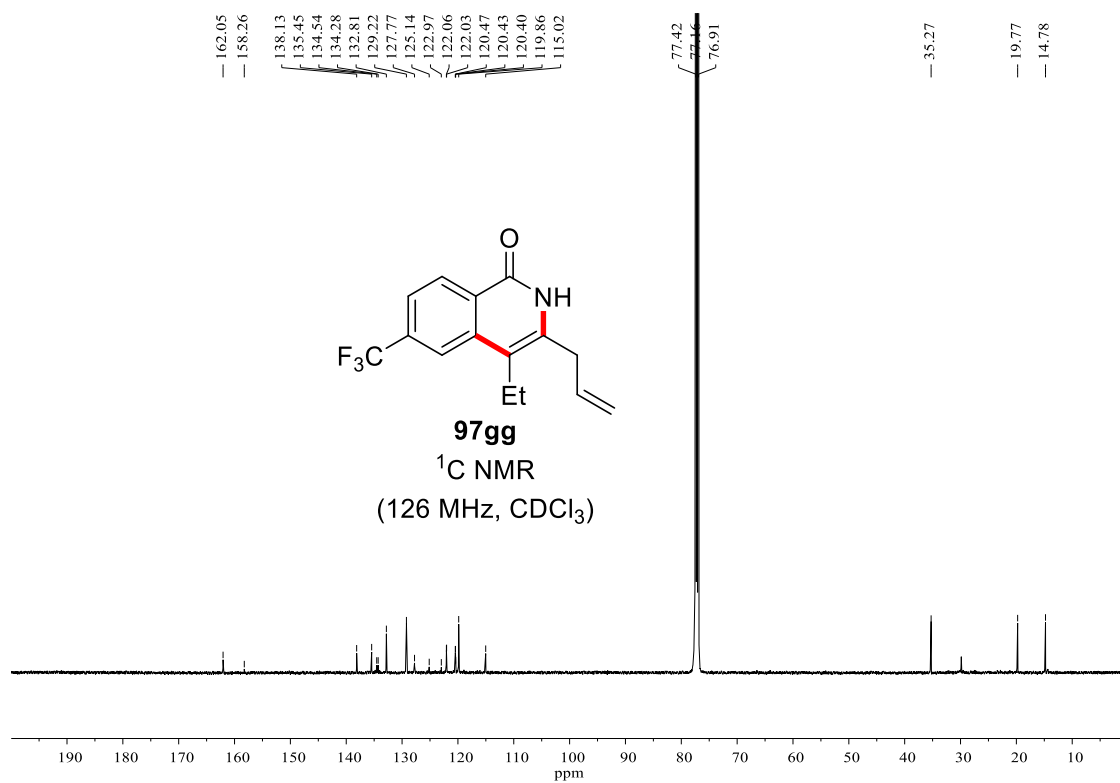
# NMR Spectra



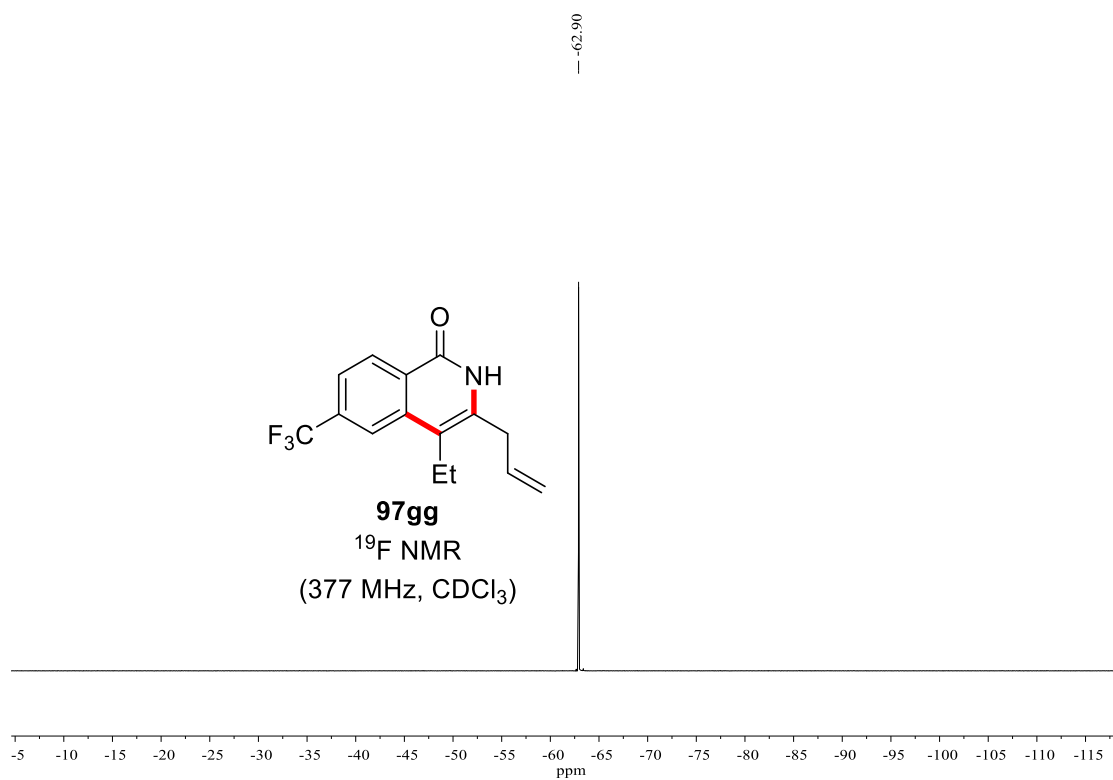
**97gg**  
 $^1\text{H}$  NMR  
 (400 MHz,  $\text{CDCl}_3$ )



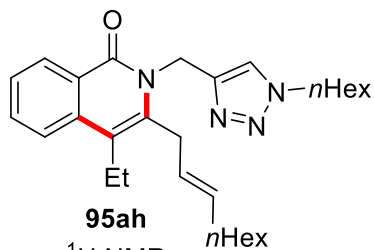
**97gg**  
 $^{13}\text{C}$  NMR  
 (126 MHz,  $\text{CDCl}_3$ )



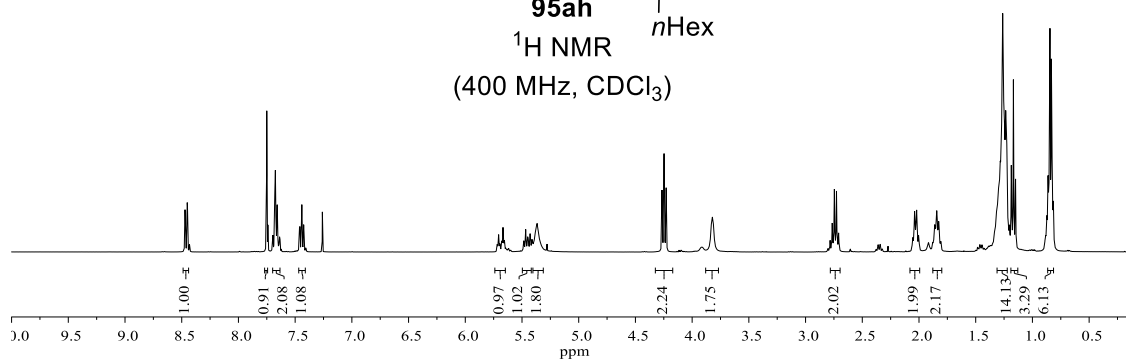
## NMR Spectra



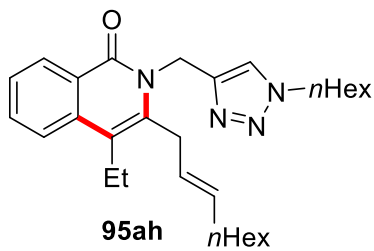
# NMR Spectra



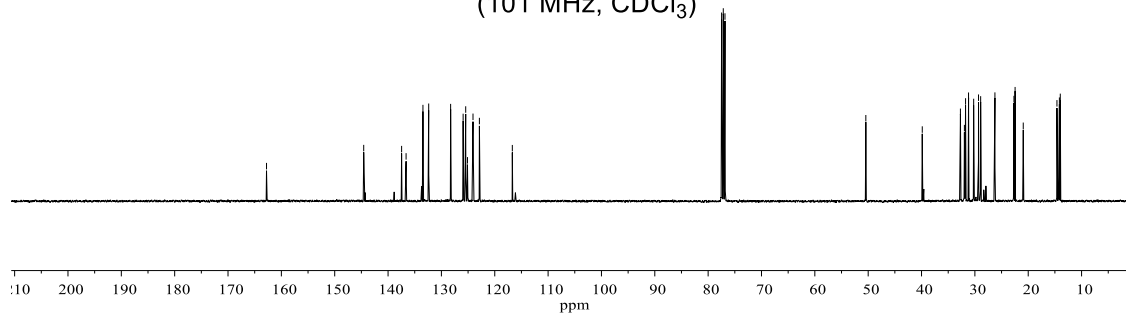
$^1\text{H}$  NMR  
(400 MHz,  $\text{CDCl}_3$ )



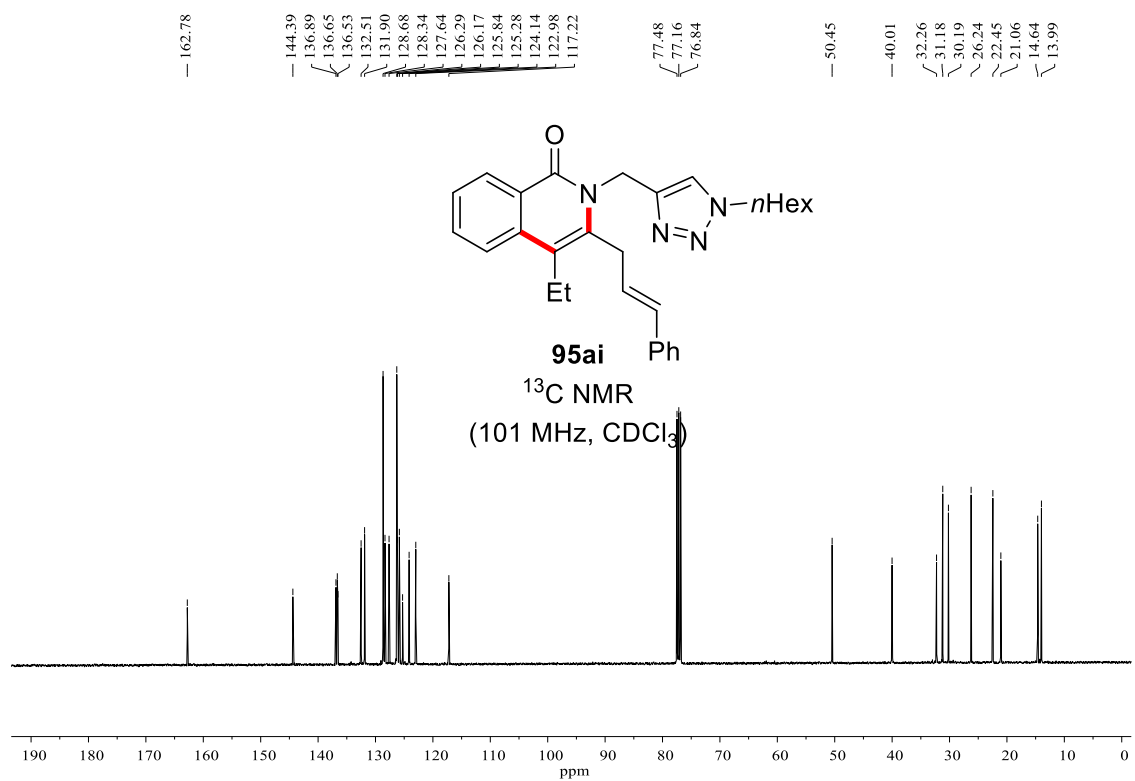
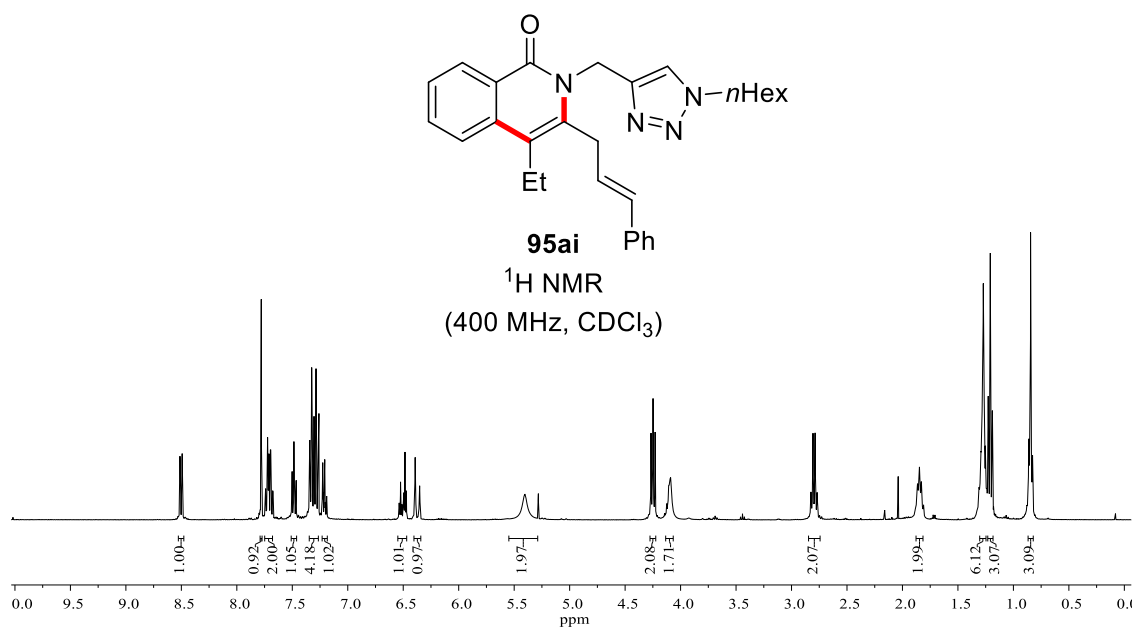
162.78, 144.56, 137.46, 136.62, 133.46, 132.38, 128.27, 125.93, 125.45, 125.11, 124.08, 122.88, 116.71, 77.48, 77.16, 76.84, 50.44, 39.86, 32.71, 31.96, 31.75, 31.19, 30.23, 29.32, 28.92, 26.24, 22.67, 22.46, 20.93, 14.61, 14.16, 13.99



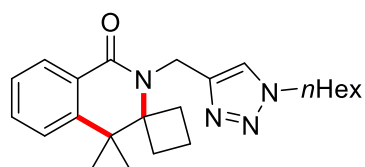
$^{13}\text{C}$  NMR  
(101 MHz,  $\text{CDCl}_3$ )



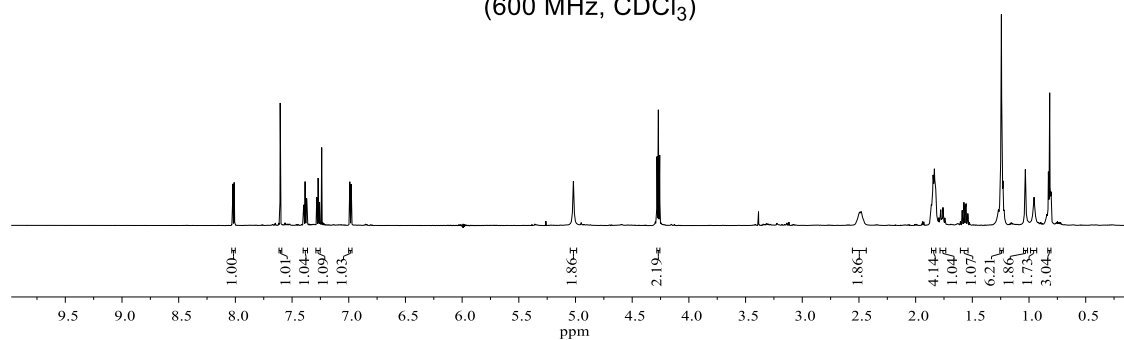
# NMR Spectra



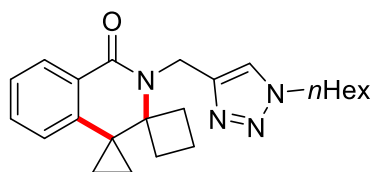
# NMR Spectra



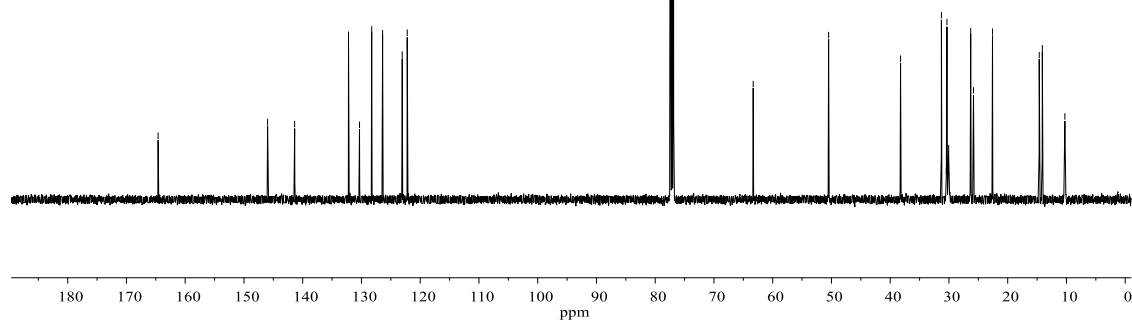
**96aa**  
 $^1\text{H}$  NMR  
 (600 MHz,  $\text{CDCl}_3$ )



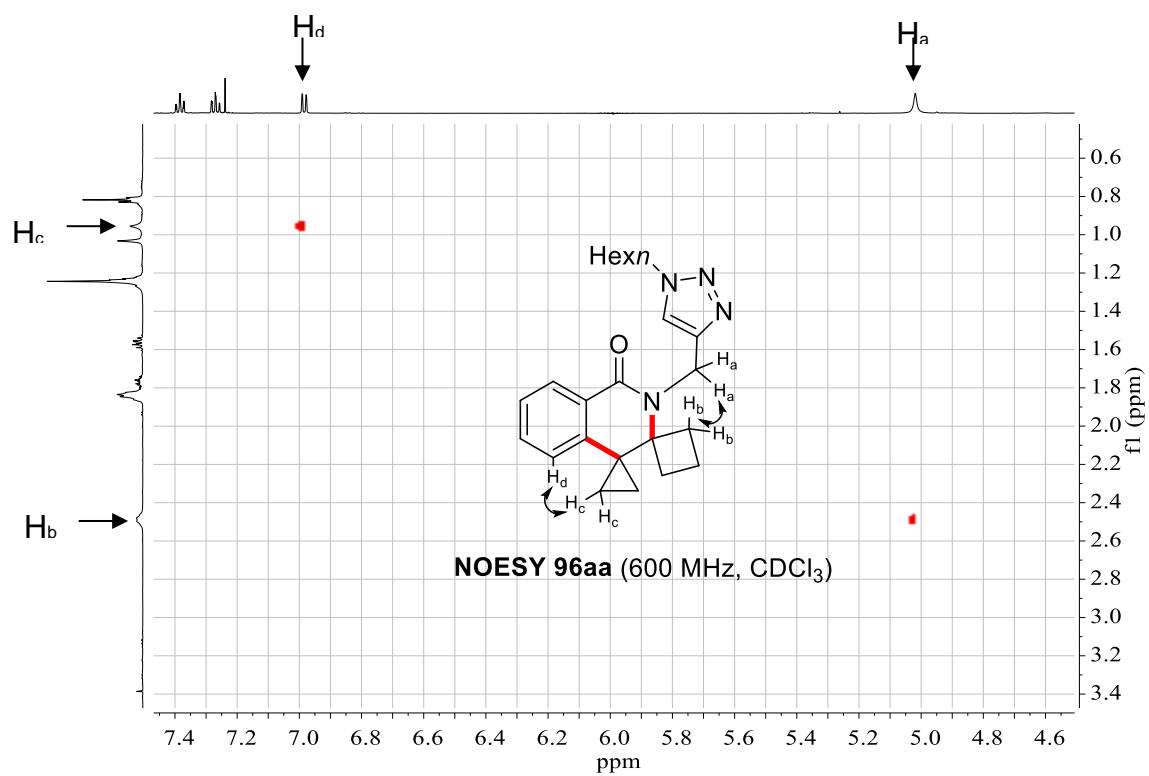
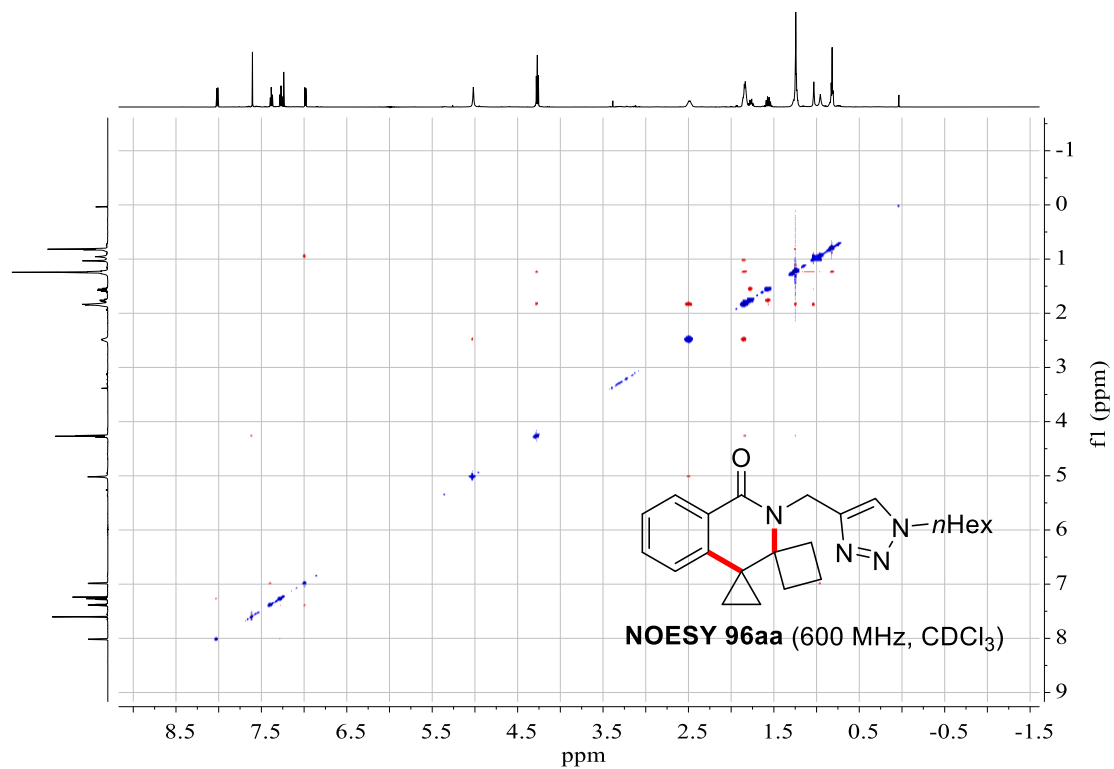
$^13\text{C}$  NMR peaks (ppm):  
 164.61, 145.98, 141.37, 132.20, 130.33, 128.25, 126.40, 123.06, 122.21, 77.41, 77.16, 76.91, 63.32, 50.48, 38.24, 31.28, 30.45, 30.34, 30.05, 26.30, 25.82, 22.59, 14.63, 14.10, 10.27



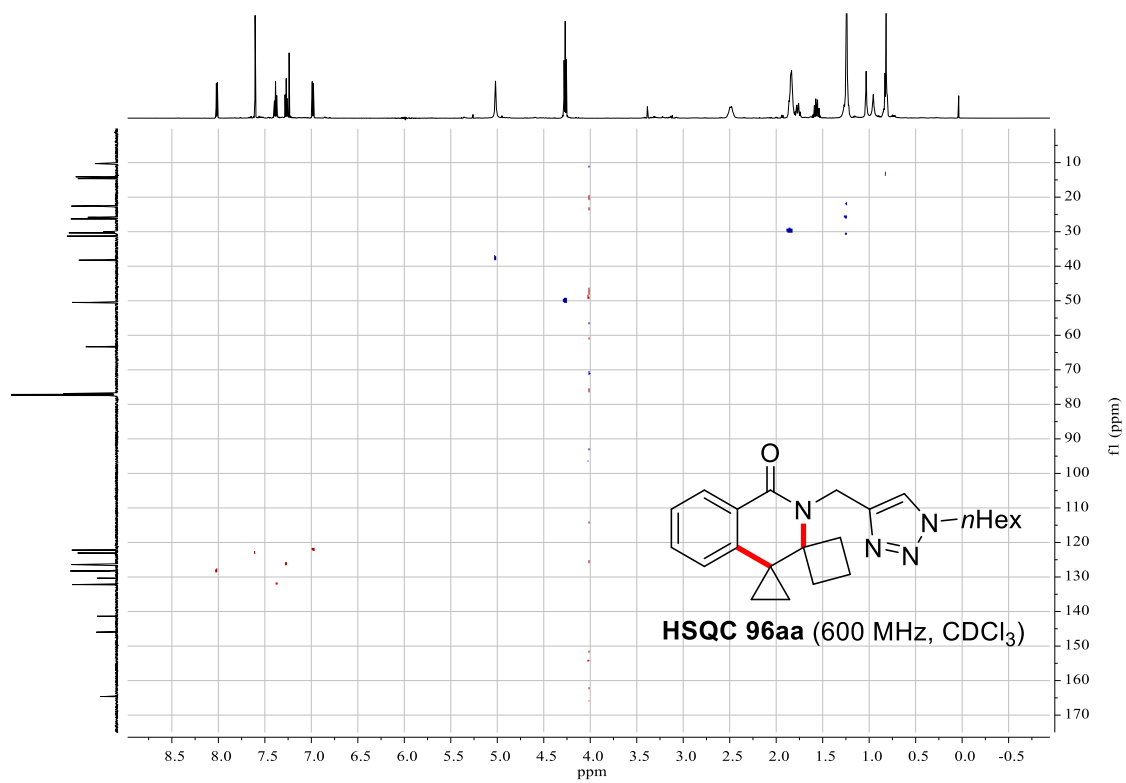
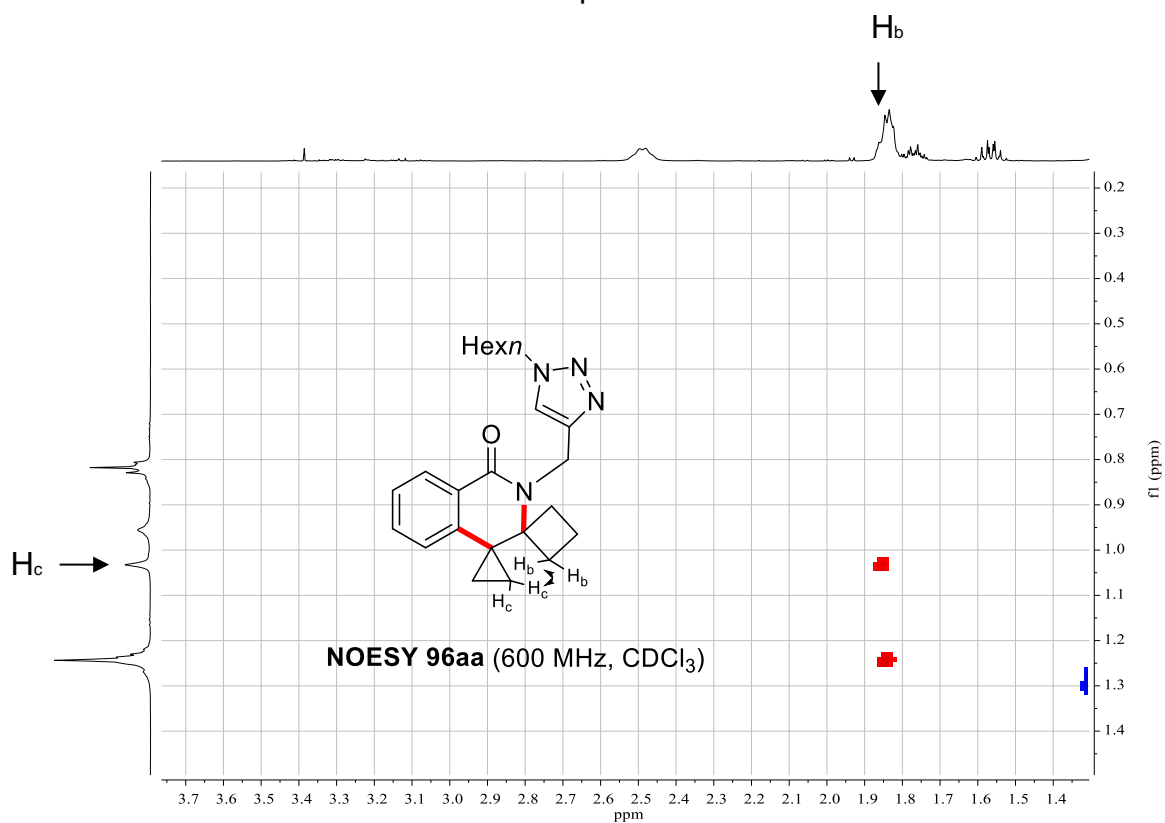
**96aa**  
 $^{13}\text{C}$  NMR  
 (126 MHz,  $\text{CDCl}_3$ )



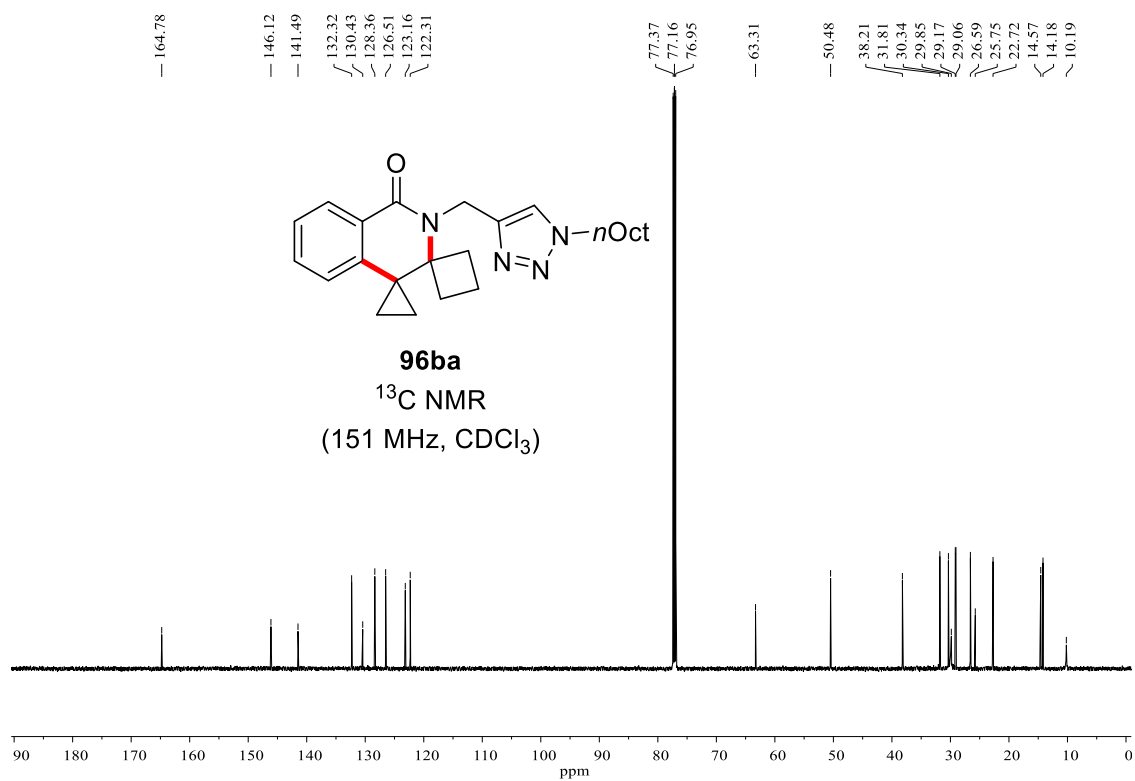
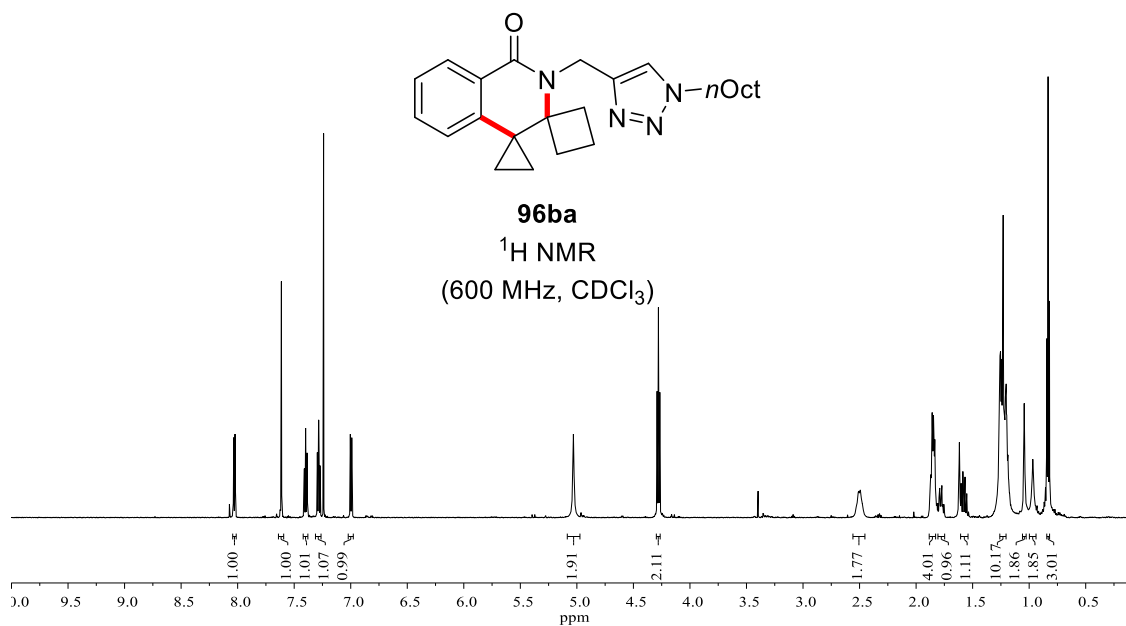
# NMR Spectra



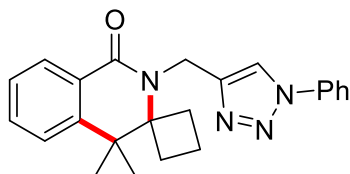
# NMR Spectra



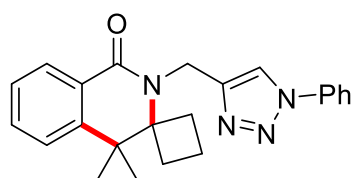
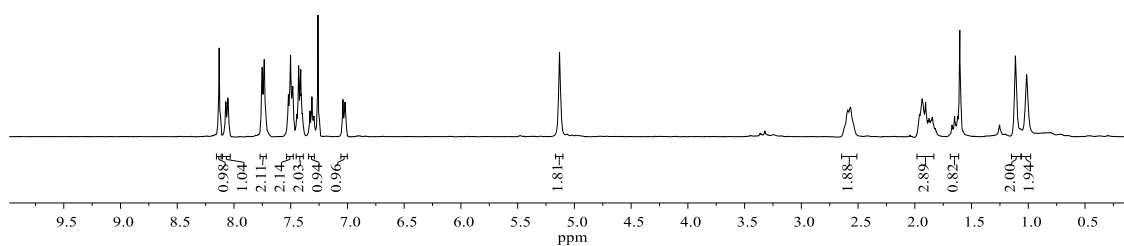
# NMR Spectra



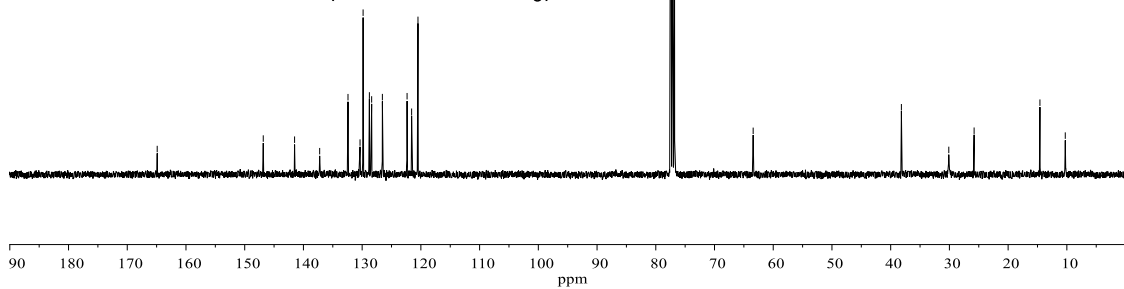
# NMR Spectra



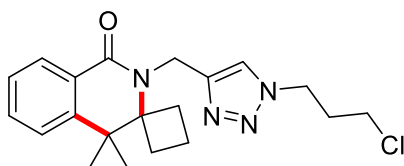
**96ya**  
 $^1\text{H}$  NMR  
 (400 MHz,  $\text{CDCl}_3$ )



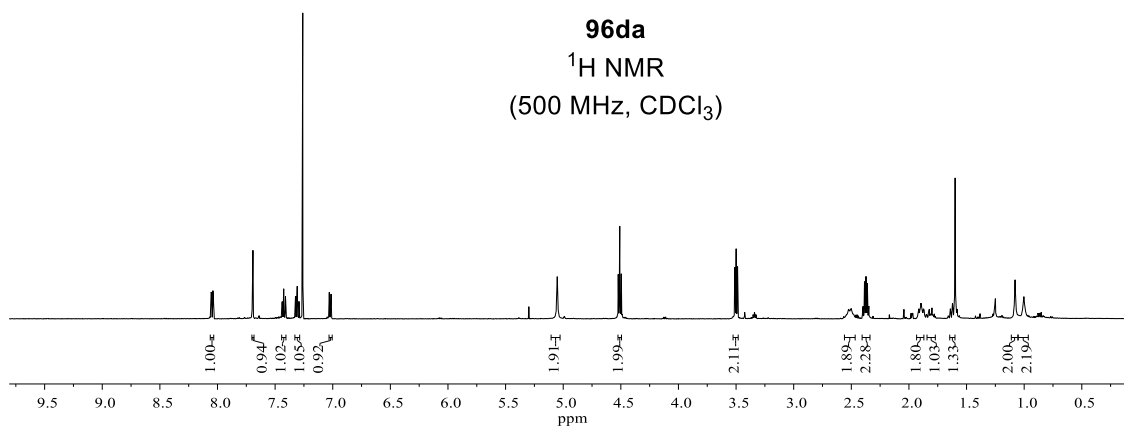
**96ya**  
 $^{13}\text{C}$  NMR  
 (101 MHz,  $\text{CDCl}_3$ )



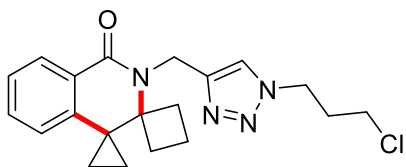
# NMR Spectra



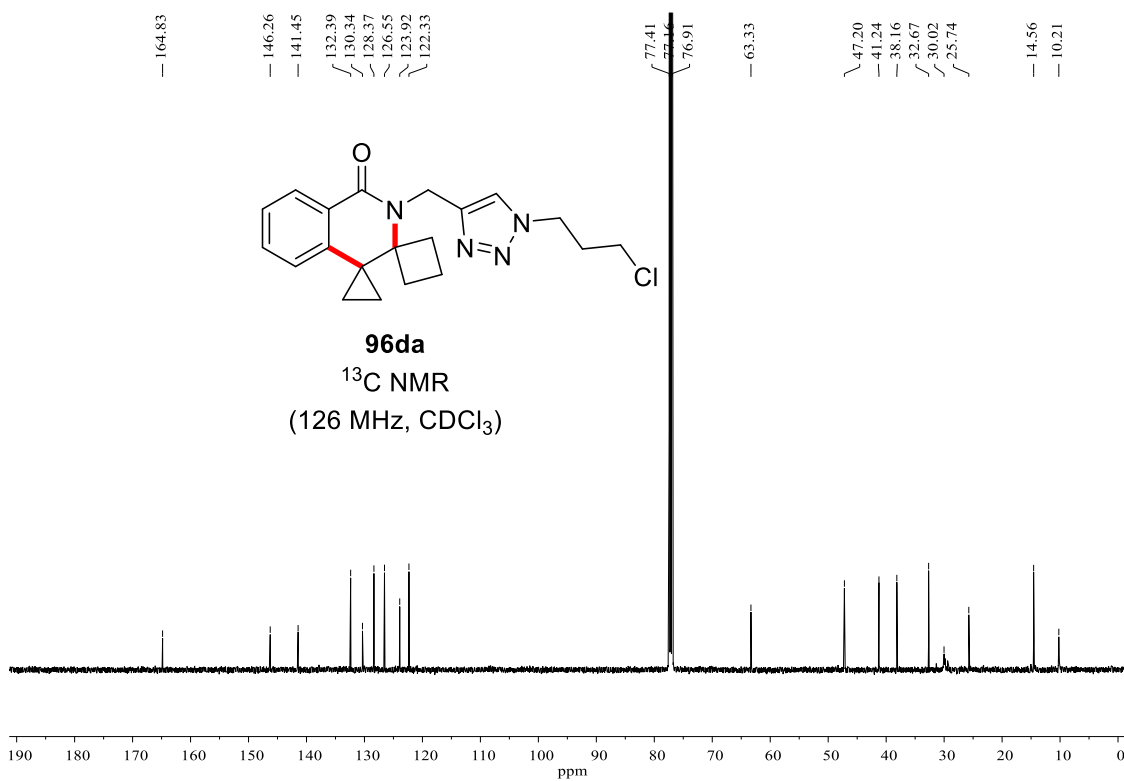
**96da**  
<sup>1</sup>H NMR  
 (500 MHz, CDCl<sub>3</sub>)



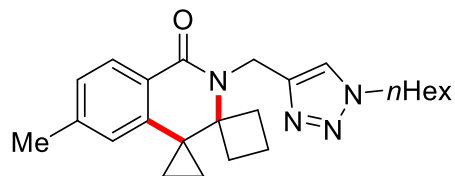
164.83  
 146.26  
 141.45  
 132.39  
 130.34  
 128.37  
 126.55  
 123.92  
 122.33  
 77.41  
 77.16  
 76.91  
 63.33  
 47.20  
 41.24  
 38.16  
 32.67  
 30.02  
 25.74  
 14.56  
 10.21



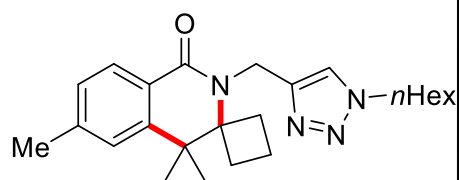
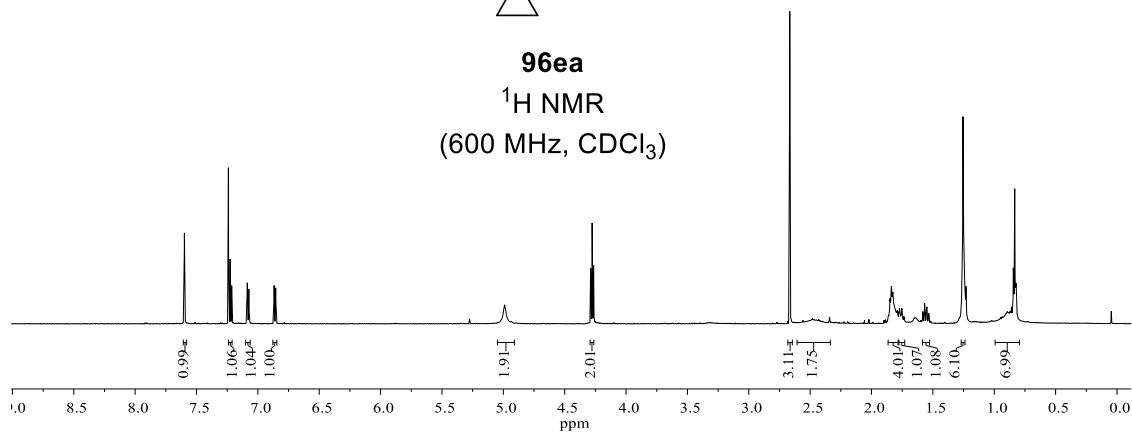
**96da**  
<sup>13</sup>C NMR  
 (126 MHz, CDCl<sub>3</sub>)



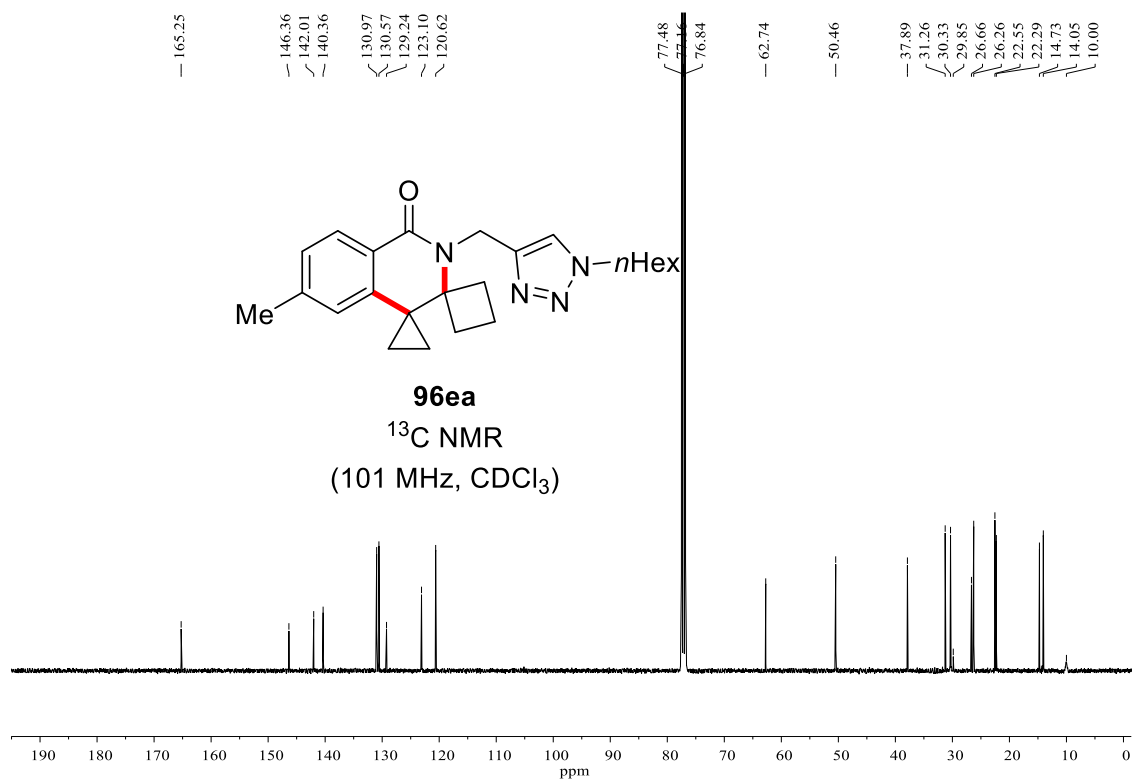
# NMR Spectra



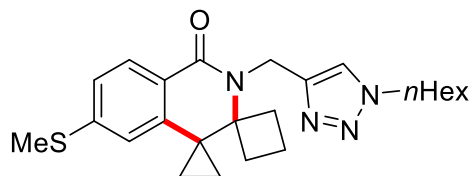
**96ea**  
 $^1\text{H}$  NMR  
 (600 MHz,  $\text{CDCl}_3$ )



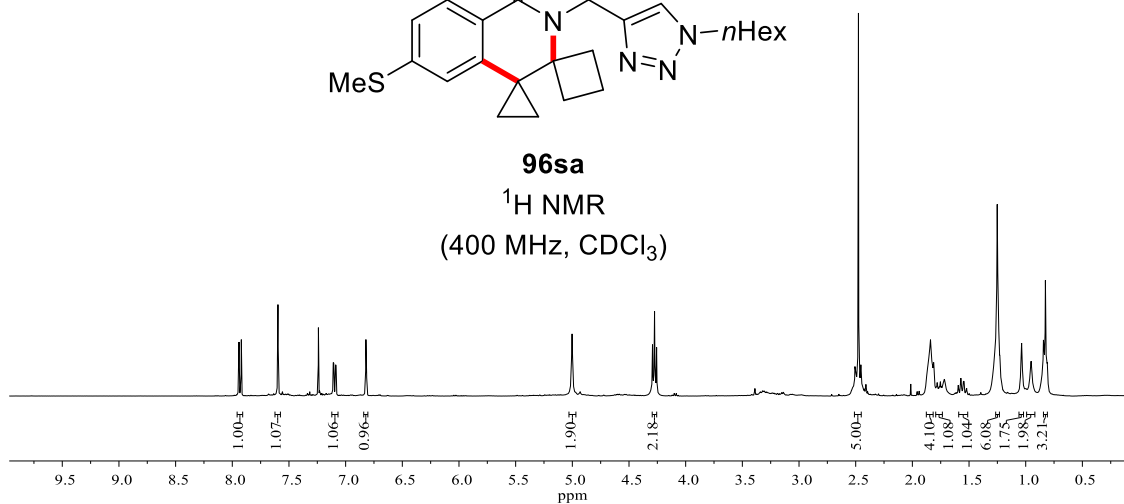
**96ea**  
 $^{13}\text{C}$  NMR  
 (101 MHz,  $\text{CDCl}_3$ )



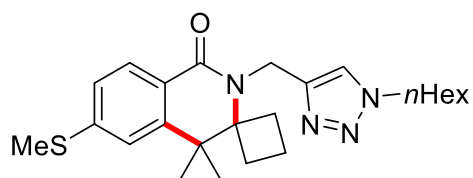
# NMR Spectra



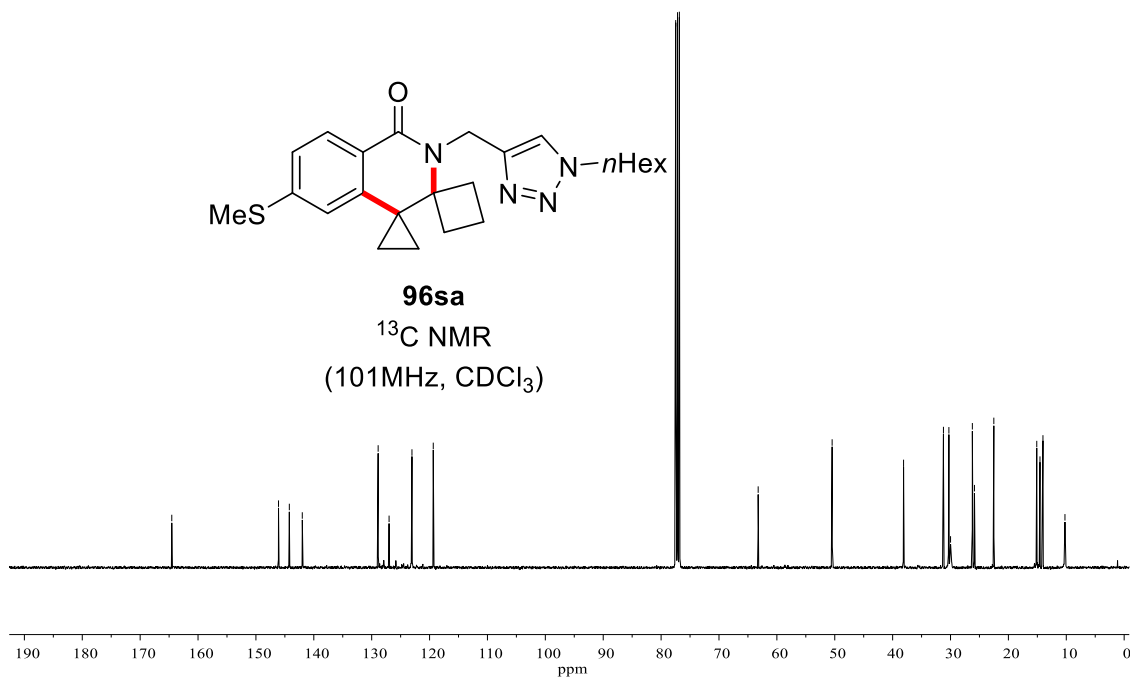
**96sa**  
 $^1\text{H}$  NMR  
 (400 MHz,  $\text{CDCl}_3$ )



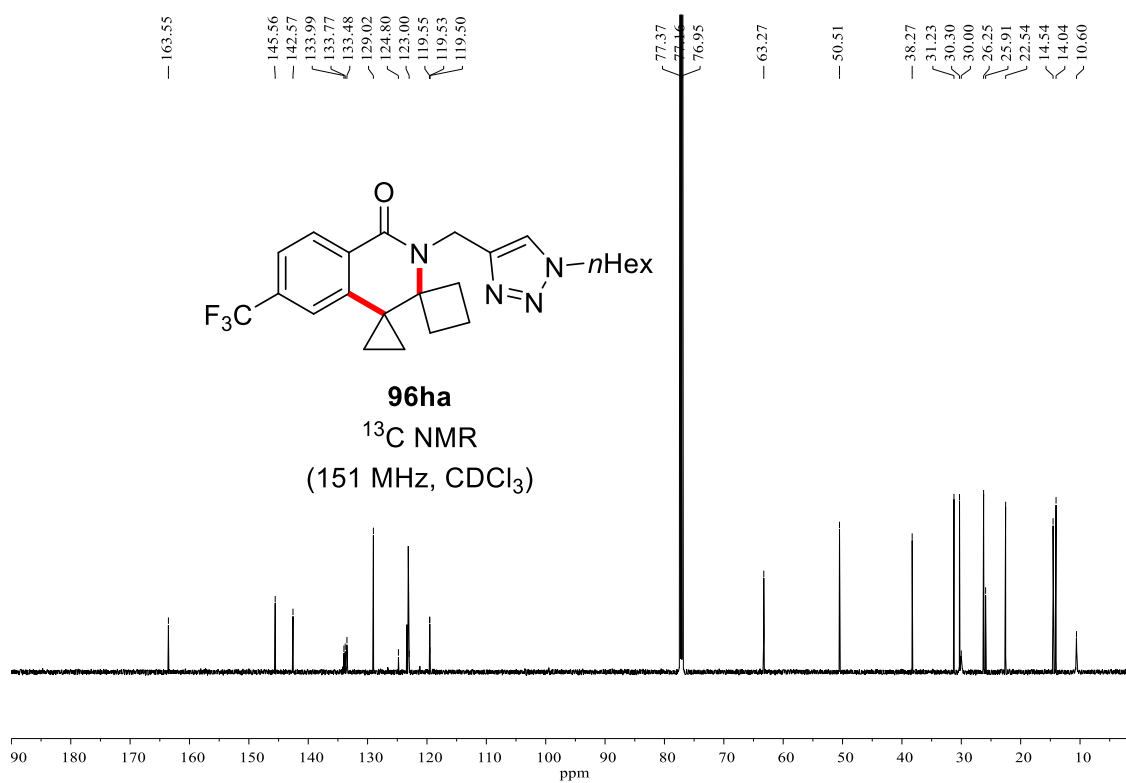
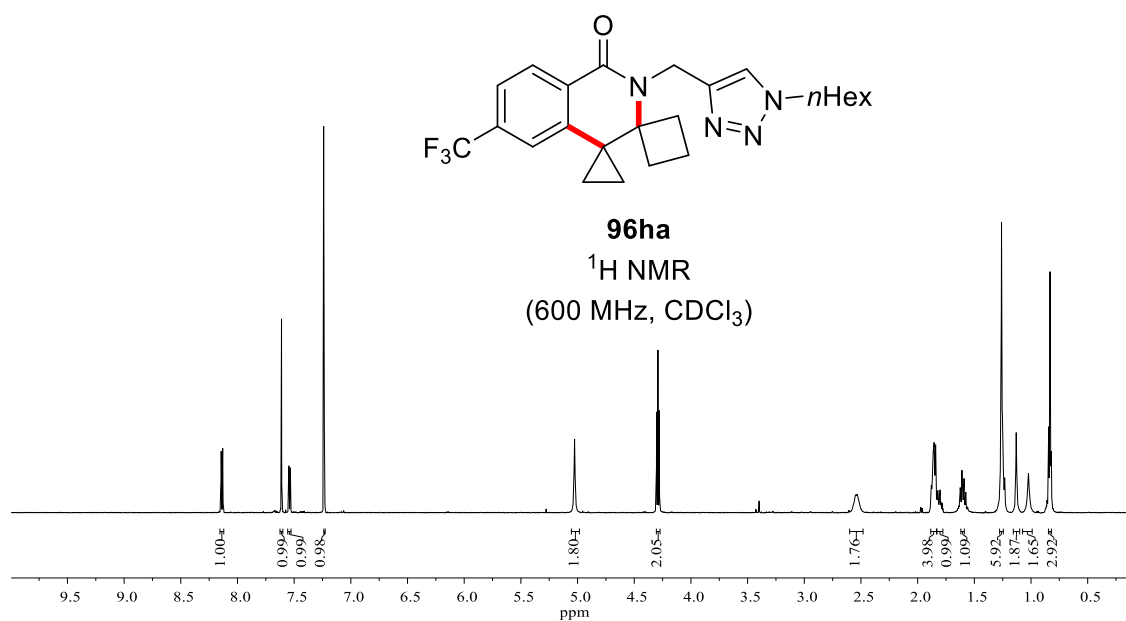
$^13\text{C}$  NMR chemical shifts (ppm): 164.54, 146.10, 144.23, 141.99, 128.88, 127.00, 123.11, 123.04, 119.36, 77.48, 77.16, 76.84, 63.23, 50.45, 38.11, 31.22, 30.28, 30.00, 26.23, 25.86, 22.52, 15.10, 14.54, 14.03, 10.23.



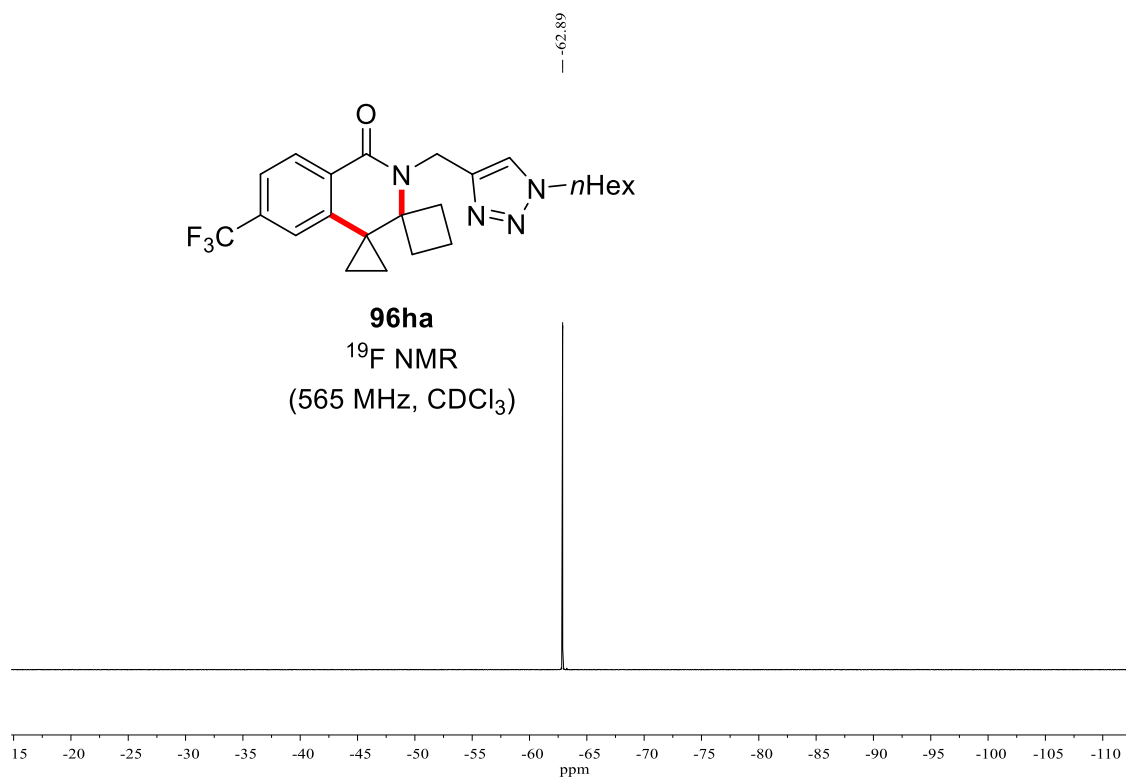
**96sa**  
 $^{13}\text{C}$  NMR  
 (101MHz,  $\text{CDCl}_3$ )



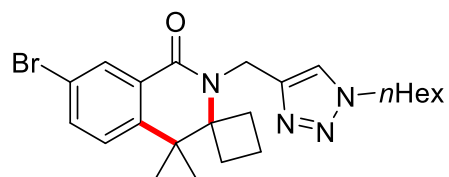
# NMR Spectra



# NMR Spectra

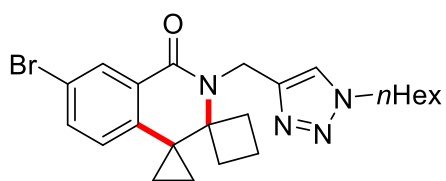
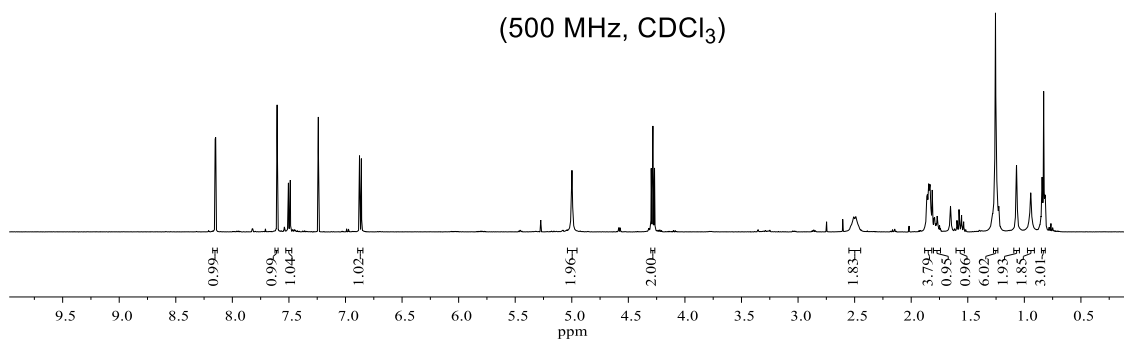


# NMR Spectra



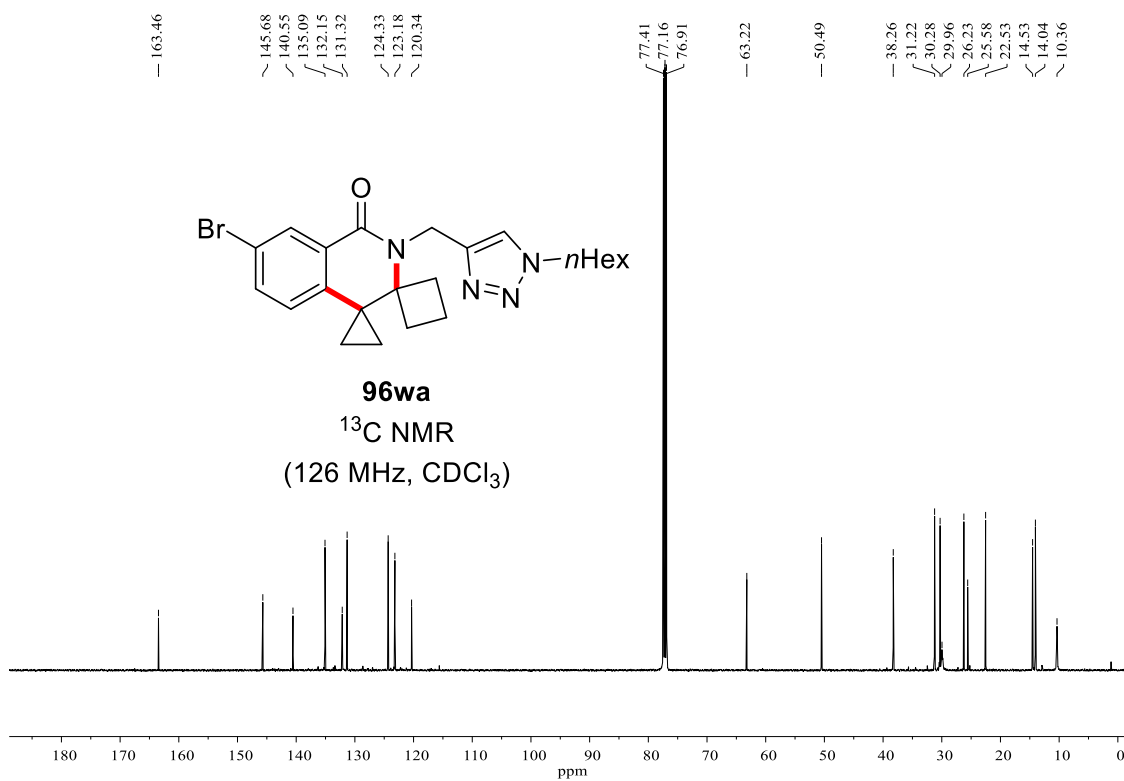
**96wa**

$^1\text{H}$  NMR  
(500 MHz,  $\text{CDCl}_3$ )

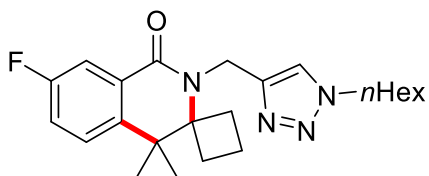


**96wa**

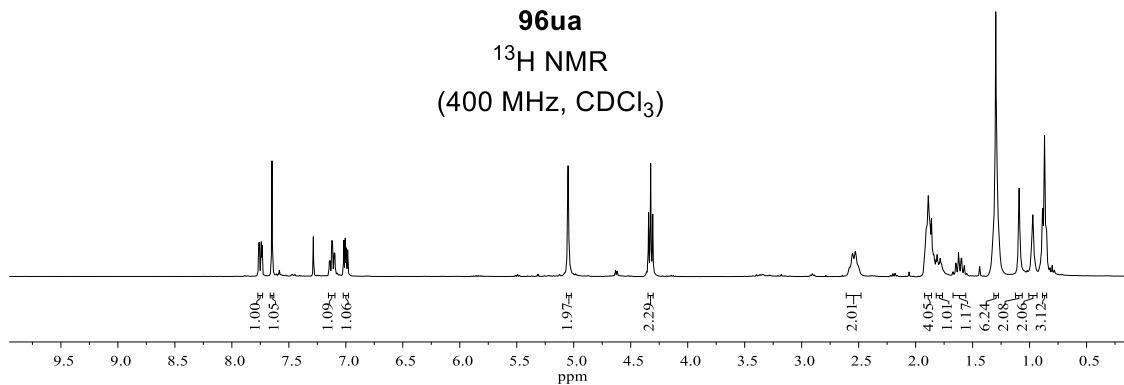
$^{13}\text{C}$  NMR  
(126 MHz,  $\text{CDCl}_3$ )



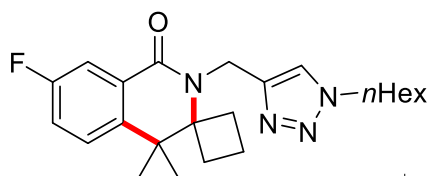
# NMR Spectra



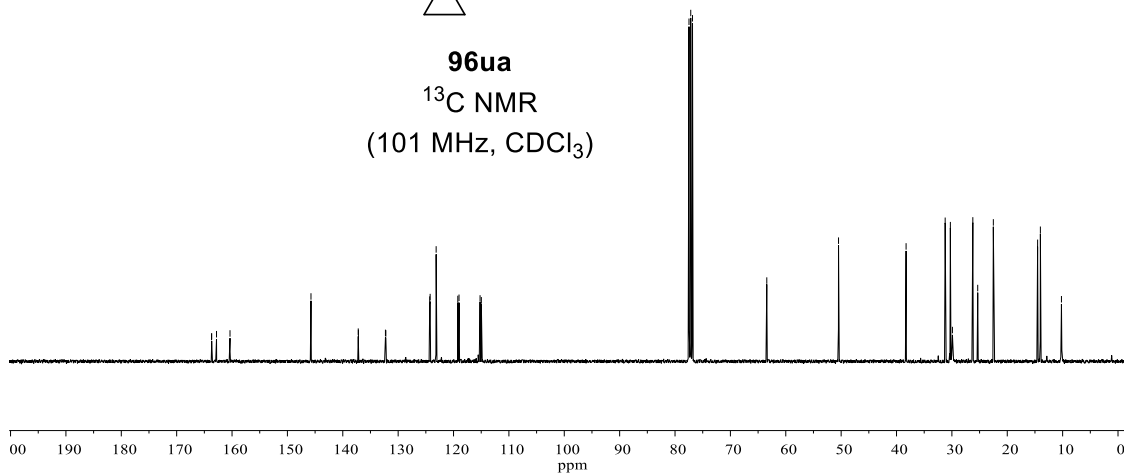
**96ua**  
 $^1\text{H}$  NMR  
 (400 MHz,  $\text{CDCl}_3$ )



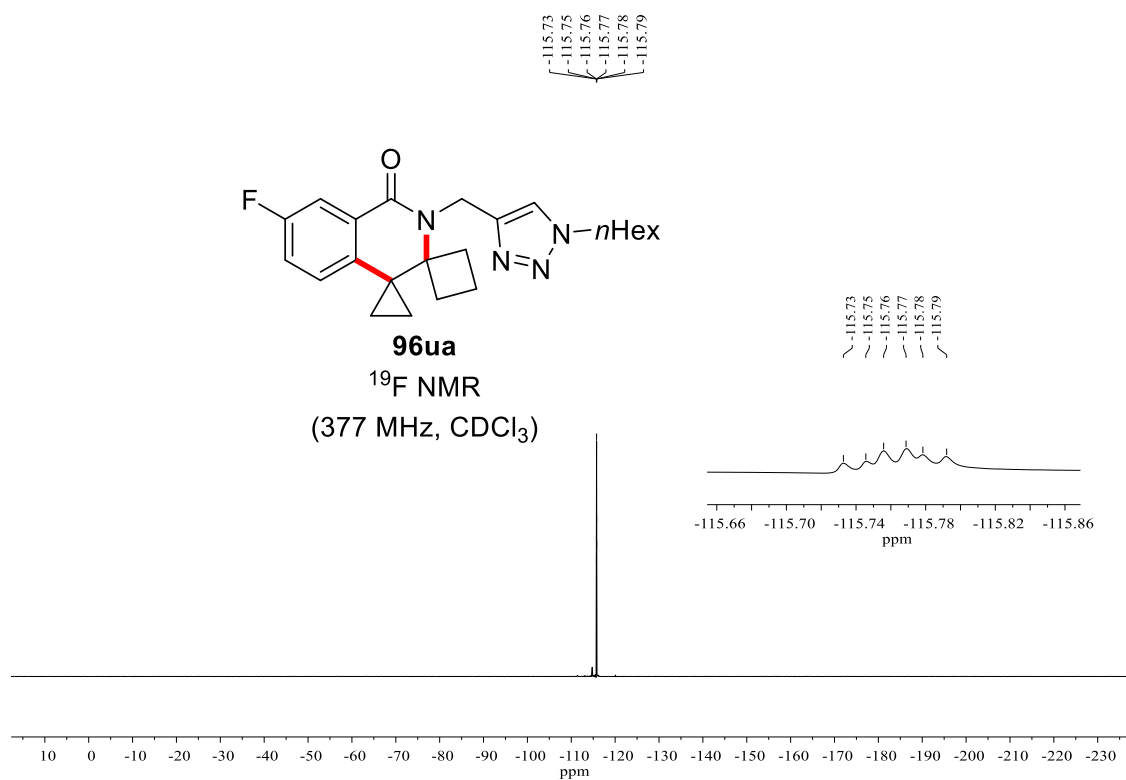
163.70  
 163.68  
 162.80  
 160.37  
 — 145.74  
 137.21  
 137.18  
 132.30  
 132.22  
 124.30  
 124.23  
 123.14  
 119.23  
 119.01  
 115.21  
 114.98  
 77.48  
 77.16  
 76.84  
 — 63.43  
 — 50.47  
 38.27  
 31.21  
 30.28  
 29.90  
 26.22  
 25.34  
 22.51  
 14.52  
 14.02  
 10.21



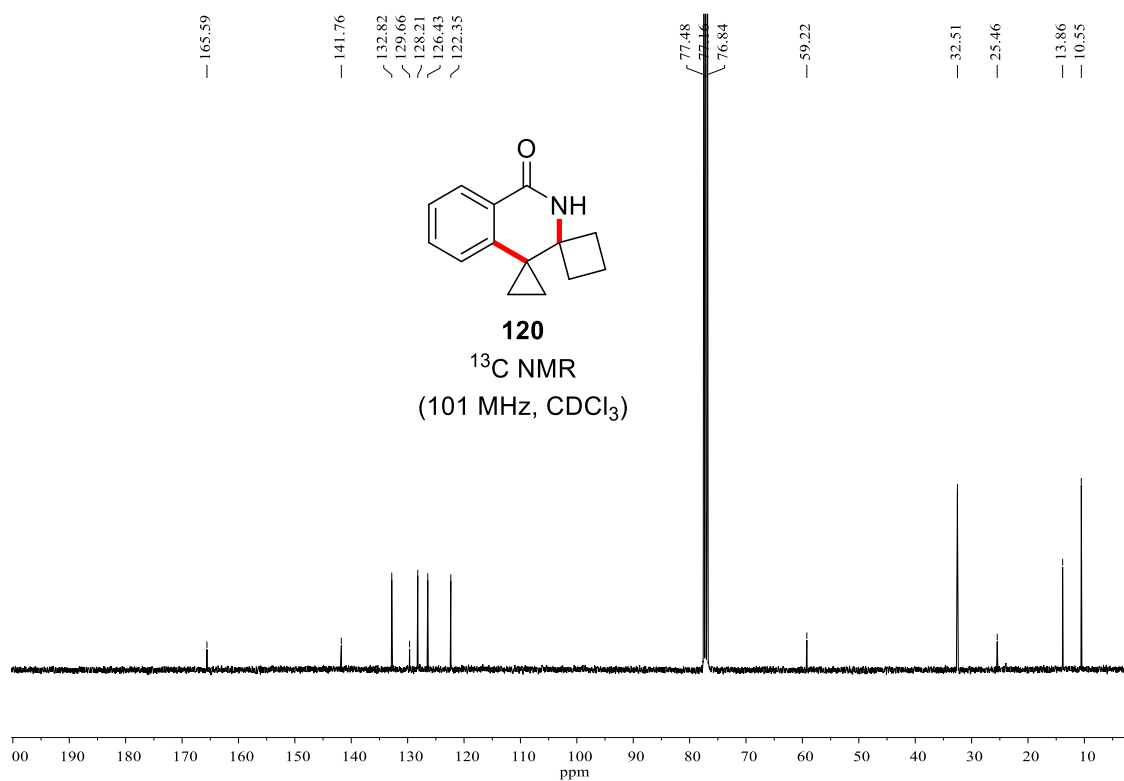
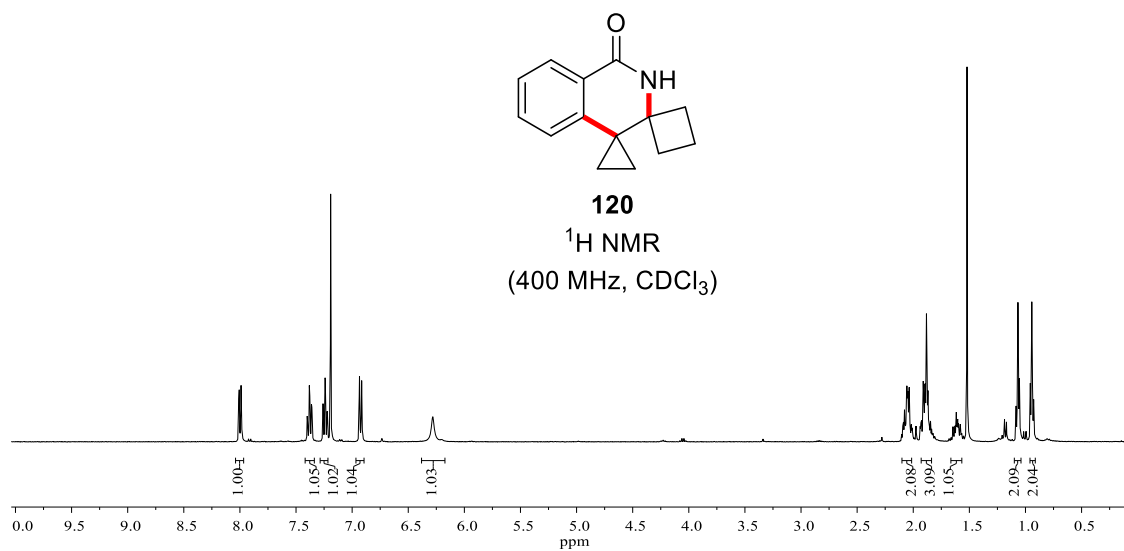
**96ua**  
 $^{13}\text{C}$  NMR  
 (101 MHz,  $\text{CDCl}_3$ )



# NMR Spectra



# NMR Spectra



## **Erklärung**

Ich versichere, dass ich die vorliegende Dissertation in dem Zeitraum von  
Oktober 2016 bis Oktober 2020 am Institut für Organische und Biomolekulare  
Chemie der Georg-August-Universität Göttingen

auf Anregung und unter Anleitung von

**Herrn Prof. Dr. Lutz Ackermann**

selbstständig durchgeführt und keine anderen als die angegebenen Hilfsmittel  
und Quellen verwendet habe.

Göttingen, den 05.11.2020

---